Supporting Documents for Quantitative Metric 3.3.3

Submitted to NAAC

By

Gandhi Institute For Technology (GIFT), Bhubaneswar

Gandhi Institute For Technology (GIFT)

Bhubaneswar

Number of books and chapters in edited volumes/books published and papers published in national/ international conference proceedings per teacher during last five years					
Year	**2015-16**	**2016-17**	**2017-18**	**2018-19**	**2019-20**
Number of books and chapters in edited volumes/books published and papers published in national/ international conference proceedings	193	155	125	160	213
Number of Full time teachers year wise during last 5 years	149	148	149	151	145
Average %	**5.7**				

Active Power Management of Isolated Renewable Microgrid generating Power from Rooftop Solar Arrays, Sewage Waters and Solid Urban Wastes of a Smart City using Salp Swarm Algorithm

Amar Kumar Barik
Electrical Engineering Department
NIT Silchar
Silchar, India
akbeee@gmail.com

Dulal Chandra Das
Electrical Engineering Department
NIT Silchar
Silchar, India
dulal_nit@yahoo.co.in

***Abstract*— This work is a maiden attempt to manage the active power of an isolated renewable microgrid with Rooftop solar arrays, Micro-hydro generator, Biomass fired combined heat and power, Aqua-electrolyzer, and Fuel cells, by optimized load frequency control using a recent Salp Swarm Algorithm. The effort has put on to propose the mathematical model of a renewable microgrid generating power from solar irradiances, urban solid wastes, and sewage waters of a smart city like Bhubaneswar, for a dual objective of power and waste management. The importance of choosing the above combination of resources for microgrid is the effective co-compensation with climatic changes between solar PV and micro-hydro units naturally. Since sufficient solar energy is available during summer, but the water potential reduced subsequently for micro-hydro power generation. In other hands, during monsoon, water potential is highly available as rainwater adds to the sewage, but there are insufficient sunrays for PV units. The Biomass-based CHP is considered to give support to microgrid during non-availability of solar energy. It becomes a great challenge to coordinate between generation and load demand efficiently with the considered sources of renewable energy due to their inherent dependency towards climatic variations. To overcome this issue, the responses of the system are studied for different scenarios of renewable sources availability and load changes for optimal frequency control. The proposed microgrid is simulated with MATLAB-Simulink for four different scenarios and the optimized responses are reported to be competent in maintaining power frequency within the acceptable limit.**

Keywords*— *Aqua-electrolyzer, Combined heat and power, Fuel cell, Micro-hydro power, Rooftop solar PV, Salp swarm algorithm.

I. INTRODUCTION

Bhubaneswar, the capital city of Odisha is developing as one of the smart city of our country. It's historic monuments, rich heritage and urbanisation attracts people from different corners of the country as well as the foreign tourists, which intensify population density in the city day-by-day. This leads to various socio-ecological issues in the city. Some major issues for a smart city are reliable power management, proper waste management, and suitable communication facilitation etc. This paper attempts to discuss some short of resolution towards first two issues using waste to energy concepts along with renewable energy harnessing for the city. The proposed idea is to develop zone-wise distributed generation (DG) based renewable microgrids that convert solid wastes and sewage water into electricity which could be supplied to meet the domestic consumer demand of that zone only, supported with the power from rooftop solar photovoltaic (RSPV) arrays [1]. This may reduce loading of the conventional grids, which provide power to industries, commercial buildings and bulk power consumers of the city.

The Ministry of New and Renewable Energy (MNRE), India had initiated National Solar Mission programs to promote grid connected RSPV units [2]. Incorporating this mission, the power from solar energy could be harnessed during normal day time by the RSPV arrays mounted on roof of the taller buildings of the city [3]. The municipal solid wastes of the city collected daily needs to be segregated as recyclable and non-recyclable masses near the dumping yards. The non-recyclable wastes could be used for power generation in Biomass fired combined heat and power (BCHP) plant after suitable processing and mixing with standard biomasses (such as agricultural residues) [4]. The wastes after incineration reduced to small fraction of the original and these BCHP residues could be used for land fill, thereby reducing the chances of environmental pollution of the city.

The waste waters of every household of a specific zone of city could be channelized to a common sewage canal and stored in a small reservoir, outskirt of the city for settling down the dissolved wastes, and prior water treatment. A small-head dam could be constructed on that reservoir and power could be generated using Micro-hydro turbine generator (MHTG) units, from those treated waste waters before they flow to the mainstream or river [5]. This reduces the chances of river water pollution. The excess power produced with multiple MHTG units during rainy days could be utilized by an Aqua-electrolizer plant (AE) to produce Hydrogen (H_2) gas and stored, to be used as fuel in Hydrogen Fuel Cell (FC) units during peak demand hours [6, 7]. There is possibility of such microgrids for Bhubaneswar, near *Kuakhai* and *Daya* rivers, close to dumping yards or at the ends of sewage canals depending on the availability of land, resources and other feasible aspects.

978-1-5386-4581-9/18/$31.00 ©2018 IEEE

Optimal Load-frequency Regulation of Bio-Renewable Cogeneration based Interconnected Hybrid Microgrids with Demand Response Support

Amar Kumar Barik
Department of Electrical Engineering
NIT Silchar, Silchar,
Assam, India 788010
Email: akbeee@gmail.com

Dulal Chandra Das
Department of Electrical Engineering
NIT Silchar, Silchar,
Assam, India 788010
Email: dulal_nit@yahoo.co.in

***Abstract*— This work is an earliest attempt to study the load-frequency regulation of Wind, Solar-thermal, Micro-hydro, Biogas, and Biodiesel generating unit based interconnected hybrid microgrids with Demand response support. The linearized models of each renewable units are established for the proposed interconnected two-unequal hybrid microgrid system along with demand response strategies. The load-frequency responses of the proposed system are studied using Particle swarm optimization tuned classical PID controllers for different scenarios of source and load variations. Initially, the responses of system with micro-hydro and biogas units, are studied, subsequently connecting Wind and Solar-thermal units, which witness the increment in oscillations with penetration of renewable units. Then, the oscillations are reduced optimally by the inclusion of biodiesel generator and demand response supports. Finally, the responses are studied for simultaneous variations in renewable-sources and load-demands, reporting satisfactory regulation of load frequency with demand response contributions.**

Keywords*— Biodiesel-engine generator, Biogas-turbine generator, Microhydro-turbine generator, Solar-thermal power, Demand response contribution.

I. INTRODUCTION

The growing demand of power for a populous, developing nation like India with depleting conventional resources in current scenario, motivates to think of green-eco-friendly sustainable resources. Ministry of New and Renewable Energy (MNRE), India had recently initiated some programs to promote bio-renewable cogeneration based power production [1]. The available renewable energies from a single source might be too little in comparison to recent power demand. Hence, we need to design hybrid or multi-source generator based microgrids to meet the power demand of a locality effectively [2]. The nearby hybrid-microgrids could be further interconnected for exchange of surplus renewable energies among them to meet the varying consumer demands with optimal utilization of renewable resources and operational economy. Sometimes, the over penetration of renewable power generators in microgrid may lead to precarious frequency oscillations [3], because of their intermittent, non-dispatchable nature, which extend a great challenge to stabilize the system response within nominal limits [4]. There is a possibility to reduce these oscillations using Demand response contribution (DRC) strategies as discussed by Bao et al. for frequency control in conventional [5] and multi-area power systems [6]. Apart from the crucial loads in the microgrids, there are some electrical appliances such as water heaters, freezers, refrigerators, plugged-in hybrid electric vehicles (PHEV), and heat pumps, which are basically considered as non-essential loads that could be participated in contributing the demand responses (DR). The combination of some of these available DR devices supporting microgrid for frequency control by temporarily increasing or decreasing their power consumption, could be termed as Demand response contribution (DRC) units [5].

Some works with hybrid microgrids using Solar Photovoltaic arrays (SPV)/ Solar thermal power (STP) units and Wind turbine generator (WTG) units are recently reported, that harness cleanest form of renewable energy from sunlight and wind. The load frequency control (LFC) of isolated hybrid systems with Organic Rankine cycle (ORC) based Parabolic trough collector (PTC) type STP/WTG/diesel units are reported using Genetic Algorithm (GA) in [7] and using Particle Swarm Optimisation (PSO) in [8]. The efficacy of frequency responses of two interconnected microgrid with WTG and SPV are discussed in [9]. The waste water based Micro-hydro turbine generator (MHTG) is reported in [10], which utilised sewage water for power generation. The SPV, Biogas-Turbine Generator (BGTG) & Biodiesel Engine Generator (BDEG) based hybrid microgrid is reported in [11] which utilised Solar-energy, biogas from anaerobic digestion of bio-degradable wastes, and biodiesel from transesterification of energy-crop based vegetable oils respectively.

With motivation from these literatures, we put effort to propose bio-renewable cogeneration based interconnected hybrid microgrids with parabolic trough collector based STP, MHTG, BGTG, and BDEG units, and investigate the frequency responses for optimal load-frequency regulation with DRC. The main focus of the work are:

(a) Incorporation of DRC for load-frequency control in multi-unit based interconnected renewable microgrids without any energy storage devices.

(b) Responses of the systems are tested with variations of available DRC units.

(c) Simultaneous source and load variations are considered in both the interconnected microgrids for sensitivity study.

Rest of the paper are organized as follows. Section II illustrates the modelling of each components of proposed microgrid systems. The analysis of simulated results towards reduction of oscillations in microgrids are briefly discussed for interconnected modes in III, and IV concludes the paper.

978-1-5386-8235-7/18/$31.00 ©2018 IEEE

Demand Response Supported Optimal Load-Frequency Regulation of Sustainable Energy based Four-Interconnected Unequal Hybrid Microgrids

Amar Kumar Barik
Email: akbeee@gmail.com

Dulal Chandra Das
Email: dulal_nit@yahoo.co.in

Rasananda Muduli
Email: erasa.knp@gmail.com

Department of Electrical Engineering, NIT Silchar, Silchar, Assam, India 788010.

***Abstract* – The work is engrossed on optimal load-frequency regulation of 4-interconnected unequal hybrid microgrids with demand response support. It's a maiden attempt to include solar/wind based renewable systems with bio-energy based generating units for distributed co-generation as well as their interconnected coordination with a dual objective of waste and power management of Bhubaneswar city. Since the renewable resources are extremely nature dependent and affected by climatic variations, the suitable bioenergy based generators are included in each microgrid to meet the consumer demands with optimal allocation of resources. This work incorporated demand response contribution units to each microgrid and studied the coordinated responses of interconnected system for 4-different extreme scenarios of climatic variations with real-time recorded solar and wind data including realistic loading pattern. The proposed system is designed and simulated in Simulink, for optimal frequency regulation using Particle swarm optimization tuned classical PID controllers. The results are found competent enough to maintain load-frequency within acceptable limit with demand response support in all these 4-cases.**

***Keywords* – Bioenergy based generation system, Renewable energy systems, Demand response contributions, Solar Thermal power.**

I. INTRODUCTION

The developing economy, population growth, and modern life-style in current scenario exaggerate power demand and intensify environmental pollution along with growing industrialisation and deforestation. This leads to various socio-ecological issues, further it's a challenge to resolve the issues with reliable power and waste management of the community. This work puts an earliest effort to propose some combined resolution towards these issues incorporating waste-to-energy concepts with coordinated Renewable and Bioenergy based sustainable sources by means of distributed generations (DG), considering optimal utilisation of sunrays, wind, sewage waters, agricultural and domestic/urban solid-wastes of Bhubaneswar, the capital city of Odisha.

The power from available renewable resources could be optimally harnessed using Renewable energy systems (RES) like, Wind turbine generators(WTG) [1], Solar thermal power (STP) units [1], Solar photovoltaic (SPV) units [2]. These resources being intermittent in nature, could be supported by suitable Bioenergy based generation systems (BEGS), such as Biodiesel-engine generator (BDEG) [3], Biogas-turbine generator (BGTG) [3], Biomass-fuelled combined heat and power (BCHP) [2], and Micro-hydro turbine generator (MHTG) [2] units. The concept is proposed to develop zone-wise DG with bio-renewable cogeneration based hybrid microgrids (μGs) which convert community wastes (sewage water and solid wastes) into electricity to meet the demand of domestic consumers, with demand response contribution (DRC) [4] support. The harnessed sustainable green-power reduces the conventional grid loading with subsequent waste-reduction to support the environment. Apart from the crucial loads in the microgrids, there are some electrical appliances such as Water-heaters (WH) [5], Freezers/Refrigerators (FR) [5], plugged-in hybrid electric vehicles (PHEV) [6], and Heat-pumps (HP) [7] , etc., which are basically considered as non-essential loads and could be participated in contributing the demand responses (DR). The combination of some of these available DR devices supporting microgrid for frequency control by temporarily increasing or decreasing their power consumption, could be termed as DRC units[4]. We consider the zone-wise charging stations of PHEV as DRC units of corresponding μG in this work.

Some works reported recently with solar-bioenergy cogeneration based isolated microgrids harnessing power from solid-urban-wastes and sewage-waters [2]. The community based isolated renewable μG with SPV, BDEG and BGTG units are reported utilising suitable garbage and wastes for power production [3]. Sometimes all the potential resources or suitable landscapes may not be available at the same location to be included in a single μG for isolated mode of operation. So, we need to think for designing DG based hybrid μG to be installed at the suitable location nearest to the available resources for economic power generation. Further these hybrid-μGs could be interconnected for coordinated supply and demand side management with DRC. The real-time frequency regulation with DRC strategy [8] of isolated microgrid using particle swarm optimization (PSO) based DRC strategy reported in [9]. The LFC of 3-interconnected system with DRC is reported in [10]. The PSO tuned classical PID controllers are reportedly used for LFC of bio-renewable cogeneration based interconnected hybrid microgrids with demand response support [11]

Motivated with these literatures, a waste-to-energy based bio-renewable energy cycle is presumed with coordination of proposed 4-interconnected microgrids as shown in Fig. 1. It is

978-1-5386-6971-6/19/$31.00 ©2019 IEEE

A storage based Virtual Synchronous System for Load-frequency regulation of interconnected Hybrid Microgrids using Selfish-herd optimiser

Amar Kumar Barik
Department of Electrical Engineering
National Institute of Technology Silchar, Silchar,
Assam, India 788010
Email: akbeee@gmail.com

Dulal Chandra Das
Department of Electrical Engineering
National Institute of Technology Silchar, Silchar,
Assam, India 788010
Email: dulal_nit@yahoo.co.in

***Abstract*— This paper is mostly focused on overcoming typical challenges due to renewable energy integration in hybrid microgrids, by incorporating coordinated energy storage-based virtual synchronous system (VSS). The work is initiated by proposing an unequal interconnected hybrid microgrid including Wind, Solar-thermal, Micro-hydro, Biogas, Biodiesel generating units with Battery and Super-capacitor based VSS. The load-frequency responses of the proposed system are compared for different scenarios of source and load variations with classical PID controllers using a recent Selfish-herd optimiser algorithm. Initially, the system responses are compared with 4-optimisation techniques to confirm the superior one. Then the system responses are compared with 3-scenarios of extreme source variations to analyse the effect of renewable penetration and VSS. Finally, the system frequency variations are reduced adequately by the inclusion of the proposed VSS and the responses of each scenarios are recorded.**

Keywords*— Biodiesel generator, Biogas generator, Microhydro generator, Selfish-herd optimizer, Solar-thermal power, Virtual synchronous system, Wind generator.

I. INTRODUCTION

The emergent global power demands with exhausting fossil resources are encouraging to search for green-eco-friendly sustainable resources. However, the power harnessed from locally available single renewable resources might not be reliably sufficient as compared to their demand. Hence, there is a need for designing multi-source generator based hybrid microgrid (hmG) to supply quality power locally[1]. The nearby hybrid microgrids (hmGs) could be further interconnected for exchange of surplus powers to meet the varying consumer demands with optimal utilization of renewable resources and operational economy [2,3]. Mostly, the excess of renewable power penetration in hmG might lead to hazardous fluctuations of system frequency [3,4], due to their intermittent and non-dispatchable nature. This encompasses an abundant challenge for stabilising the frequency responses within nominal system limits [4,5]. There are two possible ways to overcome this issue by managing the demand or supply. Some recent literature reported the load management concept using demand response contributions [6,7] to reduce frequency fluctuations. However, it is still a challenge to avail such reliable demand response contributors in locality, though this method is comparatively economic. Whereas, the supply side management is little easier by including some reliable storage unit, but more costly as compared to the demand side management. In this context, some literature has reported the application of suitable energy storage based Virtual inertia generators [8,9,10] for supporting the system inertia. The combination of some suitable energy storage systems like Super capacitors (SC) and Battery stacks (BS) with fast-switching power electronic converters could provide inertia support like synchronous generators of the microgrid and hence termed as Virtual synchronous system (VSS) in this work. This VSS unit is expected to support the hmG for frequency regulation by charging/discharging itself during uncertain source/load variation.

Some works reported on hmGs recently are using Renewable energy system (RES) like Wind turbine generator (WTG) and Solar thermal power (STP) units that harness clean energy from wind and sunlight respectively. The load frequency control (LFC) of isolated hybrid systems with Organic Rankine cycle (ORC) based Parabolic trough collector (PTC) type STP/WTG/diesel units are reported in [11] and [12] with Particle swarm optimisation (PSO). The frequency regulation of Biogas generator (BGG) & Biodiesel generator (BDG) based hybrid hmG using Grasshopper optimisation algorithm (GOA) is reported in [13]. The frequency regulation of hmG using Salp swarm algorithm (SSA) is reported in [14] with waste water based Micro-hydro generator (MHG) and storage units. The land requirement of linear Fresnel reflector (LFR) type STP unit [6,7] is 65% less compared to similar PTC type [11,12]. Recently, a swarm based Selfish-herd optimiser (SHO) algorithm is reported in [15] which have very few applications in LFC of hmG. Most of the literature reported on LFC of hmGs have either used the classical proportional-integral-derivative (PID) controller or compared the responses of new controllers like fuzzy [16] or fractional order [17,18] controllers with PID responses. Also, the PID controller are very robust, cheaper, and effortlessly designed to link with optimisation algorithms for tuning as reported and discussed in several literature.

Motivated with these literatures, this work endeavours to study the system responses during renewable penetration by proposing two-unequal interconnected waste-to-energy (WTE) based hmGs. The concept WTE based hmG is illustrated in Fig. 1, with 50Hz system frequency including storage (SC+BS) based VSS units. It is assumed that the first microgrid (hmG1) consists of LFR type STP, BGG, BDG1 and VSS1 units; whereas, the second microgrid (hmG2) consists of WTG, MHG, BDG2, and VSS2 units. The major contributions of the work are:

(a) Design and incorporation of VSS with combined energy storage units like super capacitor and battery stacks for LFC in multi-unit based unequal interconnected hmG.

978-1-7281-7034-3/20/$31.00 ©2020 IEEE

Vermicomposting Technique for Starch based Food Wastes by using Eisenia Fetida and its Optimization by ANN

[1]Amar Kumar Das, [2]Saroja Kumar Rout, [3]Patitapaban Panda

[1] Asst. Professor, Dept. of Mechanical Engineering, Gandhi Institute For Technology(GIFT),Bhubaneswar.

[2]Professor, Dept. of Computer Science & Engineering, Gandhi Institute For Technology (GIFT), Bhubaneswar.

[3]Professor, Dept. of Civil Engineering, Gandhi Institute For Technology (GIFT), Bhubaneswar.

Abstract— **Due to the lack of awareness and imprudent food habits of modern man, a substantial volume of food waste is being generated in India. The disposal of which imposes a major and unwarranted challenge for maintenance of a hygienic environment. Discussing the contemporary methods of waste management, Vermicomposting is regarded as a promising technique to convert such organic solid wastes into organic compost through biological activities. In this study, composting by Eisenia Fetida using high starch-based food wastes with cattle manure in different conditions has been undertaken. The addition of starchy food wastes like rice in cow dung was found to promote the biological decomposition of organic matter, cellulose, and lignin and improve the nutrient quality like Nitrogen, Phosphorous, and Potassium (NPK) significantly. Furthermore, the prime factors which influence the composting, as well as growth of the worm, like temperature, pH, moisture content, sizing of organic substrate, aeration, etc., has been optimized using Artificial Neural Network (ANN) for better results. By changing the simulation it prepares the neural system in the three performance functions as mse, msereg and sse, and the transfer function transig, logsig and purelin to valid the outcomes. It was observed that 20-25% of food wastes mixed with cattle manure under 30°C, pH of 7.0-7.5, 1-2 mm substrate, and 70% moisture content in bean were the optimum combination for vermicomposting by Eisenia Fetida. Hence, the conversion of starchy food wastes into organic manure by vermicomposting is found as a cost-effective and eco-friendly technique. However, the influences of other ambient conditions are not included in the analysis.**

Keywords—Vermicomposting, NPK Value, Eisenia Fetida, Organic manure, ANN.

I. INTRODUCTION

Municipal Solid Waste (MSW) can be regarded as the waste produced from domestic and industrial usages. India is the second-largest nation accounting for a population of 1.21 billion, with rapid urbanization and prosperity [1]. In developing countries such as India, waste biomass from domestic, rural, urban, and industrial sources is the key cause of organic pollution [2]. Management of solid waste is one of the most daunting problems facing a severe pollution problem in metropolitan cities due to the production of enormous amounts of solid waste. This paper provides an evaluation of the current state of municipal solid waste management (MSWM) in Indian cities. Disposal in landfills requires a large scale area and burning or incinerating of wet food items may lead to more energy consumption. The spaces required for making a landfill will reduce in the near future due to an increase in population.[3] Potential sites for the municipal landfill are likely to generate harmful gases such as methane and carbon dioxide which are contemplated as greenhouse gases subsidizing climate changes globally[4]. The landfill also contributes to lowering the soil fertility level, leading to poor crop growth. Hence to overcome this crisis, an eco-friendly and hygienic method can opt which is regarded as composting [5]. The source of composting and vermicomposting-related materials and biological activity make it extremely difficult to determine the rate of application of vermicomposting and its suitability as a modification of the soil. MSW is produced generously which is a burden from a waste disposal point of view [6]. The biological conversion of organic waste to biofertilizer is termed as Vermicomposting. The agent which widely contributes to the conversion of organic wastes into organic compost is earthworm [7]. There are approximately 1800 species of earthworms among which 6-7 varieties of earthworms are used to break down the complex compounds present in the organic residue and food waste [8].

The earthworm intakes these wastes and the end product produced is the worm humus which is otherwise termed as vermicast. These castings are rich in nutrients like nitrogen, phosphorus, potassium, calcium, sodium, magnesium, iron, etc. which can be used directly as a fertilizer to boost up the plant growth [9]. Vermicompost, when compared with locally available chemical fertilizer, is considerably richer in nutrients, cheap in cost, and an environmentally friendly way

to sustainably recycle the organic wastes to bio-fertilizer. Strong paper mill sludge, textile mill sludge, winery waste, guar gum industrial waste, etc. are some industrial sludges tested for vermicomposting.[10]

Depending on the waste materials being used for compost preparation, the nutrient content in vermicompost varies. If one of the waste materials is heterogeneous, the compost would have a wide variety of nutrients available. If one waste material is heterogeneous, only those nutrients will be available[11]. In Odisha, the staple food is rice, hence a considerable amount of food waste generated is from rice. The present study reveals the role of earthworm in the transformation of valuable organic manure from starch food waste. The outcome showed that Eisenia Fetida vermicomposting is effective in converting sludge into nutrient-rich manure within a short period.

This paper aims to find out the parameters responsible for effective composting and substantially optimizing such parameters for better enrichment in vermicompost as the end product.

II. MATERIALS AND METHODS

A brief comparison between chemical fertilizer and vermicompost is given below in Table-1. The table shows the increment in potential nutrients values of compost required for the growth of a plant in Vermi based that of Chemical fertilizer.

Table-1. Potential nutrients values

Variables	Chemical Fertilizer	Vermicompost
pH	7.8	6.8
Nitrate / Nitrogen	156.50 ppm	902.20 ppm
Potassium	0.48%	0.70%
Phosphorus	0.35%	0.47%
Total Nitrogen	0.80 %	1.94 %

Figure 1 shows the schematic diagram of the worm bin prepared for vermiculture and subsequently producing the compost. It is made of standard size by (6 ft x 4.5 ft x 5ft) and occupied with a maximum volume of 70-80% of total capacity. The preparation of vermicompost is done by providing suitable bedding materials for the earthworms. The vermicompost bed is prepared by the materials such as Dry Cow Dung, watering at proper intervals, Cooked Rice Wastes, Shredded Cardboard materials or papers, dry neem leaf, and eggshell powders as per the required intake of raw materials. Earthworms are used for the digestion of the bedding materials. Dry cow dung which is free from lumps is also spread evenly. The purpose of using dry cow dung is because it is free from any unusual odor compared to wet cow dung. Water is sprinkled on the dry cow dung for it to retain moisture which will be favorable in digesting the waste. Moisture content is an essential factor, as the earthworms breathe through their skin, they need enough moisture to prosper otherwise their skin dries out and consequentially leading to the death of earthworms. The dung is mixed thoroughly at regular intervals for proper aeration. Rice waste is added to the bin and it is allowed to decompose for about 2-3 days with proper moisture content. The rice wastes with cow dung proportionately 70:30 are used in our worm bin. The decomposition allows partial digestion of complex materials of the sample, making it suitable for the earthworms to consume.

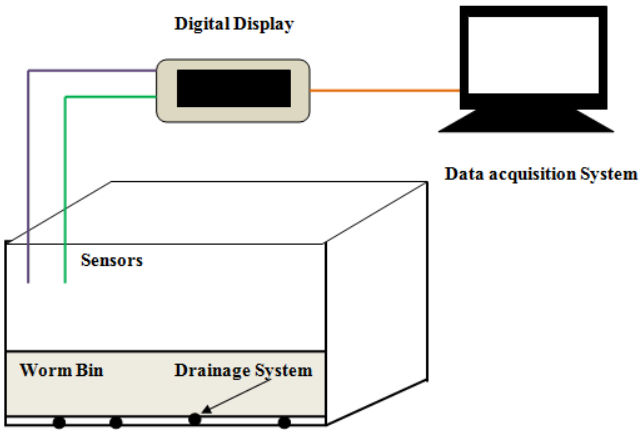

Figure 1 Experimental Worm Bin

The worm bin consists of a sample tray having a porous surface at the bottom to drain out the excess water. The temperature, pH, and humidity of the bin are measured and recorded by sensors assisted data acquisition system. Using temperature and humidity sensors, vermicomposting areas are kept under control. Through the IoT devices & Cloud storage platform, optimal levels for both temperature and humidity are preserved is represented in Figure 1. In this process, Eisenia Fetida was used for preparing compost due to its potential stability with the environment, high reproductive rate, and ease of availability.

Earthworm (Eisenia Fetida) is introduced to the bin. The moisture content is maintained by spreading shredded cardboard material or papers on top of the bin and sprinkling water at a regular interval of 1-2 days. The shredded cardboard also acts as food material for the earthworm. The earthworm eats the food waste and after digestion excretes a lightweight material which is also called worm humus or vermicompost. This process takes up to 24- 28 days, the vermicompost produced is black/brown in color, rich in nutrients required for the healthy growth of plants. The whole process is carried out at different temperature conditions to get optimized values of nutrients.

Figure 2 Compost prepared using Eisenia Fetida

The vermicompost then undergoes some nutrient tests in order to measure the necessary nutrients (N-P-K) available in the compost.

Nutrient tests for vermicompost nitrogen (N), phosphorus (P), and potassium (K) are conducted on vermicompost samples. The findings found after research are included in Table 2.

Table-2 NPK values under different Conditions

Temperature (0 C)	pH Value	C/N ratio	Organic Carbon (OC)%	Moisture (%)	N %	P%	K %
30	6.1	5.1:1	6.28	29	1.23	1.53	0.63
31	6	5:1	6.1	30	1.10	1.62	0.72
32	6.2	4.8:1	6.3	31	1.22	1.52	0.68
33	6.2	4.9:1	6.2	35	1.15	1.54	0.64
34	6.17	5.8:1	6.18	31.8	1.19	1.54	0.65
35	6.12	5.4:1	6.23	30	1.21	1.54	0.62
36	6.14	5.3:1	6.32	33	1.24	1.54	0.61
37	6.15	5.5:1	6.35	35	1.28	1.58	0.52

For the survival of earthworms, the addition of some other organic waste (cattle dung) to food waste was appropriate. The number of earthworms increased to 30 days during the vermicomposting of food waste. Then the number of earthworms began to decline before the end of the experiment. The reduction in the number can be due to food fatigue. The best measures to test the vermicomposting process are the survival, biomass production, and reproduction of earthworms. Therefore, cattle dung, serving as an additional waste, not only decreased the processing time but also increased its consistency and transformed food waste into quality manure. The findings indicated that the higher proportion of starch food waste in cattle dung was not sufficient for the processing of cocoons. One of the important factors in the development of cocoons in various feed mixtures may be the biochemical consistency of the feed It was stressed that microbial biomass and decomposition activities during vermicomposting are also critical for determining worm biomass and cocoon production, in addition to the biochemical properties of waste.

III. Result and Discussion

Vermicomposting is now a biotechnology, and vermicompost is successful organic farming superlative. Nutrients such as available N (nitrogen), soluble K (potassium), exchangeable Ca (calcium), Mg (magnesium), P (phosphorus), and microelements such as Fe (iron), Mo (molybdenum), Zn (zinc), and Cu (copper) that can be readily absorbed by plants are released during vermicomposting and converted into soluble and available forms that provide nutrients.

Process Optimization and Validation using ANN Technique:

The Neural Network plays an important in machine learning with a backpropagation multilayer feed-forward system. This neural system is most appropriate for different machine learning applications. Neural networks can decide the condition of the brain in the MR image [12]. The Artificial Neural Network was trained and framed by Mat lab programming is represented in [13,14] with the goal that the minimum error in data preparing and most extreme relationship exist in a coefficient of the system toolbar.

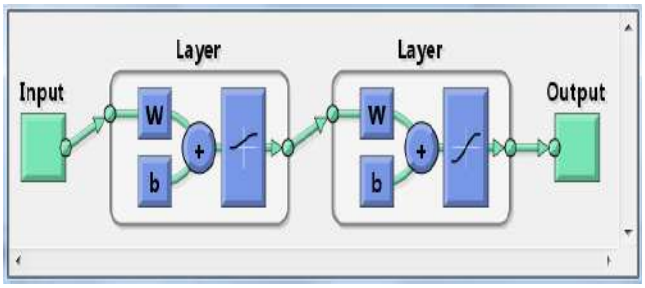

Figure 3 ANN Layout of the system using Matlab

The last attempted network was the Neural system feeding forward backpropagation with TrainBR preparation capacity, LEARNGD energy learning capacity, and SSE execution work. This procedure utilizes the ANN apparatus in Matlab programming to prepare, confirm, and test the system module. Backpropagation is the most generally utilized Neural Network [15,16].

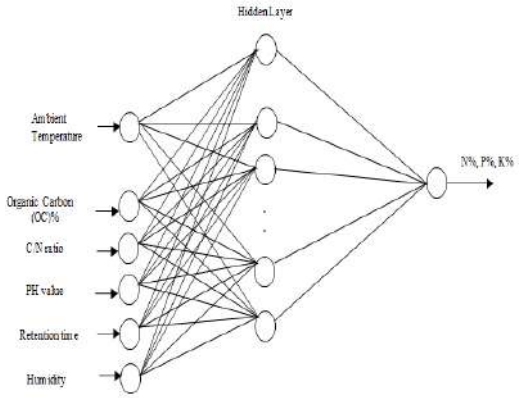

Figure 4 ANN Layout of the Vermicomposting System

Thermolysis of waste plastics into value added products and its future prospective

[1] Amar Kumar Das, [2] Suraj Biswas, [3] Binod Kumar Jena

[1]Department of Mechanical Engineering, Gandhi Institute For Technology (GIFT), Bhubaneswar

Bijupatnaik University of Technology (BPUT), Rourkela, Odisha, India.

[1]amar.das120@gmail.com, [2] sjbiswas2050@gmail.com,[3] jkbinod98@gmail.com

Abstract - Recent demand necessitates resolving environmental threats from Municipal Solid Wastes (MSW), making awareness for saving fossil fuels, controlling emissions as well as global warming. It also encourages research towards disposal and recovery of sustainable energy from wastes which becomes a recent trend to provide an effective mean to its entire beneficiary. The paper addresses various types of wastes collected from many municipalities in India and provides a better and promising solution to treat the non-biodegradable wastes like plastics. Mostly Plastic wastes are generated in bulk amount due to its flexibility and relatively inexpensiveness from the user point of view. The plastics as difficult to dispose may be subjected to a conversion process like thermolysis in the absence of air. In the experimental study, different waste plastics have undergone thermolysis at different range of temperatures and use of catalyst. A critical analysis and characterization have been made with the products extracted from this process. On the other hand, the paper highlights different parameters and their influence on the rate of production. Finally the product extracted from thermolysis is being compared with its contemporary products and tried to establish its feasibility as future prospective.

Keywords: "thermolysis, MSW, global warming, critical analysis, feasibility."

I.INTRODUCTION

Municipal solid waste (MSW) is one of the major areas of concern all over the world. In developing country like India, there is a rapid increase of municipal solid waste due to urbanization and population growth. Composition of waste varies with different factors like living standard, climatic condition, and socio-economic factor etc.The current statistics deals with the type of waste generated in India both in domestic and industrial reasons and its management in both quantitatively and qualitatively. Plastic waste is the third largest contributor to municipal and industrial waste systems after food and paper. Significant amount of energy can be produced with this technology. This could be an alternative energy resource for substituting fossil fuels. The fuels produced from this process do not contain sulphur content because there is no sulphur in the waste plastic feedstock.

Municipal solid waste (MSW) includes household garbage and rubbish, street sweeping, Construction and demolition debris, sanitation residues, trade and non-hazardous industrial refuse and treated bio-medical solid waste [1]. As per the World Bank estimates urban India produces approximately 100,000 metric tons of MSW daily or approximately 35 million metric tons of MSW annually by the year 2000 [2].

The quality and quantity of MSW generated by a particular community varies according to their socio-economic status, cultural habits, urban structure, population and commercial activities etc. Planning, designing and operation of municipal solid waste management system can be done on the basis of composition and the quantity of MSW generated in the country. The wide use of polymeric materials or plastics resulted in the accumulations of untraditional wastes not native to the mother earth life cycle.

Therefore, wastes of modern materials are accumulated without effective decomposition and recycling routes in the landfills. The increase of petroleum and petrochemical prices opened the ways for industries to invest in decomposition of plastic wastes to petro chemicals. Plastic waste pollution is increasing day by day in developed and developing countries because of their non-biodegradable nature. In India, plastic waste generated per day is about ten thousand tons that of total municipal solid waste. Due to improper segregation and recycling system for these plastic wastes, load on landfill sites increases which ultimately causes environmental pollution and affects marine biodiversity.

II.MATERIALS AND METHODS

Thermoplastic wastes mainly consist of polyethylene, terephthalate, high density polyethylene(HDPE), polyvinylchloride(PVC), low density polyethylene(LDPE), polypropylene(PE) and polystyrene(PS). For food packaging, generally polyethylene and polypropylene materials are used. These types of thermoplastic waste can be recycled by using different methods like mechanical recycling, chemical recycling, incineration, thermolysis etc.

The technology helps to save land resources by utilizing waste plastics to generate valuable energy. Currently, a majority of the waste plastic is land filled and it is not sustainable because waste plastic takes very long time to decay. The world's annual consumption of plastic which was five million tonnes in the 1950's has skyrocketed to a global production of 245 million tonnes in 2008 and waste plastic generation is rapidly increasing. Plastic waste is the third largest contributor to municipal and industrial waste systems after food and paper. Significant amount of energy can be produced with this technology. This could be an alternative energy resource for substituting fossil fuels. The fuels produced from this process do not contain sulphur content because there is no sulphur in the waste plastic feedstock

Thermolysis is one of the recycling options for plastic waste which involves heating of organic material at elevated temperature in absence of oxygen. It is one of the best methods to reduce load of plastic waste on available landfills. It converts plastic waste into different petroleum fractions which can be used in many industries as an alternative fuel for running boilers, generators, and turbines. By using suitable catalyst, process yield can be enhanced, and reaction time can be minimized which ultimately achieves efficiency in the process. The materials to be tested in this study are HDPE, LDPE, PP and PS which account for 70% of the plastics used in packaging. PVC and PET are not studied due to health concerns.

A. Characterization of Waste plastics Thermolysis

Thermolysis is a thermo-chemical conversion process in which an irreversible chemical change caused by the action of heat in absence of oxygen. Plastic is generally composed of 85% Organic Compounds, Carbon, Fabric Material and 0.9-1.25% Sulphur. Thermolysis of Plastic yields products like; Fuel Oil = (60 - 65 %), Carbon Black (Char) = (20 - 25%), Non-Condensable Gases = (10 - 15%), Moisture = (3 - 5%).

From the literature review, reaction temperature was the most important factor that influenced the whole process, however, this study has also investigated the secondary cracking process and other significant factors such as temperature, heating rate, type of plastic, catalysts, interaction between different plastics, pyrolysis process, etc. The effects of secondary cracking were investigated. This work has not been found in other researches. The second stage of the study was to optimize the operation conditions and the reactor design to produce high quality liquid fuel (diesel) from the pyrolysis of LDPE.

Thermoeconomic and Exergetic Analysis of waste plastic oil fueled with diesel in compression ignition engine

Amar Kumar Das [1], Sudhansu Sekhar Sahoo[2], Dulari Hansdah [3], Achyut Kumar Panda [4]

[1] Department of Mechanical Engineering, Gandhi Institute For Technology (GIFT), Bhubaneswar, Odisha, India.

[2] Department Mechanical Engineering, College of Engineering, Bhubaneswar, Odisha, India.

[3]Department Mechanical Engineering, NIT Jamshedpur.

[4] Department of Chemistry, VSSUT, Burla, Sambalpur, Odisha, India.

E-mail: amar.das@gift.edu.in , sudhansu@cet.edu.in, dhansdah.me@nitjsr.ac.in,achyut.panda@gmail.com

***Abstract*-Due to ever rising demand and inabundant storage of fossil fuels required for transport systems, attentions have been stared for budding potential and high enduring alternative fuels with affordable cost. With the purpose of attain higher performance and trim down environmental effects of the engine, it is indispensable to realize the mechanism to provide better enhancements in fuel economy and engine power by using renewable fuels in conventional diesel engine. The paper aims to carry out thermodynamic, exergetic and thermo economic study of a compression ignition engine operated while using various blend of wpo and its mixtures with pure diesel in order to access behavior of various performance parameters. The present work includes working with energy, exergy and cost rate energy production, fuel consumption and losses for whole system. In concluding part, the thermodynamically economic analysis was executed for equilibrium-condition engine control volume by applying and resolving energy, exergy and economic equilibrium. The results demonstrated the most excellent thermodynamic conditions, the engine attained when fueled with diesel. However, the most cost-effective working circumstances happened while fueled by 20% waste plastic oil by volume with diesel.**

***Keywords*- waste plastic oil, thermoeconomic analysis, exergy analysis.**

I. INTRODUCTION

Improvement of technique to develop resourceful and commercial energy arrangements is a most important confront in global scenario. Amid restricted conventional reserves and global increasing requirements of energy, it happen to be extra imperative to realize the methods which dilute the quality of power and its reserves and to extend an orderly solutions for upgrading the design of power systems and dropping bang to the surroundings [1].Exergy oriented financial study is used as a commanding means for systematic learning of thermal arrangements to forecast output of arrangements in addition to its financial viability [2].The energetic and exergetic analysis techniques are rendered to thermodynamically evaluate the efficiency of an energy transformation system. The energy analysis involves the thermodynamic limitation, such as uninterrupted energy loss to the environment and identifying the position of occurrence [3]. A holistic investigation of a thermal system take account of quantitative and qualitative approach of thermodynamics equally representing energy and exergy analysis so as to acquire a further useful depiction of system performance [4].In addition, the most favorable state of the system, decided by thermodynamic analysis, initiates a basically unbalanced economic condition. Therefore, it necessitates a thorough evaluation of performance of the engines using waste plastic oil-diesel blend by thermo-economic analysis. The basic objectives of the thermo economic analysis is to evaluate the products in terms of actual cost, rational basis of pricing ,informative to decision variables and allotment and restriction of the expenditures [5]. Consequently, an exergy oriented study of any thermal systems is considered as extremely valuable and functional instrument in recognizing the resources, places, kinds and

978-1-7281-7663-5/21/$31.00 ©2021 IEEE

degrees of thermodynamical limitations in addition to forecast monetary involvements in power transformation system [6,7]. However, a little research work was mentioned on thermo-economic analysis on CI engines operating with different biodiesels [8] but no work is yet being reported using waste plastic oil diesel blend. Panigrahi et al. [9], investigated on neem oil methyl ester used in biodiesel engine followed by energy and exergy analysis. They have concluded that 20% of neem oil methyl ester biodiesel could attain higher rate energy and exergy efficiency and lower rate of exergy destruction than diesel. Gouda et al.[10],also conducted the energy, exergy and emission analysis of blend of pyrolytic Kaner seed oil (KSPO) with pure diesel in a twin cylinder CI engine. They claimed that engine could produce increase in BTE and decrease in BSFC up to 15% KSPO-diesel blend to that of pure diesel. However, Lower CO and higher HC, NOx and smoke emission were also monitored with blend of KSPO and diesel. However, higher percentages of WPO blended in diesel engines can be limited due to lower calorific value, lubricity, viscosity, cetane value and blending constancy [11]. Moreover an optimum blending of wpo with diesel showed better results in performance and emission as compared to fossil fuel.

The objectives of this research were to appraise the output of diesel engines using WPO diesel blend following thermo-economic analysis. The engine brake power, fuel consumption, exhausts gas temperature and outlet water temperature was also measured and the system design equations were formulated to determine the system efficiency by using experimental data. In conclusion, energy, exergy and economic balances were conducted for establishment of thermo-economic analysis.

II. EXPERIMENT SET UP AND METHODS

A. Pyrolytic fuel mixture preparation and Characterization

In this study, the test oil was designated as Waste plastic oil (WPO) which was prepared by pyrolysis method by taking crushed plastic wastes as raw materials with Zeolite A as Catalyst disseminated in a semi batch reactor, maintained with at an optimum temperature of 500 ^{o}C by means of a PID controller. The test oil produced was further analyzed for its physio-chemical composition. These blends are denoted as D90WPO10, D85WPO15, D80WPO20, D75WPO25 and D70WPO30 where the numbers denotes the fraction of WPO and diesel in volume fraction available in the fuel mixture. The physical properties of pyrolysis oil and different blend with diesel are summarized in Table 1.

TABLE 1 Different fuel properties of WPO blended Diesel

Test Fuels	*Volumetric concentration, (%)*		*Fuel Density @15 ^{o}C (g/m^3)*	*Flash point (^{o}C)*	*Fire point (^{o}C)*	*Gross Calorific value (MJ/kg)*	*Kinematic Viscosity (cst) @30 ^{o}C*
	Diesel	*WPO*					
Diesel	100	-	835	52	57	45	2.15
D90WPO10	90	10	830.8	47.3	52.2	45.1	2.31
D85WPO15	85	15	828.7	44.95	49.8	45.15	2.39
D80WPO20	80	20	826.6	42.6	47.4	45.2	2.47
D75WPO25	75	25	824.5	40.25	45	45.25	2.55
D70WPO30	70	30	804.34	17.69	21.96	45.73	3.31

B. Test Engine and Procedure

The test engine is comprised of a 4 stroke single cylinder and direct injection Kirloskar made. The engine is facilitated with water cooling system having power rating of 3.5 kilowatt at engine speed of 1500 rpm. The engine specification particulars are demonstrated in Table 2 and diagrammatic experiment system layout is

978-1-7281-7663-5/21/$31.00 ©2021 IEEE

Performance Enhancement of Domestic Refrigeration System Using R-134a Refrigerant Blended with Graphene as Nano Additives

Amar Kumar Das and Ritesh Mohanty

Abstract Refrigeration system involved with evaporative heat transfer intends to intensify the cooling effect in domestic applications. In order to reduce the energy consumption and improve the cooling rate, various attempts have been undertaken. In this experiment, the exploitation of a refrigerating system using R-134a as refrigerant has been studied. The study also explains the thermal conductivity, dynamic viscosity and rate of heat transfer of graphene used as nano additives in evaporator tube of a vapour compression refrigeration (VCR) system. The thermal conductivity of base refrigerant rises with rise of temperature to the optimal concentration value of 0.6–0.9% by wt. in nano additives. In addition, significant improvement in the performance of refrigeration system due to the addition of nano additives in domestic refrigerant has been addressed. However, the apprehension of global warming due to potential use of R-134a as refrigerant is still a matter of concern. Hence, the paper encourages the use of nano refrigerant that leads to improvise the effectiveness, durability and energy efficiency of refrigeration without any system modification.

Keywords Refrigeration system · Nanofluid · VCR · NanoGraphene oxide

1 Introduction

Modern world undergoing a phase of liberization, urbanization and industrializations is confronted with challenges for energy security and sustainability. In order to regulate the energy loss, stringent energy policies have been implemented by governments to put a ban on energy wastes that leads to reduce energy consumption [1]. To meet such energy requirements, improvisation in performance and energy efficiency

A. K. Das (✉)
Department of Mechanical Engineering, Gandhi Institute for Technology, Bhubaneswar, India
e-mail: amar.das@gift.edu.in

R. Mohanty
Department of Mechanical Engineering, DRIEMS Polytechnic, Tangi, Cuttack, India
e-mail: ritesh.rmohanty@gmail.com

M. Ramgopal et al. (eds.), *Advances in Air Conditioning and Refrigeration*, Lecture Notes in Mechanical Engineering, https://doi.org/10.1007/978-981-15-6360-7_10

of a refrigeration system becomes a matter of concern. Extensive inspection has been supervised to scrutinize the thermal conductivity of the nanofluids. However, there is least scope of literature to explain thermal conductivity of nano refrigerant and its improvement methods [2]. Thermophysical properties of base fluid can be increased by accumulating low concentration of nanoparticles in it. This may be due to higher dispersion quality of nanoparticles that leads to augment the thermal conductivity of the refrigerant. Nanoparticles have been used as supplements in refrigerants and being accepted as a promising method of improvising the performance of the vapor compression refrigeration system (VCRS) without modifying the system components. It has been mentioned that nano refrigerant having higher thermal conductivity due to better dispersion behavior and stability can be used significantly in the refrigeration system [3].

Studies on potential properties like thermal conductivity and viscosity of nano refrigerants in comparison with conventional refrigerant used in refrigeration system have been illustrated. Various researches on nano additives encourage its use as nano refrigerants due to its promising tribological performance of compressor in a refrigeration system. According to Selvam and his colleague [4], thermal conductivity of nano refrigerant has been improved using silver nanofluid in ethylene glycol in water as base fluid. However, the thermal conductivity is found increasing with the increase in the concentration of nanoparticles and temperature. Akilu et al. [5] investigated the use of TiO_2–CuO nano composite in ethylene glycol as base fluid. The trends of increasing thermal conductivity by increase in nanoparticles volume concentration and temperature have been followed. It has been observed that an enrichment of 16.7 and 80% was gained at 2.0% volume concentration compared to base ethylene glycol at 40.4 °C. Akhavan et al. [6] discussed on the implementation of different mass fraction of CuO nanoparticles as nano refrigerant compared to R600a as base fluid. They have reported that the heat transfer of the nano refrigerant has been improved around 83% than the pure refrigerant. Nabil et al. [7] also studied heat transfer performance of TiO_2 nanoparticles in water-ethylene glycol (EG) mixture. The results have been reported on different operating temperature conditions. Prime factors like viscosity and thermal conductivity of the refrigerant were maintained at temperature range of 30–80 °C. There was a substantial rise of thermal conductivity of 15.4% at 1.5 vol.% nano concentration at 60 °C as reported. Wang et al. [8] also investigated how to improve the coefficient of performance of refrigeration system using a mixture of fullerenes (C70) and $NiFe_2O_4$ dispersed in compressor lubricant oil after solid grinding. The coefficient of performance of the refrigeration system was also found increasing by 1.23%. Bhattacharya et al. [9] investigated on the usage of Al_2O_3 as nano refrigerant and declared that a better energy saving could be achieved as compared to pure R-134a. In addition, extensive researches are desirable on thermophysical properties of hybrid nanoparticles in hydrocarbon mixtures and R-134a with GON refrigerants as additives in vapor compression refrigeration systems.

Hence, this study aims to explore the means and ways of how to improve the thermal conductivity and viscosity of the nanographene/R-134a as refrigerant. In addition, the coefficient of performance of the refrigeration cycle using the

nano refrigerant is found promising. This may be due to higher thermophysical properties of the nano refrigerant that leads to enhance the rate of heat transfer in an evaporator tube.

2 Materials and Approaches

2.1 Refrigerant Properties

A refrigerant is a substance having desirable thermodynamic properties used in the refrigeration cycle. In this experiment, the thermophysical properties of nano refrigerant are investigated by considering graphene as better nano additives in conventional refrigerant, R-134a. Table 1 shows the thermophysical properties of the graphene nanoparticles (GNO) used as additives in base refrigerant. The combined study of the thermal properties (thermal conductivity and specific heat) and the rheological properties (viscosity) of various refrigerant has been tested in the laboratory. The thermal conductivity of all nanofluids was measured using a KD2 Pro conduct meter (Decagon Devices Inc.) with the help of the transient hot wire technique [10].

The specific heat for each nanofluid was measured in a differential scanning calorimeter (DSC). The viscosity and rheological behavior of nanofluids were obtained by conducting tests under steady-state conditions using a HAAKE RheoStress rotational remoter.

Table 1 Thermophysical properties of nano refrigerants

Nano refrigerant	Density	Viscosity	Thermal conductivity
	(kg/cm^3)	(Pa s)	(W/m K)
Copper oxide (CuO)	6320	–	32.9
R-134a	1202.6	0.00019336	0.0139
Aluminum oxide (Al_2O_3)	3880	–	40
R245fa	1339	0.402×10^{-3}	0.081
Graphene nano-oxide (GNO)	2400	–	2000

A Crow Particle Swarm Optimization Algorithm with Deep Neural Network (CPSO-DNN) for High Dimensional Data Analysis

Bibhuprasad Sahu , Amrutanshu Panigrahi, Sasmita Pani, Shrabanee Swagatika , Debabrata Singh and Santosh Kumar

***Abstract*—Diagnosis of any disease at its early stage correct treatment of the patients is necessary to save productive lives. Many techniques are adopted by different researchers to diagnose the disease at an early stage, but none of them are suitable due to the course of dimension dilemma. To differentiate the gap between logical and biological variation between the samples of the considered datasets, feature selection plays an important role. From different research, it is clear that while considering the local optima, PSO algorithm converges prematurely and decreases the diversity of the population. To avoid the limitations Crow Particle Optimization (CPSO) is implemented to identify the featured genes from a high dimensional dataset. The main concepts behind this CPO are related to the bird crow which hides a large number of foods in different places securely and collects it as per the need. To understand performance of the (CPSO-DNN) we have used three different evolutionary searchings like firefly search, elephant search and squirrel search. Gradient descent based Deep neural network with soft-max activation function has been used to maximize the no of feature genes by reducing the low impact features. Simulation results demonstrate that the (CPSO-DNN) exhibits an outstandingly higher accomplishment in terms of accuracy and can be considered as a better classification model as compared to other algorithms.**

***Index Terms*—CSO, PSO, Optimization, Neural Network and Deep learning**

I. Introduction

FOR solving different optimization problems in different evolutionary algorithms are preferred by many researchers with good expected efficiency. Basically, metaheuristic algorithms [1] are inspired by natural behavior. As the real-world optimization problems are becoming large. dynamic and complex in nature, to solve these nature-inspired algorithms are considered. Some well-known machine learning searching techniques are artificial bee colony (ABC) [2],ant colony optimization (ACO) [3], cuckoo search (CS) [4], differential evolution (DE) [5], firefly algorithm (FA) [6], gravitational searching algorithm (GSA) [7], and particle swarm optimization (PSO) [8].The application of metaheuristic algorithms are not limited it also used for various applications bioinformatics[9], clustering [10], deep learning [11], DNA fragment assembly[12], flow-shop scheduling [13], feature selection [14], geographical information systems [15], image segmentation [16], job-shop scheduling [17], power system [18], traveling salesman [19], vector quantization [20], and the water reactor problem [21]. A deep neural network is a neural network with a certain level of complexity, a neural network with more than two layers and use sophisticated mathematical modeling to process data in complex ways. Now PSO is the most preferred optimization technique used, but it suffers from premature convergence. To avoid this limitation a high accuracy optimization technique is preferred [22]. Elephant search, Bat algorithm, Fish algorithm, monkey search, lion optimization, etc. In this we have concentrated on crow particle Optimization (CPO) algorithm, which is nothing but a hybrid approach of CSO and PSO.Crow Search optimization (CSO) technique is based on the behavior of the bird crow [23]. Crow is considered to be a smart bird in this world which hides is food somewhere in secrete and roam different places in the search space to divert the food position of the others with awareness probability and fight length parameters. To understand the performance of the CPSO-DNN we have used three different evolutionary searchings like firefly search, elephant search, and squirrel search.

Rest part of the paper organized into five different sections. Section II explains the related work ,section III describces the gene selection statagy , section IV descibes contain some related works in Section II, Section III classified gene selection strategy and Section IV discuss the experimental result analysis. Lastely in Section V and VI we conclude by the statics analysys of result and conclude our paper respectively.

Bibhuprasad Sahu, Amrutanshu Panigrahi and Sasmita Pani are with the Dept. of CSE, GIFT, Bhubaneswar, Odisha, India. (e-mail: prasadnikhil176@gmail.com amrutansup89@gmail.com sasmita.pani@gift.edu.in)

Shrabanee Swagatika, Debabrata Singh and Santosh Kumar are with the Dept. of CSE, ITER, 5,6 Dept. of CSIT, ITER, SOA Deemed to be University, BBSR, Odisha,India, (e-mail: shrabaneeswagatika@soa.ac.in, debabratasingh@soa.ac.in santoshkuamr@soa.ac.in)

978-1-7281-4988-2/20/$31.00 ©2020 IEEE

II. Related Work

A. Particle Swarm optimization

Many swarms in nature like birds, fish, etc. have a higher level of behavior but they give respect to some rules within the swarm population. An example point of view we can consider the bird starlings obeys three simple rules. The first rule is when a bird flies in the open sky it follows the flight velocity of neighbors (nearly seven neighbors) and maintains a distance from others. The second rule is each bird tries to fly near towards the center of the swarm to avoid the unexpected attack from others like eagles. The third rule states that short memory is used as the bird flies in the sky to search food and shelter. Focusing on the above stated three characteristics, Kennedy and Eberhart in 1995 developed particle swarm optimization (PSO) to understand swarming characteristics of birds and fish [22]. Let us consider x_i and v_i to present position (solution) and velocity respectively of a particle i. Suppose there are n particles in the swarm population. So i = 1, 2, .n.

Updating the position and velocity of the particle can be evaluated with the following equations.

$$v_i^{t+1} = v_i + \alpha\epsilon_1[\, g^{best} - x_i^t\,] + \beta\epsilon_2[x_i^* - x_i^t] \quad (1)$$

$$x_i^{t+1} = x_i^t + v_i^{t+1}\Delta t \quad (2)$$

Here ϵ_1, ϵ_2 values vary between (0, 1) which are uniformly distributed random variables. α, β are the learning parameters whose value varies between (0,2). g^{best} Presents the best position within the swarm population. x_i^* Presents individual best solution.

B. Crow Search Algorithm(CSA)

This algorithm was proposed by Askarzadeh in the year of 2016. From the broad types of birds, crows are always considered to be a smart intelligent than others especially hiding the food safely from others. Even if the intelligent capability of the crow is not less than the human being still, their brain functions fast as compare to their body size. While the crows feel the food is unsafe then they warn others using an unsophisticated communication approach. Each crow applies mirror tests for self-awareness purposes to stay active among others. Crows are considered to be a thief as they know how to steal the food from others and store safely for the future. CSA focuses on for main criteria's such as (1) the crows prefer to live like team. (2)Hiding places of the crow are memorized for long duration (3) They follow each other while roaming around air for food (4) Crows are very protective towards food so hide their food from attacker with probability of [0,1].

In CSA suppose to consider the crows identified as N, the roaming dimension space of crows are denoted as Z, we can represent the position of the crow j at time t instance at the defined search space Z is $y^{j,t}$ and j=1,2,3,4……N. and TMax and T Min represent the maximum and minimum iteration.

As the Crows having good memories the position of the hiding space $N^{j,t}$ for each t iteration and best position of the by any crow can be determined at t time instance for crow j is $N^{j,t}$. Two scenarios may occur when the crow follows the hiding place.

Scenario 1: (Does not know the hiding place)

Consider that the crow j has no idea regarding the hiding location then it will start follows the hiding place of crow z. So the by the following equation the crow j update its self-location as mentioned in equation 3.

$$y^{j,t+1} = y^{j,t+1} + Rno_j \times hl^{j,t} \times (N^{z,t} - y^{j,t}) \quad (3)$$

Here hl represents the height length (used for local search with a small value and global search for large value), Rno_j represent the randomly generated number between [0, 1]. As the crow flies in height there is an influence that searching for food capability increases.

Scenario 2 :(Know the hiding space)

When the crow has acknowledged the hiding space, then to protect its own food it first moves to the position of the location of food existence.

Another parameter considered in CSA except height length is(AP) the probability of awareness (Mainly focused in Scenario 2). This is used to maintain a balance between the exploration of large value and exploitation for small value. Scenario 1 and 2 can be expressed in equation 4.

$$y^{j,t+1} = \begin{cases} y^{j,t} + y^{j,t+1} = y^{j,t+1} + Rno_j \times hl^{j,t} \times (N^{z,t} - y^{j,t}) & , Rno_z \geq qAP^{j,t} \\ \text{Prefer a Random Position} & \text{Otherwise} \end{cases} \quad (4)$$

Here Rno_z is a random ∈ [0, 1]. The position of the crow gets an update with a fitness function or an Objective Function. The crows update the new position using equation 5.

$$N^{j,t+1} = \begin{cases} y^{j,t+1}, if\ Function\left(y^{j,t+1}\right) \geq Function\left(N^{j,t}\right) \\ N^{j,t}, Otherwise \end{cases} \quad (5)$$

.

C. Deep Learning

Deep learning is also called stacked NN (neural network) because it is categorically different from other neural networks as it consists of multi hidden layers(3nos) except the input/output layer. Deep learning does combination and aggregation activity from one layer to another. That's why deep learning considered the best choice for high dimensional datasets as it improves the complexity as abstraction level. As the dataset consists of real as well as discrete data values, finding optimal results using a gradient descent algorithm is not feasible. It is difficult to evaluate each and every hyperparameter alone to achieve a local minimum. At the starting stage, we consider small weight so the considered activation function works linearly with high gradient value.To keep the validation error minimal the learning rate of the DNN should choose efficiently.For performing better solution L1 and L2 regularization scheme is adopted to check the performance of NNs.

i) **Pseudocode for DNN**

i. Input: $Z=(Z_1, Z_2, \ldots\ldots Z_n$ *represents an input data matrix for n samples,Z1=*$(Z1_1, Z1_2, \ldots\ldots, Z1_n)^T$ *represent desired respective outputs with maximum selected attribute no of K.*

ii. Consider SS={ bias},CS=F and Ca_w*=0*

iii. While $|SS| < k+1$ *do*

iv. Assign Ca_w*=0*

v. Then hidden layers weights and input weight will get update.

vi. Average G_{wf} *calculate by using multiple time drop out.*

vii. Evaluate $j = \arg max \|G_{wf}\|$

viii. Learning rate implementing AdaDelta (used for dimension learning rate)

ix. Initialize In_{w_j} *by using Xavier initialization*

x. Perform $ss = ss \cup F_j$ *and* $CS = CS \backslash F_j$

Where SS= Chosen Set,CS=Candidate Set ,Weights of input=In_w ,w_{cs}= weight of the candidate list, Gr_w= gradient of input set, Gr_{wj}= gradient to select single feature(j) out of candidate set (c)., In_w= input weight with recently identified input weight with jth input node.SS and CC will be updated with variation of j.

D.1.4 Crow Particle Swarm Optimization(CPSO)

CPSO is a hybrid approach of both PSO and Crow search Alogothim with a target to achieve a global optimum with the help of center PSO[27]. Using the selection approach some individuals are selected in successive selection. Individual solution space for the particle is searched and the position is updated using equation 6.

$$v_{i,j}^{itr+1} = \omega v_{i,j}^{itr} + c_1 r_1 \left(p_{i,j}^{itr} - x_{i,j}^{itr}\right) + c_2 r_2 \left(p_{gbest,j}^{itr} - x_{i,j}^{itr}\right) \quad (6)$$

PSO oscillation can be adjusted by the maximum velocity V_{max} and it is shown using the following equations 7 and 8.

$$v_{max} = \left(1 - \left(\frac{itr}{itr_{max}}\right)^h\right) * V_{max0} \quad (7)$$

$$V_{max0} = \alpha * (position_{max} - position_{min}) \quad (8)$$

Here $position_{max}, position_{min}$ presents the maximum and minimum threshold position, itr denoted as the iteration position, itr_{max} presents maximum iteration, h presented as constant (positive Value), α denoted as the search space bound. By the help of the hybrid operator, some individual feature between PSO and CSA gets exchanged with the help of the selection criteria. Here Roulette-Wheel random selection approach is used.It is presented in equation 9.

$$prob_i = \frac{fitr_i}{\sum_{i=1}^{N} fitr_i} \quad (9)$$

Fn_i is known as the fitness value of individual population i. In CPSO the local search operator is used to identify the best position of the crow in PSO and CSA. Let's consider the best position of the crow c in CSA is updated as $x_{c,j}^{itr+1}$ and $x_{p,j}^{itr+1}$ presents the best position in the case of PSO. By the help of the local operator, we can evaluate the best position of the i^{th} crow using following equation 10.

$$x_{i,j}^{itr+1} = \begin{cases} x_{i,j}^{itr} & : if\ f(x_{i,j}^{itr}) < f(x_{i,j}^{itr+1}) \\ x_{i,j}^{itr+1}: & Otherwise \end{cases} \quad (10)$$

CPSO Algorithm

1. Initialization of individual population random position in both CSA and PSO
2. Identify the center crow.
3. Execute CSA and PSO
4. Implementation of the local operator to enhance the best solution
5. Implementation of the hybrid operator after a recognized iteration reached
6. Repeat 2 -6 until if criteria not achieve.

Stop if best solution Found

III. Gene Selection And Classification Strategy

The setting of the parameter done for gene selection and classification mentioned below.

- CPSO: For CSA(Total no of crows =20, flight length =1.5, Probability of awareness=0.5), for PSO(Particle count =20, inertia value(ω)=0.9-0.4, value of c1,c2=1.4,h=0.05, value of α=0.01) ,for CPSO(no of individuals =20)

Deep Learning (DNN): Activation function(AF)= Softmax , initialization of weight approach= XAVIER, Bias initialization=1.0, considered distributed function =Normal, Rate of Learning=0.1, Rate of bias learning=0.01, Rate of momentum =0.9, Update version of Stochastic gradient descent(SGD)=NESTEROVS, Value for normalization threshold =1.0, adopted loss function –Loss MCXENT, Rho parameter for ADADELTA=1.0E-6,RMS delay parameter for RMSPROP=0.95,Mean decay parameter for ADAM-0.999, Epoch count =10, Optimization algorithm=Gradient descent(GD),No of batch=50, no of Seed =1 , Decimal place considered =2.

IV. Experimental Result Analysis And Findings

In this module, we expressed our experimental performance and discussed how this proposed approach is effective result with high dimensional dataset. The Fig. 1 represents the experimental flow of entire process. The high dimension datasets mention in Table I are implemented with CPSO to identify the reduced important featured genes, it works as a feature selection algorithm. Then the reduced feature set is treated as input to Deep Neural Network (DNN) to achieve the perform better classification for gene expression dataset.

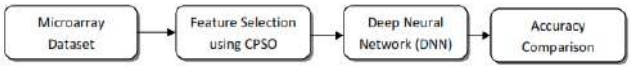

Fig. 1. Experimental process.

TABLE I
DATASET CONSIDERED FROM UCI REPOSITORY EXPERIMENT

Dataset	No of genes	No of instances	No of classes
CNS	7129	72	2
SRBCT	2308	83	4
MLL	12582	72	3
Breast Cancer	10	286	2
Ovarian Cancer	15155	253	2
Lung	12601	203	5
DLBCL	4027	47	2
Colon	2001	62	2
ALL-AML	7130	38	2
Prostate	12601	102	2

During training phase of neural network, we have adopted 10-cross validation where the available training data is subdivided into 10 sets and classification algorithm is applied 10 times. So 90% of the dataset is considered as training set for train the model and rest 10% is evaluated as the test set for testing the performance of the model. Overall 10 cross-validation is used to provide a better solution to avoid over fitting problems. The overall performance if the trained model is evaluated by calculating average accuracy and time taken to build the model. The accuracy can be predicted as the ratio between true positive and total no of samples. We have compared our results with various optimization algorithms like firefly (FFS) and Elephant search optimization (ESA).

From Table, II and III we observed that Deep learning performs better in other datasets in comparison with the CNS dataset as this dataset contain less no of instance during classification phase. Table III presents a comparative study to understand the efficiency of CPSO-DNN approach. The comparison results opine that CPSO-DNN achieves better accuracy for all considered microarray datasets. from the table it is clear that CPSO-DNN performs faster among other approaches for all datasets especially for Lymphoma, leukemia dataset as well as Prostrate cancer dataset. Normally when we are working with high dimension dataset, for achieving better accuracy the reduced no of genes plays a major role. For easy understanding of the accuracy results for different microarray datasets considered for this study is expressed in terms of the box plot. To validate the experimental results we have adopted two different significant tests such as one-way ANOVA and Post hoc Turkey HSD.

TABLE II
ACCURACY COMPARISION

				As per the literature survey								
Dataset	No of genes	No of instances	No of classes	FFS-DNN			ES-DNN			CPSO-DNN		
				No Of Reduced Genes	Built Time	Accuracy	No Of Reduced Genes	Built Time	Accuracy	No Of Reduced Genes	Built Time	Accuracy
CNS	7129	72	2	1526	0.45	56.67	1621	0.47	53.34	1211	0.39	64.89
SRBCT	2308	83	4	768	0.63	93.98	306	0.66	83.14	268	0.59	ta
MLL	12582	72	3	190	14.59	80.56	190	15.13	80.56	216	12.94	87.42
Breast Caner	10	286	2	6	0.75	65.39	6	1.09	73.43	5	0.98	79.18
Ovarian Cancer	15155	253	2	35	17.23	97.24	384	1.67	99.21	467	3.11	99.65
Lung	12601	203	5	5304	15.53	93.11	4545	2.92	94.1	4282	1.63	96.18
DLBCL	4027	47	2	1805	0.79	89.36	1717	0.44	91.49	1667	0.31	92.74
Colon	2001	62	2	562	0.43	77.43	72	0.41	79.03	351	0.37	81.59
ALL-AML	7130	38	2	2463	1.84	100	1044	0.31	92.11	1766	0.68	100
Prostate	12601	102	2	5189	1.24	87.26	4267	1.33	88.24	4066	1.18	92.19

V. STATISTICAL TEST RESULT

It is clear from the ANOVA test that P-value for F-statistics is more than 0.05, which specifies that the treatments used are not failing the condition of level of significance. Even if the performance of CPSO-DNN doesn't advise the presence of significant pairs in one ANOVA. So we prefer multiple comparative statistical tests to evaluate any new set of pairs.We consider one way ANOVA of K=2 for independent treatment for CPSO-DNN compared with ESA-DNN and ABC-SVM considering the following parameters such as k= two no of treatments, v – degree of freedom(8), α= significant level (0.01) and p-value is 0.05 respectively for Tukey-Kramer HSD Q statistical analysis. Then we evaluate posthoc Tukey HSD test to evaluate relevant treatment pairs. Below tables shows the result of different statistical analysis.

In the below Table III we compared accuracy analysis of our proposed methods with the exiting methods and also find out the execution time for all. Then in the Table IV one-way ANOVA Statistical result is evaluated and the statistics result of Turkey HSD analysis is concluded with turkey HSD interference with insignificant value shown in Table V.

TABLE III
ACCURACY COMPARATIVE ANALYSIS

Proposed method	Dataset considered	Accuracy	Execution time
ESA-DNN	ALL-AML	92.11	0.44
FFS-DNN	ALL-AML	100	0.79
Pillar NN	ALL-AML	85.6	0.87
CPSO-DNN(Ours)	**ALL-AML**	**100**	**0.68**
ESA-DNN	DLBCL	91.49	0.44
FFS-DNN	DLBCL	89.36	0.79
CPSO-DNN(Ours)	**DLBCL**	**92.74**	**0.31**
ESA-DNN	Prostate	88.24	1.33
FFS-DNN	Prostate	87.26	1.24
CPSO-DNN(Ours)	Prostate	92.19	1.18
ESA-DNN	MLL	81	15.13
FFS-DNN	MLL	80.56	14.59
CPSO-DNN(Ours)	**MLL**	**87.42**	**12.94**
ESA-DNN	SRBCT	93.98	0.66
FFS-DNN	SRBCT	92.77	0.63
CPSO-DNN(Ours)	**SRBCT**	**97.11**	**0.59**

TABLE IV
(ONE-WAY ANOVA STATISTICAL RESULT)

	Treatment	ESA-DNN	CPSO-DNN
	Obsetvation no	10	10
Oneway Anova	Sum	929.5	934.78
	Mean	92.95	93.4
	sum of squares	866493914	884558913
	Variance	28.04	19.16
	standard deviation	5.29	1.59
	standard deviation mean	1.67	1.78

TABLE V
(TUKEY HSD Q STATISTICS RESULT)

Treatments	Tukey HSD Q statistics	Tukey HSD P-value	Tukey HSD interference
ESA-DNN vs CPSO-DNN	2.65	0.8506	Insignificant

VI. CONCLUSION

From this analysis, it is clear that for achieving success with high dimensional gene expression dataset it is necessary to understand the details. As a microarray high dimensional dataset suffers from coarse of dimension so it is important to choose a better feature selection and classification mechanism to identify the level of the disease so it will be a positive opportunity to save the life of the patient. In this research the result reveals that CPSO-DNN able to identify the featured genes from the microarray dataset. This proposed method crow particle swarm optimization with deep learning results better accuracy. As we have checked our performance with different statistical methods and hence it is proved that CPSO-DNN performs better than other as compared with the literature survey. In future the proposed approach will be tested with high dimensional and high sample dataset to check the performance.

REFERENCES

[1] M. Gendreau, J.-Y. Potvin, Handbook of Metaheuristics, second ed., Springer Publishing Company, Incorporated, New York, NY,2010.

[2] D. Karaboga, An idea based on Honey Bee Swarm for numerical optimization. Technical Report TR06, Erciyes University, Oct.2005.

[3] M. Dorigo, V. Maniezzo, A. Colorni, Ant system: Optimization by a colony of cooperating agents, Syst. Man Cybern. Part B: Cybern. IEEE Trans. 26(1) (Feb. 1996), 29–41.

[4] X.-S. Yang, Chapter 9–Cuckoo search, in: X.-S. Yang (Ed.), Nature-Inspired Optimization Algorithms, Elsevier, Oxford, 2014, pp. 129–139.

[5] S. Das, P.N. Suganthan, Differential evolution: a survey of the state-of-the-art, Evol. Comput. IEEE Trans. 15(1) (Feb. 2011), 4–31.

[6] X.-S. Yang, Firefly algorithms for multimodal optimization, in: O. Watanabe, T. Zeugmann (Eds.), Stochastic Algorithms: Foundations and Applications, volume 5792 of Lecture Notes in Computer Science, Springer, Berlin, Heidelberg, 2009, pp. 169–178.

[7] E. Rashedi, H. Nezamabadi-pour, S. Saryazdi, GSA: a gravitational search algorithm, Info. Sci. 179(13) (2009), 2232–2248.

[8] J. Kennedy, R. Eberhart, Particle swarm optimization, in: IEEE International Conference on Neural Networks, Perth, Australia, 1995, Vol. 4, pp. 1942–1948.

[9] Barik S. , Mohanty S. , Mohanty S. , Singh D., " Analysis of Prediction Accuracy of Diabetes using Classifier and Hybrid Machine Learning Techniques" , ICICC-2019(2019),Springer.

[10] L. Bai, X. Cheng, J. Liang, H. Shen, Y. Guo, Fast density clustering strategies based on the k-means algorithm, Pattern Recognit. 71 (2017), 375–386.

[11] K. Li, Q. Gan, L. Yuan, Q. Fu, Optimized generation of test sequences for high-speed train using deep learning and genetic algorithm, in: IEEE 19th International Conference on Intelligent Transportation Systems (ITSC), Rio de Janeiro, Brazil, 2016, pp. 784–789.

[12] Allaoui, B. Ahiod, M.E. Yafrani, A hybrid crow search algorithm for solving the DNA fragment assembly problem, Expert Syst. Appl. 102(C) (2018), 44–56.

[13] Abdel-Basset, G. Manogaran, D. El-Shahat, S. Mirjalili, A hybrid whale optimization algorithm based on local search strategy for the permutation flow shop scheduling problem, Future Gener. Comput. Syst. 85 (2018), 129–145.

[14] Barbu, Y. She, L. Ding, G. Gramajo, Feature selection with annealing for computer vision and big data learning, IEEE Trans. Pattern Anal. Mach. Intell. 39(2) (2017), 272–286.

[15] M. Al-Abadi, A novel geographical information system-based ant miner algorithm model for delineating groundwater flowing artesian well boundary: a case study from Iraqi southern and western deserts, Environ. Earth Sci. 76(15) (2017), 534.

[16] H. Çataloluk, F.V. Çelebi, A novel hybrid model for two-phase image segmentation: GSA based Chan–Vese algorithm, Eng. Appl. Artif. Intell. 73 (2018), 22–30.

[17] K. Rameshkumar, C. Rajendran, A novel discrete PSO algorithm for solving job shop scheduling problem to minimize makespan, in: IOP Conference Series: Materials Science and Engineering, Bengaluru, India, 2018, pp. 012143.

[18] S. Jiang, Z. Ji, Y. Wang, A novel gravitational acceleration enhanced particle swarm optimization algorithm for windthermal economic

emission dispatch problem considering wind power availability, Int. J. Elec. Power Energy Syst. 73 (2015), 1035– 1050.
[19] A. El-Shamir Ezugwu, A.O. Adewumi, Discrete symbiotic organisms search algorithm for travelling salesman problem, Expert Syst. Appl. 87 (2017), 70–78.
[20] K. Chiranjeevi, U. Jena, P.M.K. Prasad, Hybrid cuckoo search based evolutionary vector quantization for image compression, in: Lu, H., Li, Y. (Eds.), Artificial Intelligence and Computer Vision, Springer, New York, NY, 2017, pp. 89–114.
[21] A.A. de Moura Meneses, M.D. Machado, R. Schirru, Particle swarm optimization applied to the nuclear reload problem of a pressurized.
[22] A. Askarzadeh, A novel metaheuristic method for solving constrained engineering optimization problems: crow search algorithm, Comput. Structures. 169 (2016), 1–12.
[23] Zhan, Zhi-Hui, Jun Zhang, Yun Li, and Yu-Hui Shi. "Orthogonal learning particle swarm optimization." IEEE transactions on evolutionary computation 15, no. 6 (2010): 832-847.

2021 International Conference on Emerging Smart Computing and Informatics (ESCI)
AISSMS Institute of Information Technology, Pune, India. Mar 5-7, 2021

CDA-SVM: A Chaotic Dragonfly Enriched Support Vector Machine for Micro array Data sets

1st Bibhuprasad Sahu
Department of CSE
Gandhi Institute For Technology
Bhubaneswar, India
prasadnikhil176@gmail.com

2nd Amrutanshu Panigrahi
Research Scholar
SOA Deemed to be University
Bhubaneswar, India
amrutanshup89@gmail.com

3rd SatyaSobhan Panigrahi
Department of CSE
Gandhi Institute For Technology
Bhubaneswar, India
satyasobhan@gift.edu.in

4th Sachi Nandan Mohanty
Department of Computer Sc.& Engineering
College Of Engineering
Pune,India
sachinandan09@gmail.com

5th Subhashree Sukla
Department of CSE
Gandhi Institute For Technology
Khurdha,Bhubaneswar, India
subhashreesukla@gift.edu.in

6th Chetan Nimba Aher
Department of CSE
AISSMS Institute of Information Technology
Pune, India
chetan.aher07@gmail.com

2021 International Conference on Emerging Smart Computing and Informatics (ESCI) | 978-1-7281-8519-4/20/$31.00 ©2021 IEEE | DOI: 10.1109/ESCI50559.2021.9396985

***Abstract*—Pattern classification method is adopted by the Support Vector Machine(SVM) which influences the accuracy of the classification by initializing the kernel parameter and selection of bio-marker genes.Identification of the most distinguished genes from the Microarray data set is itself a challenging task for the researchers. Various nature and bio-inspired optimization techniques are adopted to achieve the solution of the optimization problems. So, in this study for parameter optimization and biomarker genes were identification can be done using SVM, we have proposed a novel Chaotic dragonfly algorithm combine with SVM.The proposed algorithm is designed to evaluate various micro array cancer data sets.The designed model is divided into 3 stages such as Prepossessing of data sets (Filter stage using SMOTE,ROS,RUS),identification of the featured genes done using the feature selection phase CDA (Chaotic Dragonfly algorithm), and finally in the classification phase is done to evaluate the performance of the purposed method.In this stage the identified features from the second stage are feed to SVM classifier.The experimental study proved that CDA-SVM presented its capability to recognize the featured biomarker genes from the high dimensional data sets. Not only it performed better but also able to recognize less amount of featured genes.Out of 10 chaotic maps, Gauss chaotic map which enhances the performance of the DA.**

***Index Terms*—Microarray Dataset, DA, CDA, SVM,Chaotic theory**

I. Introduction

In machine learning field, SVM is preferred by the researchers because of the minimization of risk and vector machine dimension concept. SVM can perform better in terms to reduce the gap between error minimization in training and maximization of margin so that over-fitting problem can be solved easily. SVM is well noticed by several researchers as it achieves the global optima and it solves the problem like minima trapping. SVM performance is quite good to solve various medical diagnosis problems. The performance for SVM can be improved by considering the kernel bandwidth parameters(σ) and penalty parameter(C) of the kernel function. The penalty parameter is used the fill up the gap between error optimization(fitting) and the complexity of the model where used to present the map input space with high dimensional space as we are considering micro array data set which is suffering from the curse of dimension problem. To improvise the accuracy grid search, the gradient descent method is implemented, but the matter of concern is these above methods fall into local minima.To Avoid this various meta heuristic algorithms like harmony search,bat algorithm,particle swarm optimization,frog leaping algorithm are used to achieve global optimum for SVM.Non redundant features of the data set impacts the accuracy of the classifier so feature selection plays an vital role [1]–[5].This study provides a new direction to tackle with the parameter selection of SVM and feature selection using chaotic dragonfly algorithm.First we have explore the capability of dragonfly algorithm to evaluate optimization of the parameter and feature selection using SVM.

In this study, chao theory is introduced with dragon fly algorithm (DA).The resultant of chao enhanced dragonfly algorithm is used optimize the key parameters of the SVM to identify the optimal feature subset for SVM.The outcome of the SVM model,CDA-SVM was scrupulously validated on the micro-array data sets through ten fold cross validation considering various performance parameters like classification accuracy,sensitivity,ROC,specificity. Performance of the proposed model is compared with various hybrid SVM methods such as DA-SVM,PSO-SVM,ABC-SVM,SCA-SVM,CSA-SVM,SSA-SVM,CSO-SVM,GWO-SVM [25], [26].

The remainder section of the paper is organized as follows. We introduce the basic background details of various filter approaches such as(SMOTE,ROS,RUS) and wrapper approaches DA,CDA including the basic details of SVM classifier in second section.The third section describes the detail study of micro-array data sets.Section four describes the proposed CDA-SVM.Section five and six explains the result analysis and conclusion and future scope.

II. STUDY OF BACKGROUND THEORY

A. Filter approach

1) Sampling Techniques: Class imbalance is the one of the common issue in case of micro-array data sets as the the no of non cancer classes(major) are significantly high then the cancer classes(minor) [7], [8]. When the researchers deals with such type of data sets it became a serious issue as all the traditional learning approaches are lenient towards the major classes.This may decrease the accuracy of the classifier and the chance of false positive ratio may goes high, which is totally not advisable.This types of problems are generally called as Class imbalance issues.Re-sampling is the approach used which normally balance the classes of the micro-array data set in two ways. 1.Under-sampling (Majority one) 2.Over-sampling the (minority one).The performance of the Re-sampling depends on two basic information such as ratio gap between major and minor class and classifier characteristics which is being adopted by the researcher.Main disadvantage of re-sampling is by considering the under sampling,there may be a chance that it may eliminate the important features where as using oversampling it increases the numbers minor class artificially which may cause the over-fitting error. To encounter this above issues of micro-array data sets we have used three sampling techniques such as SMOTE,ROS,RUS for our study as filter method.Synthetic minority oversampling technique(SMOTE) is one of the well known oversampling method which generates the synthetic samples of the minor class by considering k-minority classes randomly.To achieve a balanced data set multiple re-sampling can be adopted. Random majority under sampling (RUS) is used to remove the samples from the majority class randomly. Using RUS the potential of the information lost may occur,which directly affect on performance of the classifier [8], [9].Random over-sampling(ROS) duplicates examples from the minority class in the training data set and can result in over-fitting for some models.To improve the performance of the SVM, the CURE-SMOTE algorithm is also used by some researchers for imbalanced data classification.

B. Wrapper approach

1) Dragonfly Algorithm(DA): Dragonfly algorithm was first proposed by prof. Mirijalili, with inspiration from static and dynamic mechanisms of idealized dragonflies. Hunting mechanism is the static behavior of the dragonflies in which they search for food in small geographical area with in a small group.For searching food group of dragonflies migrates from one place to another to search the preys,is considered as the dynamic mechanism for Dragonfly Algorithm [10].In DA static and dynamic mechanism presents the exploration and exploitation phases of the meta algorithm respectively [11], [12].The swarming behavior of dragonflies depends on three characteristics such as Separation,Alignment,Cohesion for creation of attraction towards foods and distraction towards enemy.To develop the swarming the behavior, the position of the dragonflies presented as $X_i = (x_i^1, x_i^2, ..., x_i^D)$,Where values of i varies between 1,2,3...N, (x_i^D) presents of the i^{th} position of the dragonfly with in the D dimension search space including N no's of search problems.The mathematical details of various parameters are stated below.

- 1. Separation describes the static collision avoidance from each other. The separation can be defined as follows

$$Sep_i = -\sum_{k=1}^{N} X - X_k \tag{1}$$

  Where X denoted as the current position of the individual dragonfly and X_k and N present the position of the K^{th} neighbor and total no of the dragonflies available in the search space.
- 2.Alignment which presents mean of velocities of all neighbor dragonflies present in the search space. It can be evaluated using below equation

$$Alig_i = \frac{\sum_{k=1}^{N} Vel_k}{N} \tag{2}$$

- 3.Cohesion defines the distance of the dragonfly with respect to center of mass.It can be defined using below equation.

$$Coh_i = \frac{\sum_{k=1}^{N} X_k}{N} - X \tag{3}$$

  Where X,N presented the current position of individual dragonfly and N denotes the total of dragonflies in the search space.
- 4.Attraction of dragonflies towards Prey(x$\hat{+}$) is evaluate as the difference of distance between the current position of the dragonfly with respect to the position of the prey(X).

$$Att_i = X^+ - X \tag{4}$$

- 5.Distraction in the search space cane be evaluated as the distance gap between the current position of the individual and enemy position.It can be evaluated using below equation.

$$Distr_i = X^- - X \tag{5}$$

According to the basic Dragon fly algorithm ,movement direction of the dragon fly cane be evaluated using step vector ΔX and position vector(X).The velocity of dragonfly can be evaluated like PSO [13]–[15].Following equation is used to evaluate the position vector of individual dragonfly.

$$\begin{aligned}\Delta X_{t+1} \quad = \quad & ValueofChaoticmapof i^{th} + iterationAlig_i \\ & + SeparationweightSep_i \\ & - CohesionweightCoh_i + enemyweightDistr_i \\ & + foodweightAtt_i + \omega \Delta X_i\end{aligned}$$

If there is either one neighbour dragonfly is present then position of the dragonfly and if no neighbour dragonfly then the position can be gets update using equation 7 and 8(Levy Flight). In the equation 8 (d) is denoted as the dimension of the position vector in the search space. The Levy flight is calculated using equation 9. Here levy fight is used to

improve the all stochastic, randomness and DA exploitative behaviors.The parameters like Separation,Alignment,Cohesion, Attraction,Distraction is used to balance the gap between exploration and exploitation [16], [17].

$$X_{t+1} = X_t + \Delta X_{t+1} \tag{6}$$

$$X_{t+1} = X_t + levyX_t \tag{7}$$

$$levy(X) = 0.01 * \frac{p_1 * \sigma}{|p_2|^{\frac{1}{\beta}}} \tag{8}$$

In the equation 9, P_1,P_2 are random variables whose value varies between [0 and 1] and β is a constant,where as σ can be calculated using equation 10.

$$\delta = [\frac{\Gamma(1+\beta) \times \sin(\frac{\Pi\beta}{2})}{\Gamma\frac{1+\beta}{2} \times \beta \times 2^{\frac{\beta-1}{2}}}]^{\frac{1}{\beta}} \tag{9}$$

where

$$\Gamma(x) = (x-1)! \tag{10}$$

C. Chaotic Map Concept

To achieve the optimal search solution of a given problem chaos optimization theory is used as it is a nonlinear phenomenon where a small change in initial condition changes affects the nonlinear change in the future characteristics or behavior.chaotic optimization concept is one of the recent algorithm , the main logic behind this technique is transformation of parameters from chaos to the solution space.Using chaotic motion properties like randomness, ergodicity, and regularity is search the global optimum in the search space.Due to the simplicity and convergence speed of chaotic map theory it is preferred by the researchers to integrate with various meta heuristics algorithms to improve the accuracy.The objective of this study is identify the best chaotic map combine with Dragonfly algorithm to detect the suitable feature subset and improvise the accuracy [18]–[20], [27].

D. Chaotic DA (CDA)

In CDA is the the chaotic version of DA. The main limitation with basic DA, the corresponding parameters are randomly initialized ,So the randomness of the algorithm affected the performance of DA [21].To provide the solution of limitation of DA instead of assign the parameters randomly,in CDA the values can be substituted with chaotic values. The CDA, updating the position of the dragonflies can be done using equation (6).Value of Chaotic map of i^{th} iteration is denoted as D(i)

$$\begin{aligned}\Delta X_{t+1} = \\ D(i)[Alig_i + SeparationweightSep_i \\ - CohesionweightCoh_i + enemyweightDistr_i \\ foodweightAtt_i + \omega\Delta X_i]\end{aligned} \tag{11}$$

In CDA, the initialization of parameters (mentioned in Table 1) and position of the dragonfly can be done randomly. Each and every position of the dragonfly presents the feature subset with different no of features and lengths. The position the dragonfly can be evaluated using the fitness function (denoted in equation 13).

$$F = max(Acc + \omega_f(1 - \frac{L_f}{L_t})) \tag{12}$$

Where ω_f is defined as the weight factor(vale considered for this study is 0.9, L_f is defined as no of features .

1) Pseudo-Code of CDA:

1) Initialize the following parameters such as
   - Population size of dragonfly(M)
   - Dimension d.
   - Lower bound(LB)
   - Upper bound(UB)
   - Max iteration(MAX_itr)
2) Initialize the position of the dragonfly randomly.
3) Initialization of of step Vector ΔX_k.
4) Evaluation of fitness value of dragonfly position $(F(X_k))$
5) set the value of iteration(t)=1.
6) Repeat 7 to 18
7) for $j = 1 :\leq M$
8) Calculate the B(t) Chaotic map Value.
9) Update all parameters of Dragon flies algorithm (inertia weight, separation weight ,alignment weight,food weight,iteration number).
10) Evaluate the value of Separation,Alignment,Cohesion, Attraction,Distraction.
11) if(neighbor number$\leq$ 1)
    update the velocity and position of dragonfly
    using equation 12 and 7 respectively
    else update the position vector using equation 8.
12) end if
13) If the updated position is not in search space or out of boundary then bring it back.
14) increment the iteration(t) means t=t+1.
15) Repeat until Iteration(t)$\leq Max_iteration$.
16) Produce the best solution.

TABLE I
INITIAL PARAMETERS OF CDA

Parameter Details(CDA)	Value
β,	1.5
d	31
M	50
$Lowerbound$	1
$Upperbound$	31
$MaxIteration$	50

E. SVM

All data science experts prefer SVM as a suitable binary classification approach, as it perform in a better way with different kernel functions with excellent accuracy. Basically

for evaluation of the classifier, the available data set is converted into training and test with (70-30) ratio.Here class label is recognize as the output.The main characteristic of SVM is,geometric margin between two classes are identified with minimization of the error by preventing the data points which are wrongly classified [22]–[24]. Equation(13) presents basic mathematical expression of SVM.

$$\min_{w \epsilon R^F} \frac{1}{2}[w]_2^2 + C \sum_{i=1}^{n} I(y_i, f_w(X_i)) \tag{13}$$

Here the hyper plane concept is implemented to identify the difference between two classes.Loss function $I(y, \hat{y})$ is denoted as $\hat{y}$. For evaluation of the smoothness/error , a regularization parameter C is adopted . $f_w(x_i) = \langle \phi(x_i), w \rangle$ where $\phi(x) : R^d \rightarrow R^F$ presents the mapping relationship of data set(input) from the input space R^d to feature space R^F. The value of F is chosen infinity. When the value of F is very large, then the products inner space R^F can be evaluated using the kernel function $k(x, y) = \langle \phi x, \phi y \rangle$ .Outof 4 basic SVM kernel functions (linear(L), polynomial(P), sigmoid(S), and radial basis functions (RBF)), for our study , we have considered RBF as kernel function, Which is expressed as

$$k(x, y) = \frac{\exp ||x - y||^2}{2 \times \sigma^2} \tag{14}$$

Different parameters such as C,V,and kernel parameters values can be considered wisely to evaluated the classification accuracy.

TABLE II
PARAMETER OF SVM

$C(Regulation\_parameter), 10^{-4}, 10^{-3}, 10^{-2}, 10^{-1}, 1, 10^4, 10^3, 10^2$, 10^1
$\Gamma(Kernel\_parameter), 10^{-4}, 10^{-3}, 10^{-2}, 10^{-1}, 1, 10^4, 10^3, 10^2, 10^1$

III. DATA SET DESCRIPTION

TABLE III
DATA SET DESCRIPTION

Dataset	No$_i nstances$	No of features	classes
1.Leukemia1	72	7129	2
2.Leukemia2	72	7129	3
3.Lyomphoma	45	4096	9
4.DLBCL	77	7129	2
5.COLON	62	2000	2
6.9-TUMORS	60	5726	26
7.11-TUMORS	174	12533	11
8.14-TUMORS	308	15009	9
9.PROSTRATE TUMORS	102	15009	2

IV. PROPOSED METHODOLOGY

To uncover the optimal values of SVM parameters chaotic DA algorithm is used.CDA-SVM is trained with data sets such as UCI data sets from the UCI Machine Learning Data repository.The data set considered for this study is presented in the table-3. Total 9 no of different micro array cancer data sets taken into study. The data set description table contains data set name , no of instances, no of features and no of classes. The proposed model,CDA-SVM, it begins with the data prepossessing step.For this we divide the data set into (90-10)% as training and test subsets.Different parameters of CDA-SVM such as population,maximum iteration,other parameters considered is presented in Table-1.The proposed CDA-SVM framework was implemented using 10 fold cross validation for identify the feature subset from the high dimensional micro-array data set.The performance of the proposed one is compared with different meta heuristic algorithms such as SVM methods such as CSA,PSO,ABC,SCA,CSA, SSA,CSO,GWO. A dragonfly in the search space changes randomly and the position can be evaluated with parameters presented in table 1.As the searching limit increases,it also increases the search space,which direct impact to achieve the optimal solutions. The positions of dragonflies are modified according to Eqs. (1),(2),(3),(4),(5). Until it of satisfy termination criteria (MAX_iter or best solution found),the CDA algorithm repeats its execution. .The CDA identifies the best combination of features by adaptively searching the feature space and the learning accuracy of SVM determines the fitness value of the dragonflies.The radial base function (RBF) is used as the kernel function of the SVM model.All of the codes are implemented in MAT-LAB R2018b and run on a Window 10 PC with Intel Core i5-3470K 3.20 GHz CPU and 16 GB RAM.

TABLE IV
AVERAGE ACCURACY OBTAINED BY VARIOUS ALGORITHMS

Dataset	CSO	CSA	GWO	ABC	PSO	DA	CDA
1	98.65	99.13	97.74	98.07	99.27	87.42	100
2	88.5	87.52	95.47	96.37	98.77	77.26	99.78
3	98.01	98.81	95.76	96.98	95.87	83.21	98.92
4	93.67	95.59	94.69	96.73	97.62	94.67	100
5	87.36	90.37	93.93	94.62	95.68	96.67	98.92
6	60.54	58.57	62.34	65.44	65.57	78.43	91.76
7	90.43	90.77	90.66	91.77	94.72	94.31	95.77
8	47.72	70.55	70.11	70.57	74.37	71.26	76.77
9	92.11	92.31	94.76	92.25	94.71	94.63	99.71

TABLE V
AVERAGE F1 VALUE OBTAINED BY VARIOUS ALGORITHMS

Dataset	CSO	CSA	GWO	ABC	PSO	DA	CDA
1	0.98	0.99	0.97	0.98	0.99	0.87	1
2	0.88	0.87	0.95	0.96	0.98	0.77	0.99
3	0.98	0.98	0.95	0.96	0.95	0.83	0.98
4	0.0.93	0.95	0.94	0.96	0.97	0.94	1
5	0.87	0.90	0.93	0.94	0.95	0.96	0.98
6	0.60	0.58	0.62	0.65	0.65	78.43	91
7	0.90	0.90	0.90	0.91	0.9	0.94	0.95
8	0.47	0.70	0.70	0.70	0.74	0.71	0.76
9	0.92	0.92	0.94	0.92	0.94	0.94	0.99

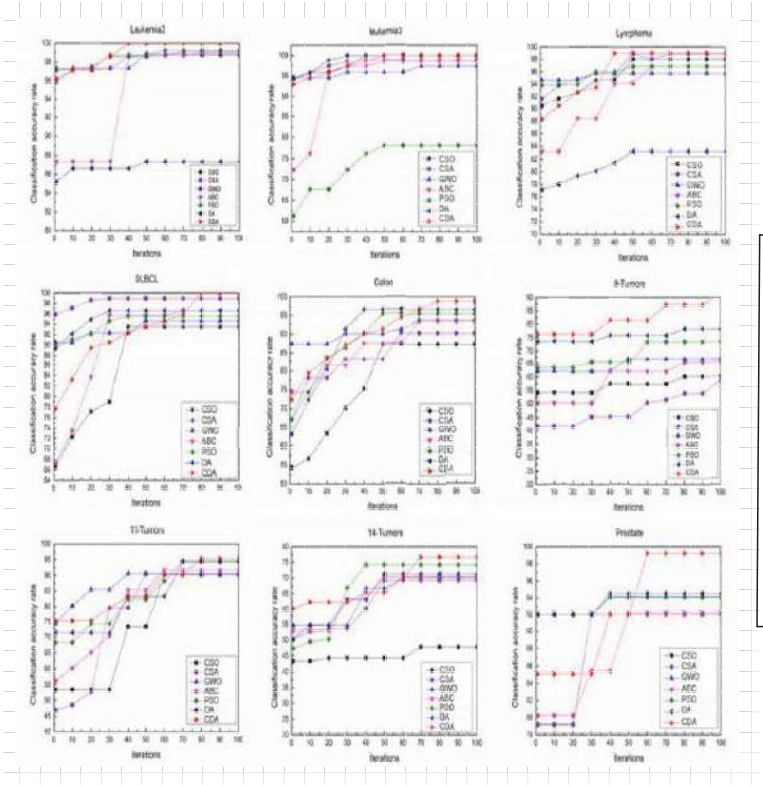

Fig. 1. Average Accuracy obtained by various algorithms

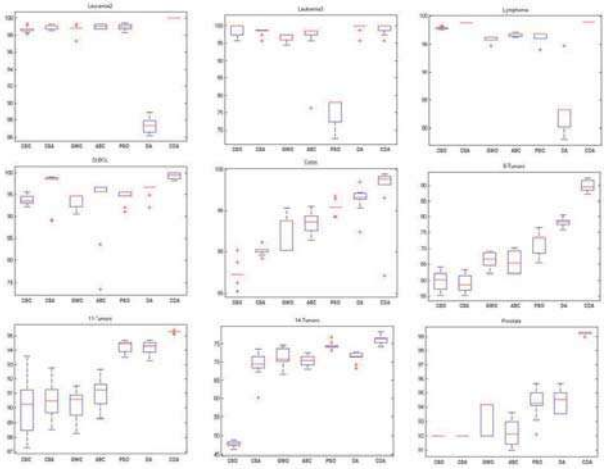

Fig. 2. Box plot presentation

V. Result analysis

The experiments are tested through implementing CSO, CSA, GWO, ABC, PSO, DA, and CDA using MATLAB.Due to the efficiency of SVM algorithm,we adopt SVM in CDA.For balanced data set, we often use the Acc as the criterion. But Acc is not efficient to represent the performance of the classifier for imbalanced problems.AUC is an indicator used to measure the classification performance in imbalanced data.F indicator is a comprehensive measure for balancing recall and precision.From the table 4 it is clear that for the

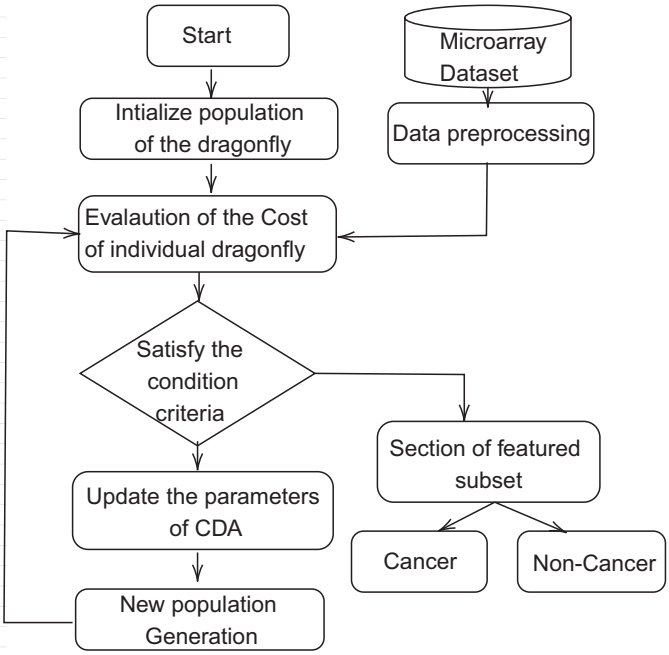

Fig. 3. Block Diagram of CDA-SVM

data set leukemia 1 and DLBCL the proposed methodology achieves 100% accuracy.In case of 11-tumor data set CDA-SVM algorithm performance is very close to the accuracy achieved by the DA.Where as in case of Lymphoma data set the CSA,CSO algorithm performs very close to the accuracy of CDA-SVM.In comparison to all data sets the proposed algorithm performs better.The performance evaluation is done using following equations (16)(17)(18).

$$ACC = \frac{True_{Pos} + True_{Neg}}{True_{Pos} + True_{Neg} + False_{Pos} + False_{Neg}} \quad (15)$$

$$Sensitivity = \frac{True_{Pos}}{True_{Pos} + False_{Neg}} \times 100 \quad (16)$$

$$Specificity = \frac{True_{Neg}}{True_{Pos} + False_{Neg}} \times 100 \quad (17)$$

Where,$True_{Pos}$ is the no's of true +ve , $False_{Neg}$ means the no's of -ve, $True_{Neg}$ represents the no's of true -ve, and $False_{Pos}$ is the no's of false +ve.AUC is the area under the ROC curve. The performance of different algorithm is compared and presented in fig-1. and fig 2 presents the performance using box-plot.

VI. Conclusion

According to the above observations, it can be concluded that the performance of CDA is superior to the other algorithms for feature selection.The main reason for the good performance of CDA is the integration of RUS,ROS,SMOTE and DA.On the one hand,IDA is able to enhance the exploitation and exploration capabilities.One the other hand,the proposed subset generation enriches population diversity and helps CDA jump out of local optimum.

REFERENCES

[1] B.Sahu,S. Mohanty, & S.Rout,A hybrid approach for breast cancer classification and diagnosis. EAI Endorsed Transactions on Scalable Information Systems,6(20),2019.

[2] B.Sahu,J. C. Badajena, A.Panigrahi,C.Rout,& S.Sethi,"7 An Intelligence-Based Health Biomarker Identification System Using Microarray Analysis."In Applied Intelligent Decision Making in Machine Learning pp. 137-161,CRC Press,2020.

[3] B.Sahu A combo feature selection method (filter+ wrapper) for micro array gene classification. International Journal of Pure and Applied Mathematics,118(16),389-401,2018

[4] B.Sahu,Multi-Tier Hybrid Feature Selection by Combining Filter and Wrapper for Subset Feature Selection in Cancer Classification. Indian Journal of Science and Technology, 12(3),1-11,2019.

[5] B.Sahu,A. Panigrahi, S.Mohanty,& S.S.Panigrahi,A hybrid Cancer Classification Based on SVM Optimized by PSO and Reverse Firefly Algorithm. International Journal of Control and Automation, 13(4), 506-517,2020

[6] W.Ke,C Wu,Y. Wu & N.N. Xiong,A new filter feature selection based on criteria fusion for gene microarray data.IEEE Access, 6, 61065-61076.2018.

[7] H.Houssein, Y.Mina, & E. H. Aboul,Nature-inspired algorithms: A comprehensive review. In Hybrid Computational Intelligence:Research and Applications(p. 1).CRC Press,2019.

[8] R. Z.Al-Abdallah,A. S. Jaradat, I.A.Doush,Y.A.Jaradat, Abinary classifier based on firefly algorithm,Jordanian Journal of Computers and Information Technology (JJCIT),496 3,2017.

[9] H.Chantar,M.Mafarja,H.Alsawalqah,A.A.Heidari,I.Aljarah,H.Faris,Feature selection using binary grey wolf optimizer with elite-based crossover for arabic text classification, Neural Computing and Applications (2019) 1–20.

[10] M.Taradeh,M.Mafarja,A.A.Heidari,H.Faris,I.Aljarah,S.Mirjalili,H.Fujita, An evolutionary gravitational search-based feature selection, Information Sciences,2019.

[11] M.Mafarja,A.Qasem,A.A. Heidari,I.Aljarah,H.Faris,S. Mirjalili,Efficient hybrid nature-inspired binary optimizers for feature selection, Cognitive Computation,578 1–26,2019

[12] S. Mirjalili, Dragonfly algorithm: Dragonfly algorithm: a new meta-heuristic optimization technique for solving single-objective, discrete, and multi-objective problems.Neural Computing and Applications, 27(4),1053-1073.2016.

[13] Y.Meraihi, A.Ramdane-Cherif, , D.Acheli, & M.Mahseur, Dragonfly algorithm: a comprehensive review and applications. NEURAL COMPUTING & APPLICATIONS,2020.

[14] R.KS,& S.Murugan, Memory based hybrid dragonfly algorithm for numerical optimization problems. Expert Systems with Applications,83, 63-78,2017.

[15] Y.hang, R.Zhu,Z.Chen, J.Gao,& D.Xia,Evaluating and selecting features via information theoretic lower bounds of feature inner correlations for high-dimensional data. European Journal of Operational Research,2020.

[16] O.A.Alomari,A.T.Khader, M A.Al-Betar,& Z.A.A.Alyasseri,A hybrid filter-wrapper gene selection method for cancer classification.In 2018 2nd International Conference on BioSignal Analysis, Processing and Systems (ICBAPS)(pp. 113-118).IEEE,July,2018.

[17] F.Fausto,A.Reyna-Orta,, E.Cuevas,Á.G.Andrade& M.Perez-Cisneros,From ants to whales: metaheuristics for all tastes. Artificial Intelligence Review,53(1), 753-810,2020.

[18] G.I.Sayed,A.Tharwat,& A. E.Hassanien, Chaotic dragonfly algorithm: an improved metaheuristic algorithm for feature selection. Applied Intelligence, 49(1),188-205, 2019.

[19] A.Tharwat,T.Gabel,& A. E.Hassanien, Parameter optimization of support vector machine using dragonfly algorithm. In International Conference on Advanced Intelligent Systems and Informatics (pp. 309-319).Springer, Cham,September 2017.

[20] M.Yasen,N.Al-Madi,&N. Obeid,Optimizing neural networks using dragonfly algorithm for medical prediction.In 2018 8th international conference on computer science and information technology (CSIT) (pp. 71-76).IEEE,July 2018.

[21] M.Duan,H.Yang, B.Yang,X.Wu,&H. Liang,Hybridizing dragonfly algorithm with differential evolution for global optimization. IEICE Transactions on Information and Systems,102(10),1891-1901,2019.

[22] B.Sahu,A.Panigrahi,& S. K.Rout,10 DCNN-SVM: A NEW APPROACH FOR LUNG CANCER DETECTION. Recent Advances in Computer Based Systems, Processes and Applications: Proceedings of Recent Advances in Computer based Systems, Processes and Applications (NCRACSPA-2019),October21-22,2019, 97,2020.

[23] B.Sahu,A.Panigrahi,S.Pani,S.Swagatika,D.Singh& S.Kumar, A Crow Particle Swarm Optimization Algorithm with Deep Neural Network (CPSO-DNN) for High Dimensional Data Analysis. In 2020 International Conference on Communication and Signal Processing (ICCSP) (pp. 0357-0362). IEEE,2020, July.

[24] B.Sahu,A.Panigrahi, S.Sukla,& B.B.Biswal,MRMR-BAT-HS:A Clinical Decision Support System for Cancer Diagnosis.Leukemia,7129(73), 48.

[25] B.Sahu,S.N.Mohanty. CMBA-SVM: a clinical approach for Parkinson disease diagnosis. International Journal of Information Technology,1-9,2021.

[26] B.Sahu,M.Gouse,C. R.Pattnaik,& S.N.Mohanty,MMFA-SVM: New biomarker gene discovery algorithms for cancer gene expression. Materials Today: Proceedings,2021.

[27] B.Sahu,S.Dash, S.N. Mohanty,& S.K. Rout,Ensemble comparative study for diagnosis of breast cancer datasets. International Journal of Engineering Technology, 7(4.15),281-285,2018

Recent Advances in Computer based Systems, Processes And Applications

10 DCNN-SVM: A NEW APPROACH FOR LUNG CANCER DETECTION

Bibhuprasad Sahu[1], Amrutanshu Panigrahi[2], Dr. Saroj Kumar Rout[3]

[1]*Department of Computer Science and Engineering, Gandhi Institute For Technology, Gramadhia, Bhubaneswar, India*

[2]*Department of Computer Science and Engineering, Gandhi Institute for Technology, Gramadhia, Bhubaneswar, India*

[3]*Department of Computer Science and Engineering, Gandhi Institute for Technology, Gramadhia, Bhubaneswar, India*

ABSTRACT: In the present scenario lung cancer is considered as a common disease which improves the death ratio. So detection of cause of the cancer in early stage may improve the survival chances of patients by identify the level and position (or) status of the tumor. Computed technology (CT) scan is considered as a new tool for classification of lung cancer implementing deep convolutional neural network (DCNN) with support vector machine (SVM). To indentify lung nodules which are cancerous and non cancerous in nature, extraction of deep features plays a vital role similarly reduction of dimensionality is important. Here we have used linear discriminate analysis (LDR). CT images are considered as an input to DCNN then it is classify by support vector machine classifier to achieve better accuracy. Comparative result shows the DCNN-SVM approach provides a sensitivity, specificity and accuracy of 97.27%, 93.66% and 98.67% respectively.

Keywords: Lung cancer, Support vector machine, Linear discriminate analysis, Neural network.

I. INTRODUCTION

Especially in noninvasive treatment and clinical assessment, medical image investigation has played matchless quality in the field of health division [1]. For easy and accurate diagnosis of disease doctors normally takes the help of different methods such as X-rays, CT images and MRI images [2]. Lung cancer is one of the main sources of death. It causes 61 million deaths per year. Lancet report claims the death ratio increases by 112% during the year (1990-2016). Discovery of lung cancer isn't a simple task because 80% of the patient is truly diagnosed at impelled stage [3]. Globally lung cancer position is seventh and tenth in case of male and females respectively. It seems to be the third most dangerous disease after breast cancer seems to be with females in India [4-5]. In image processing feature selection and dimension reduction used for proper identification of disease [6-7]. The extraction of relevant information is provided to support vector machines

for training and testing. In the article neural network modules with binarization of image preprocessing are used for image classification. Technology like SVM, KNN, and ANN are expansive and survival rate of patient is very low as it detects at only advanced stage [0-10].

The manuscript introduces an innovative CAD scheme for classification of benign and malignant characteristics from CT images using deep learning-based SVM. Here the DCNN has been introduced as a feature selection tool and is linked SVM to achieve better outcomes in the classification. Proposed method outperformed better and improvement is quite good. Section 2 of the remainder of the document includes literature study and discussion of various classifiers in section 3.Section 4 addressed the proposed methodology and section 5 included the work execution followed by conclusion of future work.

II. LITERATURE REVIEW

For the classification of breast cancer, Hiba chougard et al. presented a CAD model based on CNN. To prepare deep learning needs expansive datasets while a limited quantity of medical image information used in the transfer leaning method. CNN delivers 98.94 percent accuracy with highest results. Heba Mohsen et al. [12] has implemented DNN classifier for brain tumor classification by combining wavelet transformation and principal component analysis (PCA).An algorithm for lung nodule classification that circuits full-ISD (Texture, shape and deep model-learned data) at the level of choice. GLCM based description is used in this algorithm [13]. Sharkes, AI-Sharkavy & Ragab (2011) implemented discrete wavelet transformation (DWT) with PCA for the extraction of features. This approach enables the system to detect and classify cancer and non-cancer disease. The accuracy achieved was almost 98% [14]. Siziki et al. (2016) implemented a deep convolutional neural network (DCNN) for cancer / non-cancer mass detection. The sensitivity accuracy achieved by the above approach was 89.9% [15].Wichakam el al (2016) used the DCNN-SVM with a sensitivity accuracy of 98.44% in the prostate dataset [16]. Levy used Alexnet to identify benign and malignant masses in the DCNN dataset.

III. PRESENT CLASSIFICATION ISSUES

A neural network contains many hidden layers with having capability of modeling complex structures. As the neural network black box and also having restriction towards the ability to identify the conceivable causal relationship [18, 19].Present techniques, after the CT image are captured and segmentation applied then it is provided as input to the SVM classifier and accuracy determined.

IV. PROPOSED ARCHITECTURE OF CDNN_SVM METHODOLOGY

The suggested CAD comprises of the following steps:

(1) Enhancement of the Image (2) Feature Extraction (3) Feature Reduction (4) Classification Feature (CDNN-SVM). The CAD scheme suggested is introduced in flow of the DCNN_SVM system is represented in Figure 1.

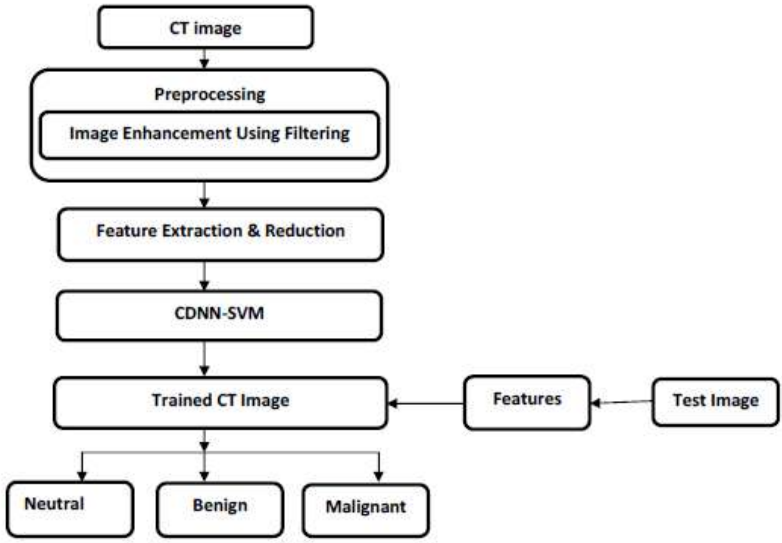

Figure 1. Flow of the DCNN-SVM system

A. Image Enhancement Phase

Some kind of noise has affected the medical database. If the image is noisy and the value of the target pixels with adjacent pixels differs between 0 and 255, then the pixel will be replaced with regard to the achieved middle value. We have considered adaptive histogram equalization for image enhancement.

B. Feature extraction and Reduction Phase

Using the extraction techniques of features, an image can be represented from the matrix-vector as compact and unique. Before classification, we conduct extraction of features to provide or determine a reduction in dimensions that will provide greater accuracy during classification. Extraction of the feature achieves the positive features of the CT images. In this study different feature techniques like histogram features, texture features and wavelet features are used for extraction of important features.

After evaluating the geometrical features for individual nodules or CT images, the featured vales are input to linear Discriminate Analysis (LDA) classifier. To differentiate between nodule and the normal anatomy structures features are

merged with LDA. Minimizing the first informational index by calculating specific important characteristics influences the difference between two data designs. Using LDA dimension reduction of features vector can perform without any data loss. The following graph represents the feature reduction time of LDA is better than other reduction methods like PCA/ICA.

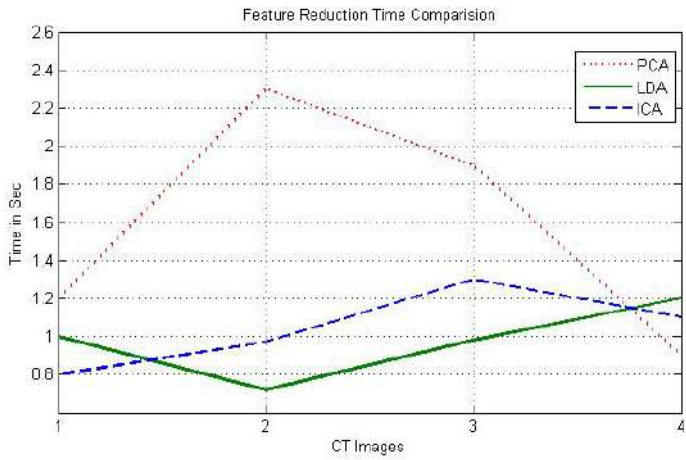

Figure 2. Feature reduction time comparisons (PCA/LDA/ICA)

C. Feature classification using CDNN-SVM

The Deep learning structure normally extends the usual neural network by incorporating higher number of hidden layers in between the input and output layer to represent the unpredictable and nonlinear type of connections. After completion of the feature selection, the combinatory step on resulting component vector is conducted with CDNN. CDNN operates with two deep methods like Deep Belief Network and Boltzmann Machine. The gravitational search algorithm is introduced to enhance the classification efficiency of the said model. The flow of deep learning model is mentioned in the Fig3.

Support Vector Machine (SVM) is used in this study as it produces high rate for classification in the lung cancer diagnosis. SVM is a kind of ML algorithm that analyzes the data which can be further used for classification. It is also a well-known supervised method which sorts data based on categories. The goal of SVM is to separate hyper planes in a high-dimensional feature space to demonstrate a computationally effective method. There are multiple hyper-planes available in capable of classifying two data sets. The one with the maximum margin is the optimum hyper-plane to be selected. The margin is represented as the width by which, before hitting a data point, the boundary could increase. Support vectors are the information points pushed up by the margin. Therefore, the objective of the SVM is to locate the optimal hyper plane that distinguishes clusters of target vectors on the opposing sides of the plane [14-17].

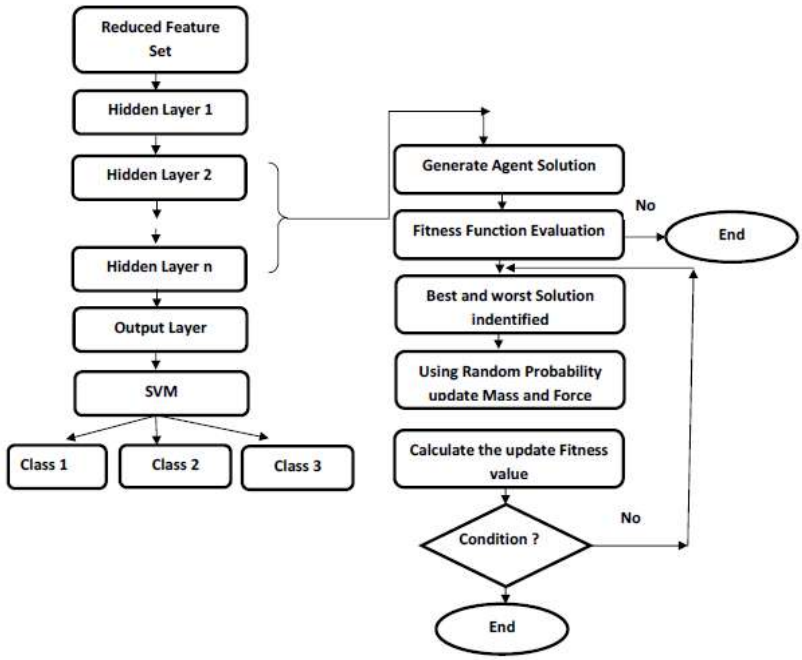

Figure 3. Block diagram of DPNN-SVM

V. SIMULATION AND RESULTS DISCUSSION

In this work, we have considered a database consists of 50 lung cancer Ct images for cancer detection purposes. The thickness of the CT image is 1.25mm attained by a single breath. The location of the nodules is acknowledged by the radiologist and dataset also provided. Ct Images are taken from UCI repository. Testing CT images are shown the below Figure 4.

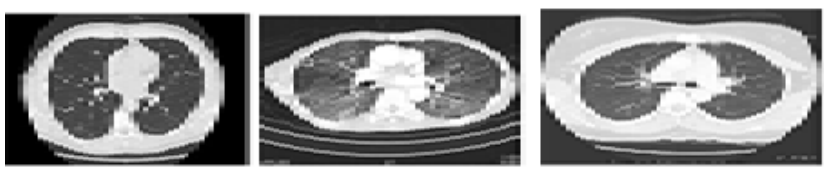

Figure 4. Sample images for experiment

A. Performance evaluation

The classification model's performance can be evaluated using performance matrices in the proposed work. There are several evaluation techniques, including the Confusion Matrix (CM), the receiver-operating curve (ROC), the region under the ROC curve (AUC), the accuracy, and the F1 score, to evaluate a classifier.

The CM is a particular table that presents the output of the classifier. The CM is usually referred to the error matrix in machine learning area. An image region, depending on the type of data, is said to be positive or negative. In addition, a decision can be either correct (real) or incorrect (false) for the detected outcome. Therefore, one of four possible categories will be the classification: True Positive (TP), True Negative (TN), False Positive (FP), and False-Negative (FN).

1. Accuracy

Accuracy is defined as the measure of the classifier's correct prediction. It provides the enormous classifier's performance ability.

$$\text{Accuracy} = \frac{\text{TP} + \text{TN}}{\text{TN} + \text{FP} + \text{FN} + \text{TP}} \tag{1}$$

2. Receiver operating characteristic (ROC)

The ROC analysis is a well-defined evaluation criteria which is being used for detecting the tasks. Initially the ROC was there for medical decision making but gradually it was also used in medical imaging. The ROC curve contains the operating points which represent the plot of True Positive Rate (TPR) as a function of False Positive Rate (FPR). The TPR and FPR are defined as sensitivity and specificity respectively. They can be evaluated by using Eqs. (3) and (4).

$$\text{Sensitivity} = \frac{\text{TP}}{\text{TP} + \text{FN}} \tag{2}$$

$$\text{Specificity} = \frac{\text{TN}}{\text{TN} + \text{FP}} \tag{3}$$

3. Area under the ROC curve (AUC)

This parameter is being used in the medical diagnostic system, which provides a model by considering the average of the points on the curve for evaluation of the model. The score of AUC should lay between 0 and 1 for the classifier performance, the model having higher score provides more adequate classifier performance.

4. Precision

Precision is defined as the proportion of the total predicted positive observations properly predicted. High precision pertains to low FPR. The following equation calculates the precision,

$$\text{Pr ecision} = \frac{\text{TP}}{\text{TP} + \text{FP}} \tag{4}$$

5. F1 score

This parameter is the precision and recall weighted average. It is used to evaluate the classifier's performance as a statistical measure. This score therefore takes into consideration both false positives and negatives. This can be formulated as,

$$\text{F1score} = \frac{2 \times \text{Re call} \times \text{Pr ecision}}{\text{Re call} + \text{Pr ecision}} \tag{5}$$

VI. EXPERIMENTAL SETUP

The suggested SVM classifier based on DCNN was implemented to mammographic images which offered the chance of each image being either benign or malignant in one of the two classes. The most commonly used lung cancer has been chosen in this task to demonstrate the techniques recommended using R. 70 images are considered for training for the lung image analysis and another 30 images are used for testing.

Table I. DCNN-SVM image classification

Phase	*Objective images*	*DCNN-SVM*			
		Normal	Cancerous	Non cancerous	Total Count
Training image	Normal	22	1	4	27
	cancerous	2	18	2	22
	Non cancerous	0	20	1	21
	Total Count	25	20	7	52
Test images	Normal	6	0	2	8
	cancerous	2	8	1	11
	Non cancerous	1	10	0	11
	Total Count	7	20	3	30

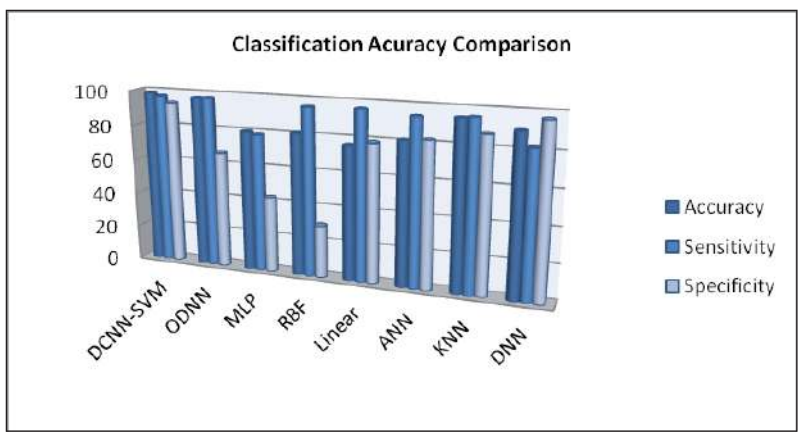

Figure 5. Comparative analysis of different classifiers

Table II. Classification comparision

	DCNN-SVM	*ODNN*	*MLP*	*RBF*	*Linear*	*ANN*	*KNN*	*DNN*
Accuracy	98.67	97.16	80.03	81.19	76.34	81.29	94.78	90.11
Sensitivity	97.26	97.41	78.66	95.89	96.34	94.22	95.53	82.18
Specificity	93.66	66.59	43.11	29.79	78.64	82.29	87.34	96.39

VII. CONCLUSION

Compared to other classification methods, the suggested CDNN-SVM with feature section LDA offers excellent classification for Lung CT images. The primary objective of this study is to identify the mass and classify the genes that are benign and malignant. The developed CAD approach reduces the labeling time without any interventions of human error. Many researchers developed different CAD approaches to achieve good better accuracy and precision to detect normal and abnormal CT lung image. The experimental outcome explains the classification performance in term of sensitivity, accuracy, specificity and its value are 97.26, 98.27 and 93.66 respectively. These outcomes suggested that the proposed CAD method is efficient to indentify the cancerous parts of a CT images. In future work we will prefer to work with high dosage CT lung cancer data for high accuracy output to classify the benign and malignant genes.

REFERENCE

1. Rattan, S., Kaur, S., Kansal, N., & Kaur, J. (2017, December). An optimized lung cancer classification system for computed tomography images. In 2017 Fourth International Conference on Image Information Processing (ICIIP) (pp. 1-6). IEEE.
2. Naresh, Prashant, and Rajashree Shettar. “Image processing and classification techniques for early detection of lung cancer for preventive health care: A survey.” International Journal on Recent Trends in Engineering & Technology 11.1 (2014): 595.
3. Li, Juntao, et al. “Adaptive multinomial regression with overlapping groups for multi-class classification of lung cancer.” Computers in biology and medicine 100 (2018): 1-9.
4. Sharma, Disha, and Gagandeep Jindal. “Computer aided diagnosis system for detection of lungcancer in CT scan images.” International Journal of Computer and Electrical Engineering 3.5 (2011): 714.
5. Bhatnagar, Divyesh, et al. “Classification of normal and abnormal images of lung cancer.” Materials Science and Engineering Conference Series. Vol. 263. No. 4. 2017.
6. Sui, Xizhao, et al. “Validation of the stage groupings in the eighth edition of the TNM classification for lung cancer.” Journal of Thoracic Oncology 12.11 (2017): 1679-1686.
7. El-Sherbiny, Bassma, et al. “Blb (brain/lung cancer detection and segmentation and breast dense calculation).” 2018 First International Workshop on Deep and Representation Learning (IWDRL). IEEE, 2018.

8. Xie, Yutong, et al. “Fusing texture, shape and deep model-learned information at decision level for automated classification of lung nodules on chest CT.” Information Fusion 42 (2018): 102-110.
9. Sharma, Disha, and Gagandeep Jindal. “Computer aided diagnosis system for detection of lungcancer in CT scan images.” International Journal of Computer and Electrical Engineering 3.5 (2011): 714.
10. Shankar, K., et al. “Optimal feature-based multi-kernel SVM approach for thyroid disease classification.” The Journal of Supercomputing (2018): 1-16.
11. Sahu, Bibhuprasad. “A combo feature selection method (filter+ wrapper) for microarray gene classification.” International Journal of Pure and Applied Mathematics 118.16 (2018): 389-401.
12. Mohsen, Heba, et al. “Classification using deep learning neural networks for brain tumors.” Future Computing and Informatics Journal 3.1 (2018): 68-71.
13. Xie, Yutong, et al. “Fusing texture, shape and deep model-learned information at decision level for automated classification of lung nodules on chest CT.” Information Fusion 42 (2018): 102-110.
14. Sahu, Bibhuprasad. “Multi-Tier Hybrid Feature Selection by Combining Filter and Wrapper for Subset Feature Selection in Cancer Classification.” *Indian Journal of Science and Technology* [Online], 12.3 (2019): n. pag. Web. 24 Sep. 2019
15. Sahu, B., Mohanty, S. N., & Rout, S. K. (2019). A Hybrid Approach for Breast Cancer Classification and Diagnosis. EAI Endorsed Trans. Scalable Information Systems, 6(20), e2.
16. Sahu, Bibhuprasad, Sujata Dash, Sachi Nandan Mohanty, & Saroj Kumar Rout. “Ensemble Comparative Study for Diagnosis of Breast Cancer Datasets.” *International Journal of Engineering & Technology* [Online], 7.4.15 (2018): 281-285. Web. 24 Sep. 2019.
17. Sahu, Bibhuprasad. “Multi filter ensemble method for cancer prognosis and Diagnosis.” International Journal of Engineering Applied Sciences and Technology [Online], 4.2 (2019): n. pag(105-109). Web. June. 2019

Hetero Leach: Leach Protocol with Heterogeneous Energy Constraint

Amrutanshu Panigrahi, Bibhuprasad Sahu, and Sushree Bibhuprada B. Priyadarshini

Abstract Wireless Sensor Networks (WSNs) are used for checking and information gathering from the physical world in various applications, for instance, condition watching, developing the board, following animals or items, social protection, transportation, and general home frameworks. Nowadays, WSNs are pulling in unfathomable thought in research. The objective of this research is to focus on clustering based routing approach in WSN. We have explained different existing clustering based routing algorithms for WSN. Initially, we have implemented one well-known algorithm LEACH with 100 no of node in a 500 × 500 flat grid. Also, we have introduced one new algorithm called HETERO LEACH which removes the disadvantages of LEACH protocol. The leach protocol works in homogeneous energy constraint, while the HETERO LEACH can work with heterogeneous energy constraints. On the other hand, all these routing protocols have been implemented and simulated using MATLAB. Subsequently, these protocols have been simulated with different parameters such as Number of packets to CH, No of Alive Nodes, and Dead Node to prove their functionality and to find out their behavior in different sorts of sensor networks. The result shows the comparison of these two protocols and the best protocol by taking the energy constraint into consideration. And finally, we have shown that the hetero leach works much better than as compared to the leach protocol.

Keywords Leach · Apteen · WSN · CH · Hetero Leach

A. Panigrahi (✉) · B. Sahu
Department of CSE, Gandhi Institute for Technology, Bhubaneswar, Odisha, India
e-mail: amrutansup@gmail.com

S. B. B. Priyadarshini
Department of Computer Science & Information Technology, Siksha 'O' Anusandhan, Deemed to Be University, Bhubaneswar, Odisha, India

D. Mishra et al. (eds.), *Intelligent and Cloud Computing*,
Smart Innovation, Systems and Technologies 194,
https://doi.org/10.1007/978-981-15-5971-6_3

1 Introduction

Wireless Sensor Network or WSN [1], are generally used for checking and for also information gathering from the physical world in various applications, for instance, condition watching, developing the board, following animals or items, social protection, transportation, and general home frameworks. WSN [2], involves an ordinarily enormous number of sensor center points, in like manner called bits. These bits are accumulated to form the data which will be transmitted towards different network elements called nodes. Sink focus focuses gather and procedure the got information so as to make it open to the client. Notwithstanding the path that in a little WSN one-jump correspondence to the sink can be executed, when all is said and done, a multi-ricochet diagram must be considered [3]. For this situation, conventional bits are responsible for executing a planning custom so as to move the data towards the sink. Since bits ought to control in doubt work unattended for quite a while, they have uncommon essentialness obstacles [4, 5]. This significantly impacts the structure of a WSN and unequivocally on the planning custom. Since correspondence is an expensive asset to the degree essentialness use, an animal control message sending section (i.e., flooding) is the time when all is said and done senseless. Or then again perhaps, the course of action of the planning custom [6], is a central edge that ought to consider tradeoffs between transmission power and sending techniques so as to give relentless quality and nature of association. Moreover, since a piece should crash in perspective on battery weariness or unmistakable reasons, a fit controlling convention to be enough adaptable to respond to a misstep by reconfiguring the edge work [7, 8].

As progression makes, WSN is snatching open passages for application in flexible affiliations [9]. There are two unmistakable ways to deal with show flexibility in a Mobile WSN environment. Subsequent techniques are there to keep up static sinks, while sensor focuses are versatile, for instance, when added to creatures in the following applications [10, 11]. For this condition, a static sink can be utilized to amass following data set away in the sensor focus focuses when the creatures are in its range. At last, the two systems can be joined, giving every single focus point get to the WSN be adaptable [12]. For instance, in a private situation for created individuals or for individuals with insufficiencies, sensors added to them can offer data to the cell phones of the accomplice work compel [13]. Despite the extra intricacy of planning customs for MWSN, pass on capacity brings the chance of diminishing the measure of jumps to the sink focus point. As exhibited by [14–16], the likelihood of having something near a sensor focus point in the degree of sink increments with the correspondence extend, the speed of the middle point, and the measure of sinks, accomplishing a reduction of the dormancy. Regardless, high portability conditions could avoid different transmissions to sufficiently pass on messages [17, 18].

2 Routing Algorithm

2.1 LEACH

In [19], the author had presented Low Energy Adaptive Clustering Hierarchy, a progressive routing calculation for sensor systems, called Low Energy Adaptive Clustering Hierarchy (LEACH). LEACH organizes the hubs in the system into little bunches and picks one of them for cluster head. At that point, the group head totals and packs the data got from every one of the hubs and sends it to the corresponding base station. The hubs picked as the group head channel out more vitality when contrasted with different hubs as it is required to send information to the base station which might be far found. Henceforth, filter utilizes irregular turn of the hubs required to be the bunch heads to equitably convey vitality utilization in the system. After various reenactments, it was discovered that just 5% of the absolute number of hubs needs to go about as the bunch heads [10]. The TDMA/CDMA is being utilized to diminish between the group and intra-bunch impacts. This convention is utilized where a consistent observation by the sensor hubs are there as the primary objective, because the information accumulation is concentrated at the BS and is being performed occasionally.

- **Operations**

LEACH operations are conducted in two phases:

1. Setup phase
2. Steady phase

In the initial stage, the clusters are formed with the corresponding cluster heads. Mean while in the second phase the data is sensed and sent back to the different base station. The steady phase takes much longer time as compared to the setup phase, as in this phase all information is gathered and distributed to the different base station.

(a) **Setup phase**: In the setup stage, a foreordained portion of hubs, p, pick themselves as group heads. It is finished by a limit denoted as T(n). The limit esteem relies on the ideal rate to turn into a bunch head-p, the current round r, and the arrangement of hubs that have not turned into the group head in the last 1/p rounds. The formulae are as follows:

$$T(n) = \frac{p}{1 - p \times \left(r \times \operatorname{mod} \frac{1}{p}\right)} \forall n \in G \tag{1}$$

Here p no of nodes sends the advertisement message to different nodes to participate in their group. The nodes receiving the message has to send an acknowledgment message to raise their flags. The node which sends the advertisement message will be elected as the CH. Similarly, different node has to participate in different clusters. In the wake of getting the affirmation message, contingent on the quantity of hubs under

their group and the kind of data required by the framework (in which the WSN is setup), the bunch heads make a TDMA plan and allots every hub a schedule vacancy, in which it can transmit the detected information. The TDMA plan is communicated to all the bunch individuals. In the event that the extent of any bunch turns out to be excessively vast, the group head may pick another bunch head for its bunch. The bunch head picked for the current round can't again turn into the group head until the various hubs in the system haven't turned into the bunch head.

(b) **Steady stage**: In this stage, the available information will be sensed from different channels and sends them to individual cluster heads by using the TDMA technique. The data will be received by the cluster head in packet format. After receiving all packets, the cluster head combines it and sends it back to the intendant recipients. The nodes present in the cluster will receive the message by implementing the CDMA technique.

2.2 Hetero Leach

In HETERO LEACH, once the cluster heads are taken then in each defined time period the CH first communicates by considering the following parameters:

Thresholds: It includes two parameters called a hard farthest point (HL) and a fragile cutoff (DL). HL is a particular estimation of a quality past in which a center point can be enacted to transmit data. DL is a little change in the estimation of a quality which can trigger a center point to transmit data again.

Schedule: It utilizes the TDMA technique for scheduling the message to different cluster-based nodes.

TC: It is commonly known as counter time which is the extreme time span between two consecutive communications. In a sensor compose, close to centers fall in a comparable gathering, sense tantamount information, and try to send their data at the same time, causing possible accidents. We present a TDMA schedule with the ultimate objective that each center point in the pack is doled out a transmission opening, as showed up in Fig. 1.

Important Features

The primary highlights of these algorithms are:

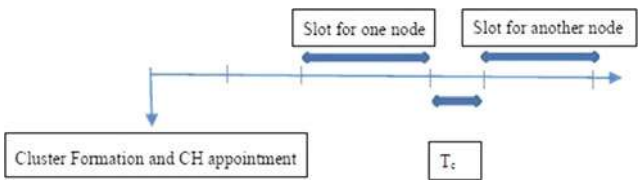

Fig. 1 Timeline for HETERO LEACH

1. By sending intermittent information, it gives the client a total image of the system. It additionally reacts right away group change time bunch development edge schedule opening for a hub I TDMA schedule and parameters to extraordinary changes, accordingly making it receptive to time basic circumstances. Hence, it consolidates both proactive and receptive approaches.
2. It offers adaptability of enabling the client to set the time interim (TC) and the limit esteems for the properties.
3. Vitality utilization can be constrained by the tally time and the edge esteems. The half breed system can imitate a proactive system or on the other hand a responsive system, by appropriately setting the check time also, the limit esteems.

3 Simulation and Result

For LEACH and HETERO LEACH WSN routing protocol, we have used Matlab Simulator A simulation environment having 50nodes,100 nodes in 500 × 300 flat grid has been created with random position. The performance of each protocol has been analyzed by considering some influencing parameters like Cluster Head, Alive Nodes, Dead Nodes, Number of Base Stations. The performance details are as follows:

CH

In a hierarchical protocol in which the maximum number of nodes transmit to cluster heads, and then it aggregates and compresses the data and forwards it to the related base station (sink). As heavy amounts of data need to be transmitted during the communication and Cluster Head is wholly responsible for delivering the packets to the intended destination. Random distribution of cluster heads in Leach makes the Network overloaded.

Alive Nodes

This value indicates the number of active nodes participating in the communication which defines the lifetime of the network. LEACH is a proactive routing protocol, hence the number of alive nodes is higher as compared to the HETERO LEACH protocol.

Dead Node

Dead node is nothing but the routing holes present in the communication path. Routing hole means the node which takes part in the communication path goes dead during the communication of the packet (Figs. 2, 3, 4, and 5).

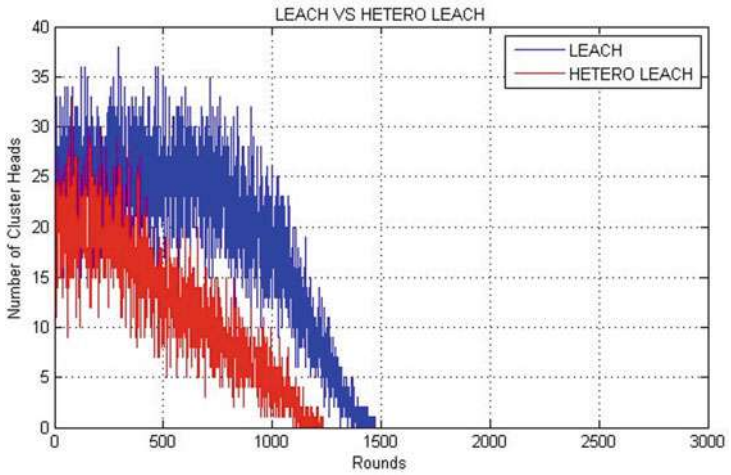

Fig. 2 Number of CH LEACH versus HETERO LEACH

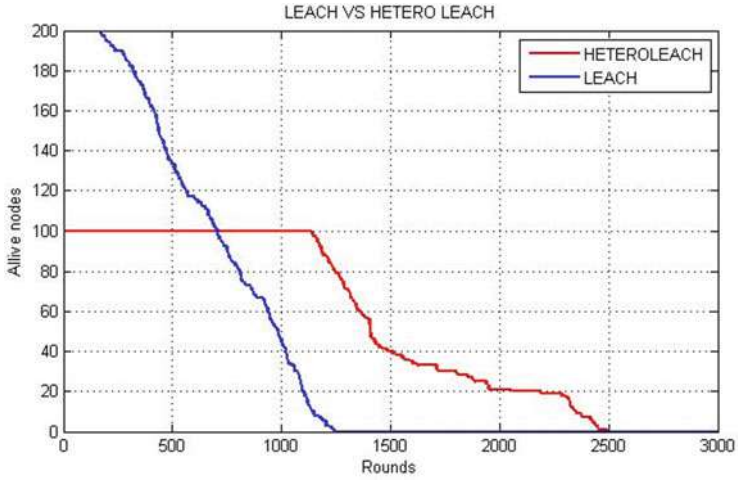

Fig. 3 Number of alive node LEACH versus HETERO LEACH

4 Conclusion

Based on the parameters, the HETERO LEACH performs better because it deals with the hybrid network with heterogeneous energy level. LEACH protocol is a proactive routing protocol, therefore, the number of nodes associated with the communication will be higher. And due to these characteristics, the number of dead nodes for LEACH protocol is also high because the probability of the node for becoming dead increases as well with the increase in the number of rounds (Table 1).

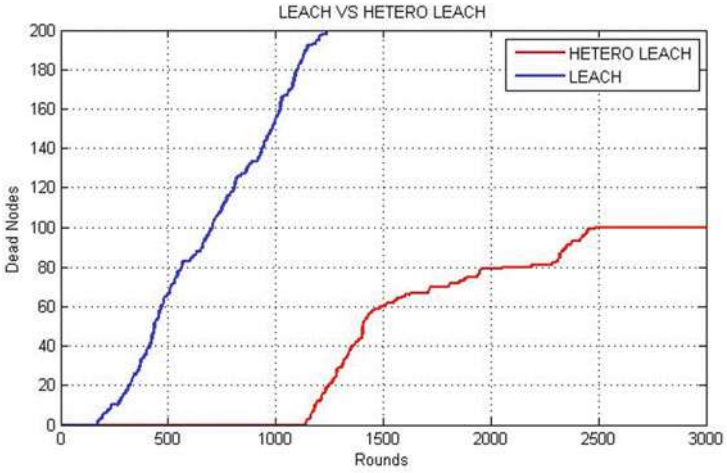

Fig. 4 Number of dead node LEACH versus HETERO LEACH

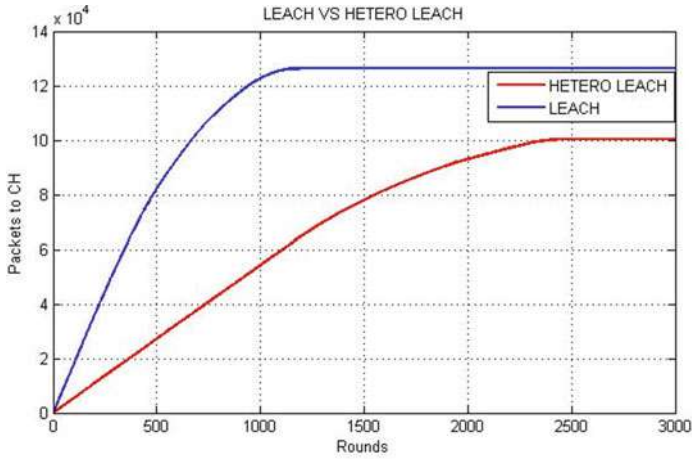

Fig. 5 Number of packets to CH LEACH versus HETERO LEACH

Table 1 Comparison of LEACH versus HETERO LEACH

Characteristic	HETERO LEACH	LEACH
Network type	Hybrid network	Proactive network
No of dead node	High	Moderate
No of alive node	High	Moderate
No of packets to BS	High	Moderate
No of packets to CH	Moderate	High
No of CH	High	Moderate
Energy efficiency	High	High

References

1. Akyildiz, I.F., Su, W., Sankarasubramaniam, Y., Cayirci, E.: A survey on sensor networks. IEEE Commun. Mag. **40**(8), 102–114 (2002)
2. Ogundile, O., Alfa, A.: A survey on an energy-efficient and energy-balanced routing protocol for wireless sensor networks. Sensors **17**(5), 1084 (2017)
3. Calzado, C.G.: Contributions on agreement in dynamic distributed systems (Doctoral dissertation, Universidad del País Vasco-Euskal Herriko Unibertsitatea) (2015)
4. Munir, S.A., Ren, B., Jiao, W., Wang, B., Xie, D., Ma, J.: Mobile wireless sensor network: architecture and enabling technologies for ubiquitous computing. In: 21st International Conference on Advanced Information Networking and Applications Workshops (AINAW'07), vol. 2, pp. 113–120. IEEE (2007)
5. Burgos, U., Gómez-Calzado, C., Lafuente, A.: Leader-based routing in mobile wireless sensor networks. In: Ubiquitous Computing and Ambient Intelligence, pp. 218–229. Springer, Cham (2016)
6. Al-Karaki, J.N., Kamal, A.E.: Routing techniques in wireless sensor networks: a survey. IEEE Wirel. Commun. **11**(6), 6–28 (2004)
7. Choi, J.Y., Yim, S.J., Huh, Y.J., Choi, Y.H.: A distributed adaptive scheme for detecting faults in wireless sensor networks. WSEAS Trans. Commun **8**(2), 269–278 (2009)
8. Behera, A., Panigrahi, A.: Determining the network throughput and flow rate using GSR and AAL2R (2015). arXiv:1508.01621
9. Burgos, U., Soraluze, I., Lafuente, A.: Evaluation of a fault-tolerant wsn routing algorithm based on link quality. In: Proceedings of the 4th International Conference on Sensor Networks, pp. 97–102 (2015)
10. Crowcroft, J., Segal, M., Levin, L.: Improved structures for data collection in wireless sensor networks. In: IEEE INFOCOM 2014-IEEE Conference on Computer Communications, pp. 1375–1383. IEEE (2014)
11. Akkari, W., Bouhdid, B., Belghith, A.: Leach: low energy adaptive tier clustering hierarchy. Procedia Comput Sci **52**, 365–372 (2015)
12. Gómez-Calzado, C., Casteigts, A., Lafuente, A., Larrea, M.: A connectivity model for agreement in dynamic systems. In: European Conference on Parallel Processing, pp. 333–345. Springer, Berlin (2015)
13. Liang, Y., Yu, H.: Energy adaptive cluster-head selection for wireless sensor networks. In: Sixth International Conference on Parallel and Distributed Computting Applications and Technologies (PDCAT'05), pp. 634–638. IEEE (2005)
14. Manjeshwar, A., Agrawal, D.P.: APTEEN: a routing protocol for enhanced efficiency in wireless sensor networks. In: Null, p. 30189a. IEEE (2001)
15. Kafi, M.A., Challal, Y., Djenouri, D., Doudou, M., Bouabdallah, A., Badache, N.: A study of wireless sensor networks for urban traffic monitoring: applications and architectures. Procedia Comput. Sci. **19**, 617–626 (2013)
16. Ko, J., Lu, C., Srivastava, M.B., Stankovic, J.A., Terzis, A., Welsh, M.: Wireless sensor networks for healthcare. Proc. IEEE **98**(11), 1947–1960 (2010)
17. Wieselthier, J.E., Nguyen, G.D., Ephremides, A.: Algorithms for energy-efficient multicasting in static Ad Hoc wireless Networks, pp. 251–263 (2001)
18. Broch, J., Maltz, D.A., Johnson, D.B., Hu, Y.C., Jetcheva, J.G.: A performance comparison of multi-hop wireless ad hoc network routing protocols. In: MobiCom, vol. 98, pp. 85–97 (1998)
19. Heinzelman, W.R., Chandrakasan, A., Balakrishnan, H.: Energy-efficient communication protocol for wireless microsensor networks. In: Proceedings of the 33rd Annual Hawaii International Conference on System Sciences, p. 10. IEEE (2000)
20. Gómez-Calzado, C., Lafuente, A., Larrea, M., Raynal, M.: Fault-tolerant leader election in mobile dynamic distributed systems. In: 2013 IEEE 19th Pacific Rim International Symposium on Dependable Computing, pp. 78–87. IEEE (2013)

21. Anitha, R.U., Kamalakkannan, P.: Enhanced cluster based routing protocol for mobile nodes in wireless sensor network. In: 2013 International Conference on Pattern Recognition, Informatics and Mobile Engineering, pp. 187–193. IEEE (2013)

M-Throttled: Dynamic Load Balancing Algorithm for Cloud Computing

Amrutanshu Panigrahi, Bibhuprasad Sahu, Saroj Kumar Rout, and Amiya Kumar Rath

Abstract Cloud computing environment can also be called as Internet-based computing process in which there is no limitation of work. There are multiple numbers of data center (DC) available for solving multiple user requests coming from a different user base (UB). The data center is capable of negotiating multiple instructions simultaneously. But the instructions are submitted to the DC randomly. Thus, there is chance of overload for a particular DC. Hence, the load balancing plays a vital role in cloud computing to maintain the performance of the computing environment. In this research article, we have implemented throttled, round-robin, and the shortest job first loadbalancing algorithm. Also, we have proposed one more algorithm called M-throttled which has the high performance compared to others. We have taken different parameters such as overall response time and DC processing time for comparison. These are simulated by taking closest data center policy in CloudSim environment.

Keywords Data center · User base · Throttled · Round-robin · M-throttled · CloudSim

1 Introduction

Cloud computing is a dynamic system in which shared resources, data, and programs are given by the customer's prerequisite at the explicit time. It is a term which is commonly utilized if there should arise an occurrence of web. Load adjusting in distributed computing structures is very a test now. Persistently, a passed on procedure is required, since it isn't in every case basically plausible to keep up at least one inactive system which is similar to the active one to satisfy the required requests. In cloud

A. Panigrahi (✉) · B. Sahu · S. K. Rout
Department of CSE, Gandhi Institute for Technology, Bhubaneswar, Odisha, India
e-mail: amrutansup89@gmail.com

A. K. Rath
Department of CSE, VSSUT, Deputed to NAAC, Burla, Bangalore, Odisha, India

D. Mishra et al. (eds.), *Intelligent and Cloud Computing*,
Smart Innovation, Systems and Technologies 194,
https://doi.org/10.1007/978-981-15-5971-6_1

computing, the cloud can be observed as the cloud which provides the availability of resources on the Internet for different users. The end users use these resources as per the requirement. Simultaneously multiple users utilize these resources simultaneously. Cloud computing provides various services such as IaaS, SaaS, and PaaS to handle different kinds of requests coming from the end users [1]. The request coming from the end users are not homogeneous and are submitted to different data centers for execution randomly. Hence, it is very difficult to handle the heterogeneous requests by an overloaded data center. Hence, load balancing is becoming the most challenging factor in the field of cloud computing. So it is required to disseminate the stack evenly at each data center to realize an efficient client fulfillment and proper resource usage proportion. The main objectives of this mechanism are as follows [2, 3]:

- To make all the DCs equally loaded.
- To keep the performance constant.
- To maintain the execution speed in heavy traffic.

It is the method for redistributing the hard and fast burden to every processor or DCs or to make resource use fruitful and furthermore to improve the reaction time of the assignment, at the same time ousting a condition in which a bit of the DCs is over stacked, while some others are under stacked. The basic intriguing focuses while becoming such calculation are estimation of load, assessment of load, security of different systems, execution of structure, and relationship between different DCs [4]. This heap considered can be regarding CPU load, measure of memory utilized, postponement, or system load. A site or a web application can be acquired by a lot of clients at any time. It ends up troublesome for a web application to deal with all these client asks for at one time. It might even outcome in framework breakdowns. For a site proprietor, whose whole work is reliant on his entryway, the sinking feeling of site being down or not available additionally brings lost potential clients. Here, the heap balancer assumes a vital job. Cloud load balancing is the way toward disseminating remaining tasks at hand and figuring resources crosswise over at least one server. This sort of dissemination guarantees most extreme throughput in least response time [5, 6]. In this research paper, we have implemented throttled, RR, and shortest job first algorithm for calculating the efficiency of the cloud computing environment while performing the load balancing. Along with these algorithms, we have proposed one more algorithm M-throttled with an improvised performance of the network with the presence of the heavy traffic at different instances of time. The influencing parameters such as response time and process time for UB and DC are considered for the evaluation of different algorithms.

2 Literature Survey

Load balancing ensures the principal work in providing a QoS in the cloud environment. It also has been generating liberal energy for the exploration arrange. There are tons of philosophies that have adjusted to the store modifying issue in

conveyed processing. The choice involves varying customary procedures without including any swarm knowledge computations. Different load adjusting methodologies were proposed starting late and each based on various edges of figuring and techniques, e.g., using a central burden modifying approach for virtual machines [13], the arranging system on weight altering of virtual machine (VM) resources subject to inherited computations [14], a mapping course of action reliant on multi-resource burden changing for virtual machines [15], different dispersed calculations for VMs [16], weighted least-association methodology [17], and two-stage booking calculations [18]. Also, a few techniques for burden adjusting were displayed for different cloud applications, for instance, an administration-based work set for extensive scale stockpiling [19], information focus the executive design [15], and a heterogeneous cloud.

The mediocre contains approaches like [8] swarm learning figuring, counterfeit honey bee state [9, 10], and PSO [11, 12], which has the fine granularity result for the dynamic behavior of appropriated processing. In [9], the author represented an estimation for weight movement of an extraordinary weight with a changed technique of ACO. In [7], a load advertisement adjusting framework was proposed in light of underground creepy crawly state and complex framework speculation in an open appropriated registering class. This is the first occasion when that ACO and complex frameworks were united into weight modifying in conveyed processing what's increasingly procured extraordinary execution. In [8], the author offered a response for weight altering in the cloud by ACO, to grow or confine different execution parameters, for instance, CPU weight and memory limit. In [9, 10], the author displayed a novel technique for burden altering reliant on fake bumble bee settlement. PSO was in like manner grasped for weight altering in dispersed registering, for instance [11, 12].

3 Existing Algorithms

3.1 Throttled Load Balancing

In this method [16], heap balancer keeps up a database of VM with their present states (Accessible/Occupied). At any instant when a demand to allocate another VM from the DC controller reaches, it processes the record table from best till the most readily accessible VM is detected. As soon as the VM is discovered, the Heap Balancer restores the corresponding VM's ID to the DC controller. The DC controller sends the demand to VM with the identified by the corresponding ID. The DC controller informs the heap balancer of the new allotment. The heap balancer refreshes the allotment table by augmenting as needs be. When the VM wraps up the demand and the data center controller gets the reaction cloudlet, it advises the heap balancer of the VM de-assignment. The heap balancer de-assign the equivalent VM whose Id is as of now imparted. The objective of this method is to determine the response time

of every VM as VMs are having different capacities corresponding to processing efficiency.

$$RT = F_t - A_t + T_d$$

where RT = response time, F_t = finish time, A_t = arrival time, and T_d = transmission delay.

3.2 Round-Robin Load Balancing

It is the least complex calculation that utilizes the idea of time slice [8]. In this method, time is separated into numerous slices also, every datacenter is provided with a specific time slice and inside that defined amount of time the hub will play out its activities. The data center controller doles out the demand to a rundown of VMs on a pivoting premise. The first demand is allotted to an available VM which will be determined haphazardly from the gathering and afterward DC controller doles out the resulting demands in a roundabout request. If the VM is appointed the demand, then the VM is shifted to the end of the rundown. RR calculation chooses the heap on arbitrary premise and also, in this manner, prompts a circumstance where a few hubs are intensely stacked and some are daintily stacked.

3.3 SJF Load Balancing

Shortest Job First (SJF) [17] planning is a need and non-preemptive booking. In Non-preemptive methods, when the procedures are allocated for a time to a processor then the processor can't be taken by the other, until the procedure is finished in the execution section. This calculation appropriates the heap haphazardly by first checking the extent of the procedure and after that exchanging the heap to a virtual machine, which is gently stacked. All things considered that procedure measure is least; this procedure will first need to execute whether we guess most reduced estimated process executed in least time. The heap balancer spreads the heap on to various hubs known as spread range technique. Shortest Job First (SJF) calculation can be said to be ideal with a normal holding up time negligible, which improves the framework execution.

4 Proposed Algorithm: M-throttled

In this calculation, the heap balancer keeps up a rundown table of VMs and the amount of requesting and by assigned to VM. At first, all VMs have zero portions.

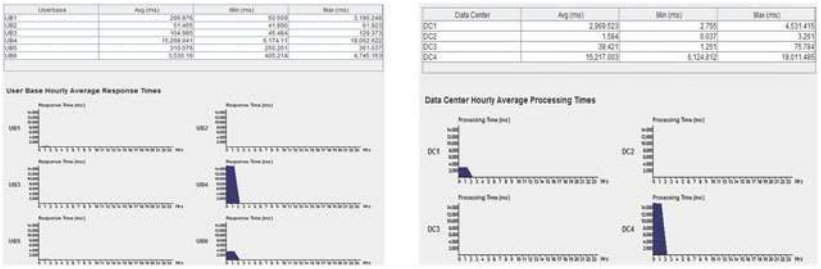

Fig. 1 UB RT and DC PT using RR algorithm

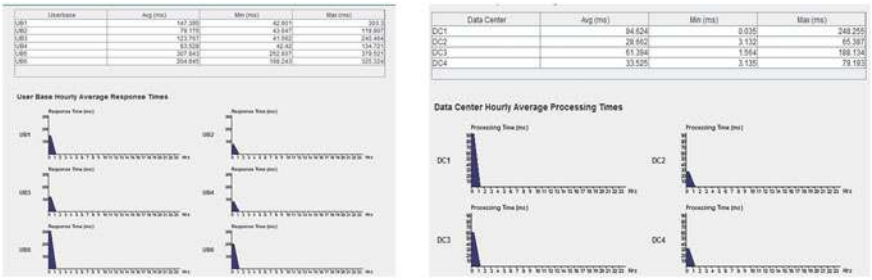

Fig. 2 UB RT and DC PT using throttled algorithm

Right when an interest to assign another VM from the DC controller comes to, it forms the rundown table and perceives the base stacked VM. If there are multiple, the chief recognized is picked. The heap balancer reestablishes the machine IDs to the DC controller. The DC controller provides the interest to the VM recognized by its identified ID. The DC controller illuminates heap balancer about the newly generated task. The heap balancer invigorates the task table augmenting the distribution with that VM. Right when the VM wraps up the interest and DC controller gets the interested cloudlet, it educates the heap balancer regarding the corresponding VM's appropriation. The heap balancer revives the dissemination table by diminishing the assignment of the VM by one. In M-throttled algorithm, a correspondence exists between the stack balancer and the data center controller for reviving the rundown table provoking an overhead that makes the delay in giving response to the showed up sales (Figs. 1, 2, 3, and 4).

5 Implementation

In this simulation, six datacenters DC1, DC2, DC3, DC4, DC5, and DC6 with closed data set policy have been adapted during the simulation. In this, different arrangement parameters can be set like number of user bases, number of tasks produced by

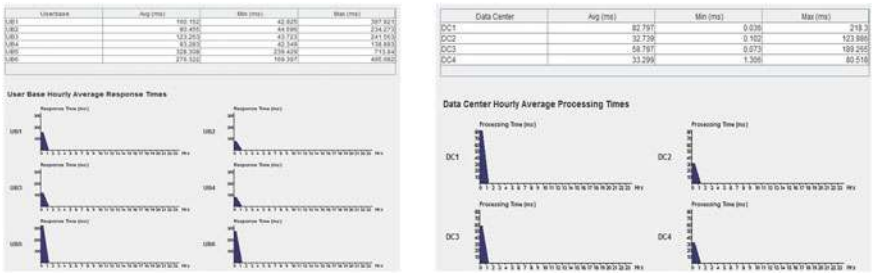

Fig. 3 UB RT and DC PT using SJF algorithm

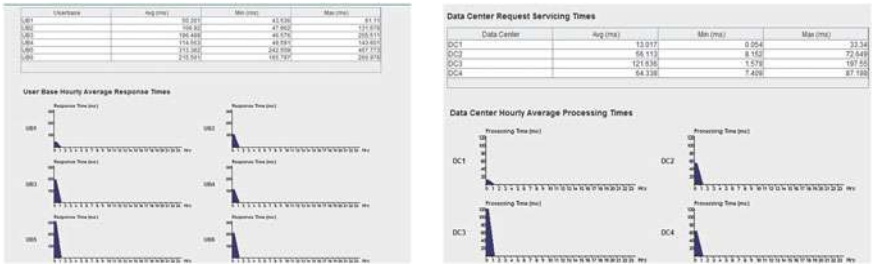

Fig. 4 UB RT and DC PT using M-throttled algorithm

each user base per hour, number of VMs, number of processors, processing speed, available bandwidth, etc. Based on the parameters, the result incorporates reaction time, handling time, fetched, etc. UB response time (RT) and DC processing time (PT) are considered for the evaluation purpose (Tables 1 and 2) [16].

6 Conclusion

We have studied the concepts of load balancing and its vital effects on cloud computing environment. Different algorithms provide the solution for the existing problem of load balancing among different data centers to maintain the efficiency of the network. The performance of the strategies such as throttled, round-robin, shortest job first, and M-throttled time has been studied by taking some influencing parameters such as response time and processing time. A comparison has been done on the basis of some predefined parameter such as UB response time and DC processing time. With the presence of heavy traffic in each region the UB response time and the DC processing time, the M-throttled algorithm performs much better than that of other existing algorithms.

Table 1 DC configuration

Parameter	Value used
VM image size	10000
VM memory	1024 Mb
VM band	1000
DC-Arch	X86
DC-OS	Linux
DC-Machine	20
DC-Memory/machine	2048 Mb
DC-Storage	100000 Mb
DC-Band	10000
DC-Processors/Machine	4
DC-Speed	100MIPS
DC-Policy	Time Shared/Space Shared
DC grouping UB based	1000
DC grouping request based	100
Instruction length	250

Table 2 Region configuration

Cloud analyst region id	Users (M)
0	4.4
1	1.1
2	2.6
3	1.3
4	0.3
5	0.8

References

1. Velte, A.T., Velte, T.J., Elsenpeter, R.C., Elsenpeter, R.C.: Cloud Computing: A Practical Approach, p. 44. McGraw-Hill, New York (2010)
2. Randles, M., Lamb, D., Taleb-Bendiab, A.: A comparative study into distributed load balancing algorithms for cloud computing. In: 2010 IEEE 24th International Conference on Advanced Information Networking and Applications Workshops, pp. 551–556. IEEE (2010)
3. A Vouk, M.: Cloud computing–issues, research and implementations. J. Comput. Inf. Technol. **16**(4), 235–246 (2008)
4. Alakeel, A.M.: A guide to dynamic load balancing in distributed computer systems. Int. J. Comput. Sci. Inf. Secur. **10**(6), 153–160 (2010)
5. http://www.ibm.com/press/us/en/pressrelease/22613.wss
6. http://www.amazon.com/gp/browse.html?node=20159001
7. Randles, M., Odat, E., Lamb, D., Abu-Rahmeh, O., Taleb-Bendiab, A.: A comparative experiment in distributed load balancing. In: 2009 Second International Conference on Developments

in eSystems Engineering, pp. 258–265). IEEE (2009)
8. Shah, M.M.D., Kariyani, M.A.A., Agrawal, M.D.L.: Allocation of virtual machines in cloud computing using load balancing algorithm. Int. J. Comput. Sci. Inf. Technol. Secur. (IJCSITS) **3**(1), 2249–9555 (2013)
9. Moges, M., Robertazzi, T.G.: Wireless sensor networks: scheduling for measurement and data reporting. IEEE Trans. Aerosp. Electron. Syst. **42**(1), 327–340 (2006)
10. Pallis, G.: Cloud computing: the new frontier of internet computing. IEEE Internet Comput. **14**(5), 70–73 (2010)
11. Armbrust, M., Fox, A., Griffith, R., Joseph, A.D., Katz, R., Konwinski, A., Lee, G., Patterson, D., Rabkin, A., Stocia, I., Zaharia, M.: Above the Clouds: A Berkeley View of Cloud Computing, pp. 1–23. EECS Department, University of California (2009)
12. Bhadani, A., Chaudhary, S.: Performance evaluation of web servers using central load balancing policy over virtual machines on cloud. In: Proceedings of the Third Annual ACM Bangalore Conference, p. 16. ACM (2010)
13. Rimal, B.P., Choi, E., Lumb, I: A taxonomy and survey of cloud computing systems. In: 2009 Fifth International Joint Conference on INC, IMS and IDC, pp. 44–51 (2009)
14. Zhang, Z., Zhang, X.: A load balancing mechanism based on ant colony and complex network theory in open cloud computing federation. In: 2010 The 2nd International Conference on Industrial Mechatronics and Automation, vol. 2, pp. 240–243. IEEE (2010)
15. Hiranwal, S., Roy, K.C.: Adaptive round robin scheduling using shortest burst approach based on smart time slice. Int. J. Comput. Sci. Commun. **2**(2), 319–323 (2011)
16. Wickremasinghe, B., Calheiros, R.N., Buyya, R.: Cloudanalyst: a cloudsim-based visual modeller for analysing cloud computing environments and applications. In: 2010 24th IEEE International Conference on Advanced Information Networking and Applications, pp. 446–452. IEEE (2010)
17. Waheed, M., Javaid, N., Fatima, A., Nazar, T., Tehreem, K., Ansar, K.: Shortest job first load balancing algorithm for efficient resource management in cloud. In: International Conference on Broadband and Wireless Computing, Communication and Applications, pp. 49–62. Springer, Cham (2018)
18. Buyya, R., Ranjan, R., Calheiros, R.N.: Modeling and simulation of scalable cloud computing environments and the cloudsim toolkit: challenges and opportunities. In: 2009 International Conference on High Performance Computing and Simulation, pp. 1–11. IEEE (2009)
19. Bo, Z., Ji, G., Jieqing, A.: Cloud loading balance algorithm. In: Proceedings of the 2010 2nd International Conference on Information Science and Engineering (ICISE), pp. 5001–5004. Hangzhou, China (2010)

Inverse Kinematics Solution of a 6-DOF Industrial Robot

Kshitish K. Dash, B. B. Choudhury and S. K. Senapati

Abstract A vital part of many industrial robot manipulators is to reach required position and orientation of end effectors so as to complete the pre-defined task. To get this, one should have knowledge of kinematics, i.e. inverse kinematics (IK). Though inverse kinematics never gives a closed form solution, it is too difficult to solve such problem of an industrial robot. There are so many analytical and other simulation methods which are adopted to solve this IK problem for our 6-DOF industrial pick and place robot. In this paper, artificial neural networks (ANN) are used and simulated by using MATLAB.

Keywords Industrial robot · Inverse kinematics · ANN

1 Introduction

Kinematics of robot indicates the analytic behaviour of the movement of robot manipulator. By taking appropriate kinematics models of an industrial robot, the kinematic behaviour, i.e. inverse kinematics and forward kinematics, can be analysed. These two spaces utilized as a part of kinematics demonstrating are known as Cartesian space and Quaternion space. The alteration among two Cartesian coordinate takes place in form of rotation and a translation as soon in Fig. 1. So many methods are adopted to solve forward kinematics and inverse kinematics problems of an industrial pick and place robot. out of different method Jacobian matrix and Denvit-Hertenberg theory is useful for analytic solution of straight forward kinematics and Screw theory is useful for inverse kinematic solution.

K. K. Dash (✉) · B. B. Choudhury · S. K. Senapati
Indira Gandhi Institute of Technology, Sarang, Dhenkanal 759146, Odisha, India
e-mail: kdash76@gmail.com

B. B. Choudhury
e-mail: bbcigit@gmail.com

S. K. Senapati
e-mail: sukantasenapati63@gmail.com

J. Nayak et al. (eds.), *Soft Computing in Data Analytics*,
Advances in Intelligent Systems and Computing 758,
https://doi.org/10.1007/978-981-13-0514-6_19

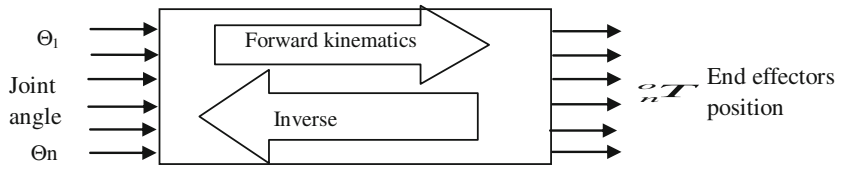

Fig. 1 Schematic portrayal of inverse and forward kinematics

Denavit–Hartenberg (D-H) gives common alteration between two joints, and it requires four parameters. The parameters used here are known as the D-H parameters. The kinematics of robot ordered in form of forward kinematics and inverse kinematics. Forward kinematics issue is simple, and also, there is no complication deriving the equations. Therefore, there is dependably a forward kinematics arrangement of a controller. Inverse kinematics is a considerably more troublesome issue than forward kinematics. The solution of the backwards kinematics issue is computationally extensive where some have solution, some have no solution, some have redundancy problem takes quite a while in the continuous control of controllers.

2 Literature Review

Li et al. [1] studied 6-R robot for virtual reality and analysed the virtual reality. The simulation is done by using EON software. The inverse kinematics of this robot is simulating by MATLAB, and the result is validating for the virtual reality using both the software. Lazar et al. [2] developed a robot manipulator control by using visual serving. The paper describes how integrating reference and image prediction novel architecture are used for the prediction camera velocity and time variation consider by interaction matrix. A simulation is done to improve its efficiency for a 6-DOF manipulator. Chen et al. [3] developed a paper to increase the inverse kinematics behaviour of a 6-DOF robot. The two coordinates are considered here as reference coordinate and tool coordinate. The screw motion calculated for each link based on reference coordinate. At last, a new algorithm is used to improve the efficiency of inverse kinematics. Duka [4] developed a paper inverse kinematics and forward kinematics of articulated robot. D-H theory is adopted to solve 4-axis articulated robot problem and considering the corresponding data inverse kinematics value also calculated. A comparison takes place between experimental data with calculated data for 4-axis articulated manipulator. Adrin et al. [5] developed a paper ANFIS-based inverse kinematics solution. They have discussed a 3-DOF planer manipulator which is considered to get effectiveness of this approach. The data obtained from forward kinematics is transfer for inverse kinematics and accepted the accuracy of the different joint angles. Dash et al. [6] developed a paper

inverse kinematics of industrial using ANN. The end effectors' position is calculated by considering different joint angle. The multilayer neural network is used to train the data, and the analytical data is validate with ANN trained value. Chandra and Rolland [7] present 3RPR planer parallel manipulator where simulated annealing and relay collaborative met heuristics. The given method gave promise results. Henten et al. [8] devolved autonomous robot for harvesting. In this paper, the 3D image system implemented for controlling and to avoid collision-free motion during harvesting and 7-DOF manipulator was used to make more comfortable harvesting. Husty et al. [9] taken new algorithm to solve IK of 6-R manipulator. Here kinematics image considers to identify the displacement of each point, and the solution is made in two phase. In first phase, two joint angle value calculated algorithm by using and other four calculated by inverse kinematics equation. Srinivas et al. [10] accepting end-focuses for all segments of a multi-segment trunk are known and subtle elements are applying single-segment converse kinematics to each segment of the multi-segment trunk by adjusting for coming about changes in introduction. At last, an approach which registers per-area end-focuses given just a last segment endpoint gives an entire answer for the multi-segment converse kinematics issue. Iliukhina et al. [11] devolved modelling 5-DOF manipulator where the piece of research went for making mechanical controller controlled by methods for brain–computer interface for enhancing family unit confidence of people with incapacities and growing the extent of their movement. The mechanical controller gives plausibility of self-satisfaction in fundamental family works, and it shows a numerical model of the kinematics of the automated controller. Khuntia et al. [12] modelled a heuristics allocation of multitask robot. Here it has been created thinking about the earth, the framework parameters and the robots' capacities. An answer calculation has been created and executed to acquire the outcomes.

3 Inverse Kinematics

Backward kinematics is the inverse of forward kinematics. The position of end effectors calculated, after determining all joint angle position. The inverse kinematics solves the problem like end effectors position, what are the relating joint positions. In contrast with the forward kinematics issue, the arrangement of the converse issue is not generally conjugal. The end effectors position can be reached in several configurations according to position vectors. Our main aim is to solve 6-DOF industrial robot using artificial neural networks (ANN) and simulated the solution by using MATLAB.

The inverse kinematics model is shown in Fig. 2 whose angle can be calculated like $\theta_1, \theta_2, \theta_3 \ldots = f - (p)$. The arrangement is figured in two stages, first uses an area vector from the wrist to the wrist. The vector takes into consideration the arrangement of the initial three primaries DOF that finish the worldwide movement.

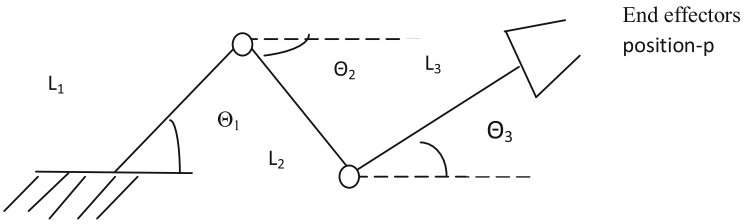

Fig. 2 Structure of 3-R arm

The last 3-DOF is discovered utilizing the computed estimations of the first 3-DOF and the introduction matrices T4, T5 and T6. The modelling is done here using D-H method for forward kinematics, and the values are obtained for end effectors with various corresponding joint angle position.

$$T = A_1 A_2 A_3 A_4 A_5 A_6 \tag{1}$$

where T is the target position Θ_i is the joint variable.

4 Denavit–Hartenberg Theory

D-H parameters are one of the most useful theories to take care of forward kinematics issue of automated arms. The D-H formalization takes place by using only four parameters to describe the spatial relationship between successive link coordinate frames as shown in Fig. 3. The 6-DOF robot solution made by introducing two constraints to the placement of those frames: The axis x_i is perpendicular to the axis z_{i-1}, and the axis x_i intersects the axis z_{i-1}.

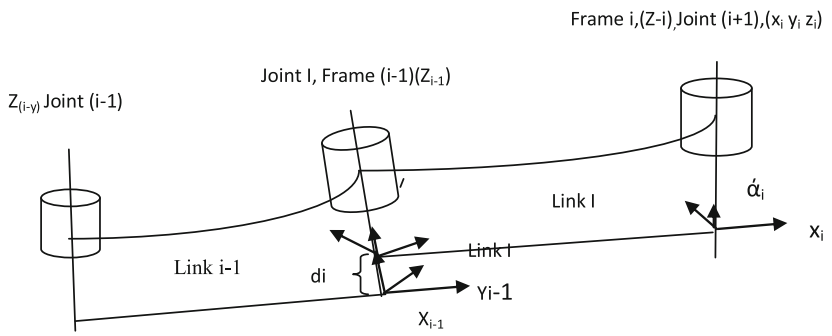

Fig. 3 D-H architecture

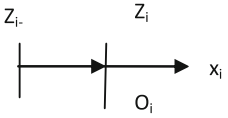

Fig. 4 D-H architecture for two axis

Frame i is rigidly attached to link joint i + 1. The frame is assign as D-H convention, i.e. D-H_1 x_i perpendicular to z_{i-1}, D-H_2 x_i intersects the axis z_{i-1}

Assign Z-axis as axis of motion. If Z_i and Z_{i-1} don't intersect and not parallel each other then x_i act along the common normal from origin O_i which is the meeting point between Z_i and the general normal line.

From Fig. 4 if Z_i and Z_{i-1} are parallel and do not intersect, then O_i can be consider anywhere along Z_{i-1} axis. The y_i value can be obtain by cross product of two axis when both Z_i and Z_{i-1} are intersect each other, Generally cross product that two axis each other. To get the above value from the frame i − 1 to frame i, some necessary steps to be followed then after we can get the equation like as stated below

$$T_i^{i-1} = T_z(d_i)T_z(\theta_i).T_x(a_i)T_x(\alpha_i) \tag{2}$$

$$= \begin{bmatrix} 1 & 0 & 0 & 0 \\ 0 & 1 & 0 & 0 \\ 0 & 0 & 1 & d_i \\ 0 & 0 & 0 & 1 \end{bmatrix}$$

$$\begin{bmatrix} Cos\,\theta_i & -Sin\,\theta_i & 0 & 0 \\ Sin\,\theta_i & Cos\,\theta_i & 0 & 0 \\ 0 & 0 & 1 & 0 \\ 0 & 0 & 0 & 1 \end{bmatrix} \begin{bmatrix} 1 & 0 & 0 & a_i \\ 0 & 1 & 0 & 0 \\ 0 & 0 & 1 & 0 \\ 0 & 0 & 0 & 1 \end{bmatrix} \begin{bmatrix} 1 & 0 & 0 & 0 \\ 0 & Cos\,\alpha_1 & -Sin\,\alpha_i & 0 \\ 0 & Sin\,\alpha_i & Cos\,\alpha_i & o \\ 0 & 0 & 0 & 1 \end{bmatrix}$$

$$= \begin{bmatrix} Cos\,\theta_i & -Cos\,\alpha_i Sin\,\theta_i & Sin\,\alpha_i Sin\,\theta_i & a_i Cos\,\theta_i \\ Sin\,\theta_i & Cos\,\alpha_i Cos\,\theta_i & -Sin\,\alpha_i Sos\theta_i & a_i Sin\,\theta_i \\ 0 & Sin\,\alpha & Cos\,\alpha_i & d_i 0 \\ 0 & 0 & 0 & 1 \end{bmatrix}$$

By considering 6-DOF architecture of Aristo as shown in Fig. 5, the parameters are calculated as stated Table 1. After getting parameter by using D-H principle, the joint angle for different position for inverse kinematics can be calculated.

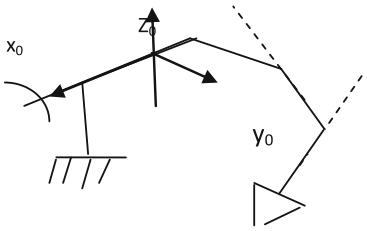

Fig. 5 6-DOF robot position

Table 1 D-H parameter value

DOF.	θ_i	A	a_i	d_i
1	90	O	0	184
2	89.28	O	150	158
3	91.61	79.71	0	300
4	92.18	90	250	150
5	92.51	0	0	378.5
6	95.02	63.9	0	64.0

$$\theta_1 = \tan^{-}\left[\lambda q_y - d_2 q_x / \lambda q_x + d_2 q_y\right] \tag{3}$$

$$\theta_3 = \tan^{-}\left[\frac{q_x^2 + q_y^2 + q_z^2 - d_4^2 - a_2^2 - d_2^2}{\pm\sqrt{4d_4^2 a^2 - \left(q_x^2 + q_y^2 + q_z^2 - d_4^4 - a_2^2 - d_2^2\right)^2}}\right] \tag{4}$$

$$\theta_2 = \tan^{-}\left[\frac{q_z(a_2 + d_4 s_3) - d_4 c_3(\pm\sqrt{q_x^2 + q_y^2 - d_z^2}}{q_z d_4 c_3 - (a + d_4 s_3)\left(\sqrt{q_x^2 + q_y^2 - d_2^2}\right)}\right] \tag{5}$$

$$\theta_4 = \tan^{-}\frac{C_1 a_y - S_1 q_x}{C_1 C_{23} q_x + S_1 C_{23} q_y - C_{23} q_z} \tag{6}$$

$$\theta_5 = \tan^{-}\left[\frac{(C_1 C_{23} C_4 - S_1 S_4) q_x + (S_1) C_{23} C_4 + C_1 S_4) q_Y - C_4 S1_{23} q_z}{C_1 S_{23} q_x + S_1 S_{23} q_y + C_{23} q_z}\right] \tag{7}$$

$$\theta_6 = \tan^{-}\left[\frac{-(S_1 C_4 + C_1 C_{23} S_4) nx + (-C_1 C_4 - S_1 C_{23} S_4) n_y + (S_4 s_{23}) n_z}{-(S_1 C_4 + C_1 C_{23} S_4) + C_1 C_4 - S_1 C_{23} S_4 + S_4 S_{23}}\right] \tag{8}$$

The above equation is used to calculate the joint angle value experimentally for different position of end effector.

5 Artificial Neural Network

The neural system design of this arrangement as appeared in Fig. 6 and the neurons are completely associated with this system. In this network, 18 nodes have been used to train the network. A sigmoid capacity is utilized as an exchange work among neurons, and there are three components of the system input. The initial three components speak to Cartesian position, and other six speak to the joint edge of various hubs. The showing informational index was set up keeping in mind that the end point position where ANN can be utilized for the inverse kinematics controller.

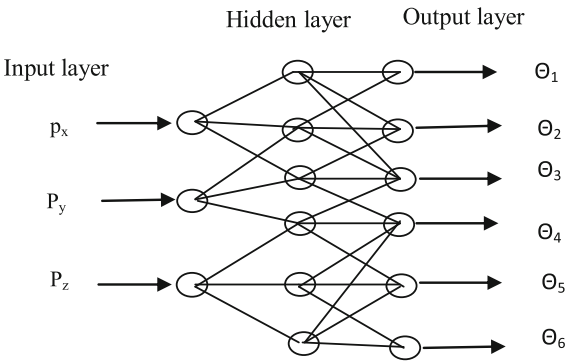

Fig. 6 Multilayer neural network

$$Ahi(t) = \sum_{k=1}^{i} WT_{ik} I_k + \sum_{k=1}^{m} Wh_{ik} f(Ah_k(t-1)); \tag{9}$$

The actuation work which is utilized as a part of concealed layer and the yield of the system is a weighted total of the shrouded unit output.

6 Results and Discussion

With reference to above equation and considering some equation from author [6], a number of joint angle value calculated which is shown below. From the table, it is observed that obtain joint angle value is varying within the maximum and minimum value of manipulator joint angle with a different position of end effector.

6.1 Experimental Data of Industrial Robot

See Table 2.

6.2 Specification of Industrial Robot

By taking number of experimental data, the neural network trained and obtained performance curve as shown in Fig. 7 (Tables 2 and 3).

Table 2 Joint angle and position of manipulator value

Θ_1	Θ_2	Θ_3	Θ_4	Θ_5	Θ_6	p_x	p_y	p_z
90	−89.98	90	0	90	0	0.30	378.88	393.84
89.85	−89.82	89.28	3.25	88.50	4.68	2.29	281.47	394.37
89.56	−89.78	91.61	5.25	85.00	7.84	2.56	380.14	394.74
89.20	−89.59	92.18	11.85	83.74	10.91	7.38	383.33	382.24
88.51	−89.22	92.51	17.17	79.71	15.46	8.11	390.57	375.52
86.45	−87.81	95.02	22.92	76.98	21.74	0.52	395.10	351.48
82.39	−85.56	95.44	26.56	63.93	24.37	29.85	414.98	336.66

Fig. 7 Performance curve

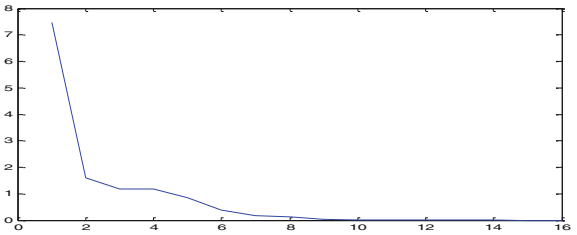

Table 3 Joint angle specification

Minimum	Maximum	Home	Axis
−250°	90°	90°	Base
−90°	45°	90°	Shoulder
90°	−45°	−90°	Elbow
0°	340°	0°	Wrist
−90°	90°	90^0	Pitch
0°	340^0	0^0	Roll

The Levenberg–Marquardt (LM) algorithm is used to get the performance curve very fast. It is an iterative technique to get performance curve. The curve shows that the experimental value is nearly close to the theoretical value, and its errors are decrees with higher DOF.

The training rate is adapted for different epochs. Fig. 8 shows the change of the training rate decreasing with the number of epochs. By increasing the DOF, the joint angle value is closer with the train data.

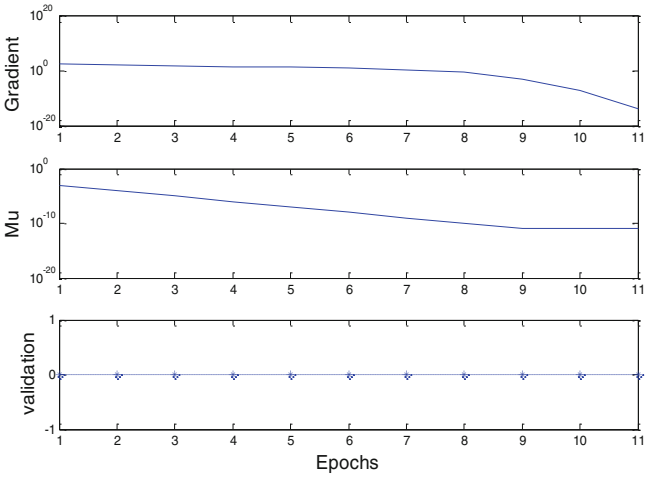

Fig. 8 Validation curve

7 Conclusion

From the analysis, it is observed that the calculated value of all joint angle of the industrial 6-DOF industrial robot is nearly equal to the experimental data. Out of different joint angle θ_1, θ_3, θ_4, θ_5 values are nearly equal to experimental data and θ_2, θ_6 values match 60% with experimental joint angle values. The trained value obtained by using neural network for the inverse kinematics gives approximate value after high training sample which is a big drawback of this paper.

References

1. Li, W.J., Song, Z.H., Zhu, Z.X., Mao, E.R.: Analysis and simulation of 6R Robot in virtual Reality. IFAC-PapersOnLine **49**(16), 426–430 (2016)
2. Lazar, C., Burlacu, A., Copot, C.: Predictive Control Architecture for Visual Servoing of Robot Manipulators (2011)
3. Chen, Q., Zhu, S., Zhang, X.: Improved inverse kinematics algorithm using screw theory for a six-dof robot manipulator. Int. J. Adv. Robot. Syst. (2015)
4. Duka, A.V.: Anfis Based Solution to the Inverse Kinematics of a 3-DOF Planar Manipulator. INTER-Eng-2014 (2014)
5. Parhi, D.R., Deepak, B.B.V.L., Nayak, D., Amrit, A.: Forward and inverse kinematic models for and articulated robotic manipulator. Int. J. Artif. Intell. Comput. Res. **4**(2) 103–109 (2012)
6. Dash, K.K., Choudhury, B.B., Khuntia, A.K., Biswal, B.B.: A Neural Network Based Inverse Kinematic Problem. IEEE. 978-1-4244-9477-4/11/$26.00 ©2011
7. Chandra, R., Rolland, L.: On solving the forward kinematics of 3RPR planar parallel manipulator using hybrid metaheuristics. Appl. Math. Comput. **217**(22), 8997–9008 (2011)

8. Van Henten, E.J., Schenk, E.J., van Willigenburg, L.G., Meuleman, J., Barreiro, P.: Collision-free inverse kinematics of the redundant seven-link manipulator used in a cucumber picking robot. Bio Syst. Eng. **106**(2), 112–124 (2010)
9. Husty, M.L., Pfurner, M., Schröcker, H.: A new and efficient algorithm for the inverse kinematics of a general serial 6R manipulator. Mech. Mach. Theory **42**(1), 66–81 (2007)
10. Srinivas, N., Matthew, A.C., Bryan, A.J., Ian, W.: A geometrical approach to inverse kinematics for continuum manipulators. In: Proceedings of IEEE/RSJ International Conference on Intelligent Robots and Systems, Nice, France, pp. 3565–3570 (2008)
11. Iliukhina, V.N., Mitkovskiib, K.B., Bizyanovaa, D.A., Akopyan, A.A.: The modeling of inverse kinematics for 5 DOF manipulator. Procedia Engineering **176**, 498–505 (2017)
12. Khuntia, A.K., Choudhury, B.B., Biswaland, B.B., Dash, K.K.: A Heuristics Based Multi-Robot Task Allocation. IEEE. 978-1-4244-9477-4/11/$26.00 ©2011

Design & Analysis of an Unipolar DC-Microgrid system under Variable loading Condition

Sudhansu Bhusan Pati
Research Scholar
School of Electrical Engineering, KIIT Deemed to be University

Subhasree Kundu
Assistant Professor
School of Electrical Engineering, KIIT Deemed to be University

S.K Barik
Assistant Professor
School of Electrical Engineering, KIIT Deemed to be University

Sushree Shataroopa Mohapatra
Research Scholar School of Electrical Engineering, KIIT Deemed to be University

Abstract— **The use of power electronics-based instruments has increased the harmonics in the AC distribution system, which is very tedious to control. They are for the DC distribution system may be adopted to avoid such a harmonics problem. The advantages of the DC system over the AC system have made it possible to design the DC micro grid system where the point of generation and the point of utilization are closer to each other. However, the protection of DC micro grid is and very critical issue from a control and operation point of view as there is no zero-crossing. A substantial increase in the DC fault current may lead to a permanent shutdown of DC lines. To address these issues in this paper a research work has been carried out for checking the variation of load on the performance of protection features in a DC micro grid system. The system has been investigated with a Matlab Simulink model.**

Keywords—DC microgrid, Unipolar, Power Quality, loading, common mode voltage

I. INTRODUCTION

In the recent trades of power system power system producing clean and green energy from the available resources is a very critical challenge. However to meet the global energy demand it is require to interconnect more number of renewable based sources to the traditional grid most of the renewable sources produces DC power against traditional generating units,.Again the modern lifestyle also demands DC power at the point of its utilization. These electronic devices produce harmonics in the AC system which ultimately affects the power quality . It is also very difficult to manage a large power system with this limited controllability. Therefore it is quite easier to control the power if it can be utilies at the point of production . This creates a new window in the power system in the from of micro grid. Micro grid is of 2 types i.e. ac micro grid and DC micro grid

DC micro grid is more user friendly and at the same time we can transfer $\sqrt{2}$ times of AC power. This is because of absence of reactive power drop as absorbed in ac system. The DC micro grid also reduces the use of power conversion circuit as used for integrating the renewable sources into the traditional grid. This increases the robotsness and efficiency of the. In contradiction to the above advantages the DC micro grid requires some additional protection features for protecting the equipment from conveter circuit during failure condition. Some of the renewable based generation system injects AC current (component) to the DC line and thereby affecting the performance of DC micro grid.

Variable loading condition a failure of earthing resistance increases the chances for large amount capacitor discharge current heavy discharging current if not protected. Then it may damage the nearest load connected to that resistance. Therefore it is require operate micro grid in exactly in coordination with the loads conacted to the system.

DC grid can be utilised for powering of many electronic loads which can be chosen according to the requirement. Different DC to DC conversion technique has been used for interconnecting the DC sources. Every DC sources has its own prons and cons. Solar PV system although efficient and reliable from available Dc power but as it is environment depended, its output may disturb the main DC line. Similar kind of power quality disturbances can also be experienced from energy storage devices such as battery and fuel cell. Therefore these devices requires some voltage establishing circuit as its output. Although DC micro grid increases the reliability of the system but it require some special attention for its protection features as it does not have the zero crossing point like AC system it also require some protection features while connecting or powering the Dc micro grid from AC sources. Unlike grounding feature in AC system, the dc grounding suffers from corrosion issues. This requires anticorrosion treatment from time to time.

In the last decade a number of research and debate has been carried out over the DC mirco grid architecture, power quality issues and load variations. Most of the disturbances are coming out due to the interfacing of AC sources and converter presence in the DC system. The harmonics injected from the AC utility system also creates a number of disturbance which can be eliminated by suitably designing and active power filter and placing the same at the point of interconnection. Apart from the issues as mentioned above variation of load and its impact on the Dc micro grid is the least researched area . In order to elaborate the above mentioned points this paper is organised as follows: (i) The section two des cribes about the architecture of DC micro grid system in terms of voltage polarity (iii) modelling of different components involved in Dc

micro grid disturbance (iv) this section represent the analysis of load variation in an unipolar DC micro grid system (v) this section represent the overall conclusion and future scope of the work

II. DC MICROGRID ARCHITECTURE

Like ac distribution system, the DC distribution system also consist of two wire and three wire transmission line. The two wire transmission line is turned as unipolar whereas the three wire transmission lines is termed as bipolar. The two system has its own advantages and disadvantages at different voltage levels. Fig.1 shows the unipolar DC micro grid architecture where both the electrical sources and loads are connected to the positive and negative leads of the DC system. Here the power or energy is transmitted at the same potential therefore during the design and evaluation stage it is required to select the dc voltage of some magnitude for all the appliances. This architecture can support for transmitting the power at higher voltage like AC system. However, the conversion circuit must be designed to handle this voltage. It is also worthwhile to note here that due to absence of asymmetry in the DC system it is quite unbalanced conditions. The advantages of the system is that the design is very simple and flexible which makes it feasible to operate the system in off grid area where AC infrastructure is not available. It is also beneficial for those operations where point of production and point of utilization are not far away. Long transmission of dc micro grid can be possible with solid state transformer. Due to limited availability of pole of this system is not feasible for those areas where voltage sensitivity is an issue. It is because a single fault can affect the permanent shut down of entire system. Apart from this advantage it also suffers from limited availability of voltage level.

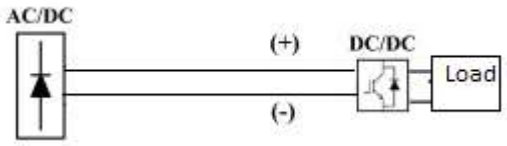

Fig 1. Uni-Polar DC Micro Grid

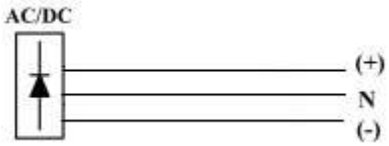

Fig 2. Bi-Polar DC Micro Grid

The different disadvantages presented in the unipolar micro grid system can be overcome by bipolar DC system. The bipolar DC system can provide three types of voltage level such as $+V_{dc}$,$-V_{dc}$ and $2V_{dc}$. Unlike unipolar DC system the bipolar DC system will provide a more reliable system as because a fault in any one of the line does not affect the voltage in other line. Again due to availability of different voltage level a number of loads can be connected to the system.

III. OVER LOADING FAULT ANALYSIS

Design and analysis of short circuit current in a DC micro grid environment under varying loading condition is very much essential. In general, there are two types of fault mainly occurring in DC system and they are terminal to terminal fault and terminal to ground fault. Terminal to terminal fault is the most Sevier fault and all the devices staring from protection devices to connected loads must be designed based on this level of current. In DC micro grids architecture there are two types of fault analysis such as steady state and transient state fault analysis.

$$I_{cap}(t) = \frac{vdc}{2Rc} e^{-t/\tau c} \quad \text{----------(1)}$$

Equation (1) shows the converter fault current appearing at the dc terminal during transient fault condition. Under this condition the fault current basically depends upon the discharging circuit resistance and capacitance and thereby affecting the stability in the circuit.

$$V_c = \frac{V_o \omega_o}{\omega} e^{-\delta t} \sin(\omega t + \beta) - \frac{I_o}{\omega C} e^{-\delta t} \sin \omega t \quad \text{----------(2)}$$

Similarly, equation (2) shows the discharging voltage of the converter capacitor and that of the discharging cable current is shown in equation (3). From this equation it can be found that the discharging current of cable strictly depends on the initial state of the system and harmonics present in the system.

$$I_{cable} = C\frac{dvc}{dt} = -\frac{Io\omega o}{\omega} e^{-\delta t} \sin(\omega t - \beta) - \frac{Vo}{\omega L} e^{-\delta t} \sin \omega t \quad \text{-----(3)}$$

where $\delta = R/2L$, $\omega = \sqrt{1/LC - (R/2L)^2}$, $\omega o = \sqrt{\delta^2 + \omega^2}$, and, $\beta = \arctan(\omega/\delta)$.

$$t_1 = t_0 + (\pi - \gamma)/\omega \quad \text{----------(4)}$$

where $\gamma = \arctan[(V_0\omega_0 C \sin\beta / V0\omega 0 C \cos\beta - I_0)]$.

$$V_{ga} = V_g \sin(\omega st + \alpha) \quad \text{----------(5)}$$

$$I_{ga} = I_g \sin(\omega st + \alpha - \varphi) + [I_{g|0|} \sin(\alpha - \varphi 0) - I_g \sin(\alpha - \varphi)]$$

$$= I_g \sin(\omega 0t + \alpha - \varphi) + I_{gt} e^{-\frac{t}{\tau}} \quad \text{----------(6)}$$

where $\varphi = \arctan[\omega_s (L_{ac+L})/R]$, $\tau = (L_{ac} + L)/R$

$$i_{vst} = i_{D1} + i_{D2} + i_{D3} = i_{ga}) ,(>0) + i_{gb} ,(>0) + i_{gc} ,(>0) \quad \text{---------(7)}$$

Therefore, excessive transient current can be limited by suitably placing an active filter into the circuit. Similarly, equation (4) shows the time taken by the system drop down the capacitor voltage into zero.

IV. RESULT ANALYSIS

In order to investigate the variation of load on the performance of DC micro grid system the following setup was designed in the MATLAB SIMULINK model.

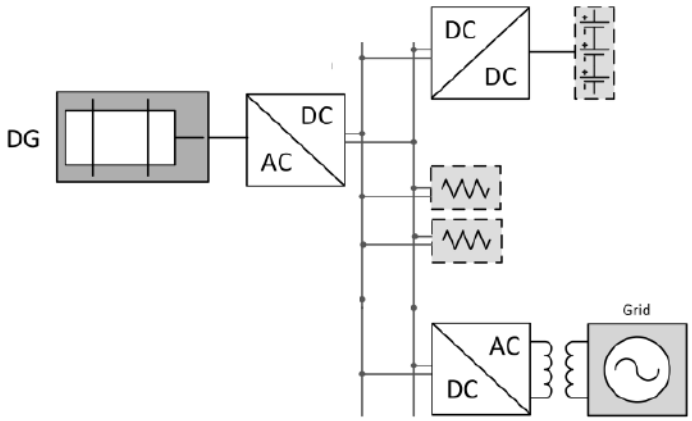

Fig.3 The proposed DC Micro Grid Architecture [1]

The proposed DC micro grid consist of three different types of load and three different types of source. The sources consist of a 9 MVA small hydro plant along with 2MW fuel cell. The total AC power is converted into a DC system of 780V. The load consists of DC load and variable AC load connected through some converter. The two AC load consist of varying frequency type load i. e50 Hz and 55 Hz respectively. Both the load is of 400kWand 200kW respectively. Fig.(iii) shows the proposed architecture of variable DC load connected to the DC micro grid system.

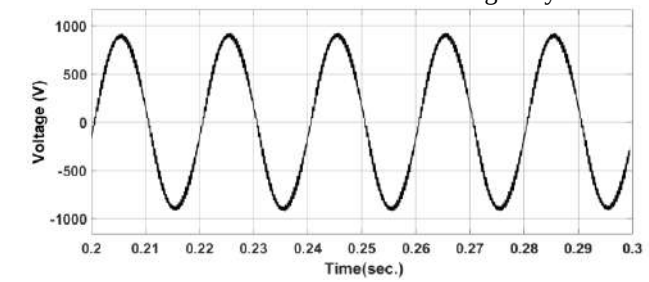

Fig.4. Load-1 AC system Voltage

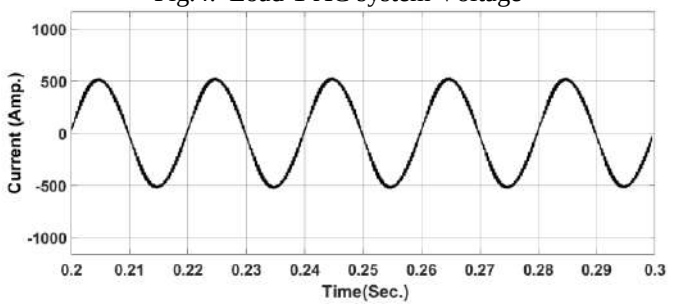

Fig.5. Load-1 AC system Current

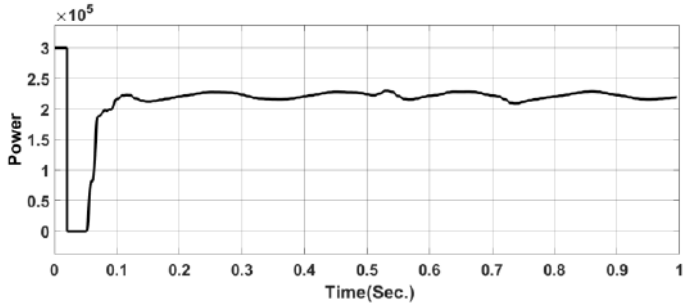

Fig.6 Load-1 AC power drawn by the system

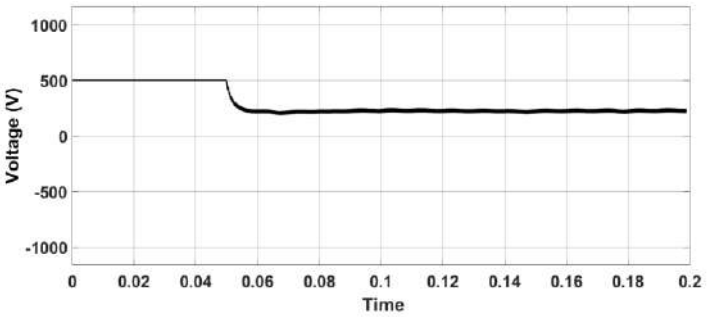

Fig.7 DC fuel cell voltage using Boost converter

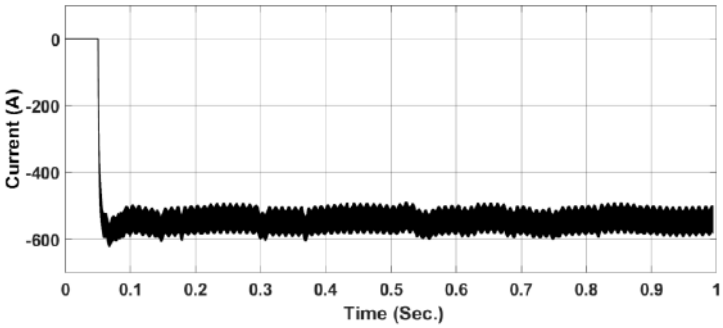

Fig.8. DC fuel cell current using Boost converter

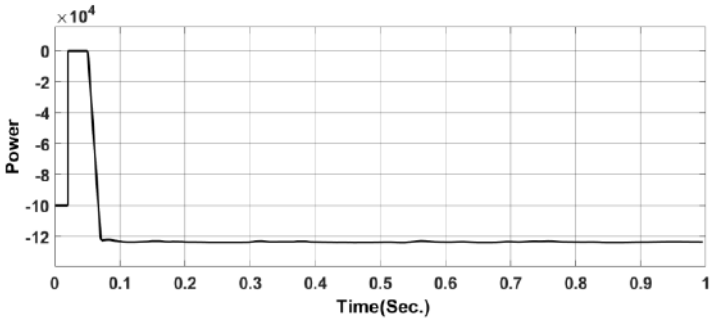

Fig.9 DC fuel cell power using Boost converter

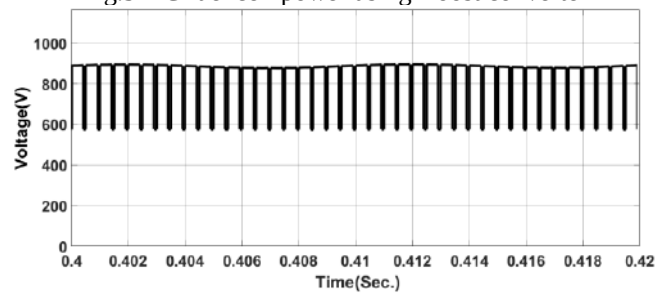

Fig.10 DC Motor terminal voltage

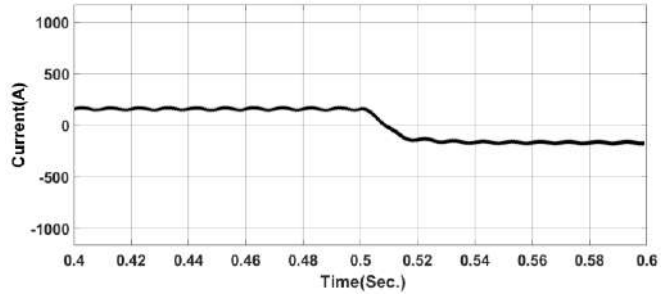

Fig.11 DC Motor current drawn by the system

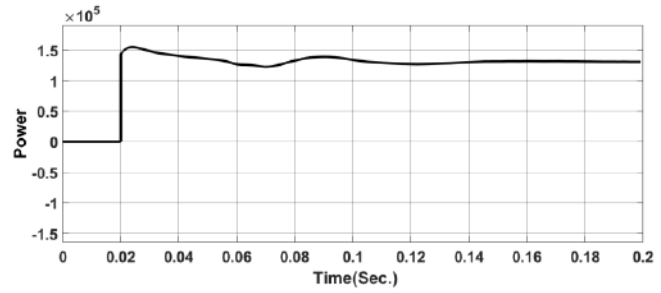

Fig.12 DC motor Power drawn by the system

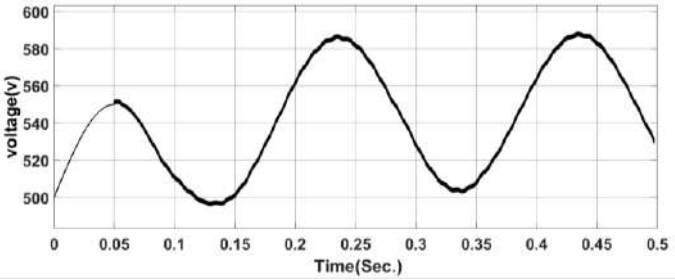

Fig.13 variable load-2 voltage

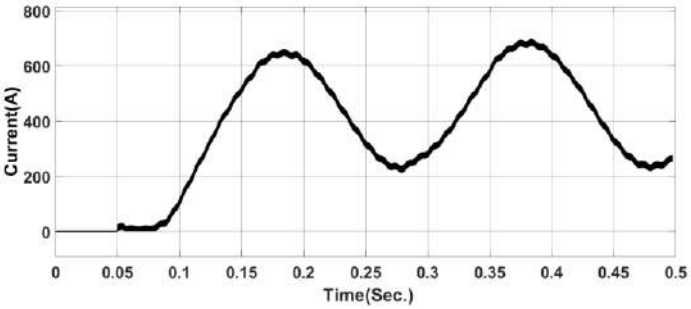

Fig.14 Variable Load-2 Current

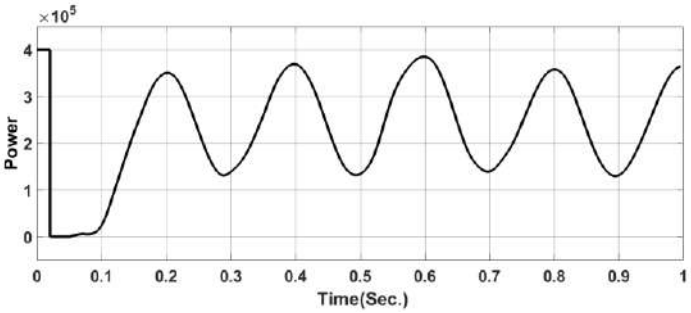

Fig.15 variable load-2 power

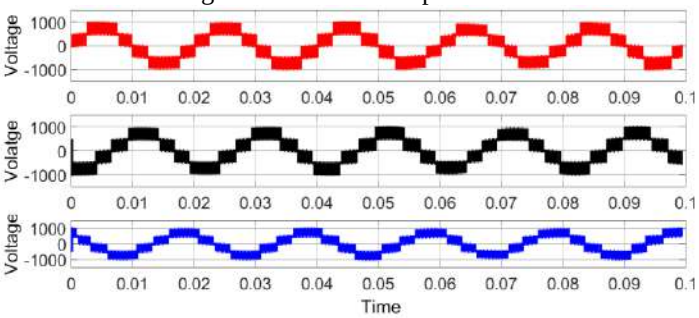

Fig.16 three phase rectifier voltage

Fig.(iv) shows the load voltage and load current. Here 100% load is connected thereby 750V AC is maintained across it. Fig.(v) shows real power drawn by load. Here it can be noticed that at time 0.13 the system gets established itself for three cycles and after that it undergo and oscillation for five cycles. If the oscillation persists for them then some protection device has to be connected. Similar kind of situation is also shown in fig.(vi) which shows the performance of DC motor connected through some converter. Fig.(vii) shows the boost converter voltage connected exactly at the intermediate position of the DC distribution line. Here a voltage of 250V has been maintained throughout the simulation. Fig.(viii) shows the current available in the system when a sudden voltage sag for 0.2 sec. During this time DC micro grid behaves as an islanding mode where the current drops down to – 200.

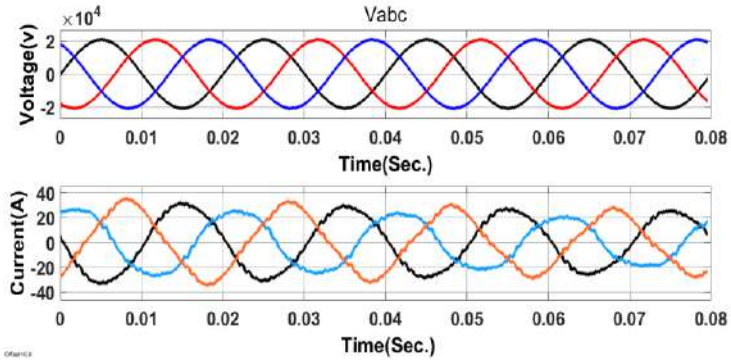

Fig.17 Active Filter Voltage & Current

During this mode of \operation, the total harmonic distortion present across the interfacing of AC-DC system is 4.39%.

V. CONCLUSION

The variation of load profile has been investigated in this paper. The load has been varied in three steps such as loading under 80%, 100% and 125% of the capacity. The presented result shows that, when load increases beyond 112% the inverter starts injecting DC harmonics resulting the oscillation of the system voltage at PCC. Again chances for terminal to ground short circuit also increases. Therefore, while designing the protection feature for DC microgram emphasis must be given to different fault position from feeder side to Bus side.

ACKNOWLEDGMENT

The Authors would like to thank the School of Electrical Engineering KIIT University, for providing necessary laboratory facility for successfully completing the research work carried out in this research paper.

REFERENCES

[1]. de Carvalho Neto, João & Salazar, Andrés. (2015). One-Cycle Control applied to a bidirectional Buck-Boost converter in energy storage applications. 1-6. 10.1109/COBEP.2015.7420204.

[2]. Justo JJ, et al. AC-microgrids versus DC-microgrids with distributed energy resources: a review. Renew Sustain Energy Rev 2013;24:387–405.

[3]. Chowdhury S, et al. Microgrids and active distribution networks. London, United Kingdom: The Institution of Engineering and Technology; 2009. Lasseter RH. MicroGrids. IEEE Power Eng Soc Winter Meet 2002;1:305–8.
[4]. Liang T, et al. From laboratory microgrid to real markets – challenges and opportunities. In: Proceedings of IEEE international conference on power electronics and ECCE Asia (ICPE & ECCE); 2011. p. 264–271.
[5]. Meliopoulos APS. Challenges in simulation and design of microgrids. IEEE Power Eng Soc Winter Meet 2002;1:309–14.
[6]. Govardhan MD, Roy R. Notice of violation of IEEE publication principles: a review on key issues of microgrid. IEEE PES Innov Smart Grid Technol2011:322–7.
[7]. Ustun TS, et al. Modeling of a centralized microgrid protection system and distributed energy resources according to IEC 61850-7-420. IEEE Trans Power Syst 2012;27:1560–7.
[8]. Jiang W, et al. The overview of research on microgrid protection development. In: Proceedings of international conference on intelligent system design and engineering application (ISDEA); 2010. p. 692–697.
[9]. Basak P, et al. A literature review on integration of distributed energy resources in the perspective of control, protection and stability of microgrid.Renew Sustain Energy Rev 2012;16:5545–56.
[10]. Chen J, et al. The overview of protection schemes for distribution systems containing micro-grid. In: Proceedings of power and energy engineeringconference; 2011. p. 1–4.
[11]. Conti S. Protection issues and state of the art for microgrids with inverter interfaced distributed generators. In: Proceedings of international conference on clean electrical power (ICCEP); 2011. p. 643–647.
[12]. Brucoli M, Green TC. Fault behaviour in islanded microgrids. In: Proceedings of the 19th international conference on electricity distribution. CIRED, Vienna; 2007.
[13]. Shi S, et al. Protection of microgrid. In: Proceedings of the 10th IET international conference on developments in power system protection (DPSP2010); 2010. p. 1–4.
[14]. Eissa MM, et al. A novel back up wide area protection technique for power transmission grids using phasor measurement unit. IEEE Trans Power Deliv2010;25:270–8.
[15]. Begovic M, et al. Wide-area protection and emergency control. Proc IEEE 2005;93:876–91.
[16]. erzija V, et al. Wide-area monitoring, protection, and control of future electric power networks. Proc IEEE 2011;99:80–93.
[17]. Tianqi X, et al. A novel communication network for three-level wide area protection system. In: Proceedings of IEEE power and energy society general meeting conversion and delivery of electrical energy in the 21st Century; 2008. p. 1–8.
[18]. Wen-Di Z, Jin-Ding C. A multi-agent system for distributed energy resources control in microgrid. In: Proceedings of the 5th international conference on critical infrastructure (CRIS); 2010. p. 1–5.
[19]. Naduvathuparambil B, et al. Communication delays in wide area measurement systems. In: Proceedings of the thirty-fourth southeastern symposium on system theory; 2002. p. 118–122.
[20]. Al-Nasseri H, et al. A voltage based protection for micro-grids containing power electronic converters. In: Proceedings of IEEE power engineering society general meeting; 2006.
[21]. Al-Nasseri H, et al. Protecting micro-grid systems containing solid-state converter generation. In: Proceedings of international conference on future power systems, 2005.

Authors Biography

Btech from College of Engineering, Bhubaneswar in Electrical and Electronics Engineering.Mtech in Power Electronics and Drives from SOA University.Now PhD Scholar at KIIT University.Having 10 years of teaching experience in different Private College

Shubhasri Kundu has received B.Tech in Electrical Engineering from Jalpaiguri Govt. Engg. College (WBUT) in 2007 and M.Tech. in Mechanical Engineering (Mechatronics) from National Institute of Technology Rourkela, India in 2011. She has awarded with Ph.D. degree from the same place in 2016. Her research interest is mobile robot navigation in all terrain (surface and underwater) using AI based computational techniques.

Dr. Barik has thirteen years of experience in teaching in undergraduate and postgraduate level. He has also an excellent research career in the area of Solar Photovoltaic Grid Integrated System.He has a number of research publications in SCI, Scopus indexed journals.

Sushree Shataroopa Mohapatra has born in Bhubaneswar in 1991.She has received her B.Tech,M.Tech degree from BPUT & KIIT University in 2012 & 2014 respectively.She joined Maharaja Institute of Technology in July, 2014 Since 2017 she has been with Gandhi Institute for Technology(GIFT)as an Assistant Professor.
She is continuing her Ph.D from 2017 in KIiT university.Her main areas of research interest are Microgrid Protection, Islanding Detection and its control.
She is a life member of Solar Energy Societyof India and The Institution of Engineers , India.

Available online at www.sciencedirect.com

ScienceDirect

Materials Today: Proceedings 5 (2018) 20727–20735

materialstoday: PROCEEDINGS

www.materialstoday.com/proceedings

ICMPC_2018

Impact of milling time and method on particle size and surface morphology during nano particle synthesis from α-Al_2O_3

Nabnit Panigrahi[a], Rajeswari Chaini[a], Ayusman Nayak[a],Purna Chandra Mishra[b,*]

[a] *Department of Mechanical Engineering, Gandhi Institute for Technology, Bhubaneswar, Odisha, India*
[b]*School of Mechanical Engineering, Kalinga Institute of Industrial Technology, Deemed to be University, Bhubaneswar-24, India*

Abstract

In this paper, ball milling of Industrial Alumina (α-Al_2O_3) powder was studied with varied milling time. For reducing the size of the particle Ball milling top down approach is adopted. The average size of micro level alumina was 70 µm. The conversion was carried out by grinding process at two different stations for different time periods. Rotational speed, balls to powder ratio, water to powder ratio and milling time are the parameters included in this study. The scanning electron microscopy (SEM) result of the sample which was carried out by Insmart System for 120 hours ground materials indicates non contaminated particle but, did not give any clear picture of size. The grinding work by ball milling was carried out for 10 hours after rinsing of the jar with alumina. The result indicates that the size of Alumina is reduced from 70 µm to 1.4 µm with grey color agglomeration particles.

Selection and/or Peer-review under responsibility of Materials Processing and characterization.

Keywords: Alumina powder, ball milling, particle size reduction, scanning electron microscopy, transmission electron microscopy

1. Introduction

Nanotechnology is considered to be a multidisciplinary and an interdisciplinary area of Research and development. The wide-ranging of applications that nanotechnology is and will be catering to speaks of its omnipresence.Nanotechnology finds a defining role to play in the field of agriculture, energy, electronics, medicine, healthcare, textiles, transport, construction, cosmetics, water treatment etc., as suggested by many researchers worldwide [1].In this context, a particle is defined as a small object that behaves as a complete unit with respect to

* Corresponding author. Tel.: +0-674-654-0805;
*E-mail address:*pcmishrafme@kiit.ac.in

Selection and/or Peer-review under responsibility of Materials Processing and characterization.

its transport and properties.Nanoparticles in nanofluids are made of metals, oxides, carbides or carbon nano tubes and the size ranging from 1 to 100 nanometer (10^{-9} mm).The materials include in nanoparticles are namely, oxide ceramics (Al_2O_3, CuO), Metal carbides (SiC), Nitrides (AlN, SiN), Metals (Al, Cu), Non-metals (Graphite, Carbon nanotubes), Layered (Al + Al_2O_3, Cu + C). A nanofluid are the new class engineered fluid with high thermal conductivity obtained by suspending nanometer size (1-100nm) particles is a base fluid like water, Ethylene- or tri-ethylene-glycols and other coolants, Oil and other lubricants, Bio-fluids and Polymer solutions. In other words, nanofluids are nanoscale colloidal suspensions containing condensed nanomaterials and it is agglomerate-free stable suspension for long durations without causing any chemical changes in the base fluid [2]. Solid and liquid phase are the two phases in the system. Nanofluid have been found to possess boosted thermo physical properties for instance thermal conductivity, thermal diffusivity, viscosity, and convective heat transfer coefficients compared to those of base fluids like water or oil.[3]. Nanoparticles suspended in different base fluids can alter the momentum and heat transfer features of the velocity and thermal boundary layers by significantly increasing the liquid viscosity and thermal conductivity[4]. Owing to the outstandingfeatures of nanofluids, it finds wide applications in enhancing heat transfer. Most engineering products bring about from nanotechnology will be imperilled to heat transfer analysis, as thermal considerations have always been an essential part of any new design. Researchers realized that the obtainablemarcoscale data were inadequate to forecast fluid flow and heat transfer characteristics in heat exchangers and many engineering devices.Cooling plays a significant role in most of the engineering devices. Conventional methods adopted were providing fins to increase the surface area, increase pump power for increasing the flow rates. Also conventional heat transfer fluid like engine oil, ethylene glycol and water have naturally poor thermal conductivity compared to solids and also conventional fluid do not work with the emerging “miniaturized” knowledge due to chance of clogging the tiny channels of these devices. However, novel and superior cooling technology is the want of the hour.

Alumina, silicon, aluminum, copper, and silver shows higher magnitude heat transfer rate in increasing order. The thermal conductivity of silver, alumina and engine oil is 429 W/m-K, 40 W/m-K and 0.145 W/m-K correspondingly. Dispersing solid particles in fluids to enhance thermal conductivity give the basic concept of nanofluids. The foremost challenge is the quick settling of these solid particles in fluids. Nanoparticles differs from microparticles by better dispersion behavior, less clogging and abrasion and much larger surface area to volume ratio.

Theoretical and experimental investigations have been conducted by many researchers for production, preparation and its steadiness. Nanofluids were first originated by Choi and Eastman in 1995 at the Argonne National Laboratory, USA. Since then, there has been rapid development in the synthesis techniques for nanofluids [5]. Sridhara and Sathapathy have abridged the fundamentals of nano fluid, its preparation methods and the factors effecting the thermal conductivity boost in the Al_2O_3 base nano fluid [2]. PramodWarrier and AmynTeja concluded that the decrease in the thermal conductivity of the solid with particle size must be considered when developing models for the thermal conductivity of nanofluids.[6] A number of investigations revealed that the nanofluid heat transfer coefficient could also be increased by more than 20% in case of very low nano particles concentrations[7-8]. Das et al. concluded that nanofluids show great potential for use in cooling and the connected technologies. Oxide nanoparticles-based nanofluids are relatively less promising in the enhancement of thermal conductivity of fluids. Also the enhancement diminishes rapidly with the increase in particle size [9]. Researchers discovered that nanofluids has shown numerous distinct properties with large enhancements in thermal conductivity as compared to the base liquid, temperature and particle size dependence reduced friction coefficient , and significant increase in critical heat flux [10-14]. Mishra et al. studied that the thickness of nano fluid depends on many parameters such as base fluids, particle volume fraction, particle size, particle shape, temperature, shear rate, pH value, surfactants, dispersion techniques, particle size distribution and particle accumulation [15].

The current study focused on the conversion of micro alumina to nano alumina by top down approach and wet grinding process, characterization of ground particles and investigation on the effect of grinding time on the characteristics of the particles.

2. Materials and methods

Top down process is a traditional route scaling down processes acquainted in macro and micro engineering. In top down approaches an outside force is applied to a solid particles which is then break-up into smaller particles. Concerted incremental improvement in the entire manufacturing process transforms precision engineering into ultra precision engineering. The stiffness of the parts of mechanical devices used to form objects is particularly

significant. Material is removed by grinding. A characteristic of particles in grain refining process is that their surface energy upturns, which causes the combination of particles to increase. In dry grinding method the solid substance is ground as a result of shock, a compression, or by friction, using such popular methods as a jet mill, hammer mill, a shearing mill, a roller mill, shock shearing mill a ball mill and a tumbling mill. It is tough to obtain particle less than 3 μm size by means of dry grinding since condensation of small particles takes place simultaneously with pulverization. But, in wet grinding the solid substrate is carried out using a tumbling ball mill, a planetary mill or a vibratory ball mill, a centrifugal fluid mill, an agitating beads mill, a flow conduit beads mills an annular gap bead mill or a wet jet mill. The wet process is appropriatefor averting the condensation of the nanoparticles so formed, and thus it is possible to obtain highly dispersed nano particles. A distinctive synthetic method for nanoparticles for the top-down methods is given in Fig.1.

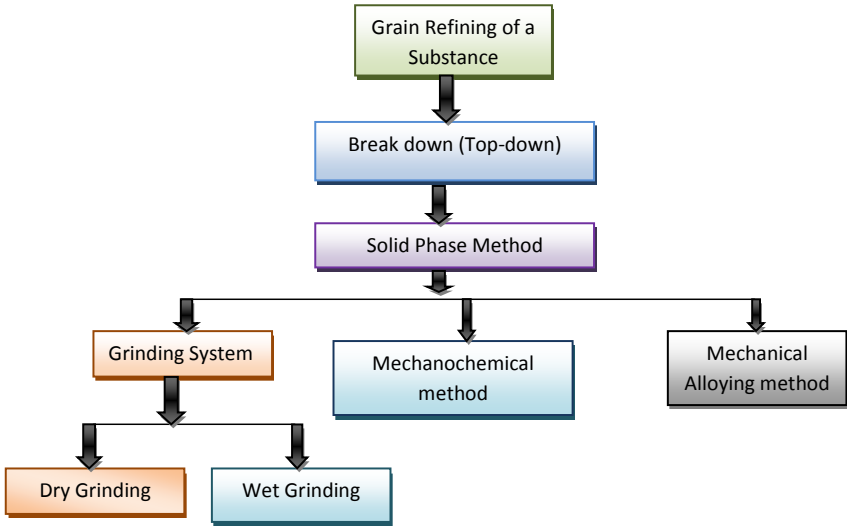

Fig.1. A distinctive synthetic method for nanoparticles for the top-down approaches

The average particle size of the raw material is found to be 68.308 μm which has been tested in PSA (Particle Size Analyzer). The tested report is shown in Fig. 2.

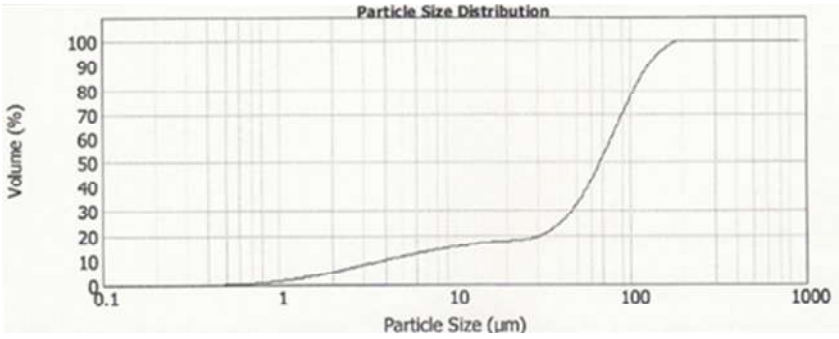

Fig.2. The average particle size of alpha alumina sample

The conversions from micro to nanoparticles were carried out by wet grinding process at two different stations for different time periods.

- Station I
- Station II

3. Results and discussion

3.1 Station I results

The 1st phase of grinding work was carried out for 80 hrs, 120 hrs and 140 hrs. The Field emission - Scanning electron microscope (FE-SEM) and Energy dispersive X-Ray spectroscopy (EDS) testswere carried out in Indian institute of chemical technology (IICT) Hyderabad. FE-SEM data for 120 hours ground sample at different magnification is shown in Fig. 3.EDS result of 120 hours sample is shown in Fig. 4.The FE-SEM data for 140 hours ground sample at different magnification is shown in Fig. 5.EDS result of 140 hours sample is shown in Fig. 6.

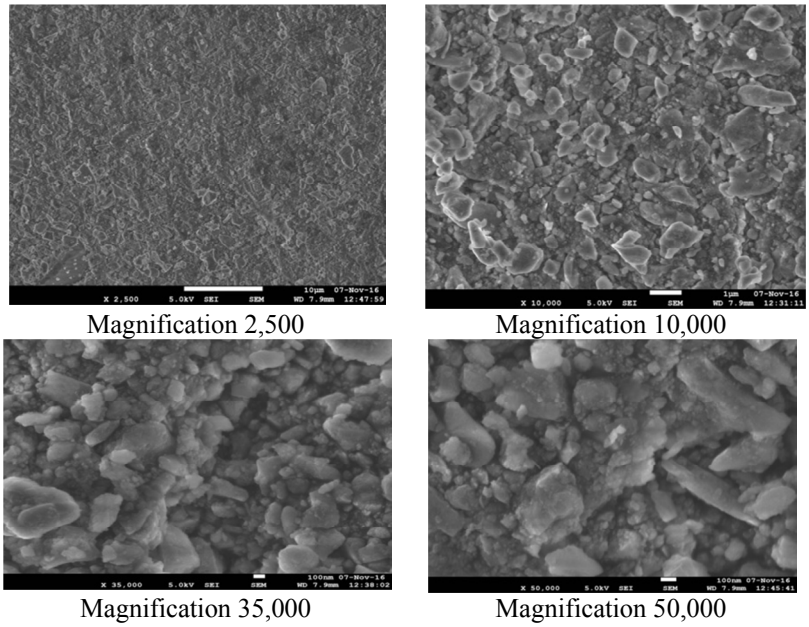

Fig. 3. FE-SEM data for 120 hours ground sample at different magnification.

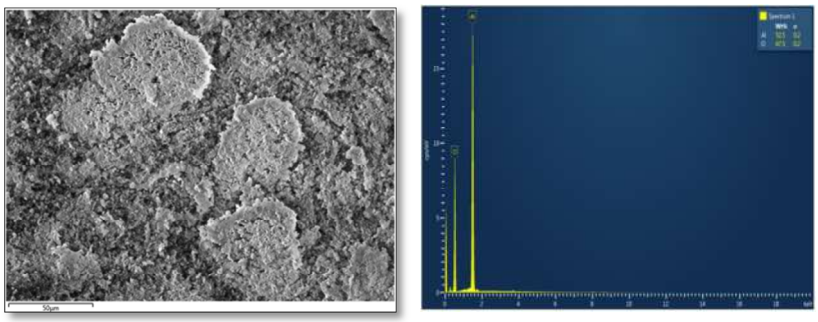

Fig.4. EDS result of 120 hours sample

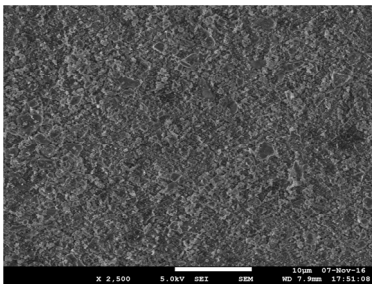

Magnification 2,500

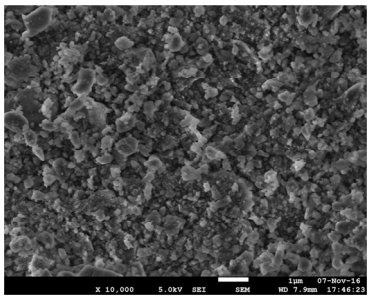

Magnification 10,000

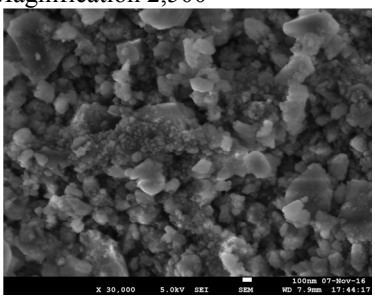

Magnification 30,000

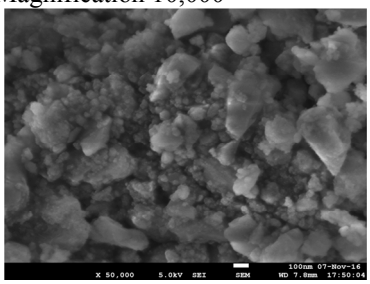

Magnification 50,000

Fig. 5. FE-SEM data for 140 hours ground sample at different magnification.

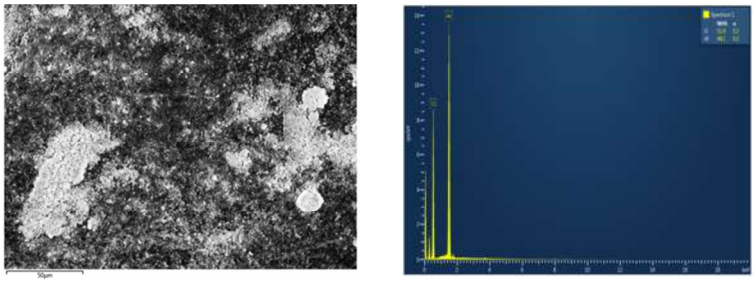

Fig.6. The EDS result of 140 hours sample

Fig. 5 and Fig. 6 indicated that the size of the Alumina is not as per our requirement and is above 100 nm. The ground samples indicates that there was no contamination but does not give any clear picture of size. Thus, the above said sample has been tested for TEM and PSA to get a clear picture of size shown in Fig. 7 and Fig. 8.

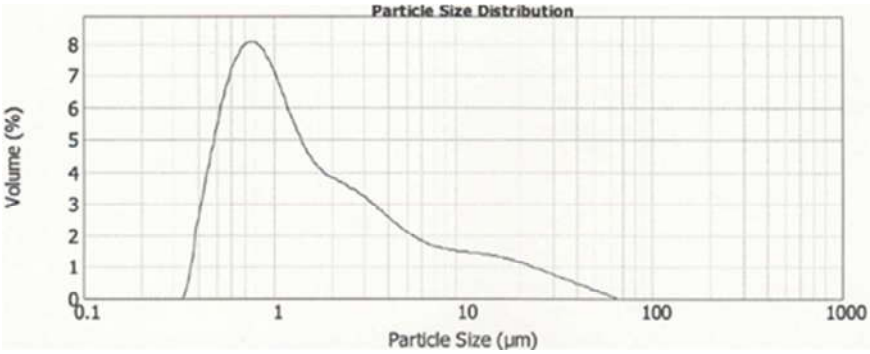

Fig. 7. Particle size analysis of 120 hours ground alumina

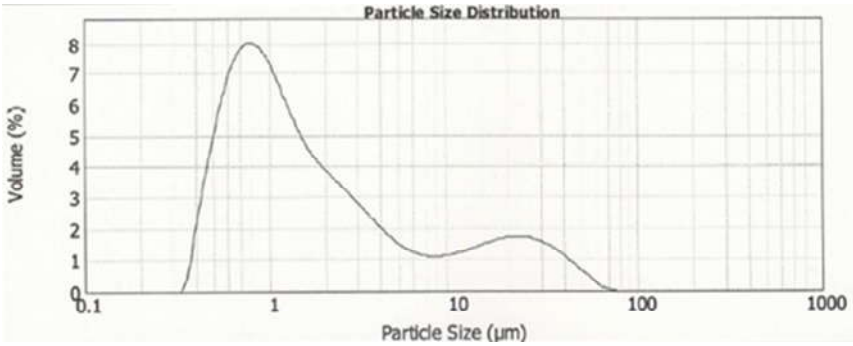

Fig. 8. Particle size analysis of 140 hours ground alumina

The above result showed that the average particle size of 120 hours ground sample was 1.268 µm and for 140 hours ground sample was 1.301 µm. Thus further grinding is required for the above ground sample to achieve nano.

3.2 Station II results

The grinding process was carried out in a dual drive mill which is a planetary ball mill shown in Fig. 9. The material of jar and balls are made up of stainless steel and the size of ball is of 10 mm diameter. The principle behind this is that during the mechanical alloying the powders are cold welded and fractured. The mill comprises of a single turn disc and double bowls. The turn disc rotates in one direction while the bowls rotates in the reverse direction. The centrifugal forces, created by the rotation of the bowl around its own axis composed with the rotation of the turn disc, are applied to the powder mixture and balls in the bowl are interchangeably synchronized. Thus friction caused from the hardened milling balls ground the powder mixture. Thus the powder mixture is fractured and cold weld under high energy impact.

Initially the jars were rinsed with sample alumina for 10 hours as previously the jars were exposed to iron oxide material shown in Fig. 10. 220 gm of alumina per jar (2 jars) was placed in the ball mill and was ground for 5 hours and 10 hrs in their dual drive mill laid open to high-energy collision from the balls.

Fig. 9 Planetary ball mill and jar

Fig.10.10 mm stainless steel grinding balls before rinsing and after rinsing with Al_2O_3.

The ground sample was collected by rinsing with toluene acid shown in Fig. 11.

Fig. 11.The ground sample collection after rinsing with toluene.

The above ground sample was tested for particle size analysis. The report is shown in Fig. 12 and Fig. 13. The average size of particles milled at different times and at different stations are shown in Table 1.

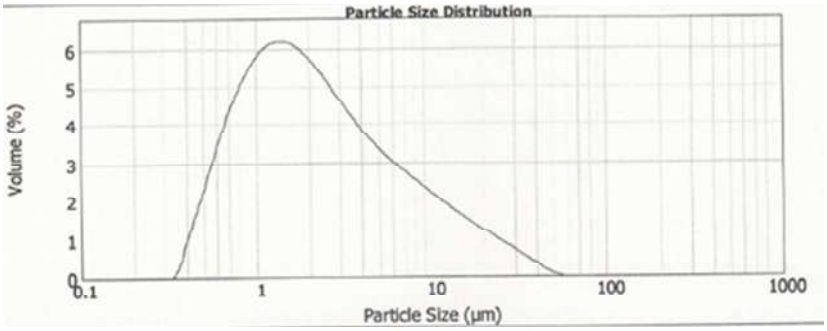

Fig.12. Particle size analysis of 5 hours ground alumina

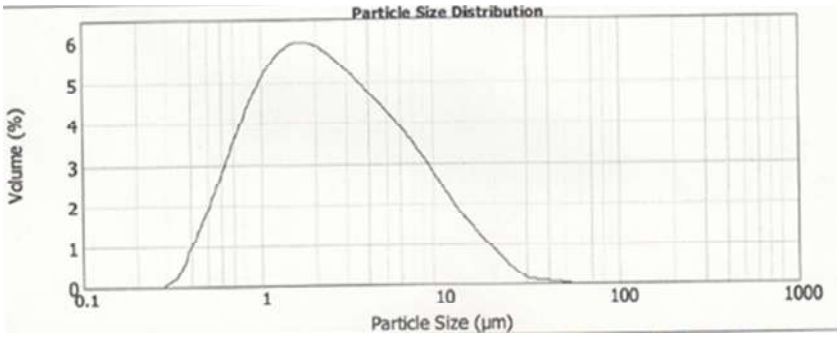

Fig .13. Particle size analysis of 10 hours ground alumina.

Table 1 The average size analysis result of different machines ground for different hours

Sl. No.	Work Station	No of hours ground	Average size (µm)
1	Raw Material (α-Al_2O_3)	0	68.308
2	Station-I	120	1.268
3	Station-I	140	1.301
4	Station-II	5	2.052
5	Station-II	10	2.306

After grinding in different ball mills and looking to their average sizes, it has been observed that the average size of every sample is about 1 micron. This might be because of the particle agglomeration or coating of some other material. Leaching process was carried out for removing the coating, hopeful that the size will reduce to nano size. Result of the leaching with 10 % HCL shown in Fig.14, is not satisfactory, followed by higher percentage of HCL leaching with 30%.

Fig. 14. Sample with 10% leaching.

Leaching of ground Alumina powder with higher concentration (20% and 30%) of HCL has been carried out shown in Fig. 15 and the samples are sent for characterization.

Fig. 15. Sample with 30% leaching.

4. Conclusions

- Micro sized α-Al_2O_3as received from National Aluminum Company Limited (NALCO) was successfully converted to nano alumina.
- The alumina powders were converted to nano size through wet grinding process at different times to investigate the effect of grinding time on characteristics of the particles.
- It was observed that the more was the grinding time the lesser was the particle size.

Acknowledgements

The authors greatly acknowledge the assistance of IMMT, Bhubaneswar, NALCO India Ltd., Talcher and IICT, Hyderabad, India for the nanoparticles preparation and characterization.

References

[1]A. Kumar, RIS Discussion Papers, RIS-DP # 193 (2014) 1-33.

[2]V. Sridhara, L. N. Satapathy, NanoscaleRes. Lett. 6 (2011) 456.

[3]W. Yu, H. Xie, J. Nanomater. 2012 (2012) Article ID 435873, doi:10.1155/2012/435873.

[4]Edel, Z. J. Doctoral dissertation, Michigan Technological University (2013).

[5] S. U. S. Choi and J. A. Eastman, No. ANL/MSD/CP—84938, CONF-951135--29, ASME Int. Mech. Eng. Cong. Exh. San Francisco, Calif, USA, 1995.

[6]P. Warrier, A. Teja, Nanoscale Res. Lett. 6 (2011) 247.

[7]Y. Xuan, Q. Li, Int. J. Heat Fluid Flow, 21(2000) 58.

[8]H. U. Kang, S. H. Kim, J. M. Oh, Exp. Heat Transf. 19 (2006), 181.

[9] S. K. Das, S. U. S. Choi, H. E. Patel, Heat Transf. Eng., 27 (2006) 3-19.

[10]K. S. Gandhi, Current Sci., 92(2007) 717-18.

[11]C. H. Chon, K. D. Kihm, Appl. Phys.Lett. 87 (2005), 153107-1 to 3.

[12]B. Yang, Z. H. Han, Appl. Phys. Lett. 89 (2006) 08311-1 to 3.

[13]K.M. Kostic, Proc. MN2006, Multifunctional nanocomposites. Honolulu, Hawaii. Sept 2006, 20-22.

[14]D. Yulong, H. Alias, D. Wen, R.A. Williams, Int. J. Heat Mass Transf., 49 (2006) 240-250.

[15]S. Mukherjee, P. C. Mishra, S. K. S. Parashar, P. Chaudhuri, Heat Mass Transf. 52 (2016) 2575-2585.

2019-20 C.

Predictive Modeling and Optimization of Technological Response Parameters in Nd:YAG Laser Microgrooving of Titanium Alloy Using Combined RSM-PSO Approach

Samir Kumar Panda, Sudhansu Ranjan Das and Debabrata Dhupal

Abstract The present work focuses on modeling and optimization during Nd:YAG laser microgrooving of Ti_6Al_4V titanium alloy material with an objective to find the optimum process parameters settings for the groove upper width as well as depth and heat-affected zone. The experiments are performed as per Box–Behnken design of experiments (BBDOEs) with four process parameters (diode current, pulse frequency, scanning speed, and number of passes) for parametric optimization in order to control the technological response characteristics of the precision microgrooves on Ti_6Al_4V titanium alloy. Analysis of variance (ANOVA), response surface methodology (RSM) and particle swarm optimization (PSO) are subsequently proposed for predictive modeling and process optimization. The methodology described here is expected to be highly beneficial for manufacturing industries.

Keywords Laser microgrooving · TI_6AL_4V · ANOVA · RSM · PSO

1 Introduction

The recent technology has been advancing to infinite extent in search of newer materails and alloys with high hardness, strength and less weight which are very difficult to be machined with the conventional machining processes for achieving the required accuracy and precision. Nowadays, there is a vast demand for the well-finished products of titanium alloy materials with high accuracy and complex integrated designs. Such features on a component can be achieved only through the advanced manufacturing process, especially by laser beam machining. In case of micromachining the feature size is less than 1 mm. Hence lasers are increasingly employed for a precise micromachining because their beams can be focused accurately on microscopic areas, and attributed to a number of advantages which are normally applicable to whole range of the materials processing applications, like, non-contact processing,

S. K. Panda · S. R. Das (✉) · D. Dhupal
Veer Surendra Sai University of Technology, Burla 768018, India
e-mail: das.sudhansu83@gmail.com

L. Vijayaraghavan et al. (eds.), *Emerging Trends in Mechanical Engineering*,
Lecture Notes in Mechanical Engineering,
https://doi.org/10.1007/978-981-32-9931-3_17

high productivity, eradication of the finishing operations, minimized cost of processing, and enhanced the quality of product, maximize material utilization, green manufacturing and minimize the heat-affected zone. The above-cited advantages can only be obtained with appropriate selection of process parameters. Researchers have employed various methods MRA [1, 2] and ANN [3, 4] for mathematical modeling in order to predict the responses and Taguchi method [5], RSM [6, 7], GA [8, 9], PSO [10, 11] for optimization the controlled process parameters during laser micromachining process, that have been explored as productivity and reliable tool in advanced computing technology for high-quality frameworks since it gives a straight-forward, skilled, and systematically optimize the output, such as cost, quality, and performance. The proper utilization, along with appropriate adjustment of machining controllable process parameters are of main importance for achieving fine grade of microgrooves, which generally utilize proper time and effort due to the frequently changing behavior of the laser micromachining process. Thus, the present study focuses on development of mathematical models and multi-response parametric optimization during laser microgrooving of titanium alloy (Ti_6Al_4V) through Nd:YAG laser treatment using statistical approach such as response surface methodology (RSM) followed by, computational approach like particle swarm optimization (PSO).

2 Experimental Procedure

A 75 W diode-pumped Nd:YAG laser (make: Sahajanand, model: SPRIGO LD) was used to conduct the experiments which has assist gas supply unit. During experiment, the laser beam (focal length of 77 mm) has been set at surface of the workpiece as the focal plane which resulted in laser beam spot size around 21 μm. In the present research, Ti_6Al_4V titanium alloy plate of dimension (75 mm * 25 mm * 5 mm) is considered as the workpiece material for experimentation, subjected to microgrooving by multiple laser pulses (DPSS Nd:YAG laser treatment) with actual peak power vary between 0.7–5 kW.

In the current investigation diode current, pulse frequency, scan speed, and number of pass are considered as the input process parameters which influence the technological response characteristics of laser microgrooving such as, upper width, heat-affected zone and groove depth. The different process parameters and their values are shown in Table 1. Using the abovementioned process parameters (4) each with five different levels, a well-designed experimental layout is formulated in conformance with Box–Behnken design of experiments (BBDOEs) which is consisting of thirty-one (31) number of trials. Design of experimental plan with actual value of process parameters, measured response are presented in Table 2. All the experiential trials for laser engraving are performed with argon gas. The upper width (GWD), heat affected zone (HAZ) and groove depth (GD) of machined microgroove is measured by utilizing scanning electron microscope (make: Hitachi, model: SU3500).

Table 1 Process parameters and levels

Parameters	Symbols	Units	Levels				
			−2	−1	0	1	2
Diode current	X_1	amp	18.5	20	21.5	23	24.5
Pulse frequency	X_2	kHz	28	31	34	37	40
Scan speed	X_3	mm/s	40	50	60	70	80
Number of passes	X_4		9	10	11	12	13

The schematic view of experimental work and methodology proposed in the current study, is presented in Fig. 1.

3 Results and Discussion

3.1 *Development of Response Model*

The results of response characteristics, i.e., groove width (GWD), groove depth (GD) and heat-affected zone (HAZ) which were obtained in accordance of BBDOEs, were analyzed in Minitab 16 through response surface methodology (RSM) and developed the mathematical models to find-out the best-fit of correlation between the abovementioned response (GWD, GD, HAZ) of the microgrooved component with the input parameters such as diode current (X_1), pulse frequency (X_2), scanning speed (X_3) and number of passes (X_4). Regression equations in the second-order (i.e., quadratic model) for the responses are presented by:

$$\begin{aligned} Y_{\mathrm{GWD}} = {} & -2663 + 37.6X_1 + 47.5X_2 - 1.29X_3 + 303.1X_4 + 2.199X_1^2 + 0.272X_2^2 \\ & + 0.00573X_3^2 - 3.052X_4^2 - 1.458X_1X_2 - 0.1708X_1X_3 - 5.958X_1X_4 \\ & + 0.0604X_2X_3 - 3.354X_2X_4 + 0.194X_3X_4 \end{aligned} \tag{1}$$

$$\begin{aligned} Y_{\mathrm{HAZ}} = {} & 1189 - 54X_1 - 2.93X_2 - 14.64X_3 - 15.2X_4 - 0.428X_1^2 \\ & - 0.4888X_2^2 - 0.008X_3^2 - 1.4X_4^2 + 0.915X_1X_2 + 0.3287X_1X_3 \\ & + 2.437X_1X_4 + 0.2694X_2X_3 - 0.073X_2X_4 - 0.0731X_3X_4 \end{aligned} \tag{2}$$

$$\begin{aligned} Y_{\mathrm{GD}} = {} & 2222 - 383.7X_1 + 166.7X_2 + 10.03X_3 - 238X_4 + 9.370X_1^2 \\ & - 0.49X_2^2 - 0.1816X_3^2 + 20.09X_4^2 - 5.083X_1X_2 + 1.408X_1X_3 \\ & + 7.58X_1X_4 + 0.521X_2X_3 - 4.71X_2X_4 - 3.088X_3X_4 \end{aligned} \tag{3}$$

To avoid the misleading conclusion, statistical analysis is performed for the proposed RSM models (GUW, HAZ, and GD) by employing ANOVA in order to check

Table 2 Design of experimental plan and experimental results

Run	Coded values				Actual settings				Responses		
	X_1	X_2	X_3	X_4	Diode current (amp)	Frequency (kHz)	Scan speed (mm/s)	No. of passes	GUW (μm)	HAZ (μm)	GD (μm)
1	1	1	−1	−1	23	37	50	10	334.0938	48.865	244.989
2	0	0	0	−2	21.5	34	60	9	277.406	62.684	378.406
3	−1	−1	1	1	20	31	70	12	309.968	36.978	252.364
4	−1	1	−1	−1	20	37	50	10	303	41.787	295.25
5	0	0	0	0	21.5	34	60	11	305.5	62.314	323.75
6	0	0	0	2	21.5	34	60	13	297.781	58.471	457.197
7	0	−2	0	0	21.5	28	60	11	301.281	52.196	291.781
8	−1	1	1	−1	20	37	70	10	304.343	47.865	395.177
9	−1	1	1	1	20	37	70	12	315.75	37.362	331.666
10	−1	−1	−1	−1	20	31	50	10	258.468	71.265	240.197
11	0	0	0	0	21.5	34	60	11	299.25	66.764	335.5
12	0	0	0	0	21.5	34	60	11	292.25	64.764	327
13	2	0	0	0	24.5	34	60	11	335.281	74.184	452.197
14	−1	−1	1	−1	20	31	70	10	256.875	47.225	272.562
15	1	−1	−1	−1	23	31	50	10	320	68.037	264.375
16	1	−1	−1	1	23	31	50	12	329.718	71.378	425.177
17	0	0	0	0	21.5	34	60	11	301.25	65.939	334.75
18	1	−1	1	−1	23	31	70	10	310.968	58.190	387.677
19	0	0	2	0	21.5	34	80	11	301.156	56.196	311.822
20	−1	1	−1	1	20	37	50	12	301.093	32.953	352.677

(continued)

Table 2 (continued)

Run	Coded values				Actual settings				Responses		
	X_1	X_2	X_3	X_4	Diode current (amp)	Frequency (kHz)	Scan speed (mm/s)	No. of passes	GUW (μm)	HAZ (μm)	GD (μm)
21	0	0	0	0	21.5	34	60	11	300.75	69.014	304.75
22	−1	−1	−1	1	20	31	50	12	312.5	70.862	355.687
23	0	0	0	0	21.5	34	60	11	304.75	64.264	304.875
24	0	0	−2	0	21.5	34	40	11	303.031	69.759	217.781
25	1	1	−1	1	23	37	50	12	301.875	59.875	338.479
26	1	−1	1	1	23	31	70	12	319.75	66.512	424.791
27	0	2	0	0	21.5	40	60	11	317.906	44.959	347.822
28	1	1	1	1	23	37	70	12	306.593	80.378	393.156
29	0	0	0	0	21.5	34	60	11	303.25	63.239	341.375
30	1	1	1	−1	23	37	70	10	319.25	74.537	413.354
31	−2	0	0	0	18.5	34	60	11	303.906	50.471	391.406

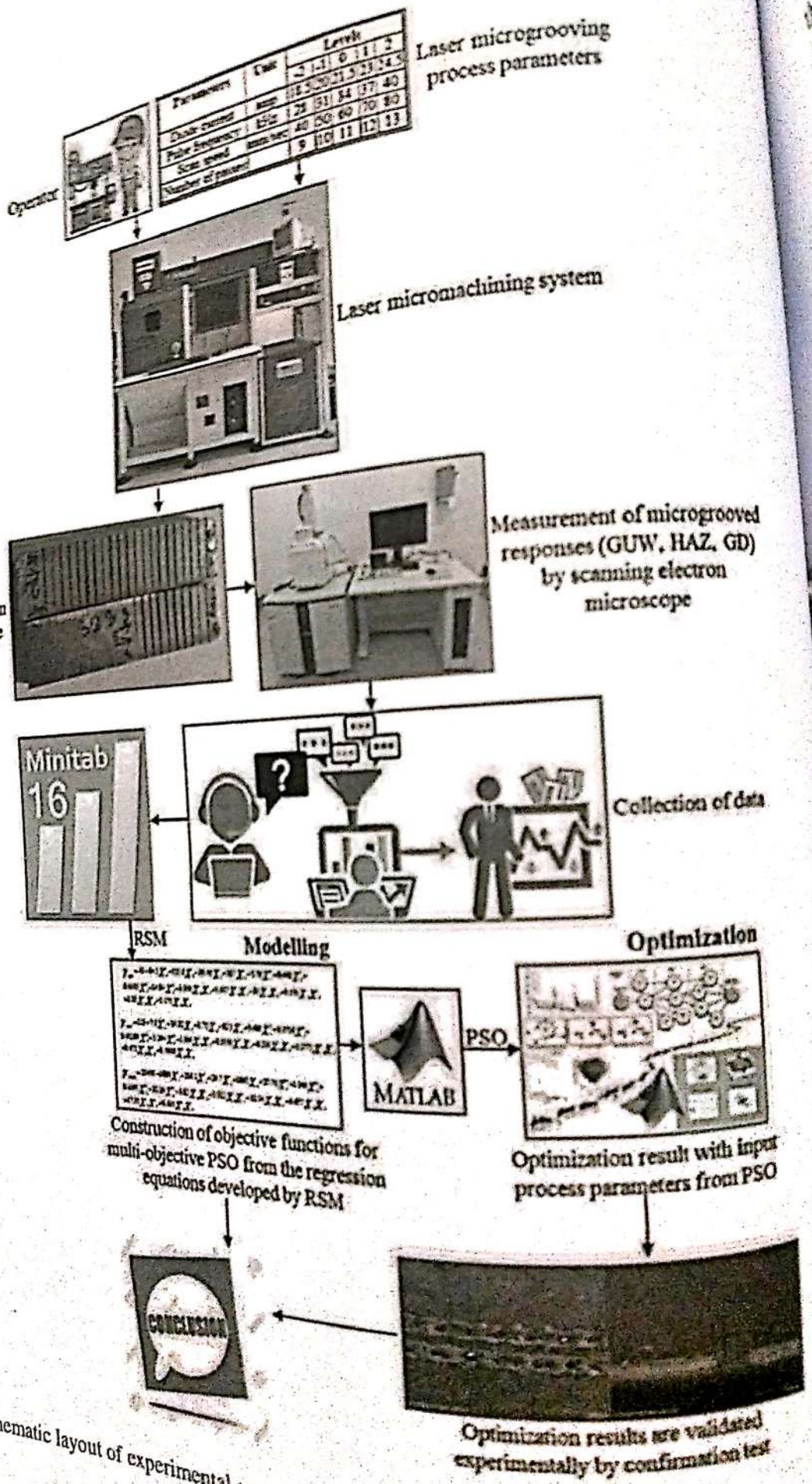

Fig. 1 Schematic layout of experimental setup and methodology proposed

their adequacy and validity, as shown in Table 3. The estimate F-value of the models for GUW, HAZ, and GD are 27.14, 25.15, and 31.05, respectively, which shows the excellent significance of model because of lower magnitude of F-table value (2.46) at 95% of confidence level. Moreover, it can be clearly seen that the developed quadratic models are statistically significant as the P (probability) value is under 0.05. Particularly, the model developed using RSM for groove width, groove depth and heat-affected zone explain the R^2 values (i.e., co-efficient of determination) of 0.959, 0.956, and 0.964, respectively, which are very close to unity (1) ensuring the excellent fit for the model with greater statistical significance. Finally, normal probability plot combined with Anderson–Darling test for GUW, HAZ, and GD is shown in Fig. 2, which ensures that the residuals distributed fairly close to a straight line indicating that the errors are dispersed normally and specifying that the terms associated with the model are significant. With p-value (0.103 for GUW, 0.055 for HAZ, and 0.11 in case of GD) received from Anderson–Darling test is greater than significance level value (0.05), which confirms the adequacy of models as no reason was observed for the rejection of null-hypothesis. Hence, the proposed predictive can be utilized for particle swarm optimization.

3.2 *Response Optimization Using PSO*

Alternative method like GA, claimed to be more efficient for simultaneous optimization of multiple responses. However, the computational effort required by PSO to arrive to such high-quality solutions is less than the effort required to arrive at the same high-quality solutions by the GA, which pursuits us to consider PSO in the present study. PSO is a soft computing approach which relies on some programming commands to generate the global optimal result. The regression Eqs. (1)–(3) developed by RSM approach for groove width, heat affected zone thickness and groove depth are utilized in generation of objective function for PSO. The minimum and maximum values of the process parameters were used as constraints for the objective function. For multiple response optimizations using PSO, the following equation is proposed by taking into consideration of all the responses simultaneously optimized and optimum parameter settings can be considered by the objective function:

$$Z_{\text{GLOBALMIN}} = W_1 * \frac{Y_{\text{GWD}}}{Y_{\text{GWDMIN}}} + W_2 * \frac{Y_{\text{HAZ}}}{Y_{\text{HAZMIN}}} + W_3 * \frac{Y_{\text{GD}}}{Y_{\text{GDMIN}}} \tag{4}$$

Figure 3 presents the convergence plot, which aims to optimize the abovementioned three laser microgrooving responses in the presence of PSO specific parameters. Here, the initial swarm size is set at 50 with maximum number of iteration of 100. The constants $C1$ and $C2$ are taken as 2. By solving the optimization problem with PSO, it was found that the Z_{MIN} value is 0.2949, occurring at a weightage of 0.80 (W_1) to upper width. Also 10% i.e. weightage of 0.1 (W_1 and W_3) equal importance has been given to other two responses (heat affected zone thickness and groove

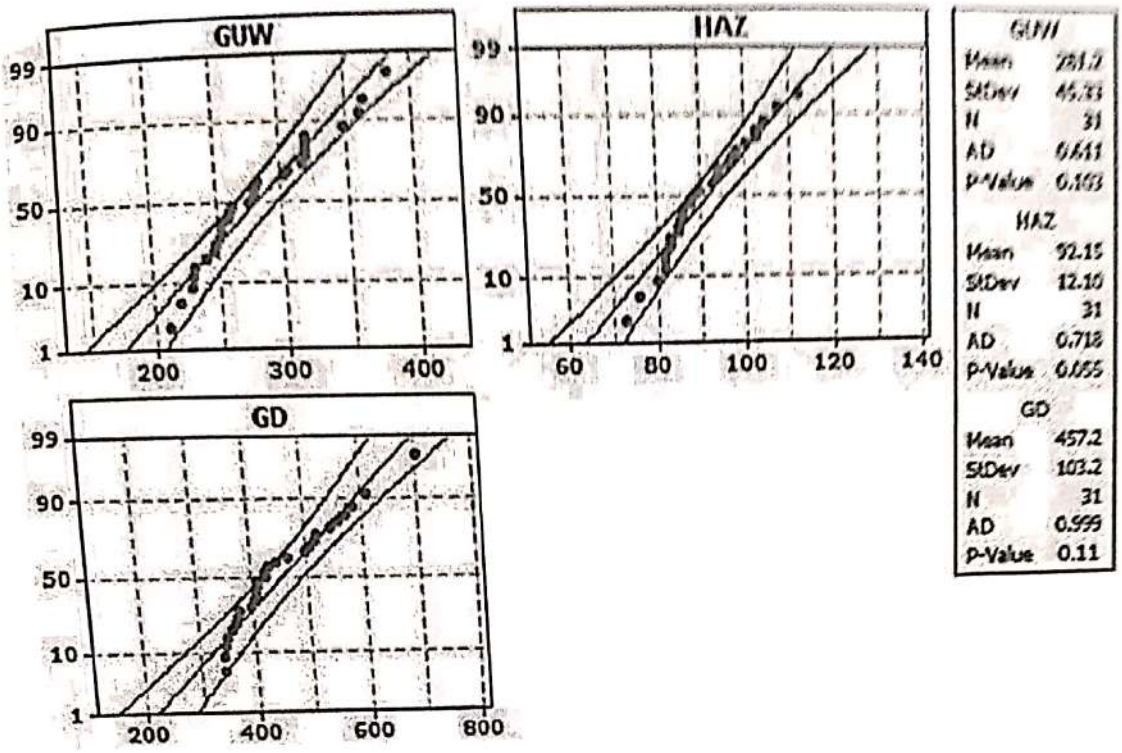

Fig. 2 Normal probability plot for technological response characteristics of laser microgroove

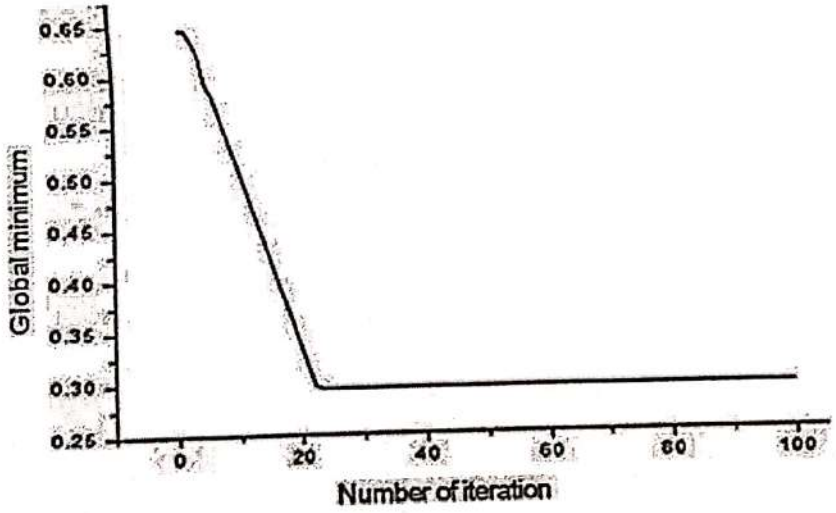

Fig. 3 Optimal convergence curve for multi-objective PSO

depth). Moreover, it can be concluded that the optimal solution occurs at sudden decrease in global minimum with a less processing time due to lesser complexity as well as significant improvement in computational efficiency of PSO algorithm. The optimal process parameters setting for microgrooving variables in laser machining of titanium alloy (Ti_6Al_4V) are diode current 18.5 amp, pulse frequency 40 kHz, scan speed 40 mm/s, no. of passes 13, with estimated groove width (GWD) of 0.124 mm, heat affected zone (HAZ) of 0.123 mm and groove depth (GD) of 0.232 mm. Finally, an additional experiment is performed with the optimal configuration (suggested by

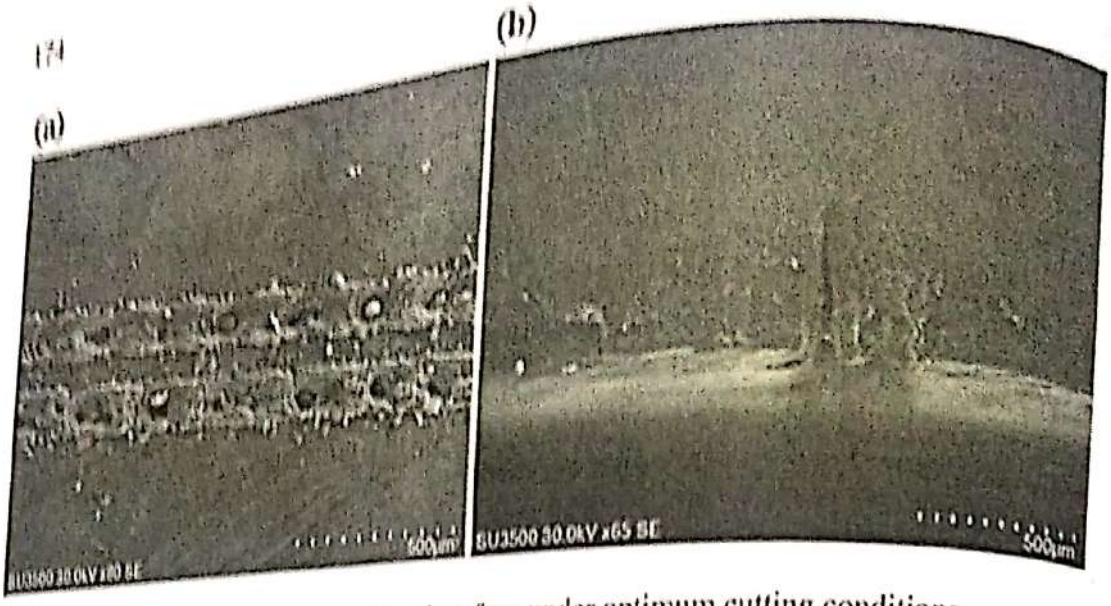

Fig. 4 SEM micrograph showing machined surface under optimum cutting conditions

PSO) in order to observe the machined microgroove using scanning electron microscope (SEM), shown in Fig. 4.

4 Conclusions

In the present work, laser engraving has been carried out on Ti_6Al_4V substrate using argon gas. The experiments were modeled using CCD based RSM approach. Empirical models proposed for the technological response characteristics such as, groove upper width as well as depth and heat-affected zone have R-square value close to one and P-value less than 0.05, which ensured the greater statistical significance with excellence of fit for the model. The normal probability plot ensures that the residuals distributed fairly near to a straight line showing the normality dispersion of errors as well as implying the sources associated with the models are significant. Anderson–Darling test for model show adequate, as P-value is over 0.05 at 95% confidence level. The regression equations developed in RSM approach were used to generate the objective function for the PSO approach, which demonstrated the ability to optimize and to accurately model the technological response characteristics of microgroove through advances in computer technology. By solving the optimization problem with PSO, corresponds to optimal setting of process parameters (diode current = 18.5 amp, pulse frequency = 40 kHz, scan speed = 40 mm/s, number of passes = 13) with estimated upper width 0.124 mm, heat affected zone 0.123 mm and depth 0.232 mm. The suggested multiple approaches (experimental, statistical, and computational) are reliable methodologies for improving laser microgrooving process and can be used in model predictive control, real-time process monitoring, and optimization in different machining process.

References

1. Dhupal D, Doloi B, Bhattacharyya B (2009) Modeling and optimization on Nd:YAG laser turned micro-grooving of cylindrical ceramic material. Opt Lasers Eng 47:917–925
2. Kibria G, Doloi B, Bhattacharyya B (2013) Predictive model and process parameters optimization of Nd:YAG laser micro-turning of ceramics. Int J Adv Manuf Technol 65:213–229
3. Biswas R, Kuar AS, Biswas SK, Mitra S (2010) Artificial neural network modelling of Nd:YAG laser microdrilling on titanium nitride—alumina composite. J Eng Manuf 224:473–482
4. Kibria G, Doloi B, Bhattacharyya B (2014) Modelling and optimization of Nd: YAG laser micro-turning process during machining of aluminum oxide (Al_2O_3) ceramics using response surface methodology and artificial neural network. Manuf Rev 1:1–8
5. Kuar AS, Acherjee B, Ganguly D, Mitra S (2012) Optimization of Nd:YAG laser parameters for microdrilling of alumina with multiquality characteristics via Grey-Taguchi method. Mater Manuf Processes 27:329–336
6. Kibria G, Doloi B, Bhattacharyya B (2012) Optimisation of Nd: YAG laser micro-turning process using response surface methodology. Int J Precis Technol 3:14–36
7. Biswas R, Kuar AS, Mitra S (2015) Process optimization in Nd:YAG laser microdrilling of alumina–aluminium interpenetrating phase composite. J Mater Res Technol 4:323–332
8. Nandi S, Kuar AS (2015) Parametric optimisation of Nd:YAG laser micro-drilling of alumina using NSGA II. Int J Mach Mach Mater 17:1–21
9. Mohammed MK, Umer U, Al-Ahmari A (2017) Optimization of laser micro milling of alumina ceramic using radial basis functions and MOGA-II. Int J Adv Manuf Technol 91:2017–2029
10. Kalita K, Shivakoti I, Ghadai RK (2017) Optimizing process parameters for laser beam micro-marking using genetic algorithm and particle swarm optimization. Mater Manuf Process 32:1101–1108
11. Dhupal D, Mohanty S, Dixit SR, Das SR, Nanda BK (2018) Micromachining on Al-SiC based metal matrix composite using DPSS laser. Mater Today: Proc 5:11304–11318

Available online at www.sciencedirect.com

ScienceDirect

Materials Today: Proceedings 5 (2018) 24133–24140

materialstoday: PROCEEDINGS

www.materialstoday.com/proceedings

IConAMMA_2017

Experimental Study on $Ca_3(PO_4)_2$-Al_2O_3 Bio-ceramic Composite Using DPSS Laser

Samir Kumar Panda[a*], Debabrata Dhupal[b], Bijoy Kumar Nanda[c]

[a]PhD scholar,VSSUT,Burla,768017, India
[b]Professor,Production Engineering,VSSUT,Burla,768017, India
[c]Professor,Production Engineering,NIT, Rourkela,769004, India

Abstract

The DPSS lasers are mostly used in industries for laser based micromachining. The present experimental study investigates the laser micro grooving operation on a sheet of Calcium phosphate-Alumina ($Ca_3(PO_4)_2$-Al_2O_3) bio-ceramic composite for bio-medical applications. The $Ca_3(PO_4)_2$-Al_2O_3 bio ceramic has been fabricated by adding 20% weight of alumina with calcium phosphate to enhance the mechanical properties of the bio-ceramics. Bio ceramics were initially used as alternatives to metals to increase their biocompatibility. $Ca_3(PO_4)_2$-Al_2O_3 bio ceramics shows the properties like bioactive and bio resorbable compounds.. Pulse frequency, pulse width, diode current and gas pressure has been taken as input parameters. Upper width, lower width and micro-grooving depth deviation has been considered as the output parameters for this present experiments for machining at different parametric combinations. This peper reports theoretical and experimental results of micro-grooved bio-ceramics with thicknesses of 3 mm by using pulsed DPSS laser. Taguchi based experimental design has been adopted to carry out experiments. Then Gray Relational Analysis (GRA) based multi response optimization of input process parameters for the outputs characteristics are performed to get the optimal conditions. The optimum machining parameters were found as; pulse frequency= 3 KHz, pulse width = 5% of duty cycle, diode current = 24 Amp and gas pressure=1.0 Kgf/cm^2.Validity of the model has been checked through experiments and the error in upper width, lower width and micro-grooving depth deviation in the validation experiments are found to be satisfactory with minimal errors. Also Scanning Electron Microscopy (SEM) images after conformation test examined from cross-sections of the micro-grooved bio-ceramic samples.

Selection and/or Peer-review under responsibility of International Conference on Advances in Materials and Manufacturing Applications [IConAMMA 2017].

Keywords: Bio-ceramics, Micro grooving, Taguchi, GRA

* Corresponding author. Tel.: +919438418034
E-mail address: samir_panda001@yahoo.com

ıtroduction

he research on biomaterials has been primarily driven by the increasing demand for hard tissue replacement. ever these materials are not useful for long term uses, because of the problems related to their durability and tioning in body fluid environment.

of the most interesting area of engineering involves development of various biomedical devices. Some of them be implantable. For example catheters, heart valves, orthodontic wires, fracture fixation plates, pacemakers, ous filling formulations, total joint replacement prostheses etc. All implantable items must be prepared from olerable materials to be acceptable by the body fluid without any kind of unwanted side effects [1-2] Bio-mics based on calcium phosphates are biocompatible and osteo-conductive and they can be bound to bone ıout an intervening fibrous connective tissues[3].

The biomedical applications of $Ca_3(PO_4)_2$-Al_2O_3 bio ceramics include spinal fusion, maxillofacial ɔnstruction, artificial bone grafts, bone augmentations, bone fillers, periodontal disease repairs and after tumour gery. Several laser materials processing techniques like micro-drilling, micro-cutting, micro-grooving, scribing, have been successfully explored and are in the centre of research for last 15 years through in-depth research vities[4]. Laser micro-grooving on bio-ceramics is in high demand in the engineering industries because of its le applications in various fields like health care and bio-medical engineering applications[5].

DPSS Nd:YAG LASER with average power of 75w has been used. A schematic diagram of Nd-YAG laser beam chine has been shown in figure-2 [5].The assist gas helps in removing the molten material from the groove zone ectively. Recent requirement with regard to the quality, flexibility, speed and production costs of the micro-ıchining process are becoming increasingly stringent. [6,7]. The process parameter like assist gas pressure plays important role in laser micro machining[8]. Different assisted gases have different reactions with the working ıterial. Oxygen and nitrogen are reactive gases used for micro-machining of composite material. Oxygen has been ed as assist gas which reacts with calcium phosphate-Alumina liberating heat energy. This reaction is exothermic nature which produces heat energy that adds to the beam energy and acts as secondary source of energy 10],[11],).Nitrogen can be used to get high edge quality and shielding effect on the work piece material but due to ɔnomic aspect it is not recommended for this purpose.

Experimental Procedure

In this study, calcium phosphate ($Ca_3(PO_4)_2$) has been used as a matrix of the composite. Calcium phosphate)7% pure) with non-toxic impurities for human consumption, commercially available alumina (α-Al_2O_3, 99.4% ure) has been used as ceramic filler in the composites. As part of this study, 20% by weight of alumina in the $Ca_3(PO_4)_2$ powder has been added to fabricate the sample by cold compaction followed by sintering at 1050 °C as he presence of 20 wt% Al_2O_3 in ($Ca_3(PO_4)_2$) bio ceramics does not allow pore size in the bulk to increase in this naterial, thereby showing higher strengths[12].

2.1 Laser Micro-grooving Procedure

Calcium phosphate-Alumina composite specimen of square cross section of size (20 x 20) mm having a mean thickness of 3 mm was used as work piece material. A square cross section micro groove has been shown in figure-1 [5]. The machining was done by Nd:YAG solid state laser at different parametric combinations as per the experimental planning. A CNC diode pumped Nd:YAG laser operated on pulsed mode & manufactured by M/s Sahajanand Laser technology. The specification of the Nd-YAG laser has been indicated on table-1.This system mainly consists of various sub-systems such as power supply unit, beam delivery unit, oxygen air supply unit, Nd:YAG rod, X,Y,Z axis movement, cooling unit, CNC controller for and a Q-Switch unit. Exact groove specification with desirable dimension was represented in the below diagram.

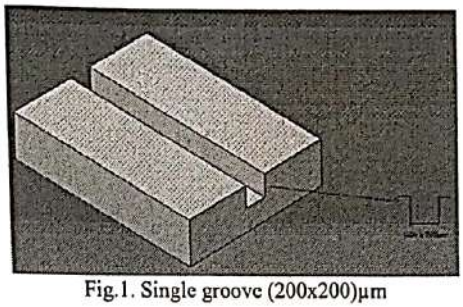

Fig.1. Single groove (200x200)µm

his research work, fabrication of micro-groove has been investigated. Nd:YAG lasers are used to produce grooves on $Ca_3(PO_4)_2$-Al_2O_3 composite. Taguchi based experiments have been designed for the mentations.

Table 1. Specifications of Nd:YAG laser machine set-up

Specification	Description
Type of laser	Nd-YAG laser 1064 nm
Operating mode	Pulsed Q-swiched
Mirror reflectivity	front mirror 80%, Rear mirror 100%
Laser beam diameter	1mm
Pulse width	120 ns
Spot diameter	21µm
Mode of beam	Fundamental mode

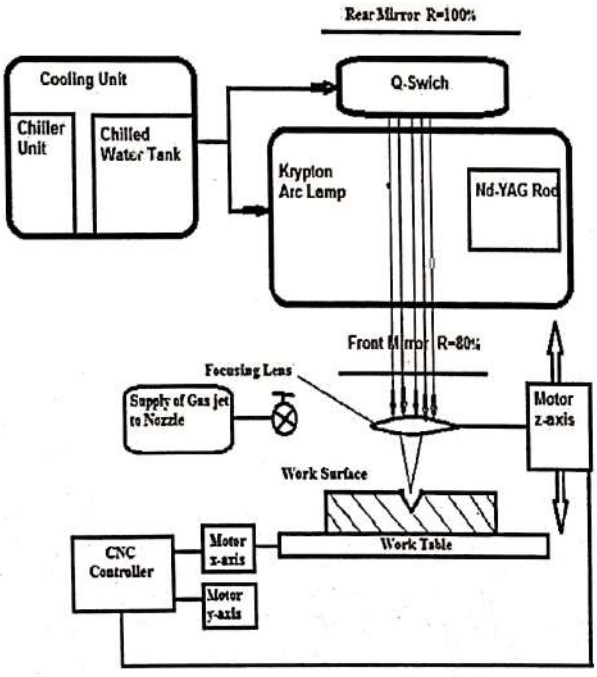

Fig.2. Schematic diagram of Nd:YAG laser beam machine set up.

thodology

esign of Experiment

guchi design matrix is particularly considered for optimization of single output response performance eteristics. The performance is calculated by signal to noise (S/N) ratio characteristics for every individual runs. uality characteristics of S/N ratio are of three different types of output response viz. Smaller is better, larger is and nominal is better. For this experimental investigation, a statistical design software Minitab 16® is used for n as well as optimizing the process parameters for betterment of the output response.

guchi method has been used for designing of the experiments to find out the critical parameters to get num settings for each input parameter. To get approximate result and the dependency of the output parameters, llowed L_{25} design. In this paper the process parameters are pulse frequency, pulse width, diode current and gas sure. The respective process parameters and their design levels are given in the table 2. Grey Relational ysis (GRA) has been implemented to convert the multi objective optimization problem to a single objective nization [13].

Table 2. Process parameters and experimental design level

Parameters	Units	Code	Level				
			1	2	3	4	5
Pulse frequency	KHz	F	3	4	5	6	7
Pulse width	%	D	5	10	15	20	25
Diode current	Amp	I_D	16	18	20	22	24
Gas pressure	Kgf/cm^2	P	0.2	0.4	0.6	0.8	1.0

Table:3 Experimental result with GRG

Run	F	D	I_D	P	D_U	D_L	D_D	Normalized value			GRC			GRG
								D_U	D_L	D_D	D_U	D_L	D_D	
1	3	5	16	0.2	0.011	0.027	-0.010	0.734	0.743	0.584	0.653	0.661	0.546	0.620
2	3	10	18	0.4	0.001	0.028	-0.047	1.000	0.728	0.847	1.000	0.648	0.766	0.805
3	3	15	20	0.6	0.034	0.022	0.071	0.152	0.835	0.000	0.371	0.751	0.333	0.485
4	3	20	22	0.8	0.015	0.027	-0.020	0.648	0.733	0.657	0.587	0.652	0.593	0.611
5	3	25	24	1	0.007	0.024	-0.051	0.836	0.796	0.879	0.753	0.710	0.805	0.756
6	4	5	18	0.6	0.022	0.044	-0.050	0.465	0.427	0.869	0.483	0.466	0.792	0.581
7	4	10	20	0.8	0.022	0.038	0.012	0.450	0.534	0.426	0.476	0.518	0.466	0.486
8	4	15	22	1	0.016	0.013	-0.010	0.620	1.000	0.584	0.568	1.000	0.546	0.705
9	4	20	24	0.2	0.019	0.022	-0.004	0.527	0.829	0.541	0.514	0.745	0.521	0.594
10	4	25	16	0.4	0.020	0.030	0.018	0.504	0.690	0.383	0.502	0.617	0.448	0.522
11	5	5	20	1	0.032	0.039	-0.068	0.202	0.528	1.000	0.385	0.514	1.000	0.633
12	5	10	22	0.2	0.030	0.039	-0.010	0.242	0.512	0.580	0.398	0.506	0.543	0.482
13	5	15	24	0.4	0.001	0.024	0.068	0.996	0.799	0.023	0.992	0.713	0.339	0.681
14	5	20	16	0.6	0.020	0.056	-0.020	0.514	0.205	0.653	0.507	0.386	0.590	0.495
15	5	25	18	0.8	0.002	0.068	-0.004	0.971	0.000	0.541	0.945	0.333	0.521	0.600
16	6	5	22	0.4	0.030	0.057	-0.022	0.247	0.193	0.669	0.399	0.383	0.602	0.461
17	6	10	24	0.6	0.024	0.029	-0.003	0.414	0.710	0.534	0.460	0.633	0.517	0.537
18	6	15	16	0.8	0.028	0.027	0.013	0.299	0.741	0.415	0.416	0.659	0.461	0.512
19	6	20	18	1	0.015	0.030	-0.047	0.646	0.691	0.850	0.585	0.618	0.770	0.658
20	6	25	20	0.2	0.040	0.047	0.005	0.000	0.366	0.476	0.333	0.441	0.488	0.421
21	7	5	24	0.8	0.008	0.027	-0.003	0.810	0.732	0.529	0.724	0.651	0.515	0.630
22	7	10	16	1	0.009	0.031	-0.020	0.797	0.673	0.656	0.711	0.605	0.592	0.636
23	7	15	18	0.2	0.019	0.030	-0.008	0.535	0.689	0.567	0.518	0.617	0.536	0.557
24	7	20	20	0.4	0.029	0.059	0.007	0.284	0.165	0.462	0.411	0.374	0.482	0.422
25	7	25	22	0.6	0.029	0.043	-0.014	0.285	0.451	0.612	0.411	0.477	0.563	0.484

zy relational analysis

ps followed in GRA are:

Normalization of experimental data.
The Grey Relational Coefficient (GRC) is evaluated from the normalized data
Grey Relational Grade (GRG) is then evaluated by taking average of the Grey Relational Coefficients (GRC)
Analysis of Variance is conducted for the input parameters with the GRG and the parameters which affect the process are found out.
Then optimum levels of the machining parameters are found out.

Normalization

cates better performance in micro grooving process for upper, lower and depth deviations are "lower the '. For grey relational analysis, for 'lower is better' response we normalized by equation (1).

$$k)=\frac{x_{i\max}(k)-x_i(k)}{x_{i\max}(k)-x_{i\min}(k)} \quad (1)$$

e $x_i^*(k)$ is the normalized data and $x_i(k)$ is the observation data for i^{th} experiment by using k^{th} response. mallest values and largest values of $x_i(k)$ in k^{th} response are $x_{i\min}(k)$ and $x_{i\max}(k)$ respectively.

Determination of Grey Relation Coefficient (GRC)

Relation Coefficient (GRC) ζ_i(k) for the k^{th} response characteristics in the i^{th} experiment may be expressed uation 2, after pre-processing the data.

$$:\frac{\Delta_{\min}+\zeta\Delta_{\max}}{\Delta_i(k)+\zeta\Delta_{\max}} \quad (2)$$

ere, $x_0^*(k)$ = represents reference sequence.

$x_j^*(k)$ = represents the comparability sequence

$\varsigma \in [0, 1]$ is the distinguished factor; whose mostly accepted value is 0.5.

$\Delta_i = \left|x_0^*(k)-x_j^*(k)\right|$, is the difference in the absolute values between $x_0^*(k)$ and $x_j^*(k)$

$\Delta_{\min} = \min_{\left(\forall j\in i\right)} \min_{(\forall k)}\left|x_0^*(k)-x_j^*(k)\right|$ = minimum value of x_i.

$\Delta_{\max} = \max_{\left(\forall j\in i\right)} \max_{(\forall k)}\left|x_0^*(k)-x_j^*(k)\right|$ = maximum value of x_i.

2.3 Calculation of grey relation grade

After calculating the GRC values, the respective Gray Relational Grade (GRG) values may be calculated by using Equation 3 as given below.

$$\frac{1}{m}\sum_{k=1}^{n} w \times \zeta_i(K) \quad (3)$$

re, γ_i is the Grey Relational Grade (GRG), 'w' the weight factor, 'm' is the number of run and 'n' is the ber of response. The GRC and the respective GRG for each experiment for micro grooving operation are then ilated. The higher value of GRG is very close to the product quality for optimal process parameters.

Results and Discussions

robability plot graph estimates cumulative distribution function from all samples by plotting each observation es against its estimated cumulative probability. The scales are transformed so that the fitted distribution forms a ght line. A good distribution fit is one where the observations are near to the fitted line. For the current rvation, 95% confidence level has been taken and the respective probability plot is shown in the Fig. 4. Here all points approximately follow the straight line, which fairly efficient to the output response.

n this experimental study, upper deviation, lower deviation and depth deviations have been measured in laser o grooving operation of Calcium phosphate-Alumina bio ceramic composite. The smaller values of the onses indicate better dimensional accuracy and groove quality of the micro grooved part. Therefore the present eriments are referred to as "smaller-the-better" type.

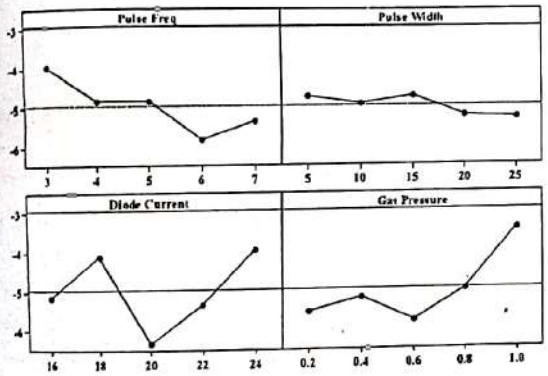

Fig. 3. Main effect plot for GRG for laser micro grooving

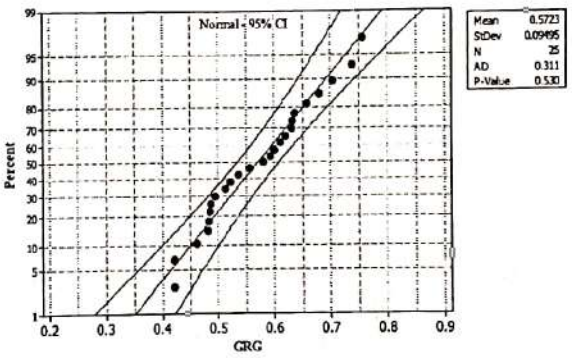

Fig. 4. Probability Plot on GRG for laser micro grooving

By using the grey relational analysis, multiple responses are converted to a single response, i.e., GRG, for the se in optimization. Four micro grooving process parameters are considered for optimizing the upper deviations, wer deviations and depth deviations, simultaneously. The experimental data found in Table 3 can be used to aluate the normalized upper deviations, lower deviations and depth deviations. These normalized values are used evaluate GRC's for both responses using equation (3). The GRG is calculated from GRC for every experimental n using equation (4). The experimental run verse GRG plot has been shown in Fig. 3. The maximum value of RGs obtained is 0.805. Higher value of GRG indicates that, comparability sequence has a good correlation with e reference sequence. The graphical representation as shown in Fig. 3 is main effect plot for GRG which exposes ie optimum machining parameters.

Table 4 ANOVA for Gray Relational Grade

Source	DF	Adj SS	Adj MS	F	P	Rank
Pulse frequency	4	0.052917	0.013229	4.80	0.029	3
Pulse width	4	0.005911	0.001478	0.54	0.071	4
Diode current	4	0.083523	0.020881	7.58	0.008	1
Gas pressure	4	0.078321	0.019580	7.11	0.010	2
Error	8	0.022029	0.002754			
Total	24					

S = 0.0524744 R^2 = 90.92% R^2 (adj) = 72.77%

The result of analysis of variance for GRG is shown in the Table 4. From all significant coefficients the highest F ue is obtained for diode current, Equal to 7.5%, means it has highest effect on response followed by gas pressure, se frequency and pulse width. As the P value is less than 0.05 represents the significant of the parameter, pulse quency, diode current and gas pressure showing significant value whereas pulse width not. The R^2 and Adj. R^2 ue obtained from the ANOVA i.e. 90.92% and 72.77 % respectively. This concludes the fitness of the model with pect to output response.

For the current experimental model the confirmatory test is carried out with the optimal parameter setting i.e. "3-24-1.5" evaluated from mail effect plot. The respective experimental as well as

Confirmatory experiment:

he predicted value of GRG ($\hat{\gamma}$) at the optimal level of the machining parameters can be found out by equation (4).

$$\hat{\gamma} = \gamma_m + \sum_{i=1}^{q} \left(\overline{\gamma_i} - \gamma_m\right) \quad (4)$$

Where γ_m is the mean of GRGs of all experiments, $\overline{\gamma_i}$ is the mean of GRG at the optimal level of i^{th} parameter, nd q represents number of machining parameters which affects GRG.

For demonstration, the initial machining parameters had been assumed to be F=5 KHz, D=10% duty cycle, I_D= 2 Amp and P= 0.2 Kgf/cm^2. With these settings, the experimental values of upper, lower and depth deviation were 0.030mm, 0.039 mm and -0.010 mm respectively. We have shown in Table 5 the optimal parameters and the predicted upper deviation, lower deviation, depth deviation and the GRG.

Table 5. Confirmation experiment results

	Optimal machining parameters	
	Initial Experiment	Optimum Experiment
Setting level	$U_D L_D D_D$	$U_D L_D D_D$
Upper width deviation	0.030mm	0.018mm
Lower width deviation	0.039mm	0.024mm
Depth deviation	-0.010mm	-0.008mm

From the above table we can see that upper deviation decreased by 40%, lower deviation decreased by 38.46% and depth deviation decreased by 20%. Thus, it is concluded that the quality may be highly improved by this study.The predicted optimized responses agree with actual responses at optimal parameter settings. The SEM image after the confirmatory test has been shown in the Fig. 5.

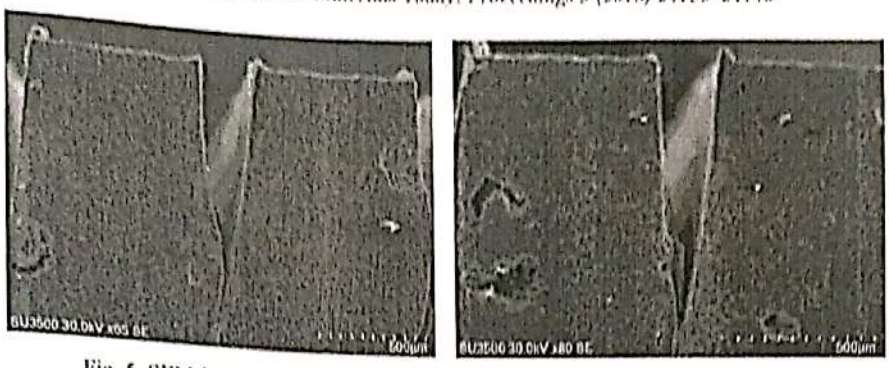

Fig. 5. SEM-image showing the upper surface, lower surface and depth of micro groove

Conclusions

Laser micro-grooving is an alternate process to micro machining when small grooves are needed. Experiments have been conducted successfully on Calcium phosphate-Alumina bioceramic composite using DPSS Nd:YAG laser operating on pulsed mode. Predefined range of process parameters according to the design of experiments were employed to obtain the responses viz. upper width, lower width & depth deviations. The experimental analysis gives following results:

- The optimum settings of micro grooving parameters are found to be F = 3 KHz, D = 5 % duty cycle, I_D = 24 Amp and P=1.0 Kgf/cm^2. A confirmatory test has been conducted and the overall improvement of in GRG was observed.
- From the main effect plots, it has been concluded that, the upper deviation varies with the lamp current and attains minimum value at medium level of lamp current with low pulse frequencies.

References

[1] P. Ducheyne, K. Healy, D. E. Hutmacher, D. W. Grainger, C. J. Kirkpatrick, Comprehensive Biomaterials (2011) 3672.

[2] B.D Ratner, A.S. Hoffman, F.J. Schoen, J.E. Lemons, Biomaterials Science, 3rd edition; Eds.; Academic Press: Oxford, UK, 2013; p. 1573.

[3] G. Selvaduray, L. Sheet, Materials Science Technology 9 (1993) 463-473.

[4] E. Fernández, F. J. Gil, M. P. Ginebra, F. C. M. Driessens, J. A. Planell, S. M. Best, Journals of Materials Science, 1999; Volume 10, Issue 3, pp 169–176.

[5] D. Dhupal, B. Doloi, B. Bhattacharyya, International Journal of Machine Tools & Manufacture 48 (2008) 236–248.

[6] A.K Dubey, V Yadava, Journals of Materials Process Technology, 2008, 195(1–3):15–26.

[7] R.K. Jain, Production Technology, Khanna Publishers, New Delhi, 2005.

[8] K. Farooq, A. Kar, Journal of Applied Physics 1998;83:12.

[9] J. Yang, J. Yu, Y.Cui, Y. Huang,.Ceramic Intnternational 2012;38:3643–8.

[10] T. M. Yue, W. S. Lau, Material and Manufacturing Process 11.1 (1996): 17-29.

[11] Woo Chun Choi, George Chryssolouris, , 1995 J. Phys. D: Appl. Phys. 28 873 .

[12] Vaibhav Trivedi, Anupam Srivastav, Rahul bhatnagar, Mohd Javed, Journal of Mechanical and Civil Engineering ,2016, PP 63-67.

[13] Shreemoy Kumar Nayak, Jatin Kumar Patro, Shailesh Dewangan, SoumyaGangopadhyay, Procedia Materials Science 6 (2014) 701 – 708

Node Localization by using Fuzzy Optimization Technique in Wireless Sensor Networks

Saroj kumar Rout[1], Amiya Kumar Rath[2], Chidananda Bhagabati[3], Pradyumna Kumar Mohapatra[4]

[1]*Research Scholar, Department of Computer Science Engineering, Sikshya 'O' Anusandhan University, Bhubaneswar, Odisha, India.*

[2]*Department of Computer Science & Engineering, Veer Surendra Sai University of Technology (VSSUT), Burla,Sambalpur, Odisha, India.* [3]*Department of Computer Science & Engineering, Krupajal Engineering College,Bhubaneswar, Odisha India.* [4]*Department of Electronics & Telecommunication, Orissa Engineering College, Bhubaneswar, Odisha India.*

Email-{ [1]rout_sarojkumar@yahoo.co.in, [2]amiyaamiya@rediffmail.com, [3]*c.bhagabati@gmail.com,*[4]*er_pradyumna@yahoo.co.in* }

Abstract- Localization in Mobile Sensor Network presents, a never seen before challenge in this modern era. Localization algorithms somehow able to manage to solve the problem in a practical deployment. The following dossier article comes up with an idea to solve the trilateration problem. We propose Fuzzy Based Eminence of Trilateration (FBEOT) that helps in defining an efficient and dynamic mapping of nodes and relationship among ranging noise factor with objects. It is specific in FBEOT, that we design a dynamic Fuzzy optimization localization method, in which the most efficient and powerful node is selected for trilaterations process of localization in sensor network. To confirm this Dynamic Framework, combination of fuzzy optimization & TDOA technique with an efficient protocol is used. FBEOT is suitable in calculating trilateration accuracy factor and also the proposed localization method significantly improves localization performances.

Keywords- GPS, Localization, Confidence, Wireless Sensor Network (WSN), Fuzzy logic, TDOA.

I. INTRODUCTION

Wireless Sensor Networks (WSNs) are often arranged for one particular use, and often their location remains unknown. Through localization, a physical framework milieu can be provided to sensor readings. The information will have a minimal effect if the exact location of sensor node is unknown. Besides, some applications need the node position, like vehicle tracking system [1]. So localization is essential in WSN research. Hence, Localization is defined as the process of estimating and computing the exact position or coordinates of sensor nodes [2]. This idea and facts show the researchers to find the solution of localization problem. The manual configuration technique is an easy way but quite impractical for larger networks i.e. sensors at volcanoes or portable sensors. A second way can be using Global Positioning System (GPS) as an external hardware to each sensor. The other option of using GPS is constrained due to power consumption, cost, and inability to use it indoor, hence creates a necessity for using nodes inside [3]. Different localization algorithms helps in estimating the location of sensors by using the data related to initially unknown location information and the few sensor nodes absolute positions as well as the distance between sensor nodes & bearing measurements. The anchor node locations are known globally and hence are equipped with an external hardware, GPS. In global coordinate system, these anchors help in determining the sensor network location. Due to some of the following reasons, most sensors don't know their locations e.g., constraints on size & cost, deploying environment (GPS is inaccessible in some places), deployment of sensors (sensors may be scattered), energy consumption etc. These sensors with no information about their location are called as unknown nodes. Node localization algorithm helps for estimating unknown node location.

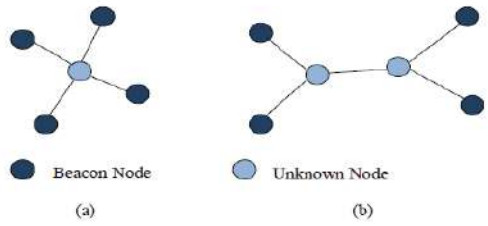

Figure 1(a) Beacon Node and 1(b) Unknown Node

A. CATEGORIES OF LOCALIZATION ALGORITHMS.

Range-based localization: In this method, the distance between a sender and a receiver can be calculated by using the received signal strength or the time-of-flight of communication signal which is sent to the receiver by the sender. However, the accuracy of the estimation completely relies on local environment, medium of transmission and intricate hardware.

Range-free localization method: In this method, there is no need of calculating absolute point-to-point distance by using received signal strength because the hardware design is very simple and the reference nodes have pre-knowledge about their location, which ultimately suits the use of WSNs. Functioning of localization algorithm can be increased and amended by using various optimization techniques like Fuzzy Logic [4-8], Monte Carlo Optimization [9], Neural Network

[10] etc. or by doing amalgamate of localization algorithms [11, 12].

The purpose of the paper is to present an innovative fuzzy optimization localization algorithm called Dynamic trilateration. This algorithm helps in keeping the average location error low. In this paper, we explore and analyze TDOA based trilateration algorithm for localization in wireless sensor networks and a new localization algorithm is proposed.

The remaining parts of the paper are organized as: In Section II, Description of the trilateration, TDOA and Fuzzy system. In Section III, Represents Algorithm Design & proposed method. In Section IV, simulation and result. Finally Section V, Concluding remarks.

II. DYNAMIC TRILATERATION

A. Trilateration

Calculation of node location with help of the distances between unknown node and considering specific anchor point with their location coordinate value is called as trilateration. The position at which the sensor must be placed is determined by using anchor coordinate and sensor's distance to the anchor (Generally, the distance between the sensor and anchor is estimated through TDOA measurement). The sensor must be placed inside the circumference of anchor node circle which is centred at the anchor's position value. In 2D space, the distances in between three non-co-linear anchors are required to obtain the point of intersection of three circles, known as unique location. In 3D environment four anchors are essential for estimating the distance value so that the unique location (intersection point) is obtained.

This method specifies two cases:

1. The unknown node is present in the intersection of three dynamic anchor nodes which is shown in Figure 2.
2. The unknown node may be present in three dynamic anchor node's overlapping region where there is no common intersection point. This is represented in Figure 3.

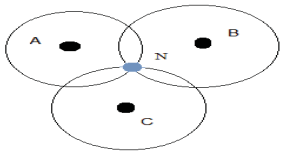

Figure 2. Trilateration by using TDOA technique A,B,C are anchor node and N is the sensor node

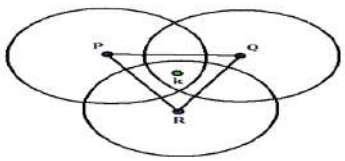

Figure 3: Trilateration by using TDOA technique P, Q, R are anchor node and K is the sensor node (Trilateration problem)

B. Trilateration Problem

This problem is found in case of 2D node location finding process where the unknown sensor nodes are not present at the 3 anchor nodes intersection point. Suppose an unknown node 'N'and it's position is not known, the three anchor nodes A, B & C are participated for finding the location of unknown node 'N' .The coordinate finding process of unknown node *N* facing the trilateration problem. 'Q' and 'R' are the anchor nodes for drawing the circle for location finding process. The circles show errors for finding centre and radius measurement, hence the circles don't intersect at a single point and it overlaps in a small region in sensor field in which node 'k' is present .The two circles intersects each other at two points. Three circles intersecting each other at six points are given in figure 3. There are three inner points that are closely associated and three outer points that are loosely associated with each other. It defines closely three associated points are nearer to each other, while the remaining are far apart. Unknown node 'K' is present at middle of three inner intersection point. So fuzzy optimization and centroid technique is used for location calculation.

C. Fundamental Centroid

Three closely associate inner intersection points are found.

The position of non-anchor node are calculated using fundamental centroid technique [13].

The basic principle of centroid method is, an unknown node surrounded by the polygon vertices should take into consideration the sensor field with unknown sensor node in the centroid of polygon represented in Figure 4.

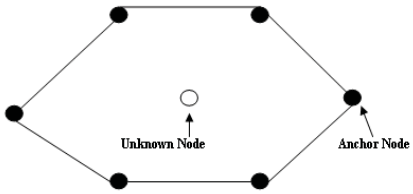

Figure 4. Node association in Centroid Technique

The relation that helps in estimating the unknown node coordinate point after successfully receiving the message is given in equation 1.

$$(X_{est,}Y_{est}) = \left(\frac{X_1+\ldots\ldots\ldots X_n}{n}, \frac{y_1+\ldots\ldots\ldots y_n}{n}\right) \quad (1)$$

Where n stands for countable powerful anchor nodes that is mapped with sensor node. The efficient algorithm never provides best result. So edge weight is essential for updating the reference node for solving this problem. This technique increases the performance of equation 1, it defines and represents anchor nodes weight in TDOA form by the given formula [14]:

$$(X_{est,}Y_{est}) = \left(\frac{X_1\, w_1+\ldots\ldots\ldots X_n\, w_n}{\sum_{i=1}^{n} w_i}, \frac{y_1\, w_1+\ldots\ldots\ldots y_n\, w_n}{\sum_{i=1}^{n} w_i}\right) \quad (2)$$

III. ALGORITHM DESIGN AND PROPOSED APPROACH

Radio Frequency (RF) and Ultrasound signals were used for proposing node localization algorithm for distance measurement purposes. The mobile anchor node localizes unknown sensor nodes in the specified sensor field when the distance factor between mobile anchor node and sensor node belongs to their reception range.

The proposed localization algorithm is categorised into two distinct steps. In first step anchor node localization is performed. In the second step there are some unlocalized node which are not covered by mobile anchor node. The unknown nodes which are localized by mobile anchor nodes are considered as stationary anchor nodes that participates in localization process The efficient node localization algorithm is specified and represented section I.

A. Supposition

The node localization method proposed is represented in the following suppositions: The static unknown node is placed and deployed in sensor field in an ad-hoc manner and these nodes are mainly self-configured in nature. The powerful efficient moving anchor node transmitting it's location information in sensor field. The powerful GPS device is attached with mobile anchor node. So it reduces the energy consumption in sensor node with static sensor node.

B. Distance Measurement

The time-of-flight method for signaling is a good distance measurement technique. The distance is measured through the satellite. A radio altimeter plays an important role to represent of the altitude [14].The distance measurement technique is computed by considering ultrasonic signal and radio signal sent by the mobile anchor node. When unknown sensor node receives RF signal, it activates its ultrasonic receiver to receive the ultrasonic pulse which arrives a short time later. Then based on signal arrival time we find time of difference between different signals with unknown node and mobile anchor node as shown in Figure 5. By considering the following diagram we represent the efficient distance measurement method for location finding process.

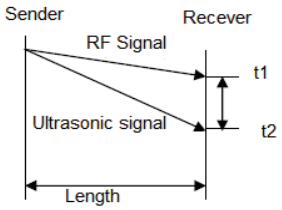

Figure 5. Distance measurement using TDOA method

$$\text{Lenth}(d) = (R_c - U_s) \times (t_2 - t_1) \qquad (3)$$

Where

R_c: It represents radio signal propagation speed.

U_s: The propagation speed of the ultrasound/acoustic signal

C. Fuzzy Logic

Fuzzy logic plays important role with unique feature to represent human thought and provide good solution for many control problems. This is a robust method and provides a better noise free reliable input and design for qualitative system [15-17]. Fuzzy system provides fuzzy set, linguistic variables like "low", "High", etc. This represents range of real value through which it is mapped between domain and fuzzy membership function. The truth value ranges between 0 to 1 for membership function is used for each point. Fuzzy system uses many membership function for representation like triangular, Gaussian, sigmoid, etc [18] based on shape of function. The fuzzy systems have important components that describe different parts like inference engine, fuzzifier and defuzzifier. The crisp input value is described by fuzzifier along with it's corresponding fuzzy sets and assigns fuzzy set's truth value or degree of membership. The inference engine describes fuzzified values based on rules. The rules is represented in IF-THEN rules based on fuzzy input and output present in fuzzy set. Fuzzy implication operators AND, OR, etc are also used. The predicate truth describes rules such as MIN-MAX and bounded arithmetic sums. Inference engine process all the rules in parallel manner. The fuzzy inference performs fuzzification of the input values using the fuzzy operators like AND or OR in antecedent part, implication from condition to consequent, aggregation of consequences and finally the defuzzification.

1. PROPOSED ALGORITHM

(NODE LOCATION COMPUTATION)

Step-1. The unknown sensor node receives two different signals having different signal strength, one RF signal and other ultrasonic signal from the anchor node. Then the signal arrival time difference is calculated between the RF signal and ultrasonic signal to find the distance value between unknown sensor node and powerful mobile anchor node.

Step-2. The input and output fuzzy linguistic variables in Mamdani FIS are as follows { very very low (VVL), very low (VL), low (L), medium low (ML), medium (M), medium high (MH), high (H), very high (VH), very very high (VVH)} and {Far, Intermediate, Near}.

Step-3. The rule based formulated using (If-Then rules). In this study, two inputted parameter each having nine linguistic variable such as { very very low (VVL), very low (VL), low (L), medium low (ML), medium (M), medium high (MH), high (H), very high (VH), very very high (VVH)}and the distance is computed as output.

Step-4. Once fuzzy rules are generated, a fairly fuzzification and bins are to be constructed based on the fuzzy rules in next step. With help of dynamic matrix which holds fuzzy output variable in column and number of trials in rows for representing the average.

Step-5. After bin construction process is completed, defuzzification process is carried out by using Jacobi's defuzzifier technique. Anchor node value J_k is calculated given below:

$$J_k = (a,b,c) = \left(\left(\frac{\sum Lt_n}{|Lt|} \right)_x , (pt_c)_x , \left(\frac{\sum Gt_n}{|Gt|} \right)_x \right) \quad (4)$$

Where *Pt, Lt, Gt* stands for fuzzy distance and it describes as.
Pt – the column C hold all point of centroid method.
Lt –the column C holds all point and value less than pt.
Gt - the column C holds all point and value greater than pt.

Step-6. Using the J_k value the node location(x,y)is fuzzified using Jacobi equation
Z = { (Pt+(Lt-Pt) rd , Gt-(Gt-Lt) rd } (5)

where rd represents random value ranges between 0 to 10.

Step-7. By help of series of iterations the value of Z = {x, y} is computed until it converges. The converged value gives the location of the sensor node.

IV. SIMULATION AND RESULTS

Node location is find by centroid method. The weights of anchor nodes have important role in centriod relation which is consider fuzzy system output for result simulation. The Mamdani fuzzy takes TDOA value as input and to maps the outputs, it is consider as weights of anchor nodes.

The mamdani method's input membership function is TDOA value from the moving anchor nodes, it is divided into nine different distinct membership function of triangular is represented as very very low (VVL), very low (VL), low (L), medium low (ML), medium (M), medium high (MH), high (H), very high (VH), very very high (VVH) is given in Figure 6. Range of input membership functions varies *[TDOA$_{min}$,TDOA$_{max}$],* where TDOA$_{min}$ stands for minimum value and TDOA$_{max}$ stands for maximum TDOA value is presented by each static sensor node from each of the mobile anchor node.

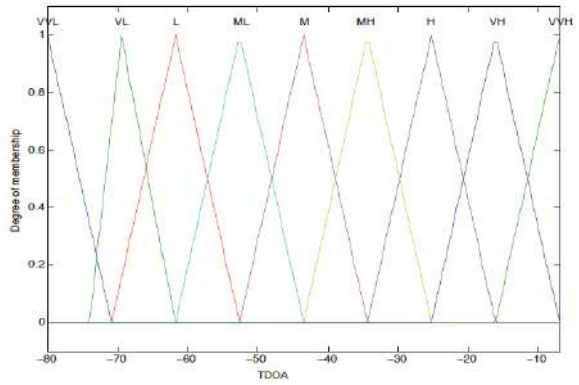

Figure 6.membership function for input value

The fuzzy membership function is divided in to different distinct linear function that is VVL, VL, L, ML, M, MH, H,VH and VVH.The weighted value of anchor node is represented in range *[0,E$_{max}$]* where *E$_{max}$* stands for maximum value as 1(one).

The fuzzy rules are represented by mamdani system is maintaining and based on the strength of TDOA. Here nearer to anchor node and far from anchor node the unknown sensor node is represented based on signal power. It is represented in Table 1 of Mamdani fuzzy system.

Table 1.Datastructure for fuzzy rules

Fuzzy RULES	IF TDOA VALUE IS	THEN WEIGHT REPRESENTS
RULE 1	VVL	VVL
RULE 2	VL	VL
RULE 3	L	L
RULE 4	ML	ML
RULE 5	M	M
RULE 6	MH	MH
RULE 7	H	H
RULE 8	VH	VH
RULE 9	VVH	VVH

Figure 7. Represents the TDOA value associated with the fuzzy system's surface.

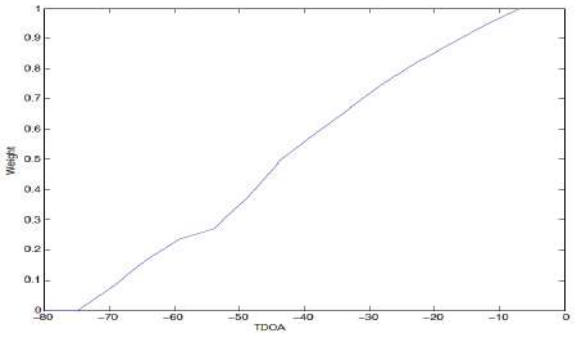

Figure 8. TDOA vs. Fuzzy Weight (Surface).

1. Location estimated Algorithm.

This paper used a good location estimated algorithm that is centroid technique. In this process equ.(2) of centroid formula is simulated using number of reference nodes. Figure 9 describes location calculation in centroid method and Figure 10 shows node location finding error in a constant area.

A. Location calculation in Centroid Method

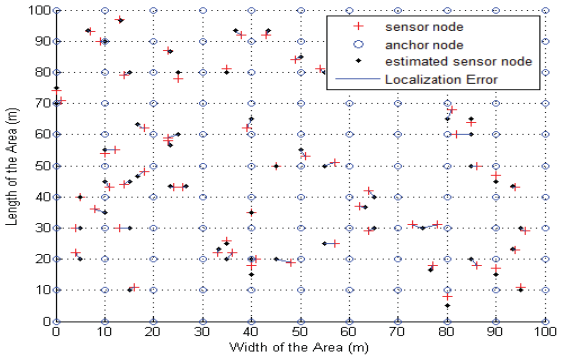

Figure 9. Node location calculation

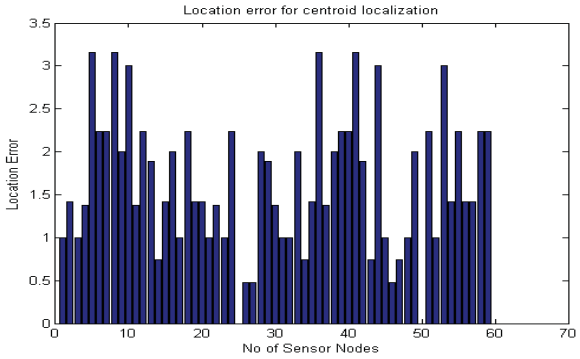

Figure 10. Node location calculation error (m)

Figure 11 represent the location calculation of a sensor node in Mamdani fuzzy method with constant density of nodes. And Figure 12 describes localization error using Mamdani fuzzy from result accuracy point of view.

B. Location calculation in Mamdani Fuzzy Method

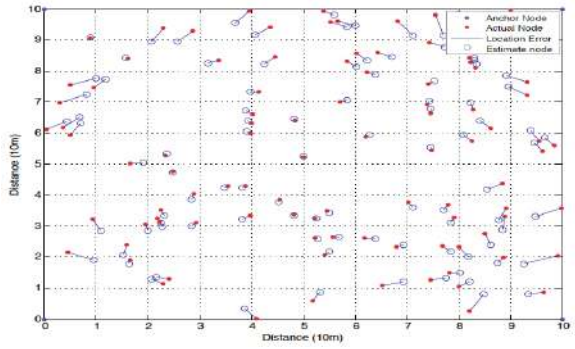

Figure 11. Node location calculation by Mamdani fuzzy technique

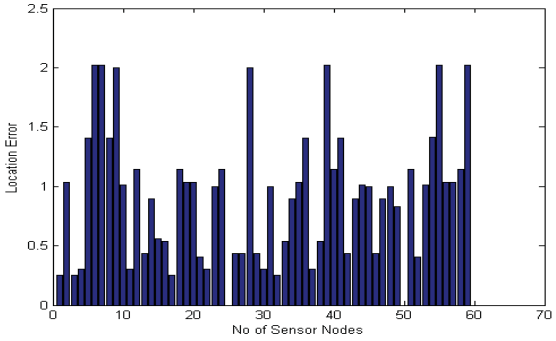

Figure 12. Node location calculation error (m)

By considering five different anchor nodes to estimate unknown node's location it adapt the TDOA method for distance estimation process with help of edge weight which is calculated using Mamdani fuzzy system. The red circle points indicate exact location of sensor node and empty circle represents estimated location of unknown sensor nodes. The link between exact and estimated point shows localization error that is shown in Figure 11.

Table 2.Node localization errors Comparison between general centroid method and Proposed fuzzy based Method.

Approachs	Node Localization Errors		
	Max. error	Min. error	Avg. error (m.)
General Centroid Method	3.1235	0	1.5024
Proposed fuzzy based Method	2.1341	0	0.8745

Figure 13 shows the average Localization error in proposed mamdani fuzzy based method is better than that of general centroid method localization process. From this figure, we found that the average localization error is less as compared to centroid method.

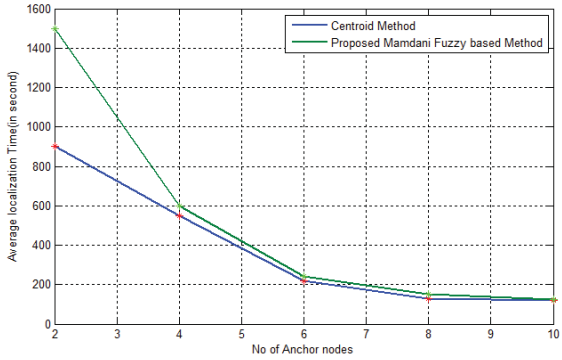

Figure 13. Average localization error vs No of anchor nodes in sensor networks.

V. CONCLUSION

In this paper, a better result is achieved by the Weighted Centroid Approach. The TDOA distance finding method has important role for node localization process. Mamdani fuzzy inference system is a better and efficient ways to calculate node location during the localization process. The important TDOA value is used as input parameter in Mamdani fuzzy system as map to the outputs, it is considered as weight parameters of anchor node to the wireless sensor node. Hence location finding error is identified in actual and computed coordinate node through modified trilateration. The efficient weighted centroid technique is treated as more preferable than the simple weighted method. The proposed optimized mamdani fuzzy method with modified trilateration is efficient from result accuracy point of view and with help of less number of anchors used.

REFERENCES

[1] M.Tubaishat, Z.Peng, Q.Qi and S.Yi, "Wireless sensor networks in intelligent transportation systems", Wireless Communication and.Mobile Computing. vol.9, issue 3, pp. 287- 302, March 2009.

[2] J. Aspnes, T. Eren, D.K. Goldenberg, A.S. Morse, W. Whiteley, Y.R. Yang, B.D.O. Anderson, and P.N. Belhumeur, "A Theory of Network Localization," *IEEE Trans. Mobile Computing,* vol. 5, no. 12, pp. 1663-1678, Dec. 2006.

[3] W Ren, "A rapid acquisition algorithm of WSN-aided GPS location", Proc. - Int. Symp.Intell. Inf. Technol. Secur. Informatics, IITSI.,pp. 42-46,2009.

[4] F. Larios,J. Barbancho,F. J. Molina and C. Leon, " Locating sensors with fuzzy logic algorithms" , IEEE Workshop On Merging Fields of Computational Intelligence and Sensor Technology - CompSens , 2011. DOI: 10.1109/MFCIST.2011.5949514

[5] Mostafa Arbabi Monfared ,Reza Abrishambaf, Sener Uysal, "Range Free Localization of Wireless Sensor Networks Based on Sugeno Fuzzy Inference", SENSORCOMM 2012 , The Sixth International Conference on Sensor Technologies and Applications, PP. 36 – 41,August 19, 2012.

[6] Chuanhui Huang, Zhan Xu, Xiu Li Re, "Analysis and Improvement for MDS Localization Algorithm", pp. 12 – 15,June 2012,IEEE

[7] Velimirović Andrija S., Đorđević Goran Lj., Velimirović Maja M.and Jovanović Milica D., "Fuzzy Set-Based Approach to Range-Free Localization in Wireless Sensor Networks.", vol. 23, issue. 2, PP. 227-244,2010.

[8] Sukhyun Yun, Jaehun Lee, Wooyong Chung and Euntai Kim. "Centroid Localization Method in Wireless Sensor Networks using TSK Fuzzy Modeling", IEEE 2009,pp 639–642.

[9] M.Vasim babu and Dr.A.V.Ramprasad, "Discrete ntithetic Markov Monte Carlo based Power Mapping Localization Algorithm for WSN", Advanced Communication Control and computingTechnologies(ICACCCT),IEEEInternational Conference on, pp. 56 –62,August 2012, DOI:10.1109/ICACCCT.2012.6320741.

[10] Runjie LIU, Kai SUN and Jinyuan SHEN, "BP localization algorithm based on virtual nodes in wireless sensor network", 6th International Conference on Wireless Communications Networking and Mobile Computing (WiCOM),pp. 1 – 4, 2010 IEEE**,**
DOI: 10.1109/WICOM.2010.5601391

[11] Shuang Tian, Xinming Zhang, Pengxi Liu, Peng Sun, Xinguo Wang, "A RSSI-based DV-hop Algorithm for Wireless Sensor Networks", IEEE 2007 International conference on Wireless communication,Networking and Mobile computing.pp. 2555–2558. DOI:10.1109/WICOM.2007.636.

[12] Yingqiang Ding, Hua Tian, Gangtao Han. "A Distributed Node Localization Algorithm for Wireless Sensor Network Based on MDS and SDP" ,proceeding of International Conference on Computer Science and Electronics Engineering, pp. 624-628,2012.

[13] Y. Sukhyun, L. Jaehun, and Wooyong 2009. A soft computing approach to localization in wireless sensor networks. *Expert Systems with Applications,* Vol. 36, No. 4, pp. 7552–7561, May 2009.

[14] G. Sarigiannidis, "Localization for Ad Hoc Wireless Sensor Networks. Netherlands", Technical University Delft, August 2006.

[15] Nissanka B.Priyantha, Anit Chakraborty, and Hari Balakrishnan, "The Cricket Location- Support System", Proceedings of 6th Annual ACM/IEEE International Conference on Mobile Computing and Networking (MobiCom 2000), pp. 32-43, August 2000.

[16] G.J. Jordt, R.O. Baldwin, J.F. Raquet, B.E. Mullins, "Energy Cost and Error Performance of Range-Aware, Anchor-Free localisation Algorithms", Ad Hoc Networks, Vol. 6, pp. 539-559, 2008.

[17] E. Elnahrawy, B. Nath, "Poster Abstract: Online Data Cleaning in Wireless Sensor Networks", Proc. of 1st International Conference on Embedded Networked Sensor Systems, 2003 , pp. 294-295.

[18] A.A. Allahverdiyev, "Cargo Transportation Routing Under Fuzzy Conditions", International Journal on Technical and Physical Problems of Engineering (IJTPE), vol.3,issue 6, pp.45—48, March 2011.

[19] De, "A Distributed Algorithm for localisation Error Detection-Correction, Use in In-Network Faulty Reading Detection: Applicability in Long Thin Wireless Sensor Networks", Proc. of the IEEE Wireless Communications and Networking Conference, pp. 1-6, April 2009.

Channel Equalization as an Optimization Problem

[1]Pradyumna Kumar Mohapatra, [2]Pradeep Kumar Jena, [3]Sunil Ku. Bisoi, [4]Saroj Kumar Rout, [5]Siba Prasad Panigrahi

[1,3]Department of electronics & Telecommunication, Orissa Engineering College, Bhubaneswar, Odisha, India

[2]Department of Mechanical Engineering,GITA, Bhubaneswar, Odisha, India.[4]Department of Computer Science & Engineering,Krupajal Engineering College, Bhubaneswar, Odisha, India.[5]Department of Electrical Engineering,GITA, Bhubaneswar, Odisha, India.

Mail-{er_pradyumna@yahoo.co.in}

***Abstract*-Equalization at the receiver is very much essential in communication system. It not only reduce the noise, ISI or CCI but to give a best possible signal to us. In this paper we have applied different optimization techniques like algorithms at the equalizer so that will get a desired signal . We proposed two algorithms, one is LSL (Least Squares Lattice) based on least square method which one of the most attractive properties is on excellent convergence velocity in order to estimate prediction error and also it has a reduced computational complexity. We have proposed another algorithm is variable length CMA which is applied on mixed phase channel for QAM signals. This method gives better convergence rate and also reduce MSE.**

Keywords-- ***Inter symbol interference (ISI), Least Squares Lattice (LSL),Channel equalization.***

I. INTRODUCTION

Channel equalizers are placed at the receiver to cancel out the interferences such as ISI , CCI and ACI in the presence of noise which is additive in nature. We are more focused at the receiver side in which equalizer is the main part which involves of large part of the computations. Basically adaptive filtering techniques mainly used as linear equalizers have long been used for this purpose. In digital communication the process which is to used to reduce ISI caused by multipath fading is called as channel estimation and equalization. Especially ISI is more complex in broadcast environments such as cellular communication. Hence, suitable channel equalization algorithms are essential to guarantee the performance of communication systems. ACI and CCI comes about in transmission systems due to various techniques such as frequency, time or space. Co-channel interference (CCI) mainly comes when the signal is contaminated by one more signal occupy the similar occurrence group. MMSE is the main criteria in channel equalization is. It also known as cost function. The formula which can be used as $E[|e(k)|^2]$.Where $e(k) = Y(K) - d(k)$.In this paper we have applied different equalization techniques at the receiver and compare their results to make sure which technique approaches the optimum performance. In adaptive channel equalization we use training sequence to reduce ISI. However the main difficulty of this move towards is that the it causes a lessening of the valuable signal rate with respect to the total signal rate[25]. One of the great advantages of blind channel equalization is that without use of training sequence and consider a few a priori arithmetical in sequence on the contribution order we can recover original signal. CMA is one of the algorithm which is being used in blind channel equalization but it has some disadvantage because of its slow convergence [1],[2].To overcome this difficulty a techniques names as (M-CMA) [5], (N-CMA) [3], (FCMA) [4] and (VSS-CMA) have been developed.

The remaining parts of the paper are organized as: In Section II, Description of the Adaptation Algorithms. In Section III, Represents ADAPTIVE SIGNAL PROCESSING ALGORITHM. In Section IV, represents PRAPOSED LSL ALGORITHM,VLCMA ALGORITHM and simulations. Finally Section V, Concluding remarks.

II. ADAPTATION ALGORITHMS

In a digital communication system and its equivalent model shown in figure 1. $X(K)$is the binary input sequence for k^{th} instant time .The system model with equalizer shown in fig 1.The channel output say $y_1(k)$ at time instant k as:$y_1(k) = \sum_{i=0}^{N-1} h_i\, x(k-i)$ (1)

Where ,$h_i(i = 0,1,2,\ldots N-1)$ are the channel tap values and N is the length of the FIR channel. We have applied different algorithms that possess different merits in terms of their performance.

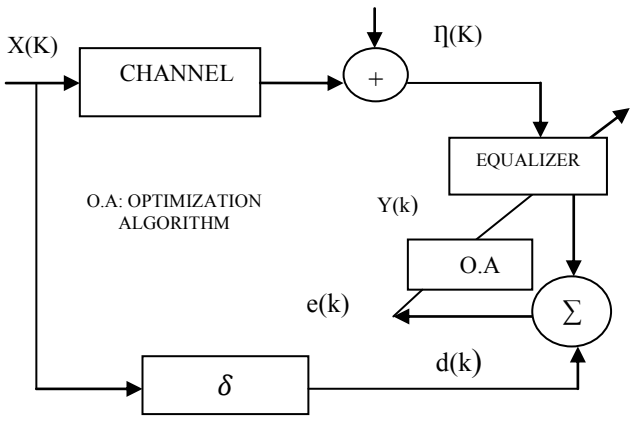

FIGURE 1. Equalization Model

978-1-5090-4620-1/16/$31.00 ©2016 IEEE

A. LEAST MEAN SQUARES ALGORITHM (LMS)

It is one of the most popular adaptive algorithm which is being used in digital communication system. The filter which is adapted using gradient descent method which updates the coefficients by taking a step in the way of the negative gradient of the objective function, i.e.,

$$W_{k+1} = W_k - \frac{\mu\,\partial jw}{2\,\partial w(k)} \qquad (2)$$

where μ determines the stability and convergence. It must be selected in the range $0 < \mu < 2/tr\{R\}$ to guarantee the stability in the mean-squared sense .Since this algorithm is matured in the literature we have applied and changed some of the parameters to study the stability as well as convergence velocity.

PERFORMANCE ANALYSIS OF EQUALIZER

SIMULATION-- 1

Now we present the performance result for a channel whose transfer function is

$$H(Z) = [\,0.0976\ 0.2873\ 0.3360\ 0.2210\ 0.0964]$$

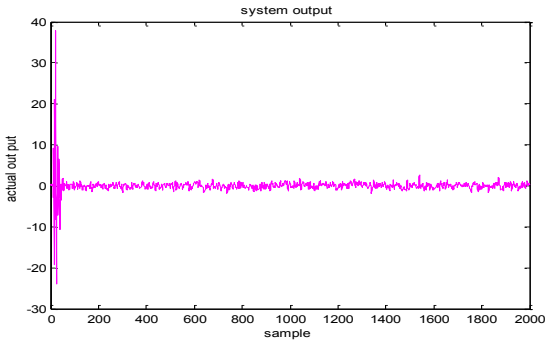

FIGURE 2: System output

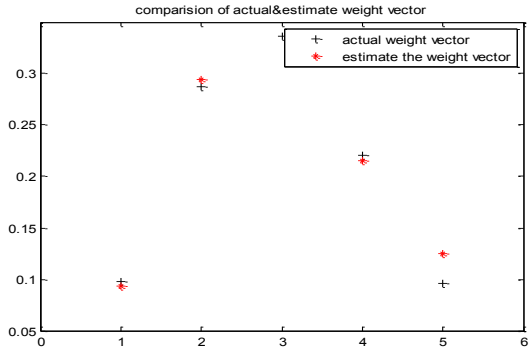

FIGURE3:COMPARISION OF ACTUAL AND ESTIMATE WEIGHT VECTOR

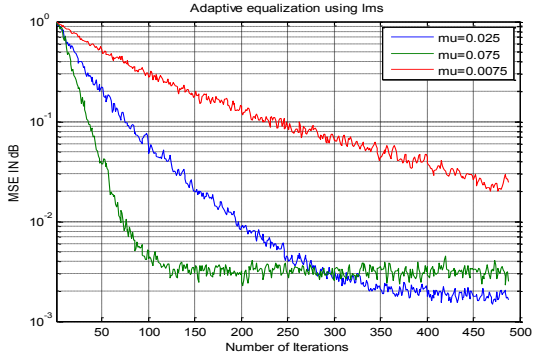

FIGURE4: CONVERGENCE CURVE OF DIFFERENT VALUES OF μ

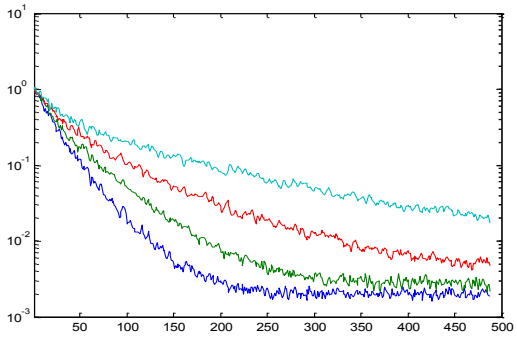

FIGURE 5: CONVERGENCE COMPARISON OF DIFFERENT VALUES OF rou=(2.9, 3.1, 3.3,and 3.5) at mu=0.04 (X axis MSE in dB) Y-axis (number of iteration)

B. NLMS ALGORITHM

NLMS is an extended method of LMS. The problem of the previous method is that it is susceptible to the scaling of its input. Therefore it very hard to choose a parameter μ that assurance the stability. One of the most appreciable thing in NLMS is because of its shows far better stability with unidentified signals[20] and the step size parameter is chosen based on the current input values.

SIMULATIONS-- 2

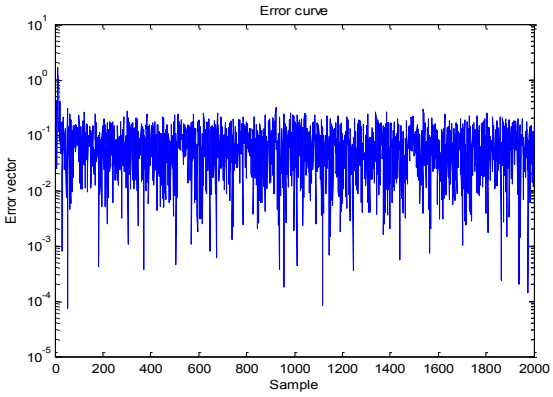

FIGURE 6: ERROR CURVE

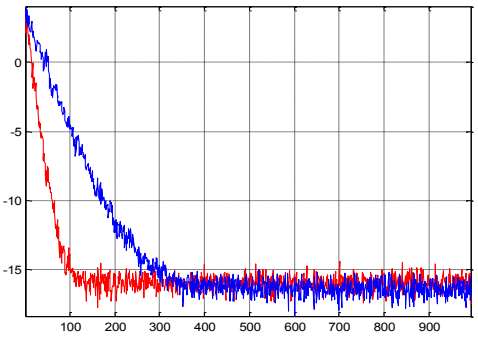

FIGURE 7: CONVERGENCE COMPARISON OF LMS AND NLMS (X axis MSE in dB) Y-axis (number of iteration)

C. RLS ALGORITHM

In this method recursively locate the coefficients of the filter that reduces a weighted linear least squares cost function relating to the input signals..The exponential weighted sum of errors squares can be described as a cost function i.e,

$$J_W = \sum_{m=1}^{k} \lambda^{k-m}\, e^2(m) + \delta\lambda^H\, W^H\,(m)W(m) \qquad (3)$$

SIMULATION 3

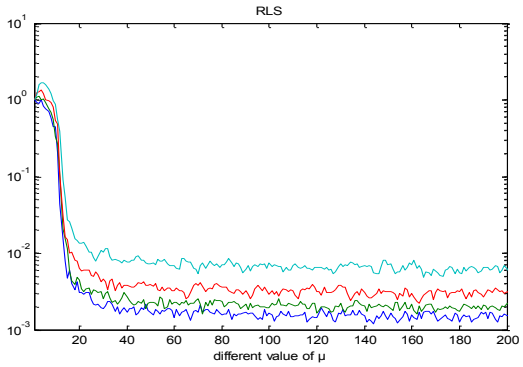

FIGURE 8: LEARNING CURVE OF DIFFERENT VALUES OF rou=(2.9 3.1 3.3 3.5)

D. FAST RLS ADAPTIVE FILTERING ALGORITHMS

As far as this algorithm is concerned it can make good change between computational complexity and convergence speed .This algorithm is separated in to two parts i.e a Prediction part and a Filtering part. The former give to the later an adaptation gain (or Kaman gain) vector to recognize the unidentified system. One of the attractive property of this method is a outcome of attractive improvement of no longer needed come from the explanation of four transversal filtering difficulty every connected during their use of the similar contribution information. One of the advantage of FRLS algorithm in the filtering part is robustness to numerical errors. The coefficients of the adaptive filter weight are adjusted by a FRLS algorithm.

SIMULATION 4

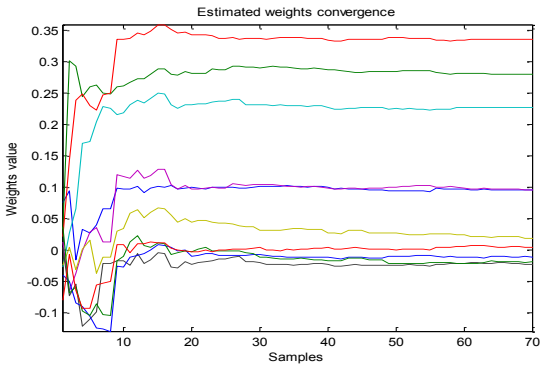

FIGURE 9: ESTIMATED WEIGHTS CONVERGENCE

- SIMULATION OF THE ADAPTIVE FILTER

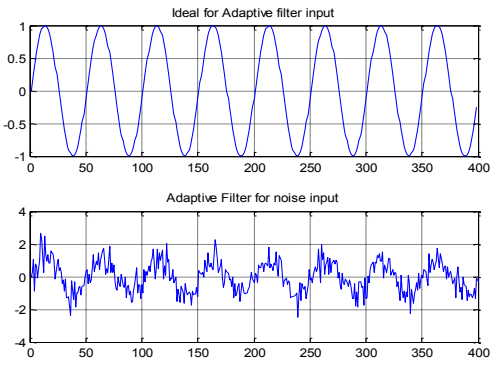

FIGURE10: IDEAL FOR ADAPTIVE FILTER INPUT AND ADAPTIVE FILTER FOR NOISE INPUT.

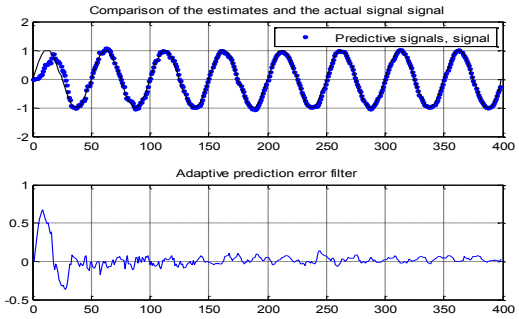

FIGURE11 COMPARISON OF THE ESTIMATE AND ACTUAL SIGNAL AND ADAPTIVE PREDICTION ERROR FILTER.

III. ADAPTIVE SIGNAL PROCESSING ALGORITHM [16,17]:

We have used some adaptive signal processing algorithms which can be investigated against ALE(Adaptive Line Enhancer) a kind of adaptive filter to extract a periodic abnormal signal including noise in the channel. Here we have used LMS , RLS, LSL, GAL algorithms for said problems..Choosing these four algorithm LMS ,RLS, and GAL (Gradient Adaptive Lattice) algorithm based on gradient method and LSL (Least Squares Lattice) algorithm based on least square method. When prediction error is estimated in LSL algorithm, least square method is fundamental principle. This algorithm has attractive properties on excellent convergence velocity in order to estimate prediction error. Among these algorithm LSL is superior on convergence velocity than LMS and GAL. Equations (4) and (5) shown below where Y_t is the output signal ,$X_t$is the sum of input and noise signal.

$$Y_t = -\sum_{n=1}^{P} W_n X_{t-n} \qquad (4)$$

$$X_t = S_t + n_t \qquad (5)$$

Where $e_t = S_t - X_t$ prediction error, $W_n, P$are coefficient and order of adaptive filter, respectively.

- SIMULATION 5

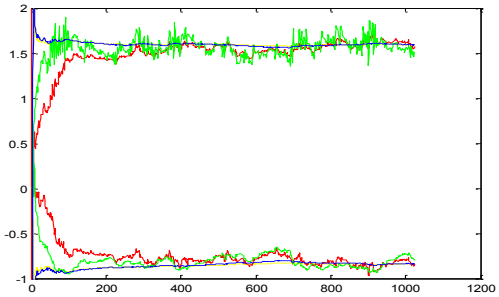

FIGURE12: TRAJECTORIES OF EQUALIZER TAPS (LMS , RLS, LSL, GAL)

IV. PROPOSED ALGORITHMS

A. PROPOSED LSL ALGORITHM

In this algorithm [15] one of the most attractive properties is on excellent convergence velocity in order to estimate prediction error. It has a reduced computational difficulty and make use of both a priori and a posterior estimation error as shown in the equation

$$\delta_N{}^{m+1} = \lambda\delta_{N-1}{}^{m+1} + \frac{g_n{}^m r_{N-1}{}^m}{\varphi_{N-1}{}^m} \quad (6)$$

$$G_N{}^{m+1} = G_N{}^m - \frac{\{\delta_N{}^{m+1}\}^2}{R_{N-1}{}^m} \quad (7)$$

$$R_N{}^{m+1} = R_{N-1}{}^m - \frac{\{\delta_N{}^{m+1}\}^2}{G_N{}^m} \quad (8)$$

$$\eta_N{}^{m+1} = -\frac{\{\delta_N{}^{m+1}\}^2}{R_{N-1}{}^m} \quad (9)$$

$$\gamma_N{}^{m+1} = -\frac{\{\delta_N{}^{m+1}\}^2}{G_N{}^m} \quad (10)$$

$$g_N{}^{m+1} = g_N{}^m + \eta_N{}^{m+1} r_{N-1}{}^m \quad 11)$$

$$r_N{}^{m+1} = r_{N-1}{}^m + \gamma_N{}^{m+1} g_N{}^m \quad (12)$$

$$\emptyset_{N-1}{}^{m+1} = \emptyset_{N-1}{}^m - \frac{\{r_{N-1}{}^m\}^2}{R_{N-1}{}^m} \quad (13)$$

In this algorithm the most important property is because of it has fast convergence speed and at initial stage few root mean square errors. Comparing GAL and LMS ,GAL is more superior than of LMS because of its convergence property .As far as noise elimination ability is concerned LSL is superior than GAL and LMS.

B. PROPOSED VLCMA ALGORITHM

One of the most suitable algorithm used for QAM signals is constant modulus algorithm(CMA)[1]. The technique which is used without the use of training series for adaptive equalization is called as blind equalization. In CMA it has got some disadvantages i.e the convergence rate is slow and large (MSE)[18] and phase is not actual in nature. The performance enhancement in convergence behaviour can be done by another blind equalization method i.e Modified constant modulus algorithm (MCMA) [8].It also take care of phase error and frequency offset at the same time. To speed up convergence rate and reduced steady state MSE, the method is proposed called as variable length constant modulus algorithm(VLCMA) which is based on stochastic gradient descent method. The selection of μ is one of the most vital part to achieve stability .If we will decrease the value of μ MSE can be lower level but algorithm can converge very slowly. A big μ can give faster convergence rate at the price of higher MSE. Variable length constant modulus algorithm (VLCMA) is proposed where the arriving signal slander in the constellation plane .In this method during the transient stages response of equalizer will be spotted approximately a big area of the transmitted data code but in the stable state the response of equalizer will lie in a close neighborhood. Hence length of the step size can be varied i.e, it can be increase in transient stages and can be decreased in steady state stages to achieve increase convergence rate and lower MSE in stable state. VLCMA[5] is a modified form of CMA which can reduce phase error and frequency offset .It's cost function is

$$J_K = J_K(Real) + J_K(Imaginary) \quad (14)$$

Similarly $y(k) = y_k(Re) + y_k(Im)$ (15)

The above terms can be identified as real and imaginary part of the equalizer output[6].

$$J_K(Real) = E[(|y_k(Re)|^2 - A(Re))]^2 \quad (16)$$

$$J_K(Imaginary) = E[(|y_k(Im)|^2 - A(Im))]^2 \quad (17)$$

Where

$$A(Re) = \frac{E(|Re\{X_k\}|^4)}{E(|Re\{X_k\}|^2)} \quad (18)$$

$$A(Im) = \frac{E(|Im\{X_k\}|^4)}{E(|Im\{X_k\}|^2)} \quad (19)$$

Error can be obtained using stochastic process and can be written as $e_k = Re\{e_k\} + jIm\{e_k\}$ (20)

Where $Re\{e_k\} = Re\{y_k\}(|Re\{y_k\}|^2 - A(Re))$ (21)

$Im\{e_k\} = Im\{y_k\}(|Im\{y_k\}|^2 - A(Im))$ (22)

Now we know the equation is of the form $W(\mathrm{K}+1) = W(\mathrm{K}) - \mu.\mathrm{e(k)}.\mathrm{X}^*(\mathrm{K})$ (23)

It is similar to that of CMA. From the above equation assuming real and imaginary part of the error signal is equal to zero .In ideal equalization, we obtain $(|Re\{y_k\}|^2 - A(Re)) = 0$ and $(|Im\{y_k\}|^2 - A(Im)) = 0$

The above equation indicates that modified algorithm attempts to create the real part of equalizer output lie on $\pm\sqrt{Re}$,and and imaginary part of equalizer output lie on $\pm\sqrt{Im}$.To minimise noise and selection of proper parameter the algorithm converges to a zero-forcing filter with probability close to one. The proposed method taking some modification [21],[22] and considering some delays from 1 to N in the error auto correlation function so that we can improve performance and rate of convergences.

CMA criterion can be verified error function i.e

$$\widehat{e_k} = \widehat{e_k}(\delta - x_k) \quad (24)$$

Similar to the gradient descent algorithm the weight [1], [2] can be

$$w(k+1) = w(k) + \mu\hat{e}(k)v^*{}_{k-i} \quad (25)$$

To improving the convergence speed and performance the proposed method considers the lags from 1 to *N* in the error autocorrelation functions, consider $\delta_k$estimation of the autocorrelation functions between $\hat{e}_k$previous error functions $\hat{e}_{k-1}, \hat{e}_{k-2}, \ldots.\hat{e}_{k-N}$ given by

$$\delta_k = \beta\delta_{k-1} + (1-\beta)\sum_{i=0}^{N-1} |\hat{e}_k\hat{e}^*{}_{k-i}|^2 \quad (26)$$

After that the equation can be

$$\mu_{k+1} = \alpha\mu_k + \gamma\delta_k \quad (27)$$

Where α, β, γ are positive parameters.

SIMULATION 6

In this simulations VLCMA is compared with CMA considering with 16-QAM signals. The response of the channel [23] whose transfer function is h=[1,0.1294-j*0.483] used in this simulations . Here number of the tap is used as 7 with the initialization of centre tap put to one and other taps put to zero.SNR is set to 25dB. Both CMA and VLCM μ=0.001, N=10000.

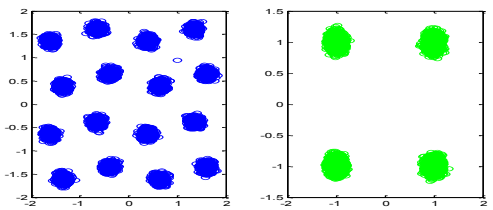

FIGURE13: 16-QAM SIGNALS, EQUALIZEDSYMBOLS

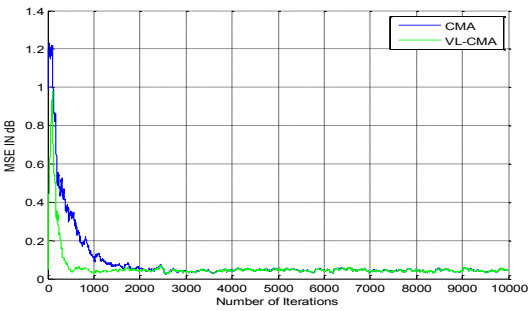

FIGURE14: LEARNING CURVES OF (CMA and VLCMA)

SIMULATION 7
COMPARE BETWEEN CMA & LMS:

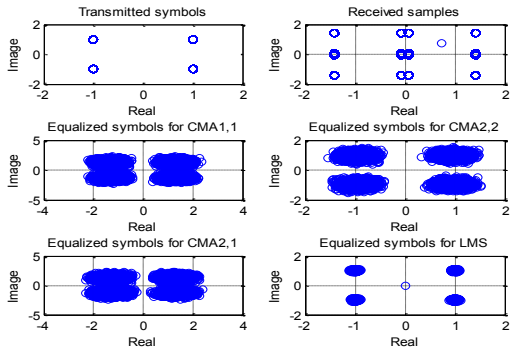

FIGURE15: TRANSMITTED SYMBOLS, RECEIVED SYMBOLS & EQUALIZED SYMBOL USING CMA AND LMS.

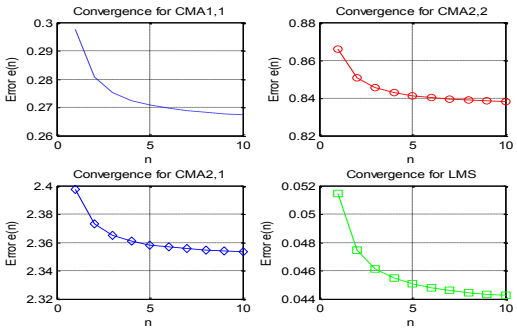

FIGURE16: MSE COMPARISON OF LMS AND CMA

COMPARISON BETWEEN LMS , RLS AND KALMAN FILTER:

In the figure… below plot of weight trajectories and MSE of three algorithms. From the figure we conclude that adaptive Kaman filter ,MSE achieved remarkable value as compared to LMS and RLS. Rate rate of convergence is also faster than LMS&RLS equalizer [13].

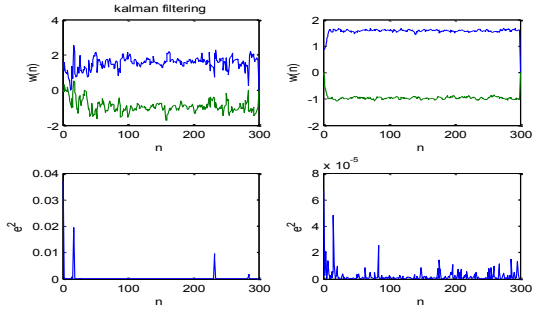

FIGURE 17: MSE AND WEIGHT TRAJECTORIES OF KALMAN FILTER

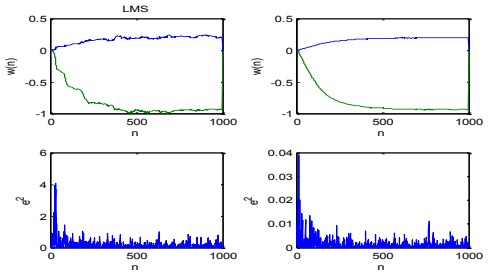

FIGURE 18: MSE AND WEIGHT TRAJECTORIES OF LMS

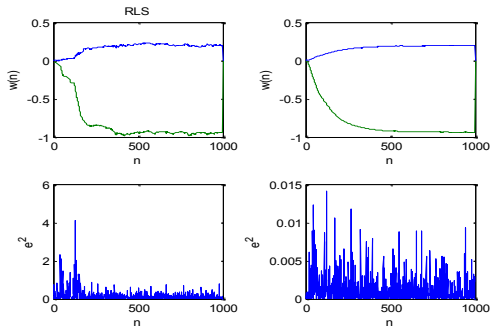

FIGURE 19: MSE AND WEIGHT TRAJECTORIES OF RLS

TABLE 1 COMPARISONS WITH THIS THREE EQUALIZERS

TYPES OF EQUALIZER	ITERATIONS	CHANNEL	MSE
KALMAN FILTER	300	AWGN	0.0027
LMS	1000	MULTIPATH	0.031
RLS	1000	MULTIPATH	0.027

V. CONCLUSION

In this paper we have analyzed different optimization techniques such as LMS,NLMS,RLS,FAST RLS,LSL,CMA,VLCMA and KALMAN FILTER algorithm based on channel equalization using different channel models. Among all these techniques it has been shown that our proposed methods i.e LSL and combinations of CMA and VLCMA provides an efficient way for channel equalization.

REFERENCES

[1] Godard, D. N., \Self-recovering equalization and carrier tracking in two-dimensional datacommunication systems," IEEE Transactions on Communications, Vol. 28, 1867{1875, 1980.

[2] TREICHLER, J. R., AGEE, B. G. A new approach to multipath correction of constant modulus signals. IEEE Trans. Acoust. Speech, Signal Process., 1983, vol. ASSP-28, p. 459-472.

[3] JONES, D. L. A normalized constant modulus algorithm. In IEEE Conference Record of the Twenty-Ninth Asilomar Conference onSignals, Systems and Computers 1995. Pacific Grove (USA), 1995, vol. 1, p. 694-697.

[4] OZEN, A., KAYA, I., SOYSAL, B. Variable step-size constant modulus algorithm employing fuzzy logic controller. Wireless Personal Communications, July 2010, vol. 54, no. 2, p. 237-250.

[5] K. N. Oh and Y. O. Chin, "Modified constant modulus algorithm:Blind equalization and carrier phase recovery algorithm," in Proc.IEEE Int.Conf. Communication., vol. 1, 1995, pp. 498–502.

[6] Roozbeh Hamzehyan, Reza Dianat, and Najmeh Cheraghi Shirazi"New Variable Step-Size Blind Equalization Based onModified Constant Modulus Algorithm" International Journal of Machine Learning and Computing, Vol. 2, No. 1, February 2012.

[7] M. Arezki, A.Namane, A. Benallal, P. Meyrueis and D. Berkani," Fast Adaptive Filtering Algorithm for Acoustic Noise Cancellation" Proceedings of the World Congress on Engineering 2012 Vol II WCE 2012, July 4 - 6, 2012, London, U.K.

[8] Oh, K. N. and Y. O. Chin, \Modifed constant modulus algorithm: Blind equalization and carrier phase recovery algorithm," 1995 IEEE International Conference on Communications,Vol. 1, 498{502, June 1995.

[9] S. Haykin, Adaptive Filter Theory, 4th ed., NJ, Prentice-Hall, 2002.

[10] J.G. Proakis, Digital Communications, 4th ed., McGraw-Hill, 2000.

[11] Jaymin Bhalani, A.I.Trivedi and Y.P.Kosta "Performance comparison of Non-linear and Adaptive Equalization Algorithms for Wireless Digital Communication**,"** IEEE 2009.

[12] .M.D.Miranda,Dept.of Electron. Eng, Sao Paulo Univ,Brazil,M.Gerken,M.T.M .DaSilva" Efficient implementation of error-feedbackLSL algorithm"ElectronicsLetters,Vol35,Issue16,IEEE 5 Aug1999 1308-1309.

[13] LinghuiWang,Wei He, Kaihong Zhou and Zen Huang "AdaptiveChannel Equalization based on RLS Algorithm" IEEE pp.105-108,April 2011.

[14] LinghuiWang,Wei He, Kaihong Zhou and Zen Huang "AdaptiveChannel Equalization based on RLS Algorithm" IEEE pp.105-1 08,April 2011.

[15] Hiromitsu Ohta" Acoustic diagnosis technique for a failurerolling bearing by Adaptive signal processing Algorithm".11th International Congress on sound and vibration ,St.Petersberg Russia, July 2004.

[16] [16].Y. Iiguni, Adaptive Signal Processing Algorithm, 1-21(Baifukan 2000) in Japanese.

[17] H. Ohta and K. Seto, " Acoustic Diagnosis on a Rolling Bearing Based on Presumption of a DivisionTerm by Locally Stationary AR Model", The 32 nd International Congress and Exposition on Noise Control Engineering, CD-ROM(2003).

[18] Wei Xue1; 2, Xiaoniu Yang1, and Zhaoyang Zhang" A Variable Step Size Algorithm for Blind Equalization of QAM Signals2",Progress In Electromagnetics Research Symposium Proceedings, Cambridge, USA, July 5{8, 2010.

[19] MERVE ABIDE DEMİR, ALI OZEN "A NOVEL VARIABLE STEP SIZE ADJUSTMENT METHOD BASED ON AUTOCORRELATION OF ERROR SIGNAL FOR THE CONSTANT MODULUS BLIND EQUALIZATION ALGORITHM" RADIOENGINEERING, VOL. 21, NO. 1, APRIL 2012.

[20] LEE, K.A.; GAN,W.S; "IMPROVING CONVERGENCE OF THE NLMS ALGORITHM USING CONSTRAINED SUBBAND UPDATES," SIGNAL PROCESSING LETTERS IEEE, VOL. 11, PP. 736-739, SEPT. 2004.

[21] ZIPF, J. G. F., TOBIAS, O. J., SEARA, R. A VSSLMS algorithm based on error autocorrelation. In 16th European Signal Processing onference (EUSIPCO 2008). Lausanne (Switzerland), August 2008, p. 25-29.

[22] OZEN, A. A novel variable step size adjustment method based on channel output autocorrelation for the LMS training algorithm. International Journal of Communication Systems (Wiley-Blackwell), 2011, vol. 24, no. 7, p. 938-949.

[23] Li, X. L. and X. D. Zhang, \A family of generalized constant modulus algorithms for blind equalization," IEEE Transactions on Communications, Vol. 54, No. 11, 1913{1917, 2006.

M-Throttled: Dynamic Load Balancing Algorithm for Cloud Computing

Amrutanshu Panigrahi[1], Bibhuprasad Sahu[2],Saroj Kumar Rout[3], Amiya Kumar Rath[4]

[1, 2, 3] Department of CSE, Gandhi Institute For Technology, Bhubaneswar, Odisha
[4] Department of Computer Science & Engineering, VSSUT, Burla , Odisha
Deputed to National Assessment and Accreditation Council (NAAC) Bangalore, India.

Abstract. In cloud computing environment can also be called as internet based computing process in which there is no limitation of work. There are multiple number of Data Center (DC) available for solving multiple user requests coming from different User Base (UB). The Data Center are capable of negotiating multiple instruction simultaneously. But the instructions are submitted to the DC randomly. Thus there is chance of overload for a particular DC. Hence the load balancing plays a vital role in cloud computing to maintain the performance of the computing environment. In this research article we have implemented Throttled, Round Robin and the Shortest Job First load balancing algorithm. Also we have proposed one more algorithm called as M-Throttled which has the high performance as compared to other. We have taken different parameter such as Overall Response Time, Datacenter Processing Time etc for comparison. These are simulated by taking closest data center policy in Cloudsim environment.

Keywords: Data Center, User Base, Throttled, Round Robin, M-Throttled, CloudSim.

1 Introduction

Cloud computing is an on demand system in which shared resources, data, programs are given by the customer's prerequisite at the explicit time. Its a term which is commonly utilized if there should arise an occurrence of Web. The entire Web can be seen as a cloud. Capital and operational expenses can be reduced by utilizing distributed computing. Load balancing in cloud computing frameworks is extremely a test now. Continuously a conveyed process is required. Since it isn't in every case basically plausible to keep up at least one inactive system which is similar as the active one to satisfy the required requests. In cloud computing the cloud can be observed as the cloud which provides the availability of resources on the internet for different users. The end users uses these resources as per the requirement. Simultaneously multiple users utilizes this resources simultaneously. Cloud computing provides various services such as IaaS, SaaS, PaaS to handle different kinds of requests coming from the end users [1]. The request coming from the end-users are not homogeneous and are submitted to different

data centers for execution randomly. Hence it is very difficult to handle the heterogeneous requests by an overloaded data center. So the load balancing plays a vital role in cloud computing.

But load balancing is becoming the most challenging factor in Cloud Computing. It is required to disseminate the stack evenly at each data center to realize a efficient client fulfillment and resource utilization proportion. The goal of the load balancing are as follows [2,3]

- To make all the DCs equal loaded.
- To keep the performance constant
- To maintain the execution speed in heavy traffic.

It is a procedure of reassigning the all-out load to the individual processors or DCs or to make resource usage successful and to improve the response time of the activity, all the while expelling a condition in which a portion of the DCs are over stacked while some others are under stacked. The imperative interesting points while growing such calculation are : estimation of load, examination of load, security of various framework, execution of framework, association between the DCs [4] . This heap considered can be regarding CPU load, measure of memory utilized, postponement or System load. A site or a web-application can be gotten to by a lot of clients anytime of time. It ends up troublesome for a web application to deal with all these client asks for at one time. It might even outcome in framework breakdowns. For a site proprietor, whose whole work is reliant on his entryway, the sinking feeling of site being down or not available additionally brings lost potential clients. Here, the heap balancer assumes a vital job. Cloud load balancing is the way toward disseminating remaining tasks at hand and figuring resources crosswise over at least one servers. This sort of dissemination guarantees most extreme throughput in least response time [5,6].

In this research paper we have implemented the throttled, round robin and shortest job first load balancing algorithm to calculate the performance of the cloud computing environment. Along with these algorithms we have proposed one more algorithm M-throttled with an improvised performance of the network with the presence of the heavy traffic at different instance of time. The parameters like response time and process time of UB and DC are considered for the evaluation of different algorithms.

2 Literature Survey

Load balancing assumes a fundamental job in giving Quality of Service (QoS) ensures in cloud registering, and it has been producing generous enthusiasm for the exploration network. There are a lot of methodologies that have adapted to the heap adjusting issue in distributed computing. The top notch comprises of differing customary methodologies without using any sort of swarm insight calculations. Many load balancing approaches were proposed as of late and each centered around various angles of calculations and strategies, e.g., utilizing a focal load adjusting approach for virtual machines [13], the planning methodology on burden adjusting of virtual machine (VM) assets dependent on hereditary calculations [14], a mapping arrangement dependent on

multi-asset load adjusting for virtual machines [15], versatile dispersed calculation for virtual machines [16], weighted least-association methodology [17], and two-stage booking calculations [18]. Also, a few techniques for burden adjusting were displayed for various cloud applications, for instance, an administration based model for extensive scale stockpiling [19], information focus the executives design [20], and a heterogeneous cloud [21].

The inferior contains approaches [8] use swarm knowledge calculations, fake honey bee state [9, 10], and particle swarm streamlining [11, 12], which is better for the dynamic circumstance of distributed computing. With self-sorted out conduct, these social bugs can be imitated all things considered, or with important changes, to take care of undifferentiated from issues in distributed computing. In [9], the author proposed a calculation for burden conveyance of an outstanding burden with an adjusted methodology of ACO from the point of view of cloud or matrix organize frameworks. In this methodology, the ants just refreshed a solitary outcome set constantly in the procedure, as opposed to refreshing their own outcome set. In [7], a heap adjusting system was proposed in light of subterranean insect state and complex system hypothesis in an open distributed computing league. This is the first time that ACO and complex systems were brought together into burden adjusting in distributed computing what's more, acquired great execution. In [8], Mishra, R. et al. gave an answer for burden adjusting in the cloud by ACO, to expand or limit diverse execution parameters, for example, CPU burden and memory limit. Notwithstanding, few elements were considered as pheromones to discover target hubs when utilizing ACO in the over three methodologies. In [9,10], the author exhibited a novel methodology for load adjusting dependent on counterfeit honey bee settlement. PSO was likewise embraced for burden adjusting in distributed computing, for example, [11,12].

3 Existing Algorithms

3.1 Throttled Load Balancing:

In this method, heap balancer keeps up a record table of VM with their present states (Accessible/Occupied). At the point when a demand to assign another VM from the DC Controller reaches, it processes the record table from best till the most readily accessible VM is detected. As soon as the VM is discovered, the Heap Balancer restores the VM ID to the DC Controller. The DC Controller sends the demand to VM recognized by the corresponding ID. The DC Controller informs the Heap Balancer of the new allotment. The Heap Balancer refreshes the allotment table by augmenting as needs be. When the VM wraps up the demand and the Data Center Controller gets the reaction cloudlet, it advises the Heap Balancer of the VM de-assignment. The Heap Balancer de-assign the equivalent VM whose Id is as of now imparted. The objective of this method is to determine the response time of every VM as VMs are having different capacity corresponding to processing efficiency.

$$\mathbf{RT= F_t\text{-}A_t\text{+}T_d}$$

Where RT= Response Time, F_t=Finish Time, A_t= Arrival Time, T_d= Transmission Delay.

3.2 Round Robin Load Balancing:

It is the least complex calculation that utilizes the idea of time slice. In this method, time is separated into numerous slices also, every datacenter is given a specific time quantum and inside this time quantum the hub will play out its activities. In this calculation, the Data Center Controller dole out the demand to a rundown of VM's on a pivoting premise. The first demand is allotted to a VM picked haphazardly from the gathering and afterward Data Center Controller doles out the resulting demands in a roundabout request. Once the virtual machine is appointed the demand, the VM is moved to the end of the rundown. In this mechanism, there is a superior distribution idea known as Weighted RR in which one can dole out a weight to each VM so that in the event that one VM is prepared to do taking care of twice as much burden as the other, the incredible server gets a weight of 2. In such cases, Data Center Controller will allocate the two solicitations to the ground-breaking VM for each demand allotted to a more fragile one. RR Calculation chooses the heap on arbitrary premise, also, in this manner prompts a circumstance where a few hubs are intensely stacked and some are daintily stacked.

3.3 Shortest Job First

Shortest Job First (SJF) planning is a need and Non-Preemptive booking. Non-Preemptive methods, when the allocated time a processor then the processor can't be taken the other, until the procedure is finished in the execution. This calculation appropriates the heap haphazardly by first checking the extent of the procedure and after that exchanging the heap to a Virtual Machine, which is gently stacked. All things considered that procedure measure is least, this procedure will get first need to execute whether we guess most reduced estimated process executes in least time. The heap balancer spreads the heap on to various hubs known as spread range technique. Shortest Job First (SJF) calculation can be said to be ideal with a normal holding up time is negligible, which improves the framework execution.

4 Proposed Algorithm: M-Throttled

In this algorithm, the Heap Balancer keeps up a list table of VM's and the quantity of solicitations presently designated to VM. Initially all VMs have zero allotments. At the point when a demand to designate another VM from the DC Controller reaches, it processes the list table, and recognizes the minimum stacked VM. In the event that there are more than one, the principal distinguished is chosen. The Heap Balancer restores the machine IDs to the DC Controller. The DC Controller sends the demand to the VM distinguished by that ID. The DC Controller informs the Heap Balancer about the new

assignment. The Heap Balancer refreshes the assignment table augmenting the allotment with that VM. At the point when the VM wraps up the demand and DC Controller gets the reaction cloudlet, it informs the Heap Balancer of the VM distribution. The Heap Balancer refreshes the distribution table by reducing the assignment of the VM by one. In M-Throttled Algorithm, a correspondence exist between the heap Balancer and the Data Center Controller for refreshing the list table prompting an overhead. This overhead makes delay in giving reaction the arrived solicitations.

5 Implementation

In this simulation six datacenters DC1, DC2, DC3, DC4, DC5, and DC6 with closed data set policy has been adapted during the simulation. In this different arrangement parameters can be set like number of user bases, number of task produced by each user base per hour , number of VMs, number of Processor, Processing speed, available bandwidth etc. Based on the parameters the result incorporates reaction time, handling time, fetched etc. UB Response Time (RT) and DC Processing Time (PT) are considered for evaluation purpose.

Table 1 DC Configuration

Parameter	Value Used
VM Image Size	10000
VM Memory	1024Mb
VM Band	1000
DC-Arch	X86
DC-OS	Linux
DC-Machine	20
DC-Memory/machine	2048Mb
DC-Storage	100000Mb
DC-Band	10000
DC-Processors/Machine	4
DC-Speed	100MIPS
DC-Policy	Time Shared/Space Shared
DC Grouping UB based	1000
DC Grouping Request based	100
Instruction Length	250

Table 2 Region Configuration

Cloud Analyst Region id	Users
0	4.4M
1	1.1M
2	2.6M
3	1.3M
4	0.5M
5	0.8M

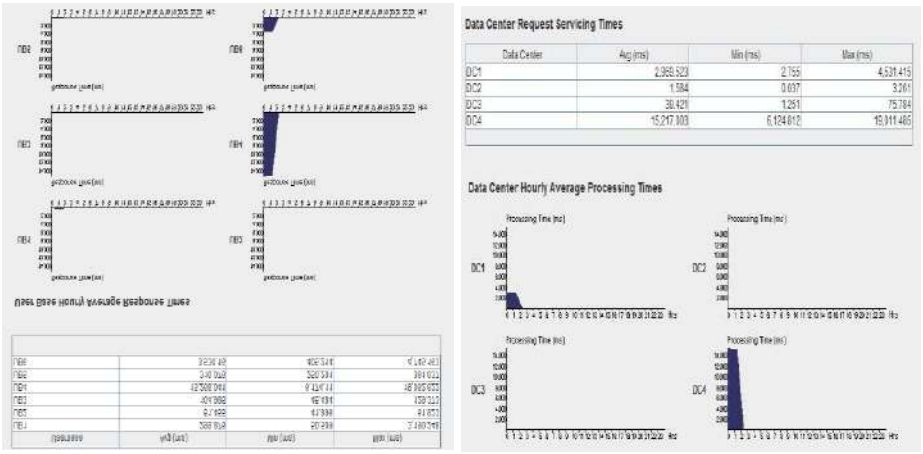

Fig. 1. UB response time and DC processing time using RR Algorithm

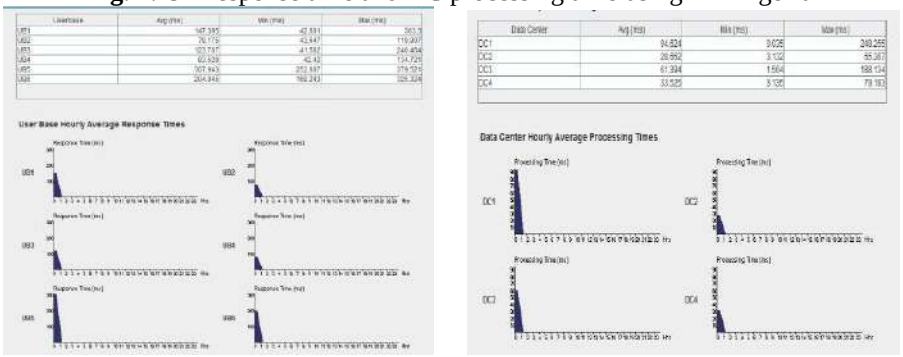

Fig. 2. UB Response time and DC processing time using Throttled Algorithm

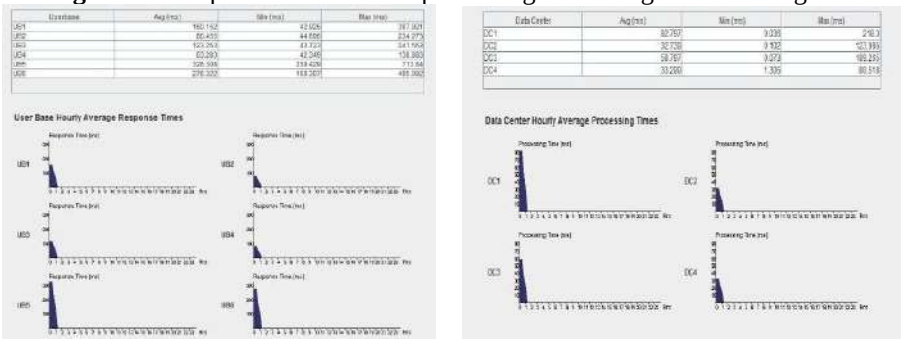

Fig. 3. UB Response time and DC processing time using SJF Algorithm

Fig. 4. UB Response time and DC processing time using M-Throttled Algorithm

6 Conclusion

We have studied the concepts of load balancing and its vital effects on cloud computing environment. Different algorithms providing the solution the existing problem of load balancing among different Data Center to maintain the efficiency of the network. The performance of the strategies such as Throttled, Round Robin, Shortest Job First and M-Throttled with respect to the response time and the processing time has been studied. A comparison has been done on the basis of some predefined parameter such as UB Response time and DC processing time. With the presence of heavy traffic in each region the UB response time and the DC processing time the M-throttled algorithm performs much better than that of other existing algorithms.

References

[1] Velte, A. T., Velte, T. J., Elsenpeter, R. C., & Elsenpeter, R. C. (2010). *Cloud computing: a practical approach* (p. 44). New York: McGraw-Hill.

[2] Randles, M., Lamb, D., & Taleb-Bendiab, A. (2010, April). A comparative study into distributed load balancing algorithms for cloud computing. In *2010 IEEE 24th International Conference on Advanced Information Networking and Applications Workshops* (pp. 551-556). IEEE.

[3] A Vouk, M. (2008). Cloud computing–issues, research and implementations. *Journal of computing and information technology*, *16*(4), 235-246.

[4] Alakeel, A. M. (2010). A guide to dynamic load balancing in distributed computer systems. *International Journal of Computer Science and Information Security*, *10*(6), 153-160.

[5] http://www-.ibm.com/press/us/en/pressrelease/22613.wss

[6] http://www.amazon.com/gp/browse.html?node=20159001

[7] Randles, M., Odat, E., Lamb, D., Abu-Rahmeh, O., & Taleb-Bendiab, A. (2009, December). A comparative experiment in distributed load balancing. In *2009 Second International Conference on Developments in eSystems Engineering* (pp. 258-265). IEEE.

[8] Pacheco, P. (1997). *Parallel programming with MPI*. Morgan Kaufmann.

[9] Moges, M., & Robertazzi, T. G. (2006). Wireless sensor networks: scheduling for measurement and data reporting. *IEEE Transactions on Aerospace and Electronic Systems*, *42*(1), 327-340.

[10] Pallis, G. (2010). Cloud computing: the new frontier of internet computing. *IEEE internet computing*, *14*(5), 70-73.

[11] Armbrust M., Fox A., GriffithR., Joseph A. D., Katz R., Konwinski A., Lee G., Patterson D., Rabkin A., Stocia I. and Zaharia M. (2009) Above the Clouds: A Berkeley View of Cloud Computing, EECS Department, University of California, 1-23.

[12] Bhadani, A., & Chaudhary, S. (2010, January). Performance evaluation of web servers using central load balancing policy over virtual machines on cloud. In *Proceedings of the Third Annual ACM Bangalore Conference* (p. 16). ACM.

[13] Rimal, B. P., Choi, E., & Lumb, I. (2009, August). A taxonomy and survey of cloud computing systems. In *2009 Fifth International Joint Conference on INC, IMS and IDC* (pp. 44-51).

[14] Zhang, Z., & Zhang, X. (2010, May). A load balancing mechanism based on ant colony and complex network theory in open cloud computing federation. In *2010 The 2nd International Conference on Industrial Mechatronics and Automation* (Vol. 2, pp. 240-243). IEEE.

[15] Hiranwal, S., & Roy, K. C. (2011). Adaptive round robin scheduling using shortest burst approach based on smart time slice. *International Journal of Computer Science and Communication*, *2*(2), 319-323.

[16] Wickremasinghe, B., Calheiros, R. N., & Buyya, R. (2010, April). Cloudanalyst: A cloudsim-based visual modeller for analysing cloud computing environments and applications. In *2010 24th IEEE international conference on advanced information networking and applications* (pp. 446-452). IEEE.

[17] Wickremasinghe, B., Calheiros, R. N., & Buyya, R. (2010, April). Cloudanalyst: A cloudsim-based visual modeller for analysing cloud computing environments and applications. In *2010 24th IEEE international conference on advanced information networking and applications* (pp. 446-452). IEEE.

[18] Buyya, R., Ranjan, R., & Calheiros, R. N. (2009, June). Modeling and simulation of scalable Cloud computing environments and the CloudSim toolkit: Challenges and opportunities. In 2009 international conference on high performance computing & simulation (pp. 1-11). IEEE.

[19] Bo, Z.; Ji, G.; Jieqing, A.(2010), Cloud Loading Balance algorithm. In Proceedings of the 2010 2nd International Conference on Information Science and Engineering (ICISE), Hangzhou, China, 4–6; pp. 5001–5004.

[20] Hiranwal, S., & Roy, K. C. (2011). Adaptive round robin scheduling using shortest burst approach based on smart time slice. *International Journal of Computer Science and Communication*, *2*(2), 319-323.

[21] Wickremasinghe, B., Calheiros, R. N., & Buyya, R. (2010, April). Cloudanalyst: A cloudsim-based visual modeller for analysing cloud computing environments and applications. In *2010 24th IEEE international conference on advanced information networking and applications* (pp. 446-452). IEEE.

Algorithm Aspects of Dynamic Coordination of Beacons in Localization of Wireless Sensor Networks

Saroj kumar Rout, Ashray Mehta, Amulya Ratna Swain, Amiya Kumar Rath, Manas Ranjan Lenka
Research scholar, Department of Computer Science Engineering, Sikshya O Anusandhan University, Bhubaneswar, Odisha India,
School Of Computer Engineering,KIIT University, Bhubaneswar, India
Department of Computer Science Engineering, VSSUT, Burla, Sambalpur Odisha India
Email: {rout_sarojkumar@yahoo.co.in, ashray.mehta@gmail.com, swainamulya@gmail.com, amiyaamiya@rediffmail.com, manasy2k3@gmail.com}

***Abstract*—Wireless Sensor Networks(WSNs) consists of hundreds of nodes which are of low power, low cost, and tiny devices. The main functionality of these nodes is to sense the environment and send the sensed data to the observer. In order to validate and get the significance of sensing data, location information of the sensor node needs to be combined with the sensed data. In addition to this, there are many other issues of WSN such as routing, coverage, etc. which also need the location information of sensor nodes. Several approaches, including range-based and range-free, have been proposed to calculate positions for randomly deployed sensor nodes. In this paper, we proposed a distributed technique for localization of sensor nodes using few mobile anchor nodes. These mobile anchor nodes move in the network space and periodically broadcast beacon messages about their location. Static sensor nodes receive these messages as soon as they come under the communication range of any mobile anchor node and compute their position based on the range based technique. Another contribution of this paper is to identify the importance of mobile anchor node over static anchor node in localization. The performance of the proposed algorithm is carried out using the Castalia simulator. The simulation result shows that mobile anchor node provide better accuracy as compared to static anchor node for sensor node localization.**

***Keywords*-Localization, Mobile Sensor Nodes, Range Base, RSS, Dynamic Beacon**

I. Introduction

WSN consists of a number of self-organized sensor nodes that are deployed to sense the environment, collect the data, and process it with constraint resources. WSNs have many applications in different areas like military, search and rescue operation, environment monitoring, and other commercial use. The performance and reliability of WSN depend upon the accurate location of the sensor nodes. Among large number of WSN applications, there are various application such as tracking the exact location of moving targets [1], [2], helping traffic routing [3], [4] and providing the geographic network coverage [5], etc., which use the sensor localization information for self-organization and configuration of networks. Therefore, localization should be considered as an implicit feature of a wireless sensor network.

978-1-4673-7437-8/15/$31.00

Integral to such sensor node, location awareness operation is the important technique that is used to locate the exact position of every sensor node. The constraints related to cost and power consumption make it practically infeasible to outfit each node in a network with a global positioning System (GPS) [6].On the other hand, it may be achievable to setup a few number of sensor nodes with GPS known as beacon node. These beacon nodes can be considered either static or mobile depending on its suitability and can be used to locate the exact coordinates of the sensor nodes. In such a situation, either the range based or the range free technique can be applied. The range-based technique [7], [8], [9], [10] can use inter-node distance measurement through some special hardware, information such as RSS to find the position of a sensor node. In contrast, the range-free technique [11], [12], [13] does not make use of any extra hardware information, rather each and every sensor nodes utilizes the existing beacon signals in order to calculate the sensor nodes location approximately.

The localization problem has received a significant attention in recent literature. Most of the current localization schemes have been proposed by using static anchor nodes. Although the cost and energy efficiency of static anchor based location scheme are low, still it does not give better accuracy. Looking at the performance of static anchor based location scheme, we proposed a mobile anchor based localization scheme that provides better accuracy and energy efficiency. The mobile beacon node is the best-utilized sensor node to find the coordinates of other sensor nodes in WSNs [14], [15]. The determination of the accuracy of a sensor node location is done by using the knowledge of the route that the mobile beacon node has traveled and how often the signal is emitted. In this paper, a distributed methods to localize the sensor nodes is proposed with the help of some moving beacon.

Our proposed localization method is based on the RSSI technique using a smaller number of mobile anchor nodes and static anchor nodes. In this localization method with the constant area and constant density of a sensor node is

represented which gives different average localization error with respected to sensor field in the localization process. Our Proposed method delved into mobile anchor nodes and established that they are energy efficient as well as they are required less in number than only static anchor nodes.

This paper is organized in the following manner. Section II describes the related work in the area of sensor node localization. Section III describes the proposed algorithm that uses the RSSI information of a moving beacon node. Section IV highlights upon the simulation results of the proposed Algorithm. Section V concludes the paper.

II. Related Work

The phenomena by which sensor nodes determine their location is known as localization. Apart from this, we can simply define localization as a mechanism for inventing of space relationship between objects. A large number of localization methods are static [6], [12] where network and the static beacon nodes are used to find the location of each node in WSN. The static localization method is further divided into two types, i.e. range based and range free. In order to measure the exact distance or angle between an unknown node and a beacon node, range-based localization method follows received signal strength(RSS),time of arrival(TOA),time difference of arrival(TDOA) or angle of arrival(AOA) and uses different methods such as trilateration,maximum likelihood or triangulation to find the unknown sensor node coordinate points.

The two significant demerits of range-based localization are:

1) Require costly additional hardware support.
2) Distance measurement errors are caused by fading and noise[16].

To overcome these drawbacks, range-free localization methods do not need any hardware support or component for measuring distances and angle.

RSS is a vital parameter used in both range-based and range-free localization methods. The RSS method clearly defines how precisely can be employed to indicate the actual transmission range. There are numerous range-based localization methods [8], [9], [10] directly use it to find the distance between two sensor nodes. Signal fading and background noise causes unstable radio transmission, which could further create a major variance of RSS .As a result, RSS have some distance measurement error, it ultimately reflects on the position calculation of sensor node inaccurately. The sensor node range-free localization methods [11], [12], [13] also employing RSS to localize sensor nodes in WSNs. In these methods, RSSs are not used for calculating absolute distances. As a replacement, these methods evaluate the value of RSS with each other to capture the relative distance and relationship among nodes.The model [17] find RSS shows the path loss using referenced distance and path loss exponent and also a random variable.

The mobile anchor localization methods [14], [15], [18], [19], [20] with the help of mobile beacon node, reduce the static localization problem. Galstyan et al. [20] propose a distributed on-line algorithm for localizing unknown node by using the mobile beacon. In [19], the authors come up with a localization scheme (REKF) with the valuable assistance of some moving robots in a Delay-Tolerant Sensor Network (DTN). Various approaches are presented in the literature to resolve the issues of localization. Different assumptions are also taken with respect to their network and sensor capabilities.

In some specific models of localization which particularly use GPS as the source, the localization process is straightforward. However, in a localization model that uses mobile anchor nodes to assist sensor nodes with the discovery of location, the mobile anchor nodes are either manually arranged according to their location or else supplied with a GPS server which they can use to find their location. Mobile anchor nodes, after providing their location information to a sensor node, then help them in estimating their location.

The literature survey clearly showed that an optimal algorithm could not be defined yet, and thus a suitable localization algorithm needs to be designed on the specificities of the situations, taking into account the size of network, as well as the deployment method with node density and the expected results. Our proposed method delved into mobile anchor nodes and established that they are energy efficient as well as require less in number than only static nodes. In those systems, only a small number of anchors are necessary for constructing the global coordinates, which significantly reduces the system cost.

III. Distributed Localization Using A Dynamic Beacon Node

In this section, a range-free distributed localization method has been proposed . It uses a mobile beacon for estimating the positions of sensor nodes in the ideal environment. Here we first focus on how a node uses the broadcasting signal message from the beacon to confine its estimation area when the beacon is moving in a straight line. Then the upper bound of the estimation error to the real position of a node is calculated.

Periodically beacon nodes exchange their location information to their neighbors. It is to be assumed that a beacon node moves in a straight line or zig jag motion in the deployment area of a sensor network. At a certain time interval called the broadcasting intervals, the mobile beacon node broadcasts a message that is the special message that holds its current position. The physical point is denoted by the position of the beacon at which it broadcasts a message. It is also assumed that a node can receive messages from the beacon only if the node is within the transmission range of the beacon. Two states are defined for every node,i.e. in and out. Also, two dynamic transitions from these two states,i.e. arrival and departure are defined by us. In The whole process of localization, a node merely computes its distance from other nodes situated in its vicinity utilizing one or more characteristics of received signal. The Location calculation depends on the signal feature is further classified into 3 main groups as triangulation, triliteration, and multilateration. RSSI (Received Signal Strength Indicator) is always available in many sensor platforms such as mica2

and TelosB. The most widely used assumption in the ideal situation is that, if the distance between the beacon node and the sensor node is the smallest then the calculation of co-ordinates of the node using RSSI value will be more accurate.

PROPOSED ALGORITHM

In this work, we categories all the sensor nodes into two types viz. anchor and non-anchor node. At the very beginning, all the anchor nodes send beacon packets to their neighbors. The beacon packet consists of the anchor node location and the node id. Once a non-anchor node receives the beacon packet, it stores the beacon location along with the RSSI value. After receiving beacon packet from minimum three beacon/anchor nodes, each non-anchor node calculates its location using the triliteration method by taking into consider the distance calculated through the RSSI value of the corresponding beacon node and its location .

A non-anchor node stores maximum five number of beacon information from the anchor nodes. The selection of beacon node information altogether depends upon the RSSI value. Hence, the beacon information having best RSSI value along with the beacon node location get stored. Among those five beacon information, a non-anchor node selects three beacon node information based on the following criteria.

The three beacon node information with higher RSSI value will be given first preference, provided the three circles drawn through the beacon/anchor node location as the center point of the circle, and distance between the beacon node and non-anchor node calculated through the RSSI value as the radius of the circle should intersect with each other. In order to satisfy the above criteria, each node stores more than three beacon information. If none of the three beacon information from the five beacon information stored at the non-anchor node satisfies the above condition, then these beacon information will not be currently considered for calculating non-anchor node location.

Since the beacon nodes are mobile, and these nodes are broadcasting their beacon information in a regular interval, a non-anchor node updates the beacon information depending upon its RSSI value. A non-anchor node may also store more than one beacon information from some beacon node provided this beacon information do not contain same beacon location. As a non-anchor node updated the collected beacon information, the non-anchor node updates its location by taking the average of its previous computed location and the new calculated location.

IV. SIMULATION RESULTS

In this section, we report selected simulation results about the performance gain from the large-scale wireless sensor networks under different system settings. we describe the simulation of our proposed localization algorithm in terms of location error, energy efficiency, and throughput. We use Castalia simulator to simulate our proposed algorithm .In our simulation, we have varied the number of nodes from 100 to 1000, which are randomly deployed using uniform distribution in different parts of deployment area with a

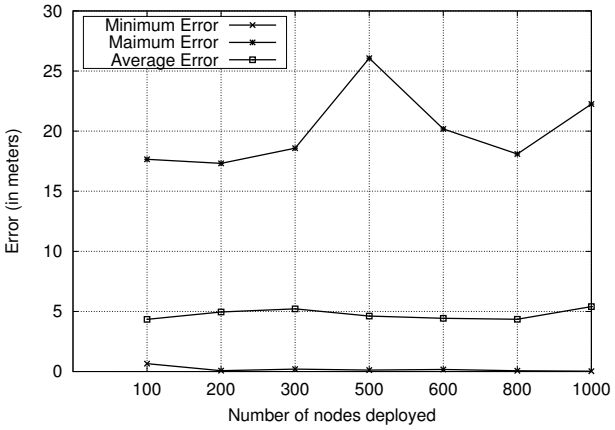

Fig. 1. minimum, maximum, average localization error

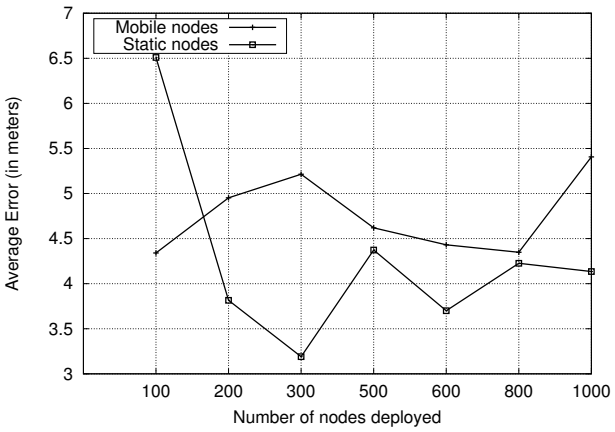

Fig. 2. average localization error in 50*50 area with mobile vs static anchor nodes

fixed density and fixed area. Simulation result shows that our localization scheme outperforms the existing localization algorithms in terms of location error, energy efficiency, and throughput.

Figure 1 shows that with increase in the number of sensor nodes in constant area the localization error remains almost the same.

Figure 2 shows the results of the constant area (50*50) with different size of the network with mobile anchor nodes vs static anchor nodes. It shows that the average localization error is less in static anchor nodes as compared to mobile anchor nodes.

In Figure 3, we have taken the deployment area of (250*250) for different size of the network with mobile anchor nodes vs static anchor nodes. It shows that the average localization error is less in mobile anchor nodes as compared to static anchor nodes.

From Figure 2, 3 we can conclude that as the deployment

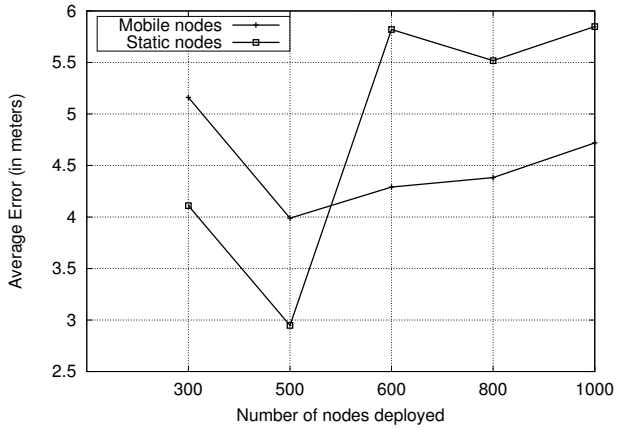

Fig. 3. average localization error in 250*250 area with mobile vs static anchor nodes

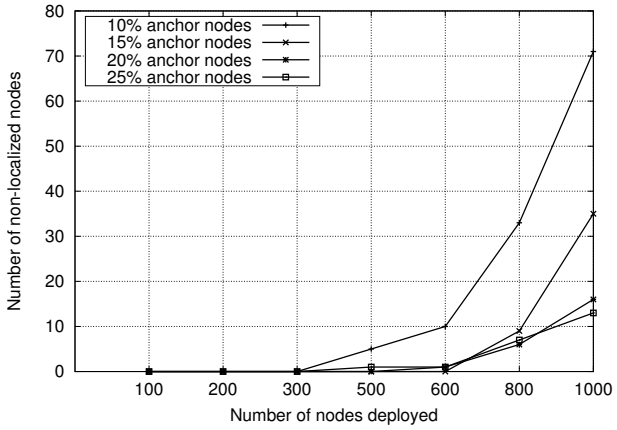

Fig. 5. Number of non-localized nodes in different size network with varying the % of mobile anchor nodes

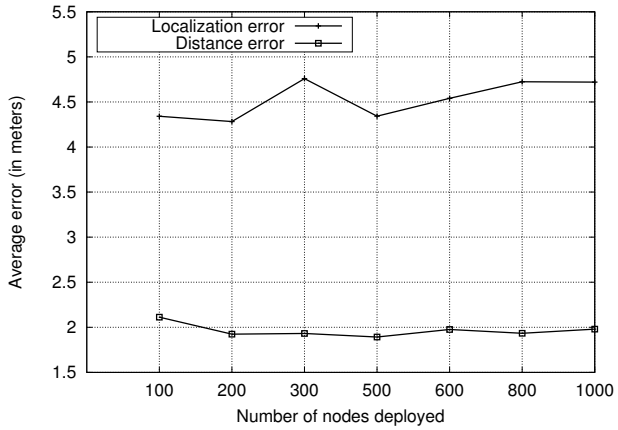

Fig. 4. localization error vs distance error with mobile anchor nodes

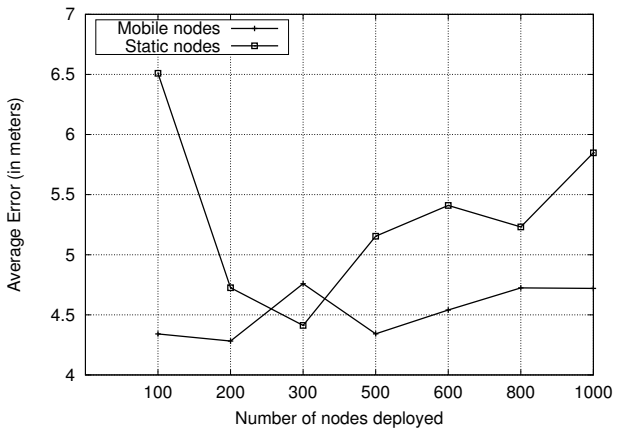

Fig. 6. average localization error with mobile vs static anchor nodes in different size networks with constant density

area increases the average localization error is minimized in mobile anchor nodes as compared to the static anchor nodes.

Figure 4 tells that at the system level, using absolute values of RSS for distance estimation and its errors of impact in localization.This graph proves the RSSI distance error effects the average node localization errors in a constant density of nodes. The error in RSSI was bound to propagate to the localization error. In the above simulation work shows that even a minimal spike in the error of distance calculation process resulted in a bigger spike for the average localization errors. It indicates the reduction of error in RSSI will reduce the average localization error.

Figure 5 shows how more no. of anchor nodes help in improving the localization accuracy. As the localization algorithm, used here is based on RSSI, but the anchor nodes can be move around their sensor field. This can be remarkably helpful in the localization process. But some nodes are at the edge of the deployment area, so they cannot receive signals from sufficient number of anchor nodes to localize, still mobile anchor nodes yields some numbers of non-localization nodes in different turns. When we are taking 10% mobile anchor nodes then the no of non-localized nodes are more in numbers. But when it becomes 25% it remarkably decreases in numbers.

Figure 6 depict localization results from some configurations were tested while keeping the node density constant. On the above graph, we have taken mobile anchor nodes compare to static anchor nodes with constant node density. The comparison shows that the mobile anchor nodes yield average localization errors which are minimum as compared to that with static anchor nodes.

Figure 7, depicts the number of non-localized nodes in a different size network with constant density using mobile vs static anchor node. It clearly shows that the number of non-localized nodes are quite less when we use the mobile anchor nodes.

The effect of the number of anchor nodes for WSN localization is shown in Figure 8. As the number of anchor

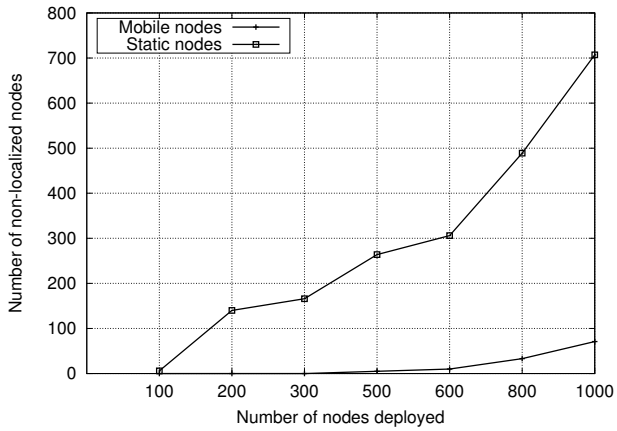

Fig. 7. Number of non-localized nodes in mobile vs static anchor nodes

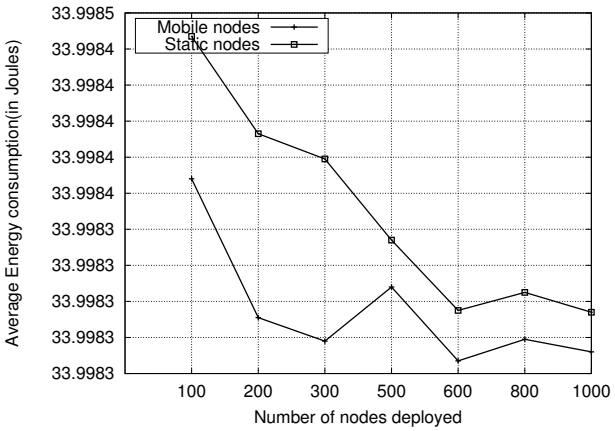

Fig. 9. Average energy consumption with mobile vs static anchor nodes

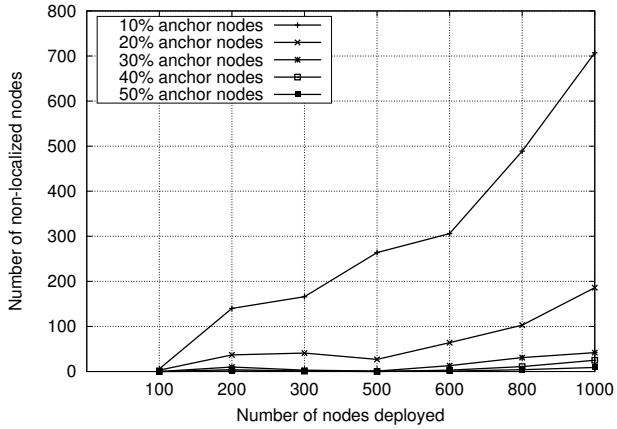

Fig. 8. Number of non-localized nodes with varying the % of the anchor nodes

nodes increases the number of non-localized nodes get reduced.

Figure 9 shows the average energy consumption in different size network with mobile vs static anchor nodes. From this figure, we found that the average energy consumption is less with mobile anchor nodes as compared to that with static anchor nodes.

V. Conclusions

As wireless sensor networks have become a key technology and are used in more and more for solving industrial and environmental problems. Hence, defining an effective localization algorithm is one of the important tasks. The existing literature shows that an optimum algorithm could not be defined yet, and thus the choice of a suitable algorithm has to be chosen on the specificities of the situations, taking into account the size of the network, type of nodes, as well as the deployment methods and the expected results.

In this paper, we proposed a localization algorithm that uses the mobile anchor nodes that periodically send beacon information to their neighbors to compute their approximate location. The proposed algorithm is based on the RSS value. From the simulation, we found that with variation in RSS value, the localization error is also varying. The localization error is further reduced by receiving multiple beacons from the different mobile anchor nodes from different position during their mobility. In addition to this, we have also analyzed the importance of mobile anchor nodes over static anchor nodes in sensor nodes localization. The most significant advantages of mobile anchor node over static anchor node are that with less number of mobile anchor nodes the localization over the whole WSN is achieved, which is preferable for energy constrained WSN.

References

[1] W. Zhang and G. Cao, "Dctc: Dynamic convoy tree-based collaboration for target tracking in sensor networks," *IEEE TRANSACTIONS ON WIRELESS COMMUNICATION*, vol. 3, no. 5, pp. 1689–1701, 2004.

[2] J. Liu, J. Reich, and F. Zhao, "Collaborative in-network processing for target tracking," *EURASIP J. Appl. Signal Process.*, vol. 2003, pp. 378–391, Jan. 2003.

[3] Y.-B. Ko and N. H. Vaidya, "Location-aided routing (lar) in mobile ad hoc networks," *Wirel. Netw.*, vol. 6, no. 4, pp. 307–321, Jul. 2000.

[4] M. Mauve, A. Widmer, and H. Hartenstein, "A survey on position-based routing in mobile ad hoc networks," *Netwrk. Mag. of Global Internetwkg.*, vol. 15, no. 6, pp. 30–39, Nov. 2001.

[5] T. Yan, T. He, and J. A. Stankovic, "Differentiated surveillance for sensor networks," in *Proceedings of the 1st International Conference on Embedded Networked Sensor Systems*, ser. SenSys '03. New York, NY, USA: ACM, 2003, pp. 51–62.

[6] B. Hofmann-Wellenhof, H. Lichtenegger, and J. Collins, *Global Positioning System: Theory and Practice*. Springer-Verlag, 1997.

[7] J. Hightower, R. Want, and G. Borriello, "SpotON: An indoor 3d location sensing technology based on RF signal strength," University of Washington, Department of Computer Science and Engineering, Seattle, WA, UW CSE 00-02-02, February 2000.

[8] P. Bahl and V. N. Padmanabhan, "Radar: an in-building rf-based user location and tracking system." Institute of Electrical and Electronics Engineers, Inc., March 2000.

[9] N. Patwari and A. O. H. III, "Using proximity and quantized rss for sensor localization in wireless networks," 2003.

[10] N. B. Priyantha, A. Chakraborty, and H. Balakrishnan, "The cricket location-support system," in *Proceedings of the 6th Annual International Conference on Mobile Computing and Networking*, ser. MobiCom '00. New York, NY, USA: ACM, 2000, pp. 32–43.

[11] K. Yedavalli, B. Krishnamachari, S. Ravula, and B. Srinivasan, "Ecolocation: A sequence based technique for rf localization in wireless sensor networks," in *In Proceedings of the Fourth International Symposium on Information Processing in Sensor Networks (IPSN*. Inc, 2005, pp. 285–292.

[12] T. He, C. Huang, B. M. Blum, J. A. Stankovic, and T. Abdelzaher, "Range-free localization schemes for large scale sensor networks," in *Proceedings of the 9th Annual International Conference on Mobile Computing and Networking*, ser. MobiCom '03. New York, NY, USA: ACM, 2003, pp. 81–95.

[13] T. He, C. Huang, B. M. Blum, J. A. Stankovic, and T. F. Abdelzaher, "Range-free localization and its impact on large scale sensor networks," *ACM Trans. Embed. Comput. Syst.*, vol. 4, no. 4, pp. 877–906, Nov. 2005.

[14] L. Hu and D. Evans, "Localization for mobile sensor networks," in *Proceedings of the 10th Annual International Conference on Mobile Computing and Networking*, ser. MobiCom '04. New York, NY, USA: ACM, 2004, pp. 45–57.

[15] N. B. Priyantha, H. Balakrishnan, E. Demaine, and S. Teller, "Mobile-Assisted Localization in Wireless Sensor Networks," in *IEEE INFOCOM*, Miami, FL, March 2005.

[16] P. Bergamo and G. Mazzini, "Localization in sensor networks with fading and mobility," *IEEE Transactions on Mobile Computing*, 2005.

[17] T. Rappaport, *Wireless Communications: Principles and Practice*, 2nd ed. Upper Saddle River, NJ, USA: Prentice Hall PTR, 2001.

[18] R. Stoleru, T. He, and J. A. Stankovic, "Walking GPS: A Practical Solution for Localization in Manually Deployed Wireless Sensor Networks," in *IEEE LCN04*, Cahrlottesville,VA, 2004.

[19] P. N. Pathirana, N. Bulusu, A. V. Savkin, and S. Jha, "Node localization using mobile robots in delay-tolerant sensor networks," *IEEE Transactions on Mobile Computing*, 2005.

[20] A. Galstyan, B. Krishnamachari, K. Lerman, and S. Pattem, "Distributed online localization in sensor networks using a moving target," in *Proceedings of the 3rd International Symposium on Information Processing in Sensor Networks*, ser. IPSN '04. New York, NY, USA: ACM, 2004, pp. 61–70.

Energy Efficient and Cost Effective Secure Node Localization with Key Management in Wireless Sensor Networks

Saroj Kumar Rout[1], Amiya Kumar Rath[2], Chidananda Bhagabati[3]

[1]*Research scholar, Department of Computer Science Engineering,*
Sikshya 'O' Anusandhan University, Bhubaneswar, Odisha, India.
[2]*Department of Computer Science & Engineering, Veer Surendra*
Sai University of Technology (VSSUT),Burla, Sambalpur, Odisha, India
[3]*Department of Computer Science & Engineering, Krupajal Engineering College, Bhubaneswar, Odisha India.*
[1]*rout_sarojkumar@yahoo.co.in,* [2]*amiyaamiya@rediffmail.com,* [3]*c.bhagabati@gmail.com*

Abstract: **Wireless Sensor Network has a wide range of application in the field military operation, tracking, and data acquisition in hazardous environments. It is a vital and essential thing to guarantee the security and resilience of sensor networks. The wireless sensor node localization plays an important role for collecting meaningful information from an exact location. During node localization process security is a vital issue to protect the data losses from unauthorised person. In this research work, we introduce efficient and effective secure node localization and a dynamic key management solution for wireless sensor networks. In this scheme we present secure node authentication with distance measurement and we call secure information verification by malicious node cleaning. Also we present key management schemes; it is assumed that key information is stored in very powerful and reliable sensor node and not in individual nodes. It is an important issue for protecting the powerful node by which the sensor network can be made secure, energy efficient and cost effective because moving anchor node plays a major role during localization process.**

Keywords: **Wireless Sensor Network, Node localization, Security, key management,key distribution.**

I. INTRODUCTION

A wireless sensor network has many applications in different field and plays a vital role for decision making and data processing. It is used in dynamic routing [1], sensor node key distribution [2] and description of authentication mechanism [3]. Sensor node localization in secure manner is a critical problem, how to maintain secure process in localization and trace association between anchor node and unknown node. Localization is necessary for solving object tracking, animal movement in forest and different vehicle tracking [4], and detection of fire at exact position in the forest [5]. Incorrect node location value may lead to alarms of the object [6]. The sensor nodes deployed in a sensor field with respect to different environment has a possibility of threats and risks.

Therefore secure localization is essential for validating and protecting the data. In this paper a Secure Node Authentication With Distance Measurement System (SNADMS) is represented. The localization correctness is represented by cleaning the malicious node in sensor network with some key management strategies.

The rest of the paper is organized as follows. Secure sensor node localization is represented in the Section II. Secure node authentication with distance measurement by diffusion protocol and malicious node cleaning is described in section III. Section IV describes reliable key management schemes in WSN. Conclusion is discussed in Section V.

II. RELATED WORK

A huge number of nodes are present in the sensor network and these nodes are of two categories. One is the anchor node and the other is unknown sensor node. Anchor node coordinate value is known by GPS device which is attached with anchor node so that it helps unknown node for location computation process. Sensor node localization process comprises of 2-type: Range based and Range free. Range based techniques are described in [7],[8] and range free methods are described in [9],[10].localization based on range based method uses RSSI(Received Signal Strength Indicator) for distance and angle measurement [11], sensor node distance is calculated by TOA(Time of Arrival) [12], and other efficient technique is Time Difference of Arrival(TDOA) [13] and AOA (Angle of Arrival) [14] and DV-HOP localization algorithm in wireless sensor network[15].

In position determination point of view, it is two types: such as Terminal-based approaches and Infrastructure-based approaches [16], [17]. In terminal-based method is called self localized system. Infrastructure based scheme is based on anchor node. The location value of unknown node is computed by efficient trilateration method in sensor network [15], multilateration method and triangulation method [14]. Localization attack can be possible in both cases. Once the sensor node is hacked then that node sends false location information. An efficient key management scheme is define in[20],intelligent defense mechanism for security in wireless

sensor network and managements with applications of trust in wireless sensor networks is also define in[21],[22]

III. THE DETAIL PROPOSED APPROACH

The objective of our proposed approach is identify the malicious node which sends inconsistency data from the fair node sets. For reliable purpose two-dimensional localization is used. Our proposed algorithm is associated with fairly three dimensions.

Definition: The wireless sensor network is mathematically represented as G(V,E),where V specifies set of nodes (anchor nodes and unknown sensor nodes) E specifies set of active edges which are within the transmission range (t_g) and they communicate with each other. It defines reliability and consistent of node when they are projected on a single Euclidean plane and maintains the association between them.

Problem: Given transmission range set is defined, $N_t(v)$ where the set containing sensor node along with its supported neighbours and its reliable distance set(D_t). Its distance is represented in sensor fields as.

$\{dm_{ij}|dm_{ij} = dm_{ji}, i,j \in N_t(v), i \neq j\}$,the largest supporting reliable subset of $N_t(v)$.

The proposed work is represented as two important phases: such as distance calculation by TDOA and malicious node cleaning. The first phase is describing the distance measurement by TDOA method by using diffusion protocol in high secure manner. In second phase set the supporting consistency range subset which contains strongly associated neighbour nodes in a virtual local plane. Once two phases operation is completed then anchor node can communicate with unknown node from the secure and malicious cleaning node set. In alternatively local coordinate system can be reconciled into the dynamic global supporting system. The mobile anchor node is in network and it updates its position value periodically.It is described as the attacker collect all the distance based information from honest node then it manipulates the data and sends false location information in the network. To protect from such attack a dynamic protocol is proposed in this paper.

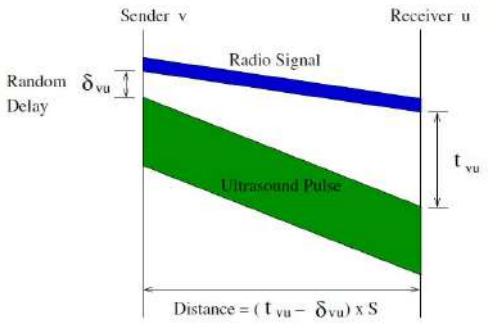

Fig. 1. Ranging Process in Phase 1

Phase I: Secure Node Authentication with Distance Measurement by Diffusion Protocol.

A hacker is sited in a secrete place and silently collects the distance information between anchor node and unknown sensor node's location coordinate value. As a result a false distance and location value is transmitted by hacker to the network. To protect the network from such attack the distance computation are announced in an atomic manner with help of diffusion protocol. This protocol uses a reliable dynamic ranging technique .It is based on TDOA (Time Difference Of Arrival Technique) [18], wireless sensor network provides a dynamic fine grain localisation system based on transmission range to calculate unknown nodes coordinate value [19].

Diffusion protocol described in two well-defined steps

Step 1: Distribute node distance Encrypted Measurements

(1) Select a node v, $v \in V(G)$ by using *diffusion_msg+random number in secure location computation process.* Let $N_t(v)$ is the strongly associated neighbour in transmission range of v in participation.

(2) Select two strongly associated node v,u such that v,$u \in V(G)$ and $u \in N_t(v)$ then v sends a special RF signal to u in a certain propagation speed after some time delay interval δvu ,v sends another special signal that is ultrasonic signal to u and maintains delay time δvu , in top secret . Receiver node maintains a record containing the time tvu until the special ultrasonic signal arrives.

(3) When two signal are collected from every node in $N_t(v)$ v performs encryption of δvu, t_{uv} where every $u \in N_t(v)$ *with* symmetric encryption method by help of fresh random generated key k. Then node v broadcasts this information to its associated neighbours .If a node fails to represent it's report it will dropped for l $N_t(v)$.

Step 2: Divulge Measurements of node atomically

(1) When all the diffusion message is collected from each and every node $N_t(v)$ (after fixed time gap),v makes known the encrypted key k. Once any node fails to tell its encryption key process then it will dropped from $N_t(v)$.

(2) When encryption key is received from all the nodes $N_t(v)$, then v starts it's distance computation dm_{ij} in between i and j node in $N_t(v)$. So the distance computed as $(t_{ij}- \delta_{ij}) \times C$, where C denotes ultrasonic signal's propagation speed. t_{ij} is associated with diffusion message from j and δij is attached in diffusion message from i.

In this algorithm defines that due to some random delay node U can't compute location value of v even if it receive both ultrasound and RF signal. The node v's data is disclosed when each and every node $N_t(v)$ ranging data is declared in step-1. When symmetry key information is disclosed in step-2 then

node's N_t *(v)* calculated the distance v. so malicious node can't fake any distance information. We deduced a symmetric key concept ranging value is to be encrypted to maintain data secure. This ranging value is verified whether it is generated by a node.

Phase II: Malicious node cleaning

Algorithm 1. Approximate cleaning

1. Set m = *1* to s_i
2. For $v \in V(G)$ choose two neighbours of v is m and n respectively in random manner
3. Set and define local coordinate supporting system L_{cs} using $v,m,n,dm_{vm},dm_{vn},dm_{mn}$
4. Set and initialize sensor graph $G(V,E)$
5. for strongly associated each neighbour $k \in Nt(v)$ do
6. compute the value of location $k,pk,$ *on* L_{cs} by trilateration of dm_{kv}, dm_{km} *and* dm_{kn} from v,m,n
7. end for
8. set and the node v in $V(G)$ is created with location pv
9. for each neighbour $k \in Nt(v)$ do
10. set and node k is created in $V(G)$ with pk as location
11. end for
12. taking pair nodes strongly associated $m,n \in V(G)$ *and it ranges value* dm_{mn} do
13. $dc_{mn} = |pm - pn|$
14. if $|dm_{mn} - dc_{mn}| < \mathcal{E}$ then
15. create reliable edge $e(m,n)$ in $E(G)$
16. end if
17. end for
18. set and define largest support transmission range set C save it
19. end for
20. from support transmission range set C choose one with the largest size.

In this algorithm malicious node can cleaning efficiently. In this cleaning method first node v takes two nodes m, n which is the neighbour node of v in random manner. Then distance is calculated between v, m, n by considering v as origin. A efficient local coordinate system L_{cs} is created .A consistency subset is created using v's coordinate system by considering graph G(V,E),where V consists of v and it's neighbour nodes and E holds edge value. Initially graph G is empty k's location is find by local system L_{cs} using trilateration method .The node v,m,n and k whose distances are dm_{kv}, dm_{km} *and* dm_{kn} .The four nodes v,m,n and k's relative location's are unique in global coordinate system. Once we mapped the neighbours on local system . Then we compare with measured distance and projected distance of m,n nodes $dc_{mn} = |pm - pn|$ is computed from the local system L_{cs} when $dc_{mn} \geq \mathcal{E}$,the edge between m,n is not consider in E .This cleaning procedure is continuing iterative manner.

IV. PROPOSED KEY MANAGEMENT SCHEMES

The protocols for key distribution and key exchange being used earlier, which are based upon infrastructures using third parties seems to be improper for comparatively larger networks, from the angles of network topology, limitation arises in transmission range factor, association between nodes and its operation and also network boundary. It provides a good solution for this in which keys are pre distributed when sensor node is deployed in the field. The keys are installed in the sensor nodes for its secure connection. In case of hostile networks, key management and authentication are of much importance. Four schemes are being proposed here assuming that key information's are stored only at the cluster nodes as the entire network can be secured by protecting the cluster head. The schemes are-authentication, pair-wise key establishment, addition of new nodes, group wise authentication in existing networks. The key description and management technique is represented in detail manner.

(a) Association of Authentication method in between two different Sensor Nodes-

Authentication is given the first priority between the nodes when a node wants to communicate with another. Consider the 1st case where communication between two sensor nodes A and B are explained in detail here. The powerful anchor node is considered as head node for a cluster that records a information set which contains not only sensor node keys i.e. K1, K2, K3...Kn but also stores individual sensor node's ids and encrypted form of ids with individual keys i.e.(IDA) K1, (IDB)K2, (IDC)K3,…… (IDC)Kn before deployment. Each and every node maintains its stack which contains its ids and encrypted form of id along with its keys.

The sensor node A contains IDA and (IDA)K1 .Similarly IDB and (IDB)K2 is assign and maintain by B. For the authentic purpose MAC operation is perform by A with its (IDA)K1 along with randomly generated number i.e $A\alpha$. Then sensor node A send IDA||Aα|| MAC {(IDA)K1|| Aα} message to node B.Once the message is received by sensor node B,then it started its MAC calculation for validation purpose.

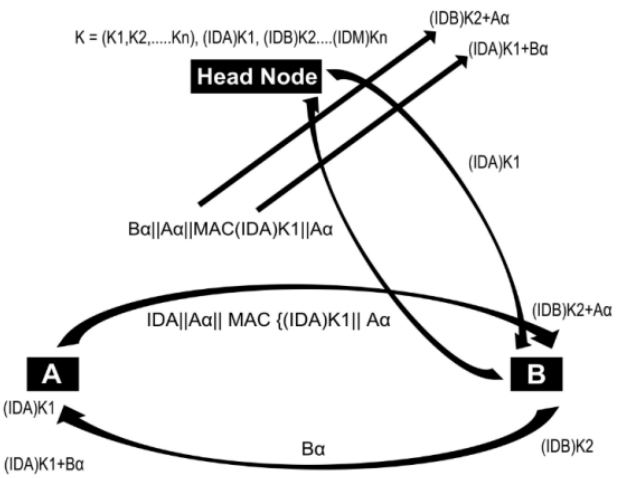

Fig. 2. Authentication Procedure

The powerful head node contains the key. A random number *Bα.* is generated by node B. upon receiving message from node A and node B sends message i.e. Aα||Bα||IDB ||H{(IDB)K2}|| IDA. IDB is recognised and authenticated node by calculating the hash over the {(IDB)K2},it is with head node . Once it ia authenticated by head node the validity is provided to sensor node A by sending (IDA) K1 to node B. Then node B calculates MAC {(IDA)K1|| Aα} and compares it with A's MAC. If there is a match, the sensor node is honest and valid, so a safe communication is possible.

The Aα sent from the Node A to Node B in the first step is used to change the {(IDB)K2is changed by using the Aα. Then node B sends request for authentication to head node & also asks for {(IDA) K1}. The (IDB) K2of B has been changed to (IDB) K2+ Aα, so that any one copying the communication between B and head node can't use it. After authentication, the cluster head can directly send Bα to A, and updating of (IDA) K1 to (IDA) K1+Bα is carried out at A & head node. After every authentication, he nodes change their Id values, which strengthens the security of the network. So authentication is given the topmost priority in the proposed scheme.

(b) Key Pairs maintain between two Individual Sensor Nodes

Each authenticated node knows each other's id. So they need a key pair for safe communication. For example consider two sensor' node's id is X and Y having its key X_d, They wants to maintain communication to each other. Node X compute its key X_dX as $X_dX = F\ X_d\ (X)$ & pair wise key $X_dXY = X_d\ X\ (Y) = F\ X_d\ (XY)$, Y compute its key $X_d\ Y$ as $X_d\ Y = F\ X_d\ (Y)$& pair wise key $X_d\ XY = X_d\ Y\ (X) = F\ X_d\ (XY)$. Once key setup phase is completed then start to transmit message to each other. A message 'Msg' is encrypted as Msg'= X_d XY(Msg). A counter is maintaining for store transmitted message.

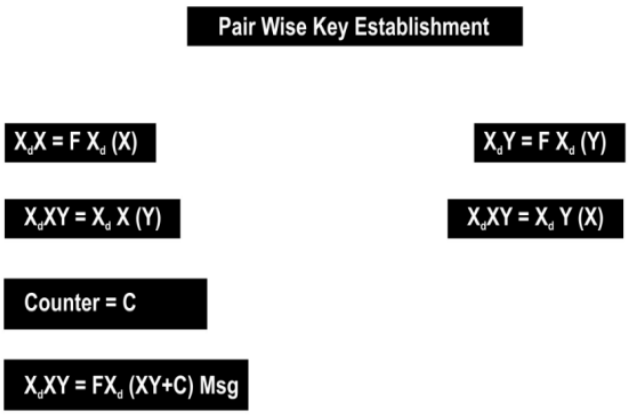

Fig. 3. Key pairs maintain between two individual sensor node

With each transmission the value of the counter is incremented by 1 at both the ends, In order to encrypt the same message differently with different permutation and combination manner. So that the attacker get confused to decipher the key. On every transmission the value of the counter gets incremented by the value 'c' along with the updation in pair wise key value i.e. $X_d\ XY = F\ X_d\ (XY+C)$. A message Msg can be encrypted as Msg'= X_d XY(Msg) = F X_d (XY+C)(Msg).

(c) Scheme for Addition of a new node into an existing Sensor Network

New nodes should be added regularly, as nodes can be damaged because of power loss. It is assumed that before deployment the head node has all sensor node's key and encrypted its id with its corresponding key .New node addition procedure is described here in the given figure. For example suppose Sensor node X

wants to be added into the network where sensor node A and Sensor node B are its two neighbours .The powerful Anchor node that is the head node consists keys of the sensor nodes i.e. K1, K2,…….Kn. Then encrypted data contain id of all node and encrypted own key i.e. (IDA)K1, (IDB)K2, (IDC)K3,… (IDN)Kn. The sensor node X holds it id i.e.IDX along with the encrypted form of its id and its own key and encrypted form its id with its own key i.e.(IDX)K3.MAC form of X is using its encrypted id and generated random number i.e. MAC {(IDX)K3||Xα}. Id + message is send to its neighbouring node in concatenating form its Id, random number and MAC data i.e. IDX||Xα|| MAC {(IDX)K3||Xα}. The neighbour node pass the message received to the head node, with the own encrypted id to the message sent by X i.e. (IDA)K1||IDX ||Xα|| MAC {(IDX)K3|| Xα}. The head node identifies the message and then checks for the authentication of the message i.e. IDX ||Xα|| MAC {(IDX) K3|| Xα}, by calculating its MAC IDX ||Xα|| MAC {(IDX) K3|| Xα} K3 is available with the head node. The computed MAC and the existing MAC are compared in the receive message at the head node. In case the two MAC's matches then it is conforms that node X is a authentic node and and node X is added to the sensor network by sending the message to node A

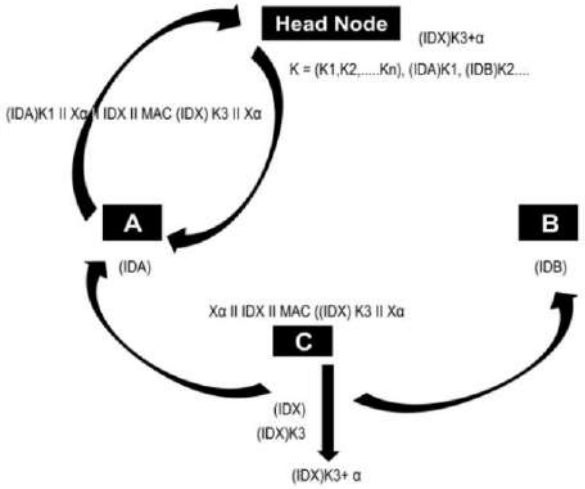

Fig. 4. Addition of new sensor node mechanism

K3+ Xα is encrypted with its id and the new key. Similarly the new sensor node changes its key K3 to K3 + Xα after requesting for adding its neighbour sensor node.

(d) Inter Group Authentication Scheme

Let us now consider a sensor network consisting of several sensor nodes belong to one particular group. All the activities in the network are being monitored by the base station .It performs the functions like assigning individual ids, group id and creation of a group key for the existing sensor nodes. When a new group is added in the existing group with the communication range, then the authentic procedure is maintained be the new arrival group member in Figure 5 A, B, C, D nodes are attached to existing group. Then their id and group id is assign by base satiation individually i.e. GID1 and also key i.e. KG1 is created as group key for the existing member. Each node stores its own id,group id along with its own key and encrypted form of the group id assign by the group key. The base station assigns its own id, group id i.e. GID2 and group key i.e KG2 for the newly arrive sensor node.

The node of other group key member needs to authenticate before the communication. In figure 5 G, H, I belongs to the sensor node of new group. We assume in the same transmission and communication boundary contains nodes are D, C, B of the existing group and the node G from new group. Inter group security mechanism is described as, the new arrival group nodes will decides the neighbouring group and after that it transmits its request to all the neighbours nodes in its neighbour group. Then it set and initialize the transmission range and make its communication When the node receive the broadcast request then immediately responds to the receiving request. This strategy follows probabilistic method. Where security depends upon the number of response received from the dedicated sender that requesting for the communication initiation. If number of node increase security responsibility and other factor is increase.

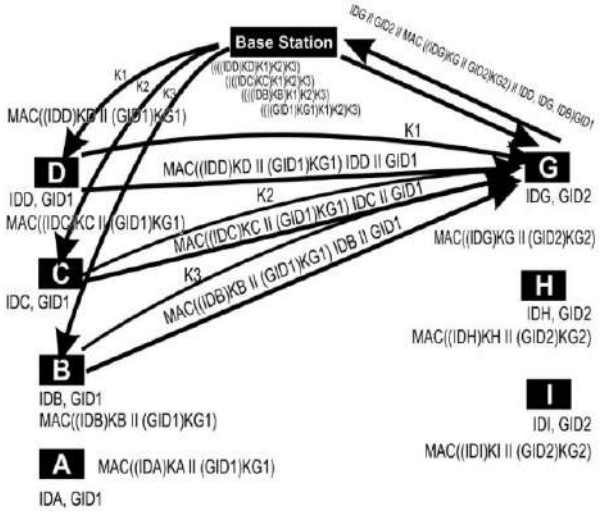

Fig. 5. Inter group authentication mechanism

Step 1: A concatenated message is sent by the sensor node upon receiving the request. The concatenated message consists of encrypted form of MAC of its id, group id. The sensor nodes D,C,B of first group sends message of other group sensor node G. Sensor node D sends message MAC ((IDD)KD||(GID1)KG1) || IDD || GID1 to G. Similar process is adopted by the sensor nodes B,C and sends the messages to G.The base station calculates the MAC ((IDD)KD||(GID1)KG1) and insert them into node D prior to development. Each node has MAC generated by the base station.

Step 2: In the effective ways MAC is calculated from the MAC received, node id and the group id. Since the key for id and group id is unavailable at the receivers end, hence a concatenated message is sent new group node G sends message IDG|| GID2|| MAC ((IDG) KG || (GID2) KG2) || (IDD||IDC||IDB) GID1 to the base station successful authenticate the rest of the id are checked for validity.

Step 3: Separate keys are created by the base station for the sensor nodes belonging to the first group. Three number of keys are generated. The encrypted form of the node id and group id of the first group encrypted by its key.

i.e.((IDD)KD),((IDC)KC),((((IDB)KB),((GID1)KG1). It is again encrypted with new generated key and finaly sends the encrypted id and group id i.e ((((IDD)KD)K1)K2)K3,((((IDC)KC)K1)K2)K3,((((IDB)KB)K1)K2)K3and((((GID1)KG1)K1)K2)K3.It becomes computationally infeasible to decrypt any of the encrypted data.

Step 4: The generated keys are sent by the base station to the respective sensor nodes. Sensor nodes D, C, B receives k1, k2 and k3 from the respected base station.

Step 5: The allocated keys are sent to the nodes of the second group by the first group node.

Step 6: The decryption of the encrypted ids are done by the new group members to get ((IDD) KD), ((IDC) KC), ((((IDB) KB), ((GID1) KG1) on receiving keys from 1st group. Node g computes the MAC and match with the MAC received in step 1. Based on matching authentication is successful.

V. CONCLUSION

In this research work we represent a local dynamic map which maintain with a reliable subset of ranging claim .The efficient and reliable method aims at finding and cleaning the malicious node. In this approach provides authentication to the coordinate values of the honest node and Provide a secure system for localization process. The proposed approach provides the better secure localization system and hence clean malicious node gives the better system. The proposed approach provides efficient key management and cost analysis technique and hence provides a reliable secure localization system.

REFERENCES

[1] B. Karp, and H. T. Kung, "GPSR: Greedy Perimeter Stateless Routing for wireless networks," in Proceedings of the 6th Annual International Conference on Mobile Computing and Network, 2000, pp. 243–354.

[2] D. Liu, and P. Ning, "Location-based pairwise key establishments for static sensor networks," in Proceedings of the 1st ACM workshop on Security of ad hoc and sensor networks, 2003, pp. 72–82.

[3] N. Sastry, U. Shankar, and D. Wagner, "Secure verification of location claims," in Proceedings of the 2nd ACM workshop on Wireless security, September 2003.

[4] J. Yick, B. Mukherjee, and D. Ghosal, "Wireless sensor networks: a survey," Computer Networks, vol.52, no. 12, pp.2292–2330, August 2008.

[5] I. F. Akyildiz, W. Su, Y. Sankarasubramaniam, and E. Cayirci, "Wireless sensor networks: a survey," Computer Networks, vol. 38, no. 4, pp. 393–422, March 2002.

[6] Y. Zeng, J. Cao, J. Hong, and L. Xie, "Secure localization and location verification in wireless sensor networks," in IEEE 6th International Conference on Mobile Adhoc and Sensor Systems, October 2009, pp. 864–869.

[7] S. Zhu and Z. Ding, "A simple approach of range-based positioning with low computational complexity",IEEE Transactions on Wireless Communications, vol. 8, no. 12, December 2009.

[8] M. Heidari, N. Alsindi, and K. Pahlavan, "Udp identification and error mitigation in ToA-based indoor localization systems using neural network architecture," IEEE Transactions on Wireless Communications, vol. 8, no. 7, July 2009.

[9] S. Lee, E. Kim, C. Kim, and K. Kim, "Localization with a mobile beacon based on geometric constraints in wireless sensor networks," IEEE Transactions on Wireless Communications, vol. 8, no. 7, pp. 5801–5805, December 2009

[10] H. Chen, Q. Shi, H. Vincent Poor, and K. Sezaki, "Mobile element assisted cooperative localization for wireless sensor networks with obstacles," IEEE Transactions on Wireless Communications, vol. 9, no. 3, March 2010.

[11] P. Bahl, and V. Padmanabhan, "RADAR: An In-Building RF-Based User Location and Tracking System," in Proceedings of the 19th Annual Joint Conference of the IEEE Computer and Communications Societies, vol. 21, 2000,pp. 755–784.

[12] A. Harter, A. Hopper, P. Steggles, A. Ward, and P. Webster, "The anatomy of a context-aware application," in Proceedings of the 5th Annual ACM/IEEE International Conference on Mobile Computing and Networking, 1999,pp. 59–68.

[13] L Girod and D. Estrin,"Robust range estimation using acoustic and multimodal sensing," in Proceedings of the IEEE/RSJ International Conference on Intelligent Robots and Systems, 2001, pp. 1312–1320.

[14] D. Niculescu and B. Nath, "Ad hoc positioning system (APS) using AoA," in Proceedings of the Twenty-Second Annual Joint Conference of the IEEE Computer and Communications Societies, vol. 3, April 2003, pp. 1734–1743.

[15] Xu Chun-Xia & Chen Ji-Yu, "Reseaech On The Improved DV-HOP Localization Algoritm In WSN", International Journal of Smart Home, Vol. 9, No. 4 (2015), pp. 157-162 .

[16] L. Doherty, K. Pister, and L. Ghaoui, "Convex position estimation in wireless sensor networks," in Proceedings of the 20th Annual Joint Conference of the IEEE Computer and Communications Societies, vol. 3, 2001, pp. 1655–1663.

[17] Y. Shang, W. Ruml, Y. Zhang, and M. Fromherz, "Localization from mere connectivity," in Proceedings of the 4th International ACM Symposium on Mobile Ad Hoc Networking & Computing, 2003, pp. 201–212.

[18] A. Ferreres, B. Alvarez, and A. Garnacho, "Guaranteeing the authenticity of location information," IEEE Pervasive Computing, vol. 7, no. 3, pp. 72–80, July 2008

[19] A. Savvides, C. Han, M. Strivastava, Dynamic fine-grained localization in ad-hoc networks of sensors, in: MOBICOM, 2001.

[20] Seung-Hyun Seo and Elisa Bertino, "Effective Key Management in Dynamic Wireless Sensor Networks", IEEE Transactions On Information Forensics And Security, Vol. 10, No. 2, February 2015.

[21] E. Sandeep Kumar, S. M. Kusuma, and B. P. Vijaya Kumar, "An Intelligent Defense Mechanism for Security in Wireless Sensor Networks", International Conference on Communication and Signal Processing, April 3-5, 2014 India, 2014 IEEE.

[22] G. Han, J. Jiang, L. Shu, J. Niu and H. C. Chao, "Managements and applications of trust in wireless sensor networks: A Survey," J. Comput. Syst. Sci., vol. 80, no. 3, 2014.

Comprehensive Review to Analyze the Islanding in Distributed Generation System

Sushree Shataroopa Mohapatra
School of Electrical Engineering
KIIT Deemed to be University
Bhubaneswar, India
mshataroopa@gmail.com

Dr. Manoj Kumar Maharana
School of Electrical Engineering
KIIT Deemed to be University
Bhubaneswar, India
mkmfel@kiit.ac.in

Sudhansu Bhusan Pati
School of Electrical Engineering
KIIT Deemed to be University
Bhubaneswar, India
sbpati.eee@gmail.com

Abstract- **The cumulative infiltration of small sized Renewable Energy Sources (RES) into prevailing grid has generated novel challenges. µG (µG) is a controllable unit for the grid as well as for the user side. It can meet its distinctive demands, ease feeder loss and safeguard local voltage stability. They can be coupled and separated from the grid to facilitate both grid-connected and islanded mode of operation. Islanding is a condition in which a distribution system gets electrically secluded from the rest of the network, owing to a fault at inflow side or any other disturbance, and yet remains to be strengthened by the Distributed Generation (DG) system coupled to it. Keeping track of different parameters alike Voltage, frequency, Impedance, real power(P), reactive power(Q), voltage(V) at the point of common coupling (PCC) is of great use to decide about islanding at any desired location.**

In today's scenario islanding detection is a vital phase. This study reviews about various islanding detection technique with their virtues and failings. It gives a comprehensive idea about different control schemes intended in line with the obligatory functions and probable operating conditions. Henceforth, the review can motivate the researcher on finding novel technique for detection of islanding in real time scenario for better power quality.

Keywords— Islanding, Distributed Generation, Microgrid, Voltage, Frequency, Controllers

I. INTRODUCTION

The furthermost important feature that extricates a Microgrid (µG) from a conventional grid is its controllability which makes the µG act as a controllable coordinated module when connected to a network. A micro grid is a decoct version of the centralized power system having following features.

- It is reliable & Flexible
- It is more secure
- It is resilient
- It can save money
- It can store & incorporate renewable energy

An interconnected µG shown in Fig.1 can achieve better stability and controllability with a distributed control structure. Interconnecting µGs to the central grid have the significance like availability, Operations/stability, Economic. The µG controller act as the edge concerning the utility grid and the loads pointing towards optimal power management.

According to IEEE 1547.4 a µG system must be capable of operating in parallel to the central grid or independently in isolation from the central grid. The islanded operation of µG can fetch numerous assistances to the utilities, which embraces the following:

- Improve customer's reliability
- Resolving overload problems
- Settling power quality issues
- Allow maintenance of system parameters without customer's intervention

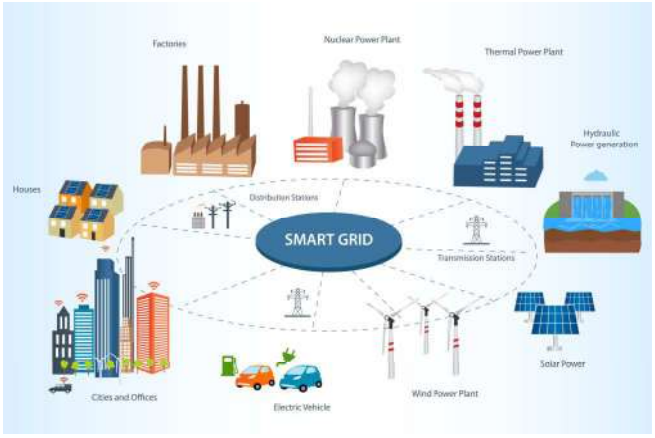

Fig.1. Smart Grid Layout

In islanded mode, a DG must supply the µG with seeded values for the system voltage(V) and frequency(f) variables. The RMS value and the frequency(f) of the AC voltage must be regulated by the inverter in a voltage source inverter mode. During islanded operation it may be anticipated for the converter to continue to supply a critical load when the central grid is disconnected. Additional criterion related to the islanding detection relates to the device involved in grid-interactive detection. The device has created an alternating current (AC) that corresponds to the output power existing on the grid [1]. Specifically, the grid-interactive inverter should counterpart the voltage, frequency, and phase of the connected power line. The main island state in which the portion of the electrical power system (EPS) was strengthened exclusively by more than one local EPS's via the PCC while the portion of the EPS was electrically secluded from the rest part of the system. Based on planned and unplanned event, there is a different two-variable portion of EPS is involved which makes islanding detection in real time a subject of significant study [2]. In general, detection of islanding can be categorized into passive methods that look for a grid transient occurrence, active methods that evaluate the grid by directing signals from the

978-1-7281-8774-7/21/$31.00 ©2021 IEEE

2021 1st International Conference on Power Electronics and Energy (ICPEE) | 978-1-7281-8774-7/21/$31.00 ©2021 IEEE | DOI: 10.1109/ICPEE50452.2021.9358542

inverter or from the distribution point of the grid [3]. Fig.2 represents different methods available for detection of islanding in a power network. Some techniques can be used by the utility to identify the conditions that would cause the inverter-based techniques to malfunction and purposely upset certain conditions to turn off the inverters. A μG controller severs the local path from the network and forces the DGs to power the intact local load via a dedicated switch [4].

From the view point of nuclear power plant Islanding is an extraordinary approach of action for a nuclear reactor. In this mode, the power plant is cut off from the grid, and only the power produced by the reactor itself is used to power the cooling systems. Islanding has become a standard practice for certain reactor to restore the electricity production when the power plant gets disconnected from the grid. During the balanced state, even if the load and output were matched, additional transient signals can be produced by the failure of the grid [5].

At different operating conditions countless control methods of Distributed Energy Resources (DER) unit are shortened in Table.I. Micro grids can operate either in grid connected or islanded mode to achieve uninterruptible power supply for the local loads. In order to bone up the above said operating conditions, it is indispensable to address all the issues related to modelling and control of μG.

Table. I. Control Methods of DER Units at different operating conditions.

Status	Operation	Function	Control Methods
Grid-Forming Unit	Control the system voltage(V) & frequency(f) by stabilizing generation power & load demands throughout the islanded operating mode	Voltage and Frequency Control (V & f control)	Hybrid AC Voltage control & Current Control, Indirect Current Control and AC Voltage Control
		Load Sharing	Voltage & Frequency Control, Active Current Sharing
Grid-Feeding Unit	Regulate the output active power and reactive power depending upon the power dispatched strategies/frequency(f)/voltage(V) discrepancy of the load/feeder	Power Dispatch (P_{disp})	Current Control and AC Voltage Control, VOC And Virtual Flux, Direct Power Control
		Real Power(P) And Reactive Power (Q) Support	Unity Power Factor Control, Positive Sequence Control, Constant Real and Reactive Power Control
Grid-Supporting Unit	Manages to excerpt maximum power (P_{max}) from the key energy sources & the essential reactive power to support grid voltage sags and local demand of reactive current	Real Power Output (P_{out})	MPPT
		Reactive Power(Q) Support	AC Voltage Control

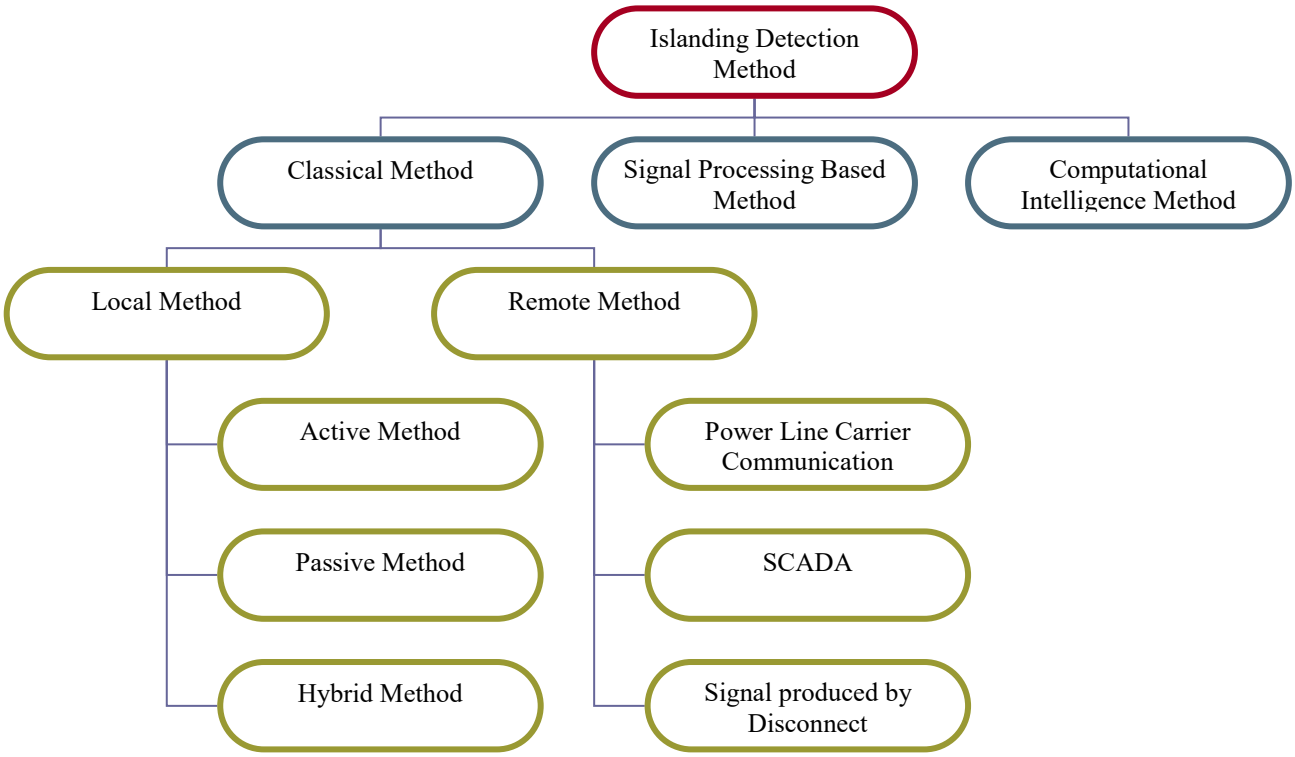

Fig.2. Methods for Detecting Islanding

II. NEED AND IMPORTANCE OF ISLANDING

In the power industry, an islanded distribution generation system is the most significant at present. With the rise in the contribution of DER to the output of electricity, the possessions of the power network are gaining more importance [6]. Islanding has turn out to be a key problem nowadays with the rise in the usage of Distributed Generators (DG) in a power grid. If the local loads proceed to control a portion of the distributed system, then this condition is called the Islanding condition. Distributed generation has become a norm in power engineering in recent times [7]. This goes well in close association with the popular growth of society, where minute-scale solutions and proximity consider reactions to several dilemmas. Numerous incidents in the power network led DG sources to be the new face of higher amount of electricity generation.; Nevertheless, DG can accommodate a cost-effective replacement for critical devices [8]. Therefore, it would take paramount expense and time to design extra power sources and configure the transmission system, though it may not be obtainable in both cases. The islanding condition can be defined as the state in which a distribution system is electrically detached from the power network, but continues to be controlled by the DG attached to it. This is not an active power source in a distribution system and power is also not supplied during the upstream transmission line fault detection, but with DG, this postulation is no longer right. Current uses show that DG is needed for islanding detection by all utilities to be efficiently isolated from the network at the earliest.

III. FACTORS INFLUENCING ISLANDING IN DISTRIBUTED GENERATION SYSTEM

The contribution of the short-circuit fault current (I_{fsc}) in the course of the interconnected and islanded mode has a vital role in Islanding event. With this regard the integration of DG services into µG distribution networks improves the protection issues. The Distributed Generation services influenced by some key factors which are listed below.

A. Reliability and Security

The current µG safety systems ought to be developed and intended with certain new methodologies to obtain new features such as self-healing, resilience to system anomalies, plug and play, high reliability, and security [9]. A µG is connected via a distributed network (DN) to the system to improve certain parameters such as safety, power quality, reliability, and stability which are estimated, in addition to the aids of the DG system [10]. when islanding is observed, power obtained through the micro grid and device reliability can be significantly improved to function independently [11].

B. Bidirectional Power Flow

The incorporation of the DG (synchronous, asynchronous, and inverter interfaced DG and ESS (short-term, long-term) modifies the faces of the network which in turn degrades the performance i.e., bidirectional power flow, low inertia device, and variable impedance in the overall system. The security systems are mutually affected by these variables and, in the event of any lack of cooperation, the efficacy of the intact network deteriorates [12].

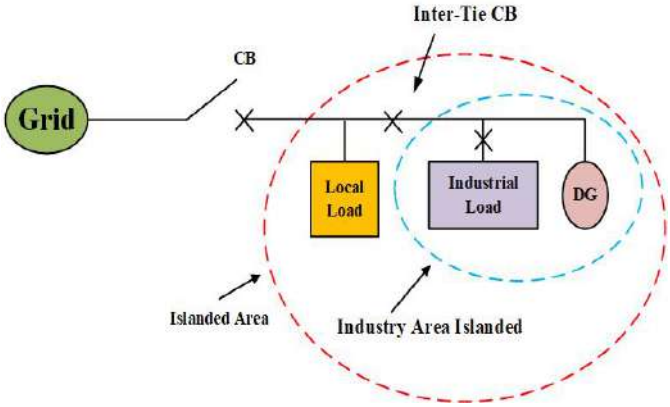

Fig.3. Principle of Islanding

C. Short Circuit Current

With a varied choice of service from the grid-connected mode to the islanded mode, the amount of short circuit current (SCC) changes dramatically. The support of DGs to the level of SCC also depends on the µG system's form, scale, and position of the DGs and ESS integration into the electrical power network [13].

D. Communication Infrastructure

The communication infrastructure and information collection can be defined contingent on two variables, the same as local information without communication and wide-area contact calculation. µG security, however, is affected by the combination of these two items [14].

E. Time Delay

With reference to the µG digital security architecture; it has been found that the time delay felt close to communication links shows a dynamic stinct [15].

F. Relay

The type of relay and synchronization of relays affect the complete planning of a µG security scheme [16].

G. Fault Analysis

The major factors in µG safety are the methods of processing skewed signal data and perceiving the fault without delay [17].

IV. CRITICAL BARRIERS OF ISLANDING

The traditional distribution network usually operates centrifugally and the flow of power from the power plant to the customer is unidirectional. Over-current-based safety devices are suggested for this type of network as the severity of the SCC is associated with the place where the fault occurred.

A. Reactive Power Injection

The increase in voltage is caused by certain things due to the erratic features of the PV source and the discrepancy between demand and output [18]. In reality, the enactment boosting of the PV system can be achieved by restraining the overall generation of PV output and sinking the infiltration rate of the PV network.

B. Energy Storage and Power Flow Control Methods

Some problems may be caused by the incorporation of the huge number of RES into the power network, such as critical voltage stability disputes. In this regard, incorporation of high-level RES into the grid has come to picture [19]. To ensure that it is apposite to incorporate some suggestions, such as the introduction of new stowing technologies espoused for voltage regulation: by means of the growth of grid-connected RESs, the ESS constraint became essential.

C. Non-Availability of Zero Crossing Current

Although an arc event is accompanied by the breaker operation in AC and DC networks, the action of AC breakers completely governed by the AC system's zero-crossing current, and after firing, it enables the arc to be separated within half a cycle [20]. Circuit breakers and fuses are the defensive devices in the traditional method that have been economically accessible and commonly especially for DC networks. Across low-impedance device, the fuses function in the nous that the metal wire melts instantly when a strong current flow through the fuse. It is usually selected according to the system's time ratings, current ratings, and voltage ratings for smooth and reliable service.

D. Low Voltage Crossing

With the rise in PV cohort across the network, a major challenge is modelled to preserve the stability and reliability of the grid. According to the grid code, the photovoltaic device should be associated to the network within the voltage dips which is termed as low voltage passage capability need [21].

E. Unbalance Voltage Control

When PV integration increases, unbalanced voltages induce some effects on the electric power system [22]. This is likely to suffer severely for this cause, and this will give rise to instability in the situation of unbalance. Active power filter in the distribution line is used for voltage imbalance compensation via the generation of negative sequence voltage (NSV) in series.

V. CURRENT TRENDS AND DEVELOPMENTS IN DISTRIBUTED GENERATION SYSTEM

The task of updating electricity delivery to integrate emerging technology is great, and electricity utilities are expected to work tirelessly on this agenda while making investments to ensure that current networks keep their electricity supply obligations safe and stable from a variety of sources in the aspect of conflicts and adverse environmental conditions [23]. Implementing vehicle-to-grid (V2G) technology, electric vehicles (EV) are becoming easy to deal with tools in distribution networks and are allowing many ancillary services (e.g., peak power shaving, voltage management, spinning reserve, etc.) to be offered [24]. This occurrence has progressive effects on the process of DG, nevertheless at the same time challenges the deployment of DG. An optimization model for the joint implementation of charging stations for electric vehicles and distributed generation resources, which comprehensively considers the portion of electric vehicles in the vehicle-to - grid context. The integration of DGs, such as wind turbines or photovoltaics, creates formerly unknown load flow situations that can threaten the operational protection of power systems [25].

The growing installation of DG systems in Germany, especially in rural areas, coincides with the low hosting capacity due to the historical dimension of the network. The various control practices smeared to the DG systems, counting the control of the active & reactive power, the handling of the load frequency, and the identification & control of the island mode of operation of the generation units, are the key themes found [26]. The diverse control approaches such as PID, stable, predictive, and fuzzy, with its solicitations are found. Specifically, solicitations for the association of generation units and the regulation of the DC-AC (inverter) electric power adaptation system are witnessed. Some of the recent methodologies and advantages are elaborated in the following Table. II [27].

VI. PERFORMANCE METRICS AND ANALYSIS OF DISTRIBUTED GENERATION SYSTEM

To analyze the performance metrics of a distributed generation system two major cases have been replicated with the aid of certain mathematical formulation [29]. The observed currents after islanding are zero as the measurement is performed in an open circuit island field. There are numerous criteria and test environments, containing multiple load quality variables, to assess the efficiency of island detection methods. The productivity of the IDMs (Islanding Detection Method) depends primarily on the timely and precise implementation of the appropriate process [30]. The operational capacity of an IDMs is defined by three major performance indices: NDZ (Non-Detection Zone), parallel RLC load, and load quality factor. A good procedure in these drastic circumstances demonstrates the effectiveness of IDMs. If the islanding state under such circumstances is successfully identified by a method, the dominance of the method is highlighted and fulfilled by the international standards.

A. Motivation of the Research Study

In real life, to encounter the rising demand for energy feeding, the incorporation of non-conventional energy sources into the grid is increasing. Islanding in the power grid is a big problem for a DG which can be mitigated using the impedance drift method [31] Islanding happens when a segment of the power supply in the interconnected system is withdrawn from the grid and the local charge remains to be distributed. The islanding condition occurred in a μG with distributed energy expansion may cause real dangers due to line fault. The islanding defects severely disrupt the normal operation of a DG [32]. Therefore, a few islanding techniques are used by analysts to protect the DGs from active, passive and hybrid disturbances. Communication-based strategies are more expensive than different approaches because of the criteria for the implementation of assurance framework and reconfiguration of security scheme [33].

The localized algorithms interpret isolation mode, monitor, and modify the basic network parameters, such as voltage(V), reactive power(P), frequency(f), and so on, such as active and passive techniques. Still, the passive methods

are ignored to consider islanding conditions if the mechanism has a low power imbalance [34]. Quite active approaches are the active techniques; the threshold values are normally fixed analytically as opposed to passive strategies, which can be misdirected and problematic. Most islanding detection techniques depend on the steady-state nature of the parallel RLC load, where the strength of the active load is directly proportional to the voltage square. Active load regulation, however, varies with voltage(V) and grid frequency shifts, which can also contribute to frequency(f) instability and have a major effect on the identification of islands.

TABLE II. Recent Methodologies and its Advantages [28]

Si. No	Method	Process	Advantages	Drawbacks
1.	Passive Method	Reflexively observe a series of electrical measures at PCC & analyses the response	i. Fast response time (4ms)	i. Large NDZ ii. Shortcoming in setting of threshold value.
2.	Active Method	Injects agitation into the grid strictures incessantly at regular interims & explores the retort	i. Minimizes NDZ ii. Improve detection accuracy iii. Response time 13-0.95ms	i. Continuous injection of disturbance signal have negative influence on power quality.
3.	Hybrid Method	Inherits the anticipated sorts of both passive(primary) and active (secondary) technique	i. Response time 0.12s	i. Incorporates desirable features of both the techniques.
4.	Remote Method	Utilize communication amid the utility and the DG to sense an existence of an Islanding incident	i. Includes nonappearance of NDZ ii. No deprivation of PQ iii. Effective in multi-DG environment iv. Response time within 200ms	i. Requires additional instrument making system expensive.
5.	Signal Processing Based Method	Observes numerous strictures at the PCC & smears a method to derive unseen sorts which are further utilized for event classification	i. Proficient of digging out unseen sorts of some signal ii. Gives information about mode of being the system iii. Minimizes NDZ	NA
6.	Intelligent Method	Intelligence-based practices can lever several factors concurrently, it is probable to train the DG for numerous islanding circumstances and improve the precision of recognition.	i. Can lever several parameters simultaneously ii. Enhance accuracy of detection	NA

B. Proposed Research Objective

There are three remarkable extents in this section, such as data generation, feature extraction and identification, classifications for the detection, classification of the island and non-island occurrences in the DG system. The negative sequence part of the PCC voltage is detached in the process of dataset generation [35]. To eliminate the negative voltage of the series the signal is tested, and the sequence analyzer runed through the non-stationary signals. Integrating distributed generation (DG) power with electricity systems offers potential energy security and efficient solutions with limited impacts on the environment. Leading concerns related to DG integration is accidental islanding.

A new Eradicate liability passive islanding detection system, which takes into account the dynamic load behavior. It is evaluated under noise conditions for the measured voltage signal and the corresponding resistance derivative. The islanding detection index that regulates the frequency based on time [36]. With ensemble empirical mode decomposition (EEMD) for detection, the model voltage signal was initially preprocessed. Then, autoregressive signal modeling has been used at the PCC with the grid to pull out signal structures from voltage and frequency signals. In spite of that, suitable guidelines are being anticipated to set a reasonable threshold [37]. The threshold values used to distinguish among the islanding phase and other non-islanding cases are thus removed, even with a zero-power misalliance between generation and load.

C. Contribution of Research Study

The main objective is to build a framework using an effective sharing technique to manage large-scale data processing and probing operations. The shredding approach is implemented by applying efficient shred partitioning and efficient shard selection techniques to improve the efficiency of distributed processing systems. A classification experiment with an extensive range of real-time data will test the suggested method. For the study of the output of the proposed algorithm, the classification models such as a decision tree and multilayer perceptron outcomes must be noted and plotted. It is expected that the proposed algorithm would yield better results for classification models. Through simulation, the sensitivity study of these parameters is determined in terms of load volatility, fault events, and load

switching on different events, insulating and non-islanding voltage drops [39].

D. Application and Advantage

Distributed generation units reduce reliance on major power plants. This effects in eradicating the need to erect immense power generation and deferral of new capacity. It also cuts the reliance on the long-distance national transmission grid, which probably reduces the charge of mounting new transmission lines and reduces transmission congestion [40]. It enhances or preserves system reliability by having aback-up generation. It also improves the flexibility of system operators, increases energy security by varying energy sources and reducing dependence on a complex large system [41]. The application of the distributed energy source poses new concerns regarding unintended islanding behaviour in which grid security issues are prompted, thus endangering the safety of utility staff. These many decades contain thousands of researchers' discoveries and developments of the anti-islanding system to meet the need for grid safety. The distributed generation units interconnect with the electrical supply network through a three-phase inverter, whereby the active and reactive power management applications rely on inverter control strategies [42].

Conclusion

Islanding confers to the state where in µGs form in consequence of severing the central power source deprived of preventing the integration of DG sources. Integrating DG sources through electric systems offers potential energy security and a stable solution with limited impacts on the environment. One of the most important concerns related to DG integration is accidental islanding. The persistence of the article is to deliver ways to detect islanding in the power network. By analyzing a statistic poised of diverse indicators such as voltage amplitude, event time period, unbalanced degree, device frequency, grid impedance, and power angle, the islanding pattern has been identified. For an islanded µG, DG disconnection is necessary only if the generation from DGs is not adequate to meet the local load requirements to elude power misbalance and grid failure. However, if the generation from DGs is adequate to maneuver native loads plus the islanding event is deliberate, a load controlling activity for the uninterrupted supply of previous loads has to be accomplished. After going through various methods adopted for islanding detection, it is established that Intelligent technique along with signal processing-based method can play a major role in perceiving islanding events in an intricate cross DG network. Ultimately, the review will guide the researcher towards effective islanding discovery in a DG for better energy consumption in real-time scenarios.

REFERENCES

[1] R. M. Radhakrishnan, A. Sankar and S. Rajan, "Synchrophasor based islanding detection for µGs using moving window principal component analysis and extended mathematical morphology", IET Renewable Power Generation, vol. 14, no. 12, pp. 2089-2099, 7 9 2020, doi: 10.1049/iet-rpg.2019.1240.

[2] Jetty Rajesh Reddy, Alagappan Pandian, Chilakala Rami Reddy, "An efficient learning based RFMFA technique for islanding detection scheme in distributed generation systems", Applied Soft Computing, Volume 96, 2020, 106638, ISSN 1568-4946, doi: 10.1016/j.asoc.2020.106638

[3] Sindhura Rose Thomas, Venugopalan Kurupath, Usha Nair, "A passive islanding detection method based on K-means clustering and EMD of reactive power signal", Sustainable Energy, Grids and Networks, Volume 23, 2020, 100377, ISSN 2352-4677, doi: 10.1016/j.segan.2020.100377

[4] S. Admasie, S. B. A. Bukhari, T. Gush, R. Haider and C. H. Kim, "Intelligent Islanding Detection of Multi-Distributed Generation Using Artificial Neural Network Based on Intrinsic Mode Function Feature", Journal of Modern Power Systems and Clean Energy, vol. 8, no. 3, pp. 511-520, May 2020, doi: 10.35833/MPCE.2019.000255.

[5] Picioroaga, Irina, Mircea EREMIA, Valentin ILEA, and Cristian BOVO. "Resilient operation of distributed resources and electrical networks in a Smart City context,". The UPB Scientific Bulletin, Series C 82, no. 3 (2020): 267-278.

[6] Afshin Taheri Kolli, Navid Ghaffarzadeh, "A novel phaselet-based approach for islanding detection in inverter-based distributed generation systems", Electric Power Systems Research, Volume 182, 2020, 106226, ISSN 0378-7796, doi: 10.1016/j.epsr.2020.106226.

[7] Kanupriya, and Durgesh Vishwakarma. "A Review Article of Facts Based Islanding Phenomenon Reduction and Enhancement of Grid Efficiency", International Journal of Scientific Research & Engineering Trends Volume 6, Issue 3, May-June-2020, ISSN (Online): 2395-566X.

[8] Azeem, F., Narejo, G.B. & Shah, U.A. Integration of renewable distributed generation with storage and demand side load management in rural islanded µG. *Energy Efficiency* 13, 217–235 (2020). doi:10.1007/s12053-018-9747-0

[9] Vieira, Thiago Correia, Ahda Pionkoski Grilo, Julio Carlos Teixeira, and Ricardo Caneloi dos Santos. "Methodology for Assessing the Risk of Unintentional Islanding of Distributed Wind Generators Using Passive Schemes." Journal of Control, Automation and Electrical Systems 31, no. 1 (2020): 177-188.

[10] P. Buduma, S. J. Pinto and G. Panda, "Loss of Utility Detection and Seamless Operation of Distributed Generation System," in IEEE Transactions on Industry Applications, vol. 56, no. 3, pp. 3149-3158, May-June 2020, doi: 10.1109/TIA.2020.2976800.

[11] Radhakrishnan, Rohikaa Micky, Ashok Sankar, and Sunitha Rajan. "A combined islanding detection algorithm for grid connected multiple µGs for enhanced µG utilisation." International Transactions on Electrical Energy Systems 30, no. 2 (2020): e12232.

[12] Sarangi, Swetalina, Binod Kumar Sahu, and Pravat Kumar Rout. "Distributed generation hybrid AC/DC µG protection: A critical review on issues, strategies, and future directions." International Journal of Energy Research 44, no. 5 (2020): 3347-3364.

[13] Antonio Colmenar-Santos, Ana-Rosa Linares-Mena, Enrique-Luis Molina-Ibáñez, Enrique Rosales-Asensio, David Borge-Diez, "Technical challenges for the optimum penetration of grid-connected photovoltaic systems: Spain as a case study", Renewable Energy, Volume 145, 2020, Pages 2296-2305, ISSN 0960-1481, doi: 10.1016/j.renene.2019.07.118.

[14] Reddy, Ch Rami, and K. Harinadha Reddy. "Passive islanding detection technique for integrated distributed generation at zero power balanced islanding." International Journal of Integrated Engineering 11, no. 6 (2019): 126-137.

[15] Diahovchenko, I., Kolcun, M., Čonka, Z. et al. "Progress and Challenges in Smart Grids: Distributed Generation, Smart Metering, Energy Storage and Smart Loads". Iran J Sci Technol Trans Electr Eng 44, 1319–1333 (2020). Doi:10.1007/s40998-020-00322-8

[16] M. A. Mohamed, A. Almalaq, E. Mahrous Awwad, M. A. El-Meligy, M. Sharaf and Z. M. Ali, "An Effective Energy Management Approach within a Smart Island Considering Water-Energy Hub," in IEEE Transactions on Industry Applications, doi: 10.1109/TIA.2020.3000704.

[17] Nienhuis, J. H. and Lorenzo-Trueba, J.: Simulating barrier island response to sea level rise with the barrier island and inlet environment (BRIE) model v1.0, Geosci. Model Dev., 12, 4013–4030, doi: 10.5194/gmd-12-4013-2019, 2019

[18] David Ribó-Pérez, Paula Bastida-Molina, Tomás Gómez-Navarro, Elías Hurtado-Pérez, "Hybrid assessment for a hybrid µG: A novel methodology to critically analyse generation technologies for hybrid µGs", Renewable Energy, Volume 157, 2020, Pages 874-887, ISSN 0960-1481, doi: 10.1016/j.renene.2020.05.095.

[19] Fan, Guangkuan, Zhenyu Zhang, Hao Tian, Xin Yang, Jianhua Bai, Xuefeng Jia, and Yunfei Wang. "Reliability Assessment of Distribution Network with Distributed Generation based on BP Neural Network." In Journal of Physics: Conference Series, vol. 1549, no. 5, p. 052014. IOP Publishing, 2020.

[20] Zhu, Huimin, Shun Yuan, and Chunlai Li. "Network communication monitoring system of distributed PV power generation system." International Journal of Communication Systems (2020): e4517, doi: 10.1002/dac.4517.

[21] B. Pancha, R. Shrestha, and A. Jha, "Islanding Detection in Distributed Generation Integrated Thimi – Sallaghari Distribution Feeder Using Wavelet Transform and Artificial Neural Network", *JIE*, vol. 15, no. 2, pp. 55-61, Jul. 2019.

[22] Reddy, C. R., & Reddy, K. H. (2019). Passive Islanding Detection Technique for Integrated Distributed Generation at Zero Power Balanced Islanding. *International Journal of Integrated Engineering*, *11*(6), 126-137.

[23] Reddy, C.R., Reddy, K.H. A New Passive Islanding Detection Technique for Integrated Distributed Generation System Using Rate of Change of Regulator Voltage Over Reactive Power at Balanced Islanding. J. Electr. Eng. Technol. 14, 527–534 (2019). Doi: 10.1007/s42835-018-00073-x

[24] Reza Zamani, Mohammad Esmail Hamedani Golshan, Hassan Haes Alhelou, Nikos Hatziargyriou, A novel hybrid islanding detection method using dynamic characteristics of synchronous generator and signal processing technique, Electric Power Systems Research, Volume 175, 2019, 105911, ISSN 0378-7796, doi: 10.1016/j.epsr.2019.105911.

[25] Ahmadipour, Masoud and Hizam, Hashim and Othman, Mohammad Lutfi and Mohd Radzi, Mohd Amran (2019) *Islanding detection method using ridgelet probabilistic neural network in distributed generation.* Neurocomputing, 329 (15). pp. 188-209. ISSN 0925-2312

[26] S. R. Mohanty, N. Kishor, P. K. Ray and J. Catalao, "Comparative study of advanced signal processing techniques for islanding detection in a hybrid distributed generation system," 2015 IEEE Power & Energy Society General Meeting, Denver, CO, 2015, pp. 1-1, doi: 10.1109/PESGM.2015.7285854.

[27] S. K. G. Manikonda and D. N. Gaonkar, "Comprehensive review of IDMs in DG systems," in IET Smart Grid, vol. 2, no. 1, pp. 11-24, 3 2019, doi: 10.1049/iet-stg.2018.0096.

[28] Ch, Rami Reddy, and K. Harinadha Reddy. "Islanding Detection Techniques for Grid Integrated DG–A Review." International Journal of Renewable Energy Research (IJRER) 9, no. 2 (2019): 960-977.

[29] M. Gholami, Islanding Detection Method of Distributed Generation Based on Wavenet, International Journal of Engineering (IJE), IJE TRANSACTIONS B: Applications Vol. 32, No. 2, (February 2019) 242-248

[30] S. Murugesan and V. Murali, "Active Unintentional Islanding Detection Method for Multiple-PMSG-Based DGs," in IEEE Transactions on Industry Applications, vol. 56, no. 5, pp. 4700-4708, Sept.-Oct. 2020, doi: 10.1109/TIA.2020.3001504.

[31] M. Malakondaiah, K. K. Boddeti, B. Ramesh Naidu and P. Bajpai, "Second harmonic impedance drift-based islanding detection method," in IET Generation, Transmission & Distribution, vol. 13, no. 23, pp. 5313-5324, 3 12 2019, doi: 10.1049/iet-gtd.2018.6838.

[32] Liu, X., Zheng, X., He, Y., Zeng, G., and Zhou, Y., "Passive Islanding Detection Method for Grid-Connected Inverters Based on Closed-Loop Frequency Control", Journal of Electrical Engineering & Technology, vol. 14, no. 6, pp. 2323–2332, 2019. doi:10.1007/s42835-019-00181-2.

[33] R. Bakhshi-Jafarabadi and J. Sadeh, "New voltage feedback-based islanding detection method for grid-connected photovoltaic systems of μG with zero non-detection zone," in IET Renewable Power Generation, vol. 14, no. 10, pp. 1710-1719, 27 7 2020, doi: 10.1049/iet-rpg.2019.1174.

[34] J. Ke, Z. Zhengxuan, Y. Zhe, F. Yu, B. Tianshu and Z. Jiankang, "Intelligent islanding detection method for photovoltaic power system based on Adaboost algorithm," in IET Generation, Transmission & Distribution, vol. 14, no. 18, pp. 3630-3640, 18 9 2020, doi: 10.1049/iet-gtd.2018.6841.

[35] G. Wang, F. Gao, J. Liu, Q. Li and Y. Zhao, "Design consideration and performance analysis of a hybrid islanding detection method combining voltage unbalance/total harmonic distortion and bilateral reactive power variation," in CPSS Transactions on Power Electronics and Applications, vol. 5, no. 1, pp. 86-100, March 2020, doi: 10.24295/CPSSTPEA.2020.00008.

[36] J. Ke, Z. Zhengxuan, Z. Qijuan, Y. Zhe and B. Tianshu, "Islanding detection method of multi-port photovoltaic DC micro grid based on harmonic impedance measurement," in IET Renewable Power Generation, vol. 13, no. 14, pp. 2604-2611, 28 10 2019, doi: 10.1049/iet-rpg.2019.0271.

[37] Y. Lee, J. Kim and B. Han, "Islanding Detection Method for Inverter-Based Distributed Generation by Injecting Second Order Harmonic Current," 2019 10th International Conference on Power Electronics and ECCE Asia (ICPE 2019 - ECCE Asia), Busan, Korea (South), 2019, pp. 2860-2865.

[38] Xing Xie, Chun Huang, Danni Li, A new passive islanding detection approach considering the dynamic behavior of load in μG, International Journal of Electrical Power & Energy Systems, Volume 117, 2020, 105619, ISSN 0142-0615, doi: 10.1016/j.ijepes.2019.105619

[39] Reddy, V. R., & Sreeraj, E. S. (2019, December). A Feedback Based Hybrid Islanding Detection Method and Voltage Ride-Through of One Cycle Controlled PV Inverter. In 2019 National Power Electronics Conference (NPEC) (pp. 1-6). IEEE.

[40] Reddy, J. & Alagappan, Pandian & Dhanasekharan, R & Reddy, Ch & Lakshmi, B & Devi, B. Neelima. (2020). Islanding detection of integrated distributed generation with advanced controller. Indonesian Journal of Electrical Engineering and Computer Science. 17. 1626-1631. 10.11591/ijeecs. v17.i3. pp1626-1631.

[41] Anudeep, Bhatraj and Nayak, Paresh Kumar. "Sequence Component-Based Improved Passive Islanding Detection Method for Distribution System with Distributed Generations" *International Journal of Emerging Electric Power Systems*, vol. 20, no. 2, 2019. doi.org:10.1515/ijeeps-2018-0292.

[42] D. Zhang, L. Yu, X. Wen, B. Xu, J. Ding and C. Luo, "Islanding Detection Method for Inverter Cluster Based on Interharmonic Impedance Measurement," 2019 IEEE 3rd Conference on Energy Internet and Energy System Integration (EI2), Changsha, China, 2019, pp. 883-888, doi: 10.1109/EI247390.2019.9062209.

American Journal of Electrical and Electronic Engineering, 2019, Vol. 7, No. 4, 94-98
Available online at http://pubs.sciepub.com/ajeee/7/4/2
Published by Science and Education Publishing
DOI:10.12691/ajeee-7-4-2

Principle of Coherence Optical Systems-Current Applications and Future Challenges

Arun Agarwal[1,*], Kabita Agarwal[2], Gourav Misra[3], Subrat Kumar Panda[4]

[1]Department of ECE, Institute of Technical Education & Research (ITER), Siksha 'O' Anusandhan Deemed to be University, Khandagiri Square, Bhubaneswar-751030, Odisha, India
[2]Department of Electronics and Instrumentation Engineering, College of Engineering & Technology (CET), Ghatikia, Kalinga Nagar, Bhubaneswar-751003, Odisha, India
[4]School of Electronic Engineering, Dublin City University, Glasnevin, Dublin 9, Ireland
[4]Department of ECE, Gandhi Institute For Technology (GIFT), Gramadiha, PO-Gangapada, Bhubaneswar-752054, Odisha, India
*Corresponding author: arunagrawal@soa.ac.in

Received August 10, 2019; Revised September 15, 2019; Accepted September 20, 2019

Abstract This paper reviews the concept of coherent optical systems as future digital optical communication systems having capacity of achieving 100Gbps speed. While the transmission capacity increases in wavelength-division multiplexed (WDM) system, coherent technologies have been in large interest in recent years. The interest lies in finding methods of increasing the bandwidth demand with multilevel modulation formats based on coherent technologies. We also discuss about requirements and challenges in implementation of respective digital receivers and associated signal processing.

Keywords: *optical systems, WDM, coherent, bandwidth, signal processing, digital receivers*

Cite This Article: Arun Agarwal, Kabita Agarwal, Gourav Misra, and Subrat Kumar Panda, "Principle of Coherence Optical Systems-Current Applications and Future Challenges." *American Journal of Electrical and Electronic Engineering*, vol. 7, no. 4 (2019): 94-98. doi: 10.12691/ajeee-7-4-2.

1. Introduction

In the 1980s Coherent optical fiber communications were studied extensively mainly because high sensitivity of coherent receivers could be used for a higher transmission distance; however, due to the rapid progress in high-capacity wavelength-division multiplexed (WDM) systems using erbium-doped fiber amplifiers (EDFAs) their research and development have been interrupted for nearly 20 years behind.

In 2005, there was a large interest in the topic because of the digital coherent receivers which does not depend upon any complicated process rather uses variety of spectrally efficient modulation formats such as M-ary phase shift keying (PSK) and quadrature amplitude modulation (QAM). By this process the phase information are not being lost and different offset like chromatic dispersion and polarization-mode dispersion can be compensated. Taking these aspects into consideration the coherent optical is being in research in the field of optical communication systems.

2. The New Coherence Optical Communication Transmission

2.1. Digital Communication

Digital modulation is the mapping of digital sequence i.e. the binary data in analog form or signal. In digital modulation scheme a block of k bit data's are mapped into one modulation level M, where $M = 2^k$ to generate a signal $S_m(t)$, where m lies between $1 \le m \le 2^k$ .In this way it is possible to increase the transmitted bit rate by transmitting k number of bits of information in every T_s sec.

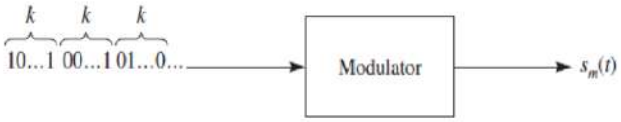

Figure 1. Generation of $S_m(t)$

There are different modulation schemes in which $S_m(t)$ can be used are pulse amplitude modulation (PAM), phase shift keying (PSK), quadrature shift keying (QAM).

In PAM the amplitude of the signal is varied. Suppose a signal $S_m(t)$ be like,

$$S_m(t) = A_m \cos(2\pi f_c t)$$

Where, $A_m = 0,1,2 \ldots (M-1)$.

In PSK the phase of the signal is varied. Suppose a signal $S_m(t)$ be like,

$$S_m(t) = g(t)\cos\left(2\pi f_c t + \frac{2\pi}{M}(m-1)\right).$$

In QAM both the amplitude and phase of the signal are varied. The signal $S_m(t)$ be like,

$$S_m(t) = I_m g(t)\cos(2\pi f_c t) + Q_m g(t)\sin(2\pi f_c t)$$

Where, $I_m, Q_m = \pm 1, \pm 3, \ldots\ldots (\pm M - 1)$.

2.2. Phase Modulation

Phase modulators are used to achieve Optical amplitude modulation (AM) in a Mach–Zehnder configuration which are driven in a push–pull mode of operation. Optical IQ modulation can be consists of a push–pull type MZM in parallel, with one of the MZM given a π/2 phase shift.

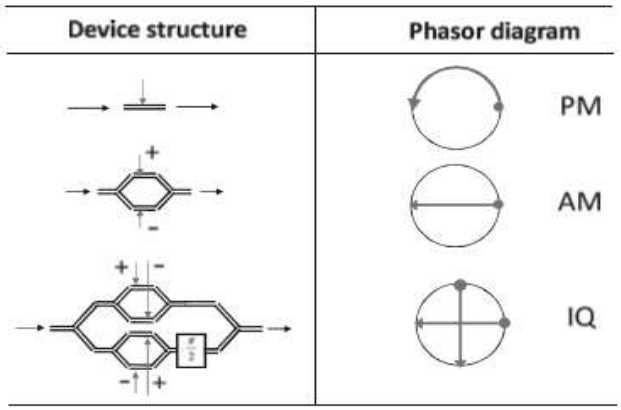

Figure 2. Device structure and the phasor diagram comparison among phase modulation, amplitude modulation, and IQ modulation.

Phase modulation depends on the wavelength λ, electrode length (interaction length) l_{el}, and the change of the effective refractive index Δn_{eff}. Considering only the Pockels effect, the change of the refractive index can be assumed to be linear w.r.t. the applied external voltage u(t):

$$\varnothing_{PM}(t) = \frac{2\pi}{\lambda}\Delta n_{eff}(t).l_{el} \sim u(t).$$

Transfer function: $E_{out}(t) = E_{in}(t)e^{i\frac{u(t)\pi}{v_\pi}}$.

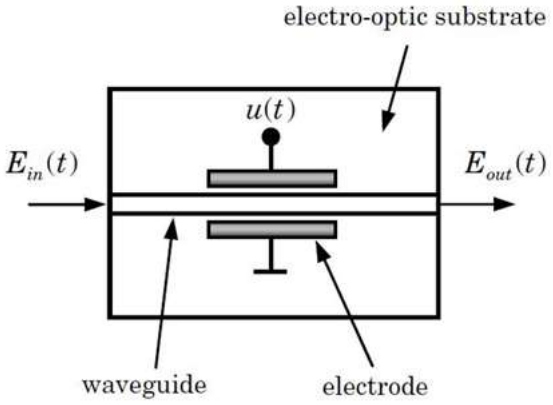

Figure 3. Device structure of phase modulation

2.3. Mach-zehender Modulation

When two phase modulators are placed parallel using an interferometric structure a mach zehender is formed. In a MZM the incoming light is split into two branches, with different phase shifts applies to each path, and then they recombined. The output of MZM is a result of interference, ranging from constructive (the phase of the light in each branch is the same) to destructive (the phase in each branch differs by π).

Transfer function:

$$E_{out}(t) = E_{in}(t)(e^{i\varnothing_1(t)} + e^{i\varnothing_2(t)})$$

$$\varnothing_1(t) = \frac{u_1(t)\pi}{v_\pi}$$

$$\varnothing_2(t) = \frac{u_2(t)\pi}{v_\pi}$$

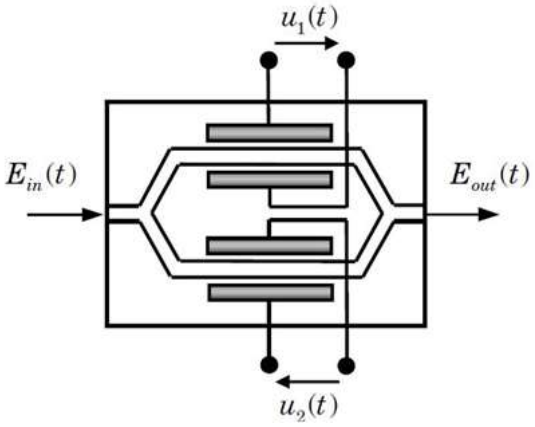

Figure 4. Device structure of MZM

When MZM is operating in push-push condition, $u_1(t) = u_2(t)$.
When MZM is operating in push-pull condition, $u_1(t) = -u_2(t)$.

In push-push condition the MZM works as a pure phase modulation system and in push-pull as pure amplitude modulation system.

In push-pull condition, $u_1(t) = -u_2(t) = \frac{u(t)}{2}$.

In push-pull operation the field (E) and the power (P) transfer function of the MZM is,

$$E_{out}(t) = E_{in}(t)\cos\left(\frac{\Delta\varphi_{MZM}(t)}{2}\right) = E_{in}(t)\cos\left(\frac{u(t)\pi}{2v_\pi}\right)$$

$$\frac{P_{out}(t)}{P_{in}(t)} = \frac{1}{2} + \frac{1}{2}\cos\left(\Delta\varphi_{MZM}(t)\right) = \frac{1}{2} + \frac{1}{2}\cos\left(\frac{u(t)\pi}{v_\pi}\right)$$

$$\Delta\varphi_{MZM}(t) = \frac{u(t)\pi}{v_\pi}.$$

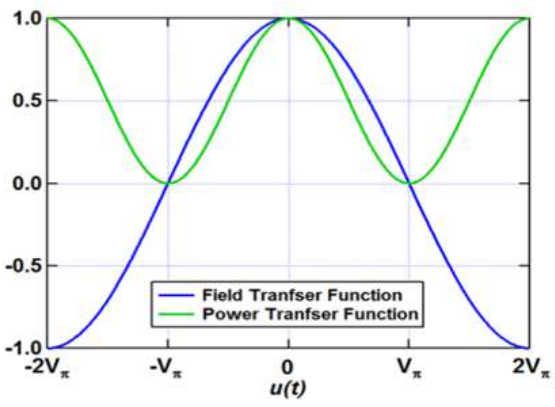

Figure 5. Field and power transfer function

When MZM, bias voltage is at quadrature point i.e. $V_{bias} = -\frac{v_\pi}{2}$ and modulate with a inpute voltage swing of v_π peak-to-peak. In this condition the MZM acts as a pure amplitude modulation technique (example: on-off keying).

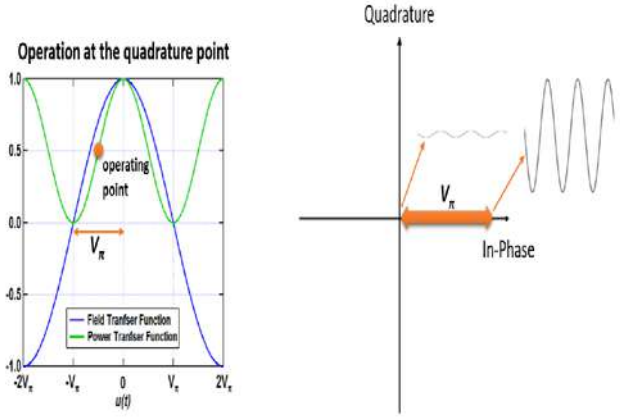

Figure 6. Operation at Quadrature point

When MZM, bias voltage is at minimum transmission point i.e. $V_{bias} = -v_\pi$ and modulate with an input voltage swing of $2v_\pi$ peak-to-peak, in addition to amplitude modulation, a phase change of π occurs every time the input, u(t), crosses the minimum transmission point (example: BPSK).

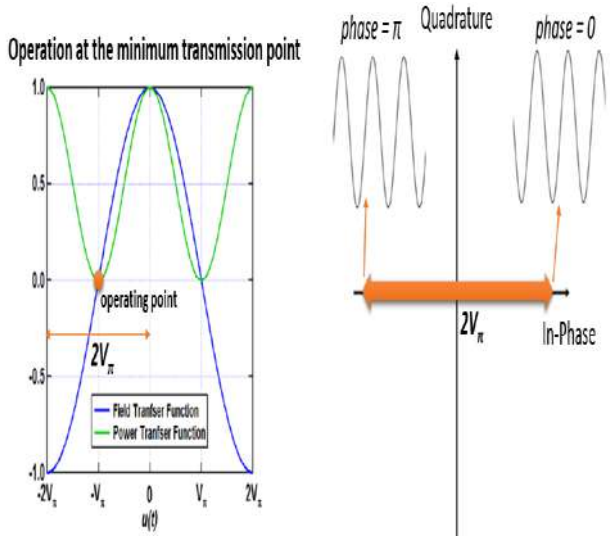

Figure 7. Operation at minimum point

2.4. Optical IQ Modulator

Here MZMs working in push-pull condition are placed parallel to one another with a $\frac{\pi}{2}$ phase shift to the second MZM.

The transfer function of dual drive MZM is:

$$\frac{E_{out}(t)}{E_{in}(t)} = \cos\frac{E_{out}(t)}{E_{in}(t)}$$

$$= \cos\left(\frac{\Delta\varphi_I(t)}{2}\right) + \cos\left(\frac{\Delta\varphi_Q(t)}{2}\right).e^{i\frac{\pi}{2}}$$

$$E_{out}(t) = E_{in}(t)\left[\cos\left(\frac{\Delta\varphi_I(t)}{2}\right) + i\cos\left(\frac{\Delta\varphi_Q(t)}{2}\right)\right]$$

$$\Delta\varphi_I(t) = \frac{(V_I + V_{DC})\pi}{v_\pi}$$

$$\Delta\varphi_Q(t) = \frac{(V_Q + V_{DC})\pi}{v_\pi}.$$

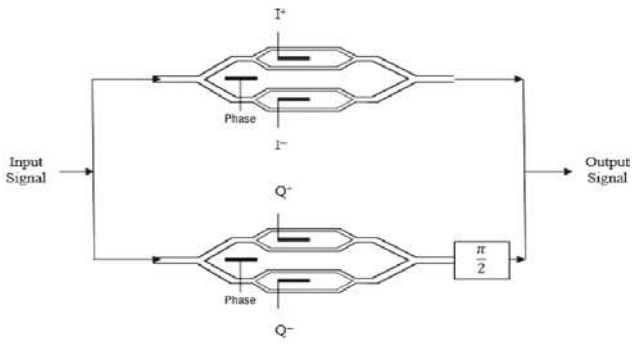

Figure 8. MZM IQ Modulator

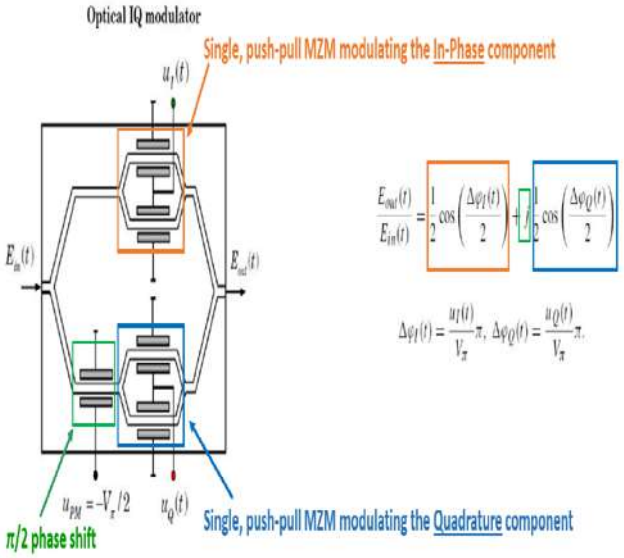

Figure 9. Dual-Nested IQ (In-Phase, Quadrature) Mach-Zehnder Modulator (with each MZM biased at minimum transmission point)

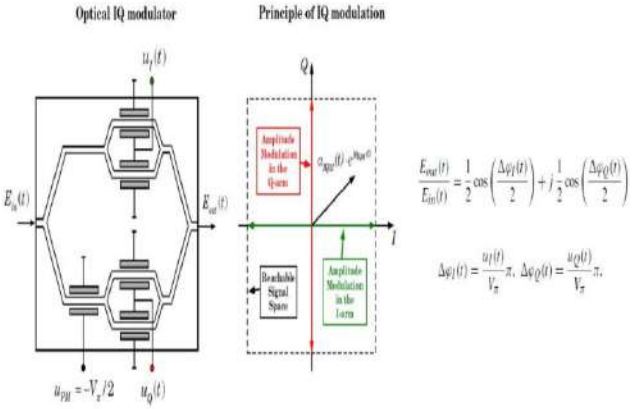

Figure 10. Dual-Nested IQ (In-Phase, Quadrature) MZM(with each MZM biased at minimum transmission point) and principle behind it.

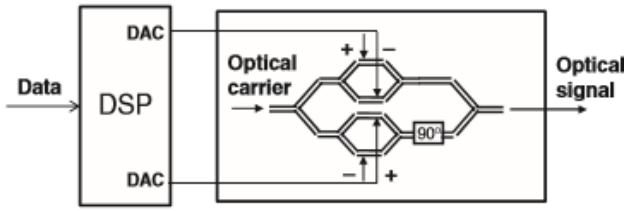

Figure 11. DSP based optical transmitter

3. Direct Detection Scheme

Through direct detection at the optical receiver the digital information is recovered in the intensity modulated format by help of a photodiode that helps in converting the power of the optical carrier into electrical current. The photocurrent that is produced is directly proportional to the square of the signal amplitude.

$$I_{ID} \propto E_S \cdot E_S' = \left(A_S e^{j(\omega_s t+\varphi)}\right) \cdot \left(A_S e^{-j(\omega_s t+\varphi)}\right) = A_S^2$$

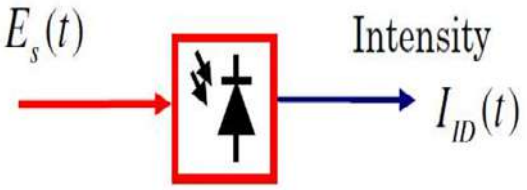

Figure 12. Photodiode working

3.1. IQ Demodulation Formats

An IQ demodulator mixes the received modulated carrier with a Continuous Wave (CW) Local Oscillator (LO), and a 90-degree shifted version of the LO the signal is down-converted from the carrier frequency down to baseband, and the in-phase and quadrature components can be recovered. Its functionality is to essentially obtain the complex envelope (and therefore, the data) of a modulated carrier.

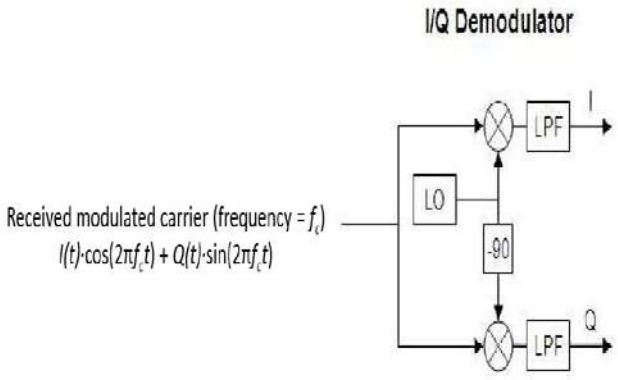

Figure 13. IQ demodulator

3.2. 90° Hybrid

In an optical demodulator, the used IQ demodulator is a 90 degree hybrid. It is used to mix the received signal with the local oscillator signal and also the shifted local oscillator signal.

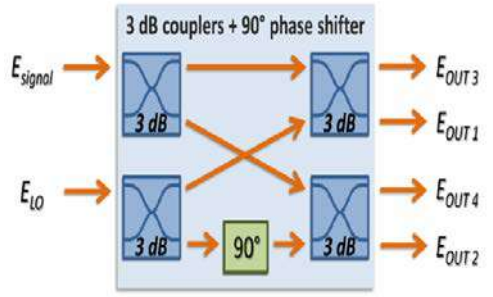

Figure 14. 3dB coupler with 90 degree phase shift

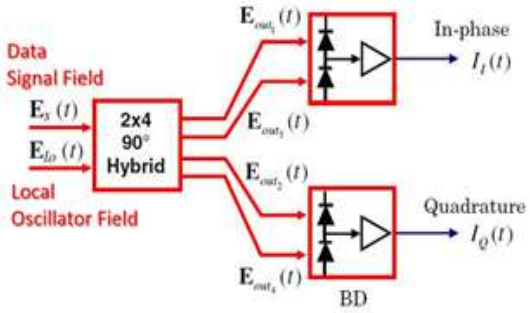

Figure 15. Coherence receiver

$$E_1(t) = \frac{1}{2}\left(E_s(t) + E_{LO2}(t)\right)$$

$$E_2(t) = \frac{1}{2}\left(E_s(t) - E_{LO2}(t)\right)$$

$$E_3(t) = \frac{1}{2}\left(E_s(t) + iE_{LO2}(t)\right)$$

$$E_4(t) = \frac{1}{2}\left(E_s(t) - i\,E_{LO2}(t)\right)$$

$$I_I(t) = R\sqrt{P_S P_{LO2}}\cos\left(\theta_s(t) - \theta_{LO2}(t)\right)$$

$$I_Q(t) = R\sqrt{P_S P_{LO2}}\sin\left(\theta_s(t) - \theta_{LO2}(t)\right)$$

$$I(t) = I_I(t) + iI_Q(t)$$

$$I(t) = R\sqrt{P_S P_{LO2}}\,e^{i\left(\theta_s(t) - \theta_{LO2}(t)\right)}$$

3.3. Polarization Diversity Coherent Receiver

Two coherent receivers are employed to detect the two orthogonal polarizations of the received signal (the polarizations are separated using a Polarization Beam Splitter).

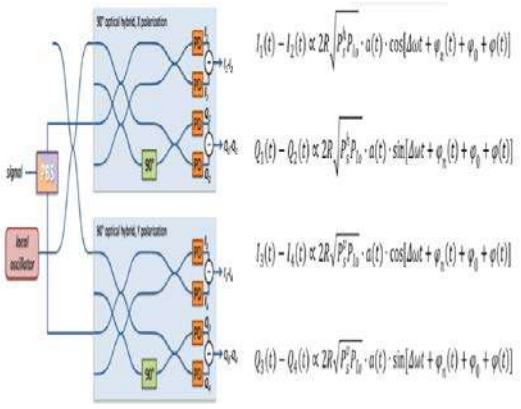

Figure 16. PD coherent receiver

4. DSP Advantages

1. Recent developments in high-speed ADCs and ASICs have enabled the use of real-time DSP algorithms to demodulate Gbit/s coherent optical signals.
2. By DSP processing it is possible to compensate for the “incoherence” (frequency offset and phase noise) of the Tx and LO lasers.
3. Advanced RF/wireless comms concepts finally applicable for ultra-high speed optical communications.
4. State-of-the-art: 100 Gbits/s optical transceivers are a commercial reality and deployed by major telecom operators today (DP-QPSK at 25 Gbaud symbol rate).
5. DSP can also be used to compensate for link impairments:

i. Chromatic Dispersion (CD)
ii. Fiber nonlinearities
iii. Bandwidth limitations

6. Higher rates and longer transmission distances
7. Universal transceivers using the same hardware in all parts of the network; rate and format is determined by the software.
8. More transparent and upgradable networks Lower cost

5. Conclusion and Future Work

The progress in coherence optical is very rapid in past years. In the future years it can use in

1. long distance communications,
2. high speed coherence receiver can be
3. tunneble local oscillator with narrow line-width
4. more flexible DSP with high error correction rate
5. Hybrid integration of planar light-wave circuits (PLCs) for phase and polarization diversities, double balanced photodiodes, and a local oscillator is an important technical task, which enables cost reduction of the coherent receiver and improves system stability.

References

[1] www.photonics.ntua.gr/.../Lecture_4_CoherentOptical_DSP.pdf.
[2] Kazuro Kikuchi, M. Nakazawa et al. (eds.), , “Coherent Optical Communications: Historical Perspectives and Future Directions”, High Spectral Density Optical Communication Technologies, Optical and Fiber Communications Reports 6, C Springer-Verlag Berlin Heidelberg 2010.
[3] Monika Nehra and Deepak Kedia, Design of Optical I/Q Modulator Using Dual-drive Mach Zehnder Modulators in Coherent Optical-OFDM System, J. Opt. Commun. 2018; 39(2): 155-159.

Materials Today: Proceedings xxx (xxxx) xxx

Contents lists available at ScienceDirect

Materials Today: Proceedings

journal homepage: www.elsevier.com/locate/matpr

Effect of quenching and partitioning treatment on low carbon medium manganese alloyed steels-A short review

Swetapadma Mishra, RenuPrava Dalai *

Department of Metallurgical and Materials Engineering, VSSUT Burla, Sambalpur, Odisha, India

ARTICLE INFO

Article history:
Received 18 September 2020
Received in revised form 24 November 2020
Accepted 1 December 2020
Available online xxxx

Keywords:
Quenching-partitioning heat treatment
Alloyed medium Mn steel
Alloying elements
Reversed austenite
Martensite

ABSTRACT

The present review work is on the effect of the quenching-partitioning heat treatment technique on the alloyed medium Mn steel. Medium Mn steel with alloying elements gives an ultrahigh strength and a multiphase microstructure. Nowadays, to fulfill the demands of the automotive industries, these steels need high strength with a higher amount of ductility. Mechanical properties of the alloyed medium manganese steel depend on reversed austenite and fresh martensite. The quenching-partitioning parameters modify the fraction (volume) of reversed austenite and martensite. The alloying elements like Al, Si, Ni, and Cr further change the amount of the reversed austenite and martensite, which enhances the strength, hardness, and toughness of this steel. Hence in this review work, a detailed study is carried out to give an idea about the effect of the quenching-partitioning treatment with different alloying elements on the low carbon alloyed medium Mn steels.

Selection and peer-review under responsibility of the scientific committee of the 1st International Conference on Energy, Material Sciences and Mechanical Engineering

1. Introduction

Medium Mn steels provide a superb combination of strength and ductility, fall under the category of advanced- high-strength-steels (AHSS). Austenite nucleates in medium Mn steel in the inter-critical annealing method. In this method, mainly the partition of carbon and manganese occurs in the martensite to reverse austenite. This partition helps to stabilize the reverse austenite by developing the retained austenite. For the medium Mn steel, a relatively higher temperature above 900 K is the inter-critical annealing temperature to reverse the austenite [1]. Due to this inter-critical method of heating, tempering occurs in the medium Mn steel. As a result, there is a significant reduction in hardness because of a reduction in the solid-solution carbon content and dislocation density. Hence, according to the researcher's suggestions, there are some difficulties to improve the mechanical properties for the inter-critical annealing method of heat treatment with maintaining the required amount of retained-austenite [2]. Recently in the case of manganese steel, researchers are mainly concentrating on the low or medium Mn steels with 3-12 wt% of Mn. These steels are categorized under the third generation AHSS. The current research on the third-generation AHSS focuses on the application of the quenching-partitioning method of heat treatment on the medium Mn steel to fulfill the property gap of the first and second-generation AHSS [3,4]. For these steels, elemental partitioning occurs at the time of annealing, which changes the microstructure during hot rolling, cooling, annealing, and inter-critical annealing [5]. The quenching-partitioning process has three stages, such as initial quenching in between the start and finish temperature of martensite (M_S-M_F), then secondary partitioning, and the third stage is the final quenching [6]. The quenching-partitioning method of heat treatment is generally useful for the improvement of the mechanical properties of the alloyed medium Mn steels [7]. Application of the quenching-partitioning method of heat treatment on the medium Mn steel gives better mechanical properties than the inter-critical annealing, which mainly depends on the stability of the retained austenite. Alloying elements (C, Mn, Al, Si, and Ni) help to enhance the austenite stability and the fraction of retained-austenite in volume [8]. The amount of retained-austenite should be high to improve the rate of work hardening in the low carbon alloyed medium Mn steel [9]. Hence the current review work gives a clear idea about the effect of the quenching-partitioning method of heat treatment on the Al, Si, Ni, and Cr added low carbon medium Mn steel.

* Corresponding author.
E-mail address: rpdalai_mme@vssut.ac.in (R. Dalai).

https://doi.org/10.1016/j.matpr.2020.12.107

Selection and peer-review under responsibility of the scientific committee of the 1st International Conference on Energy, Material Sciences and Mechanical Engineering

2. Quenching-partitioning of steel

The quenching-partitioning method is useful for the automobile industries to improve the strength and ductility along with fuel-saving and passenger safety for the automotive steels. Speer et al. first attempted the quenching-partitioning process for the enhancement of the mechanical properties into the steel. A microstructure with low carbon martensite and retained-austenite helps to increase the strength and ductility of steel [10,11]. Past research findings suggested that the high-strength of quenching-partitioning steel is due to the martensite laths. However, good ductility is because of the transformation induced plasticity (TRIP) effect [12-16]. In recent times researchers are trying for a new heat treatment technique like quenching-partitioning, which improves the mechanical properties. The quenching-partitioning process generally occurs in three stages. The first stage is the initial quenching, followed by partitioning with quenching as the last stage. Full or partial austenitization occurs in the initial stages of quenching. Quenching temperature is in between the MS and room temperature (R_T), which controls the amount of primary martensite [17]. In the partitioning stage, heat treatment to higher temperatures results in the diffusion of carbon. At the R_T, there is carbon enrichment in the austenite, which results in its stabilization. Insufficient enrichment of carbon helps martensite transformation in the final quenching stage to R_T [18,19]. The presence of carbon and manganese improves the stability of austenite. The addition of alloying elements like Al, Si, and Ni creates a path for carbon partitioning in the austenite by lowering the precipitation of carbide [20]. Quenching-temperature (Q_T), partitioning-temperature (P_T), and partitioning-time are the three parameters that improve the mechanical properties of the steel by altering the microstructure [21].

3. Quenching-partitioning of medium Mn steel

Fig. 1 shows the quenching-partitioning heat treatment schedule used for the medium Mn steel. Medium Mn steels show their inability to bainite formation, low hardenability during partitioning treatment [9,22]. S. Ayemanpudi et al. observed that higher partitioning temperature, i.e., 450 to 600 °C compared to 400 °C, helps to initiates cementite precipitation. Pearlite also formed on the bulky austenite, which results in a lower amount of retained-austenite. According to their study, they revealed that higher partitioning temperature on medium Mn steel gives an idea to avoid or lower the reactions [23]. Inter-critical annealing, followed by the quenching-partitioning, generates unstable untransformed austenite. However, manganese partitioning helps to stabilize the newly developed reversed austenite. This austenite with different stabilities enhances the mechanical properties of the medium Mn steel. For the quenching-partitioning method of heat treatment on medium Mn steel, the carbon content is between 0.1 and 0.3 wt%. When the carbon content is more than 0.3 wt%, then twins generate which may create the quenching cracks and lowers the toughness [24]. H. Pan et al. applied the quenching-partitioning treatment on medium Mn steel. They observed that the quenching-partitioning process of heat treatment enhances the yield strength [25].

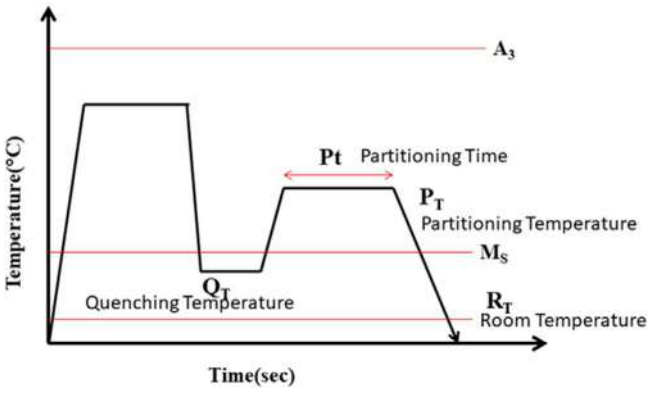

Fig. 1. Quenching-partitioning heat treatment schedule used for the medium Mn steel.

3.1. Effect of quenching and partitioning on Si added medium manganese steel

F.H. Akbary et al. applied the quenching-partitioning method to 0.3 wt%C, 3.5 wt%Mn, and 1.6 wt%Si steel. They observed that austenite present in the higher Mn regions more stable than lower Mn regions. Hence, the fraction of initial martensite amount in volume is less in the higher manganese regions. Due to partitioning in the higher Mn regions, less carbon partitioning, not able to stabilize the austenite. Hence, a more amount of secondary martensite transformation occurs in this region. They concluded that microstructural inhomogeneity is more distinct for higher quenching temperatures [26]. E. De Moor et al. developed 3 to 5 wt% Mn and 1.59 to 1.6 wt% Si with 0.2 to 0.29 wt% C steels. They determined the effect of quenching-partitioning on the tensile strength and retained-austenite volume fraction for the steels. Fully austenitization of the developed steels gives better mechanical properties [27]. J. Hidalgo et al. used the quenching-partitioning heat treatment to 1.5 wt% Si added 4.5 wt% medium Mn steel. They investigated the fracture mechanisms of the steel at two partitioning temperatures, i.e., 400 and 500 °C, respectively. Pearlite transformation, carbide precipitation in the C enriched austenite after partitioning at 500 °C, creates more ductile behavior than partitioning at 400 °C. However, for both the partitioning temperature, manganese segregation promotes brittle fracture because of higher hardness [9]. Z. Dai et al. designed a new quenching-partitioning heat treatment with local equilibrium or para equilibrium at the austenite–martensite interface and used in Si added Mn steel. The interface present between the austenite and martensite changed to austenite and martensite. This change depends upon the quenching-partitioning parameters and the alloy composition. It also provides a new aspect to design future quenching-partitioning steel [28]. Table 1 shows the effects of quenching-partitioning on Si added low carbon medium Mn steel.

3.2. Effect of quenching and partitioning effect on al added medium manganese steel

Z. R. Hou et al. developed a 0.15 wt%C, 5 wt% Mn, and 1.5 wt% Al added medium Mn steel. Initially, they used the inter-critical annealing method and then quenching the steel with water and then partitioning the steel. They observed that there is a refinement of the ferrite grains Presence of more number of ultrafine ferrite grains and retained-austenite enhance the ductility of this steel [29]. This steel also provides good mechanical properties with tensile elongation. B. B. He et al. designed a 2 wt% Al added medium Mn steel. They observed the application of the quenching-partitioning method of heat treatment provides excellent tensile strength with good ductility [30]. S. Kaar et al. concluded that the quenching-partitioning treatment to a 1.3 wt% Al and 4.5 wt% Mn steel accelerates the transformation kinetics. The amount of the retained-austenite increases as the quenching temperature increases [31]. D. H. Kim et al. reported that quenching-partitioning treatment at room-temperature enhances the yield strength of 0.21 wt%C, 10.2 wt%Mn, and 1.94 wt% Al steel [32].

Table 1
Effect of quenching-partitioning on Si added low carbon medium manganese steel.

Chemical composition in wt %	Quenching and partitioning temperature and time	Findings
0.3C-3.5Mn-1.6Si [26]	Austenitization temperature and time (900 °C and 180sec), quenching temperature (180 °C or 240 °C), partitioning temperature and time (400 °C and 5sec).	Microstructural inhomogeneity is more distinct for higher quenching temperatures.
0.2C-3Mn-1.6Si [27]	Austenitization temperature and time (840 °C and 120 sec), quenching temperature 210 °C and partitioning temperature and time (400 °C and 30sec).	Give a better combination of microstructure and properties.
0.3C-3Mn-1.6Si [27]	Austenitization temperature and time (820 °C and 120 sec), quenching temperature at 200 °C and partitioning temperature and time (400 °C and 30sec).	
0.3C-5Mn-1.6Si [27]	Austenitization temperature and time (780 °C and 120 sec), quenching temperature at 160 °C, and partitioning temperature and time (400 °C and 30sec).	
(0.15–0.3)C-(1.5–3)Mn -(1–2)Si [9]	Initially, heated to a temperature above Ac_3 and then slow cooling to Ar_3, i.e., approximately 740 °C, quenching temperature in between the M_S-M_F temperature and then reheated to a higher temperature for a couple of minutes.	Manganese segregation promotes brittle fracture mechanisms because of higher hardness.
0.25C-2.1Mn-1.1Si[28]	Austenitization temperature and time (900 °C for 180sec), quenching temperature at 230 °C/260 °C/290 °C. The partitioning temperature and time (400 °C and 120 sec).	To tailor the microstructure, the interfacial partitioning of manganese plays an important role.
0.59C-2.9Mn-2Si [28]	Austenitization temperature and time (900 °C for 180sec), then quenching to room temperature. The partitioning temperature and time (400 °C and 120 sec).	

Table 2
Quenching-partitioning treatment on Al added low carbon medium manganese steel.

Chemical composition in wt %	Quenching and partitioning temperature and time	Findings
0.15C-5Mn-1.5Al[29]	Austenitization temperature and time (750 °C for 15mins), then water quenching to 20, 40, 60, and 80 °C for 2sec. Partitioning temperature at 400 °C for 100sec.	A higher amount of retained-austenite provides higher tensile strength and elongation. However, ductility enhances due to the presence of ultrafine ferrite.
0.2C-10Mn −2Al[30]	The cast and forged steel after air cooling tempered at 300 or 350 °C.	Due to the TRIP effect, it exhibits higher mechanical properties.
0.2C-4.5Mn-1.3Al[31]	Austenitization at 900 °C for 120 sec, then quenched in the temperature range 130–330 °C for 10 sec, and then reheated to 350, 400, and 450 °C for 600 sec, respectively.	The final quenching temperature controls the microstructure. The fraction of primary martensite and retained-austenite depends on the quenching temperature.
0.21C–10.20Mn–1.94Al[32]	Initially austenitized at 1200 °C for one hour and then hot-rolled. Annealing at 650 °C for one hour. The annealed sample was cold-rolled and then again heat-treated at 700 and 750 °C for one hour. The 750 °C annealed sample is tempered at 100 °C, 200 °C, or 300 °C for 20 min to partition C.	High yield strength (1GPa), tensile strength (1.5GPa), and ductility (19.5%).

Table 3
Effect of quenching-partitioning on both Si-Ni and Si-Cr added low carbon medium Mn steel.

Chemical composition in wt%	Quenching and partitioning temperature and time	Findings
0.19C- 5.7Mn- 1.6Ni- 1.4Si[33]	Austenitization temperature and time (900 °C and 180sec), quenching temperature (180 °C or 240 °C), and partitioning temperature and time (400 °C and 5sec).	The addition of Ni enhances the retained austenite fraction in volume. As a result, enhancement in mechanical properties such as tensile strength and hardness. The retained-austenite fraction in volume and stability increases with Ni content, which further enhances the tensile strength and hardness.
0.244C-1.379Mn-1.386Si-0.033Ni[7]	Austenitization temperature and time (840 °C and 120 sec), quenching temperature (210 °C), and partitioning temperature and time (400 °C and 30sec).	A higher fraction of retained-austenite in volume and stability of retained-austenite does not always provide higher mechanical properties.
0.209C-1.436Mn-1.444Si-1.012Ni[7]	Austenitized temperature and time (820 °C and 120 sec), quenching temperature (200 °C), and partitioning temperature and time (400 °C and 30sec).	
0.279C-1.409Mn-1.458Si-1.986Ni[7]	Austenitization temperature and time (780 °C and 120 sec), quenching temperature (160 °C), and partitioning temperature and time (400 °C and 30 sec).	
(0.15–0.3)C-(1.5–3)Mn-(1–2)Si[34]	Initially, heated to a temperature above Ac_3 and then slow cooling to Ar_3, i.e., approximately 740 °C, quenching temperature (between M_S – M_F) and then reheated to a higher temperature for a couple of minutes.	Low carbon martensite with carbon enriched austenite phases gives higher tensile strength and ductility. These phases are formed by controlling partitioning conditions.

Table 2 represents the effects of quenching-partitioning on Al added low carbon medium Mn steel.

3.3. Effect of quenching and partitioning effect on Ni and Si added medium manganese steel

A. Maribel et al. developed a low carbon, 6 wt%Mn-2 wt%Ni added medium Mn steel and used four three different partitioning temperatures, i.e., 400, 550, 600, and 650 °C. From their comparative analysis, they observed that the retention of austenite depends on the amount of alloying elements and partitioning conditions. However, they also observed that the higher partitioning temperature was not able to give a significant improvement in the tensile strength properties [33]. K. Kim et al. applied the quenching-partitioning treatment on a Ni added 0.3C-1.5Mn-1.5Si (wt%) steel. The addition of Ni with the quenching and partitioning heat treat-

ment technique increased the fraction of retained austenite in volume and its stability. Further grain refinement occurs with increasing the retained- austenite fraction in volume, with the weight percent of Ni. The quenching-partitioning method of heat treatment helps to enhance the mechanical properties of this Ni added steel. Table 3 shows the effects of quenching and partitioning on both Si-Ni, and Si-Cr added low carbon medium Mn steel.

3.4. Effect of quenching and partitioning effect on Si and Cr added medium manganese steel

E. J. Seo et al. analyzed the role of quenching-partitioning treatment on a Si (1.6 wt%), Cr (1 wt%) added medium Mn steel. They observed the presence of low carbon martensite, which gives high strength to this steel. It also offers better mechanical properties because of a large fraction of retained austenite in volume [9,34].

4. Conclusions

Q_T, P_T, and P_t are the controlling parameters for the quenching-partitioning process of heat treatment. This process alters the microstructure through the reverse austenite and martensite. It changes the mechanical properties such as hardness, strength, toughness, and ductility of low carbon alloyed medium Mn steel. This method of heat treatment provides better mechanical properties to this steel compared to the other heat treatment methods. Alloying elements like Al, Si, Ni, and Cr with the quenching-partitioning improves the mechanical properties. These alloying elements create a path for carbon partitioning to austenite by lowering the carbide precipitation during the partitioning stage.

Declaration of Competing Interest

The authors declare that they have no known competing financial interests or personal relationships that could have appeared to influence the work reported in this paper.

Acknowledgements

The authors would like to acknowledge VSSUT Burla, Sambalpur, Odisha, India, for their support to complete this review work.

References

[1] T. Tsuchiyama, T. Inoue, J. Tobata, D. Akama, S. Takaki, Scrip. Material. 122 (2016) 36–39.
[2] Y. Ma, Mater. Sci. Tech. 33 (15) (2017) 1713–1727.
[3] B.C. De Cooman, J.G. Speer, Steel Res. Inter. 77 (2006) 634–640.
[4] K. Steineder, D. Krizan, R. Schneider, C. Beal, C. Sommitsch, Acta Mater. 139 (2017) 39–50.
[5] B. Wolfgang, H. Christian, Metals. 9 (10) (2019) 1–4.
[6] J. Speer, D.K. Matlock, B.C. De Cooman, J.G. Schroth, Acta Mater. 51 (2003) 2611–2622.
[7] K. Kim, S.J. Lee, Mater. Sci. Eng. A 698 (2017) 183–190.
[8] L. Wang, J.G. Speer, Metal. Micro. Analy. 2 (2013) 268–281.
[9] J. Hidalgo, C. Celada-Casera, M.J. Santofimia, Mater. Sci. Eng. A 754 (2019) 766–777.
[10] E.J. Seo, L. Cho, B.C. De Cooman, Metall. Mater. Trans. A 46 (2015) 27–31.
[11] J.G. Speer, F. Rizzo, D. Matlock, D.V. Edmonds, Mater. Res. 8 (2005) 417–423.
[12] S.S. Nayak, R. Anumolu, R.D.K. Misra, K.H. Kim, D.L. Lee, Mater, Sci. Eng.A 498 (2008) 442–456.
[13] M.J. Santofimia, L. Zhao, R. Petrov, J. Sietsma, Mater. Charact. 59 (2008) 1758–1764.
[14] C.Y. Wang, J. Shi, W.Q. Cao, H. Dong, Mater. Sci. Eng. A 527 (2010) 3442–3449.
[15] J.G. Speer, E. De Moor, K.O. Findley, D.K. Matlock, B.C. De Cooman, D.V. Edmonds, Metall. Mater. Trans. A 42 (2011) 3591–3601.
[16] E. Moor, S. Lacroix, A. Clarke, J. Penning, J.G. Speer, Metall. Mater. Trans. A 39 (2008) 2586–2589.
[17] C.C. Casero, C. Kwakernaak, J. Sietsma, M.J. Santofimia, Mater. Des. 178 (2019) 1–12.
[18] K. Dorien, P. Roumen, F. Cecilia, K. Leo, Mater. Sci. Eng.A 615(2014) 107–115.
[19] S. Ebner, C. Suppan, A. Stark, R. Schnitzer, C. Hofer, Mater. Des. 178 (2019) 1–10.
[20] G. Mandal, S.K. Ghosh, S. Bera, S. Mukherjee, Mater. Sci. Eng.A 676(2016)56-64.
[21] D. De Knijf, E.P. Da Silva, C. Fojer, R. Petrov, Mater. Sci. Tech. 31 (2015) 817–828.
[22] C. Lawrence, E.J. Seo, B. De Cooman, Scrip. Material. 123 (2016) 69–72.
[23] S. Ayenampudi, C. Celada-Casero, J. Sietsma, M.J. Santofimia, Material. 8 (2019) 1–11.
[24] Li, Xiao Gang, Ai Min Zhao, Hong Hong Zheng, Shao Heng Sun, and Hong Xiang Yin, Mater. Sci.Forum 850 (2016) 659–63
[25] H. Pan, M. Cai, H. Ding, S. Sun, H. Huang, Y. Zhang, Mater. Sci. Technol. 35 (2019) 807–814.
[26] F.H. Akbary, J. Sietsma, R.H. Petrov, G. Miyamoto, T. Furuhara, M.J. Santofimia, Scripta Material. 137 (2017) 27–30.
[27] E. De Moor, J.G. Speer, D.K. Matlock, J.H. Kwak, S.B. Lee, ISIJ Inter. 51 (2011) 137–144.
[28] Z. Dai, R. Ding, Z. Yang, C. Z. Hao Chen, Acta Material. 144(2018) 666-678.
[29] Z.R. Hou, X.M. Zhao, W. Zhang, H.L. Liu, H.L. Yi, Mater. Sci. Tech. 34 (2018) 1168–1175.
[30] B.B. He, M. Wang, L. Liu, M.X. Huang, Mater. Sci. Tech. 35 (2019) 2109–2114.
[31] S. Kaar, R. Schneider, D. Krizan, C. Beal, C. Sommitsch, Metals 9 (3) (2019) 1–13.
[32] D.H. Kim, J.H. Kang, J.H. Ryu, S.J. Kim, Mater. Sci. Tech. 35 (2019) 2115–2119.
[33] A. Maribel, G. Teresa, D. Molino, A. Eider, D. Artem, I. Calderon, D.C. Martin, S. Daniele, S.M. Ayenampudi, Metals 10 (2020) 862.
[34] E.J. Seo, L. Cho, B.C. De Cooman, Metall. Mater. Trans.A 45(2014) 4022–4037.

Materials Today: Proceedings xxx (xxxx) xxx

Contents lists available at ScienceDirect

Materials Today: Proceedings

journal homepage: www.elsevier.com/locate/matpr

A comparative study on the different heat-treatment techniques applied to high manganese steel

Swetapadma Mishra, Renuprava Dalai *

Department of Metallurgical and Materials Engineering, VSSUT, Burla, Sambalpur 768018, Odisha, India

ARTICLE INFO

Article history:
Received 30 September 2020
Received in revised form 26 November 2020
Accepted 14 December 2020
Available online xxxx

Keywords:
Hadfield steel
Single-step heat-treatment
Double-step heat-treatment
$(Fe, Mn)_3C$ carbides
Heating rate
Cooling rate

ABSTRACT

Hadfield manganese steel is the first choice by the mining and mineral processing industries because of its high work hardening rate, high wear resistance, ductility, and toughness properties. Sometimes Hadfield steel fails to give a better combination of these properties due to precipitation of the brittle carbides at the grain boundaries of austenite. Controlling of these $(Fe, Mn)_3C$ carbides provide high strength, ductility, toughness along with high work-hardening property and also a high wear and corrosion resistance to the steel. A suitable heat-treatment process helps to achieve carbide-free austenite grains, and it provides better mechanical properties. Hence, in the present investigation, a comparative analysis is carried out, which gives an idea about the different heat-treatment process parameters such as the heat-treatment sequence, temperature, heating rate, and cooling rate. A single-step or double-step heat-treatment process is applicable for the Hadfield steel. Recently it is reported that the double-step heat-treatment process is more efficient than the single-step heat-treatment. In the double-step heat-treatment process, initial heating up to 650 °C with a holding time of 3hrs and then heating up to 1100 °C with a holding time of 3hrs followed by water quenching dissolves the carbides for the Hadfield steel. To achieve a higher cooling rate in the heat-treatment process, water, salt solution, or a mixture of water and salt solution is used as the quenching media. From the present investigation, it is clear that a higher cooling rate, along with the double-step heat-treatment, gives a better combination of strength and ductility to Hadfield steel.

Selection and peer-review under responsibility of the scientific committee of the International Conference on Materials, Processing & Characterization.

1. Introduction

Equipment's used in the mining and mineral processing industries, always dealing with carrying the heavyweight ores, rocks, and stones [1-4]. This type of equipment needs high wear resistance capacity to sustain for a longer time. The wear conditions vary from low to severe wear, such as adhesive, abrasive, impact abrasion,and fatigue wear. Hadfield manganese steel, with its unique combination of properties such as high work hardening, ductility, and wear resistance able to withstand all these types of wear [5-8]. So there is always a demand for Hadfield steel by the mining and mineral industries. The as-cast Hadfield steel contains the brittle $(Fe, Mn)_3C$ carbides, and these carbides reduce the ductility and lower the wear resistance property [9]. The other limitation of this steel is its low yield strength. Hence in the last two decades, researchers are trying to enhance the yield strength, along with ductility and wear resistance capacity of this steel by adding alloying elements and by adopting some new heat treatment techniques. Their main aim is to remove or lower the amount of the brittle $(Fe, Mn)_3C$ carbide phase. The addition of alloying elements like Cr, V, Mo precipitates complex carbides at the grain boundaries in the as-cast steel [10]. The presence of these carbides improve the strength and hardness of the Hadfield steel but generate stresses and promote brittle fracture [11–15]. Austenite stabilizing elements such as Al and Ni enhances the hardness and ductility of the Hadfield manganese steel [16–19]. This improvement in mechanical properties increases the wear resistance of Hadfield steel. It is mentioned in the literature that the austenitization temperature of Hadfield steel is from 1010 °C to 1120 °C for sufficient time and then quenching in water [20]. The solutionizing treatment depends on the austenitizing temperature, holding time, and quenching rate. Higher austenitizing temperature coarsens the austenite grains. Heating for a longer time at higher temperatures

* Corresponding author.
E-mail address: dalai.renu@gmail.com (R. Dalai).

https://doi.org/10.1016/j.matpr.2020.12.602
2214-7853/
Selection and peer-review under responsibility of the scientific committee of the International Conference on Materials, Processing & Characterization.

creates decarburization and loss of manganese [21,22]. Slow quenching precipitates a higher amount of (Fe, Mn)$_3$C carbides [23]. Hosseini and Limooei studied the effect of the solution annealing cooling rate on the precipitation of the carbides. They reported with increasing the cooling rate of the quenching solution, the (Fe, Mn)$_3$C carbide volume fraction decreases [24]. Sant and Smith observed that the solution annealing temperature of 950 to 1050 °C and rapid quenching provides a carbide free homogeneous austenite structure. As a result, the presence of a large amount of carbon in the austenite gives high ductility, toughness, and work-hardening property to the steel [22]. Hence to get 100 percent austenite grains with smaller grain sizes, researchers apply some new heat treatment techniques. The present work aims to analyze the effect of different heat-treatment processes, heating, and cooling rate on the microstructure and mechanical properties of Hadfield manganese steel.

1.1. Single-step heat-treatment process

A. Souad and H. Ali studied the effect of a new heat treatment process on a Cr and Ni added Hadfield manganese steel. In the first case, they heated the samples with a heating rate of 6 °C/min for three different temperatures (600, 1080, and 1100 °C), with a holding time of 1hr. In the second case, heating the steel samples at temperatures like 600, 1020, and 1050 °C with a heating rate of 12 °C/min for a holding time of 1hr and then quenching with water. They observed (Fe, Mn, Cr)$_3$C cementite precipitate at the austenite grain boundaries. With increasing the weight percentage of Cr and Ni, the amount of (Fe, Mn, Cr)$_3$C cementite increases, which refines the microstructure. The heat-treated steel samples have martensite and non-transformed austenite. Heat-treatment at 1050 °C is not able to dissolve the (Fe, Mn, Cr)$_3$C cementite. However, increasing the heat-treatment temperature and decreasing the heating rate dissolves these secondary carbides or (Fe, Mn, Cr)$_3$C cementite. As a result, hardness, coefficient of friction, and wear resistance of the Cr, and Ni added Hadfield manganese steel improved [25]. Fig. 1 shows a heat-treatment cycle used for a Cr, and Ni added Hadfield manganese steel.

G. Tęcza and S. Sobule heat-treated the steel samples at three different temperatures at 1100, 1150, and 1200 °C, respectively. They observed the applied heat-treatment temperature and time are not sufficient to develop a complete austenite phase without any carbide [26]. U.Gurol used a heat-treatment cycle, which consists of initial heating of the samples up to 650 °C with a holding time of 3hrs. Then heating the heat-treated samples to 1100 °C at a heating rate of 1.67 °C/min, and then again with a holding time of 3hrs. After this heat-treatment cycle, the samples are water quenched. They observed that the developed solution annealing or heat-treatment cycle able to completely dissolve the (Fe, Mn)$_3$C cementite carbides for the 1 wt%C Hadfield steel. For higher wt% of C in Hadfield steel, this cycle is not able to dissolve the carbides completely. But with increasing the solution annealing temperature, the amount of dissolution increased. But higher solution annealing temperature increased the grain size and reduced the mechanical properties. Among the five steel samples (0.7 wt%C-17 wt%Mn, 1 wt%C-13 wt%Mn, 1 wt%C-17 wt%Mn, 1 wt%C-21 wt% Mn, and 1.3 wt%C-17 wt%Mn), the 1 wt%C-17 wt%Mn Hadfield steel shows better tensile strength and ductility [27]. Fig. 2 depicts the heat treatment cycle applied for the five high manganese plates of steel (0.7 wt%C-17 wt%Mn, 1 wt%C-13 wt%Mn, 1 wt%C-17 wt% Mn, 1 wt%C-21 wt%Mn, 1.3 wt%C-17 wt%Mn).

S. A. Torabi et al. used a cyclic solution annealing at 1100 °C for 2 hrs. They rapidly quenched the steel after annealing in water by stirring. They observed this solution annealing temperature, and rapid quenching in water developed a complete austenite phase without any precipitation of carbides [28]. A. F. Khan et al. applied a heat treatment cycle to a 1.46 wt%C, 1.03 wt%Si, 12.54 wt%Mn steel. The heat treatment cycle consists of heating the steel sample at (1050 °C + 470 °C + 850 °C) for some time off (1/3 hr + 5hrs + 4hrs) and then quenched with (water + air + water) respectively. For this heat treatment cycle, the microstructure consists of finely dispersed (Fe, Mn)3C cementite carbides within the austenite grains. Due to the presence of carbides in the austenite grains, the hardness increases from 9 to 25 HRC. They also reported that this heat treatment cycle provides high hardness and toughness to the Hadfield steel [29]. S.H. M Anijdan and M. Sabzi studied the effect of heat treatment process parameters on two as cast Hadfield steel blocks with the chemical composition of 1.21 wt% C, 12.67 wt%Mn, 0.41% Si, 0.019 wt% P. They solutionized the Hadfield steels at 1100 °C for 2hrs. After heating, they quenched with water and 3%NaCl solution. Fig. 3 shows the optical micrographs of as-cast, water quenched, and salt bath quenched samples for the 1.21 wt%C, 12.67 wt%Mn steel. They observed that the austenite grain size is smaller for the water quenched samples compared to the salt bath quenched samples. However, the amount of the (Fe, Mn)3C carbide is more for the water quenched sample than the salt bath quenched sample. As a result, the salt bath quenched sample provides lower values of hardness, tensile strength, and yield strength. However, the salt bath quenching gives higher toughness compared to the water quenched sample [30]. M. B. Limooei and Sh. Hosseini studied the effect of heat treatment process parameters such as austenitizing temperature, austenitizing time, and quenching rate on the 1.23 wt%C, 13.32 wt%Mn, 1.91 wt%Cr, and 0.49 wt% Si added Hadfield manganese steel by using the Taguchi method. They observed that the heat treatment parameters affect the austenite grain size and amount of carbide. The optimized heat

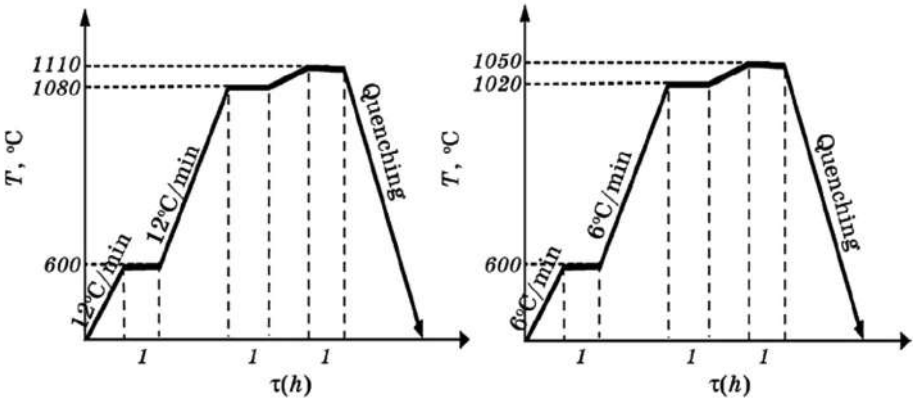

Fig. 1. Heat treatment cycle used for a Cr and Ni added Hadfield manganese steel [25].

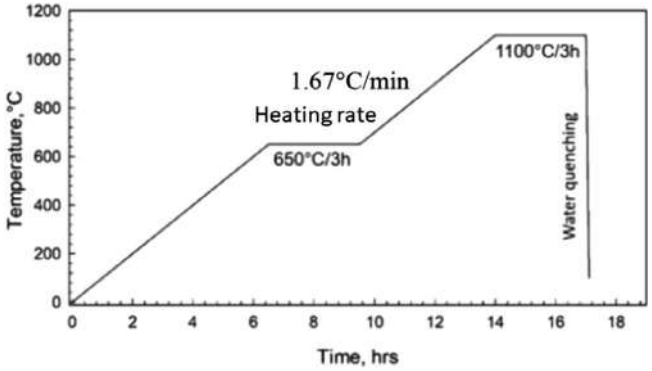

Fig. 2. Heat treatment cycle for high manganese steels (0.7 wt%C-17 wt%Mn, 1 wt% C-13 wt%Mn, 1 wt%C-17 wt%Mn, 1 wt%C-21 wt%Mn, 1.3 wt%C-17 wt%Mn) [27].

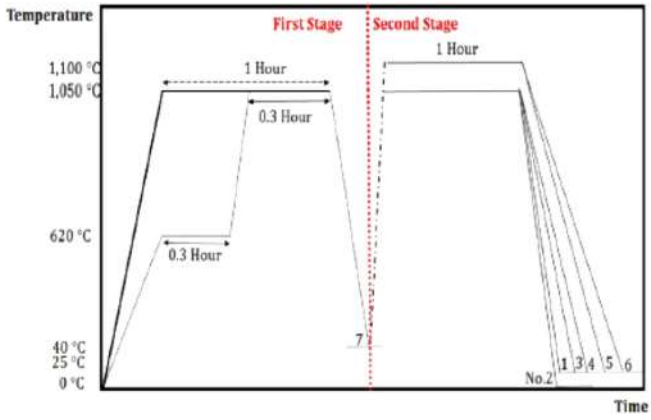

Fig. 4. A two-stage heat treatment cycle for Hadfield manganese steel [32].

treatment process parameters are the austenitizing temperature (1050C), austenitizing time (1.5 h), and quenching solution (0% salt) [24].

1.2. Double- step heat- treatment process

R. Lencina et al. applied an austenitization temperature of 1120 °C for a time of 1hr, and then water plus salt quenched with a 4% salt solution in two Hadfield steel having 12.5 wt% Mn and 16.68 wt% Mn with approximately 1.4 wt% C. They observed that 16.68 wt% Mn gives higher wear resistance than the 12.5 wt% Mn Hadfield steel [31]. M. Azadi et al. developed a new double-step heat-treatment technique for the high manganese Hadfield steel. Fig. 4 shows the double-step heat-treatment cycle applied to a 1.2 wt%C-17.5 wt%Mn-1.7 wt%Cr Hadfield manganese steel. In a resistance furnace, in the first step, the steel is heated to 620 °C for a time of 20 min. Then the steel is austenitized to a temperature of 1050 °C for a time of 20mins, followed by water quenching. However, in the second step of heat-treatment, the steel samples are put into the furnace after reaching the austenitizing temperature (1050 or 1100 °C) with a holding time of 1hr followed by quenching with water + 0 wt% salt, a mixture of water and ice, water + 1.5 wt% salt, water + 3 wt% salt respectively. However, the ice plus water solution lowered the hardness value due to the higher cooling rate, but the grain size (115 μm) was less compared with the other heat-treated samples. The increasing solution annealing temperature from 1050 °C to 1100 °C increased the amount of carbide dissolution. The double-step heat-treatment process is more efficient to improve the hardness and toughness than the single-step heat-treatment process [32]. S. Hosseini et al. optimized the heat-treatment process parameters (austenitizing temperature, time, and quenching solution) for a 1.32 wt% C-13.32 wt% Mn-1.91 wt% Cr-0.49 wt%Si Hadfield steel. They have used nine heat treatment cycles with different (water + salt) solutions as quenching medium and measured the grain size, carbide volume fraction, and hardness for the steel. They found that austenitizing temperature of 1100 °C for 3hrs holding time with a water + 1.5% salt quenching and 3% salt quenching gives a better combination of hardness and toughness because of the lower volume fraction of carbide [33]. For complete removal of the carbides, the austenitizing temperature is in the range of 30–50 °C above the upper critical temperature. With a low heating rate and high quenching rate, dissolve all the carbides. B. Bandanadjaja and E Hidayat used a two-stage heat treatment process for the improvement of impact toughness of the Hadfield steel. Initially, the steel is heated at a lower temperature up to 600–700 °C to enhance the growth rate of pearlite. It generates smaller austenite grains in the austenitization stage. After initial heating, austenitization is carried out at higher temperatures up to 980–1000 °C. They observed that this two-step heat-treatment process provides 25% higher toughness than the conventional single-stage heat-treatment process [34].

2. Conclusions

(i) Increasing the heat-treatment temperature and decreasing the heating rate dissolves the secondary carbides or (Fe, Mn)$_3$C cementite.

(ii) The austenite grain size is smaller for the water quenched sample compared to the salt bath quenched sample, and the amount of the (Fe, Mn)$_3$C carbide is more for the water quenched sample than the salt bath quenched sample.

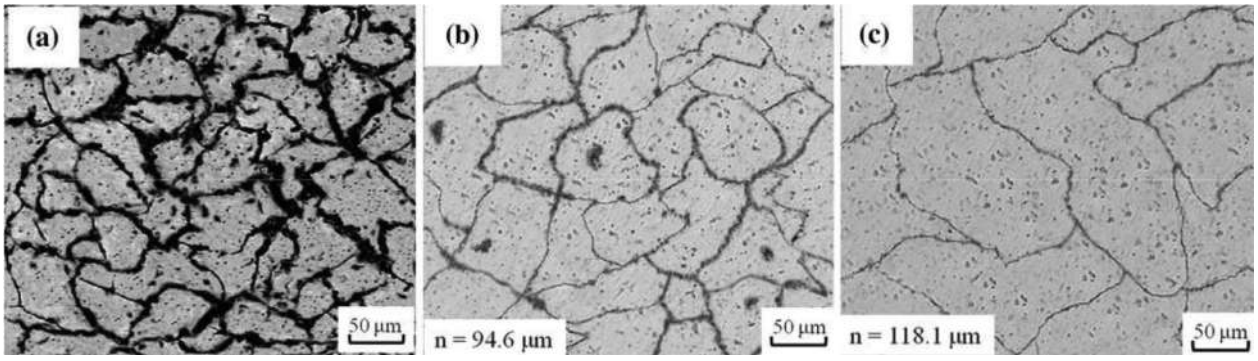

Fig. 3. Optical micrograph of a hadfield steel (1.21 wt%C, 12.67 wt%Mn, 0.41% Si, 0.019 wt% P) (a) as cast, (b) water quenched and (c) 3 wt% NaCl salt bath quenched [30].

(iii) The double-step heat-treatment process is more efficient to improve the hardness and toughness than the single-step heat-treatment process.

Declaration of Competing Interest

The authors declare that they have no known competing financial interests or personal relationships that could have appeared to influence the work reported in this paper.

Acknowledgements

The authors acknowledge VSSUT Burla, Odisha, India, for supporting and providing the facilities to complete this work.

References

[1] C. Okechukwu, O.A. Dahunsi, P.K. Oke, I.O. Oladele, M. Dauda, Int. J. Eng. Technol. 3 (2017) 83–90.
[2] J.O. Olawale, S.A. Ibitoye, M.D. Shittu, Mater. Res. 16 (2013) 1274–1281.
[3] S.A. Balogun, D.E. Esezobor, J.O. Agunsoye, J. Min. Mater. Charact. Eng. 7 (2008) 277–289.
[4] S.R. Allahkaram, IJE Trans. B: Appl. 21 (2008) 55–64.
[5] R.W. Smith, A. DeMonte, W.B.F. MacKay, Can. Metall. Quart. 42 (2003) 333–342.
[6] E. Bayraktar, F. Khalid, L. Christophe, J. Mater. Proces. Tech. 147 (2004) 145–154.
[7] R. Dalai, S. Das, K. Das, Can. Metal. Quar. 53 (2014) 317–325.
[8] C. Chen, L. Bo, H. Ma, D. Sun, F. Zhang, Trib. Intern. 121 (2018) 389–399.
[9] M.K. El-Fawkhry, A.M. Fathy, M.M. Eissa, H. El-Faramway, Inter. J. Met. Cast. 8 (2014) 29–36.
[10] A. Souad, H. Ali, Intern. J. Metalcasting (2020), https://doi.org/10.1007/s40962-020-00479-2.
[11] G. Tecza, A. Garbacz-Klempka, Arch. Foundary Eng. 16 (2016) 163–168.
[12] J.O. Agunsoye, T.S. Isaac, A.A. Abiona, J. Miner. Mater. Charact. Eng. 1 (2013) 24–28.
[13] E.G. Moghaddama, N. Varahrama, P. Davami, Mater. Sci. Eng. A 532 (2012) 260–266.
[14] Y.S. Ham, J.T. Kim, Si Y. Kwak, J. K. Choi, W.Y. Yoon, Chi. Foun. 7(2010)178-182.
[15] R. Dalai, S. Das, K. Das, Int. J. Miner. Metall. Mater. 26 (2019) 64–75.
[16] Z. Zhou, Z. Zhang, Q. Shan, Z. Li, Y. Jiang, R. Ge, Metals 9 (2019) 1–14.
[17] Y.N. Dastur, W.C. Leslie, Metall. Mater. Trans. A 12 (1981) 749–759.
[18] M. Abbasia, S. Kheirandisha, Y. Kharrazi, J. Hejazia, Mater. Sci. Eng. A 513–514 (2009) 72–76.
[19] K. Panchal, Inter. J. Sci. Dev. Res. 1 (2016) 817–825.
[20] D.K. Subramanyam, A.E. Swansiger, H.S. Avery, Austenitic Manganese Steels, tenth ed., ASM International Handbook 1990.
[21] A.K. Srivastava, K. Das, Mater. Sci. 43 (2008) 5654–5658.
[22] S.B. Sant, R.W. Smith, J. Mater. Sci. 22 (1987) 1808–1814.
[23] K.N. Jang, T.K. Kim, K.T. Kim, Nuc. Eng. Tech. 51 (2019) 249–256.
[24] S. Hosseini, M.B. Limooei, World Appl. Sci. J. 15 (2011) 1421–1424.
[25] A. Souad, H. Ali, Metallophys. Adv. Technol. 41 (2019) 607–620.
[26] G. Tecza, S. Sobula, Arch. Foundry Eng. 14 (2014) 67–70.
[27] U. Gurol, S. Can Kurnaz, J. Min. Metall. Sect. B-Metall. 56(2020)171-182.
[28] S.A. Torabi, K. Amini, M. Naseri, Int. J. Adv. Des. Manuf. Technol. 10 (2017) 75–83.
[29] A.F. Khan, A.M. Rana, M.U.I. Islam, T. Abbas, Pak. J. Appl. Sci. 1 (2001) 317–320.
[30] S.H.M. Anijdan, M. Sabzi, J. Mater. Eng. Perf. 27 (2018) 5246–5253.
[31] R. Lencina, C. Caletti, K. Brunelli, R. Micone, Proc. Mater. Sci. 9 (2015) 358–366.
[32] M. Azadi, A.M. Pazuki, M.J. Olya, Metall. Micro. Analy. 7 (2018) 618–626.
[33] S. Hosseini, M.B. Limooei, M. Hossein Zade, E. Askarnia, Z. Asadi, Int. J. Chem. Mol. Nucl. Mater. Metall.Eng. 7(2013)582–586.
[34] B. Bandanadjaja, E. Hidayat, J. Phys. Conf. Series 1450 (2020) 1–9.

A comparative study of harmonic elimination of cascade multilevel inverter with equal dc sources using PSO and BFOA techniques

[1]Rupali Mohanty, [2] Gopinath Sengupta,[3]Sudhansu bhusana Pati
[1]Department of EEE,[2]Department of EEE ,[3]Department of EEE
[1] GIFT ,Bhubaneswar ,[2]GIFT Bhubaneswar ,[3]GIFT Bhubaneswar

Abstract: *Eliminating harmonics using a multilevel inverter with equal separate dc sources using heuristic techniques from the electric drives of renewable energy sources is considered. Solving a nonlinear transcendental equation set describing the harmonic-elimination problem with equal dc sources reaches the limitation of contemporary computer algebra software tools using the resultant method. The proposed approaches in this paper can be applied to solve the problem in a simpler manner. In this paper two proposed methods solve the asymmetry of the transcendental equation set, which has to be solved in cascade multilevel inverters. Simulation and experimental results are provided for an 11-level cascaded multilevel inverter to show the validity of the proposed methods, and a comparative analysis is done for eliminating the harmonics in a multilevel inverter.*

Keywords: Harmonics, Equal voltage source, Cascade Multilevel inverter, Particle swarm optimization, Bacteria foraging optimization algorithm

I. INTRODUCTION

Harmonics must always be limited below threshold level prescribed by standards [1]. Several techniques have been proposed to cancel out high amplitude harmonics to eliminate or reduce the need for filtering while meeting the standard requirements. The most interesting one includes programmed harmonic elimination [2] and multilevel converters, which do not require high frequency switching as the PWM (Pulse Width Modulation) techniques do. Therefore the multilevel converters have attracted much attention in high power application. Multilevel voltage-source inverters are a suitable configuration to reach high power ratings and high quality output waveforms besides reasonable dynamic responses [3]. Among the different topologies for multilevel converters, the cascaded multilevel inverter has received special attention due to its modularity and simplicity of control. The principle of operation of this inverter is usually based on synthesizing the desired output voltage waveform from several steps of voltage, which is typically obtained from dc voltage sources. There are different power circuit topologies for multilevel converters. The most familiar power circuit topology for multilevel converters is based on the cascade connection of an's' number of single-phase full-bridge inverters to generate a ($2s$ + 1) number of levels. To control the output voltage and to eliminate the undesired harmonics in multilevel converters with equal dc voltages, various modulation methods such as sinusoidal pulse width modulation (SPWM), space vector PWM techniques are suggested in [4] and [5]. Another approach is to choose the switching angles so that specific higher order harmonics such as the 5th, 7th, 11th, and 13th are suppressed in the output voltage of the inverter. This method is known as Selective Harmonic Elimination (SHE) or programmed PWM techniques in technical literature [6]. Such method is associated with the arithmetic solution of nonlinear transcendental equations which contain trigonometric terms. This set of nonlinear equations can be solved by iterative techniques such as the Newton–Raphson method. However, such techniques need a good initial guess which should be very close to the exact solution patterns. Furthermore, this method finds only one set of solutions depending on the initial guess. Therefore, the Newton–Raphson method is not feasible to solve the SHE problem for a large number of switching angles if good initial guesses are not available.

In this paper the total harmonics are reduced by selected harmonics elimination technique in cascade multilevel inverters. In literature

there are several techniques are proposed to do so. In this paper PSO and BFOA techniques are proposed to minimize the THD. In this the asymmetry of the transcendental equation set are solved and the simulation results for an 11-level cascaded multilevel inverter are discussed and a comparative analysis is done among these methods.

II. CASCADE MULTILEVEL INVERTER

The cascaded H-bridge multilevel inverter consists of a series of single-phase H-bridge inverter units, as shown in Fig. 1. It is modular in nature and can be extended to any required number of levels. It is supplied from several separate dc sources (SDCSs), which may be obtained from batteries, solar cells, or ultra-capacitors. Each SDCS is connected to a single-phase H-bridge inverter and can generate three different voltage outputs, $+Vdc$, 0, and $-Vdc$.This is accomplished by connecting the dc source to the ac output side by using different combinations of the four switches of a inverter. The ac outputs of the modular H-bridge inverters are connected in series such that the synthesized voltage waveform is the sum of all of the individual inverter outputs.Level of inverter can be calculated by the formula: n=2s+1.where "s" is number of individual source connected.

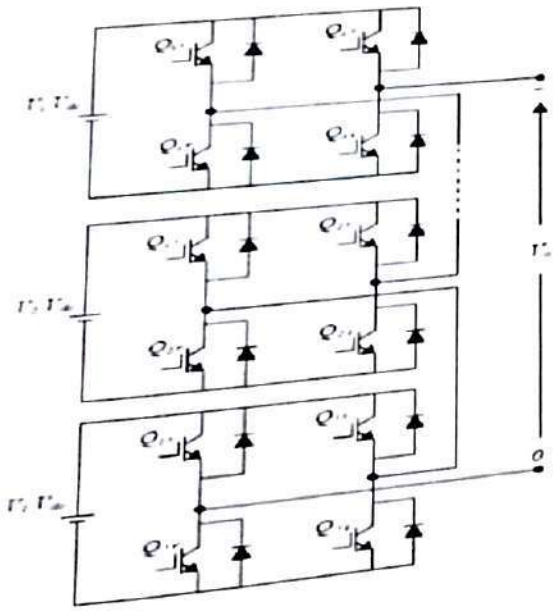

Fig(a)

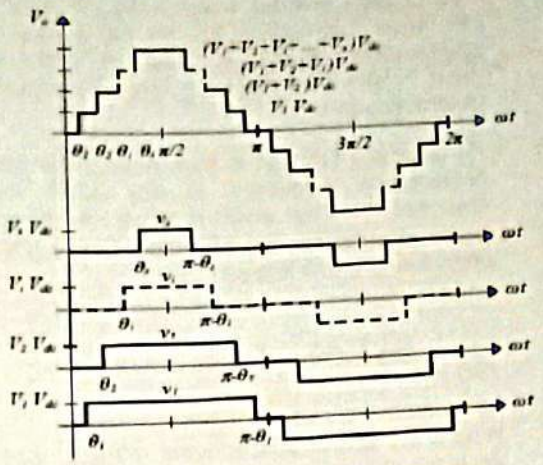

Fig(b)

A.PROBLEM FORMULATION

Assuming the equal DC source is applied to each of the inverter and taking into consideration the characteristics of the inverter waveform Fourier series expansion of stepped output voltage waveform of the multilevel inverter with equal dc sources can be expressed as:

$$Vo(\omega t)=\sum_{n=1,3,5}^{m}\frac{4vdc}{n\pi}\{\cos(n_{\varphi}1)+\cos(n_{\varphi}2)+\cos(n_{\varphi}3)+\cos(n_{\varphi}4)+\cos(n_{\varphi}5)\}\sin(\omega t) \quad \ldots\ldots\ldots\ldots\ldots\ldots\ldots 1$$

Where vdc is the nominal dc voltage.equation 1 has 5 variables (φ1, φ2, φ3, φ4, φ5) .

Where 0< φ1< φ2< φ3< φ4< φ5<π/2. and a set of solutions is obtainable by equating s-1 harmonics to zero and assigning a specific value to the fundamental component, as given below:

$$\cos(\varphi 1)+\cos(\varphi 2)+\cos(\varphi 3)+\cos(\varphi 4)+\cos(\varphi 5)=m$$

$$\cos(3\varphi 1)+\cos(3\varphi 2)+\cos(3\varphi 3)+\cos(3\varphi 4)+\cos(3\varphi 5)=0$$

$$\cos(5\varphi 1)+\cos(5\varphi 2)+\cos(5\varphi 3)+\cos(5\varphi 4)+\cos(5\varphi 5)=0 \quad \text{----------2}$$

$$\cos(n\varphi 1)+\cos(n\varphi 2)+\cos(n\varphi 3)+\cos(n\varphi 4)+\cos(n\varphi 5)=0$$

Where m = V1/(4Vdc/π) and the modulation index ma=m/s.

For 11 level inverter where s=5, 3rd ,5th ,7th ,9th order harmonics will be eliminated if single phase Supply is given. In 3 phase case triple harmonics are eliminated automatically.

An objective function is then needed for the optimization procedure. In this paper the objective Function which is to be minimized is the total harmonics distortion (THD). The objective function is given by:

$$f(t) = \frac{\sqrt{\sum_{n=3,5,7}^{49}(Vn)^2}}{V1} \quad \ldots 3$$

Where V1 is the fundamental voltage and Vn is the nth order harmonics voltage.

III. PARTICLE SWARM OPTIMIZATION

Particle Swarm Optimization was developed by Kennedy and Eberhart (1995) as a stochastic optimization algorithm based on social simulation model . The algorithm employs a population of search points that moves stochastically in the search space. Concurrently, the best position ever attained by each individual, also called its experience, is retained in memory. The development of particle swarm optimization was based on concepts and rules that govern socially organized populations in nature, such as bird flocks, fish schools, and animal herds.

A. PSO ALGORITHM FOR MINIMIZATION OF THD

Let $Vi = [Vi1, Vi2, \ldots, Vis]$ be a trial vector representing the ith particle of the swarm to be evolved. The elements of Vi are the solutions of the harmonic minimization problem, and the dth element of that is corresponding to the dth switching angle of the inverter. The step-by-step procedure to solve the SHE problem with equal dc sources is as follows.

1) Get the data for the system. At the first step, the required parameters of the algorithm such as population size M, maximum iteration number *iter*max, etc., are determined and the iteration counter is set to *iter* = 1.

2) Generate the initial conditions of each particle. Each particle in the population is randomly initialized between 0 and $\pi/2$; similarly, the velocity vector of each particle has to be generated randomly within $-Vmax$ and $Vmax$.

3) Evaluate the particles. Each particle is evaluated using the fitness function of the harmonic minimization problem. the cost function is given as follows:

$$f(t) = \frac{\sqrt{\sum_{n=3,5,7}^{49}(Vn)^2}}{V1}$$

4) Update the personal best position of the particles. If the current position of the particle is better than it's previous personal best position, replace Pi with the current position Xi. In addition, if the best position of the personal bests of the particles is better than the position of the global best, replace Pg with the best position of the personal bests.

5) Update the velocity and vectors. All particles in the population are updated by velocity and position update rules (4) and (5), respectively.

6) Termination criteria. If the iteration counter *iter* reaches *iter*max, stop; else, increase the iteration counter *iter* = *iter* + 1 and go back to step(3).

IV. BACTARIA FORAGING OPTIMIZATION ALGORITHM

Bacteria Foraging Optimization Algorithm (BFOA) was proposed by Passino. The key idea of the new algorithm came from the application of group foraging strategy of a swarm of *E.coli* bacteria in multi-optimal function optimization. Bacteria search for nutrients in a manner to maximize energy obtained per unit time. Individual bacterium also communicates with others by sending signals A bacterium takes foraging decisions after considering two previous factors. For searching nutrients the bacterium moves by taking small steps which known as chemotactic movement Mathematical modeling, adaptation, and modification of the algorithm might be a major part of the research on BFOA in future.

A . BFOA ALGORITHM FOR MINIMIZING THE THD

Let $Vi = [Vi1, Vi2, \ldots\ldots Vis]$ be a trial vector representing the ith bacterium step of the swarm to be evolved. The elements of Vi are the solutions of the harmonic minimization problem, and the dth element of that is corresponding to the dth switching angle of the inverter. The step-by-step

procedure to solve the SHE problem with equal dc sources is as follows.

1) get the data for the system. at the first step the required parameters of the of the algorithmsuch that chemotactic step, reproduction count, elimination dispersal count is set to 1.

2) Generate the initial condition of each bacterium. Each bacterium step in the population is randomly initialized between 0 and $\pi/2$. Similarly the direction vector of each bacterium randomly generated within $-V_{max}$ and V_{max} .

3) Each bacterium is evaluated by using objective function of the harmonic minimization problem i.e THD.

$$f(t) = \frac{\sqrt{\sum_{n=3,5,7}^{49}(Vn)^2}}{V1}$$

4) Generate the random vector Δ(i) with each element Δm(i),m=1,2,..... *Vis* a random number on [-1,1].update the step of the bacterium .compute the objective function. If the current step is better than the previous then replace the step with current one. This will continue till the maximum chemotactic step.

5) For the given reproduction count and elimination dispersal count for each bacteria the minimum objective function value find out. Sort bacteria and chemotactic parameters c(i) in order of ascending cost f(t) .the bacteria with highest f(t) values die and the remaining bacteria with best values split. This will be continued till maximum reproduction count.

6) For i= 1,2,3 eliminate and disperse each angel. To do this if a angel is eliminated simply disperse another one to a random location. And calculate the objective function value to get a minimum value. if the elimination dispersal count reaches its maximum value stop else increase the dispersal count and go back to step (3).

V. EXPERIMENTAL RESULT

A. FOR PARTICLE SWARM OPTIMIZATION

in order to validate the computational result as well as the simulations,experimental results are presented for a single phase 11 lavel cascade H-bridge inverter.The program was developed in matlab and the fitness function i.e the THD was minimized.The THD result up to 49th harmonics was calculated with a supply voltage of 12V.The THD result upto 49th harmonics is 6%.The angle for which this result has come is as below.

θ_1=5.2338^0, θ_2=16.3852^0, θ_3 =30.9033^0 , θ_4 =42.9065^0 , θ_5 =62.6564^0.

The fourier transform analysis has done and the figure is shown below

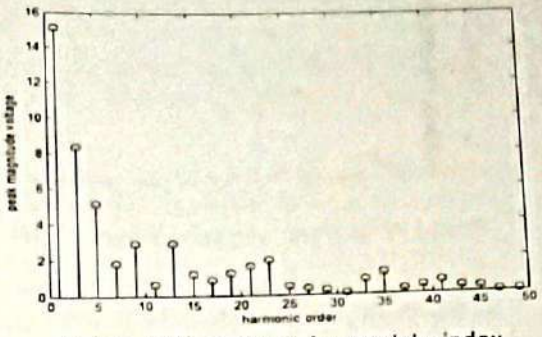

Fig(c) FFT analysis for module index 0.8

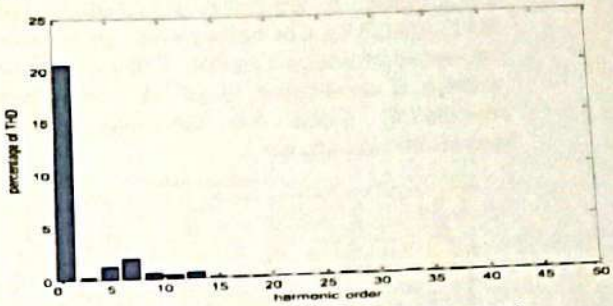

Fig(d) FFT analysis with percentage of THD

B. FOR BACTARIA FORAGING OPTIMIZATION ALGORITHM

.The THD result up to 49th harmonics was calculated with a supply voltage of 12V.The result is given below.

THD=7.2% The angle for which this result has come is as below.

θ_1 = 8^0 θ_2 = 24^0 θ_3 = 29^0 θ_4 = 49^0 θ_5 = 63^0.

The fourier transform analysis has done and the figure is shown below

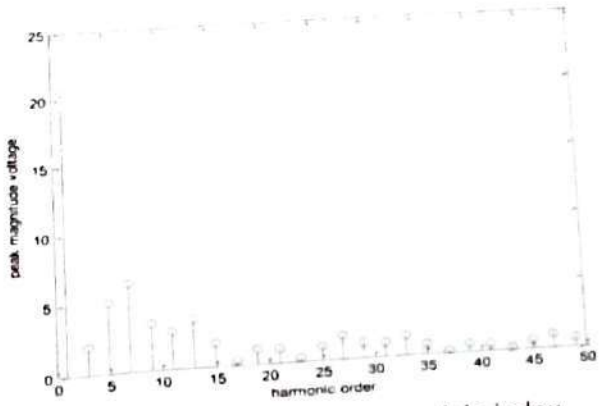

Fig(e) FFT analysis for module index 0.8

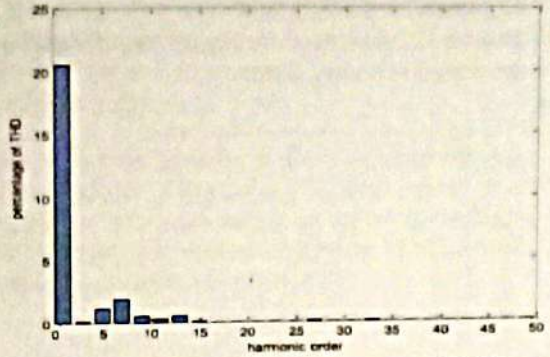

Fig(f) FFT analysis with percentage of THD

C. SIMULATION RESULT

To validate the computational results for switching angles which was found out from the program a simulation is carried out in MATLAB/SIMULINK software for an 11-level cascaded H-bridge inverter. The nominal dc voltage is considered to be 12 V and with modulation index 0.8 the line voltage waveform was shown.

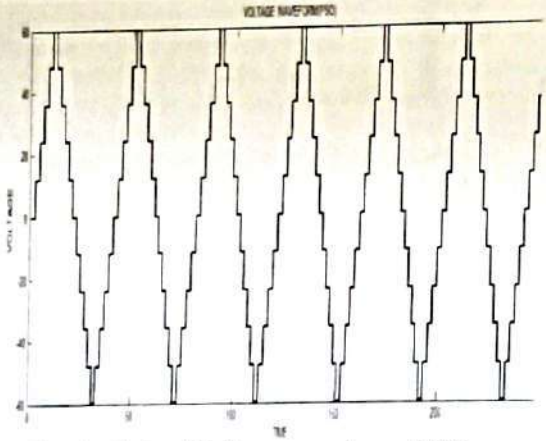

Fig(g) Output Voltage waveform (PSO Techniques)

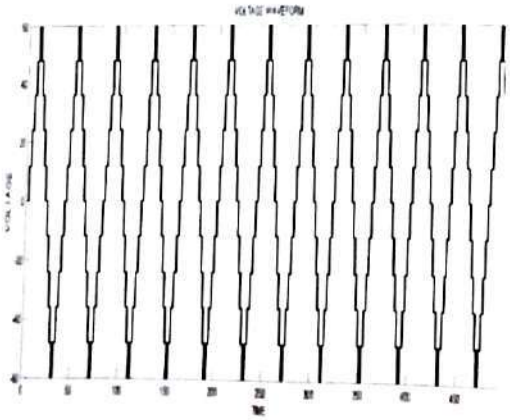

Fig(h)

Output Voltage waveform (BFOA Techniques)

VI. CONCLUSION

In this paper programs are developed on different heuristic technique to solve the SHE problem with equal D.C sources in H-bridge cascade multilevel inverter. The PSO and BFOA techniques presented in this thesis achieve this objective and includes:

1. Development of algorithm for minimization of THD.

2. Application of this algorithm in multilevel inverters with equal dc sources which are used in power system to convert the dc power to ac power.

3. Development of simulation to validate the result.

This concludes that when the resultant approach reaches the limitation of contemporary algebra software tools, the proposed methods are able to find the optimum switching angles in a simple manner. The simulation and experimental results are provided for an 11-level cascaded H-bridge inverter to validate the accuracy of the computational results. From the experiment we found that the percentage of THD is more in BFOA technique than that of PSO technique.

VII. REFERENCES

1. IEEE recommended practices and requirements for harmonic control in electrical power system IEEE standard,519-1992.

2. M. Sarvi, M. R. Salimian, "Optimization of Specific Harmonics in Multilevel Converters by GA&PSO", UPEC2010 31st Aug - 3rd Sept 2010.

3. H. Taghizadeh and M. Tarafdar Hagh,"Harmonic Elimination of Cascade Multilevel Inverters with Nonequal DC Sources Using Particle Swarm Optimization" IEEE transactions on industrial electronics, vol. 57, no. 11, november 2010.

4. D. G. Holmes and T. A. Lipo, "Pulse Width Modulation for Power Converters".Piscataway, NJ: IEEE Press, 2003.

5. S. Kouro, J. Rebolledo, and J. Rodriguez, "Reduced switching-frequency modulation algorithm for high Power multilevel inverters," IEEE Trans.Ind. Electron., vol. 54, no. 5, pp. 2894–2901, Oct. 2007.

6. W. Fei, X. Du, and B. Wu, "A generalized half-wave symmetry SHE-PWM formulation for multilevel voltage inverters," IEEE Trans.Ind. Electron., vol. 57, no. 9, pp. 3030–3038, Sep. 2010.

7. Burak Ozpineci, Leon M. Tolbert' 2, John N. Chiasson2, "Harmonic Optimization of Multilevel Converters Using Genetic Algorithms", 2004 35th Annul IEEE Power Electronics Specialisu Conference.

8. Swagatam Das, Arijit Biswas, Sambarta Dasgupta, Ajith Abraham "Bacterial Foraging Optimization Algorithm: Theoretical Foundations, Analysis, and Applications"

9. Hai Shen, Yunlong Zhu, Xiaoming Zhou, Haifeng Guo, Chunguang Chang, "Bacterial Foraging Optimization Algorithm with Particle Swarm Optimization Strategy for Global Numerical Optimization"

10. Leon M. Tolbert, John N. Chiasson, Zhong Du, Keith J. McKenzie, "Elimination of Harmonics in a Multilevel Converter", IEEE transactions on application industry,vol.41,n0.1,January/februry 2005.

11. Jagdish Kumar, Biswarup Das, Pramod Agarwal, "Selective Harmonic Elimination Technique for a Multilevel Inverter", Fifteenth National Power Systems Conference (NPSC), IIT Bombay, December 2008.

★ ★ ★

A review on Segmentation Techniques of Image Processing

Jyostna Mayee Behera[1],Kirti Bhandari[2],Kamalpreet Kaur[2],Sukanta Behera[3]
([1,3]GIFT,Bhubaneswar ,[2]Dr. B R Ambedkar National Institute of Technology, Jalandhar)

Abstract:
The various image segmentation techniques for partitioning an image into multiple segments, so that the representation should be valuable. There are now a wide assortment of image segmentation techniques, some considered general purpose and some deliberate for specific classes of images. These practices are separated on the basis of various properties such as detecting discontinuities and similarities. It is a great challenge for image analysis to have a accurate partitioning of image so that reliability of segmentation maintained.

Keywords: *Image segmentation, thresholding, feature based clustering, region based segmentation, model based segmentation, graph based segmentation*

I. Introduction

The image segmentation technique is to clump pixels into significant image surfaces, objects, or natural parts of objects. Segmentation usage in various vicinity such as object recognition, finger print recognition, medical imaging and computer guided survey. The image several images namely light intensity (visual) image, range image (depth image), nuclear magnetic resonance (MRI), thermal image and many more. A challenging problem is to region with boundaries insufficiencies just like missing edges or lack of texture contrast between regions of interest and background. This review paper attempts to incorporate all these points to limited extent. However, by no means is it exhaustive survey

II. Segmentation Techniques

Based on the following two properties of image, different techniques are classified

Detecting Discontinuities
Detecting Similarities

Detecting Discontinuities

The Detecting Discontinuities are based upon a difference of their gray levels in an image as illustrate an edge detection [1]. Signal rises with rapid evolution such as transient signal in dynamic systems may undergo abrupt changes such as sharp change in first or second derivative

However, Fourier analysis is usually not able to detect the events. The purpose of this example is to show how analysis by wavelets can detect the exact instant when a signal changes and also the type and amplitude of the change.

DetectingSimilarities

The *Detecting Similarities* are based upon the predefined criteria, that divides the proposed image into a segments whose pixel values on grouping gives the same results correspondence to the original image[1],followed by image segmentation algorithms that point up different techniques.

Classification of these techniques are as follows:

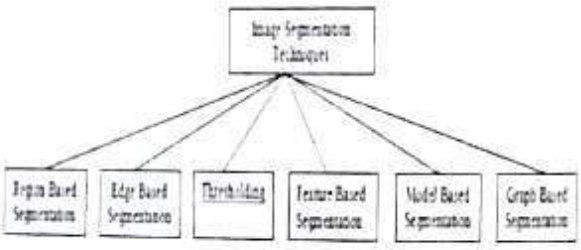

Figure 1: Classification of Segmentation Techniques

A. Region based segmentation

Firstly region is defined as a set of associated pixels with similar properties. Interpretation of an image will be correct, if it is partitioned into regions that correspond to objects or parts of an object.

The partitioning into regions is done often by using gray values of the image pixels [6,4]. As following two techniques are very supportive in region based segmentation:

Region Growing

Region Splitting and Merging

1. Region Growing

Region growing is a technique that combines pixels based upon predefined criteria into sub regions or larger regions [7]. It can be processed in four steps:-

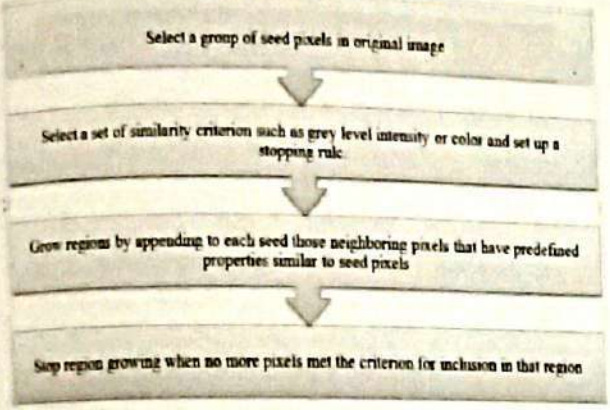

Figure 2: Steps of Region Growing

2. Region Splitting and Merging

As for choosing a seed points, image can be divided into a set of arbitrary unconnected regions which then merged into a region .Region splitting and merging is usually implemented using a theory based on quad tree data.

B. Edge Based Segmentation

The boundary between two regions with relatively distinct gray level properties is known as *Edge*. A basic feature of image, that include rich information that is very significant for obtaining the image characteristic used for object recognition. Using this technique, object boundaries are represented, and helpful in identifying the objects. The most commonly used discontinuity based operators on this techniques are Robert's edge detection, Sobel Edge Detection, Prewitt edge detection, Kirsh edge detection, Robinson edge detection, Marr-Hildreth edge detection, LoG edge detection and Canny Edge Detection [9] which can easily implemented also.

C. Thresholding

The simplest property that pixels in a region can share its intensity, called thresholding. Naturally, region can be segmented through thresholding by the separation of light and dark regions [10]. It is beneficiary to separate out the regions of the image corresponding to objects in which we are interested, from the regions of the image that correspond to background. [11,12].

Threshold techniques can be categorized into two classes:

Global Threshold

Local Threshold

D. Feature based clustering

The clustering in an image segmentation is defined as the process of identifying groups of similar image primitive. Clustering techniques can be classified into following two categories:

Supervised Clustering

Unsupervised Clustering

1. *Supervised clustering*: Human interaction is included to decide the clustering criteria. It includes hierarchical approaches such as relevance feedback techniques, Log-Based Clustering, Hierarchical Clustering, Retrieval Dictionary Based Clustering, K-Means Algorithm. These clustering techniques are:

   i. *Relevance feedback*: A relevance feedback approach allows a user to interact with the retrieval algorithm by providing the information of which images in relevance to the query.

   ii. *Log–Based Clustering*: Information retrieval process is maintained that is based on retrieval system logs. [13].

   iii. *Hierarchical Clustering*: It is the procedure of integrate a different

images that building as a cluster in the form of a tree and then developing step by step in order to form a small cluster.

iv. *Retrieval Dictionary Based Clustering:* Formation of cluster is formed by calculating the distance between two learned patterns. As these learned patterns are classified into different clusters followed by a retrieval stage [13].

v. *K-Means Algorithm:* In K-means algorithm data vectors are grouped into predefined number of clusters. At first, the centroids of the predefined clusters are initialized randomly [14].

2. *Unsupervised clustering:* This type of clustering decides the clustering criteria by itself.

E. Model based segmentation

Markov Random Field (MRF) based segmentation is well-known as Model based segmentation. MRF has an inbuilt region smoothness constraint which is used for color segmentation. Components of the color pixel tuples are measured as independent random variables for further processing. MRF is combined with edge detection for identifying the edges accurately [15]. MRF has spatial region smoothness constraint and there are correlations amongst the colour components [16].

F. Graph based segmentation

Ina Graph based segmentation, from a given image, image features are extracted which is used to construct a graph based upon different supervised learning algorithms. After building a graph, apply state-of-the-art graph-cut algorithms to solve the problem efficiently [19].Let G = (V, E) be an undirected graph with vertices $v \in V$, the set of elements to be segmented, and edges $(vi, vj) \in E$ corresponding to pairs of neighbouring vertices has a corresponding weight W (vi, vj)[20] which is a measure of the dissimilarity between the two pixels connected by that edge. In the graph-based approach, a segmentation S is a partition of V into components such that each component (or region) $C \in S$ corresponds to a connected component in a graph G = (V, E'), where $E' \subseteq E$. [20]

III. Conclusions and Future Scope

As paper, signifies the classification techniques of image segmentation that shows potential to future as the universal procedurals and has become the focus of contemporary research. Homogeneity of images, spatial characteristics of the image continuity, texture, image content are the various factors for segmenting an input image. Thus, there is no single method which gives effective results for all type of images. After the analysis of different techniques of image segmentation, it is observed that a hybrid solution for image segmentation consists of two or more techniques is being the best approach to solve the problem of image segmentation.

References

[1] Waseem Khan, "Image Segmentation Techniques: A Survey", Journal of Image and Graphics, Vol. 1, No. 4, December 2013, available at http://www.joig.org/uploadfile/2013/1226/20131226051740869.pdf

[2] Sujata Saini and Komal Arora, " A Study Analysis on the Different Image Segmentation Techniques", International Journal of Information & Computation Technology ISSN 0974-2239 Volume 4, pp. 1445-1452, 2014, available at http://www.ripublication.com/irph/ijict_spl/ijictv4n14spl_13.pdf

[3] Rajeshwar Dass, Priyanka and Swapna Devi," Image Segmentation Techniques", IJECT Vol. 3, Issue 1, ISSN: 2230-7109 (Online) | ISSN: 2230-9543 (Print), Jan-March 2012.

[4] Rafael C. Gonzalez and Richard E. Woods, "Digital Image Processing", 2nd ed., Beijing: Publishing House of Electronics Industry, 2007.

[5] H. G. Kaganami and Z. Beij, "Region Based Detection versus Edge Detection", IEEE Transactions on Intelligent information hiding and multimedia signal processing, pp. 1217-1221, 2009.

[6] K. K. Singh and A. Singh, "A Study of Image Segmentation Algorithms for Different Types of Images", International Journal of Computer Science Issues, Vol. 7, Issue 5, 2010.

[7] Hassana Grema Kaganami and Zou Beiji, "Region-Based Segmentation versus Edge Detection", Intelligent Information Hiding and Multimedia Signal Processing, 2009. IIH-MSP '09. Fifth International Conference, pp. 1217 – 1221, DOI: 10.1109/IIH-MSP.2009.13, 2009.

[8] Nikita Sharma, Mahendra Mishra and Manish Shrivastava, " Colour Image Segmentation Techniques and Issues: An Approach", International, W. X. Kang, Q. Q. Yang, R. R. Liang, "The Comparative Research on Image Segmentation Algorithms", IEEE Conference on ETCS, pp. 703-707, 2009.

[9] Muthukrishnan and Radha, "Edge Detection Techniques For Image Segmentation" , International Journal of Computer Science & Information Technology (IJCSIT), Vol 3, No 6, Dec 2011, available at http://airccse.org/journal/jcsit/1211csit20.pdf

[10] http://homepages.inf.ed.ac.uk/rbf/CVonline/LOCAL_COPIES/MORSE/threshold.pdf

[11] http://www.ancient-asia-journal.com/articles/10.5334/aa.06113/

[12]Salem Saleh Al-amri , N.V. Kalyankar and Khamitkar, " Image Segmentation by Using Threshold Techniques", Journal Of Computing, Volume 2, Issue 5, ISSN 2151-9617, May 2010, available at https://arxiv.org/ftp/arxiv/papers/1005/1005.4020.pdf

[13] Santanu Bhowmik and Viki Datta ," A Survey on Clustering Based Image Segmentation", International Journal of Advanced Research in Computer Engineering & Technology, Volume 1, ISSN: 2278 – 1323, Issue 5, July 2012, available at, http://ijarcet.org/wp-content/uploads/IJARCET-VOL-1-ISSUE-5-280-284.pdf

[14] Sriparna Saha and Sanghamitra Bandyopadhyay", A new symmetry based multiobjective clustering technique for automatic evolution of clusters", Journal Pattern Recognition, Volume 43, Issue 3, pp 738-751, March 2010.

[15] J. Luo, R. T. Cray and Lee, "Incorporation of derivative priors in adaptive Bayesian color image segmentation", Proc. ICIP'97, Vol. 3, pp. 58-61, Oct 26-29, 1997.

[16] J. Gao and J. Zhang M. G. Fleming, "A Novel Multiresolution Color Image Segmentation Technique and its application to Dermatoscopic Image Segmentation", Image Processing, vol 3, pp 408–411, 2000.

[18] Tamas Sziranyi, Josiane Zerubia, LaszLo Czuni, David Geldreich and Zoltan Kato, "Image Segmentation Using Markov Random Field Model in Fully Parallel Cellular Network Architectures" , Real-Time Imaging 6, DOI 10.1006/rtim.1998.0159,pp. 195-211 (2000), available at, https://www.inf.u-szeged.hu/~kato/papers/rti2000.pdf

[19] Pedro F. Felzenszwalb and Daniel P. Huttenlocher, "Efficient Graph-Based Image Segmentation", International Journal of Computer Vision 59(2), pp. 167–181, 2004

☆ ☆ ☆

Multiband Monopole Antenna With complimentary Split Ring Resonator for WLAN and WIMAX Application

Pravanjana Behera[1], Ajeeta Kar[2] Monalisa Samal[3], Subhransu Sekhar Panda[4], Durga Prasad Mishra[5]

[1,2,3,4,5]Asst. Professors, Gandhi Institute For Technology, Bhubaneswar

Abstract— This paper presents a compact multi band monopole antenna with complimentary split ring resonator element for WLAN (2.4/5.8GHz), WIMAX(3.5) applications. The proposed complimentary split ring resonator antenna(CSRA) has novel design which provides 21.35%(2.42GHz), 38%(3.7GHz) and 13.8%(5.78GHz) impendence bandwidth at operational frequency bands. This antenna have good radiation pattern at resonant frequencies 2.42 GHz & 3.7 GHz,5.78GHz. The design and analysis of the proposed antenna have been carried out by means of Ansoft HFSS 14.0 based on finite difference time domain(FDTD) method . Electrical permittivity, permeability property of complimentary split ring resonators is measured using MATLAB also presented in this paper.

Index Terms— CSRR, WLAN, WIMAX, Monopole antenna, Multiband

I. INTRODUCTION

Antenna is a transducer which convert Electromagnetic wave to Electromagnetic radiation. Antennas which are working properly more than one frequency region either for transmitting or receiving purpose are known as multiband antennas [1]. Such antennas are usually used for dual band, tri-band, penta-band , hepta-band Applications. Naturally multiband antennas are more complex than the single frequency resonating band. We will investigate compact multiband monopole antenna with complimentary split ring resonators for WLAN and WIMAX application .

Rapid development of various wireless local network(WLAN), WIMAX applications have forced researchers to use novel antenna for mobile and base station called miniaturised multi band and wideband antenna . Today the most popular wide spread WLAN protocols have been IEEE 802.11 b/g, which is used the 2.4 GHz ISM band(2.4-2.484 GHz),IEEE 802.11y, which is used the 3.6 GHz band(3.6-3.7 GHz) and IEEE 802.11a which employs the 5 GHz U-NII band (5.725-5.850 GHz).The WIMAX licensed band (3.3-3.8 GHz).In this context preferably all those bands are achieved using a single antenna.

A monopole antenna is the best antenna for multiband and wideband application. Due to their appealing features of wide bandwidth, simple structures, ominidirectional patterns and ease of construction, planar metal-plate monopole antennas have been proposed for such applications [2]

In this context a printed rectangular monopole antenna (PRMA), which is a rectangular microstrip antenna(RMSA) with etched ground plane. Complimentary split ring resonator provides negative permittivity & may negative permeability which has the ability to tuned the antenna at certain frequency.

Tuning a particular frequency can be achieved by taking the monople antenna length is equal with quarter wavelength. But due to complimentary split ring resonator the rectangular monopole antenna length further reduced and can be tuned to particular frequency according to the shape, size, structure of the split ring resonator. For improving impedance bandwidth various types of transition between the feed line and patch has been adopted. Such region is known as feed region .The feed regions include rectangular microstrip feed region.

II. DESIGN AND METHODOLOGY

The objective to study the behavior of complimentary split ring resonator & to design an antenna using this CSRR element.

A. Complimentary split ring resonator

CSRR is an artificial metamaterial which does not depend upon crystal & lattice of an atom or molecule. It only depends on shape, size and structure. CSRR are excited by means of a dynamic electric field with a non-negligible component in the axial direction and these particles make the artificial line where they are inserted to behave as a negative permittivity[3][4]. CSRR is known as a resonance particle. But resonance of this particle depends upon always shape and size. CSRR means etching of split ring resonator from the metal coated substrate. With this we have investigated the multi resonance behaviour of split ring resonator. And the optimum size of CSRR particle design is presented here ,which provides a resonance frequency at 2.42GHz, 3.5 GHz, 5.78GHz.

Here the substrate is FR4 epoxy with dielectric constant ε_r=4.4, having tangent loss tanδ= 0018. The substrate is of length l3=22 mm & width w=20 mm. Fig 1 (a) shows a rectangular substrate with metal coating, from which a split ring resonator is etched. And becomes a complimentary split ring resonator. Here l1=12mm, l2=4.5mm, w1=10mm.Fig 1(b) shows a microstrip line withl4=12mm,w2=14mm, l5=5mm ,w3=4mm. The air box having dimension 20 x 22 x 11.67 $(mm)^3$. The excitation is the wave port given to the CSRR & microstrip ground plane to two ports. The port to port distance is 20mm.

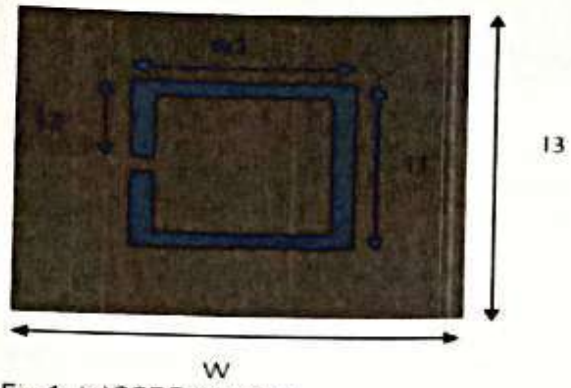

Fig 1 (a)CSRR top view

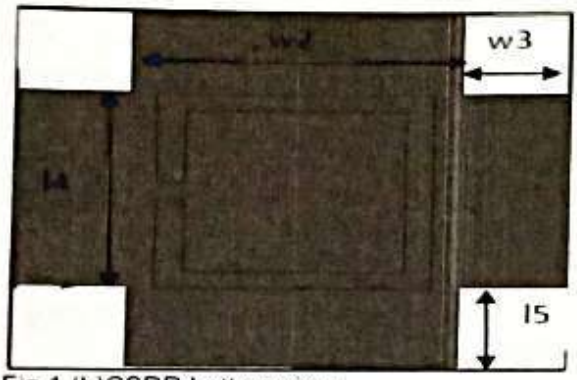

Fig 1 (b)CSRR bottom view

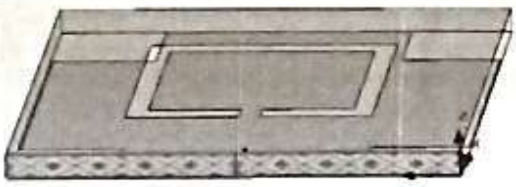

Fig1(c) Waveport applied in YZ Plane

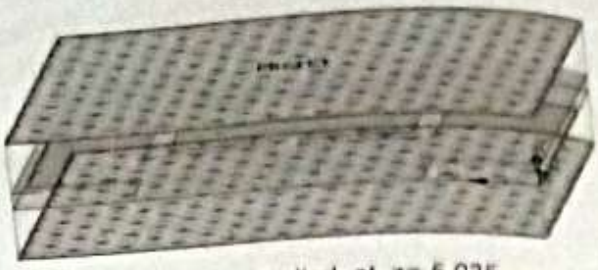

Fig 1 (d)PEC boundary applied at z=-5.035, 6.635 plane & PMC in ZX plane. The air box XY plane applied as PEC & ZX plane as PMC.

SIMULATION & RESULT

The above design is simulated in ANSOFT HFSS 14 which is developed by using finite difference time domain method.

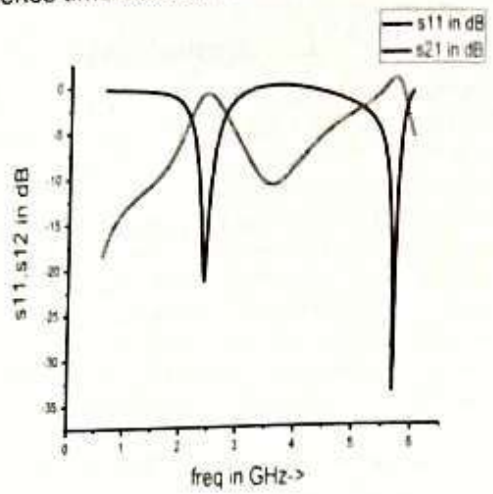

Fig 2(a) Reflection and transmission coefficient vs. frequency.

From the above figure we observe that this complimentary split ring resonator tuned to three resonance frequencies around 2.42,3.6,5.7 GHz. 2.4 Ghz, 5.78 GHz provides band stop resonating frequency & 3.6 GHz provides band pass resonating frequency.

CSRR MEDIUM PARAMETER STUDY

To find out whether on those resonant frequency Ɛ & μ negative or not S-parameters retrieval technique is useful in obtaining the material parameters, when analytical techniques become increasingly difficult to apply (e.g. Scattering object has complex geometry). This procedure extracts the effective permittivity, effective permeability, index of refraction by inverting the reflection-transmission results considering the metamaterial as a homogeneous effective medium. S-parameters retrieval provides complete information on the material parameters of the sample in a direct manner. S-parameters measurement and retrieval can

form the basis of a semi automated metamaterial characterization procedure. To extract effective medium parameter from the normal incidence scattering parameter data, the Nicolson-Ross-Weir (NRW) approach [5] and the corrections were implemented. The NRW approach begins by introducing the composite terms.

$v1=s21+s11$ .....(1)

$v2=s21-s11$ .....(2)

$s11=res11+j*ims11$ .....(3)

$s21=res21+j*ims21$ .....(4)

$\mu=\frac{2}{jk_0d}\frac{1-v_2}{1+v_2}$ .....(5)

$\varepsilon=\frac{2}{jk_0d}\frac{1-v_1}{1+v_1}$ .....(6)

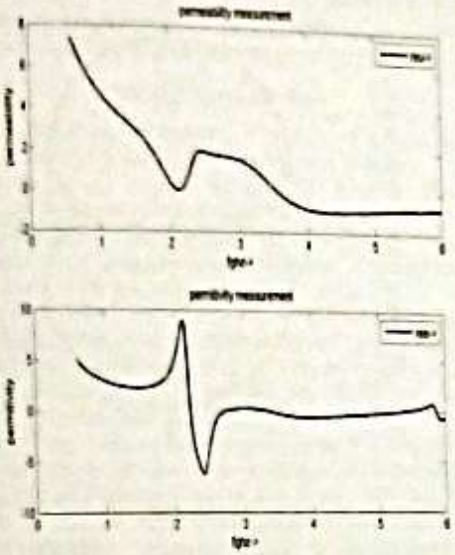

Fig 2(b) CSRR Permeability and permittivity curve with respect to frequency.

Using above formula a MATLAB program had been developed. We observed that electrical permittivity is negative around 2.45 GHz and 5.7GHz ,thus giving two resonant frequencies . The electrical permeability is also negative around 3.5 GHz, that provides another resonance frequency.

Summary -From the above study we observed that a Complimentary split ring resonator has dynamic multi frequency tunable capability, which depends upon the CSRR size, shape & structure. This unit can be embedded in any radiator which provides WLAN,WIMAX resonant frequency. So length of antenna only depends upon this resonating CSRR element. So antenna length can be reduced less than quarter wavelength.

III. Monopole Antenna With Complimentary Split Ring Resonator

A monopole antenna is mainly used for its appealing features, such as wide impedance bandwidth, ominidirectional, ease of construction. The antenna consists of three parts feed line, feed region and radiating patch. A feed region is introduced between 50 Ω feed line and the main patch to smooth the current path thus providing wider impedance bandwidth. In monopole antenna the length of the ground is important . Generally we take partial ground. To achieve the lower cut-off frequency at 2.4 GHz the radiating patch is a rectangular microstrip with a complimentary split ring resonator. The antenna is fabricated in a standard 1.6 mm FR4 epoxy substrate material with dielectric constant ε_r=4.4 at 2.42 GHz. The width of the monopole antenna is 26mm. The effective dielectric constant ε_{re} is calculated from the equation

$$\varepsilon_{re}=\frac{\varepsilon r+1}{2}+\frac{\varepsilon r-1}{2}\left[1+12\frac{h}{w}\right]^{-0.5} \quad \text{.....(7)}$$

ε_{re} =3.989

The wave guide wavelength (λ_g) can be calculated from free space wavelength (λ_0), as

$\lambda_g = \lambda_0(\varepsilon_{re})^{0.5}$ .....(8)

λ_g=62.1mm

Now quarter wavelength become 15.5 mm. So to resonate at 2.42 GHz the quarter monopole antenna patch length should be 15.5mm. But due to complimentary split ring resonator the length of the patch had taken 14mm to resonate at 14 GHz. The substrate dimension is 39x30mm.The microstrip feed line width w1=3mm is kept fixed at to achieve 50Ω impedance. A microstrip feed region of 3.5x1mm² is introduced between 50Ω feed line and radiating patch for smooth current flow .The radiating patch was composed of two side by side CSRR that covers an area 26x14 mm². On the other face of the substrate a ground plane of 22.2x30mm² was etched .The final dimension of the antenna was recorded as: L=3, k=22.2, w=30,w1=26, l1=22, l2=14, l3=10, w1=26, w2=8(all dimensions are in mm).

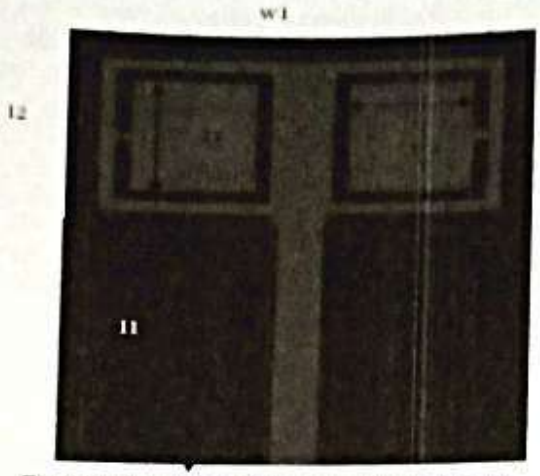

Fig 3(a) Top view of the proposed antenna

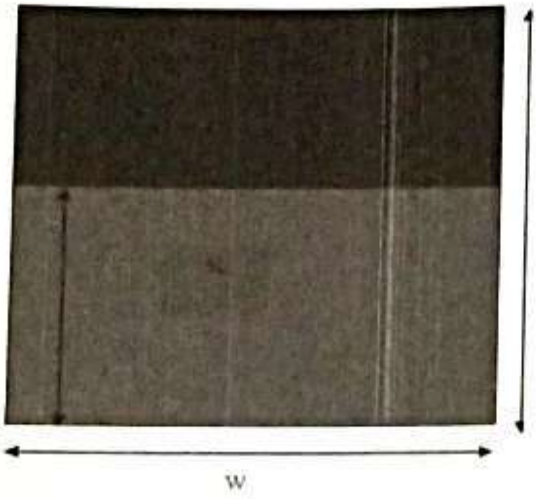

Fig 3(b) Bottom view of the proposed antenna

IV. SIMULATION & RESULT

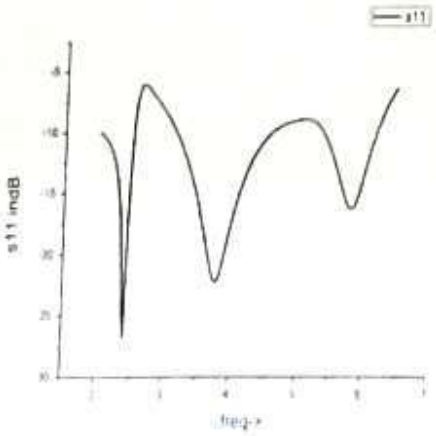

Fig 3(b) Return loss vs frequency curve

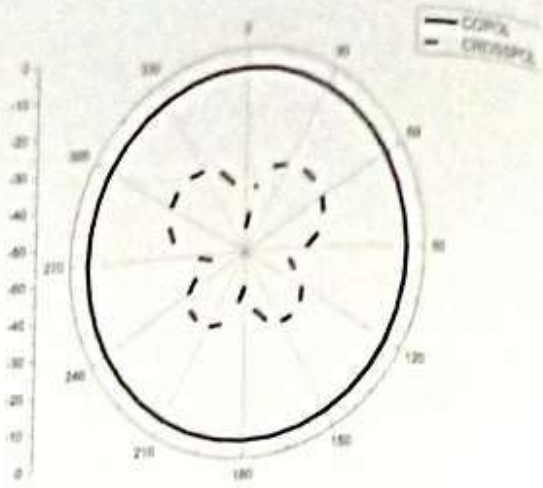

Fig 3(c) H-plane at phi=0°

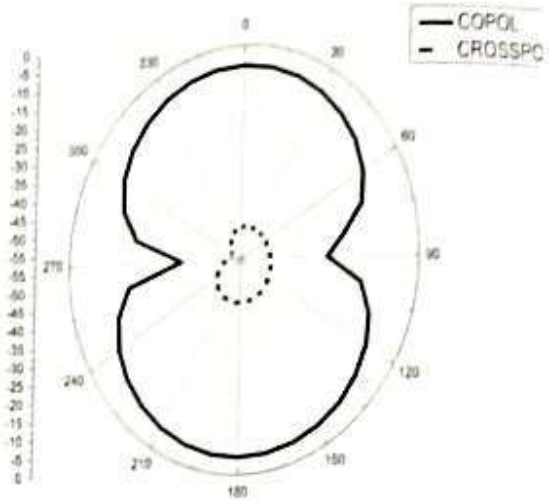

Fig 3(d) E-plane at phi=90°

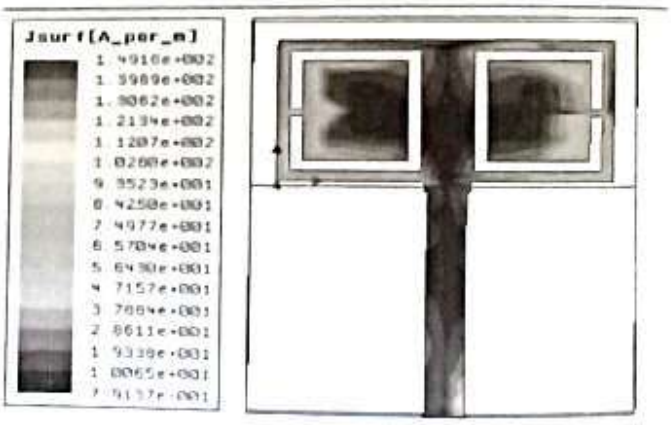

Fig 3(e) Magnitude of surface current density(J_{surf} in A/m)

Based on the designed parameter the simulated results are shown. Here our desired

resonant frequency are 2.42 GHz with 21.35%, 3.7GHz with 38% bandwidth & 5.78 GHz with 13.8% bandwidth respectively. Hence the proposed antenna almost covers all WLAN band and WIMAX band. Radiation Patterns of the proposed antenna design also computed and the corresponding polar plots of 2.42 GHz are displayed.

V. CONCLUSION

In this paper a multiband resonating frequencies are achieved by using complimentary split ring resonators monopole antenna for WLAN WIMAX applications is presented. The proposed antenna is compact and dynamically tuned to different frequencies which only depends upon the shape and size of resonating structure. It is simulated and observed it can cover almost all WLAN, WIMAX operation bandwidth. And at 2.42 resonant frequency the planar monopole antenna has preserved ominidirectional property . So it can fully meet the requirements of ISM band.

VI. REFERENCES

[1] C. A. Balanis, "Antenna Theory: Analysis and Design, "John Wiley & Sons, 1996, 3rd Edition.

[2] W. Choi, J. Jung, K. Chung and J. Choi, "Compact Wideband Printed Monopole Antenna with Frequency Band- Stop Characteristic," *IEEE Antennas and Propagation Society International Symposium*, Vol. 3A, 2005, pp. 606- 609.

[3] A. M. Nicolson and G. F. Ross, "Measurement of the Intrinsic Properties of Materials by Time Domain Tech-niques," *IEEE Transactions on Instrumentation and Measurement*, Vol. 19, No. 4, 1970, pp. 377-382. doi:10.1109/TIM.1970.4313932

[4]W. B. Weir, "Automatic Measurement of Complex Dielectric Constant and permeability at Microwave Frequencies," *Proceedings of the IEEE*, Vol. 62, No. 1, 1974, pp. 33-36. doi:10.1109/PROC.1974.9382

[5]P. K. Kadaba, "Simultaneous Measurement of Complex Permittivity and Permeability at Microwave Frequencies," *IEEE Transaction on Instrumentation and Measurement*, Vol. 33, No. 4, 1984, pp. 336-340. doi:10.1109/TIM.1984.4315236

A Novel SIW Corrugated H-plane horn antenna

[1]Anil Kumar Nayak, [2]Shashibhusan Panda,[3]Saumendra Behera
[1,3]Department of Electronics and Communication Engineering, Department of Electronics and Communication Engineering
Gandhi Institute For Technology Bhubaneswar-752054 India, [2]Kurpajal Engineering College, Bhubaneswar-751002, India

***Abstract*—A novel H-plane Substrate Integrated Waveguide (SIW) horn antenna is designed in this paper. A new type of SIW feeding technique is presented that has well high gain and radiation efficiency. The feeding section of the horn antenna uses stepped transformer for the improvement in the impedance bandwidth. The corrugated horn section is used to increase the radiation characteristics of the proposed antenna. The center frequency of the proposed SIW horn antenna is 18.48 GHz. It has a gain of 7.03 dBi, impedance bandwidth 1.3 % and the radiation efficiency of 93.38%.**

***Keywords*—SIW, impedance bandwidth, Stepped, RL, gain and efficiency**

I. INTRODUCTION

Recently, the rectangular horn antenna is one of the preeminent widely used antennas in microwave applications. However, substrate-integrated-waveguide (SIW) horn antennas are not as frequently used as metallic rectangular horn antennas because of the low front-to-back ratio (FTBR) and impedance mismatch [1].Using the stepped transform can improvement the FTBR and matching impedance. The upper and lower triangular corrugated shape SIW structure has been considered in 2-D (pyramidal shape in 3-D). The corrugated unit helps improvement the radiation characteristics of antenna like conventional horns such as increasing in gain.

The RF circuit component must be compact in size and light in weight .SIW technology promising and emerging candidate for RF and microwave circuit because the structure have the advantages of convectional metallic waveguide, namely high power handling capacity, high quality factor and low loss radiation [2]

In this paper we present a NSIW H-plane horn antenna, this antenna is integrated by using single substrate. It is to fabricate and the structure is compact. To remove the higher order mode in the wave guide, the thickness of the substrate is kept constant. At the lower frequency region, the width of SIW becomes large. As a result the flare angle changing of SIW is challenging task for the researcher. By using stepped transform technique the impedance bandwidth can be increasing considerable [3].We achieve the gain of 7.03 dBi and efficiency of 93.38% at 18.48 GHz (K-band).The structure is developed on Roger RT/duroid 5880 substrate with the permittivity (ε_r) of 2.2, height or thickness (h) Of 2.54 mm and loss tangent of 0.0009 and a working frequency of 18.48 GHz are used in all simulated result. All the simulated result is gotten from Ansoft HFSS that is associated with Finite Element Method (FEM).

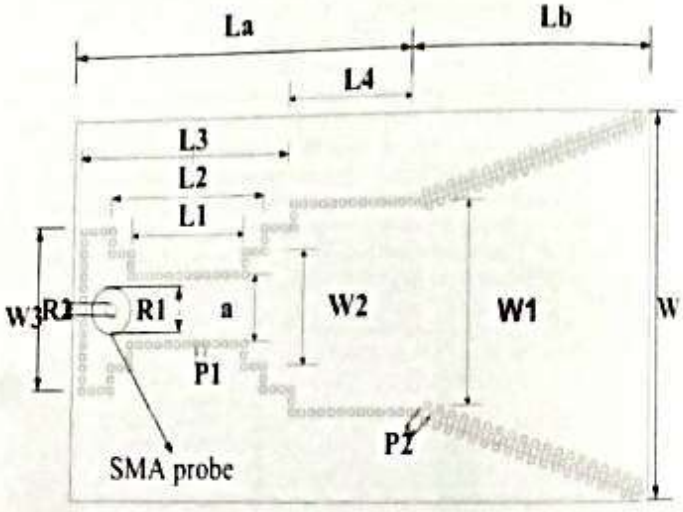

Fig.1.A Novel SIW H-plane horn antenna, top view

II. CONCEPT OF NSIW H-PLANE HORN ANTENNA

The large emphasis placed on horn antenna research was inspired by need to reduce spillover efficiencies and cross polarization loss and increase aperture efficiencies of large reflection used in radio astronomy and satellite Communication using the convectional feed aperture efficiencies of 50-60% microwave radiometry.

However efficiencies' of order of 75-80% can be obtained with improved feed system utilizing corrugated horn. [6].The NSIW H-plane hom antenna is shown in Fig 1. It consist of 50Ω feed line, ground plane and metallic vias on the both sides indicates in Fig 1.But in this paper efficiencies of the order of 90-95% can be obtain with improve the gain and improve feed systems utilizing the stepped transform .Configuration of a horn is shown in Fig 1.One end, it is open circuited whereas in the case of a SIW there is metallic vias on the both side. As the opposite of wall is open circuited, it is act as a magnetic wall.Consequantly in the waveguide section propagate the Transverse Electric with the dominant mode i.e. TE_{10} mode.

III. ANTENNA DESIGN

Fig 1.shows all the dimension of parameter of proposed a NSIW H-plane horn antenna. The antenna has been design on low cost and easily available Roger RT/duroid 5880 (tm) substrate of dielectric constant (ε_r) of 2.2,height or thickness (h) of 2.54 and loss tangent (tan δ) of 0.0009.It consist of 50Ω feed line, ground plane metallic vias on the both sides.

TABLE 1.

Parameters	Dimensions (mm)	Parameters	Dimensions (mm)
La	43.3	W1	21.6
Lb	28.2	W2	12
L1	14.4	W3	16.8
L2	19.2	a	7.2
L3	27.7	R1	2.5
L4	15.6	R2	0.746
W	40	P2	1.5
P1	1.2	d	0.8

A 50Ω feed line design by a SMA probe of inner diameter R1 and outer diameter R2.The distance between two vias and radius of vias are important factor of the design of any kind of SIW antenna. Using the following equation, where w_{eff} is the width of the waveguide [4, 5].

$$W_{eff} = a - 1.08\frac{d^2}{p_1} + 0.1\frac{d^2}{a} \quad (1)$$

The empirical equation is very accurate when p_1/d is smaller than three and d/a smaller than 1/5.

In our design the center to center distance p_1 between two vias is 1.2mm and also center to center distance p_2 of corrugated part is 1.5mm and diameter of vias is 0.8mm each. his dimension of this antenna is 71.5 x 40 x 2.54 mm^3. The details dimension of proposed a novel SIW H-plane horn antenna in table I.

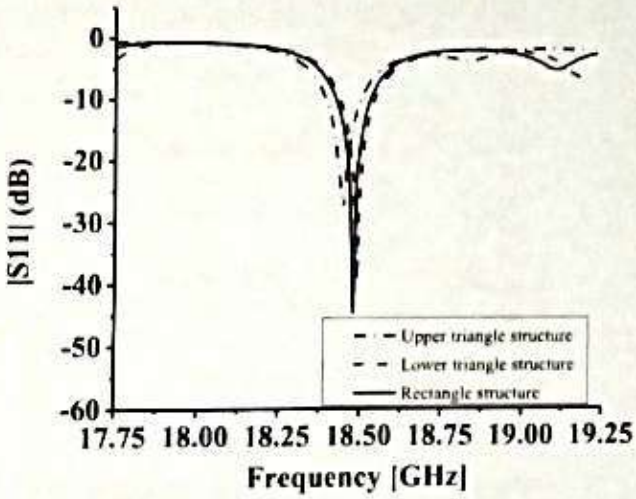

Fig.2. Simulated $|S_{11}|$ parameter.

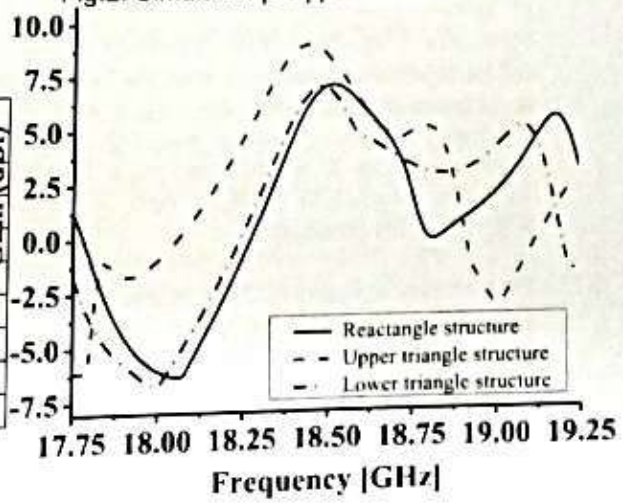

Fig.3.Peak gain versus frequency (Simulated by Ansoft HFSS)

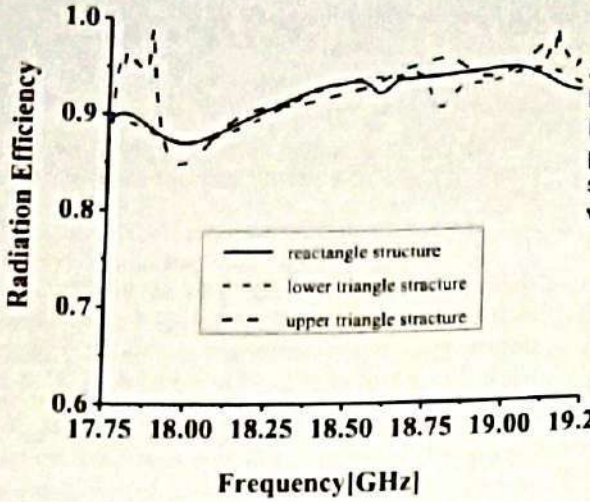

Fig.4.Efficiency versus frequency (Simulated by Ansoft HFSS)

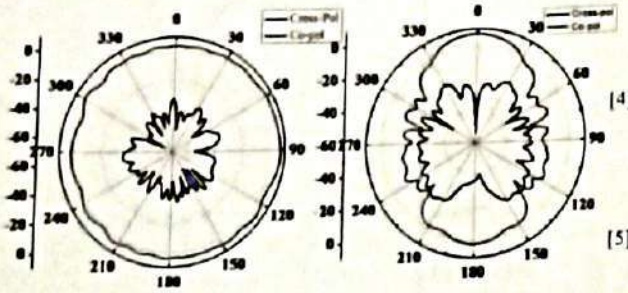

(a)

(b)

Fig.5.Radiation pattern of the antenna (a) H-plane at 18.48 GHz (b) E-plane at 18.48 GHz. (Simulated by Ansoft HFSS)

IV. RESULTS AND DISCUSSION

The NSIW H-plane horn antenna is designed to operate at 18.48GHz. The return loss of the proposed NSIW is presented Fig 2.for the three structure. It is observed from the Fig 2. That the return loss at 18.48 GHz is 44.53 dB with 1.28% of bandwidth..

The maximum gain of 7.03 dBi is obtained at resonant frequency for NSIW H-plane horn antenna shown in Fig 3.The maximum efficiency of NSIW H-plane horn antenna at 18.48 GHz is 93.38% is achieved shown in Fig 4.This type of antenna radiates normal to its surface, so the elevation pattern for $\varphi = 0^0$ and $\varphi = 90^0$ are important for measurement. Fig 5. (a) and (b) are shows the H-plane and E-plane. The radiation pattern at 18.48 GHz, and we observed that cross polarization level very less in both cases

V. CONCLUSION

In this work, a novel SIW H-plane horn antenna has been proposed. This antenna is basically miniaturized version of convectional H-plane horn antenna without degrading its performance. This antenna can be used for the speed radar, surveillance, imaging and wireless applications.

REFERENCES

[1] H.Y.Taso,D.H.Yang,J.C.Cheng,J.S.Fu and W.P.Lin, "W-Band SIW H-plane Horn Antenna Devlopment," *in proc. HSIC/IEEE Des Conf.*, pp. 185-187, 2012.

[2] H.Wang,D.G.Fang,B.Zhang and W.Q.Che,"Dielectric Loaded Substrated Intigrated H-plane horn antennas, " *IEEE Trans.Antenna Propag.*,vol.58,no.3,pp.640-647,2010.

[3] V.Kumari,W.Bhowmik and S.Srivastava, "Design of High-Gain SIW and HMSIW H-plane Horn Antenna using metamaterial," *in IJMAW/CambrigeUniversity press*, pp. 1-8, 2014.

[4] D.Deslandes and K.Wu, "Accurate modelling wave mechanism &design consierdations of Substrate Intigrated Waveguide.," *IEEE Trans.Microw.Theory Tech*, vol. 56,no-6, pp. 2516-2026, 2006.

[5] F.Xu and K.Wu, " Guided wave and leakge characteristic of Substrate Intigrated Waveguide," *IEEE Trans.Microw.Theory Tech*, vol. 53,no-1, pp. 66-73, 2005

[6] M.Oliaei and M.S.Abrishamian, "Corrugated SIW Kband horn antenna," *In Proc. of AEU/Elsevier*, vol. 68,no-12, pp. 1199-1204, 2014.

Production of biodiesel from non-edible tree-borne oils and its fuel characterization

[1]Nabnit Panigrahi, [2]Amar Kumar Das, [3]Kedarnath Hota
[1] Gandhi Institute For Technology,[2] Gandhi Institute For Technology, [3]Gandhi Institute For Technology

Abstract: *This article intends to extract oil from non-edible seeds like neem, polanga, mahua and simarouba in the form of crude vegetable oil. The extracted oil was used for biodiesel production by following esterification and transesterification process. Different methods were adopted for the determination of fuel properties namely density, viscosity, calorific value, flash point, fire point, cloud point, poor point, cetane no, carbon residue, copper strip corrosion, iodine value, saponification value and moisture content of sample fuels following the standards procedure. The result of fuel properties obtained for the sample fuels are compared with diesel fuel. Pertaining to fuel properties, the tested fuels show akin fuel properties as diesel fuel.*

Index Terms: Biodiesel, diesel, fuel properties, vegetable oil

I. INTRODUCTION

India being a developing country requires much higher level of energy to sustain its rate of progress. India's energy demand is expected to grow at 5.2%. India is the world's 5th largest energy consumer for about 4.1% of the world's energy and moving fast enough to become the 3rd largest consumer after US and China. India's import bill on import of petroleum products is 5,27,765 crore in 2015-16.

Many research works have been carried out on edible and non-edible methyl ester and various conclusions were drawn [1-3]. The use of edible vegetable oils for biodiesel production is been a great concern because they compete with food materials. Hence, the contribution of non-edible oils such as neem, mahua, polanga and Simarouba oil will be significant as a non-edible plant oil source for biodiesel production [4-6]. Considering the oil contents of seeds and availability potential of neem, mahua, polanga and simarouba oils, the present investigation on biodiesel production and determining the physical and chemical properties of the said biodiesel and comparing with diesel were undertaken with the following specific objectives given below.

The main objectives of the study can be stated as the following

- To extract vegetable oil from the seeds
- To convert the vegetable oil to biodiesel
- To prepare the blends of biodiesel (B10).
- To determine some important fuel properties of the sample fuel and compared with diesel

II. MATERIALS AND METHODS

A. Oil Extraction

Considering the number of non-edible oil seed bearing tree species having tremendous potential of biodiesel production in Odisha, Neem(*Azadirachta Indica*), Mahua (*Madhuca Indica*), Polanga (*Calophyllum inophyllum*) and Simarouba (*Simarouba glauca*)tree borne oils were selected for present investigation. Details of some of the tree-borne oil seed plants are given in Table 1 referred from [7-8].

Table1 Oil Extractions of selected Oil Seed Plants

Sl. No	Botanical Name	Common Name	Oil (%)
1	*Azadirachta indica*	Neem	20-50
2	*Madhuca indica*	Mahua	35
3	*Calophyllum inophyllum*	Polanga	50-73
4	*Simarouba glauca*	Simarouba	60-75

The extraction of vegetable oil from seeds is commonly categorized as:

- Mechanical extraction by expeller.
- Chemical extraction by solvent extraction.

For mechanical expeller, the dry fruits were collected in a drum, and the kernels were separated. Later the kernels were dried and then fed into the oil extraction machine. The pure vegetable oil obtained by pressing followed by filtration and is collected in a drum.

In solvent extraction, oil from solid material was extracted by repeated washing with an organic solvent which was hexane. In this method 50 gram of kernel was dried, ground into small

particles and placed in the thimble. The thimble was placed in an extraction chamber, which was suspended above a flask containing the solvent. The flask was heated and the solvent evaporates and moves up in to the condenser where it was converted in to a liquid and trickles into the extraction chamber containing the sample. When the solvent surrounding the sample exceeds a certain level it overflows and trickles back down into the boiling flask. At the end of the extraction process which lasts for 7 hours. The solvent was removed by rotary evaporator to recover the required oil. The collected oil from expeller was tested for FFA (Free fatty acid).

The FFA of oil was found to be more than 1.5. Therefore, a two-step transesterification process was required for these feed stocks. Line diagram of biodiesel production is shown in Fig 1.

Fig 1 Line diagram of biodiesel production

B. Preparation of biodiesel

Esterification Reaction

For the pre-treatment, 5 litre of the above oil was heated up to 60°C, and then methanol (6:1 molar ratio of methanol: oil) and acid catalyst (0.5% v/v) were added. The reactants were stirred at a speed of 1600 revolution per minute at a temperature of 60°C for 2 hours. This decreased the acid value significantly. The top layer methanol was separated out by decantation process and the oil layer was taken for transesterification. Once the reaction was completed, it was dewatered by passing over a hydrous Na_2SO_4 and then fed to the transesterification process.

Transesterification Reaction

The above esterified oil were filtered and pre-processed to remove water and contaminants if any and then fed directly to the transesterification process along with any product of the acid esterification process. The oil was pre-heated to 65° C and a mixture of methanol and the catalyst KOH was added to the oil. The molar ratio of MeOH / oil was 6:1 and catalyst concentration was 1% w/w of oil. A part of the alkali catalyst was used to neutralise the residual amount of acid and the remaining as catalyst for transesterification. Once the reaction was completed, the product was allowed to stand overnight to separate the layers. The upper biodiesel layer was washed with hot distilled water to remove the excess methanol, catalyst and traces of glycerol. The washed ester layer was dried under the vacuum to remove the moisture and methanol, and again it was passed over a hydrous Na_2SO_4. The biodiesel so obtained were designated as methyl ester. Laboratory Scale-Biodiesel Production Unit is shown Fig. 2.

Fig 2 Biodiesel production unit

C. Preparation of biodiesel blends

Fuel blends were prepared from above prepared biodiesels and diesel. Diesel was blended with biodiesel in different proportions to form B10(10% biodiesel + 90 % diesel). Photograph of sampleoil with biodiesel blends is shown in Fig. 3.

Fig. 3 Sample Oil and Biodiesel

D. Fuel Properties

Fatty Acid Profile

Fatty acid profile of oil samples is given in Table 2.

Table 2 Fatty Acid Profile of Sample Oils as shown in [9]

Fatty Acid	Neem oil	Mahua oil	Polanga oil	Simaroub a oil
C_{16}	14.9	24.5	12.01	12.3
C_{17}	-	-	-	0.1
C_{18}	14.4	22.5	12.95	27.3
$C_{18:1}$	61.9	37.5	34.09	54.6
$C_{18:2}$	7.5	14.3	38.26	2.3
C_{1}	-	-	0.3	0.2

8 3				
C_{20}	1.3	1.5	-	1.2
C_{21}	-	-	-	0.4

Flash Point Fire Point

A Pensky Martens closed cup type apparatus was used in the study for determination of flash point and fire point shown in Fig. 4 a. In the experiment, the sample was filled in the test cup up to the specified level and heated with the help of a heater in such a way that the temperature rise was approximately 5°C per minute with uniform stirring. At every 1°C rise in temperature, the flame was introduced for a moment with help of a shutter. The fire point was recorded at that temperature when the fuel gives sufficient vapor that catches fire at least for five seconds.

Cloud Point and Pour Point

The apparatus mainly consists of 12 cm high glass tubes of 3 cm diameter. The tubes were enclosed in an air jacket, which is filled with a freezing mixture of crushed ice and sodium chloride crystals. The glass tube consists of fuel sample was taken out from the jacket at every 1°C interval as the temperature falls, and inspected for cloud formation. The point, at which a haze was first observed at the bottom of the sample, was taken as the cloud point.

For determining the pour point, the sample was pre-heated to 48°C and then cooled to 35°C in air before it was filled in the glass tube. Thereafter, the cooled samples were placed in the apparatus and withdrawn from the cooling bath at 1°C interval for checking its flow ability. The pour point was taken to be the temperature 1°C above the temperature at which no motion of fuel was observed for five seconds on tilting the tube to a horizontal position. Three replications were made for the fuel.

Density

Density is defined as mass per unit volume. The relative density of the selected fuels at 15°C was determined. The empty pycnometer of 50 ml capacity was weighed by an electronics balance. The pycnometer was then filled with fuel sample and weighed. The samples were maintained at 15°C by keeping them in a temperature control chamber. The weight of the empty pycnometer was subtracted from the weight of the filled ones to get the weight of the fuel sample. Three replicates were taken for each sample and their mean was calculated. This value when divided by the volume of the fuel sample gave the density of the fuel sample at 15°C. The density of the distilled water at 15°C was also determined. The Pycnometer is shown in Fig. 4b. Density was then calculated from the given Eqn 1.

$$Relative density = \frac{Density of the fuel at 15^{\circ}C}{Density of the water at 15^{\circ}C} \quad (1)$$

Viscosity

Kinematic Viscometer is used for measuring viscosity shown in Fig. 4 c. The sample was introduced into the viscometer, invert the viscometer, immerse tube into the liquid and suction is applied which causes the sample to rise to etched line. The tube was inserted into a holder and placed at constant temperature bath for about 15 minutes to reach the equilibrium temperature. Vertical alignment of the tube may be accomplished in bath by suspending a plumb bob in the tube. Suction was applied to the tube so that the sample was raised a short distance above the mark. Same procedure was repeated to get the exact data. The viscometer constants vary for different size of the tubes and are given inn Appendix-I. Kinematic viscosity in centistokes was then calculated by using Eqn. 2.

$$Kinematic Viscosity = Viscometer constant \times t \quad (2)$$

Where,

t = flow time, s

Vis constant of the viscometer= 0.0336 cSt/s

Calorific value

Calorific value of fuel was determined by a closed vessel called bomb calorimeter shown in Fig. 4 d.

Sample fuel (1 gram) was placed in the crucible. Pure oxygen was then admitted through the oxygen valve till pressure inside the bomb rises to 30 atmospheres. The bomb was then completely submerged in a known quantity of water contained in a large copper vessel. When the bomb and its contents had reached steady temperature, fuse wire was heated up electrically. The fuel ignited and continued to burn till whole of its burnt. The heat, liberated by the combustion of fuel, is absorbed by this water and apparatus. The gross calorific value was calculated using Eqn. 3.

$$H_c = \frac{(m_w + m_e)C_w(t_2 - t_1)}{m_f} \quad (3)$$

Where,

m_f= Mass of fuel sample burnt in bomb, kg ; m_w= Mass of water filled in the calorimeter, kg ; m_e= Water equivalent of apparatus, kg ; C_w = Calorific value of water, kJ/kg K; t_2 = Final temperature of water, ^{0}C ; t_1 = Initial temperature of water, ^{0}C

Cetane No.

Cetane Number indicates the readiness of the fuel to self-ignite when exposed to the high temperatures and pressure in the diesel engine combustion chamber. Higher the cetane number, better its ignition properties. It affects engine performance parameter like combustion, stability, smoke, noise and emission of CO and hydrocarbons.

The cetane number is an indicator of the quality of fuel's combustion during ignition while it is under compression. It is one of several important measures of fuel's quality and specifically indicates the fuel's ignition delay. This is the period of time that elapses between a fuel's injection into the combustion chamber and the start of its combustion. A higher cetane number means that fuel has a shorter ignition delay. Cetane index is given in Eqn 4.

$$\textbf{Cetane Index} = 46.3 + \frac{5458}{s.v} - (0.225 \times i.v) \quad (4)$$

Where,

s.v= Saponification value. *i.v* = Iodine value

Cetane number is nearly equal to cetane index as per the equation given below also reported by [10]:

Cetane Number = Cetane Index – (1.5 to +2.6)

Carbon Residue

The test was conducted by using Conradson's apparatus shown in Fig. 4 e. In this method, 10 g weight of each fuel sample was weighed free of moisture and other suspended matter in to an iron crucible. The crucible was then placed in the centre of skid more crucible of the apparatus and the sand was levelled in the large sheet iron crucible and then the skidmore crucible was set on it in the exact centre of the iron crucible. Thereafter, the covers were applied to both skidmore and iron crucible loosening the latter fitting to allow free exit to the vapour as it formed. The fuel sample was then heated with a high flame from gas burner for 20 minutes. When the smoke appeared on the chimney, immediately the burner was moved or tilled so that the gas flame placed on the sides of the crucible for the purpose of igniting the vapour, after that the ignited vapour was burnt uniformly with the flame above the chimney. When the vapour ceased to burn and no further smoke was observed, the burner was adjusted and the heat was held as at the beginning to make the bottom and the lower part of the sheet iron crucible a cherry red appearance about 15 minutes. The cover of skidmore was then removed with a tong and it was cooled and weighed. The percentage of carbon residue on the original sample was then calculated using the equation 5given below:

$$\textbf{Carbon residue}\ (\%) = \frac{\textbf{mass of carbon residue g}}{\textbf{mass of test sample g}} \times 100 \quad (5)$$

Copper Strip Corrosion Test

The corrosiveness of a fuel is measured using the copper strip corrosion test. A polished copper strip was immersed in a specific volume of the sample being heated under specific temperature and time. At the end of the heating period the copper strip foil was removed, washed and the colour tarnish level were assessed against the ASTM copper strip corrosion standards. The model is shown in Fig. 4 f and Fig. 4 g.

Iodine value

Iodine value, also called Iodine number, is the mass of iodine in grams absorbed by 100 g of the oil/fat. The iodine value is a measure of the degree of un-saturation of an oil or fat. It is a constant for particular oil or fat. It is an useful parameters in studying oxidative rancidity of oils since higher the un-saturation, greater is the possibility of the oil to become rancid.

Halogens add across the double bonds of unsaturated fatty acids to form addition compounds. Iodine mono chloride (ICL) was allowed to react with the fat in the dark. Iodine gets incorporated into the fatty acid chain wherever the double bond exist. The amount of iodine consumed was then determined by titration of the iodine released (after adding KI) with standard sulphate and comparing with a blank in which the fat was omitted. Hence the measure of iodine absorbed by an oil or fat gives the degree of un-saturation. The reaction in the test is given below as per [11]:

The iodine value of the sample is determined by the Eqn. 6 given below.

$$\textbf{Iodine Value} = \frac{V \times N \times 0.1269}{\textbf{Mass of oil in gram}} \times 100 \quad (6)$$

Where,

V = Volume of $Na_2S_2O_3$ (blank experiments - test experiments); N= Normality of $Na_2S_2O_3$ solution

1 ml of 0.1N $Na_2S_2O_3$ = 0.1269gm. of Iodine

Saponification value

Saponification value represents the number of milligrams of potassium hydroxide required to saponify 1 g of fat under the conditions specified.

Saponification is the process by which the fatty acids in the glycerides of the oil/fat are hydrolyzed by an alkali. The resultant salts of fatty acids are called soaps. When the oil or fat (triglyceride) is heated with KOH (alkali) it is saponified (hydrolyzed) and release fatty acids and glycerol. It is the number of milligram of KOH required to neutralise the fatty acids resulting from the complete hydrolysis of 1 g of fat or oil. This value gives an indication of the nature of fatty acids constituent of the fat and depends upon the average molecular mass of the fatty acid constituent of fat. Thus this value is useful for a comparative study of the fatty acid chain length in oils. The greater the molecular mass (the longer the carbon chain) the smaller the number of fatty acids is liberated per gram of fat hydrolysed and therefore the smaller the saponification number and vice versa. A blank experiment was similarly treated in the absence of oil. 5 gm of oil was refluxed with 25 ml of alcoholic KOH. After saponification, remaining KOH was estimated by titrating it against standard HCl. Clarity and homogeneity of the test solution are indicators of complete saponification.

$$\text{Saponification Values (mg KOH)} = \frac{(\text{Blank experiment} - \text{Titrate experiment})}{\text{Neem oil (g)}} \times 28.06 \quad (7)$$

Where,

1 ml of 0.5 N HCl = 28.06 mg KOH

Moisture Content

Karl Fischer Moisture Analyzers shown in Fig. 4 h is used for determination of oil or water content in crude oils. In this experiment, methanol was poured into the titration vessel in such a way that the upper level of solvent was just in contact with platinum electrode. Titration was carried out by KF reagent to moisture free the vessel with continuous stirring by magnetic stirrer. Then 10 µl distilled water was added to the vessel and titration was performed to determine the titre value in mg of water consumed per ml of KF reagent. After the determination of titre value, a known quantity of sample was added to the vessel and titrated against the KF reagent which was contained in burette. The burette was driven by microprocessor controlled stepper motor with continuous stirring by magnetic stirrer. As the end point was approached, the reagent delivery was slowed down and finally stopped when the end point was reached. The amount of water present in the sample was calculated by the Eqn 8 as per [12] given below

$$\text{Moisture content \%} = \frac{\text{Volume of KF reagent consumed (ml)} \times \text{titre value} \left(\frac{\text{mg}}{\text{ml}}\right) \text{of titre}}{\text{Sample volume}} \times 100 \quad (8)$$

Fig. 4 Apparatus used for Determination of Fuel Properties

III. Results and Discussions

The oil explored from kernels by soxhlet apparatus and expeller is shown in Table 3.

Table 3 Oil Productions by Soxhlet Apparatus and Expeller

Vegetable Oils	Oil Production by Soxhlet Apparatus (%)	Oil Production by Expeller (%)
Neem (*Azadirachta indica*)	40-45	35
Mahua (*Madhuca indica*)	50	37
Polanga (*Calophyllum inophyllum*)	60	50
Simarouba (*Simarouba glauca*)	70	55

Table 3 shows that the oil production by soxhlet apparatus was 25%-40 % more than mechanical expeller, can be compared with the result given in [13]. The FFA of Neem, Mahua, Polanga and Simarouba at different conditions, are summarized in Table 4.

Table 4 FFA values of the Sample Oils

Oil samples	Before esteri-fication	After esteri-fication	After trancesteri-fication
Neem	45	3.1	0.40
Mahua	34	2.3	0.23
Polanga	42	3.2	0.39
Sima-rouba	10	1.5	0.20

From the above table the FFA of all these oil samples after transesterification were within the limit. The acid value (FFA *2) of the above tested samples were within the prescribed limits. Density, Viscosity and Calorific value of sample fuels is mentioned in Table 5.

Table 5 Densities, Viscosity and Calorific Value of Sample Fuels

Sl no.	Name of Oil/Biodiesel	Density (gm/cc)		Kinematic Viscosity (cSt)		Calorific value (MJ/Kg)
		Oil	Biodiesel	Oil	Biodiesel	Biodiesel
1	Neem	0.90	0.88	37.87	4.5	39.81
2	Mahua	0.90	0.88	37.18	4.98	39.10
3	Polanga	0.89	0.87	35.61	4.00	41.38
4	Simarouba	0.85	0.86	44.95	4.68	41.20
5	Diesel	0.82		2.85		45.339

The **density** of sample crude oil was found to be around 2-5% higher than that of biodiesel and was 5-12% higher than that of diesel. The density of tested biodiesel samples were within the limits (0.86-0.90 gm/cc) prescribed in the biodiesel standards.

The **kinematic viscosity values** of neem, mahua, polanga and simarouba crude oil were 13 to 16 times that of diesel.

The **calorific values** of neem, mahua, polanga and simarouba biodiesel were 13.8%, 15.93%, 9.5%, and 10.02 % lower than that of diesel respectively. The oxygen molecule present unites with hydrogen of the oil for combustion reacts with hydrogen as reflected by [12].

Flash Point, Fire Point, Cloud Point and Pour Point of sample fuels are given in Table 6.

Table 6 Flash Point, Fire Point, Cloud Point and Pour Point of Sample Oil/Biodiesel

Sl. no.	Bio-diesel	Flash Point (°C)	Fire Point (°C)	Cloud Point (°C)	Pour Point (°C)
1	Neem	160	170	9	2
2	Mahua	168	180	14	3
3	Polanga	148	160	13	4
4	Simarouba	146	156	19	4
5	Diesel	60	65	6.5	-20

The **flash point** of sample crude oil was found to be more than that of biodiesel. Also the flash point of sample biodiesel was quite high compared to 60°C for the diesel.

The **fire point** of oil was higher than that of biodiesel.

The **cloud point** of biodiesel was more than that of oil. The **pour point** of sample oil was quite higher than that of diesel. In general the cloud point and pour point of non-edible biodiesels were higher than that of diesel.

Cetane No. and Carbon residue of sample fuel is mentioned in Table 7

Table 7 Cetane No. and Carbon Residue of Sample Biodiesel

Sl. No	Biodiesel	Cetane No	Carbon residue, %
1	Neem	52	0.21
2	Mahua	55	0.22
3	Polanga	56	0.20
4	Simarouba	54	0.21
5	Diesel	50	0.15

The cetanes no of biodiesels were more than that of diesel which led to better combustion.

The carbon residue values of biodiesel were found more than diesel. Carbon residue of sample biodiesel was within the specified limit of **0.3%.**

The copper strip corrosion test results of sample fuel are given in Table 8

Table 8 Copper Strip Corrosion Test Results of Sample Oils

Sl. No.	Name oil	Copper strip corrosion
1	Neem	Slight Tarnish
2	Mahua	No corrosion
3	Polanga	Slight Tarnish
4	Simaroub a	No corrosion
5	Diesel	No corrosion

Copper-strip corrosion test indicates the presence of sulphur compounds.

Iodine value, Saponification value and Moisture Content of sample fuel are mentioned in Table 9.

Table 9 Iodine Value, Saponification Value and Moisture Content of Sample Fuels

Sl. no	Sample Biodiesel	Iodine Value (g I_2/100g)	Saponification Value (mg KOH/g)	Moisture content (%)

		Bio-diesel	Bio-diesel	Biodiesel
1	Neem	80	204	0.03
2	Mahua	70	194	0.04
3	Polanga	75	187	0.03
4	Simarouba	83.4	185.9	0.03
5	Diesel	-	-	0.02

The **Iodine** value, which is a measure of the degree of un-saturation of oil, was found to be within the **limit (≤ 115)** of the standard specification.

Saponification number refers to the milligram of KOH required for neutralizing the fatty acid resulting from the complete hydrolysis of 1 g of fat or oil. It affected the quality of biodiesel.

The **moisture contents** of seed given above were removed during esterification and transesterification process.

III. Conclusion

- Oil production by soxhlet apparatus was 25%-40 % more than mechanical expeller.
- The density of sample crude oil was found to be around 2-5% higher than that of biodiesel and was 5-12% higher than that of diesel.
- The kinematic viscosity values of neem, mahua, polanga and simarouba crude oil were 13 to 16 times that of diesel.
- The calorific values of neem, mahua, polanga and simarouba biodiesel were 13.8%, 15.93%, 9.5%, and 10.02 % lower than that of diesel respectively.
- The flash point of sample crude oil was found to be more than that of biodiesel. The fire point of oil was higher than that of biodiesel. The cloud point of biodiesel was more than that of oil. The pour point of sample oil was quite higher than that of diesel.
- The cetane no of biodiesels was more than that of diesel which led to better combustion.
- The carbon residue values of biodiesel were found more than diesel. Carbon residue of sample biodiesel was within the specified limit of 0.3%. Sample oils shows slight tarnish or no corrosive properties.
- The iodine value, was found to be within the limit (≤ 115) of the standard specification. Saponification number gives an indication of the nature of fatty acids constituent of the fat.
- The moisture contents of seed given above were removed during esterification and transesterification process.

To end with, it can be concluded that pertaining to fuel properties, the tested fuel shows akin fuel properties as diesel fuel which can be an alternative for diesel fuel.

REFERENCES

[1] P. K. Sahoo and L. M. Das, "Process optimization for biodiesel production from Jatropha, Karanja and Polanga oils," *Fuel*, vol. 88, pp. 1588-1594, 2009.

[2] F. Ma, and M. A. Hanna, "Biodiesel production-A review," *Bioresource Technology*, vol. 70, pp. 1- 15, 1999.

[3] A. Demirbas, "Biodiesel production from vegetable oils via catalytic and non-catalytic supercritical methanol transesterification methods," *Progress in Energy and Combustion Science*, 3, pp. 466-487, 2005.

[4] H. Raheman and S. V. Gadge, "Performance of compression ignition engine with mahua (Maduca Indica) biodiesel," *Fuel* vol. 86, pp-2568-2573, 2007.

[5] N.Panigrahi, and Mohanty, M.K. (2012) 'Experimental Investigation on the performance of Nomefuelled C.I. engines', International Review of Mechanical Engineering (I.R.E.M.E.) Vol. 6,No. 7, pp 1586–1592.

[6] N.Panigrahi, M.K.Mohanty and A.K.Pradhan, "Non-Edible Karanja Biodiesel- A Sustainable Fuel for C.I. Engine," International Journal of Engineering Research and Applications (IJERA), vol. 2, no. 6, pp. 853-860 853, November-December 2012.

[7] WEC, 2010. World Energy Council India Energy Book, 2010.
[8] EIA (Energy Information Administration), Annual energy Review, 2011 (September-2012). U.S. Energy Information Administration (2011)
[9] M. C. Navindgi, M. Dutta and B. S. Prem Kumar, "Performance of a CI Engine with Different Blends of Mahua (Madhuca Longifolia) biodiesel under Varying Operating Conditions," *International Journal of Engineering and Technology*, vol. 2, no. 7, pp. 1251-1255, 2012.
[10] V. Patel, "Cetane Number of New Zealand Diesel Report," *Office of Chief Gas Engineer, Energy Inspection Group, Ministry of Commerce Press*, Wellington, New Zealand 1999.
[11] S. R. Mishra, "Prospect and Potential of fatty acid methyl esters of simarouba glauca oil for use of biodiesel" Ph.D. dissertation, Dept. Chemistry, Utkal University, Vani Vihar, 2013.
[12] P. C. Jena, "Production of biodiesel from mixture of vegetable oils and its performance in diesel engine", Ph.D. dissertation, Dept. Agricultural and food engineering department, IIT, Kharagpur.2011.
[13] S. R. Mishra, M. K. Mohanty, P. K. Das and A. K. Pattanaik, "Production of Bio-diesel (Methyl Ester) from Simarouba Glauca Oil," *Research Journal of Chemical Sciences*, vol. 2, no. 5, pp. 66-71, May 2012.

A review on the Production and Optimal use of Ethyl alcohol as a Surrogate fuel in IC Engines extracted from Organic Materials

[1]Amar Kumar Das, [2]Ritesh Mohanty
[1] Assistant Professor, Department of Mechanical Engineering, Gandhi Institute ForTechnology, Bhubaneswar.
[2]Pre Final year Student, Department of Mechanical Engineering, Gandhi Institute ForTechnology, Bhubaneswar.

Abstract: *Depleting fossil fuel reserves and increasing cost of petroleum products become a big challenge of modern world. It has been adumbrated that by year 2032, there will be a surge of 60% of the current consumption of the fossil fuel like Petrol, Diesel, etc. Ethyl Alcohol or Ethanol (C_2H_6O) may be considered as a suitable alternative fuel by replacing fossil fuel resulting reduce in environmental emissions. The objective of this paper to enumerate Ethanol, produced by the process of fermentation and distillation from organic material suitably blended with gasoline or diesel to be used as a standard alternate fuel for IC engines. Ethanol emerges a good fuel property of high octane number, better volatility, viscosity and thermal conductivity to be used as a substitute for fossil fuel.*

Index terms: Ethanol, IC Engines, Antiknock, Fermentation, Distillation

I. Introduction

Ethanol (C_2H_6O) is a renewable fuel. It can be produced from agricultural feedstock, such as sugarcane, corn, potatoes, cassava, cellulose materials and also from forestry wood wastes and agricultural residues. Ethanol has a simple molecular structure with well-defined physical and chemical properties. Ethanol can be employed as a transportation fuel even in its original form and can also be easily blended with other fuels, such as gasoline (Petrol and Diesel). Currently, there is a lot of interest in ethanol production from organic materials, to minimize the emissions of Carbon dioxide (CO_2), Hydrocarbons (HC) which is a greenhouse gas that contributes to global warming. The addition of ethanol to gasoline results in the enhancement of the octane number in blended fuels and changes the distillation temperature, as well as reducing CO_2emissions.

Today, the reserves of petroleum based fuels are being rapidly depleted. Alcohols, such as ethanol, are colourless liquids with mild characteristic odours that can be produced by fermentation of biomass crops, such as sugarcane, wheat and wood. Using alcohols as fuel for I C engine have some advantages over gasoline. Ethanol has better anti-knock characteristics and the engine's thermal efficiency improves with the increase in compression ratio. Ethanol burns with lower flame temperature and luminosity owing to the decrease of the peak temperature inside the cylinder so that the heat loss and NOx emissions are lowered. Ethanol has high latent heat of vaporization. The latent heat cools the intake air and hence increases the density and volumetric efficiency. However, the oxygen content in ethanol reduces the heating value more than gasoline does. It is evident that ethanol can be used as a fuel in I.C Engines.

II.Production of Ethanol

A. Raw Materials

Ethyl Alcohol may be made by the fermentation process from three basic types of raw materials called as feedstock.

The three basic types of feedstock are.

Saccharine:
Sugar containing materials in which the carbohydrate (the actual substance from which the alcohol is made) is present in the form of simple, directly fermentable six and twelve carbon sugar molecules such as glucose, fructose, and maltose. Such materials include sugar cane, sugar beets, fruit (fresh or dried), citrus molasses, cane sorghum, potato, corn whey and skim milk.

Starchy Materials:
That contains more complex carbohydrates such as starch and insulin that can be broken down into the simpler six and twelve carbon sugars by hydrolysis with acid or by the action of enzymes in a process called

malting. Such materials include corn, grain sorghum, barley, wheat, potatoes, sweet potatoes, Jerusalem artichokes, cacti, manioc, arrowroot, and so on.

Cellulose Materials:

Such as wood, wood waste, paper, straw, corn stalks, corn cobs, cotton, etc., which contain material that can be hydrolyzed with acid, enzymes or otherwise converted into fermentable sugars called glucose.

B. Methods of Production of Ethanol

-Fermentation
-Distillation
-Dehydration

Fermentation is a metabolic process that converts sugar to acids, gases, or alcohol. It occurs in yeast and bacteria, and also in oxygen-starved muscle cells, as in the case of lactic acid fermentation.

Ethanol is produced by microbial fermentation of the sugar. Two major components of plants, stratch and cellulose, are both made of sugars and can, in principle, be converted to sugars for fermentation. Currently, only the sugar (e.g., sugar cane) and starch (e.g., corn) portions can be economically converted. There is much activity in the area of cellulosic ethanol, where the cellulose part of a plant is broken down to sugars and subsequently converted to ethanol.

Distillation is a process of separating the component or substances from a liquid mixture by selective evaporation and condensation.

For ethanol to be usable as a fuel, the majority of the water must be removed. Most of the water is removed by distillation, but the purity is limited to 95–96% due to the formation of a low-boiling water-ethanol azeotrope with maximum (95.6% m/m (96.5% v/v) ethanol and 4.4% m/m (3.5% v/v) water). This mixture is called hydrous ethanol and can be used as a fuel alone, but unlike anhydrous ethanol, hydrous ethanol is not miscible in all ratios with gasoline, so the water fraction is typically removed in further treatment to burn in combination with gasoline in gasoline engines.

Dehydration process is to remove the water from an azeotropic ethanol/water mixture. The first process, used in many early fuel ethanol plants, is called azeotropic distillation and consists of adding benzene or cyclohexane to the mixture. When these components are added to the mixture, it forms a heterogeneous azeotropic mixture in vapour–liquid-liquid equilibrium, which when distilled produces anhydrous ethanol in the column bottom, and a vapour mixture of water, ethanol, and cyclohexane/benzene.

When condensed, this becomes a two-phase liquid mixture. The heavier phase, poor in the entrainer (benzene or cyclohexane), is stripped of the entrainer and recycled to the feed—while the lighter phase, with condensate from the stripping, is recycled to the second column. Another early method, called extractive distillation, consists of adding a ternary component that increases ethanol's relative volatility. When the ternary mixture is distilled, it produces anhydrous ethanol on the top stream of the column.

As Ethanol is hygroscopic, means it absorbs water vapour directly from the atmosphere. Because absorbed water dilutes the fuel value of the ethanol and may cause phase separation of ethanol-gasoline blends (which causes engine stall), containers of ethanol fuels must be kept tightly sealed. This high miscibility with water means that ethanol cannot be efficiently shipped through modern pipelines, like liquid hydrocarbons, over long distances. The fraction of water that an ethanol-gasoline fuel can contain without phase separation increases with the percentage of ethanol.

From the above table we see that Ethanol is similar in nature with gasoline with high octane number. Both are liquid in nature thus storage and transportation are much similar. Both can be mixed easily and burnt. Ethanol has small molecular weight, large oxygen content and high H/C ratio. Octane number for ethanol is 100. Ethanol is oxygenated fuel with small molecules, it can burn fast and fully with oxygen inside. These characters can help to improve thermal efficiency

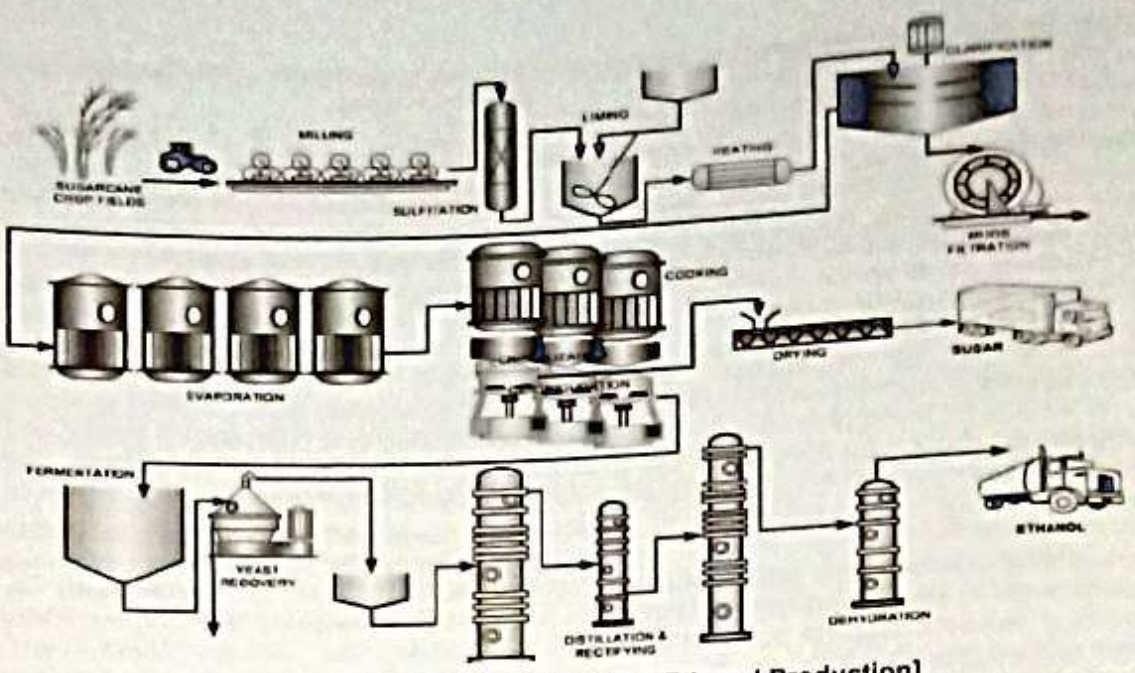

[FIG- 1 Schematic diagram of Ethanol Production]

Table-1
FUEL CHARACTERISTIC OF ETHANOL AND GASOLINE FUEL

Sl. No.	Character	Ethanol	Gasoline
01	Molecular Weight	46.12	101-106
02	Composition	C=52% H=13% O=35%	C=85% O=15%
03	Specific Gravity	0.796	0.71-0.83
04	Density (Kg/m^3)	790	710-780
05	Boiling Temperature (^{0}C)	78	27-255
06	Freezing Point (^{0}C)	-114	-57
07	Ignition Temperature (^{0}C)	423	390-420
08	Air Fuel (a/f) Ratio	9.1	14.7
09	Octane Number	100	80-99
10	Cetane Number	8	0-10

well as to achieve the cleanliness inside the engine and to reduce exhaust. With low boiling point ethanol is easy to burn and form the mixture gas which is conducive for gasoline to burn completely. Latent heat of vaporization of ethanol is three times bigger than that of petrol. So when ethanol is vaporizing, it absorbs a large amount of heat, meanwhile, the temperature of the mixed gas is lowered down. Although calorific value of ethanol is low, the heat, which the mixed gas of ethanol and gasoline produces under

theoretical air fuel ratio, is roughly the same as that of petrol.

III. Use of Ethanol in Fuel System

Gasoline is composed of C_4–C_{12}hydrocarbons and it has wide transitional properties. On the other hand, alcohol such as ethanol contains OH group that has oxygen atom and it is viewed as a partially oxidized hydrocarbon that would under-go complete combustion.

As for the combustion characteristics, the auto-ignition temperature and flashpoint of alcohol are higher than gasoline, which makes it safer for transportation and storage. The latent heat of evaporation of alcohol is 3–5 times higher than gasoline. Thus, it lowers the temperature of the intake manifold and increases the volumetric efficiency.

The enthalpy of alcohol is lower than gasoline. Therefore, more alcohol fuel is required to achieve the same energy output, which is an approximately1.5–1.8 times of gasoline fuel. The stocheometric air to fuel ratio of alcohol is about 1/2–2/3 of the gasoline, so the amount of air required for complete combustion is lesser for alcohol.

Alcohol is completely miscible with water, while the gasoline and water are immiscible. Therefore, adding ethanol causes the blended fuel to contain water, and result in the corrosion problems on the mechanical components especially for components made of copper, brass or aluminium. To reduce this problem on fuel delivery system, such materials mentioned above should be avoided. Besides, alcohol can react with most rubber and create jam in the fuel pipe. Therefore, it is advisable to use fluorocarbon rubber as a replacement for rubber.

IV.Ethanol-Research Octane Number (RON) Gasoline Blended Fuel

RON is an important parameter for vehicle combustion. Ac-cording to the past studies, the research octane number (RON) of the gasoline has been changed due to the addition of ethanol. The more ethanol is added, the higher is the RON. Increasing octane number of the fuel leads to decreases in CO and HC emissions but higher NOx emission.

The combustion duration also becomes prolong with in-creasing octane number. Longer combustion duration may result in lower thermal efficiency and increased fuel consumption. Moreover, gasoline with a high octane number is suitable for vehicles with a high compression ratio. The compression ratios of motorcycles (8–10:1) are less than gasoline cars (9–12:1). Thus, highethanol content gasoline (>15%) may not be suitable for motorcycles due to high octane number.

V.Emissions of Ethanol Blended Gasoline

Bata et al. (1989) studied different blend rates of ethanol blended with gasoline fuel for combustion in the engine and found that adding ethanol had reduced the CO and HC emissions to some degree. The reduction of CO emission is attributed by the wide flammability and oxygenated characteristic of ethanol. The study done by Palmer (1986) indicated that addition of 10% ethanol to gasoline could reduce the concentration of CO emission up to 30%. Alexandrian and Schwalm (1992) showed that the air fuel ratio (A/F) has great influence on the CO emission.

Using ethanol-gasoline blended fuel instead of gasoline alone, especially under fuel-rich conditions, it has lower CO and NOx emissions. However, studies by Chao et al. (2000) has pointed out that using ethanol-gasoline blended fuel, it increases the emission of formaldehyde, acetaldehyde and acetone, 5–14 times higher than from gasoline. Even though the emission of aldehyde will be increased when ethanol blended gasoline is used as a fuel, the damage to the environment by the emitted aldehyde is far less than by the poly-nuclear aromatics emitted from burning gasoline. Therefore, using higher percentage of Ethyl Alcohol in blended fuel can make the air quality better in comparison with burning of gasoline.

Pang et al. (2007) found that CO emission was slightly reduced (1.5–6%) from 10% (E10) ethanol blended gasoline in comparison with gasoline (RN95 -E0). The oxygenated agents (ethanol) blended with gasoline can effectively deliver oxygen to the pyrolysis zone of the burning gasoline resulting in less CO generation. In engine-out exhaust, THC emission from E10was lowerthan E0 at the torque of 3 Nm, but higher than from E0 by 2–17% under other operating conditions.

VI.Performance of an IC Engine using Ethanol Blended Gasoline:

In 1986, Palmer investigated the effect of various blend percent by volume for ethanol

and gasoline fuels in engine tests. Results indicated that adding 10% ethanol increases the engine power output by 5% and the octane number can be increased by 5% for each 10% ethanol added.
Abdel-Rahman and Osman (1997) had tested 10%, 20%, 30% and 40% ethanol of blended fuels in a variable-compression-ratio engine. They found that the increase in ethanol content increases the octane number, but decreases the heating value. The 10% addition of ethanol had the most observable effect in increasing the octane number. Under various compression ratios of engine, the optimum blend rate was found to be 10% ethanol with 90% gasoline.

Hsieh et al. (2002) determined the brake specific fuel consumption (bsfc) to demonstrate the variations of fuel consumption in the test engine using different ethanol gasoline blended fuels. The theoretical air-fuel ratio (A/F) of gasoline is 1.6 times of ethanol. Therefore the bsfc should be increasing with increase of ethanol content.

However, the fuel injection strategy tends to operate the engine at fuel rich condition. Thus, the ethanol addition produces leaning effect to enhance the combustion of fuel. Therefore, this factor makes no difference on the bsfc between using pure gasoline and using ethanol-gasoline blended fuels.

The influence of different ethanol-gasoline blended fuels on the torque output has also been investigated by performing engine test at 3,000 rpm with throttle valve opening of 40%, 60%, 80%,and 100%.It was observed that at lower throttle valve opening, the torque output is either increased or decreased by adding ethanol. However, at higher throttle valve openings (60%, 80%, 100%), the torque output increaseswith the ethanol content, which rangefrom 2% to 4%.

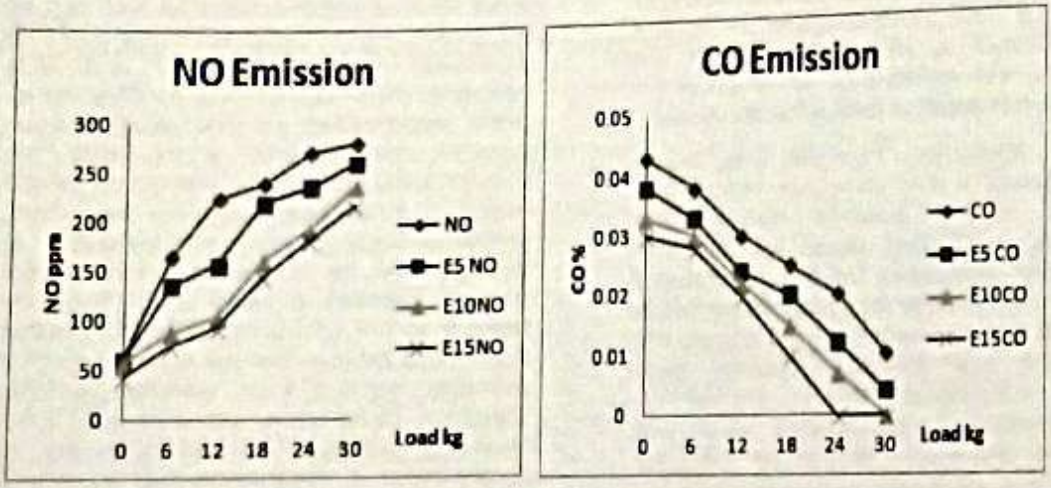

[FIG-2 NOx& CO emission by using different percentage of Ethanol blend]

As the percentage of ethanol increases, there was a reduction in CO and NOx emissions. The overall consumption of ethanol-gasoline blended fuel (E5, E10, E15, and E20) was lesser as compared with gasoline (RON 95).
CO and NOx are emitted from exhaust system due to the incomplete combustion in the combustion chamber. Therefore, lower CO and NOx emissions indicate that higher degree of combustion is achieved. By using ethanol-gasoline blended fuel, there is significant reduction in CO and THC emissions as compared with gasoline (RON 95).

It can be observed that the reduction of CO and NOx emissions become more significantas theethanol content increase. Ethanol which contains OH groups used as an oxygenate compound to raise the oxygen content of gasoline.
With additional oxygen molecule, the current air to fuel (A/F) ratio is increased and allowed the combustion occur at stoichiometric burning. In this case, the engine tends to operate in leaner conditions where combustion process of fuel is more complete. Therefore, the concentration of CO and THC emissions decreases as the fuel burning is more efficient(Wei-Dong et al.,

2001).Decrease of CO and THC concentration is also due to the lower carbon content of ethanol in comparison with gasoline.

Based on the research by Zervas et al. (2003), addition of ethanol dilutes the fuel. Hence, it enhances the combustion of CO and HC in the cylinder. Ethanol reduces the high boiling point hydrocarbon chain by increasing the number of methyl branches. This results in more completely fuel combustion in the cylinders without generated accumulation of un-burned hydrocarbon in combustion chamber emitting into the environment through the exhaust system.

American PetroleumInstitute (2010) stated that octane number of unleaded gasoline like RON 95will increase up to certain degree by adding in ethanol as an octane booster.Thus, ethanol blended with RON 95 will increase the octane number of the fuel to that of RON 97 or even higheras the content of ethanol increases. It is observed that the fuel consumption per kilometre is reduced up to 6.5% for E20.

VII.Advantages & Dis-Advantages of using Ethanol as a Fuel

Advantages:

- Unlike petroleum, ethanol is a renewable resource.
- Ethanol burns more cleanly in air than petroleum, producing less carbon (sool) and carbon monoxide
- The use of ethanol as opposed to petroleum could reduce carbon dioxide emissions, provided that a renewable energy resource was used to produce crops required to obtain ethanol and to distil fermented ethanol
- Exhaust gases of ethanol are much cleaner.
- The use of Ethanol blended fuel such as E85 Can reduce the net emissions of green house gases by as much as 38%, which is a significant amount

Dis-Advantages:

- Ethanol has a lower heat of combustion (per mole, per unit of volume, and per unit of mass) that petroleum
- Large amounts of arable land are required to produce the crops required to obtain ethanol, leading to problems such as soil erosion, deforestation, fertiliser run-off and salinity
- Major environmental problems would arise out of the disposal of waste fermentation liquors.
- Typical current engines would require modification to use high concentrations of ethanol.

VIII. Conclusion

Ethanol-gasoline blended fuel (E5, E10, E15, and E20) has reduced CO and THC emission up to 72.1 % and 58.1% respectively as compared to gasoline. There is also a reduction of fuel consumption up to 6.5%. Lesser emissions of green house effect gases into environment can be achieved by burning ethanol blended gasoline. It is viable alternative for reducing the rate of depletion of fossil fuel and a better fuel to reduce harmful gases emission into atmosphere. The results of this study can be used as the basis to determine the optimum blending proportion in future study.

IX. References

01.Lal, S. C. (2011). Engineer in Society. Non Renewable Energy, 1-2.

02.Niven, R. K. (2005). Ethanol in gasoline environmental impacts and sustainability review article. Renew Sustain Energy Rev, 35–55.

03. University of Strathclyde(2011). Energy Systems Re-search Unit.What is Ethanol?Scotland, DC: Author.

04. Huang Y. H & Wu J. H (2008). Analysis of biodiesel promotion in Taiwan. Review Sustainable Energy, 12, 76-86.

05. James Y. H & Glen E. H (1993). Petroleum Refining: Technology and Economics, New York.

06. Anderson J. E, DiCicco D. M, Glinder J. M, Kramer U, Leone T G, Raneyprblo H. E & Wallington T J(2012). High octane number ethanol-gasoline blends: quantifying the potential benefits in the United States Fuel.

07.Pang, S. B., Mu, Y., Yuan, J., & He, H. (2007). Carbon-yls emission from ethanol-blended gasoline and bio-ethanoldiesel used in engines.Journal of Atmospheric Environment, 42, 1349–1358.

08.Abdel-Rahman, A. A., & Osman, M. M. (1997). Experimental investigation on varying the compression ratio of SI engine working under different ethanol–gasoline fuel blends. International Journal of Energy Research, 21 (1), 31–40.

09.Hsieh, W., Chen, R., Wu, T., & Lin, T. (2002). Engine performance and pollutant emission of an SI engine using ethanol-gasoline blended fuels. Atmospheric Environment, 36 (3), 403–410.

10.Wei-Dong, H., Rong-Hong, C., Tsung-Lin, W., & Ta-Hui, L. (2001). Engine performance and pollutant emission of an SI engine using ethanol – gasoline blended fuels. Atmospheric Environment, 36 (3), 403–410.
11.Zervas, E., Montagne, X., & Lahaye, J. (2003). Emission of regulated pollutants from a spark ignition engine. Influence of fuel and air/fuel equivalence ratio. Environ SciTechnol, 37 (14), 3232–3238.
12.American Petroleum Institute. (2010). Determination of the Potential Property Ranges of Mid-Level EthanolBlends.
13.M .Al-Hasan, "Effect of ethanol–unleaded gasoline blends on engine performance and exhaust emission", Energy Conversion and Management 44, 1547–1561, 2003.
14.M .Abu-Zaid, O .Badran, and J .Yamin, "Effect of methanol addition to gasoline on the performance of spark ignition engines", Energy & Fuels 18, pp(312-315), 2004
15.M.V .Mallikarjun1 and Venkata Ramesh Mamilla, "Experimental Study of Exhaust Emissions & Performance Analysis of Multi Cylinder SI Engine When Methanol Used as an Additive", Volume 1 Number 3, pp .201–212, 2009
16.D.BALAJI, "Influence of isobutanol blend in spark ignition engine performance operated with gasoline and ethanol", International Journal of Engineering Science and Technology, Vol. 2(7), 2010, pp. 2859-2868.
17.Christoph Baer, Bongsoo Kim, Peter E. Jenkins, and Yong-Seok Cho, "Performance Analysis Of SI Engine With Ethyl Tertiary Butyl Ether (etbe) As A Blending Component", Energy Conversion Engineering Conference, 1990. IECEC-90. Proceedings of the 25th Intersociety
18.Alvydas Pikunas, Saugirdas Pukalskas & Juozas Grabys" influence of composition of gasoline - ethanol blends on parameters of internal combustion engines"Journal of KONES Internal Combustion Engines vol .10, 3-4 (2003).
19. Hakan Bayraktar, "Experimental and theoretical investigation of using gasoline–ethanol blends in spark-ignition engines", Renewable Energy 30 (2005) 1733–1747.
20. Hu seyin Serdar Yu cesu , Tolga Topgu l, Can C, inar,MalihOkur, "Effect of ethanol.

A Review on Performance and Emission of Waste Plastic fuel on Compression Ignition Engines

[1]Amar Kumar Das, [2]Nabnit Panigrahi
[1,2]Assistant Professor, Department of Mechanical Engineering, Gandhi Institute For Technology, Bhubaneswar.

Abstract: *Depleting fossil fuel reserves and increasing cost of petroleum products are the unsolved trouble of modern world. The treatment, management and disposal of solid waste are critically concerned in every developing country like India due to uncontrolled and increased disposal rates causing severe threat to the environment. Pyrolysis has been effectively proved as an influential alternative among other methods of waste disposal that follows waste to energy recovery. This review subscribes the effective methodology of pyrolytic conversion of plastic wastes into energy sources in regards to its technologies and products. In this review, first the different types of waste plastics are introduced followed by their sources and different waste management practices being practiced. Second part of the paper briefly summaries the Pyrolysis technology for treatment of waste plastics and the influence of important operating parameters such as temperature, heating rate and residence time in the reaction zone on the pyrolysis behaviours and products, reactor type, operating pressure and presence of catalyst. Finally, the composition, properties and uses of the pyrolytic liquid products are summarised to emphasize the suitability and sustainability of pyrolysis process for recycling of waste plastics.*

Index terms: Solid waste, pyrolysis, energy recovery,waste plastics, operating parameters, pyrolytic Liquid

I. Introduction

Throughout the world, research on waste plastics management is being carried out on war-footing. According to a nationwide survey, conducted in the year 2003, more than 15342.46Tof plastic waste is generated daily in our country, and only 40% by wt of the same is recycled, balance 60% by wt is not possible to dispose off (Guntur and Kumar). Plastic waste contributes to the solid waste streams by about 8% – 15% by weight and twice that by Volume (GOI, 1997).From this statically forecasting, it is anticipated that, the plastic waste will reach 11 million ton by the year 2020. At these crucial levels of waste plastics generation, India has to take a well planed front towards preparing a solid waste recycling and disposal. However each process has its drawbacks and economical, operational& financial limitations for practical implementation.

Plastic waste management is biggest problem now due to their non-biodegradability nature. Now plastics manage by plastics recycling technologies.

Table 1: Uses of different types of plastics [Arun Joshi, Rambir and Rakesh Punia]

Type of Plastics	Uses
Polyester	Textile fibre
PET	Carbonated drink bottles, plastics film
PE	Supermarket bags, plastics bottle
HDPE	Milk jugs, detergent bottles, thicker Plastics film, pipe
LDPE	Floor tiles, shower curtains
PVC	Agriculture (fountain) pipe, guttering Pipe, Window frame, sheets for building material
PS	Foam use for insulation of roofs and walls, Disposal cups, plates, food Container, CD and cassette box
PP	Bottle caps, drinking straws, Bumper, house ware, Fiber carpeting and rope

CI engines are the most preferred power plants than other internal combustion engines due to their excellent drivability and higher thermal efficiency. Use of fossil fuel emits high amount of oxides of nitrogen (NOx), carbon dioxide (CO2), Carbon monoxides (CO), Hydrocarbon (HC) and smoke, which will have a catastrophic effect on human health. Hence, stringent emission norms and depletion of petroleum fuels have necessitated the search for alternate fuels for diesel engine (Mani and Nagrajan). Alternative fuels should be easily available at low cost, be environment friendly and fulfil Energy security needs without sacrificing engine's operational performance. Waste to energy is the recent trend in the selection of alternate fuels. Fuels like alcohol, biodiesel, liquid fuel from plastics etc. are some of the alternative fuels for the internal combustion engines. Application of Waste Plastic Disposals reduces the experimental heavy fuel oil viscosity. The results showed that waste plastic disposal oil when mixed with heavy oil

reduces the viscosity significantly and improves the engine performance (Williams and

Elizabeth). Although Oxides of Nitrogen (NOx) emission slightly increases, the emission of particulate matters (PM), dry soot (DS) and soluble organic fraction (SOF) decreases by half at the mixing ratio of 30% by vol. Such kind of plastic materials are HDPE, LDPE, PE, PP, Nylon, Teflon, PS, ABS, and FRP.

II.Pyrolysis of Waste plastic and its property

Pyrolysis is generally considered as a thermal degradation process in the absence of oxygen. In plastic pyrolysis, the macromolecular structures of polymers are broken down into smaller molecules or oligomers and sometimes non numeric units. It breaks large hydrocarbon chain into smaller ones, but this type of pyrolysis requires higher temperature and high reaction time, presence of catalyst and other process conditions.

A. Mechanism and kinetics of pyrolysis

The degradation of polymer may be considerably different based on the way in which reaction is carried out: heat (thermal degradation),heat and catalyst (thermo catalytic degradation), oxygen (oxidative degradation), heat and oxygen (thermo-oxidative degradation),radiation (photochemical degradation), radiation and oxygen (photo-oxidative degradation), chemicals (chemical gradation),etc.

The pyrolysis process is basically enumerated as non-catalytic and catalytic in nature. The non-catalytic pyrolysis of waste plastic requires high energy, endothermic process in absence of oxygen at a temperature range of 350-500°C. In this method a suitable catalyst is used to carry out the cracking reaction. The presence of catalyst lowers the reaction temperature and time. In addition, catalytic degradation yields a much narrower product distribution of carbon atom number with a peak at lighter hydrocarbons and occurs at considerably lower temperatures. From an economic perspective, reducing the cost even further will make this process an even more attractive option.

B.Property study of pyrolytic plastic oil

Pyrolysis is a chemical degradation process in the absence of oxygen. Plastic waste are shredded and treated in a cylindrical reactor at different range of temperature varying from 300-500°C. The pyrolysis is carried out with or without the presence of catalyst. Catalyst helps in degrading the waste plastic in very simpler form and generating gas which is condensed passing through the condenser.

Table-2: Properties of Waste Plastic Pyrolysis Oil and Diesel [Power and Lawankar]

Sl. No	Properties	WPPO	Diesel
1	Density (kg/m^2)	793	850
2	Ash content (%)	<1.01%	0.045
3	Calorific Value (KJ/kg)	41,800	42,000
4	Kinematic viscosity	< 2.149	3.05
5	Cetane number	51	55
6	Flash point °C	40	50
7	Fire point °C	45	56
8	Carbon residue (%)	0.01%	0.20%
9	Sulphur content (%)	< 0.002	<0.035
10	Pour point °C	-4	3-15

The flue gas is treated through scrubber and chemicals for neutralization. Since plastic waste is processed about 300-350 °C and there is no oxygen in the processing reactor, most of the toxic are burnt [power and Lawankar].

III. Performance testing

The various performance parameters are taken into consideration to access the engine smooth operation and fuel optimisation such as brake thermal efficiency, brake specific fuel consumption and exhaust gas temperature.

A. Brake thermal Efficiency:

Brake Thermal Efficiency is defined as break power of a heat engine which is a function of the thermal input from the fuel. It is used to evaluate how well an engine converts the heat from a fuel to mechanical energy.

Different researchers have investigated on the brake thermal efficiency of internal combustion engines and suggested many methods and modifications in the process to enhance it using plastic pyrolytic oil as fuel.

As discussed by Mani and Nagrajan [1], certain combustion parameters like delay period, ignition temperature and combustion chamber pressure which can augment the efficiency of compression ignition engine. They used a batch reactor following catalytic pyrolysis method and maintained a range of temperature of 300-400C under atmospheric pressurefor 3-4 hrs.It yield 75% liquid hydrocarbon, which was a mixture of petrol, diesel and kerosene of 5%-10% residual coke. It was found that Brake thermal efficiency of plastic oil came closer to a value of diesel of27.4% at a rated 75% rated power beyond which it started decreasing which may be due to high exhaust gas temperature.

Guntur.et.al [2], had taken an initiative to blend the waste plastic fuel with diesel in different ratio and found in variation in the performance used in same engine at different loads. It was found that the engine preformed better result at 50% of blending. Mechanical efficiency of engine increases with an increase in load under all operating conditions. Mechanical efficiency of diesel is 67.5% and with WPPO10- 69.3%, WPPO30 - 70.34%, 71.49% with WPPO 50.

Kirubakaran.et.al [3], investigated on the performance and emission characteristics of a HCCI Engine running waste plastic oil. The engine modifications had been brought towards a good result in its mechanical efficiency. It was found that longer ignition delay of 0.5 CA of waste plastic than HCCI resulting rise in peak pressure by 5 bars inside cylinder which may be due to evaporation of waste plastic oil inside the cylinder by absorbing heat from combustion chamber. Cylinder pressure of HCCI is lower by 4 bars than waste plastic oil and injection timing controlled 23 degree before TDC.

Rate of Heat release is maximum in waste plastic oil by 45 J/CA than HCCI which is due to longer delay period and high F/A ratio in waste plastic oil resulting increase in exhaust gas temperature.

Mani and Nagrajan [4], investigated the plastic fuel in diesel engine using Exhaust gas recirculation (EGR) techniques and demanded the better result found in its efficiency. The engine had been charged with 100% pyrolysed plastic oil with cooled EGR at different proportion. The effiency found increasing in EGR flow rate, it increases by 0.8% at 10% load and 1.1% at full load than waste plastic oil. This is due to larger replacement of air in combustion chamber by exhaust gas through EGR system and higher flow rate of EGR reduces average temperature in combustion chamber resulting reduction in brake thermal efficiency.

According to panda.et.al [5], efficiency had been found maximum of a value of 19.96 with 10% blending with WPO using kaolin at catalyst at full load. The efficiency became closer or slightly greater compared to diesel up to 80% load which might be due to higher calorific value of WPO-Diesel blend than diesel.

As per wongkhorsub and Chindaprasert [6], they had worked on efficiency of plastic oil and tyre oil in comparison to diesel had been tested on same Diesel engine at 1500 rpm.The maximum load production from plastic pyrolysis oil is lowest of 3064 W, tyre pyrolysis oil of 3282 W and diesel of 3500 W.

Pratoomyod and Laohalidanond [7], discussed about the performance of diesel engine using plastic oil at different ratio of blending with diesel. They had used a six cylinder 4 stroke diesel engine for that purpose. Brake Torque of the engine found decreasing when running from 1800rpm to 2000 which might be due to augmentation in mechanical losses and lower heating value. It reached to the peak value of 284.85 N at 1800 rpm, 25% blending and full load.

B. Brake specific fuel consumption:

According to Guntur and Kumar, BSFC decreases for all fuel blends up to part load of 80% and higher consumption was found at full load. Waste plastic fuel with ratio of WPPO10, WPPO30, and WPPO 50 at 1500rpm with loading of 0, 20,40,60,80 and 100% of rated power was observed. BSFC decreases for all fuel blends up to part load of 80% and higher consumption would occur at full load. Rate of Heat release is found maximum in waste plastic oil by 45 J/CA than HCCI which is due to longer delay period and high F/A ratio in waste plastic oil resulting increase in exhaust gas temperature.

According to Panda.et.al, it was found maximum in case of diesel without blending of a value of 0.385 kg/kwhr at full load and went on decreasing with increase in blending concentration of WPO with diesel. As the blended fuel was having high calorific value, the engine normally consumed less fuel.

C.wongkhorsub and Chindaprasertthad found that plastic pyrolysis oil offered lowest BSFC of 294 g/kwhr with maximum break power at 3064 W. The maximum load production from plastic pyrolysis oil was found a lowest value of 3064 W, tyre pyrolysis oil of 3282 W and diesel of 3500 W.

Pratoomyod and Laohalidanond had also agreed with other researchers taking different blending ratio of oil and getting better result. Experiment revealed that the blended fuels showed decreasing order of BSFC with increase speed of engine from 800 to 1500 rpm and after 1500 rpm, it went on increasing for all blends due to excess mechanical losses and incomplete combustion.

IV.Emissions

Mani.et.al, discussed about the combustion characteristics of DI diesel engine using waste plastic oil in a batch catalytic pyrolysis process. It was found that NOx emission increased in waste plastic oil operation due to high combustion temperature, oxygen concentration, and high heat release rate and residence time for reaction as compared to diesel. They investigated that Increase in Ignition delay of waste plastic oil that

promoted premixed combustion by allowing more time for fuel to be injected prior to ignition could be another reason for increase of NOx emission.

Guntur and Ravi kumar, approached differently to study the emission by feeding the engine with different blending ratio of plastic oil with diesel. The exhaust gas temperature was found higher which might be due to high heat release rate. Concentration of HC emission for WPPO-Diesel blend was marginally higher than diesel which might be due to some local spot of non-homogeneity in concentration of air fuel mixture found in the combustion chamber due to shortage of oxygen. Reason for higher CO emission may be due to incomplete combustion and higher rate of fuel consumption at higher load.

G.Kirubakaran.et.al, investigated on another dimension of emission. They claimed that NOx formation in waste plastic oil could be controlled by using HCCI at full load which might be due to higher cylinder inside temperature, lower oxygen concentration and longer residence time,higher heat release rate and higher combustion temperature. They also discussed about availability of premixed and homogenous charge inside engine and rapid flame propagation resulting lower smoke level in plastic oil. However at high load, white smoke was found emittedwhich may be due to non availability of sufficient oxygen and abnormal combustions.

Exhaust gas temperature found decreasing with increase in exhaust gas recirculation quantity which may be due to reduction in peak combustion temperature.Mani.et.al, introduced the technique of EGR that provided an extra quantity of exhaust gas to flow inside the combustion chamber. Due to less exhaust temperature and sufficient residence time to occur the reactions, NOx emissions were quite regulated. HC emissions also regulated by optimizing injection timing at different EGR quantity and availability of excess oxygen.

As per panda.et.al, the emission of nitrogen oxides could be controlled by enriching the fuel air mixture. The reason may be due tothe Composition of plastic fuel containing long carbon chain compound resulting longer ignition delay which would produce more NOx formations. The higher HC emissions in blend compared to diesel may be due to improper spray offuel inside the combustion chamber. The gaseous HC remained unburnt along the cylinder wall. The other reason for it is due to presence of unsaturated HC in WPO, which was remained unbreakable during combustion process.

V. Conclusion

Many pioneer researchers step forward to work on area of plastic oil as an alternative fuel in DI diesel engine. Based on the review, it frames into picture that there is no significant power reduction in the engine performance on plastic pyrolysis oil blended with diesel up to 25% mixing.

1. Mechanical efficiency of pyrolytic plastic fuel with diesel found better result up to 50% blending.

2. Brake thermal efficiency of plastic fuel is found very close to diesel up to 75% of rated power.

3. EGR up to 10% results better performance in its brake thermal efficiency.

4. The volumetric efficiency of plastic blended fuels is found decreasing as compared to diesel.

5. Emissions can be reduced using HCCI by 0.8% at full load.

Hence plastic fuel of required proportion blending can be used as a better alternative fuel for transportation.

VI. References

[1] Performance, emission and combustion Characteristics of DI diesel engine using waste plastic oil,M.Mani, C.Subas, G.Nagarajan.

[2] Rajesh Guntur, P Ravikumar,Experimental investigation on the performance and emission characteristics of a Diesel Engine Fuelled with Plastic Pyrolysis oil-Diesel Blends.

[3]Nagakrshna.et.al, Performance, emission and characteristics of a HCCI Engine running waste plastic oil.

[4] M Mani,GNagarajan,S.Sampath,An experimental investigation on a DI diesel engine using waste plastic oil with exhaust gas recirculation.

[5]AcyutK.panda, S.Murgan, R K Singh,Performance and emission characteristics of diesel fuel produced from waste plastic oil obtained by catalytic pyrolysis of waste poly propylene.

[6]C.wongkhorsub, Chindaprasert,A Comparision of the use of pyrolysis oils in diesel engine.

[7]Pratoomyod,Laohalidanond,Performance and Emission Evaluation of Blends of Diesel fuel with Waste plastic oil in a Diesel Engine.

[8]Heywood J.B.Internal combustion engine fundamentals, McGraw hill publication.

[9] S.H. Hamid, M.B. Amin, A.G. Maadhah, Handbook of Polymer Degradation, Marcel Decker, New York, 1992.

[10] P.T. Williams, E.A. Williams, Interaction of plastics in mixed plastics pyrolysis,Energy and Fuels 13 (1990) 188–196.

[11] PhongHai Vu, Osami Nishida, Hirotsugu Fujita, WataruHarano, NorihikoToyoshima, Masami Iteya, Reduction of NOx and PM from diesel engines by WPD emulsified fuel, SAE Technical Paper 2001-01-0152.

[12] R. Murillo, E. Aylon, M.V. Navarro, M.S. Callen, A. Aranda, A.M. Mastral, Theapplication of thermal processes to valorise waste tyre, Fuel Processing Technology 87 (2006) 143–147.

A inverse kinematic solution of a 6-DOf industrial robot using ANN

[1] Kshitish k.Dash[1], [1] Department of Mechanical Engineering(GIFT)
Bibhuti B.Choudury[2] [2] Department of Mechanical Engineering, Indira Gandhi Institute of Technology, Sarang, India
Sukanta K.Senapati[3] [3] Department of Mechanical Engineering, Indira Gandhi Institute of Technology, Sarang, India

Abstract: An inverse kinematics problem of a robotic manipulator solved using Artificial Neural network is presented. This paper represents the Inverse kinematics problem which is really intricate in nature for robotic manipulators. Many conventional methods are insufficient to find the solution, though the joint arrangement of the manipulator is more complicated , so the neural computation are used to find the joint angles to set a particular Cartesian space and direction of the end effectors. A number of end effecter position and corresponding joint angle are calculated analytically in the work volume for a robotic manipulator. The entire real-world coordinates (x, y, z) as per the angles recorded in a file named as training set of ANN model. The designed neural model has specified the correct coordinates according to the certain angles of Cartesian coordinate. By using the ANN it is very effective to know the errors in joint angles.

Keywords: Inverse kinematics, Artificial Neural Network, 6-D.O.F Industrial Robot

1 INTRODUCTION

The ANN approaches are applied in the inverse kinematics technique leads many and particular problem. It is apposite for real time adaptive manageable of robot arm manipulators with a tolerable error. The Neural networks are competent with learning and building of complex functions, which are used in different applications like pattern recognition, approximation and fitting of data dynamic errors for checking. The Nonlinear dynamic systems are included with the robots for executing tasks repetitively. The literature confirmed the results which are found that, the neural network is valuable for various problems of inverse kinematics problem. The Artificial neural network solution of an inverse kinematics case is analyzed with addition to the background of theoretical neural representation. The neural networks are the data processing frame of interest in neuron computing. Simultaneously different sequence dispensation frame collected of a number of plain dispensation elements and to be interconnected with similar neurons like the nerve system of a human body. The fundamentals are processed and are act together locally with a bunch of inline weight connectors. The ANN arrangement trains itself in broad by the mapping and the practical association with set of participation data and consequent productivity data. The ANN model supplies up the association strength or weights linking the dispensation unit. During the learning process the weights correspond to the potency among neuron are in tune. The neural model is in contrast with establishing technique where the exact relationship between in and out to be abounding by user distinct algorithm. In this neural network behavior self-organization for tolerance of fault, association, optimization, and generalization etc. are allowed in the neural network.

2. Related work

Hariharan et al. [1] developed an instantaneous inverse kinematics of odd no DOF hyper-redundant manipulator arm with a mutual arithmetical as well as methodical approach. The work presents a novel, computationally competent method of performing inverse kinematics for universal odd no of DOF manipulators with a spherical joint at the wrist. Kinematic and dynamic uncertainties found the solution. Wei et al. [2] proposed a common move towards for inverse kinematics of nR robots. This paper uses of a semi-analytic method and a general method to solve the spatial nR robot inverse kinematics problem. It overcomes the numerical method's limits associated to accurateness. The conformal geometric space theory is used to set up general kinematic equations. Based on that, the biased breathing space vector melancholy method is used to find the relation between the angles of robot spatial rotation and the data of the space

vector. Kucuk et al. [3] developed an inverse kinematics problem for industrial robot arm with balance wrist. A new numerical algorithm is proposed for the opposite kinematics of the robot arm that cannot be solved in closed form. In direct to illustrate the presentation of the New Inverse Kinematics .A simulation results attained from NIKA are compared with those obtained from well-known Newton–Raphson Algorithm (NRA). Ras it Koker [4] presented a genetic algorithm come close to ANN base inverse kinematics of robotic arm base on inaccuracy reduction. ANN and genetic algorithms are used to solve the problem of inverse kinematics a six-joint Stanford robotic arm to minimize the error at the end effectors'. The end-effectors' location error is to defined the suitability function, and the hereditary algorithm is implemented. Fahmy et al. [5] develop Neuro-fuzzy inverse model control structure of robotic arm utilize for rehabilitation applications. They presented a new neuro-fuzzy regulator for robot arm. The inductive knowledge method is applied to make the necessary inverse model rules from in/out data set record in the off-line arrangement learn stage. The manage structure show high-quality result compare to the predictable techniques. Aggarwala et al. [6] discussed the ANN for the improvement of an inverse kinematic problem with optical detection of spectacle zone. This method shows a non-conventional method to solve the inverse kinematics problem using ANN. The technique gives an idea to promising, since it requires little computation time over other traditional methods. Fang et al. [7] proposed paper neural networks based adaptive decoupling control for three-axis gyro stabilized platform. The nonlinearity and coupling system is full-state-linear zed using feedback linearization, and neural networks are used to compensate for the disturbances and uncertainties. The stability of the proposed scheme is analyzed by the Lyapunov criterion. Comparative simulations and experiments results show the effectiveness of the proposed control approach compared with the conventional control.

transformation between two joints, which may called as the Denavit-Hartenberg parameters. It becomes a standard method to describing robot kinematics. Forward kinematic solution is more easer then to the inverse kinematics problem.

$$x = f(v) \quad (1)$$

f is known as non-linear function having frame of structure and different parameters are known. They are associates with each v a sole to x and usually an inverse mapping can have many v's related with each x. Closed form solutions and mathematical solutions are used to solve inverse and forward kinematic problem. Closed forms solved by taking the spatial geometry of manipulator and followed by the matrix of algebraic equation (1). The Mathematical technique are iterative algorithms is known as Levenberg-Marquardt (LM) and iterative in nature a mathematical solution which is generally slower than the corresponding closed form solution. This is very vital to note that the joint angle vector or the specification of the Cartesian vector can obtain with the equations (1) and (2), but to find the Cartesian velocity and acceleration we use equation (1), if f(q) at least once differentiable, then

$$v = f^{-}(x) \quad (2)$$

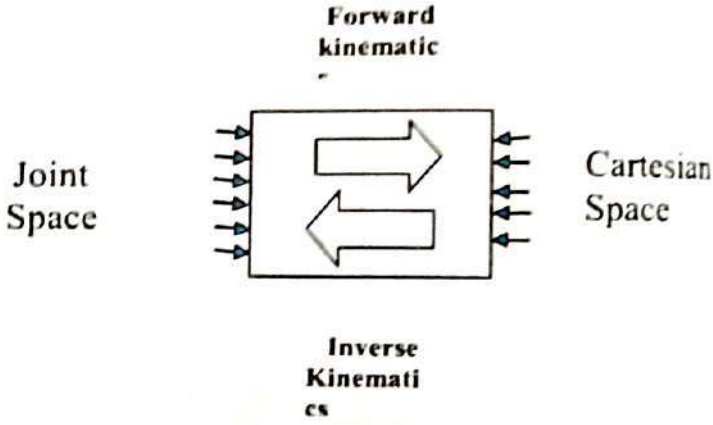

Fig.1 : Kinematics architecture

3. Inverse Kinematics for Six Axes Robots

It is very important for industrial robot manipulators to know the kinematic behaviour. To describe the kinematic model of robot arm cartesian space and joint space are generally required in the workspace. This two can be may be decomposed in form of rotation motion and a translation motion. Different path are there to represent rotation, with the following: Euler angles, Gibbs vectored. Denavit-Hartenberg algorithms require four parameters for general

$$ {}^{0}_{6}T = \begin{bmatrix} q11 & q12 & q13 & px \\ q21 & q22 & q23 & py \\ q31 & q32 & q33 & pz \\ 0 & 0 & 0 & 1 \end{bmatrix} = {}^{0}_{1}T(v1)\,{}^{1}_{2}T(v2)\,{}^{2}_{3}T(v3)\,{}^{}_{}T($$

For joint one (v1) the inverse kinematic solution have a elements of T base end-effectors, the transformation of link as follows.

$$\left[{}^{0}_{1}T(v1)\right]^{-1}{}^{0}_{6}T = \left[{}^{0}_{1}T(v1)\right]^{-1}{}^{0}_{1}T(v1){}^{1}_{2}T(v2){}^{2}_{3}T(v3){}^{3}_{4}T(v4){}^{4}_{5}T(v5){}^{5}_{6}T(v6)$$

$$\left[{}^{0}_{1}T(v1)\right]^{-1}{}^{0}_{6}T = {}^{1}_{2}T(v2){}^{2}_{3}T(v3){}^{3}_{4}T(v4){}^{4}_{5}T(v5){}^{5}_{6}T(v6)$$

$$\left[{}^{0}_{1}T(v1){}^{1}_{2}T(v2)\right]^{-1}{}^{0}_{6}T = {}^{2}_{3}T(v3){}^{3}_{4}T(v4){}^{4}_{5}T(v5){}^{5}_{6}T(v6)$$

$$\left[{}^{0}_{1}T(v1){}^{1}_{2}T(v2){}^{2}_{3}T(v3)\right]^{-1}{}^{0}_{6}T = {}^{3}_{4}T(v4){}^{4}_{5}T(v5){}^{5}_{6}T(v6)$$

$$\left[{}^{0}_{1}T(v1){}^{1}_{2}T(v2){}^{2}_{3}T(v3){}^{3}_{4}T(qv4)\right]^{-1}{}^{0}_{6}T = {}^{4}_{5}T(v5){}^{5}_{6}T(v6)$$

$$\left[{}^{0}_{1}T(v1){}^{1}_{2}T(v2){}^{2}_{3}T(v3){}^{3}_{4}T(v4){}^{4}_{5}T(v5)\right]^{-1}{}^{0}_{6}T = {}^{5}_{6}T(v6)$$

3.1 Neural networks structures

Artificial neural networks are a type of model that can perform capably multifarious non linear system in nature. The artificial neural networks have different benefits in comparison to predict computational systems in robotics. When a artificial neural networks map the three-dimensional robot between joint angle and Cartesian space by using only a back propagation algorithm. The 6R robot is chosen as one kind industrial robot manipulator due to dimensional configuration and the robot is not permit to solve inverse kinematics problems rationally.

The ANN derived from the nerve system of a human brain. Now a day's ANN starts as an important method for sorting and optimization of different kinematic problem. It is emerge as a leading learn method to perform different multifarious odd jobs in highly nonlinear vigorous environmental problem. The ANN is appropriate for designing nonlinear mapping among the in and out data set because of its large parallel interconnection between multiple patterns and the nonlinear meting out features. The Fig. 2 shows an artificial neuron network pattern, which generally include a computing element. The total is added to bias or threshold then the resultant signal is n passed through a nonlinear function known as log sigmoid function.

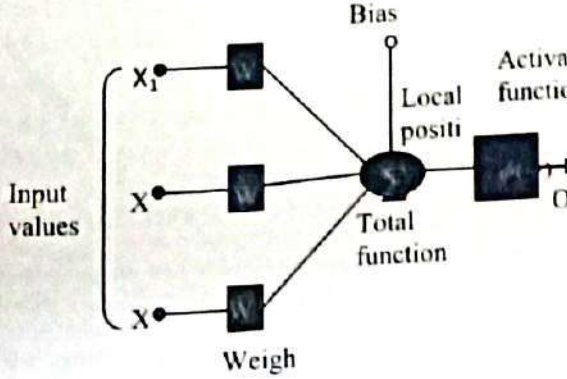

3.2 ANN applied on inverse kinematics problem.

ANN has created two problems while solving inverse kinematics of a robot arm manipulator i.e is collection of the appropriate type of artificial neural network and another one generation of perfect trained dataset. A kinematic model can develop after knowing the kinematic factors of a robot manipulator. For preparing data set experimental results gained for the manipulator are consider but it is more difficult to train it. If joint parameters are known for an industrial robot then accomplishment of this loom is measured as per the training error rate.

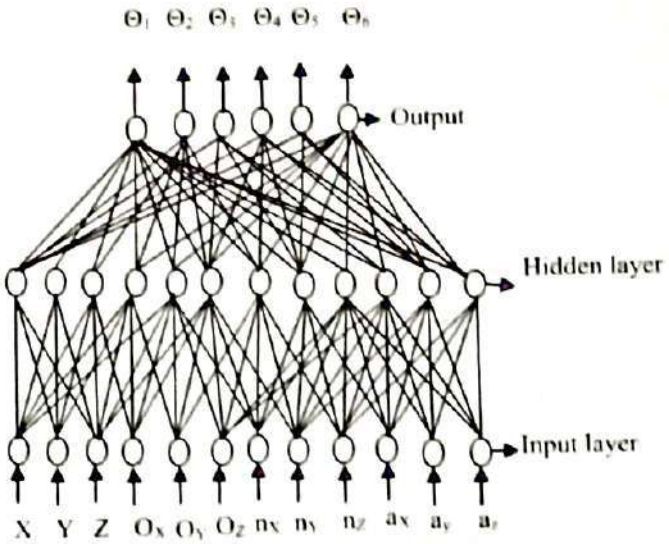

Fig 3. Three Layer Perception with six outputs

$$AHi(y) = \sum_{j=1}^{i} WTjlj + \sum_{j=1}^{n} WH_{ij} f(AHj(y-1));$$

$$i = 1,2,3.....n$$

The starting function is used here in the unknown layer and the output of the network is a weighted sum of the unknown unit o/p.

$$O_i(y) = \sum_{j=1}^{n} WO_{ij} f(AH_j(y)); i = 1,2.....n \quad (6)$$

$$E(y) = \sum_{p=1}^{PP}\left(\frac{1}{2}\sum_{j=1}^{n} e_{jp}(y)^2\right) \quad (7)$$

$$E(y)=\sum_{p=1}^{m}\left(\frac{1}{2}\sum_{k=1}^{n}\left(T_{pk}(y)-O_{pk}(y)^{2}\right)\right)$$

(8)

3 Simulation Results

The simulations are done here by using ANN with MATLAB tool box to match the input date target value i.e joint angle for industrial robot. In this analysis a 138 data sets are created and the input parameter in Cartesian position. The training and estimation the models are done here using these data sets. From the data sets having 138 data points, 99 are used as training data network, and for modernizing the desired weights. In the problem, the capacity models of the joint angles are required here as shown in Table 1. The distance between adjacent links with their ranges is mentioned in Table 2. Table 3 shows the normal positioning vector in all direction.

The above date set i.e. Joint angle and link parameter are calculated from the Ariosto Industrial robot which is available in our lab. For different position of the joint angle the end-effectors position are calculated .similar procedure we follow for other joint angle i.e. $\theta_1 to \theta_6$. While we change the joint angle we careful about the maximum and minimum range of it,

4 Simulation curve

The effectiveness of neural network is analysed and 38 nodes are nominated in the unknown layer and only 20 nodes are presented in Table 3. For the θ_1 to θ_6 are symbolized in 103 epochs for mean square error model which shows in Fig.3. In this figure the best validation performance is analysed properly

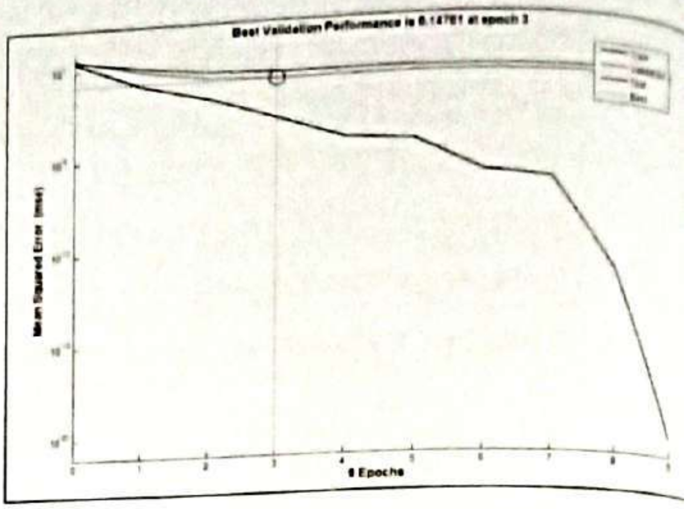

It conclude that the performance of the net work is 2.87 by choosing data division and the random test performance is 350.8441e-003,train performance is 1.2368e-003 and 147.614e-003.

Extreme value	Range	Joint
320	(-160 to 160)	Waist Joint
220	(-110 to 110)	Shoulder Joint
270	(-135 to 135)	Elbow Joint
532	(-266 to 266)	Wrist Roll
200	(-100 to 100)	Wrist Bend
532	(-266 to 266)	Wrist Swivel

d_1	d_2	d_3	d_4	d_5	d_6
184	158	300	150	378-5	640

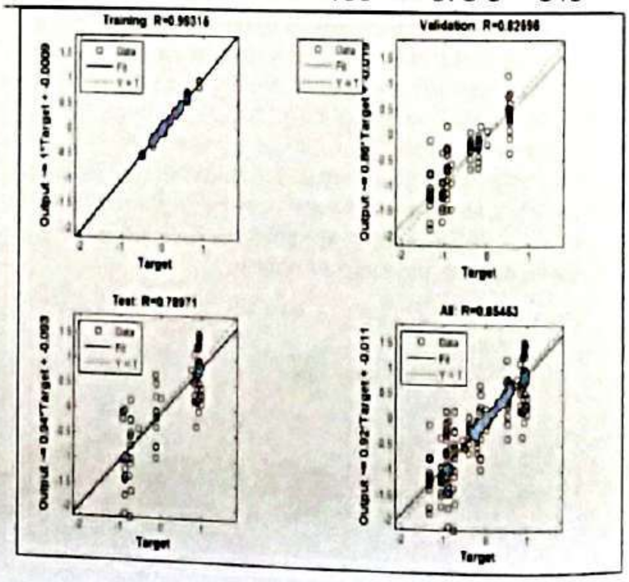

In Figure-4, P_x, P_y, Pz shows the training convergence graphs. From this figure it is

clearly visible that convergence is achieved using very few epochs. In our case multilayer neural network structure is used. Log sigmoid function is used in the unknown layer and output layer uses a linear activation function. Twenty nos. of hidden neurons have been used for simulation

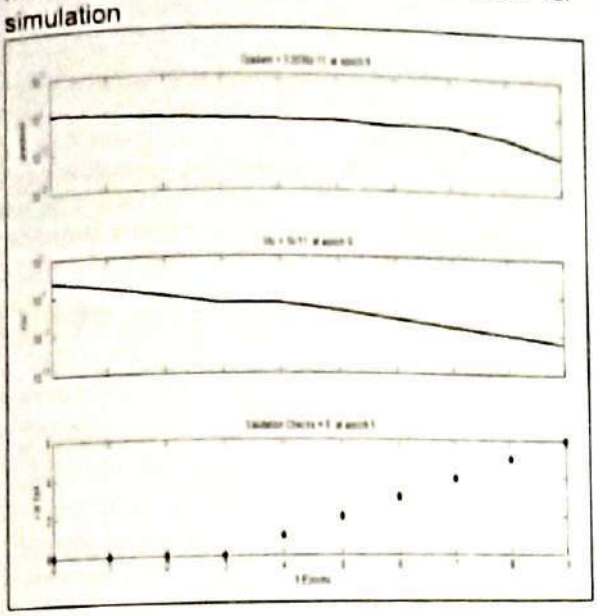

The number of epochs used in every graph and learning of the proposed network is done using Levenberg Marqdt (LM) algorithm which is very fast. Here the graph shows both input data and output data are matching each other and also vary with mean line.

5 Result and Discussions

From the result it conclude that ANN will not give good result with less no of data set but it need more number sample data set for training to attain an satisfactory accuracy. With training 60 % of the input and output data set , the matching point will very much closer to each other. For best testing 20% of data set which are not incorporated in the training set are used and got very marginal error and for validation another 20% are data set are used. For validation of the artificial neural network calculation, the errors of joint angles for 38 test points are found near mean point. Though inaccuracy result are very near by the mean line so effective error and root mean square error is calculated for each angle i.e $\theta_1, \theta_2, \theta_3, \theta_4, \theta_5$ *and* θ_6 respectively. Here we found that the errors in θ_4 and θ_5 are found to be higher as comparison to other joint angles.

References

1. Hariharan, Anantha Narayanana, Raul Ordonezas. Real-time Inverse Kinematics of (2n+1) DOF hyper-redundant manipulator arm via a combined numerical and analytical approach. Mechanism and Machine Theory 91 , (2015).
2 Yanhui Wei, Shengqi Jian, Shuang He, Zhepeng Wang.General approach for inverse kinematics of nR robots) Mechanism and Machine Theory 75 , 97–106, (2014).
3. Serdar Kucuk , Zafer Bingul, Inverse kinematics solutions for industrial robot manipulators with offset wrist. Applied Mathematical Modelling 38 (2014) 1983–1999
4. Ras it Koker, Develop a genetic algorithm approach to a neural-network-based inverse kinematics solution of robotic manipulators based on error minimization Information Sciences 222 (2013) 528–543
5. A.A. Fahmy a, A.M. Abdel Ghany , Neuro-fuzzy inverse model control structure of robotic manipulators utilized for physiotherapy applicationsAin Shams Engineering Journal (2013) 4, 805–829
6. Luv Aggarwala, Kush Aggarwal, Ruth Jill Urbani,Use of artificial neural networks for the development of an inverse kinematic solution and visual identification of singularity zone
7. Jiancheng Fang, Rui Yin , Xusheng Lei, An adaptive decoupling control for three-axis gyro stabilized platform based on neural networkMechatronics 27 (2015) 38–46.
8. Dash,K.K.,Choudhury,B.B., Khuntia,A.K.,Biswal, B.B., A Neural Network Based Inverse Kinematic Problem" IEEE, (2011), 471-476.

Experimental investigation and prediction of tensile stress for SS 304 – CP copper dissimilar metal couple joint by pulsed wave TIG welding process

[1]Bikash Ranjan Moharana, [2]Alina Dash, [3]Jukti Prasad Padhy
[1] [2] [3]Gandhi Institute For Technology, Bhubaneswar

Abstract— The current study investigates the mechanical characteristics of SS 304 – CP copper dissimilar metal joint by pulsed wave TIG welding process followed by prediction of response using FUZZY rule-based model. A statistical design of experiment based on Taguchi orthogonal array has been used for design and optimization of process parameters. The developed design model is checked for their adequacy and significance by ANOVA analysis and respective confirmation test are also carried out to check the accuracy of predicted values. The tensile stresses of all welding specimens are determined by universal testing machine (UTM). The FUZZY rule-based prediction method is used to predict the output response and also compared with the experimental results to validate the model. The metallurgical investigation of the fusion zone has been carried out using Scanning Electron Microscopy (SEM) analysis.

Index Terms— ANOVA, dissimilar metal welding, fuzzy, Taguchi orthogonal array.

I. INTRODUCTION

The importance of dissimilar metal couples in the process industries goes on increasing exponentially in opposition to that of similar metals due to an ever increase of contrasting properties requirements. These are widely used in industries like automobile, nuclear application, food processing, steam turbine, heat exchangers etc. The academic engineering fraternities are largely focused on process development and optimization for welding parameters applied to commercially available metal and alloys being used as a dissimilar couple. The stainless steel 304 and copper (ferrous and non-ferrous) dissimilar metal couple is extensively used in various industrial applications due to their complementary properties like high thermal and electrical conductivity of copper & corrosion resistance of SS 304.

A numerous research work related to dissimilar metal welding by conventional fusion welding processes has been described related to mechanical strength, microstructure analysis, parametric optimization, numerical modelling etc. of the weld bead orientation. The mechanical and metallurgical behaviour of weldpool of copper (UNSC11000) and alloy steel (En31) dissimilar metal couple by Shielded Metal Arc Welding (SMAW) explained by Velu and Bhat [1]. They failed to define any detrimental intermetallic compounds around the weld interface region. They also investigated the fracture toughness and fatigue crack growth behavior of mode-I cracked bi-metallic compact tension specimens. For getting a successful weld, they were used nickel as filler metal. The welding of Mg alloy and copper by TIG welding process explained by Liu et al. [2]. They used a Fe interlayer in between two base metals. The author reported that the oxide produced in the interface between Mg and Fe caused reduction mechanical properties of the weld. Roy et al. [3] inspected the effect of different electrodes such as Inconel (ENiCrMo3), Monel (ENiCu7) and stainless steel (E316L) over commercially pure copper and 304 stainless steel weldment by shielded metal arc welding. Defects like copper globules and porosity were observed in SS 304 weld interface. The microstructure analysis for copper weldment with Fe filler by using MIG welding process was explained by Suresh Kumar et al. [4]. The presence of copper globules embedded in the iron matrix was revealed from their microstructural analysis.

As per here concern, very limited work has been reported using pulsed wave TIG welding process for both similar as well as dissimilar metal joint. Yu et al. [5] proposed a technique to monitor the wire feed used to detect a defect in Al-Me alloy using pulsed TIG welding. Shiri et al. [6] performed the dissimilar metal welding in between CP copper and 304 SS using gas

tungsten arc welding process. Three different types of filler materials such as Ni–Cu–Fe, SS and Cu were used for the investigation of weld zone. They also concluded that the copper is a new and good candidate for gas tungsten arc welding of copper to 304 SS. Rajkumar and Arivazhagan [7] explained the role of pulsed current on weld properties of Maraging steel and AISI 4340 aeronautical steel dissimilar couple. The authors recommended that the pulsed TIG welding demonstrate superior weldability performance in every mechanical and metallurgical aspect, and it is highly reliable for joining dissimilar material combinations. The joining of marine grade alloys (Monel 400) and AISI 904L using ERNiCu-7 and ERNiCrMo-4 filler metals by pulsed current gas tungsten arc welding process is inspected by Ramkumar et al. [8]. Madadi et al. [9] investigated the hardness and dilution ratio for pulsed TIG cladding process of Stellite 6 (Co-based alloy) on carbon steel. They described that the penetration depth, and dilution increases with pulse frequency but a decrease in cladding layer hardness.

Tarng et al. [10] used neural network theory to build a relationship between process parameters and the weld pool geometry in TIG welding process. The optimization of process parameter was carried out by simulated annealing algorithm. They also verified the pool geometry by using fuzzy clustering technique. Prediction of weld bead geometry for TIG welding process by fuzzy logic was also explained by Narang et al. [11]. The weld bead geometry involves the weldment macrostructure zones and shape profile characteristics. A Neuro-Fuzzy Approach was studied by Moon and Na to Select Welding Conditions for Welding Quality Improvement in Horizontal Fillet Welding [12]. Shanben et al. [13] suggested the fuzzy inference-artificial neural network control approach may use for avoiding the difficulties of modelling as well as the control of process parameters for pulsed TIG welding process. Chi and Hsu [14] developed an intelligent decision support system based fuzzy radial basis function (RBF) neural network to established a quality prediction of output response for plasma arc welding process. Jafarian and Vahdat [15] explained a fuzzy multi-attribute approach for selecting the welding process at high pressure vessel manufacturing.

It is observed from previous literature survey pertaining to pulsed TIG welding process without using any filler material that there is a big research gap regarding process parameter optimization as well as the implementation of numerical prediction approaches in addition to mechanical as well as microstructure study of fusion zone. Very limited works are pursued for CP copper – 304 SS couple weldment. The purpose of this study to give at most useful information about welding possibilities of two dissimilar (SS 304 and copper) thin sheets using pulsed mode TIG system without filler material to the fabrication industries.

II. RESEARCH METHODOLOGY

A. Design of experiment:

Based upon the literature survey, it is observed that the Taguchi orthogonal array is one of the best alternatives for the design of experimentation among all others [16]. It is a systematic application of design for the improvement of product quality. The Taguchi design matrix uses a special orthogonal array to study every process parameter with a minimum number of experimental runs. Signal-to-noise (S/N) ratios for each factor are evaluated to assess the influence over output responses [17–19]. For the current study, three input process parameters such as peak current, scan speed, and standoff distance are taken with four levels of variations as shown in Table 1. The whole experiments are carried out according to Taguchi L16 (4 3) orthogonal array design matrix with three replicates. Therefore, total 48 numbers of samples are welded. All factor levels are equally weighted to ensure a balanced design of experiments.

Parameters	Units	Levels			
		1	2	3	4
Peak current (I_P)	Amp	80	90	100	110
Scan speed (S)	mm/min	90	120	150	180
Stand-off distance (D)	mm	0.85	1.00	1.15	1.30

B. Experimental Work

For the present research work, two different materials such as AISI 304 SS and CP copper are welded by pulsed wave TIG welding process without using any filler material. The chemical composition of for respective materials obtained by EDS analysis are listed in Table 2. In this case the butt type welding is considered maintaining zero gap in between two materials. As no groove is preferred, so the edge of the welding specimen maintained very flat i.e. making as angle of 90° as shown in Fig. 1.

Table 1: Variable process parameters for welding

Table 2: Chemical composition of AISI 304SS and copper (weight fraction, %)

	Fe	Cu	Si	Cr	Mn	Ni	C
SS	74.11	---	0.29	17.71	0.72	7.13	0.04
Cu	---	99.63	0.37	---	---	---	---

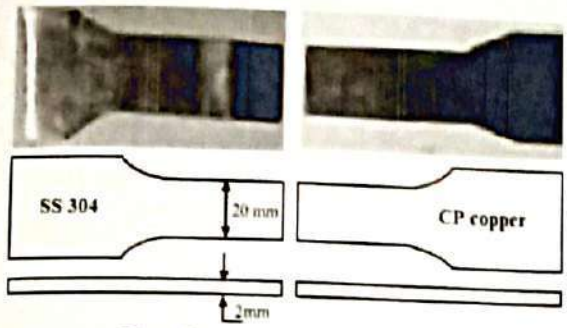

Fig.: Orientation of butt joint

All welding experiments are carried out on a "Fronius magicwave® 2200" TIG welding unit. The unit is assembled with a CNC workstation for better control in terms of accuracy over standoff distance, scan speed with respect to mounting of welding specimen. The process parameters such as electrode size, flow rate of shielding gas, frequency and ramp down time are kept constant as 1.6 mm, 10 lpm, 500 Hz and 0.75 sec respectively during all experiments.

In any welding experiments, the tensile stress is one of the most effective parameter to evaluate the quality of weld. So, tensile stress is taken as the output response for evaluation of process parameter effectiveness. The tensile tests are performed at room temperature using an automated universal testing machine Instron® 600KN. The whole experimental design matrix with respective tensile stress results are listed in Table 3.

As S/N ratio is used to evaluate the influence of process parameter over the output response, so there are three kinds of quality characteristics in S/N ratio analysis i.e. smaller-the-better, larger-the-better and nominal-the-better based on the output responses. In the present analysis, larger-the-better criterion is chosen for quality characterization of tensile stress in order to maximize the response. The respective formulation is given in "(1)".

$$S/N = -10\log_{10}\left(\sum \frac{1}{n}\, y^2\right) \qquad (1)$$

Where, y = Average tensile stress measured

n = Number of experimental runs.

The optimization of the process parameters are carried out with the help of the statistical design software Minitab 16®. The main effect plot and residual plot are given in Fig. 2 and 3 respectively. The main effect plot expresses the optimum design level for the selected design matrix. As the output response is based on larger-the-better analysis, the peak values from plot are taken as the optimum settings to maximize the response. The peak setting obtained from main effect plot is found to be "P = 100 Amp, S = 90 mm/min and D = 1.15 mm". The confirmatory test also carried out for the peak setting. The residual plot expresses the normal probability plot, residual versus fitted value as well as the histogram for normal distribution of residuals. The normal probability plot indicates a very good response as all the values are in between -2 to 2 and also the very much fitted to the normal line. Histogram shows a well fitted value with respect to the distribution line tends to a good agreement with the response. The linear regression equation for tensile stress based on the quadratic model is expressed in "(2)" as follows:

$$\text{Tensile stress} = 375.492 - 0.6425\,(I_p) - 0.9092\,(S) - 8.1667\,(D) \qquad (2)$$

Table 3 Experimental design matrix with results

Run No.	Ip	S	D	Tensile stress (MPa)	S/N ratio	Normalized value for tensile stress	Predicted Fuzzy value	Error
1	110	90	0.85	171	44.6599	0.340	0.546	0.378
2	110	120	1.00	170	44.6090	0.333	0.402	0.171
3	110	150	1.15	171	44.6599	0.340	0.391	0.132
4	110	180	1.30	116	41.2892	0.000	0.071	1.000
5	80	90	1.00	237	47.4950	0.747	0.913	0.182
6	80	120	0.85	196	45.8451	0.494	0.631	0.217
7	80	150	1.30	153	43.6938	0.228	0.386	0.408
8	80	180	1.15	137	42.7344	0.130	0.198	0.345
9	90	90	1.15	278	48.8809	1.000	0.927	-0.079
10	90	120	1.30	175	44.8608	0.364	0.397	0.083
11	90	150	0.85	169	44.5577	0.327	0.394	0.170
12	90	180	1.00	152	43.6369	0.222	0.391	0.432
13	100	90	1.30	188	45.4832	0.444	0.487	0.087
14	100	120	1.15	275	48.7867	0.981	0.971	-0.011
15	100	150	1.00	189	45.5292	0.451	0.569	0.208
16	100	180	0.85	150	43.5218	0.210	0.347	0.395

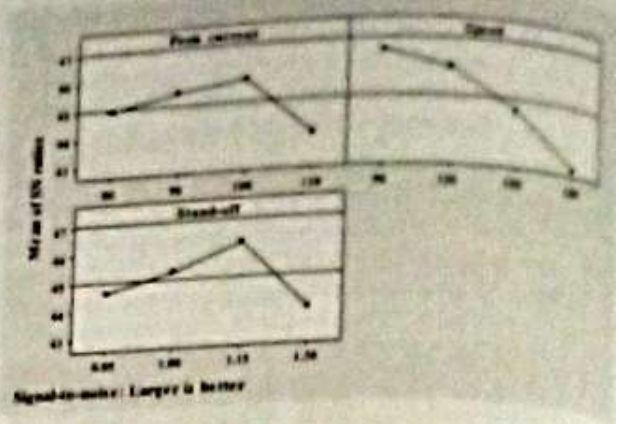

Fig. 2: Main effect plot for output response tensile stress

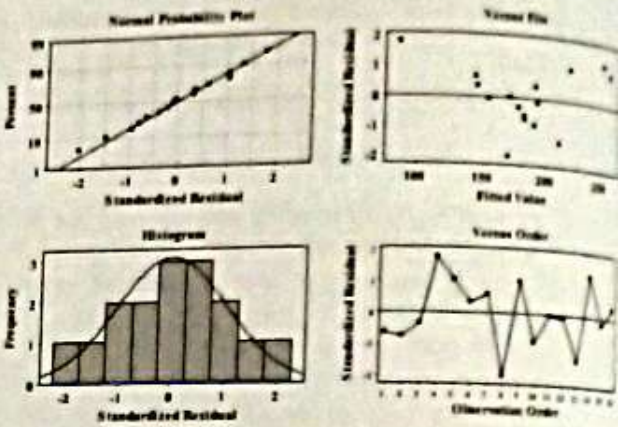

Fig. 3: Residual plot for output response tensile stress

C. *Analysis of variance (ANOVA)*

The ANOVA table investigates the effectiveness of the each process parameter for the enhancement of the weld strength. In addition to that the table also represents the suitability of the developed numerical model [16]. Here the confidence level for this design model is taken as 95 %, which reflects the significant parameter from 'P' values (as the 'P' value should be below 0.05). The 'F' value indicates the greatest effect of the process parameter over the output response. A detailed ANOVA table including R^2, adj. R^2 and the standard error values are represented in Table 4.

Table 4: Analysis of variance for output response

Source	DF	SS	Adj. MS	F	P
I_P	3	9.421	3.1403	3.74	0.080
S	3	34.872	11.624	13.8	0.004
D	3	12.766	4.2552	5.06	0.044
Error	6	5.042	0.8404		
Total	15	62.101			
S = 0.9167 R^2 = 91.9 % R^2 (adj.) = 79.7 %					

It is concluded from the ANOVA table that the scan speed and the stand-off distance give significant value whereas the peak current shows insignificant with a very minimum margin. This will be clearer from 'F' value, i.e. the scan speed obtained highest value of 13.83 followed by stand-off distance and peak current as 5.06 and 3.74 respectively. So scan speed having utmost effect on the output response compared to others two process parameters. The model adequacy represents from R^2 and adj. R^2 values. Here the R^2 and adj. R^2 value obtained from the ANOVA i.e. 91.9 % and 79.7 % respectively. This concludes the greatest fitness of the designed model with respect to output response.

D. Fuzzy logic system

A fuzzy logic system is an unique system in which the numerical data and the linguistic knowledge is simultaneously handle in an effective way. It is a nonlinear mapping of an input data (feature) vector into a scalar output, i.e., it maps numbers into numbers. Linguistic variables are the input or output variables of the system whose values are words or sentences from a natural language, instead of numerical values [20]. The system consists of a fuzzifier, membership functions, a fuzzy rule base, interface engine and difuzzifier as shown in Fig. 4. Membership functions are used in the fuzzication as well as de-fuzzication to map the non-fuzzy input values to fuzzy linguistic terms and vice versa. A membership function is used to quantify a linguistic term [10].

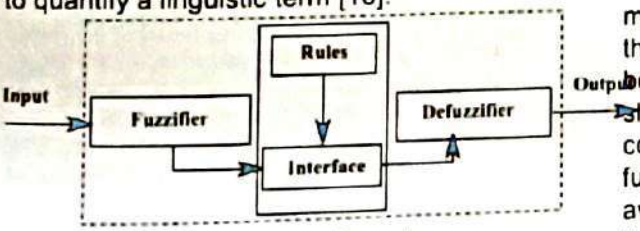

Fig. 4: Fuzzy logic system

In the present study, the tensile stress is predicted through the fuzzy logic by using MATLAB 7.6 in terms of normalized value. The inference engine i.e. Mamdani type performs fuzzy reasoning with fuzzy rules to generate a fuzzy value. These fuzzy rules are written in the form of if-then control rule. There are sixteen fuzzy rules are directly derived based on fact that larger is better characteristics. For each rule, four fuzzy subsets of Small, Medium, Large and Very large are assigned in three input membership functions and five fuzzy subset such as Very Small, Small, Medium, large and Very Large are assigned to one output membership function. The graphical presentations for both input and output membership function are shown in Fig. 5. By tracking maximum-minimum compositional operation, the fuzzy reasoning of these rules yields a fuzzy output. Lastly, the resulting fuzzy output is mapped to an output using the membership functions in the defuzzication step. These predicting fuzzy values are shown in Table 3.

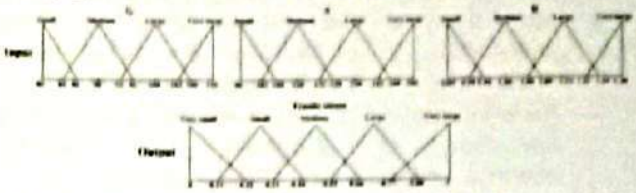

Fig. 5: Input and output membership functions

For comparing the fuzzy predicted values with the experimental results, all experimental values are first normalized using "(2)" and all respected values are listed in Table 3.

$$\text{Normalized value} = 1 - \frac{\text{Max.} - X_i}{\text{Max.} - \text{Min.}} \quad (2)$$

Where, X_i is for Value obtained for each run (i = 1, 2, 3.....16), Max is for Maximum value obtained from whole experiments and Min is for Minimum value obtained from whole experiments.

E. Comparison between experimental and predicted results

After successful welding of SS-Cu metal couple, the tensile stress (normalized) result obtained from experimental and fuzzy prediction model are listed in Table 3. The error between them also tabulated there. The comparisons between experimental and predicted results are shown in Fig. 6. The graph shows a very good comparison between two results. The proposed fuzzy logic has the modeling competence with average accordance ratio of almost 95.881 % i.e. the average error is ±4.119.

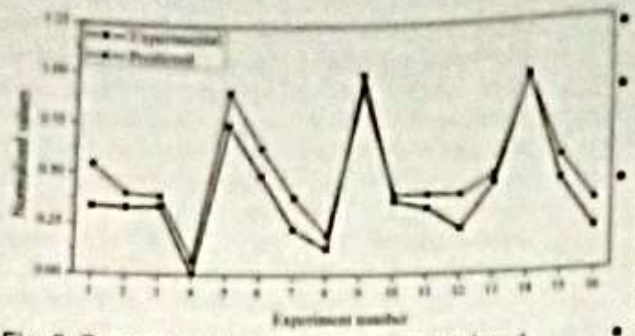

Fig. 6: Comparison between experimental and fuzzy prediction

F. Microstructure Study

Full penetration always a problem in TIG welding but here in every specimen good penetration is observed. In some cases full penetration is not obtained but achieved an acceptable penetration depth (> 85 % of the material thickness) as a whole. The welded specimens are observed under scanning electron microscope (SEM) for the proper investigation about fusion zone details. The macrostructure analyses across the fusion zone shown in Fig. 7 confirm the welds are having good sidewall fusion and good penetration depths.

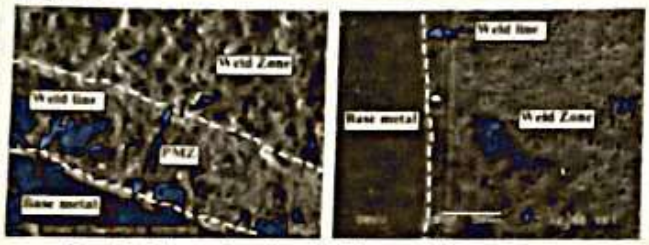

Fig. 7: Microstructure of the weld zone

Partially melting zone (PMZ) as well as the weld line is clearly visible in the image. The weld line preferably divides the weld zone and the base material. The PMZ is present in the weld zone next to the base metal clearer from the different grain size. The SEM image also represents the well distribution of two base metals inside the weld zone. The epitaxial growth of the grains happens from weld line to the weld pool, which tends to strengthen the weld.

III. CONCLUSIONS

A successful weld between two dissimilar metals i e AISI 304 SS and copper has been carried out and the following conclusions can be drawn from the investigations.

- A greater fitness of the Taguchi orthogonal design model for pulsed wave TIG welding for SS-Cu dissimilar couple, confirms from the ANOVA table and average error calculation
- Acceptable tensile stress (as varies from 190-278 MPa) is observed.
- A desired high quality dissimilar metal weld can be achieved by using optimal parameters obtained by Taguchi design.
- The fuzzy logic prediction was successfully implemented for predicting the welding output response. The average error between experimental result and fuzzy predicted is ±4.119.
- The comparison concluded that a fuzzy logic system is one of the best alternate to predict the response. Hence it can propose for real time work environment.
- The microstructure shows the well distribution of materials in the fusion zone to strengthen the joint. In addition to that the weld line and PMZ are also clearly detected.

IV. REFERENCES

[1] M. Velu & S. Bhat, "Experimental Investigations of Fracture and Fatigue Crack Growth of Copper–Steel Joints Arc Welded using Nickel-Base Filler," *Materials & Design*, Vol. 67, February 2015, pp. 244–260.

[2] L. M. Liu, S. X. Wang, & M. L. Zhu, "Study on TIG Welding of Dissimilar Mg Alloy and Cu with Fe as Interlayer," *Science and Technology of Welding and Joining*, Vol. 11, no. 523–525, Dec. 2013.

C. Roy, V. V. Pavanan, G. Vishnu, P. R. Hari, M. Arivarasu, M. Manikandan, D. Ramkumar, & N. Arivazhagan, "Characterization of Metallurgical and Mechanical Properties of Commercially Pure Copper and AISI 304 Dissimilar Weldments," *Procedia Materials Science*, Vol. 5, 2014, pp. 2503–2512.

[4] K. Suresh Kumar, G. Phanikumar, P. Dutta, & K. Chattopadhyay, "Microstructural Development of Dissimilar Weldments: Case of MIG Welding of Cu with Fe Filler," *Journal of Materials Science*, Vol. 37, no. 11, 2002, pp. 2345–2349.

[5] H. Yu, Y. Xu, N. Lv, H. Chen, & S. Chen, "Arc Spectral Processing Technique with its Application to Wire Feed Monitoring in Al–Mg Alloy Pulsed Gas Tungsten Arc Welding," *Journal of Materials Processing Technology*, Vol. 213, no. 5, May 2013, pp. 707–716.

[6] S. G. Shin, M. Nazarzadeh, M. Shanfitabar, & M. S. Afarani, "Gas Tungsten Arc Welding of CP-Copper to 304 Stainless Steel using Different Filler Materials," *Transactions of Nonferrous Metals Society of China*, Vol. 22, no. 12, December 2012, pp. 2937–2942.

[7] V. Rajkumar & N. Arivazhagan, "Role of Pulsed Current on Metallurgical and Mechanical Properties of Dissimilar Metal Gas Tungsten Arc Welding of Maraging Steel to Low Alloy Steel," *Materials & Design*, Vol. 63, November 2014, pp. 69–82.

[8] K. D. Ramkumar, S. V. Naren, V. R. Karthik Paga, A. Tiwari, & N. Arivazhagan, "Development of Pulsed Current Gas Tungsten

Arc Welding Technique for Dissimilar Joints of Marine Grade Alloys," *Journal of Manufacturing Processes*, Vol. 21, 2015, pp. 201–213.

[9] Madadi, F., F. Ashrafizadeh, and M. Shamanian. "Optimization of pulsed TIG cladding process of stellite alloy on carbon steel using RSM." *Journal of Alloys and Compounds* 510.1 (2012): 71-77.

[10] Tarng, Y. S., H. L. Tsai, and S. S. Yeh. "Modeling, optimization and classification of weld quality in tungsten inert gas welding." *International Journal of Machine Tools and Manufacture* 39.9 (1999): 1427-1438.

[11] Narang, H. K., et al. "Prediction of the weld pool geometry of TIG arc welding by using fuzzy logic controller." *International Journal of Engineering, Science and Technology* 3.9 (2011): 77-85.

[12] Moon, Hyeong-Soon, and Suck-Joo Na. "A neuro-fuzzy approach to select welding conditions for welding quality improvement in horizontal fillet welding." *Journal of Manufacturing Systems* 15.6 (1996): 392.

[13] Shanben, Chen, et al. "A Fuzzy Inference-neural Network Control of Dynamic Process of Weld Bead Width in Pulse TIG Welding [J]." *TRANSACTIONS OF THE CHINA WELDING INSTITUTION* 3 (1997).

[14] Chi, Sheng-Chai, and Ll-Chang Hsu. "A fuzzy radial basis function neural network for predicting multiple quality characteristics of plasma arc welding." *IFSA World Congress and 20th NAFIPS International Conference, 2001. Joint 9th*. IEEE, 2001.

[15] Jafarian, Mostafa, and S. Ebrahim Vahdat. "A fuzzy multi-attribute approach to select the welding process at high pressure vessel manufacturing." *Journal of Manufacturing Processes* 14.3 (2012): 250-256.

[16] Phillip J. Ross, "Taguchi Techniques for Quality Engineering" *McGraw Hill Professional*, 1996.

[17] M. Yousefieh, M. Shamanian, & A. Saatchi, "Optimization of Experimental Conditions of the Pulsed Current GTAW Parameters for Mechanical Properties of SDSS UNS S32760 Welds Based on the Taguchi Design Method," *Journal of Materials Engineering and Performance*, Vol. 21, no. 9, December 2011 pp. 1978–1988.

[18] M. Yousefieh, M. Shamanian, & A. R. Arghavan, "Analysis of Design of Experiments Methodology for Optimization of Pulsed Current GTAW Process Parameters for Ultimate Tensile Strength of UNS S32760 Welds," *Metallography, Microstructure, and Analysis*, Vol. 1, no. 2, July 2012, pp. 85–91.

[19] Y. Wang & D. O. Northwood, "Optimization of the Polypyrrole-Coating Parameters for Proton Exchange Membrane Fuel Cell Bipolar Plates using the Taguchi Method," *Journal of Power Sources*, Vol. 185, no. 1, October 2008, pp. 226–232.

[20] J. M. Mendel, "Fuzzy Logic Systems for Engineering: A tutorial", *IEEE*.

Experimental investigation and performance characterization of machining parameter inAJM process using analytical method

[1]Jukti Prasad Padhy,[2]BikashRanjan Moharana,[3]AyusmanNayak
[1][2][3]Gandhi Institute For Technology, Bhubaneswar

***Abstract*-The present investigates the performance characteristics of the process parameters in Abrasive Jet Machining using Taguchi orthogonal design matrix. The mixture of high pressure air with aluminium oxide (as abrasive particle) is used for machining of glass material. The nozzle is used to maximize the flow of abrasive particle. The machine automation was done by using the controller and driver circuit. The study established the optimum condition for the effect of over cut (OC) and material removal rate (MRR) of the said work piece. Individual optimal settings of parameters are carried out to minimize the OC and Maximize the MRR.**

***Index Terms*—Abrasive jet machining, MRR, OC, Taguchi orthogonal array.**

I. INTRODUCTION

For rising of hard and brittle material, which is very difficult-to-machine, is found to be unsuitable for machinig with conventional machining. The surface finish maynot be smooth or may be the tool or workpiece damaged by using above process.Besides, machining of these materials into complex shapes is thorny, time consuming and sometimes unfeasible.Advanced materials such as hastalloy, waspalloy, nitralloy,carbides,nimonics, heat resisting steels ,stainless steel and many other high-strength-temperature resistant (HSTR) alloys find wide application in aerospace, nuclear engineering and other industries owing to their high strength to weight ratio, hardness and heat resisting properties.Considering the importance of the difficulty, Merchant in 1960's highlighted the need for the development of newer ideas in metal machining. As a result, non-traditional machining processes have appeared to triumph over these difficulties. These non-traditional technologies do not utilize a conventional or traditional tool for metal removal, as a substitute they directly make use of some form of energy for metal machining. The classification of the machining processes, based upon the type of energy used, the mechanism of metal removal in the process, the source of energy, and the medium for transfer of those energies. Material removal may occur with chip formation or even no chip formation. In some cases microscopic size chip formation occurs. Abrasive jet machining (AJM) is one of the non-traditional methods employed for machining process in which mechanical form of energy is used. The basic mechanism of metal removal process occurs due to erosion and the transfer media is the high velocity particles. Pneumatic / hydraulic pressure happens to be the energy source.

The AJM process was started a few decades ago, till today experimental and theoretical studies have been investigated throughout the world by many researchers to develop the most efficient method. Burzynski and papini [1] implemented the narrow band level set method (LSM) on AJM for find out the surface evolution on inclined masked micro-channel in poly-methyl-methacrylate (PMMA) and glass.The result profile of glass have round bottom and curved wall and theresulting profile of PMMA have straight walls and rectangular bottoms.Ghobeity et.al [2] presented a analytical models on AJMM in which the target is oscillated transversely to the overall scan direction, by which they predicted the shape, sidewall slope, and depth ofmachined planar areas and transitional slopes inglassWakuda et.al [3] compared the machinability between AJM process and the solid particle erosion model. They concluded from the test result that the relative hardness of the abrasive against the target material is critical in the micro-machining process but it is not taken into consideration. In conventional erosion process radial crack do not propagate downwards as a result of particle impact due to no strength degradation occurs for the AJM surface.Gradeenaet. al [4] used a

cryogenic abrasive jet machining apparatus for solid particle erosion of polydimethylsiloxane (PDMS) using aluminum oxide as an abrasive at a temperature range between -178°C to 17°C and observed that optimum machining of PDMS occurred at temperature approximately at -178°C and also concluded that PDMS can be machined above its glass transition temperature. Ally et. al [5] observed that the optimum erosion rate occurred at impact angles between 200 and 300 when machining the aluminum 6061-T6, 316L stainless steel and Ti-6Al-4V alloy and taking the 50 μmAl_2O_3 as abrasive powder and found that AJM etch rate in metal was minimum when compared with the glass and polymer.

By going through many of the papers the overall conclusion drawn was that electro chemical machining and electro discharge machining are limited to the application of conductive materials which also makes high initial cost and operation cost. Similarly chemical etching requires high technical knowledge, electron beam machining laser beam machining etc. requires high investment and operating cost. Much more difficulties were faced for machining of glass, ceramic and brittle material. The above drawback motivate towards fabrication of a new AJM machine. The new AJM machine was designed, fabricated in NIT, Rourkela. The working model involved the use of a high speed stream of aluminum oxide as abrasive particles which are carried by a high pressure of air through nozzle for drill on glass as the work piece. The main objected was to minimize the over cut at the same time to maximize the material removal rate. Taguchi analysis was carried out to establish the optimum condition.

II METHODOLOGY

The AJM was put into action for designing a feasible working model. The model was designed by using CATIA software. The fabrication of the model was completed by utilizing some of the waste product also fabricating some new components.

A. Components for AJM

The main components used for fabrication of AJM are; working chamber, mixing chamber, FRL unit, nozzle, air compressor, control unit etc.

Different components of the work chamber are enclosure, work holding devices, opening and closing system and drainage system. The specification of the different material of working chamber is given in Table1.

Table 1 Specification of raw material of working chamber

Sl. No.	Raw Material	Specification
1	Mild steel sheet	880mmx440mmx1.5mm
2	Stainless steel sheet	480mmx280mmx0.5mm
3	Glass fibre sheet	760mmx760mmx5mm
4	Allen bolts with nut and washer	6mm
5	Mild steel hinges	1.5 inches

The enclosure was fabricated air tight to prevent the mixing of abrasive particle with air. The enclosure is of mild steel rectangular box of 1 mm thickness. Transparent glass fibre sheet was fitted to the box with the help of Allen bolt. The work holding device is of L-shaped to hold the work piece. The maximum size it can accommodate is 380 x 180mm. Hinge joint were used for closing and opening of the working chamber. For safe disposal of abrasive particle drainage system is provided to the enclosure. The drainage system is fabricated by Stainless steel of size (480mm x280mmx0.5mm). The model view and working model is shown in figure 1.

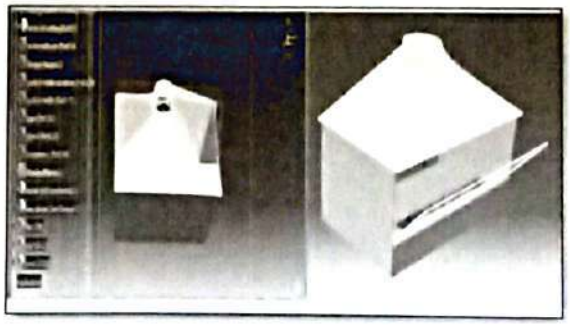

Fig.1. Model view and working model of AJM

A reciprocating air compressor of capacity 21 kgf/cm2 was used for compressing the air. Filter regulator and lubricator (FRL) was used for filtering the air and regulating the air pressure and lubrication of component. By rotating the top screw of FRL unit, pressure is controlled with in the safe limit. The mixing chamber contains three parts i.e. mixing cylinder, cam and rotor. It is used for

mixing of abrasive powder and compressed air. The cam mechanism is used for inserting the abrasive particle. The mixing cylinder was made up of mild steel, has three port. First port is used for inserting the abrasive particle and the second port is used for inserting the compressed air inside the cylinder, while third one is used for outlet of mixing of abrasive and air particle. The mixing chamber is shown in figure 2.To hold the nozzle a nozzle holder was designed and fabricated which is made up of stainless steel.

Fig. 2 Mixing Chamber

B. Machine automation

The AJM was automated by using controller, driver circuit and a stepper motor. The controller generates the electronic pulses and fed to the driver board. The driver board converts electronic pulse into motion control for motor [6]. A 4-axis controller device is used to control the movement of X,Y and Z axis controller. A software called CNC USB CONTROLLER was installed for these purposes. By using the controller, machine can move in 3-axis direction and by using different types of programming complicated shape can also be machined. Three stepper motor was used for 3-axis movement. The motor specification is given in Table 2

Table 2 Motor specification

Sl. No.	Parameter	Values
1	Voltage	2.9 V
2	Current	3.1 amps
3	Steps	200 steps/Rev

The whole machine is mounted on the X-Y table. The travel of X-Y table is 290 x 170 mm. The upper table is used for x-movement and the travelling distance is 290mm, while that of y motion the lower table is used and the travelling distance is 170mm.Finally the assembly of the AJM was carried out by using the above component and referring to the model assembly shown in Figure 3.

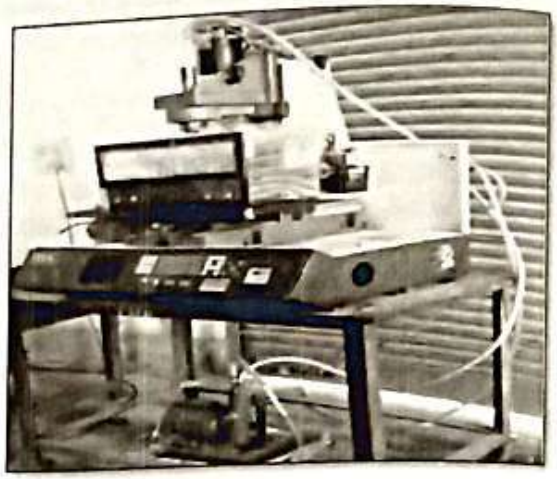

Fig. 3. Working model of AJM

C. Experimentation

Air is used as a carrier gas in the air compressor. The properties of glass which is used as a work piece and the properties of abrasive powder is shown in Table 3 and Table 4 respectively.

Table 3 Properties of glass

Chemical Composition	SiO_2 (74%), Na2O (13%), CaO (10.5%), Al_2O_3 (1.3%), K_2O (0.3%), SO3 (0.2%), MgO (0.2%), TiO_2 (0.01%), Fe_2O_3 (0.04%)
Glass transition temperature	573°C
Density	2400 kg/m^3
Refractive index	1.518

Table 4 Properties of abrasive materials

Composition	Al_2O_3
Appearance	White solid
Odor	odorless
Size	50 µ
Density	3.95-4.1 gm/cm^3
Solubility	Insoluble in water

D Conduct of experiment

The nozzle diameter of 2mm and abrasive particle size of 50 µ is kept constant. The variable factors or the machining parameters

are the Stand of Distance (SOD) and pressure (p). After conducting the experiment (drill hole) the measurement of drill hole was done by tool maker microscope and optical microscope. The final diameter of the drill hole is considered as the mean diameter of both the data of the microscopes. Also initial weight and final weight of the work piece electronic balance weight machine is used whose capacity is of 300 gram weight and 0.001 gram accuracy. Material Removal Rate (MRR) is calculated by Equation (1)

$$MRR = \frac{W_b - W_a}{t \times \rho} m^3/_{min} \quad (1)$$

Where,

W_b = Weight of the work piece before machining, kg

W_a= Weight of the work piece after machining, kg

t = Machining time, min

ρ = Density of work piece, kg/m³

In this experiment, t= 1 minute and ρ=2400 kg/m³

E. Optimal Performance Parameter

The selection of controllable parameters is a most important factor in Taguchi optimization process in order to obtain the best results. The two control parameters selected were Stand of Distance (SOD) in mm and Pressure (p) in bar which have influence on the response [8]. The two selected control parameters at three levels indicates L9 i.e. nine trials of experiments to be conducted, with the level of each parameter for each trial run as indicated on the array. Design parameters are shown in TABLE – 5. L9 Orthogonal Array is shown in TABLE -6.

Table 5 Control parameters and levels

Control Parameters	Level		
	Level 1	Level 2	Level 3
Stand Of Distance (mm)	0.7	0.8	0.9
Pressure (bar)	4	5	6

Table - 6 Orthogonal Arrays

Run Number	SOD	p
1	1	1
2	1	2
3	1	3
4	2	1
5	2	2
6	2	3
7	3	1
8	3	2
9	3	3

The next step is to determine optimal conditions for the control parameters to give the optimum responses. The response variable to be optimized was MRR for maximum value, OC with the least as much as possible. The signal optimum settings of the parameters were achieved from the signal to noise ratio(S/N) which help in data analysis and prediction of the optimum result.

III. RESULTS AND DISCUSSION

Drilled cavity on work piece as per run number is shown in Figure 4.

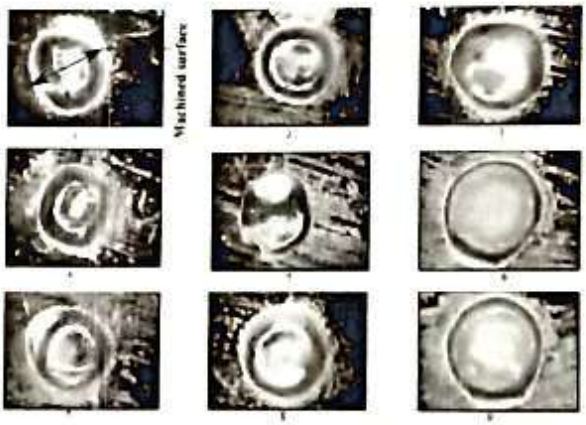

Fig 4. Drilled cavity on work piece as per run number

Experimental data are shown in Table 7 and Table 8.

Table 7 MRR versus SOD, P

Run No.	SOD(mm)	P (bar)	MRR (mm^3/min)
1	0.7	4	4.583
2	0.7	5	5.789
3	0.7	6	8.832
4	0.8	4	5.933
5	0.8	5	7.732
6	0.8	6	10.42

7	0.9	4	6.223
8	0.9	5	7.432
9	0.9	6	9.326

Table 8 OC versus SOD, P

Run No.	SOD(mm)	P (bar)	OC(mm)
1	0.7	4	0.2250
2	0.7	5	0.2976
3	0.7	6	0.4875
4	0.8	4	0.3065
5	0.8	5	0.3675
6	0.8	6	0.5075
7	0.9	4	0.2633
8	0.9	5	0.3278
9	0.9	6	0.4532

By applying the experimental data of Table 7 and Table 8 the Signal to noise (S/N) ratio graphs is shown in Figure 7 and Figure 8.

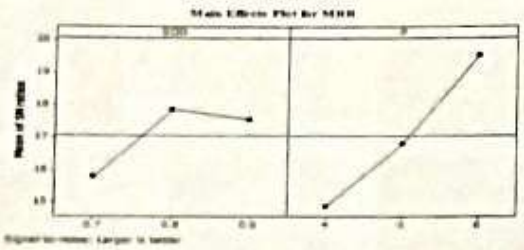

Fig. 5 Main effect plot means for MRR

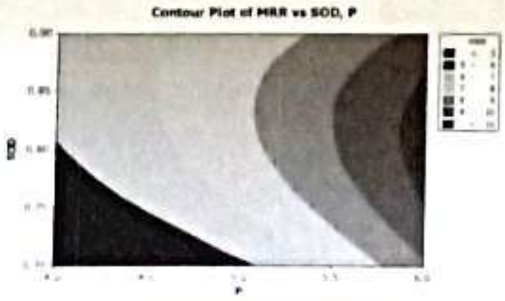

Fig 6. Contour plot for MRR

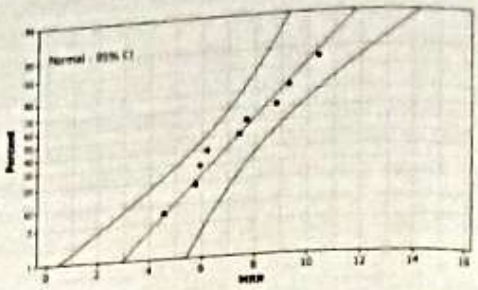

Fig.7. Probability plot for MRR

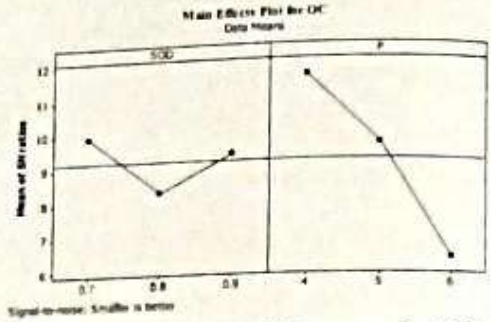

Fig. 8. Main effect plot means for OC

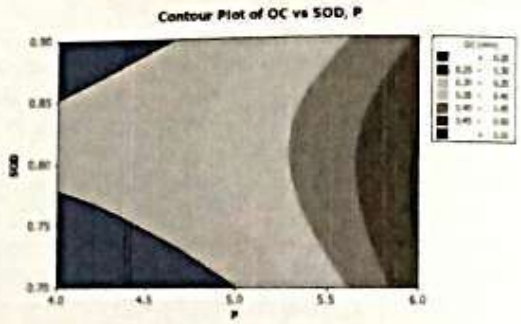

Fig.9. Contour plot for OC

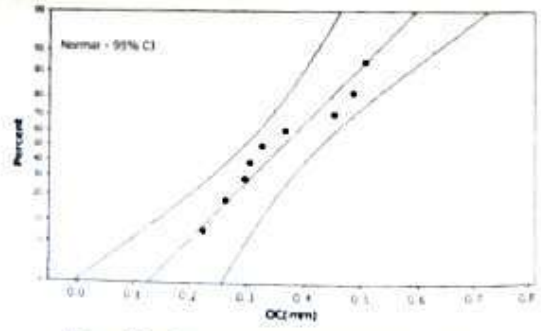

Fig.10. Probability plot for OC

From Table 7 it is observed that the pressure is directly proportional to MRR in the range of 4 to 6 bar. This is expected because an increase pressure produces strong kinetic energy which produces the higher temperature, causing more material

to erode from the work piece. The other factor SOD does not influence much as compared to pressure.

To calculate MRR, the S/N ratio with a higher the better characteristics was used. Fig. 7 indicates that at SOD 0.8 mm the MRR is maximum. It decreases with increase in SOD and also decrease with decrease in SOD. From the graph it was observed that the optimization of AZM was found to be SOD =0.8mm at p= 5 bar.

From Fig. 8 indicate that the SOD =0.7mm, the OC is minimum. It increases with SOD up to some level after that it decreases. It has also been observed that with minimum pressure the OC is found to be minimum. It further increases with increase in pressure.

IV. CONCLUSION

Design of the working model was carried out in CATIA software by considering the optimum use of available material and space.

Working chamber, nozzle holder arrangement, work holding device were fabricated in the lab as per the specification.

The AJM machine can be used for drilling and milling of glass plates or other brittle materials.

Various complicated shape can also be machined as per the programming on controller.

SOD and pressure are considered as machine parameter to study the MRR and OC.

For MRR, SOD and pressure are significant factor while pressure is significant for OC.

MRR increases with increase in pressure, but for increase in SOD, MRR increases up to some extent and then it remain constant after that it decreases.

OC increases with increases in pressure, but for increase in SOD, OC increases up to some extent only and a decrease trend is observed.

REFERENCE

[1] T. Burzynski, M. Papini (2011) , "A level set methodology for predicting the surface evolution of inclined masked micro-channels resulting from abrasive jet micro-machining at oblique incidence," International Journal of Machine Tools & Manufacture, Vol. 51, pp. 628-641.

[2] A. Ghobeitya, M. Papinib, J.K. Spelta (2009), "Abrasive jet micro-machining of planar areas and transitionalslopes in glass using target oscillation,"Journal of Materials Processing Technology, Vol. 209, pp. 5123-5132

[3] M. Wakuda , Y. Yamauchi , S. Kanzaki (2002), "Effect of workpiece properties on machinability in abrasivejet machining of ceramic materials,"Journal of the International Societies for Precision Engineering and Nanotechnology, Vol. 26, pp. 193-198

[4] A.G. Gradeena, J.K. Spelta, M. Papinia, (2012) "Cryogenic abrasive jet machining of polydimethylsiloxane at different temperatures," wear, Vol. 274-275, pp. 335-344.

[5] S.Ally , J.K. Spelt , M. Papini, (2012) "Prediction of machined surface evolution in the abrasive jet micro-machining of metal," wear, Vol. 292-293, pp. 89-99.

[6] R.K. Tyagi, (2012) "Abrasive jet machining by means of velocity shear instability in plasma," journal of manufacturing process," Vol. 14, pp. 323-327.

[7] Y. Lin, Y. Chen, A. Wang, W. Sei (2012), "Machining performance on hybrid process of abrasive jet machining and electrical discharge machining," Transactions of Nonferrous Metals Society of China (English Edition), Vol. 22, pp. 775-780.

[8] Padhy J.P and Nayak K.C (2014) "Optimization and effect of controlling parameters on AJM using Taguchi technique" IJERA, Vol.4, Issue 3(1), March 2014, pp. 598-604.

[9] Padhy J.P, Dewangana S and Biswas C.K, (2014), "Optimization of Multi-Objective Optimization of Machining Parameters of AJM using Quality Loss Function" International Journal of current engineering and Technology Special issue 3, pp-255-257.

[10] Gover P, Kumar S and Murtaza Q, (2014), "Study of Aluminium oxide Abrasive on Tempered glass in Abrasive Jet Machining using Taguchi Method. International Journal of Advance Research and Innovation, Vol. 2 (1) pp 237-241

★★★

An experimental study on some mechanical properties of epoxy/glass fiber hybrid composites modified by 10 Wt% SiO_2 micro particles.

[1]Alina Dash, [2] Bikash Ranjan Moharana, [3]Ayusman Nayak
[1] [2] [3]Gandhi Institute For Technology, Bhubaneswar

Abstract— Improvements on mechanical properties of composite materials are still under research for different applications. Fiber reinforced polymer composite is playing an vital role for interdisciplinary research. This paper summarizes the experimental results of epoxy matrix which is modified by 10 wt % SiO_2 micro ceramic particles in glass fiber/epoxy composite. The composites are fabricated by hand lay-up method. It is observed that mechanical properties like flexural strength, flexural modulus, hardness and toughness increase compare to neat epoxy but inter laminar shear strength (ILSS) decreases. Agglomeration of SiO_2 micro particles is observed in SEM analysis. The mode of failure is the combination of crack in matrix, deboning and fiber pull out.

Index Terms— Polymer Matrix Composite, Glass-fiber, Flexural strength, SiO_2

1.INTRODUCTION

From the recent and relevant published work in the area of fabrication and characterization of glass fiber reinforced composite, it is well documented that majority fillers have a positive influence on mechanical properties. Development of new composite materials or modification of existing composite material is the real challenge for most of the materials engineers. This modification can be done by addition of different ceramic powders of different sizes to achieve the required mechanical properties.

The modern use of FRP composite began in the world war-ii . Metals and ceramics are available as matrix are currently expensive so polymer are much more commonly used. And processing of PMC need not require high pressure and high temperature also equipment requires for manufacturing are simpler so PMC developed rapidly and become popular. Different materials are suitable for different applications. The use of additives can greatly affect the FRP/Composite properties. Epoxy resin has been widely used in many industrial products due to its advanced properties such as higher modulus, higher adhesive strength. Development of new composite materials or modification of existing composite material is a real challenge for most of the materials engineers. This modification can be done by addition of different ceramic powders of different sizes to achieve the required mechanical properties.

C.M. Manjunatha et al.(2010) studied the tensile fatigue behavior of a silica nano particle-modified glass fibre reinforced epoxy composite.They found that the fatigue life increased about three to four times by addition of the silica nanoparticles. In 2011 Bin Wei et al observed Strengthening of basalt fibers with nano-SiO2–epoxy composite coating. They compared by coating the basalt fiber with SiO2 nanoparticle–epoxy composite and with the pure epoxy . And found that the SiO2 nanoparticle–epoxy composite coating gave a significant increase in the tensile strength of the basalt fibers as compared with the pure epoxy coating which is an effective way in improving the mechanical properties of basalt fibers. A systematic study on the effects of silica and rubber nano-particles on the fracture toughness behavior of epoxy was conducted by Hong-Yuan Liu et al(2011) and it is observed that fracture toughness of epoxy can be significantly increased by incorporating either rubber or silica nano-particles. T.H. Hsieh et al(2010) studied The mechanisms and mechanics of the toughening of epoxy polymers modified with silica nanoparticles.Firstly they found that Young's modulus steadily increased as the volume fraction, of the silica nanoparticles was increased. And Secondly, the presence of silica nanoparticles also increase the toughness of the epoxy polymer. . Rongguo and Wenbo Luo

(2008) studied the effect of nano silica filers on mechanical properties of epoxy composite. They found that elastic moduli of the nano-SiO_2/epoxy composite are more than those of the neat epoxy resins. However, the elongation of the composites decreases with increasing SiO_2 mass fraction. Chen et al. (2008) studied effect of highly dispersed nano silica-epoxy resins with enhanced mechanical properties. It is seen that there is substantial improvement on mechanical properties of the composite with nano SiO_2 fillers. Ahmad et al. (2008) studied the effect of SiO_2 particle shape on mechanical properties of SiO_2/epoxy composite. They observed that the elongated shape of silica mineral shows the highest mechanical properties compare to other shapes and also the mechanical properties increases with increase in filler percentage. This is because of filler agglomeration, filler-matrix compatibility, bonding at interface and aspect ratio of the fused silica in the epoxy system. Johnsen et al. (2007) studied the toughening mechanisms of silica nano particle-modified epoxy polymers. They found that the glass transition temperature (T_g) was unchanged by the addition of the nano particles. However at the same time the modulus and toughness were increased with nano SiO_2 fillers.

More work is still needed to get a clear comparative study for better understanding of the mechanical response of epoxy composites modified with SiO_2 particles. Hence in this paper the mechanical properties of E-glass fiber reinforced epoxy composites with SiO_2 filler and without filler have been investigated. The analysis of the results and the relationship among composite samples are also reported. The mechanical properties are evaluated.

2. EXPERIMENTAL DETAILS

2.1 Materials

Both thermosetting and thermoplastic, are used as matrix materials for the composites. Glass is described as a thermoset plastic resin that is reinforced with glass fibers . Fibers provide strength, dimensional stability, and heat resistance. Additives provide colour and determine surface finish, and affect many other properties such as weathering and flame retardance.

All samples in this work were prepared by,

Fiber Material

Commercially available woven roving fabric E-glass fiber with silane-coupling sizing system (Saint-Gobian Vetrotex) with fiber thickness of 8 micron is used as re-inforcement.

Fig1.1:woven roving E-Glass fiber

Matrix Materials.

The epoxy resin are being widely used for many advanced composite due to their excellent adhesion to wide variety of fibers, superior mechanical and electrical properties and good performance at elevated temperature and also they have low shrinkage upon curing and good chemical resistance. . The epoxy which is used was Araldite(LY-556) an unmodified epoxy resin based on biphenyl-A-diglycidyl-ether and chemically belongs to 'epoxide' family and hardener (HY -951),aliphatic 951, aliphatic primary amine are supplied by Ciba-Geigy ,India

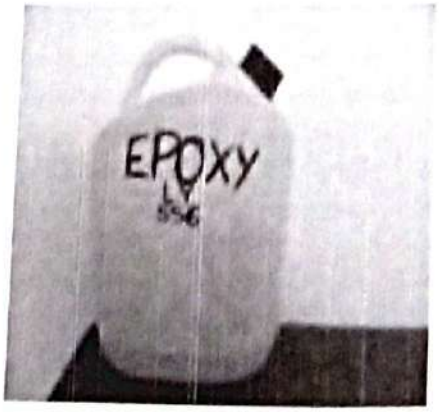

Fig 1.2 : Epoxy LY-556

Filler Material

While ceramic powder such as alumina (Al2O3), silicon carbide (SiC), silica (SiO2), titania (TiO2) etc. are widely used as conventional fillers. In this study, SiO2 (< 10 micron)) particleis used to modify the epoxy matrix, purchased from Alfa Aesar, India .

2.2. Composite fabrication

Two types of composite ,one modified with silica nano filler and other one without filler material was fabricated by hand lay-up method. Before mixing with epoxy, initially the silica powders are dried at 60 oC for 2hrs. The required amount of filler is weighted and mixed with neat epoxy.The mixture is stirred manually using a glass rod for a time period of 30 minutes. Then hardener added. After fabrication of each layer, to remove entrapped air and to achieve uniform thickness , rolling is done with a MS roller . The castings are put under load for about 72 hrs for proper curing at room temperature.

As per the ASTM standard, Specimens are cut for description by using a diamond cutter. The designations of the composites are reported in Table -1. Where C1 is the composite with filler and C2 is the composite without filler.

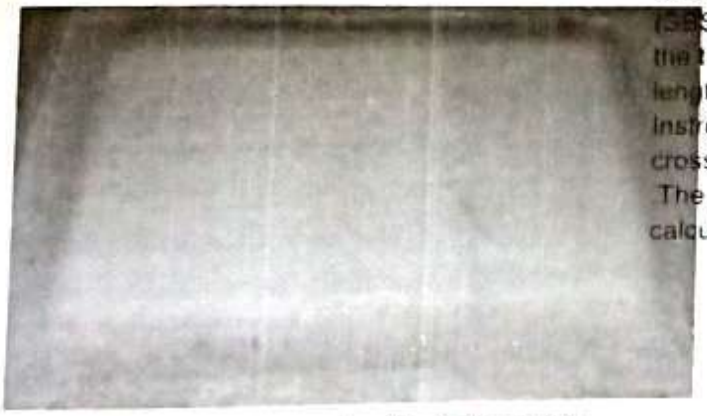

Figure 1 3 Composite after Fabrication

Table -1 Designation and composition of composite

(mm)

Designation of composites	Composition
C_1	Epoxy + 60 Wt% Glass fiber + 10 Wt % SiO_2
C_2	Epoxy + 60 Wt% Glass fiber

3. Results and Discussions

The fabricated composite is cut by means of a diamond cutter of required dimensions as per the standard and the waste part of the composite are eliminated.

Fig 1 4 Specimen for Silica modified Composite

3.1 Flexural and Inter laminar Shear Strength

The inter-laminar shear strength (ILSS) and Flexural strength (FS) are conducted as per the ASTM- D2344/D2344M-00 by short beam shear (SBS) test . The dimension of the specimen for the test is 28 mm X 11 mm X 5.5 mm and span length of 22 mm. Universal testing machine Instron 5967 is used to conduct the test. The cross head speed is maintained at 1 mm/min .The ILSS and flexural strength (FS) are calculated as per the following equations

$$ILSS = \frac{3P}{4bt}$$

$$FS = \frac{3PL}{2bt^2}$$

Where P → Maximum load (N)

B → Width of the specimen (mm)

T → Thickness of the specimen (mm)

L → Span length (mm)

It is observed that both flexural strength and modulus of is more But Inter laminar shear strength is less for SiO2 modified epoxy as compared to neat epoxy. This may be because of finer particle size (<10 micron) of silica. As decrease the particle size, increases the surface area and better adhesive bond between matrix and filler, therefore SiO2 particles gives better adhesive strength and improve the mechanical properties. Figure 1(a),(b)and(c) shows comparison of flexural strength, flexural modulus and ILSS with silica modified epoxy and neat epoxy respectively.

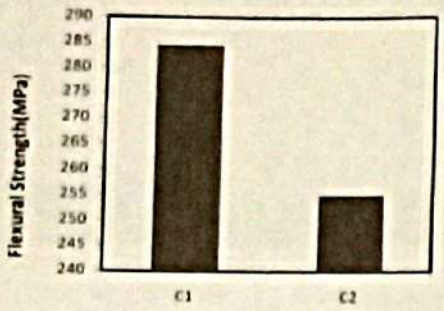

Fig:1.5:comparision of flexural strength VS micro filler

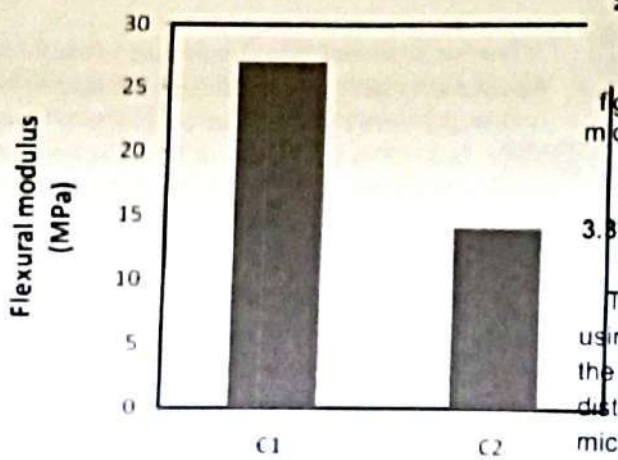

Fig 1.6 comparison of flexural modulus VS micro filler

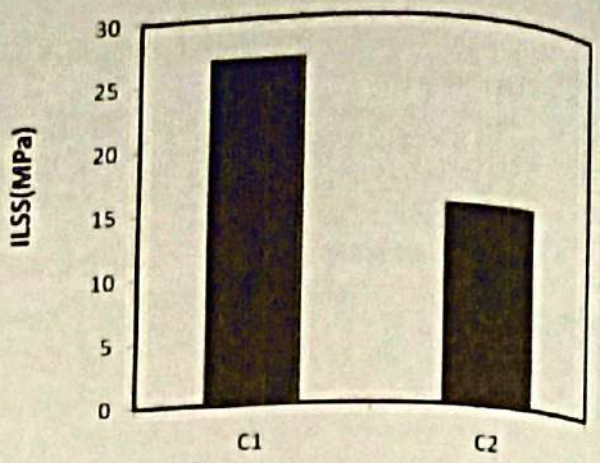

Fig:1.7: comparison of ILSS VS micro filler

3.2 Micro-Hardness

Digital Leco micro-hardness tester is used to measure the micro-hardness of the composite. It is observed that the hardness is more for SiO2 modified epoxy as compared to neat epoxy

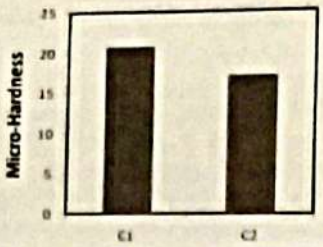

fig.1.8: comparison of micro-hardness VS micro filler.

3.3 Impact Test

The tests are done as per the ASTM D6110 using an impact tester. This is also reported that the Impact strength of neat epoxy is more. Fillers disturb the matrix continuity which can act as a micro crack initiator.

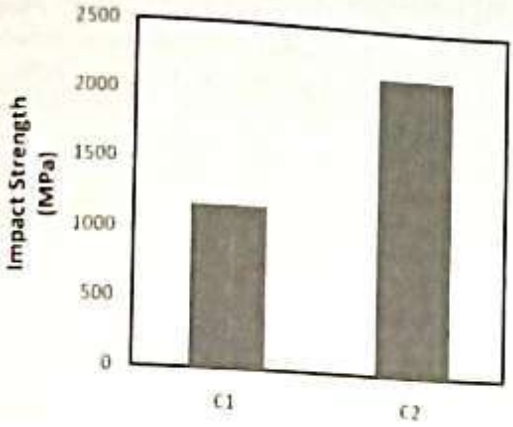

fig 1.9 comparison of Impact strength VS micro filler

3.4 SEM analysis

Fracture surface of SBS tested samples have been investigated using Scanning Electron Microscope (SEM). Figure shows the fracture surface of SiO2 modified epoxy composite. It is observed that there are pot holes in the matrix because of fabrication by hand layup technique. It is also observed that because of smaller particle size, the interface bond between filler and matrix is better.

Figure 2.0 SEM micrograph for SiO2 particle modifier

4. Conclusions

The experimental investigation concluded the following points :

- Mechanical properties like flexural strength and flexural modulus are more in case of SiO2 modified epoxy composite compare to neat epoxy.
- SEM analysis clearly indicates the mode of fracture is the combination of matrix crack, matrix/fiber debonding and fiber pull out for all types of composite.

5.References

1. C.M. Manjunatha a,*, A.C. Taylor a, A.J. Kinloch a, S. Sprenger b The tensile fatigue behaviour of a silica nanoparticle-modified glass fibre reinforced epoxy composite. Composites

2 Science and Technology 70 (2010) 193–199

3. Bin Wei a, Shenhua Song a, Hailin Cao b,c Strengthening of basalt fibers with nano-SiO2–epoxy composite coating Materials and Design 32 (2011) 4180–4186

4 Rongguo Zhaoa,b, Wenbo Luoa,b Fracture surface analysis on nano-SiO2/epoxy composite. Materials Science and Engineering A 483–484 (2008) 313–315

5 Chenggang Chen a, Ryan S Justice b,c, Dale W Schaefer c, Jeffery W Baur b,* Highly dispersed nanosilica–epoxy

resins with enhanced mechanical properties. Polymer 49 (2008) 3805–3815.

6. Milad Zamanian , Mehrzad Mortezaei , Babak Salehnia b, J.E. Jam a. Fracture toughness of epoxy polymer modified with nanosilica particles:Particle size effect. Engineering Fracture Mechanics 97 (2013) 193–206.

7. T.H. Hsieh a, A.J. Kinloch a,*, K. Masania a, A.C. Taylor a,**, S. Sprenger b. The mechanisms and mechanics of the toughening of epoxy polymers modified with silica nanoparticles. Polymer 51 (2010) 6284e6294.

8. Ahmad Farrah Noor, Mariatti Jaafar , Samayamutthirian Palaniandy, Khairun Azizi and Mohd Azizli, 2008. Effect of particle shape of silica mineral on the properties of epoxy composites. Composites Science and Technology 68, 346–353.

9. Johnsen B.B., A.J. Kinloch, R.D. Mohammed, A.C. Taylor, S. Springer, 2007. Toughening mechanisms of nano particle-modified epoxy polymers, Polymer 48,530-541.

Fabrication of Functionally Graded Composite Material using Powder Metallurgy Route: An Overview

[1]Aravind Tripathy, [2]Saroj Kumar Sarangi, [3]Rashmikant Panda
[1] Gandhi Institute For Technology (GIFT), Bhubaneswar, [2], [3] I.T.E.R., SOA University, Bhubaneswar,

Abstract: *Functionally Graded Composite Material (FGCMs) are inhomogeneous materials, consisting of two (or more) different materials, with an engineered gradient along the thickness direction having a continuously varying spatial composition. Keeping in mind the wide areas of application and the probable scope of such materials, some existing problems are discussed. As part of the present investigation, a simple case study involving Al-SiC FGCM, by powder metallurgy (PM) route is discussed. The effect of SiC addition on the density of Aluminium, densification parameters of Aluminium sintered functionally graded composite material and an overview of the current status of research on FGCMs including its future development is presented here. This review concluded that powder metallurgy (PM) is the most suitable technique certainly for mass production and up-scaling of the FGCMs. The selection was strengthened after considering the advantages of the technique such as process cost-effectiveness, reliability of the practical implementation of the process and the high capability of the process to control the quality of the FGMs.*

Index Terms: Functionally Graded Composite Material (FGCM), fabrication, Powder Metallurgy (PM), Sintering

Introduction:

Joining of two or more dissimilar materials in the laminar form often lead to failure owing to delamination because of poor bonding between the materials as well as load bearing characteristic of the materials, functionally Graded Materials (FGM) which has compositional and micro-structural gradient along its thickness direction was developed as an answer to the above mentioned failures. These works comprises of combining the metal–ceramics in a definite gradient and find their respective characteristics and compare the same with the results of other authors and recognize practical application of the new material developed in our daily use. Aiming for the best technique to be implemented, this paper presents an extensive review on the various solid state fabrication techniques of FGMs composed of metallic and ceramic phases. Fabrication techniques in this field of work have incorporated many concepts from different backgrounds of gradation and consolidation or sintering processes. However each of these processes has their own advantages and disadvantages and the best technique to be applied can be found by considering some critical issues highlighted in published literatures. FGCMs exhibit flexibility in terms of functional behavior of a single material as on one side it may exhibit metal like properties on the other side it will exhibit high temperature withstanding characteristics. This tailoring of material properties in FGCMs is done by controlling factors like chemical composition, microstructure or atomic orders etc, the property can vary along a gradient along its thickness direction [1,2]. Most theoretical works on designing, investigating and elaborating the preparation of FGMs indicates the process primarily comprises

of two steps viz. gradation and consolidation. Gradation process could be performed either by consecutive homogenization or by segregation process. Consecutive process depends on a stepwise gradient built-up of the structure from powder materials; homogenizing process shows a sharp interface between two materials is converted into a single gradient by a material transport and in segregating process, indicates the conversion of a macroscopically homogeneous material into a single gradient also by material transport which is caused by an external field such as gravitational or electric field. In order to successfully fabricate the FGMs specimens, researchers have applied the optimal combination of several methods depending on the properties of the component materials [3,4] by stacking more than one starting materials selectively until layered structure is produced. The advantage of this technique is that it is able to produce unlimited number of gradient.

In a PM process, the primary step in fabricating FGCMs is preparing the gradient (also known as gradation process) and can be based on porosity, volume fraction of the phases, particle sizes and even the chemical composition of

elemental powders. It can be construed that the gradation process is independent of the consolidation process. Thus it is immaterial, how the gradation of the structure was achieved; the consolidation is a complete new subject of study. In sintering process, the bonding of the graded layers is the primary concern and largely relies on the sintering process of the structure. The existing and most updated techniques for FGMs fabrication will be discussed in the following part of the work and optimizing the same for a particular application has been the challenge

The concept of functionally graded material (FGM) was introduced to satisfy the demand of ultra-high-temperature environment and to eliminate the stress singularities [5-6]. Normally traditional composites made out of two different materials have often been used to great satisfaction for high performance demands. However stress singularities in such composites may occur at the interfacing layers owing to mismatch of materials. Considering high temperature environment, for example in the engine combustion chamber of an air vehicle or a nuclear fusion reaction container, the relative higher disparity in thermal expansion coefficient will induce greater residual stresses resulting in cracking or debonding of the composite. Therefore the concept of FGMs was introduced to meet these challenges of multifunctional materials in these adverse operating conditions [7, 37-38].

An FGM can be prepared by continuously changing the constituents of multi-phase materials in a pre- determined volume fraction of the constituent material [8-10]. Due to the continuous change in material properties of an FGM, the interfaces between two materials disappear but the characteristics of two or more different materials of the composite are preserved. Subsequently the stress singularity at the interface of a composite can be eliminated and thus the bonding strength is enhanced. Studies reveal that the thermal residual stresses can be significantly relaxed by using an FGM [11-13]. Power-law function [14-15] and exponential function [16-21] are commonly used to describe the variations of material properties of FGMs. Because of the wide material variations and applications of FGMs, literatures corresponding to FGMs in the material constituent [22-24], and processing [9, 25] have rapidly increased in the last 10 years. Many researchers are devoted to understand the mechanics and mechanism of FGMs to offer an optimum profile for designers. Hence it has been an earnest effort at establishing one such optimal profile for a FGM using Aluminium with Silicon carbide and /Alumina here.

FGM concept may be applied for a thermal barrier using a plate or shell like structure. The metal-ceramic composite plates are widely used in aircrafts, space vehicles, reactor vessels, and other engineering applications. If a high external pressure is applied to the composite plate structure, the high stresses occurred in the structure will affect its integrity and the structure is susceptible to failure. Therefore, understanding the mechanical behavior of an FGM plate is very important to assess the safety of the plate structure. Woo and Meguid [26] applied the Karman theory for large deformation to obtain the analytical solution for the plates and shell under transverse mechanical loads and a temperature field. Reddy et al [27] investigated the static and dynamic responses of functionally graded ceramic–metal plates by using a plate finite element that accounts for the transverse shear strains, rotary inertia and moderately large rotations in the Von Karman sense. He et al. [28] studied the vibration control of the FGM plates with integrated piezoelectric sensors and actuators by a finite element formulation based on the classical laminated plate theory. Elastic bifurcation buckling of FGM plates under in-plane compressive loading was studied based on a combination of micromechanical and structural approaches [29].

Functionally Graded Composite Material-A Concept:

In case of Functionally Graded Composite Materials (FGCMs) two types of graded structures are prepared as shown in the figure below. Figure (a) a graded structure while Figure (b) a continuous structure. While in case of step wise graded structure the micro structure, feature changes in stepwise manner which is akin to a multi-layered structure with interface existing between the discreet layers. But in case of figure (b) the change in composition, microstructure occurs continuously with position. The figure below depicts the concept in a very clear manner for a FGCM [3].

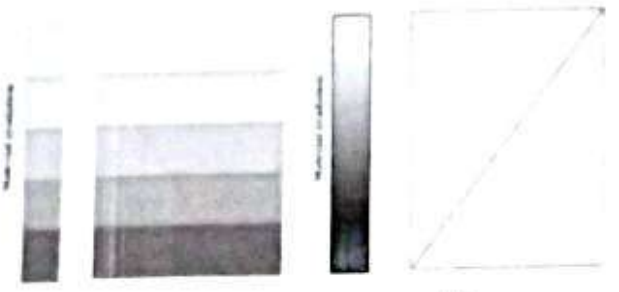

(a) (b)

Fig Schematic Diagram of concept of Gradation

FGM-Processing Techniques:

There are several different physical and chemical methods depending on type of materials, potential application and available facilities for the FGMs fabrication [30]. Basically the techniques are classified as constructive and transport based processes where each of them is composed of various sub-steps that need to be followed to complete the fabrication. By implementing constructive process which allows full and potentially automated control of compositional gradients, the gradation process is made by stacking more than one starting materials selectively until layered structure is produced. The advantage of this technique is that it is able to produce unlimited number of gradient. The transport based technique is the appropriate method for such cases as the case utilizes natural transport phenomena to create compositional and microstructural gradients during fabrication of the FGMs. The existing and most updated techniques for FGMs fabrication will be discussed in the following part of the work.

Powder Metallurgy (PM):

It is a term which covers a wide range of ways in which materials and components are made from metal and ceramic powders. P/M is also used to make intricate shape objects which are impossible to be made from other techniques. One of the most important products of this type is tungsten carbide based cutting tools. There are four basic steps in PM i.e. powder weighing, powder blending, die compaction and sintering. Compaction is generally performed at room temperature, and sintering at the elevated-temperature usually under controlled atmosphere. Secondary processing such as coining or repressing and re-sintering often follows sintering to obtain special properties or to have enhanced precision. PM is an apparent technology for the FGMs fabrication and is increasingly being used to create gradients on material. This method is appropriate for FGCMs fabrication using solid materials. In PM route, some steps are needed for the completion of the product preparation. These steps can be classified into four main steps namely: powder preparation, powder processing (weighing and mixing of powder according to desired percentage of composition), forming operations (stacking and ramming of premixed powders) and finally sintering or pressure assist hot consolidation. After completing the sintering process, optional secondary processing can be performed to enhance the performance of the structure.

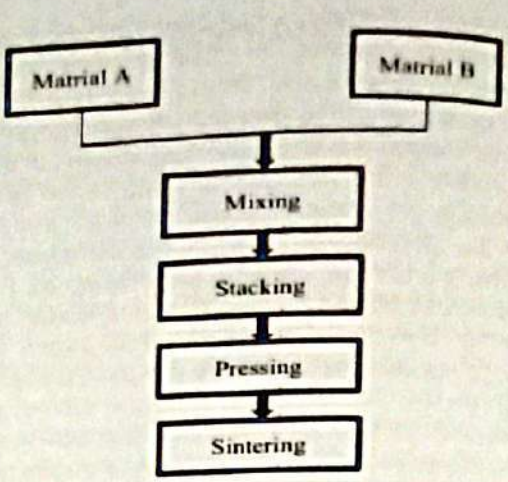

Fig: Flow process chart for Powder Metallurgy Process

Several techniques have been introduced for powder preparation such as through chemical reactions, electrolytic deposition, grinding or comminution. These techniques permit mass production rates of powder form materials and it is usually offered within controllable size range of the final grain population. For the powder processing, the main consideration is focused on the precision in weighing amounts and the dispersion of the mixed powders. These elements will influence the structure properties and should be handled in very careful way. In the subsequent processes, the forming operations is performed at room temperature while sintering is conducted at atmospheric pressure as the elevated-temperature used may cause other reaction that may affected the materials. At this stage, the atmosphere condition must be appropriate since high-temperature process has high sensitivity to the surroundings. Within a customized sintering profile for the fabrication, a new composition profile of 15 layers with crack free joint of the FGM was proposed as the optimized structure [31]. Instead of the ceramics FGM, a bulk SiC/C FGM is another pair that is successfully fabricated using hot pressing process. In term of thermal properties, the hot- pressed SiC/C FGM was found having high effective thermal conductivity at the interface of 1 mm SiC layer when compared to the specimens prepared using other methods. No cracks were found on the SiC/C coatings, thus make the FGM possess high thermal fatigue behavior.

FGCM Characteristics:

(a) Exclusive Properties of FGM's:

FGCM, as a material component with certain engineered property changing continuously in space in a particular direction as shown in figure above as a result it can overcome the

Sl. No.	FGCM Type	Requirement	Application
1	Al / SiC	Hardness & Toughness	Combustion Chambers
2	Al / C	–	Drive shaft, Turbine Rotors, Turbine Wheels
3	Si C / SiC	Corrosion Resistance and hardness	Combustion Chambers
4	Al / SiC	–	Fly wheels, Racing Car Brakes
5	Al_2O_3 / Al-alloy	Good Thermal & corrosion resistance	Rocket Nozzle, wings, Rotary Launchers, Engine casing

deficiencies exhibited by the traditional materials. Erdogan et al [32] opined through their work of the many advantages over conventional and composite materials. FGM has the following advantages:

- Residual stress and Thermal stress can be reduced using FGM coatings and interface layers.
- End point stress singularity and stress at the interface can be removed through FGM coatings.
- Reduction in crack propagating force and increasing the strength of the interface through FGM coatings
- As an interface layer to connect two incompatible materials, FGMs can effectively enhance the bond strength.

(b) Applications oriented Classifications of FGMs:

As the demand for newer materials to meet the growth and challenges of technological advancement grew with time, the concept of Functionally Graded Materials emerged with a variety of application areas [33] Considering the material combinations, FGMs are classified in to Metal / Ceramic, Ceramic/Ceramic, Ceramic/Plastic and many other combinations of materials.

Table1: List of different types of FGCM [34]

Constraints in Fabrication of FGCM:

Just as developing new engineered materials is an intriguing aspect from the user's view point, at the same point there are issues that need to be addressed and require further study mainly on the following areas [35]:

- Adequate database of the gradient material (including material system, parameters, material preparation, performance evaluation is to be developed.
- A focused research on variation of gradient material be aligned with respect to thermal stress relaxation of the materials as well as keep the road open to different applications in engineering field.
- FGMs prepared are samples of small size, simple structure. More practical valued materials are yet to be developed.
- Cost of manufacturing is high.
- Further research and evaluation of the physical properties of the material model are desired. Microscopic structure and the quantitative relation between preparation conditions have to be established in order to accurately and reliably predict the physical properties of graded materials.

Improved continuum theory, quantum (discreet) theory, percolation theory, microstructure model, advanced simulation facility with high end computing facility for simulating the material properties for theoretical prediction of the functionally graded composite characteristics

Novel design concepts of FGCMs with new research and development initiatives:

a) Design of FGCMs: T. Fukushima et al (1990) Studied about FGM design including material design, material preparation and evaluation of material properties. FGM design is a sort of reverse design process i.e first the ultimate structure of the material is conceived along with its ambient application conditions, then from the FGM design data base suitable material, various transitional components of the properties and microstructure as well as the preparation and evaluation methods and then the design is

framed up. According to Fukui. Y. et al [36], FGM design consists of three primary components:

- To determine structure and shape, Thermo-Mechanical boundary conditions and the composition distribution function.
- Identify data and composition material for thermal parameter model
- The use of suitable mathematics-mechanical calculation methods, including FEL for calculation of stress distribution of FGM, using common self developed CAD software. Use of CAD system for design of FGM is primarily aimed at optimizing the design.

b) **Fabrication of FGCMs:** When FGM preparation is undertaken the primary focus is on the appropriate means to achieve the composition of the FGM. The microstructure should be distributed as designed to achieve the designed performance of the said FGM. There are a variety of methods such as:

- Powder densification methods such as Powder Metallurgy (PM) process
- Self Propagating High-temperature Synthesis (SHS) process
- Coating Methods: Plasma Spray, Laser cladding, Electro-deposition method, Vapor deposition (physical vapor deposition and chemical vapor deposition) methods etc.

Case Study on fabrication of Al/SiC FGCM using PM route:

Many methods for producing powders have been developed and standardized for commercial exploitation, such as through electrolytic deposition, chemical reactions, grinding or comminution. These methods allow mass production rates of powder form materials. In PM process, the main criteria are focused on the precise weighing of the powders and the dispersion of the same in the mixture. These elements will affect the structural properties and hence be handled carefully.

The next step is compacting operation and is performed at room temperature while sintering is done at atmospheric pressure as elevated-temperature if used, may cause other reactions, which may affect the materials. At this stage, the ambient condition must be appropriate since high-temperature process has high sensitivity to the surroundings.

Discussed case study revealed the effect of systematic reinforcement of SiC in layers to change the physico-metallurgical properties of the functionally graded composite material and this can be tailored for and intended use. The hardness of Aluminium-Sic composites increased with increasing wt. percentage of SiC due to dispersion hardening effect. Changes in the hardness of fabricated Aluminium-SiC FGCM have bright scopes for future aerospace application programs.

Applications of FGCMs:

- FGM was originally developed for aerospace application to sustain high thermal barrier coatings such as rocket nozzle (TiAl-SiC fibers),
- Engine parts (Be-Al), Heat Exchanger panels, wind tunnel blades, Spacecraft truss structure etc. With the continuous development in the field of FGM research, it is evident that the composition, structure and properties of gradient changes can be adjusted in an effective manner suiting a particular application [39].

- The use of FGM later expanded further in to fields of industrial applications, automobile sector such as combustion chamber (SiC-SiC), Liners for engine cylinders (Al-SiC),

- CNG storage cylinder, diesel engine pistons(SiC_w / Al Alloy), Leaf springs, brake rotors, drive shafts (Al-C), Fly wheels,

- Defense applications (Special type of armour development), Applications for Naval use focusing on submarine equipments (propulsion shafts (carbon & glass fibers)), cylindrical pressure hulls, (Graphite epoxy), sonar domes (glass / epoxy) composite piping systems etc and many more.

CONCLUSION:

The development of FGMs has opened up the path to new engineered materials for exclusive applications in areas such as aerospace, automobile, Nuclear Power plant etc. This review concluded that powder metallurgy (PM) is the most suitable technique certainly for mass production and up-scaling of the FGCMs. The selection was strengthened after considering the advantages of the technique such as process cost-effectiveness, reliability of the practical implementation of the process and the high capability of the process to control the quality of the FGCMs.

It's been a great topic for Research and development as well as new application and

has found prominence in all discussions related to material science in recent time. Hence it requires new and novel approaches from all quarters, support and encouragement from research foundations, R & D Laboratories, corporate and engineering fraternity alike.

REFERENCES:

[1]. Lannutti JJ (1994), "Functionally graded materials: Properties, potential and design guidelines", Compos. Eng. 4(1):81-94.

[2]. Shukla A, Jain N, Chona R (2007), "A Review of dynamic fracture studies in functionally graded materials" Strain 43(2):76-95.

[3]. Kiebeck B, Neubrand A, Riedel H (2003). Processing techniques for functionally graded materials. Mat. Sci. Eng. A 362:81-105.

[4]. Miyamoto Y, Kaysser WA, Rabin BH, Kawasaki A, Ford RG (1999). Functionally Graded Materials: Design, Processing and applications (Materials Technology Series) 1st Ed. (Springer, 1999), 352 p.

[5]. M. Niino and S. Maeda, "Recent development status of functionally gradient materials," ISIJ International, vol. 30, no. 9, pp. 699–703, 1990.

[6]. T. Hirano and T. Yamada, "Multi-paradigm expert system architecture based upon the inverse design concept," in Proceedings of the International Workshop on Artificial Intelligence for Industrial Applications, pp. 25–27, Hitachi, Japan, 1988.

[7]. M. Yamanoushi, M. Koizumi, T. Hirai, and I. Shiota, Eds., Proceedings of the 1st International Symposium on Functionally Gradient Materials, Sendai, Japan, 1990.

[8]. Khor, K.A., Gu, Y.W., Dong, Z.L., 1997. Plasma spraying of functionally graded NiCoCrAlY/Yttria stabilized ZrO2 coating using composite powders, Composites and Functionally Graded Materials, vol. 80, pp. 89–105.

[9]. Kwon, P., Crimp, M., 1997. Automating the design process and powder processing of functionally gradient materials, Composites and Functionally Graded Materials, vol. 80, pp. 73–88.

[10]. Fumio Nogata , "Learning about design concepts from natural functionally graded materials "MD Vol 80, Composites & Functionally Graded Materials, ASME, 1997, PP. 11-18.

[11]. Y.D. Lee, F. Erdogan,"Residual/thermal stress in FGM and laminated thermal barrier coatings", International Journal of Fracture, 69 (1995), pp. 145–165.

[12]. J.T. Drake, R.L. Williamson, B.H. Rabin," Finite element analysis of thermal residual stresses at graded ceramic–metal interfaces, Part II: interface optimization for residual stress reduction, Journal of Applied Physics, 74 (1993), pp. 1321–1326.

[13]. S.H. Chi, Y.L. Chung,"Cracking in coating-substrate composites of multi-layered and sigmoid FGM coatings", Engineering Fracture Mechanics, 70 (2003), pp. 1227–1243.

[14]. Z.H. Jin, G.H. Paulino, "Transient thermal stress analysis of an edge crack in a functionally graded material", International Journal of Fracture, 107 (2001), pp. 73–98.

[15]. Y. Y. Yung and D. Munz, "Stress analysis in a two materials joint with a functionally graded material," in Functionally Graded Material, T. Shiota and M. Y. Miyamoto, Eds., pp. 41–46, 1996.

[16]. Z.H. Jin, R.C. Batra," Stresses intensity relaxation at the tip of an edge crack in a functionally graded material subjected to a thermal shock, Journal of Thermal Stresses, 19 (1996), pp. 317–339.

[17]. F. Delale, F. Erdogan, "The crack problem for a nonhomogeneous plane", ASME Journal of Applied Mechanics, 50 (1983), pp. 609–614.

[18]. P. Gu, R.J. Asaro, "Crack deflection in functionally graded materials", International Journal of Solids and Structures, 34 (1997), pp. 3085–3098.

[19]. F. Erdogan, B.H. Wu, "Crack problems in FGM layers under thermal stresses", Journal of Thermal Stresses, 19 (1996), pp. 237–265.

[20]. Z.H. Jin, N. Noda," Crack tip singular fields in nonhomogeneous materials", ASME Journal of Applied Mechanics, 61 (1994), pp. 738–740.

[21]. Erdogan F., Chen Y.F., "Interfacial cracking of FGM/metal bonds", Ceramic Coating, pp. 29–37, 1998.

[22]. S.H. Chi, Y.L. Chung, "Cracking in coating-substrate composites of multi-layered and sigmoid FGM coatings", Engineering Fracture Mechanics, 70 (2003), pp. 1227–1243.

[23]. G. Bao, L. Wang, "Multiple cracking in functionally graded ceramic/metal coatings", International Journal of Solids and Structure, 32 (1995), pp. 2853–2871.

[24]. S. Suresh, A. Mortensen, "Fundamentals of Functionally Graded Materials", Cambridge University Press (1998)

[25]. O. Kesler, M. Finot, S. Suresh, S. Sampath, "Determination of processing-induced stresses and properties of layered and graded coatings: experimental method and results for Plasma-sprayed Ni–Al2O3", Acta Materialia, 45 (1997), pp. 3123–3134.

[26]. J. Woo, S.A. Meguid, "Nonlinear analysis of functionally graded plates and shallow shells", International Journal of Solids and Structures, 38 (2001), pp. 7409–7421.

[27]. J.N. Reddy,"Nonlinear transient thermoelastic analysis of functionally graded ceramic–metal plates", International Journal of Solids and Structures, 35 (1998), pp. 4457–4476.

[28]. G.N. Praveen, K.M. Liew, "Active control of FGM plates with integrated piezoelectric sensors and actuators", International Journal of Solids and Structures, 38 (2001), pp. 1641–1655.

[29]. X.Q. He, T.Y. Ng, S. Sivashanker,

[30]. E. Feldman, J. Aboudi," Buckling analysis of functionally graded plates subjected to uniaxial loading", Composite Structures, 38 (1997), pp. 29–36.

[31] Schwartz M, "Encyclopedia of smart materials: Smart Materials", Vol. 2. (Wiley-Interscience, 2002), 1176 p.

[32]. C.S. Lee, J.A. Lemberg, D.G. Cho, J.Y. Roh, R.O. Ritchie, "Mechanical properties of Si3N4–Al2O3FGM joints with 15 layers for high-temperature applications." Journal of the European Ceramic Society 30 (2010) 1743–1749.

[33]. N. Konda, F. Erdogan, "The mixed mode crack problem in a nonhomogeneous elastic medium", Engineering Fracture Mechanics, 47 (4) (1994), pp. 533–545.
[34]. M. Gasik, A. Kawasaki, S. Ueda, in: L. Schultz, D.M. Herlach, J.V. Wood (Eds.), "Materials Processing and Development", EUROMAT'99, vol. 8, Munich, Germany, 27–30 September 1999, pp. 258–264.
[35]. V. Richter, in: B. Ilschner, N. Cherradi (Eds), 1995. FGM'94 Proceedings of the 3rd International Symposium on structural and Fundamental Gradient Materials, 1994, Presses Polytechniques et Universitaires Romandes, Lausanne, pp. 587-592.
[36]. M. Yuki, T. Murayama, T. Insawa, A. Kawasaki, R. Watanabe, in: M. Yamanouchi, M. Koizumi, T. Hirai, I. Shiota (Eds.), FGM'90, Proceedings of the 1st International Symposium on Functionally Gradient Materials, Sendai, 1990, FGM Forum, Tokyo, 1990, pp. 203–208.
[37]. Y. Fukui, "Fundamental investigation of functionally gradient material manufacturing system using centrifugal force," JSME International Journal, vol. 34, no. 1, pp. 144–148, 1991.
[38]. M. Koizumi, "The concept of FGM. Ceramic transactions," Functionally Gradient Materials, vol. 34, pp. 3–10, 1993
[39]. M. Yamanoushi and M. Koizumi, "Functionally gradient materials," in Proceedings of the 1st International Symposium on Functionally Graded Materials, Sendai, Japan, 1991
[40]. N.Cherrad, 1995, Production and Application of Functionally Graded Materials by Powder Metallurgy-European Activities, in: Proceedings of the Euro PM'95, Birmingham, UK, 23-25, pp.632-638.

[33].N. Konda, F. Erdogan, "The mixed mode crack problem in a nonhomogeneous elastic medium", Engineering Fracture Mechanics, 47 (4) (1994), pp. 533–545.
[34].M. Gasik, A. Kawasaki, S. Ueda, in: L. Schultz, D.M. Herlach,J.V. Wood (Eds.), "Materials Processing and Development", EUROMAT'99, vol. 8, Munich, Germany, 27–30 September 1999,pp. 258–264
[35].V.Richter,in: B Ilschner, N.Cherradi (Eds), 1995. FGM'94 Proceedings of the 3rd International Symposium on structural and Fundamental Gradient Materials,1994, Presses Polytechniques et Universitaires Romandes, Lausanne, pp. 587-592.
[36].M. Yuki, T. Murayama, T. Irisawa, A. Kawasaki, R. Watanabe, in: M. Yamanouchi, M. Koizumi, T. Hirai, I. Shiota (Eds.), FGM'90, Proceedings of the 1st International Symposium on Functionally Gradient Materials, Sendai, 1990, FGM Forum, Tokyo, 1990, pp. 203–208.

[37].Y. Fukui, "Fundamental investigation of functionally gradient material manufacturing system using centrifugal force," JSME International Journal, vol. 34, no. 1, pp. 144–148, 1991.

[38].M. Koizumi, "The concept of FGM. Ceramic transactions," Functionally Gradient Materials, vol. 34, pp. 3–10, 1993

[39].M. Yamanoushi and M. Koizumi, "Functionally gradient materials," in Proceedings of the 1st International Symposium on Functionally Graded Materials, Sendai, Japan, 1991

[40]. N.Cherrad, 1995, Production and Application of Functionally Graded Materials by Powder Metallurgy-European Activities, in: Proceedings of the Euro PM'95, Birmingham, UK, 23-25, pp.632-638.

☆☆☆

STUDY OF COMPRESSIVE STRENGTH OF BLENDED NANO FLYASH PPC CEMENT MORTAR

[1]Ananya Punyotoya Parida
[1]KIIT University, Bhubaneswar

ABSTRACT: Change in the surface energy, surface chemistry, and surface morphology of the particle by reducing the size of particles to nano provides an exceptional surface area-to-volume ratio and, which can be possible by altering its basic properties and reactivity. Here the recent progresses in material science with their use in various concrete researches are discussed. Nano-engineered concrete can be synthesized by incorporating Nano-sized building blocks or objects (e.g., nanoparticles and nanotubes) to control the behaviour of the material and adds novel properties by grafting molecules onto cement particles, and aggregates. Mechanical performances of a variety of materials are being influenced by this, including metals, polymers, ceramic, and concrete composites. Nano fly-ash for example, has been shown to improve workability and strength in concrete in this paper. Substitute material is named so because its particles possess size in both Nanolevel which was obtained from particle size analysis data. Further this sample is authenticated by compressive strength, SEM, XRD, acid test, alkalinity test and testing of cubes in salt water was done.

Here the strength properties of cement mortars with Nano-fly ash were experimentally studied. The rate of the reaction is proportional to the amount of surface area available for reaction. Therefore, it is plausible to add Nano-fly ash particles in order to make high-performance concrete. In this study cement is substituted with Nano fly-ash at (2%, 4%, 6% & 8% by weight) the result from the experiment shows that the compressive strengths of mortars with 6% Nano fly-ash particle is highest than those of plain cement mortars and maximum among the blended specimens at 7 and 28 days. Also it was found that the resistant towards acid and alkali is maximum in case of 6% nano flyash intringed mortar samples. It is demonstrated that the Nano incorporated particles are more valuable in enhancing strength. The results of these experiments indicate that Nano scale fly ash behaves not only as a filler to improve microstructure, but also as an element to enhance the compressive strength. It makes the construction process quick and economical.

1. INTRODUCTION

Various products generated from the Cement industry consists cement as well as releases different harmful waste into the environment which is harmful for us. The pollution may be reduced by reducing the use of cement to some extent, which indirectly reduces its production. As we know without cement concrete structures are impossible, so cement can be blended with different supplementary cementitious material to form blended cement and can be used instead of cement. Supplementary cementitious materials are those materials which are added in concrete as a part of the total cementitious component reducing the amount of cement to be used. It also helps to increase the strength of the concrete from normal to higher strength. Some of the supplementary cementitious materials such as fly-ash, micro-silica, Nano lime, Nano TiO2, Nano Fe2O3 , Nano CaCO3, Nano Al2O3 GGBS (ground granulated blast furnace slag), carbon nanotubes, calcinated shale's and many more are those which are generally blended with

cement which contributes to the chemical and physical properties.

In this experiment cement is replaced with Nano sized flyash at (2%,4%,6% & 8%).by weight respectively which reduces the voids in concrete increasing the compressive strength and enhancing different physical properties. Nano sized fly-ash possesses size around 10-9 m which makes the concrete or mortar void free. This also decreases the absorption of water in mortar and concrete.

In the recent years researchers have started using nano particles in concrete industry as admixtures to improve its strength. Nano aluminium oxide, Nano Iron oxide ,Nano zinc oxide, Nano slag, Nano silica and Nano fly ash are used in concrete .undoubtedly its production is costly but it provides better strength .from the literatures it is clear that using Nano particle in concrete mechanical

properties as well as microstructure of the specimen has been improved. Most of the researchers had done a small quantity Nano sized admixtures because of its higher cost of production.

1.1. OBJECTIVE OF PRESENT STUDY

The specific objectives of the present study are as below.

1. Preparation of nano fly ash by grinding 15hrs in ball mill.
2. Addition of nano fly ash in cement mortar.
3. Various tests to analyse the compressive strength, water absorption test, durability test.
4. For study of microstructure XRD and SEM test is to be performed.
5. Casting of mortar specimens with 2%, 4%, 6%, 8% replacement with nano flyash
6. Study the influence of compressive strength of various cement mortars with different percentage (2%, 4%, 6%, 8%) by using Nano fly-ash as partial replacement of cement at 7days, 14 days, 28 days, 56 days respectively.
7. To study the water absorption tests of various n-FA mortar samples having (2, 4, 6 and 8) % of Nano fly-ash as partial replacement with cement at 28 days.

2. EXPERIMENTAL WORK

2.1. PREPARATION OF NANO FLYASH

The attempt has been made to modify the micro sized fly ash into nano structured fly ash using High Energy Ball Mill. The smooth, glassy and an inert surface of the fly ash can be altered to a rough and more reactive state by this technique. Dry Ball milling was carried out for the total duration of 15 hours. The sample was taken out after every 5 hours of milling for characterizing. The nano structured fly ash was characterized for its crystallite size, lattice strain and percentage of crystallinity by using X-Ray Diffractometer. It was found that for the 10 hrs milling, the crystallite size was reduced from 92 nm to 29 nm and the percentage of crystallinity got reduced from 63% to 38%. The size, shape and texture of the fresh as well as nano structured fly ash were studied using Scanning Electron Microscopy (SEM).

2.2. CEMENT

Cement used in the experimental work is PORTLAND POZZOLANA CEMENT (PPC_c) conforming to IS: 1489.1.1981

2.3. N-FLY ASH

Here fly ash in terms of nano Fly ash is used as filling element in cement mortar as well as to improve the strength properties.

2.4. FINE AGGREGATE

In this project all types of casting of mortar specimens were made using Indian standard sand of three grades of equal quantities.

2.5. WATER

Clean and portable water free from colour and odour and normal pH value was used in this project for casting and curing of samples.

2.6. PREPARATION OF NANO MORTAR SPECIMEN

Using standard mix proportion of 1:3 the mortars samples prepared as per IS 2386(part 6):1963 using standard specimen cubes of size 7.06 cm, for compression testing of the specimens. n-FA were added at percentages of (2, 4, 6, 8) % respectively. These samples were cured for 7days, 28days and 56 days before test.

2.7. COMPRESSIVE STRENGTH

Sample prepared for the compression strength test is listed as below.

sl no	Sample code	Cement in gm per cube	% of n-FA added	Sand in gm per cube
1	N	200	0	600
2	N2	196	2	600
3	N4	192	4	600
4	N6	188	6	600
5	N8	184	8	600

3. RESULTS AND DISCUSSION

3.1. SEM OF NANO FLYASH

The surface morphology and the grain sizes was determined by this and results were determined in the figures given below.

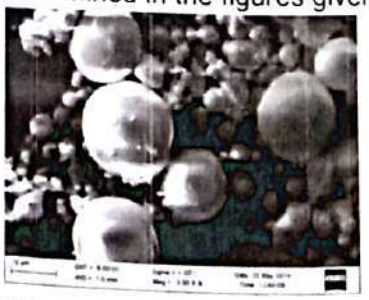

Fig 2. SEM of bulk FA

Fig 3 image of 15Hr grind nano FA sample

Fig 4 image of 0% nano flyash added mortar

Water absorption test of cubes	
Name of sample	%Water Absorption
M	1.170
M2	1.230
M4	1.001
M6	**0.899**
M8	0.986

sample

Fig 5 image of 2% nano flyash added mortar sample

Fig 6 image of 4% nano flyash added mortar sample

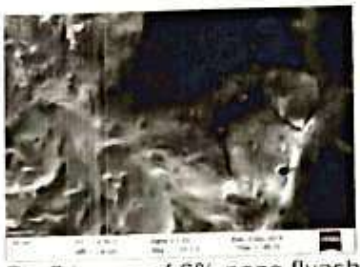

Fig 7 image of 6% nano flyash added mortar sample

Fig 8 image of 8% nano flyash added mortar sample

3.2. XRD

The X-ray technique was used to determine the particle size and percentage of crystallinity of the samples

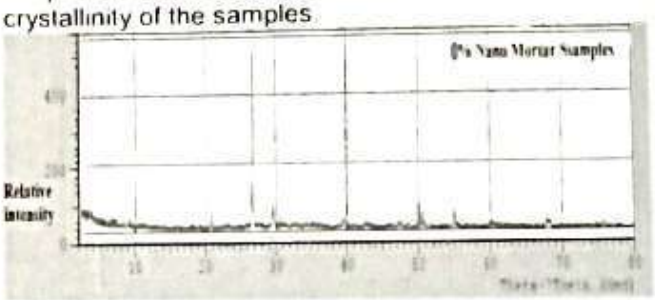

Fig 9. XRD plot for cube specimens having 0% nano flyash

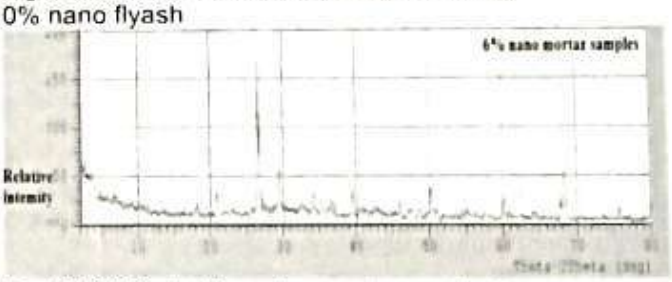

Fig 10. XRD plot for cube specimens having 6% nano flyash

3.3. COMPRESSIVE STRENGTH

Compressive strength of the prepared specimens were determined in the laboratory using compression testing machine and the results were analysed below.

No of cubes	Cube Size In cm^2	% of nano flyash in mortar	28 DAYS strength in(Mpa)	56 DAYS strength in(Mpa)
M1	49.9	0	31.463	42.345
M2	49.9	2	30.842	41.692
M4	49.9	4	33.006	41.333

M6	49.9	6	42.255	46.202
M8	49.9	8	37.595	40.361

Table: 2. Compressive Strength of cube at 28 and 56 days.

3.4. WATER ABSORPTION

The following table represents the percentage of water absorbed by the samples after curing days.

Table : 3. Water absorption relation of samples at 28 days.

4. CONCLUSION

1. The compressive strength of 2%,4%,6%,8% nano mortar specimens was found out at, 28 days, 56 days respectively.
2. The increase in compressive strength of 6% nano mortar specimens was found out to be highest among all the proportions of nano mortar specimens at 28 days, 56 days respectively.
3. From the table of water absorption it is clear that PPC mortar sample having 6 percent of nano fly ash possess least water absorption capacity.

ACKNOWLEDGEMENT

It is with immense pleasure that I express my sincere sense of gratitude and humble appreciation to Prof Dillip Kumar Bera ,School of Civil Engineering, being a constant inspiration source for me throughout this project work. Without his support and guidance, the present work would have remained a dream. I specially thank to Dr Ashoke Kumar Rath for supporting and guiding me.

All my friends and colleagues, School of Civil Engineering KIIT UNIVERSITY, are acknowledged for providing a friendly atmosphere which encouraged me throughout my work.

I take this opportunity to thank my family for their valuable support and encouragement throughout the preparation of this work. I also thank all those who have directly or indirectly helped in completion of this work. Besides this I am grateful to LARPM labs (CIPET) for determination of XRD and SEM of samples.

5. REFERENCE

[1] Minerals.usgs.gov/minerals/pubs/mcs/2012/mcs2012.pdf

[2] A.K. Mukhopadhyay, Next-generation nano-based concrete construction products: A review, in: Gopalakrishnan, B. Birgisson, P. Taylor, N. Olkhine (Eds.) Nanotechnology in infrastructure, p 207-223, Springer (2011), ISBN 978-3-642-16656-3

[3] Heikal Mohamed, AbdEL Aleem S., Morsi W. "characteristics of blended cement containing nano-silica",HBRC Journal (2013) 9, 243-55

[4] Byung-Wan Jo, Chang-Hun Kim, Ghi-ho Tae, Jong-Bin Park "Characteristics of cement Mortar with nano-SiO2 particles" ,construction and building materials 21(2007)1351-5

[5] Liu Jianzhong, Sun Wei, Miao changwen , Li Jiaping. "effect of mineral admixtures on the hydration heat of mortar in super high strength concrete" ,1st International conference on microstructure related durability of cementitious composites 13-15 october 2008, Nanjing ,china

[6] M. Cabeza, P. Merino, A. Mirand, X.R. Nó voa, Sanchez "Impedance spectroscopy study of hardened Portland cement paste", Cement and Concrete Research 32 (2002) 881–891

[7] Tamtsia T. Basile, Beaudoin J. James, and Marchand Jacques "A Coupled AC Impedance , Creep and Shrinkage Investigation of Hardened Cement Paste" NRCC-43925, Materials and Structures, v. 36, April 2003, pp. 147-155.

[8] Alaa M. Rashad , Sayieda R. Zeedan "A preliminary study of blended pastes of cement and quartz powder under the effect of elevated temperature" , Construction and Building Materials 29 (2012) 672–68

[9] Sánchez , X.R. Nóvoa , G. de Vera , M.A. Climent "Microstructural modifications in Portland cement concrete due to forced ionic migration tests. Study by impe- dance spectroscopy", Cement and Concrete Research 38 (2008) 1015–25

[10] Niloofar Salemi , Kiachehr Behfarnia, "Effect of nano-particles on durability of fiber-reinforced concrete pavement", Construction and Building Materials 48 (2013) 934–41

[11] M. Stefanidou , I. Papayianni, "Influence of nano-SiO2 on the Portland cement pastes" Composites Part B 43 (2012) 2706–10

[12] Min-Hong Zhang, Jahidul Islam, Sulapha Peethamparan, "Use of Nano-silica to increase early strength and reduce setting time of concretes with high volumes of slag" Cement & Concrete Composites 34 (2012) 650–62

[13] Rahel Kh. Ibrahim, R. Hamid, M.R. Taha "Fire resistance of high-volume fly ash mortars with nanosilica addition" Construction and Building Materials Volume 36, November 2012, Pages 779–86

[14] Min-Hong Zhang , Jahidul Islam "Use of nano-silica to reduce setting time and increase early strength of concretes with high volumes of fly ash or slag" Construction and Building Materials 29 (2012) 573–80

[15] Ye Qing , Zhang Zenan , Kong Deyu , Chen Rongshen "Influence of nano-SiO2 addition on properties of hardened cement paste as compared with silica fume" , Construction and Building Materials 21 (2007) 539–45

[16] Ali Nazari, Shadi Riahi "Al2O3 nanoparticles in concrete and different curing media", Energy and Buildings 43 (2011) 1480–8
[17] Ali Nazari , Shadi Riahi" The effects of zinc dioxide nanoparticles on flexural strength of self-compacting concrete", Composites: Part B 42 (2011) 167–75
[18] Deyu Konga, Xiangfei Dua, Su Weia, Hua Zhanga, Yang Yanga, Surendra P. Shahb, "Influence of nano-silica agglomeration on microstructure and properties of the hardened cement-based materials", Construction and Building Materials, Volume 37, December 2012, Pages 707–15
[19] G.Reddy Babu," Effect of nano-silica on properties of blended cement", International Journal of Computational Engineering Research, Vol, 03,Issue, 5
[20] A. Sadrmomtazi, A. Fasihi, F. Balalaei, A.K. Haghi "Investigation Of mechanical And physical Properties Of mortars containing silica fume and nano SiO2" , International Conference on Concrete & Development,page-1153-61
[21] Ali Nazari , Shadi Riahi" The effects of zinc dioxide nanoparticles on flexural strength of self-compacting concrete", Composites: Part B 42 (2011) 167–75
[22] Tao Meng , Yachao Yu , Xiaoqian Qian , Shulin Zhan , Kuangliang Qian ," Effect of nano-TiO2 on the mechanical properties of cement mortar", Construction and Building Materials 29 (2012) 241–245
[23] Sri Tudjono, Purwanto, Kartika Trisna Apsari, "Study the effect of adding Nano fly ash and Nano lime to compressive strength of mortar" SCESCM 2014, Procedia Engineering 95 (2014) 426 – 32
[24] Hosseinpourpia R., Varshoee A, Soltani M , Hosseini P," production of waste bio-fiber cement-based composites reinforced with nano-SiO2 particles as a substitute for asbestos cement composites" ,Construction and Building Materials Journal 31(2012) 105-11
[25] A.Boshehrian, P.hosseini, "Effect of nano- SiO2 particles on properties of cement mortar applicable for ferrocement elements", Concrete research letters , vol-2(1) march 2011
[26] L.E. Zapata-Orduz, G.Portela, O.M Suárez "Weibull statistical analysis of splitting tensile strength of concretes containing classF fly ash,micro/nano-SiO2", Ceramics International40(2014)7373–88
[27] Sayed ABD EL-Baky, Sameh YEHIA, Ibraham S. Khalil, "influence of nano silica addition on properties of fresh and hardened cement mortar", housing and building research , nanocon 2013
[28] Nima Farzadnia ,Abang Abdullah Abang Ali , Ramazan Demirboga, Nima Farzadnia ,"Characterization of high strength mortars with nano alumina at elevated temperatures", Cement and Concrete Research 54 (2013) 43–54
[29] Guanghui Bail, Wei Tengl, Xianggang Wangl, Hui Zhang and Peng Xul, "Kinetic and Processing Studies on a Novel Technology of Producing High Purity Nano-Silicon Dioxide from an Alumina Rich Coal Fly Ash with Carbon Dioxide", 2009 IEEE 978-1-4244-4630-8/09
[30] B. Karthikeyan, K. Sumanth, G. Harshavardhan, A. Rajasekharareddy and G. Dhinakaran," Microstructure analysis and Strength properties of concrete with Nano SiO2" , International Journal of ChemTech Research, ISSN 0974-4290 ,Vol 6, No 5, pp 3004-13, Aug-Sept 2014
[31] K. Thomas Paul , S. K. Satpathy , I. Manna, "Preparation and Characterization of Nano structured Materials from Fly Ash: A Waste from Thermal Power Stations, by High Energy Ball Milling" , Nanoscale Res Lett (2007) 2:397–404
[32] Yuvraj .s, vimal raj.D," Experimental Research on Improvement of Permeability Factor in Flyashed Nano Silica Concrete" ICCTET-2014,ciombatore,India, page no. 63-6
[33] Hui Li, Hui-gang Xiao, Jie Yuan, Jinping Ou "Microstructure of cement mortar with Nano-particles" science direct journal ,Composites: Part B 35 (2004) 185–9
[34] Byung-Wan Jo, Chang-Hun Kim, Ghi-ho Tae, Jong-Bin Park "Characteristics of cement Mortar with nano-SiO2 particles" ,construction and building materials 21(2007)1351-5
[35] Heikal Mohamed, AbdEL Aleem S., Movsi W.M, "characteristics of blended cement containing nano-silica",HBRC Journal (2013) 9, 243-55
[36] L.Y. Yang , Z.J. Jia , Y.M. Zhang, J.G. Dai "Effects of nano-TiO2 on strength, shrinkage and microstructure of alkali activated slag pastes", Cement & Concrete Composites 57 (2015) 1–7
[37] J. Babu Rao1 , P. Narayanaswami and K. Siva Prasad "Thermal stability of nano structured fly ash synthesized by high energy ball milling", International Journal of Engineering, Science and Technology Vol. 2, No. 5, 2010, pp. 284-99.
[38] Canadian Standards Association, Supplementary cementing materials and their use in concrete construction. CSA, Rexdale, ON, CAN-A23.5-M82, 1982
[39] American Society for Testing and Materials, Specification for fly ash and raw of calcined natural pozzolan for use as a mineral admixture in Portland cement concrete, ASTM, Philadelphia, PA, ASTM C618-78, 1978
[40] Subhash V. Patankar, Yuwaraj M. Ghugal, and Sanjay S. Jamkar "Effect of Concentration of Sodium Hydroxide and Degree of Heat Curing on Fly Ash-Based Geopolymer Mortar" Indian Journal of Materials Science, Volume 2014 (2014), Article ID 938789

Experimental Investigation Of Physical, Mechanical And Electrical Properties Of Cement Mortar Using Nano Fly-Ash

[1]Abhijit Mangaraj
[1]KIIT University, Bhubaneswar

ABSTRACT: *Mechanical performances of a variety of materials are being influenced by reducing the surface area, surface chemistry, and surface morphology of the particle this, including metals, polymers, ceramic, and concrete composites. Nano-engineered concrete can be synthesized by incorporating Nano-sized building blocks or objects (e.g., nanoparticles and nanotubes) to control the behaviour of the material and adds novel properties by grafting molecules onto cement particles, and aggregates. Micro/Nano fly-ash for example, has been shown to improve workability and strength in concrete in this paper. Substitute material is named so because its particles possess size in both Nano and micro level which was obtained from particle size analysis data. Further this sample is authenticated by compressive, flexural, water absorption, SEM, XRD and LCR tests.*

Here the strength properties of cement mortars with Nano-flyash were experimentally studied. The rate of the reaction is proportional to the amount of surface area available for reaction. Therefore, it is plausible to add Nano-flyash particles in order to make high-performance concrete. In this study cement is substituted with Nano fly-ash at (10%, 20%, 30% & 40% by weight) the result from the experiment shows that the compressive strength and flexural strength of mortars with 10% Nano fly-ash particle is highest than those of plain cement mortars and maximum among the blended specimens at 7 and 28 days. Also it was found that water absorbed by specimens cast with Nano fly-ash is less than the normal mortar. It is demonstrated that the Nano incorporated particles are more valuable in enhancing strength. The results of these experiments indicate that Nano scale fly ash behaves not only as a filler to improve microstructure, but also as an element to enhance the compressive strength. It makes the construction process quick and economical.

1. INTRODUCTION

1.1. GENERAL

Cement industry produces cement as well as releases different harmful waste into the environment which is harmful for us. The pollution may be reduced by reducing the use of cement to some extent, which indirectly reduces its production. As we know without cement concrete structures are impossible, so cement can be blended with different supplementary cementitious material to form blended cement and can be used instead of cement. Supplementary cementitious materials are those materials which are added in concrete as a part of the total cementitious component reducing the amount of cement to be used. It also helps to increase the strength of the concrete from normal to higher strength. Some of the supplementary cementitious materials such as fly-ash, micro-silica, Nano lime, Nano TiO_2, Nano Fe_2O_3, Nano $CaCO_3$, Nano Al_2O_3, GGBS (ground granulated blast furnace slag), carbon nanotubes, calcinated shale's and many more are those which are generally blended with cement which contributes to the chemical and physical properties.

In this research paper cement is replaced with Nano sized fly-ash at (10%, 20%, and 40%) by weight respectively, which reduces the voids in concrete ultimately increasing the compressive strength and enhancing different physical properties. Nano sized fly-ash possesses size around 10^{-9} m which makes the concrete or mortar void free. This also decreases the absorption of water in mortar and concrete.

Pozzolans increases the mechanical strength and durability of concrete structure when added to Portland cement. They improve strength by bringing changes in microstructure of the cementitious paste and also in the pore structure by reducing the grain size caused by the pozzolanic reactions and the effect (PE) by reducing the pores and voids by the action of the finer grains [1]. Mineral admixtures such as Micro-silica, Rice hush Ash, Fly ash, bagasse ash [2] which is rich in pozzolanic actions and

Proceedings of IIRAJ International Conference (ICCI-SEM-2k17), GIFT, Bhubaneswar, India, 18th - 19th February 2017, ISBN: 978-93-86352-38-5

fillers like lime stone fillers [3] can be used as a partial replacement for cement in high strength concrete. Several works were performed and are still going on regarding the usage of these mineral admixtures in High Strength Concrete (HSC) and High Performance Concrete (HPC).
properties [4]. Most of the works were done using silicon dioxide Nano particles [5-6]. Some of the works were also performed using Nano Al_2O_3 [7], Nano Fe_2O_3 [8] and Zinc-iron oxide Nano particles [9] as mineral admixtures in concrete. Also the use of Nano sized mineral admixtures were also studied on self-compacting concrete using SiO_2 [10, 11], Fe_2O_3 [12] and ZnO_2 [13, 14].
In addition the effects of several types of Nano particles on properties of concrete specimens which are cured in different curing media were investigated in several works [14]. From the literatures it is clear that using Nano particle in concrete mechanical properties as well as microstructure of the specimen has been improved. Most of the researchers had done using a small quantity of Nano sized admixtures because of its higher cost of production.

1.2. OBJECTIVE OF PRESENT STUDY

The specific objectives of the present study are as below.

1. Study of literature for understanding behaviour of different Nano particles in mortar/concrete.
2. Preparation of Nano fly-ash by using high energy ball milling.
3. Characterization studies of n-FA sample using PSA, XRD
4. Study the influence of compressive strength of various cement mortars with different percentage (10, 20, 30 & 40) by using Nano fly-ash as partial replacement of cement.
5. Study the influence of flexural strength of various cement mortars with different percentage (10, 20, 30 & 40) by using Nano fly-ash as partial replacement of cement.
6. To study the water absorption tests of various n-FA mortar samples having (10, 20, 30 and 40) % of Nano fly-ash as partial replacement with cement.
7. To study the AC Impedance of the sample produced from n-FA cement with respect to normal cement samples by impedance spectroscopy test.

In the recent years many finer particles are being used in concrete industry. Several works has been performed on use of Nano particles in concrete specimens as mineral admixtures to improve physical and mechanical

2. EXPERIMENTAL WORK

2.1. MATERIALS USED

2.1.1. CEMENT

Cement used in the experimental work is ORDIRARY PORTLAND CEMENT of 43 grades conforming to **IS: 8112/2013**

2.1.2. N-FLY ASH

Here fly ash in terms of nano Fly ash is used as filling element in cement mortar as well as to improve the strength properties

2.1.3. STANDARD SAND

In this project all types of casting of mortar specimens were made using Indian standard sand of three grades of equal quantities.

2.1.4. WATER

Clean and portable water free from colour and odour and normal pH value from the college campus was used in this project for casting and curing of samples.

2.2. PREPARATION OF NANO MORTAR SPECIMEN

Using standard mix proportion of 1:3 the mortars samples prepared as per IS 2386(part 6):1963 using standard specimen cubes of size 7.06 cm, for compression testing of the specimens. n-FA were added at percentages of (10, 20, 30, 40) And for flexural strength test the specimens according to ASTM standard of size (40 x 40 x 160 mm) were cast. These samples were cured for 3days, 7days and 28 days before test.

3. RESULTS AND DISCUSSION

3.1 PARTICLE SIZE ANALYSIS OF NANO FLY-ASH

for grinding in high energy ball mill Fly-ash sample was prepared from the sample collected from NALCO plant .At first the sample was sieved properly by using 90 micron sieve to take off the grains and other substances which are mixed in the sample to obtain a more homogeneous sample .then before

starting the milling process the sample was placed in hot air oven to make it moisture free for better grinding.

- The results obtained from the particle size analyser are given in table below.

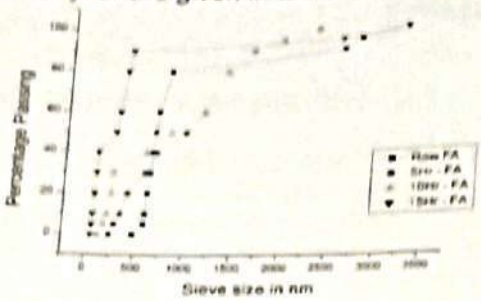

Fig 1. Relationship between % passing at various grind hours.

3.2. SEM OF NANO FLYASH

Sample name	cement %	n-Flyash %	Total Amount used for test	consistency %	Setting Time in minutes	
					initial	final
N	100	0	300 gm	30	153	230
N10	90	10	300 gm	31	160	225
N20	80	20	300 gm	32	166	230
N30	70	30	300 gm	32	175	230
N40	60	40	300 gm	33	190	255

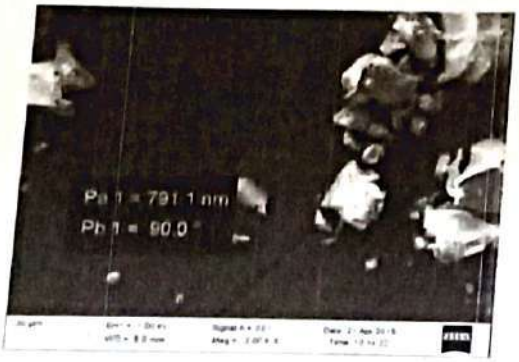

Fig 2. SEM of bulk FA

Fig 3. image of 15Hr grind nano FA sample.

The surface morphology and the grain sizes was determined by this and results were determined in the figures given below.

3.3. PHYSICAL AND RHEOLOGICAL PROPERTY

Standard Sand according to IS 650:1991(reaffirmed 2008) was used. Consistency and initial/final setting time were determined according to the IS codes, IS 4031(Part 4):1988 respectively.

Table:1 Consistency and setting time of blended cement

3.3.1. COMPRESSIVE STRENGTH

Strength developed in the mortar samples was determined in the laboratory using compressive strength testing machine and the values were represented below in the following tables.

SL NO	Sample Name	Size of Cube in cm	Mean strength in Mpa		
			3D	7D	28D
1	N	7.06	19.795	27.33	34.80
2	N10	7.06	20.785	33.34	60.24
3	N20	7.06	21.62	30.79	42.38
4	N30	7.06	19.285	25.95	32.17
5	N40	7.06	17.465	19.735	29.41

Table: 2. Compressive Strength of cube.

Specimen no	Size of prism in mm	MOR in (Mpa)	MOE in (Mpa)	Flexural Strength (N/mm²)
M	160X40X40	0.5	13.19	13.2
M10	160X40X40	0.72	14.28	17.235
M20	160X40X40	0.67	14.16	14.895
M30	160X40X40	0.58	15.84	14.185
M40	160X40X40	0.61	15.58	13.495

3.3.2. FLEXURAL STRENGTH

This test was performed for the determination of strength of the beam/prism specimens in compression and tension directions

Table:3. Flexural strength of Prism specimens

3.3.3. Water Absorption

The following table represents the percentage of water absorbed by the samples after curing days.

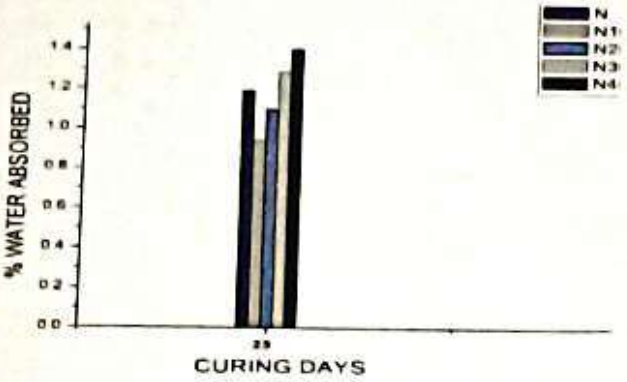

Fig : 4. Waterabsorption relation of samples.

3.4. ELECTRICAL PROPERTIES

3.4.1. AC IMPEDANCE STUDY

Electrical impedance is the measure of the opposition that a circuit presents to a current when a voltage is applied. Impedance extends the concept of resistance to AC circuits, and possesses both magnitude and phase, unlike resistance, which has only magnitude. When a circuit is driven with direct current (DC), there is no distinction between impedance and resistance.

The basis of AC impedance technique is that applying a small alternating voltage on the test material, thus resulting in the corresponding alternating current response, and the impedance of materials in a given frequency can be expressed as:

$Z(\omega) = E(t) / I(t)$

This test result shows the passage of amount of electrical charge through the samples of different proportions at different ages.

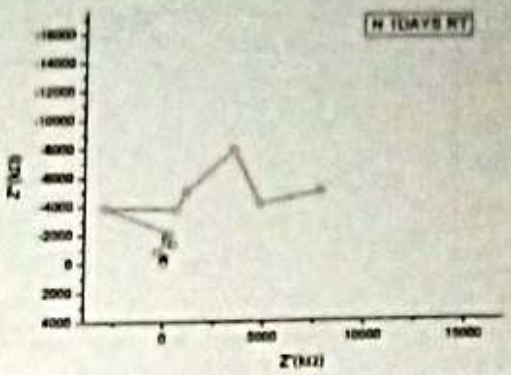

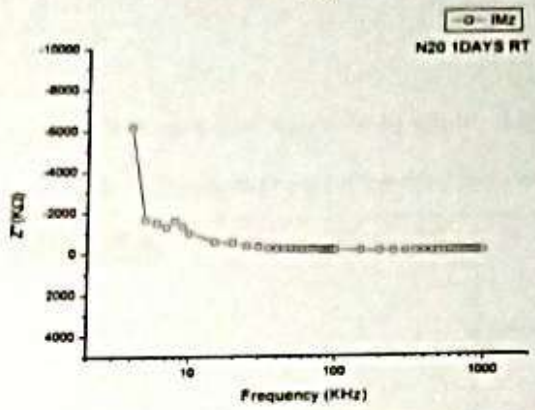

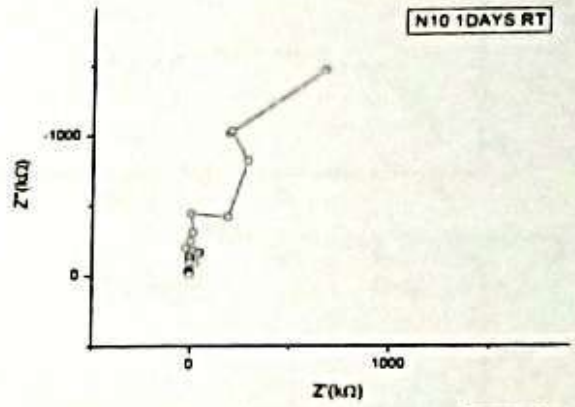

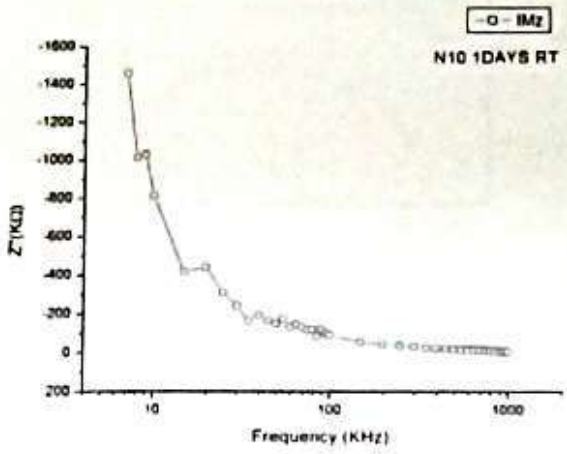

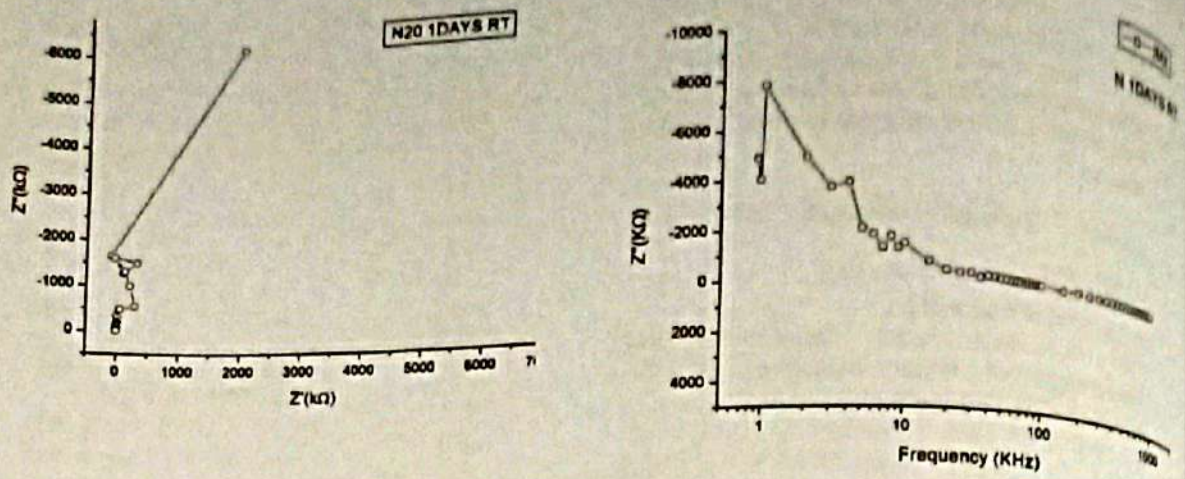

Fig 5. Study of electrical behaviour of blended cement paste samples at 1 day

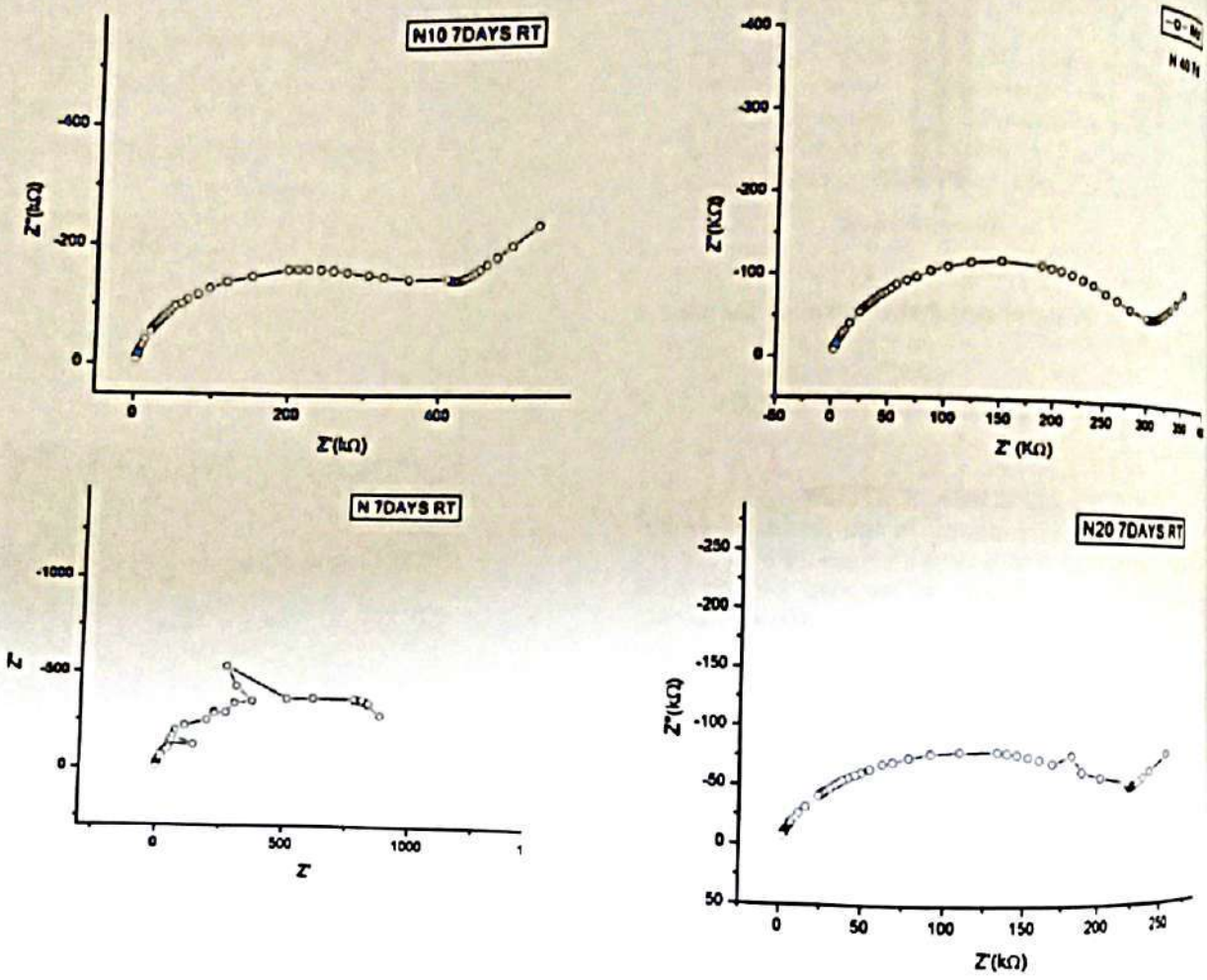

Fig: 6. Study of electrical Behaviour of samples at 7 day

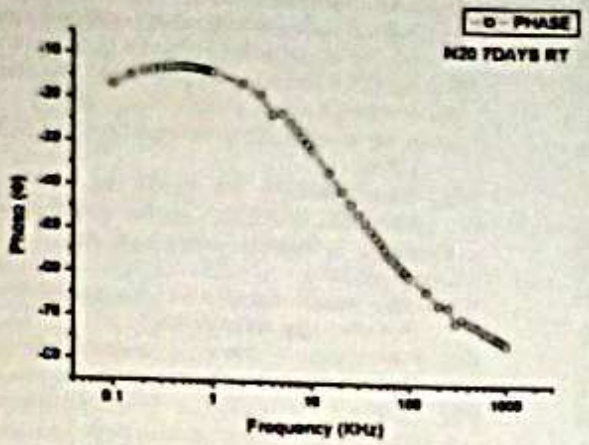

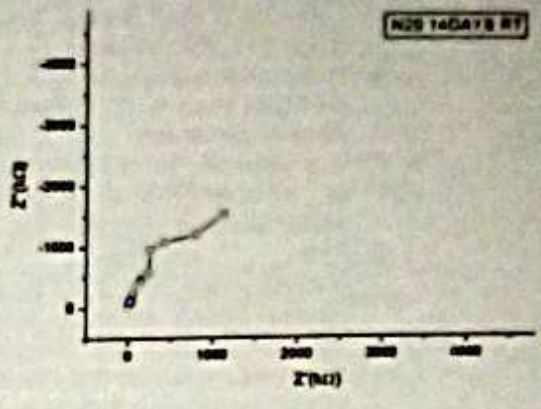

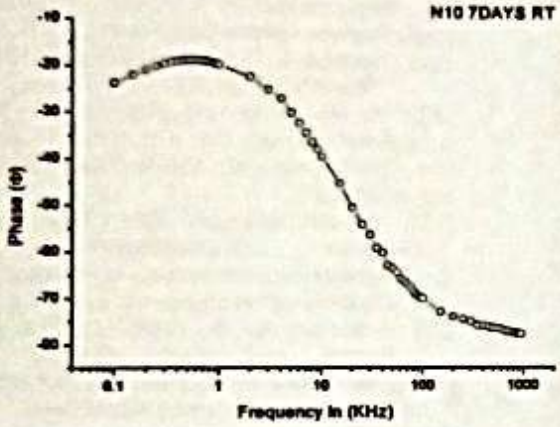

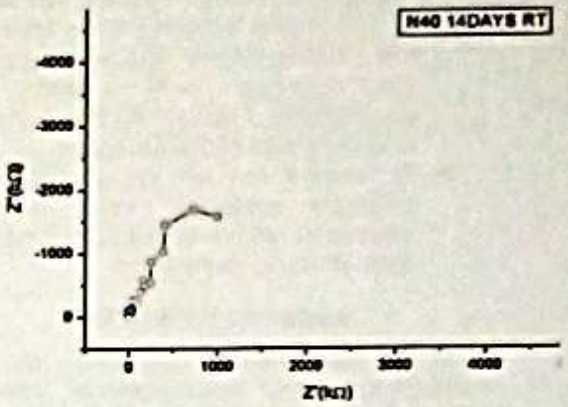

Fig: 7. Study of electrical Behaviour of samples at 14 days.

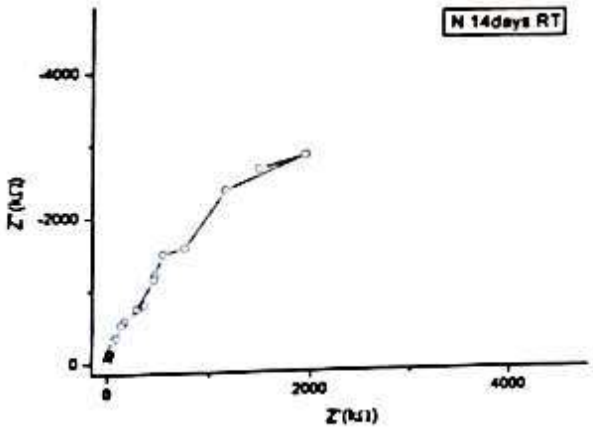

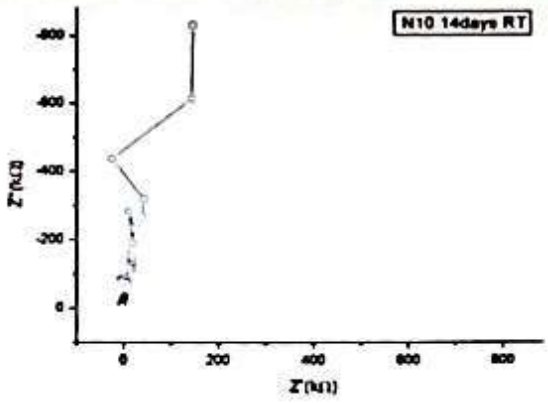

4. CONCLUSION

1. From various characterization study test it is found that 70 % flyash achieves size less than 70 nm.
2. Compressive strength enhanced to 50% with 10 % nano-flyash than that of reference sample after 28 days
3. Flexural strength value of prism cast with 10% nano flyash enhanced to 15% more than that of the reference specimen after 28 days.
4. Mortars blended with 10% nano flyash particles absorbs 22% less water than normal specimen.
5. Improvement of compressive strength is due to improved microstructure and water absorption is also less.
6. From electrical impedance spectroscopy test it is clear that the cement paste samples blended with 10% n-FA particles offers maximum resistance towards the electricity.
7. Which concludes that the pore filling capacity of mortar/ paste is maximum at 10% nano blending. This improves the microstructure and also protects the structure from external ion penetration. Finally improving the life and durability of the structure
8. At present day we are in search for alternate materials which can be effectively achieved through emerging field of nano-technology.

ACKNOWLEDGEMENT

I would never have completed my task successfully without encouragement, help and cooperation provided to me by various persons.

It is with immense pleasure that I express my sincere sense of gratitude and humble appreciation to Prof. Dillip Kumar Bera School of Civil Engineering, being a constant inspiration source for me throughout this project work. Without his support and guidance, the present work would have remained a dream. I specially thank to Dr.A.K.Rath and Dr.S.K.S.Parashar for supporting and guiding me. Special thanks to my younger ones who has supported and brought me to achieve. I take this opportunity to thank my family for their valuable support and encouragement throughout the preparation of this work. I also thank all those who have directly or indirectly helped in completion of this work.

5. REFERENCE

[1] V. Kartik Ganesh,www.engineering civil.com/theory/research papers.com, page 1,2014.

[2] Baer, D. R., Burrows, P. E., and El-Azab, A. A. (2003). "Enhancing coating functionality using Nano science and nanotechnology."

Prog. Org. Coat., 47(3-4), 342356.www.engineeringcivil.com/nanotechnology-in-civil-engineering.html

[3] Lau, Kin-Tak, and David Hui. "The revolutionary creation of new advanced materials—carbon nanotube composites." Composites Part B 33, no. 4(2002):263-277. www.engineeringcivil.com/nanotechnology-in-civil-engineering.html

[4] Mann, S. (2006). "Nanotechnology and Construction," Nano forum Report, www.nanoforum.org, May 30, 2008. www.engineeringcivil.com/nanotechnology-in-civil-engineering.html

[5] ASCE. (2005). "Report card for America's infrastructure. American society of civil engineers" "http://www.asce.org" (Mar. 8, 2008).

[6] Baughman, R. H., Zakhidov, A. A., and de Heer W. (2002). "Carbon nanotubes— the route toward applications." Science, 297(5582), 787–792. www.engineeringcivil.com/nanotechnology-in-civil-engineering.html

[7] Pilkington, http://www.activglass.com/ St. Gobain, http://www.saint-gobain.com/, 2014.

[8] Beatty, C. (2006). "Nanomodification of asphalt to lower construction temperatures." NSF Workshop on Nanotechnology, Material Science and Engineering, National Science Foundation, Washington, DC.

[9] WynandJvdM Steyn, Journal of Transportation Engineering, Vol. 135, No. 10,page 5, October 1, 2009. ©ASCE, ISSN 0733-947X/2009/10-764–772

[10] A. A. Bolonkin, Journal of Aerospace Engineering, Vol. 23, No. 4, October 1, 2010. ©ASCE, ISSN 0893-1321/ 2010/4-281–292

[11] Nanotechnology For Electronics and sensors Applications/Nano connect Scandinavia/www.nano-connect.org Chalmers University of Technology.

[12] Bolonkin, A. A. 2006. Non-rocket space launch and flight, Elsevier, London. (http://www.scribd.com/doc/24056182), (http://Bolonkin.narod.ru/p65.htm January 2005).

[13] WynandJvdM Steyn, Journal of Transportation Engineering, Vol. 135, No. 10,page 5, October 1, 2009. ©ASCE, ISSN 0733-947X/2009/10-764–772

[14] A. A. Bolonkin, Journal of Aerospace Engineering, Vol. 23, No. 4, October 1, 2010. ©ASCE, ISSN 0893-1321/ 2010/4-281–292

[15] Min-Hong Zhang ,Jahidul Islam , "Use of Nano-silica to reduce setting time and increase early strength of concretes with high volumes of fly ash or slag", Construction and Building Materials 29 (2012) 573–80

[16] M. Stefanidou , I. Papayianni, "Influence of nano-SiO2 on the Portland cement pastes", Composites Part B 43 (2012) 2706–10.

[17] RahelKh. Ibrahim, R. Hamid , M.R. Taha. "Fire resistance of high-volume fly ash

mortars with nanosilica addition", Construction and Building Materials, Volume 36, November 2012, Pages 779–86

[18] Liu Jianzhong, Sun Wei, Miao changwen , Liu Jiaping. "effect of mineral admixtures on the hydration heat of mortar in super high strength concrete" ,1st International conference on microstructure related durability of cementitious composites 13-15 october 2008, Nanjing , china

[19] NiloofarSalemi ,KiachehrBehfarnia, "Effect of nano-particles on durability of fiber-reinforced concrete pavement", Construction and Building Materials 48 (2013) 934–41

[20] Gengying Li," Properties of high-volume fly ash concrete incorporating nano-SiO2", Cement and Concrete Research 34 (2004) 1043–9

[21] Sànchez , X.R. Nóvoa , G. de Vera , M.A. Climent "Microstructural modifications in Portland cement concrete due to forced ionic migration tests. Study by impedance spectroscopy", Cement and Concrete Research 38 (2008) 1015–25

[22] Tamtsia T. Basile, Beaudoin J. James, and Marchand Jacques "A Coupled AC Impedance – Creep and Shrinkage Investigation of Hardened Cement Paste" NRCC-43925, Materials and Structures, v. 36, April 2003, pp. 147-155.

[23] Alaa M. Rashad ,Sayieda R. Zeedan "A preliminary study of blended pastes of cement and quartz powder under the effect of elevated temperature" , Construction and Building Materials 29 (2012) 672–68

[24] M. Cabeza, P. Merino, A. Mirand, X.R. No´voa, I. Sanchez "Impedance spectroscopy study of hardened Portland cement paste", Cement and Concrete Research 32 (2002) 881–891

[25] Canadian Standards Association, Supplementary cementing materials and their use in concrete construction. CSA, Rexdale, ON, CAN-A23.5-M82, 1982

[26] American Society for Testing and Materials. Specification for fly ash and raw of calcined natural pozzolan for use as a mineral admixture in Portland cement concrete, ASTM,Philadelphia, PA, ASTM C618-78, 1978

[27] Mudroch, Alena (1997). Manual of Physico-Chemical Analysis of Aquatic Sediments. Lewis Publishers, p. 30.

[28] Mc Cave, I. N., R.J. Bryant; H. F. Cook; C. A. Coughanowr (July 1986). "Evaluation of a Laser Diffraction Size AnalyzerFor Use With Natural Sediments" Journal of Sedimentary Research 56 (4): 561–564.doi: 24 October 2013.

[29] Khandaker, N.I., Ahmed, M., Garwan, M.A., 1996. Study of volcanic sediments by microbeam-PIXE, technique. Nucl. Instrum. Methods B 109/110, 587.

[30] Science, p. 18, 1888

[31] Oliver Heaviside, The Electrician, p. 212, 23 July 1886, reprinted as Electrical Papers, p 64, AMS Bookstore, ISBN 0821834657

[32] Kennelly, Arthur. Impedance(AIEE,1893) (http://ieeexplore.ieee.org/xpls/abs_all.jsp?arnumber=4768008)

[33] Alexander, Charles; Sadiku, Matthew (2006). Fundamentals of Electric Circuits (3, revised ed.). McGrawHill. pp. 387–389. ISBN 9780073301150.

[34] W.J. McCarter, R. Brousseau, The a.c. response of hardened cement paste, Cem. Concr. Res. 20 (1990) 891–900.

★ ★ ★

An overview on Public Transport System

[1] Patitpaban Panda, [2] Prof. Sudhansu Sekhar Das
[1] Department of Civil Engineering SOA University,[2] Department of Civil Engineering, VSSUT, Burla

Abstract:- In urban areas of developing countries, the majority of private vehicle ownership of two-wheelers and four wheelers are increasing. This can be attributed to many factors but can be mainly attributed to the increase in income of normal public, improvement in road quality and unreliable public transport. On the other side, increase in private vehicles has resulted in congestion on the roads, increased pollution, road accidents, thus causing the need of robust Public Transport System. In this paper the authors are exploring the causes for increase in private owned vehicles, their impact on pollution, road safety and congestion roads and ways and means to discourage the private transport and go for a viable public transport system.

Index Terms— pollution, impact, congestion and robust

I. INTRODUCTION

Over the years the two wheeler and four wheeler population in India have gone up very rapidly. There was a manifold increase in the private owned vehicles

Year	Air vehicles (000's)	Two Wheelers	Cars, Jeeps and Taxis	Buses	Goods vehicles	Others**
1991	30275	20831	3841	423	3794	3808
1996	81786	53212	8204	681	2093	3850
1997	67812	45728	6612	684	2381	4104
1998	83368	58642	5138	548	2536	4514
1999	68871	51318	5556	540	2554	4897
2000	69851	54138	5143	553	2715	5319
2001	54993	38174	7058	638	2948	5795
2002	58524	41181	7611	645	2978	6121
2003	61951	41515	8199	721	3492	6616
2004	72718	51927	9451	768	3743	6829
2005	81494	58795	10133	832	4039	7457
2006	89638	64743	11526	992	4496	7521
2007	96707	69729	12683	1150	5114	8460
2008	105158	75376	13950	1427	5603	9179
2009	114953	82402	15313	1486	6048	9713
2010	127746	91538	17109	1527	6832	11080
2011	141866	101855	19231	1604	7864	12312
2012	159493	115415	21568	1677	7618	13165
2013	182665	132550	24814	1804	8797	14511

Table: 1 Increase of Private owned vehicles in India (Source: Ministry of Road Transport and Highways)

The abnormal increase in private owned vehicles has increased in Air Pollution, Road Accidents and congestion of roads.

Private owned Vehicles: People prefer Private owned vehicles for the following reasons

1. Ease of comfort-

If you have a private car, you will not have to go to work in a crowded bus everyday and still worry about if you are going to be late. And when you want to travel in someplace, driving by yourself in your own car is the most convenient and comfortable way. The main advantage of owning a car is it

gives the freedom to travel. If you have a car then you don't need to be limited to fixed routes and timetables Moreover, a car-owner can take is/her family members with him/her and other necessary goods whenever he/she wish which might have been impossible otherwise Having more comfortable seats, ventilation or other novel technologies help people to feel better than using other methods, like a bicycle or a public bus Users have a more secure privacy compared to using public transportation.

A primary consideration of travelers should bewhether they can actually get to the places

that they wish to visit via public transportation. In some communities, routes can be very limited, which can be a major disadvantage for travellers who do not have an alternative means of getting around. If a traveler does visit a place where the main attractions or accommodation options are not near public transportation routes, he or she may need to inquire about private transportation services, such as taxicabs.

There is a limited amount of space aboard public transportation systems, which makes them inappropriate for some errands. This is a concern if you are traveling with children who have specialized needs, like strollers, or are going on a major shopping venture which could result in excessive luggage on the return trip. You may not be allowed to take these items onto public transportation with you if they will not fit under your seat or in your lap.

2. Time convenient.

As per own schedule we can go any where with our family members at any time and at any place as per our convenience.

The access time and egress time can be scheduled as per our convenience.In case of public transport we have limited choice of visiting multiple locations with in the time limit, but it is possible if we are using private vehicle.

3.Completing the work as planned.

If a person is having the private vehicle he /she can planned a programme as per his /her convenience.Work can be easily be finished in time due to availability of private vehicle which can be used when required.

4 Uncertainty of public transport in terms of time, frequency.

Waiting time for public transport has a big impact in places like Singapore, which is always hot and humid. We have to wait for 10-20 min for buses. Taxi drivers picking passengers, choosing who they want to fetch, lead to a rough estimate of 20 min wait to flag for a cab, and sometimes it is too expensive to call (people with low income or no income). We have to wait for 5-7 min wait for a train (3-4 stops).Does not stop exactly in certain location, still need to walk. Need to transfer and transfer and wait for bus/MRT. Price of public transport have been increasing (more information, look at public transport). Public transport breakdown are a big nuisance, huge waste of time. Recently, frequent breakdown of MRT, travelling time extended by an hour. Many people were late.

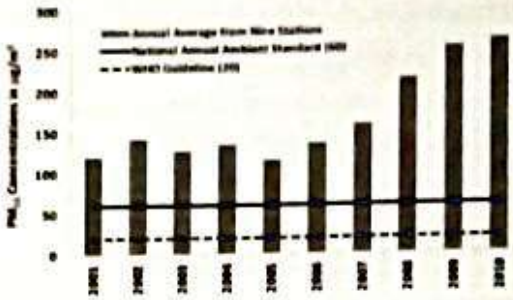

Table-2 Increase Air Pollution in India (Delhi)

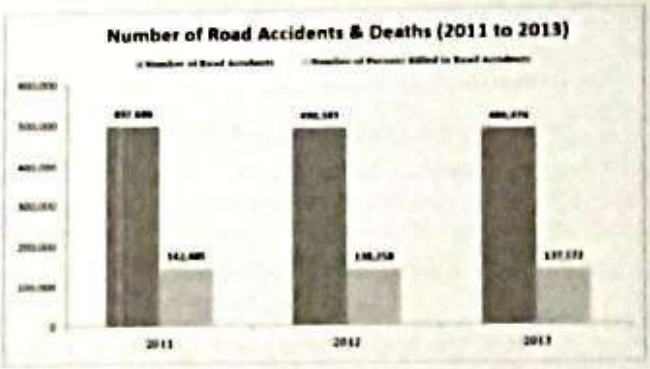

Table-3 Increase in Road Accidents

II. PUBLIC TRANSPORT SYSTEM

1. Frequency

The frequency of the public transport system is need to be increased to create affinity among regular commuters to opt public transport system.

If there is the availability of public transport system there will be less chance of opting for the private vehicle.

2. Not comfortable

Generally, public transport lacks comfort zone, hence people opt for private vehicle for their convenience. Hence the comfort zone of public transport has to be enhance.

Ex: Standardizing size of bus, incorporating AC accommodation in bus, providing sufficient sitting arrangement in bus

3. Getting reservation

Now day it is very difficult to get a conform ticket whether it is bus or train due to huge number of passengers .So, people opt for the private vehicle. Hence this problem should be eradicated and proper reservation system should be installed.

4. Increased time of travel:

If we travel by public transport system there is a most probable chance of getting delayed due to different reasons like huge no. of stoppage, breakdown of vehicle, increase of access and egress time to get in and get down from the bus. If the time of travel can be controlled as per requirement, then use of public transport can be increased

III. NEED FOR SWITCHING PUBLIC TRANSPORT SYSTEM

From the above tables and figures it is very clear that there is huge increase in private vehicle ownership and people are shifting from public transport to public transport. This is leading to increased air pollution, accidents with huge loss of life.There is a need to develop a robust public transport system so that the passengers shift from private transport to public transport which would reduce pollution, accidents and road congestion.The factors which influence passengers from shifting private to public transport are cost and time.

IV. CONCLUSION

In this paper an attempt was made to understand the increase in private owned vehicle and effects of increasing the private owned vehicles. The reason for not preferring the public transport system is analysed. The authors are working to find the ways and means to improve public transport system so that the use of private transport is discouraged

V. REFERENCES

[1] Bose, R.K. (1998). "Automotive energy use and emissions control – A simulation model to analyze transport strategy for Indian metropolises". Energy policy 26(13), Pa.,1001-1016..

[2] Shukla, A. (2004). "Planning and management of effective urban transportation systems". B.Tech project submitted to the Indian Institute of Technology – Delhi.

[3] C Singh, Y. P. (2002). "Performance of the Kolkata Metro Railway: A case study". CODATU X Pa., 337-342

[4] Sreedharan, E. (2003). "Metro rail...2500 less buses on roads!" http://www.indiainfoline.com

[5] Sreedharan E. (2001). "Delhi Metro rail. An inescapable necessity". Hindustan Times.

Parking Management: A Solution to the Urban Mobility

[1] Patitpaban Panda*, [2] Prof. Sudhansu Sekhar Das
[1] Department of Civil Engineering SOA University*,[2] Department of Civil Engineering, VSSUT, Burla

***Abstract*—Increasing vehicular traffic in urban areas is a major problem.Shifting towards private vehicle and reduction of public transport creates the strain on urban infrastructure. Leading to a congestion trap. To evade from the congestion trap, a well-proven parking management strategy is adopted taking Bhubaneswar as case study. The methodology for the work is developed taking parking charges as management tool. A stated choice experiment is to be done taking different attributes of parking to calculate the shift to public transport. The detail of the experimental design and the model development are explained in the paper.**

***Index Terms*— Stated Choice, Attributes, Demand Model, Parking**

I. INTRODUCTION

1. MOTIVATION

Efficient transport infrastructure is theprerequisite for sustainable economic development of any country. However huge investment in terms of land as well as finance is required for appreciable development of thisinfrastructure. Adding lanes to the existing roads to cater the increasing mobility demand with escalating number of vehicles have reached its limits. Especially in the urban areas, it is not possible to add to width of the roads because of extreme constraint of land availabilityeven if necessary funds can be arranged. The problem has since been recognized in the advanced developed countries, traffic control and management, more efficient use of existing roadway capacities, harmonized traffic flows, the prioritization of public transport means are some of approaches to better management of mobility in densely populated urban area.

In developing countries, the magnitude of the problem has started taking attention of planners. In recent past, the magnitude of the problem has increased many folds in Indian cities due to increase in the number of private vehicles. The affordability of middle class population has increased and the availability of cheaper cars, has further enabled the urban middle class to own cars. Hence the need of the hour is to devise a methodology to deter the use of private vehicle and encourage the use of public transport which is best suitable for a particular urban Area.

Different initiative taken by the planners patronizing public transport and imposing some restriction on the use of personalized vehicles through parking management (Bayliss, 1999), appears to be the most promising means for travel demand management. The Ministry of Urban Development, in its "National Urban Transport Policy" recognize the increasing urban road congestion and its associated air pollution. Their strategy puts primary emphasis on the need to increase the efficiency of use of road space by favoring public transport and by the use of traffic management instruments to improve traffic performance and by restraining the growth of private vehicular traffic. Some of the key points from the National Urban Transport Policy concentrate around i. Public vs personal transport and ii. In–street traffic and parking. In–street traffic and parking adoption of mechanisms restraining the use of private motors vehicles through the market mechanisms such as higher fuel taxes, higher parking fees, reduced availability of parking spaces is taken as a criteria. Present paper explain a methodology taking parking pricing as a tool to tweak the Travel Demand from Private modes (Car, Two wheelers) towards public transport taking Bhubaneswar as study area.

2. Study Area

A part of Bhubaneswar the state capital of Orissa India is taken for the study. It is one of the fastest growing cities of India. 10 million populations live ..... (Pl Describe) About ..... people from different part of state come to state capital for their official and other work. Describe the routes

3. Methodology

In order to carry out the work, it was necessary to design a suitable survey instrument, collect data from rural commuters, analyze data by developing suitable econometric models and calculate WTP values using those econometric models. The detailed methodology followed in the work is described in the following sub-sections

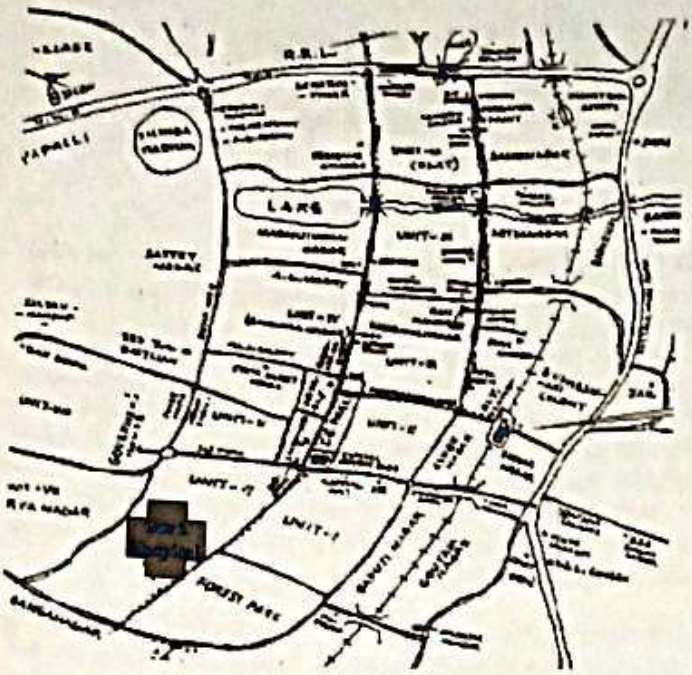

3.1 Type of Data

The RP and/or SP data collected from commuters have been used in diverse fields for calculation of WTP values (Hensher 1994; Louviere 1988a; Jose Holguin-Veras 2002). RP data is not inappropriate if it is necessary to consider attributes which are presently non-existing. On the other hand, SP data facilitates inclusion of such non-existing or hypothetical attributes and study their variability (Louviere, 1988a). Although it is not advisable to use stand-alone SP models for predictions, they can be very effective for WTP calculation (Hensher and Sullivan 2003). As the present study is aimed to calculate WTP values, SP data is found appropriate over RP data.

SP data may be collected in the form of rating, ranking, and choice. Stated choice (SC) experiments provide a framework for studying the relative marginal disutility of variations in attributes, and their correlations (Louviere et al. 2000). SC methods are well established and suitable for understanding and predicting consumer tradeoffs and choices in marketing research. They have been used extensively to model the behaviour of individuals (Hensher 2001a). Therefore, in the present work, SC method is adopted to elicit preferences by generating hypothetical profile of feeder service using various attributes and their levels

3.2 Design of the Survey Instrument

A SC survey instrument was designed for collecting behavioural data with suitable attributes and their levels describing alternative feeder services to bus stop. Well-designed SC experiments require extensive pre-testing to identify attributes, levels, and important interactions (Louviere, 1988b). The choice instruments in this study were subjected to considerab before collection of data.

3.3 Attributes and Levels

A proper specification of the attributes and th has great implications for the desi implementation of stated choice experiment producing proper SCE results. Various metho been applied to the development attributesincludes literature reviews, conceptual and policy relevant outcome m theoretical arguments, expert opinion professional recommendations, patient nominal group ranking techniques and qu research methods.In the present work attrib feeder service for SC survey were chosen ba literature, expert's judgments and reconna survey. Reconnaissance survey following attribu levels are selected for development of choice se

Table 2. Attributes and their levels

Parking Type	On Street, Off Street
Discomfort Level	AC, Non AC
Parking Time	On Street(4min, 7min, 10 Off Street (5min, 10min, 15
Headway Public Transport	5min, 10min, 15min
Access& Egress Time for Bus / Parking	5min, 10min, 15min
Parking Cost	Car (on street - Rs Rs30,Rs40, Off Street Rs Rs15,Rs20) TW (on street - Rs Rs15,Rs20, Off Street R Rs10,Rs15)
Cost of Travel /Km	Rs.1.00, Rs.1.50, Rs.2.00

Design of Choice Set

Choice sets could be formed by full factorial d considering all possible combinations. Five attrib with four levels each and one with three levels w have produced 2^2*3^5 or 972 alternatives using factorial technique. However, it was neither neces nor practically possible to include all t combinations in the SP experiment. Alternatives reduced using D-optimal design, one form of de provided by a computer algorithm (de Aguiar al.1995). Unlike standard classical designs such factorials and fractional factorials, D-optimal de matrices are usually not orthogonal and e estimates are correlated. D-optimal designs are stra optimizations based on a chosen optimality crite and the model that will be fit. The optimality crite used in generating D-optimal designs is one maximizing, the determinant of the informa matrix.Using D-optimal technique 6 combinations choice sets were generated. Each combinat contained 8 choice sets which wereincluded in e

[illegible] 1st February 2017, ISBN: 978-93-86352-18-5

questionnaire. A total of two sets of questionnaires were prepared for each type of vehicle (i.e. Two wheeler and car). A sample choice set is given below in Table- 3

Table- 3 Choice set

Vehicle	Bus	Car
Parking Type		On street
Discomfort Level	Non AC	
Parking Time		7min
Headway	15min	
A & E Time for Bus / Parking	15min	5min
Parking Cost		Rs.30/Hr
Cost of Travel /Km	Rs.1.00/KM	Rs.4.00/KM
Choice		

3.3 Econometric Model

The MNL model is used for analysis of SP and/or RP data due to its simplicity in estimation. But MNL models impose restrictions such as Independence of Irrelevant Alternatives (IIA) and also assume that the coefficients of all attributes are to be the same for all respondents in a choice experiment, whereas in reality there may be substantial variability in how people respond to attributes. Advances in logit models to overcome the restrictions of MNL completely, lead to the development of RPL or Mixed Logit (ML). In RPL model development, it is necessary to make suitable assumption about the distribution of random parameters. Generally available alternative distributions are normal, lognormal, uniform and triangular. However, all these distributions have the disadvantage of producing wrong sign to some shares due to the spread or standard deviation. It is possible to overcome the disadvantage of distribution by imposing a constraint on the spread. In a constrained triangular distribution, mean and spread are made equal to minimize the effect of spread on the estimation of values, yet producing estimates with proper sign (Hensher and Greene 2001). When mean and spread are made equal, the constrained distribution has a peak in the density function with two end points of the distribution fixed at zero and 2*mean, so that there is no free variance (scaling) parameter. Constrained triangular distribution has several advantages over the other distributions. In the present work, the constrained triangular distribution is assumed for random parameters while developing RPL models. Users' valuation of attributes may also be influenced by one or more socioeconomic attributes. The effect of socioeconomic characteristics on the mean of random parameter (called 'mean heterogeneity') is also investigated with RPL model in the present work.

3.4 Theoretical background

In econometric models based on Random Utility Theory (McFadden, 1974), the utility of each element (k) consists of an observed (deterministic) component denoted by 'V' and a random (disturbance) component denoted by 'ε',

$$U_k = V_k + \varepsilon_k \quad (1)$$

The deterministic part V_k is again a function of the observed attributes (x) of the choice as faced by the individual, the observed socioeconomic attributes of the individual (t) and a vector of parameters (β), then

$$V_k = V_k(x, t, \beta) \quad (2)$$

A probabilistic statement can be made (due to presence of the random component) as, when an individual 't' is facing a choice set, 'C_k', consisting of 'J_k' choices, the choice probability of alternative 'i' is equal to the probability that the utility of alternative 'i', U_{ik}, is greater than or equal to the utilities of all other alternatives in the choice set i.e.

$$P_{k(i)} = P_r(V_{ik} + \varepsilon_{ik} \geq V_{jk} + \varepsilon_{jk}, \text{ for all } j \in C_k, j \neq i)$$

Assuming IID (Gumbel distribution) for ε, the probability that an individual chooses i can be given by the MNL Model (McFadden, 1974; Ben-Akiva and Lerman, 1985),

$$P_k = \frac{e^{V_{ik}}}{\sum_{j \in J_k} e^{V_{ik}}} \quad (3)$$

This model can be estimated by Maximum Likelihood techniques.

The RPL model is a generalized form of MNL. It is used to account for unobserved heterogeneity and to overcome IIA limitations. Let the utility function of alternative 'i' for individual 'k' be:

$$U_{ik} = \beta x_{ik} + \varepsilon_{ik} = \beta_i x_{ik} + \hat{\beta}_k x_{ik} + \varepsilon_{ik} \quad (4)$$

Thus, each individual's coefficient vector 'β' is the sum of the population mean β_i and individual deviation $\bar{\beta}_k$, $\bar{\beta}_k x_{ik}$ are error components that induce heteroskedasticity and correlation over alternatives in the unobserved portion of the utility. This means that an important implication of the mixed logit specification is, that it is not necessary to assume that the IIA property holds. Let tastes, 'β', vary in the population with a distribution with density $f(\beta|\theta)$, where 'θ' is a vector of the true parameters of the taste distribution. If the error terms (ε_{ik}) are IID type-I extreme value, it is a RLP model (Train, 1998). The conditional probability of observing a sequence of choices is the product of the conditional probabilities

$$S_k(\beta_k) = \prod P(n(k,t)t \mid \beta_k) \quad (5)$$

Where $n(k, t)$ denotes the sequence of choices from choice sets that person 'k' chooses in situation 't'.

In the choice experiment, the sequence of choices is the number of hypothetical choices each respondent makes in the survey. The unconditional probability for a sequence of choices for individual 'n' is then be expressed as the integral of the conditional probability in (5) over all values of 'β'

$$P_k(\theta) = \int S_k(\beta) f(\beta \mid \theta) d\beta \quad (6)$$

In general the integral cannot be evaluated analytically, and one has to rely on a simulation method for the probabilities. Here a simulated maximum likelihood estimator, using Halton draws, to estimate the models, is used (Train, 1999). This type of RPL is less restrictive

than standard conditional logit models. Apart from being more difficult to estimate, literature shows that the results can be rather sensitive to the distributional assumptions and the number of draws applied in the simulation (Hensher and Greene, 2001).

II. Survey and Database

Choice data along with socioeconomic data were collected in the study area by trained enumerators during moth of February to April 2016 from 334 car and 312 two wheeler users. The data are in the process of refinements to develop the logit models.

III. Conclusion

The paper shows a process for development of logit models to be used for calculating the effect of parking pricing to tweakthe demand towards public transport. Both on street and of street parking are considered along with separate pricing for two wheeler and car parking. Access and egress distance also considered in the development of the choice set from public transport and from parking place in case of private vehicles. Though case specific same process can be used by researchers to solve similar transportation problem.

REFERENCES

Ackerberg, D. A., 2003. Advertising, learning, and consumer choice in experience good markets: an empirical examination. *International Economic Review*, 44(3),1007-1040.

Alpizar, F., and F. Carlsson. 2001. Policy implications and analysis of the determinantsof travel mode choice: An application of choice experiments to metropolitanCosta Rica. Working Paper in Economics 56. Department of Economics,Goteborg University.

Brouwer, R., Bateman, I. (2005). Temporal stability and transferability of models ofwillingness to pay for flood control and wetland conservation. *Water Resources Research*, 41(3)017.

Brouwer, R. (2006). Do stated preference methods stand the test of time? A test ofthe stability of contingent values and models for health riskswhen facing an extreme event. *Ecological Economics*, 60, 399- 406.

Ben-Akiva, M., and Lerman, S. R. 1985. Discrete Choice Analysis: Theory and Applications to Travel Demand. MIT Press, Cambridge.

Das, S. S, Maitra, B. and Manfred Boltze, 2009. Valuing Travel Attributes of Rural Feeder Service to Bus Stop a Comparison of Different Logit Model Specifications. *Journal of Transportation Engineering*, 135(6), 330-337.

de Aguiar, P. F., Bourguignon, B., Khots, M. S., Massart, D. L. &Phan-Than-Luu, R. 1995. 'D-optimal Designs', *Chemometrics and Intelligent Laboratory Systems* 30(2), 199-210.

Dong, N. and Maynard, R. A., 2013. PowerUp!. A tool for calculating minimum detectable effect sizes and minimum required sample sizes for experimental and quasi-experimental design studies. *Journal of Research on Educational Effectiveness*, 6(1), 24-67.

Eil, D., and Rao, J. M., 2011. The Good News-Bad News Effect: Asymmetric Processing of Objective Information about Yourself. *American Economic Journal: Microeconomics*, 3(2), 114-138.

Grossman, Z., and Owens, D., 2012. An unlucky feeling: Overconfidence and noisy feedback. Journal of Economic Behavior & Organization, 84(2), 510-524.

Hensher, D.A., 1994. Stated Preference Analysis of Travel Choices: The State of Practice. Transportation 21(2), 107-133.

Hensher, D. A., 2001a. The Valuation of Commuter Travel Time Savings for Car Drivers in New Zealand: Evaluating Alternative Model Specifications. *Transportation*, 28, 101-118.

Hensher, D. A., 2001b. Measurement of the Valuation of Travel Time Savings. *Journal of Transport Economics and Policy*, 35(1), 71- 98.

Hensher, D. A. and Greene, W. H. 2001. The Mixed Logit Model: The State of Practice and Warnings for the Unwary. Working Paper, School of Business, University of Sidney.

Hensher, D. A. and Sullivan, C., 2003. Willingness to Pay for Road Curviness and Road Type. *Transportation Research D*, 8, 139-155.

Jose Holguin-Veras, P. E., 2002.Revealed Preference analysis of Commercial Vehicle Choice Process. *Journal of Transportation Engineering*, ASCE, Vol. 128 (4), 236-346.

Layton, D. F. 2000. Random Coefficient Models for Stated Preference Surveys. Journal of *Environmental Economics and Management*, 40, 21-36.

Louviere, J.J. 1988a. Conjoint Analysis Modeling of Stated Preferences: A Review of Theory, Methods, Recent Developments and External Validity. Journal *of Transport Economics and Policy* 22(1): 93-119.

Louviere, J.J., 1988b. Analyzing Decision Making: Metric Conjoint Analysis. Sage University Paper Series No. 67, Newbury Park, CA.

Louviere, J. J., Hensher, D. A., and Swait, D. J. 2000. Stated Choice Methods. Analysis and Applications. Cambridge University Press.

McConnell, K. E., I. E. Strand, and S. Valdes (199 Testing temporal reliability and carry-over effect: The role of correlated responses in test-retest reliability studies, *Environmental & Resource Economic*, 12, 357– 374.

McFadden, D. 1974. Conditional Logit Analysis of Qualitative Choice Behavior. In P. Zarembka (ed.), Frontiers in econometrics, New York: Academic Press, 105-142.

Nelson, P. 1970. Information and Consumer Behavior. *Journal of Political Economy*. 78(2), 311-329.

Polyzou, E., Jones, N., Evangelinos, K.I. and Halvadakis, C.P. (2011). Willingness to pay for drinking water quality improvement and the influence of social capital. *The Journal of Socio-Economics* 40, 74-80.

Revelt, D., and K. Train. 1998. Mixed logit with repeated choices: Households'choices of appliance efficiency level. *The review of Economics and Statistics*. 80(4), 647-657.

Schotter, A., 2003. Decision Making with Naive Advice. American Economic Review, 93(2), 498-529.

Train, K., 1998. Recreation Demand Models with Taste Differences Over People. *Land Economics*. 230-239.

Train, K., 1999. Halton Sequences for Mixed Logits Working Paper, Department of Economics University of California at Berkeley.

DEMONETISATION IN INDIA: CAUSES, IMPACTS AND GOVT. INITIATIVES

Dr. Prasann Kumar Das, Prof. Nirmal Kumar Routra,
Assistant Professor, Dept of MBA, GIFT

ABSTRACT: *The demonetisation was done in an effort to stop counterfeiting of the current bank notes alleged to be used for funding terrorism, controlling black money and reducing income inequalities among the people of the country. This article has made an attempt to assess the overall profile of parallel economy in India, particularly in terms of causes, impacts and Govt. Initiatives. The results indicate that Parallel economy has been expanding very rapidly in India as well as in developing countries. It is evident from the study that Govt. Of India already introduced various issues for estimating black economy but estimation reports are not same. Indian Govt. Is more concerned about the prevalence of the parallel economy and various commissioning are formed for controlling it but results are not so impressive. Thus the paper suggests that recommendations of the commissioning or laws should be implemented correcting for reducing bad effects of black economy and it helps to reduce income inequalities and inflation in the country.*

KEY WORDS: Black money, inflation, income inequalities, parallel economy, Gross domestic product

I. Introduction:

Demonetisation is the act of stripping a currency unit of its status as legal tender. Demonetisation is necessary whenever there is a change of national currency. The old unit of currency must be retired and replaced with a new currency unit.

Demonetization is a generations' significant experience and is going to be one of the economic events of our time. Its impact is felt by every Indian citizen. Demonetization affects the economy through the liquidity side. An asset is said to be liquid if it is easy to sell or convert in to cash without any loss in its value. Its effect will be a telling one because nearly 86% (Rs 14.2 trillion) of high currency value in circulation was withdrawn without altering bulk of it. As a result of the withdrawal of Rs 500 and Rs 1000 notes, there occurred huge gap in the currency composition as after Rs 100, Rs 2000 is the only denomination.

Absence of intermediate denominations like Rs 500 and Rs 1000 will reduce the utility of Rs 2000. Effectively, this will make Rs 2000 less useful as a transaction currency though it can be a store value denomination.

Demonetization technically is a liquidity shock; a sudden stop in terms of currency availability. It creates a situation where lack of currencies squeezes consumption, investment, production, employment etc. In this context, the exercise may produce following short term/long term/, consumption/investment, welfare/growth impacts on Indian economy. The intensity of demonetization effects clearly depends upon the duration of the liquidity shocks. The move by the Govt., Is to tackle the menace of black money, corruption, terror funding and fake currency.

II. Objectives of study:

1. To analyse the causes and impact of Demonetisation in India.
2. To highlight the appropriate initiative which will be taken by Govt., To success the objective of demonetisation.

III. Research Methodology

The study is based on secondary data. The required data has been collected from various sources i.e., World Investment Report, Asian Development Banks' Reports,

various bulletins of Reserve Bank of India, that are available in internet and publications.

IV. Review of Literature

"Demonetization: Impact on the economy", by Tax Research Team, working paper number 182, NIPFP (2016)- this paper has elucidated the impact of demonetization in the availability of credit spending, level of activity and Government Finances. "The economic consequences of Demonetization of 500 and 1000 rupee notes" by M.Sabnavis, A.Sawarkar and M.Mishra in Economic Policy View November 09,2016- this paper suggested that in spite of the initial hiccups and disruptions in the system of Demonetization today, eventually this change will be well assimilated and will prove positive for the economy in the long run. "Black Money and Demonetization" by Rahul Prakash Deodhar, SSRN, November 2016. This paper has emphasized and highlighted towards control of black money, corruption and terrorism through Demonetization.

V. Causes of Demonetization

In a single master stroke, the government has attempted to tackle all three malaises currently plaguing the economy—a parallel economy, counterfeit currency in circulation and terror financing.

In addition, the Indian economy has been provided a new lease of life—a "reset" if you will—with huge positive implications for liquidity, inflation, fiscal and external deficit in the short term. Over the next two-three years, improvement in India's position on transparency and corruption in the global stage will further add to its investor appeal. With GST to be implemented soon, India is now on the path of higher growth in the medium term and long term also.

VI. Impact of Demonetization

To understand the impact of Demonetization, it is important to first understand, what is it that cash does in the economy? There are broadly four kinds of transactions in the economy: Accounted Transactions, Unaccounted transactions, those that belong to the informal sector and illegal transactions. The first two categories relate to whether transactions and corresponding incomes are reported to tax purposes or not. The third category consists largely of agents, who earn incomes below the exemption threshold and therefore do not have any tax liabilities. The use of that cash is put to for these various segments of the economy can be summarized in the form of table 1.

Table 1: Demand for Cash by various agents in the economy

Description of the activity	Unaccounted Transactions (legitimate transactions but tax not paid)	Illegal Transactions (Corruption, Crime, etc.)	Informal Sector Transactions	Accounted Transactions
Medium of Exchange	Incomes are earned through exchanges in cash, payments are made in cash	Payments for crime	Incomes are earned in cash and spent in cash	Transaction demand for money
Store of Value	Balances held in interim until alternative investment options become available (there exists a number of instruments which yield better return than cash- real estate lending in the unaccounted or informal sector and so on)	Balances held in interim until alternative investment options become available (there exists a number of instruments which yield better return than cash- real estate, lending in the unaccounted or informal sector and so on)	Savings as well as precautionary purposes (as yet unbanked in the psychological sense)	For emergences (precautionary demand for money)

(Source http://nipfp.org.in/media/medialibrary/2016/11/WP_2016_182.pdf)

1. **Liquidity crunch (short term effect):** liquidity shock means people are not able to get sufficient volume of popular denomination especially Rs 500. This currency unit is the favourable denomination in daily life. It constituted to nearly 49% of the previous currency supply in terms of value. Higher the time required to resupply Rs 500 notes, higher will be the duration of the liquidity crunch. Current reports indicate that all security printing presses can print only 2000 million units of RS 500 notes by the end of this year. Nearly 16000 mn Rs 500 notes were in circulation as on end March 2016. Some portion of this was filled by the new Rs 2000 notes. Towards end of March approximately 10000 mn units will be printed and replaced. All these indicate that currency crunch will be in our economy for the next four months.

2. **Welfare loss for the currency using population:** Most active segments of the population who constitute the 'base of the pyramid' use currency to meet their transactions. The daily wage earners, other labourers, small traders etc. who reside out of the formal economy uses cash frequently. These sections will lose income in the absence of liquid cash. Cash stringency will compel firms to reduce labour cost and thus reduces income to the poor working class.

There will be a trickle up effect of the liquidity chaos to the higher income people with time.

4. Consumption will be hit: When liquidity shortage strikes, it is consumption that is going to be adversely affected first.

Consumption ↓→ Production ↓→ Employment ↓→ Growth ↓→ Tax revenue ↓

5. Loss of Growth momentum- India risks its position of being the fastest growing largest economy: reduced consumption, income, investment etc may reduce India's GDP growth as the liquidity impact itself may last three -four months.

6. **Impact on bank deposits and interest rate:** Deposit in the short term may rise, but in the long term, its effect will come down. The savings with the banks are actually liquid cash people stored. It is difficult to assume that such ready cash once stored in their hands will be put into savings for a long term. They saved this money into banks just to convert the old notes into new notes. These are not voluntary savings aimed to get interest. It will be converted into active liquidity by the savers when full-fledged new currency supply takes place. This means that new savings with banks is only transitory or short-term deposit. It may be encashed by the savers at the appropriate time. It is not necessary that demonetization will produce big savings in the banking system in the medium term. Most of the savings are obtained by biggie public sector banks like the SBI. They may reduce interest rate in the short/medium term. But they can't follow it in the long term.

7. **Impact on black money:** Only a small portion of black money is actually stored in the form of cash. Usually, black income is kept in the form of physical assets like gold, land, buildings etc. Hence the amount of black money countered by demonetization depends upon the amount of black money held in the form of cash and it will be smaller than expected. But more than anything else, demonetization has a big propaganda effect. People are now much convinced about the need to fight black income. Such a nationwide awareness and urge will encourage government to come out with even strong measures.

8. **Impact on counterfeit currency:** the real impact will be on counterfeit/fake currency as its circulation will be checked after this exercise.

Demonetization as a cleaning exercise may produce several good things in the economy. At the same time, it creates unavoidable income and welfare losses to the poor sections of the society who gets income based on their daily work and those who doesn't have the digital transaction culture. Overall economic activities will be dampened in the short term. But the immeasurable benefits of having more transparency and reduced volume of black money activities can be pointed as long term benefits.

9. **Other Impacts**

i) ***Impact on parallel economy*** The removal of these 500 and 1000 notes and replacement of the same with new 500 and 2000 Rupee Notes is expected to - remove black money from the economy as they will be blocked since the owners will not be in a position to deposit the same in the banks, - Temporarily stall the circulation of large volume of counterfeit currency and - curb the funding for anti-social elements like smuggling, terrorism, espionage, etc.

ii) ***Impact on Money Supply*** With the older 500 and 1000 Rupees notes being scrapped, until the new 500 and 2000 Rupees notes get widely circulated in the market, money supply is expected to reduce in the short run. To the extent that black money (which is not counterfeit) does not re-enter the system, reserve money and hence money supply will decrease permanently. However gradually as the new notes get circulated in the market and the mismatch gets corrected, money supply will pick up.

iii) ***Impact on Demand*** The overall demand is expected to be affected to an extent. The demand in following areas is to be impacted particularly: Consumer goods, Real Estate and Property, Gold and luxury goods, Automobiles (only to a certain limit),

All these mentioned sectors are expected to face certain moderation in demand from the consumer side, owing to the significant amount of cash transactions involved in these sectors.

iv) ***Impact on Prices*** Price level is expected to be lowered due to moderation from demand side. This demand driven fall in prices could be understood as follows: Consumer goods: Prices are expected to fall only marginally due to moderation in demand as use of cards and cheques would compensate for some purchases.

VII. Government initiatives to make demonetization a success

The government has taken a number of steps to curb black money. Searches, seizures, surveys, and scrutiny of income tax returns are being done by the Income Tax Department. Amendments have also bee made to the Finance Act 2004 to intensi efforts to curb black money. For the succes of demonetization and smooth functioning o the economy, the Government has taken th following initiatives:

1. Controlling the election expenses.
2. Find out the root cause of generatio of black money and make emphasis to stop it. Unless this problem is tacked the menace of black money will continue to increase.
3. PAN Card is essential for all tax payers but many transactions especially those related to property and conducted in cash and are unlikely to be reported. For this it is better to create a property and wealth account in the name of an individual.
4. Government has also taken initiative in the last two years to open Dhana jan Account, which is essential to judge individual source of income.
5. Government has also taken initiatives and also motivated the people towards cashless transactions, which help to make a proper record about transactions between parties.
6. Government has also taken initiative to aware the people through mass media about the cashless transactions and income tax, etc.

VIII. Conclusion

Parallel economy is a new threat for the Indian economy. In India parallel economy is expanding very rapidly. There are many factors like Controls and Licensing System, Higher Rates of Taxes, Ineffective Enforcement of Tax Laws, Inflation, Funding of political parties etc. that influence its growth. In India amount of black money are increasing continuously which badly impacts the economic growth of the nation. Such money is a new challenge for Indian economy. Indian economy is badly affected by black money as it is underestimating GDP, increasing inequality of income, increasing illegal activities etc. Over the past 50 years, the government has at various

times announced several schemes offering opportunities to bring black money overboard but the result are not so effective. Some of these schemes are: introducing the scheme of Special Bearer Bonds, demonetizing high denomination currency notes, stringent raids and scheme of voluntary disclosures. These instruments are expected to reduce the volume of the black economy.

Black money holders will definitely lose out eventually boosting the formal economy in the long run. Short term fall in real estate prices might benefit for middle class citizens in India.

IX. References

a. Ahuja, R. (2007). Social Problems in India (2nd Ed). Jaipur: Rawat Publications.

b. Chopra, A. (2010). India targets black money. Retrieved from http://www.thenational.ae/business/economy/india-targets-black-money

c. Datta, R., & Sundharam, K. (2004). Indian Economy (49th Ed). New Delhi: S. Chand & Company Ltd. 376 & 378-379.

d. Datta, R., & Sundharam, K. (2012). Indian Economy (49th Ed). New Delhi: S. Chand & Company Ltd.

e. Dhar, P. K. (2003). Indian Economy: Its Growing Dimensions (11th Ed). Ludhiana: Kalyani Publishers

f. M.Sabnavis, A.Sawarkar and M.Mishra in Economic Policy View November 09,2016 "The economic consequences of Demonetization of 500 and 1000 rupee notes"

g. NIPFP(2016) "Demonetization: Impact on the economy", by Tax Research Team, working paper number 182,

h. Rahul Prakash Deodhar, SSRN, November 2016"Black Money and Demonetization"

★ ★ ★

BUILDING AND NURTURING HIGH PERFORMANCE THROUGH COMMUNICATION – A CASE STUDY ON A.M NAIK (LARSEN AND TOUBRO)

Bikram K. Rout, Asst. Prof. & Head, Dept. of English,
Gandhi Institute For Technology, Bhubaneswar
&
Pranati Mishra, Asst. Professor of English,
Gandhi Institute For Technology, Bhubaneswar

Communication for Organizational Success is a complex one. People in organization usually spend over 75 percent of their time in an interpersonal situation. Thus, it is no surprise to say that the root of a large number of problems is poor communication. To bring an empty space to life, takes talent, skill, imagination, and communication.

Closer home, consider what A M Naik has achieved in terms of making Larsen & Toubro (L&T) one of the most respected engineering conglomerates in the country. Now, consider his initial experience at L&T. Apart from the fact that he was not from any of the Indian Institutes of Technology (Naik did his Mechanical Engineering from Birla Vishvakarma Mahavidyalaya Engineering College in Vallabh Vidyanagar in Gujarat), his poor knowledge of English led him to make seven to eight mistakes in the first employment form he filled.

When he applied to L&T, he got a job, but the company reduced its initial offer by Rs 900 to Rs 670 a month and offered him a lower designation than what it had initially promised - all because the final interviewer thought he was a bit arrogant.

Years later, Naik attributes this to a communication gap between him and the Englishman, who was the final interviewer. "I used to think in Gujarati and then translate it into English; the Englishman perhaps misunderstood what I had intended to say," Naik said. Naik could have easily given up on the L&T job, but he did not, just to prove a point. He joined L&T on March 5, 1965, and became the workshop in-charge within one and a half years of joining the company. When he was not even 25, some 800 people reported to him. The rest is all too well known. An HR expert attributes Naik's success to his fierce desire to succeed and not let failures bother him much. He attributes this success to his strong desire to communicate his vision to the people who were his partners in the path to success at L&T. Corporate communication is the message issued by his organization, to its publics. "Publics" were both internal (employees, stakeholders, i.e share and stockholders) and external (agencies, channel partners, media, government, industry bodies and institutes, educational and general public) L&T communicated the same message to all its stakeholders to transmit coherence, credibility and ethic. If any of these essentials is missing, the whole organization may fail.

Corporate Communications help organizations explain their mission, combine its many visions and values into a cohesive message to stakeholders.

Naik flaunts his years of growing up in a village like a general his scimitar-and-baton insignia. When he was in Class 5, Naik's father, who was a high school Mathematics and Science teacher and a Gandhian shifted from Mumbai to Kharel in southern Gujarat. "And suddenly from an elite school, I came down to a floor; that, too, a gobar (cow dung) swept floor," he says, this time a smile pushing against ample jowls. Come October 2012, A.M. Naik, if all goes by his plan, will start writing a memoir. The impatient man he is, the Chairman and Managing Director of Larsen & Toubro has it all planned out for his post-retirement days. "One hundred and fifty requests have come to me to write a book," he says with no hint of exaggeration. "It will be titled 'V to W'. Village to World." Communication can nurture and create a legend out of an insignificant

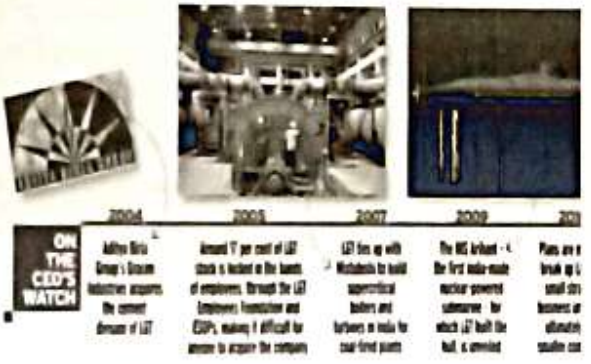

Naik had met Aditya Birla and his son Kumar, when the Birlas tried - unsuccessfully - to hire him. In 2001, when the Ambanis sold their stake to the Birlas, Kumar Mangalam Birla said to Naik : "You did not come to us, but we are coming to you." Birla wanted the cement business to be hived off from L&T, and eventually take control of L&T. However, differences arose between the L&T management and Birlas on how to go about it. Grasim Industries, the company through which the Birlas held their stake, filed a prospectus for an open offer for L&T shares. AM Naik transformed a lumbering conglomerate into India's largest engineering and construction firm. L&T today with revenues of more than USD 8 billion a year is the giant behind many massive projects in India from roads and railways to defense and nuclear power.

Key Steps to Building High Performance Corporations trough effective communication As we strive for competitiveness, high performance becomes even more critical to our success. Regardless of the stage of your company, these key steps will help you build a high performing team:

1. **Develop a diverse team cutting across cultures and communications**
   Utilize people who have different strengths and are closely aligned to the crucial business functions, customers and stakeholders. The more diverse the team, the more they are likely to be strong in achieving the whole range of thinking, action and people oriented tasks for a successful outcome. Motivation is likely to remain consistently high where team members can focus the majority of their work in areas they enjoy
2. **Generate the team purpose**

Facilitate the group to ensure clarity and accountability to the team's purpose so that the team are clear of what success looks like and are empowered to achieve it. Focus the team on achieving results by setting explicit goals.

3. **Develop crucial processes**

Developing critical processes will ensure the team has the vital framework to achieve their goals, and break through any communication barriers that prevent these processes from functioning effectively.

4. **Share the leadership and accountability**

Inspire team members to take full ownership for achieving the team purpose with the assigned resources, proposing solutions and provide performance coaching where needed to address performance issues. Be authentic, work to your own strengths and capitalize on the talents of the team members. Periodically communicate the team for feedback on your leadership so that you can adjust to get the most from each team member or the stage of the team development.

5. **Build strong relationships**

Plan focused team-building events that ensure team members recognize what effective teams look like and the team behaviors for high performance capitalize on strengths and stimulate continuous improvements. Subject to team location, encourage periodic 'get together' such as a quick lunch or morning coffee to ensure the 'human' team spirit is fostered. For virtual teams insert the social element into your conference calls with a simple icebreaker question. Remember, teams do not have to be friends, but there does need to be mutual respect and trust for high performance levels.

6. **Establish focused communication and review**

Ensure the team regularly reviews progress against their team goals and make the vital adjustments to ensure success. At the outset agree with the team the most timely and effective forms of communication for this specific team.

7. **Recognize key milestones and celebrate success**

This could range from a simple 'thank you' or 'well done' to arranging awards, gifts or bonuses to recognize effort and successful results in the most appropriate way to maintain high performance levels.

8. **Review and learn**

Review each major team experience and share these across the business Record the output and review prior to any new team coming together. This should include questions such as 'what contributed most to our team outcome?' as well as 'what could we do differently next time?

As you consider where your team is now and the best steps to help your team on their journey to becoming a high performance team, you will achieve your journey more quickly, if you bring your team along with you. So keep reviewing your progress with the team. Good and effective communication is imperative for the successful existence of any organization.

There is one topic or issue that crops up more about than any other is ***communication.*** There is little doubt that communication is a useful dustbin into which can be thrown a myriad of different issues, some big and some small.

At an organizational level, there is a need for everyone to know what and where the communication channels are so that every single person can be tied into the organization's objectives. Communication also plays a vital role in creating a compelling place to work.

At an interpersonal level, there is a need to be able to communicate openly and honestly, with team members feeling free to say what they think without fear, rancor or anger. Team members also need to listen to each other, including those voicing minority views.

We are not talking about the IT-related communications through cyberspace, but rather the interpersonal communications we have with our friends, family and co-workers. A commonly identified "best practice" among high performing teams is effective communication between team members.

Unfortunately, effective communications are not the norm in many of the organizations. Some of the most sage advice has come from the Tongue and Quill (1996 version) and it read, "Strive to communicate in a way that you cannot be misunderstood"- anonymous. Here are some dos and don'ts to effective communications and some insights to enable you to "walk the talk" and develop high performing teams.

Consider the following eight components of interpersonal communications to ensure your communications are clear and unambiguous.

- First, ensure that you have an active listener.
- Second, establish the problem or identify the requirements.
- Third, make sure there is a commitment to future action.
- Fourth, identify the conditions that will satisfy the need.
- Fifth, establish the context for the request, which may be obvious when you know someone well, but also be careful to not assume or omit critical details.
- Sixth, establish a time frame to complete the request. Seventh, indicate that you believe the person is capable of fulfilling the request.
- Finally, be sincere that the fulfillment of your request is important.
- When all these conditions are not met, you open yourself up to ambiguity and misunderstandings.

When projects are not on time, on budget, nor meeting requirements, it is often because of "misunderstandings." In industry, it is commonly accepted that poorly designed systems are the result of people poorly articulating requests. So what are the common pitfalls to effective communication?

First, making assumptions about what is or is not mutually understood.
Second, not requesting or receiving feedback to confirm what was requested.

Third, the conditions for satisfaction were not specific enough.
Fourth, the justification (for the request) was not articulated clearly or at all.
Finally, the requester is afraid of rejection or indebtedness, so the request is never made.
Now that we know what we should and should not do, I would like to highlight two actions that I think will help take teams to the next level –

- Making powerful requests and
- Following through on promises.

"We literally don't show up in our own lives until we learn to make powerful requests."(1985, Quinn and Quinn) As leaders, we should never be afraid to make requests that demand stretching a team's capabilities.

Requests have a generative and transformative power that can carry teams to greater heights of success. Similar to powerful requests, promises offer the potential to change the world. When our words align with our actions, we demonstrate commitment. **Commitment** is not an act; it is a way of life. Cohesive, high performing teams are able to deliver and follow through on promises both big and small. So when making promises at home, work or play, make sure you deliver. We communicate every day -- every minute of the day -- and sometimes in ways that we do not even realize. Be cognizant of your interpersonal communications and try to improve upon every interaction you have. We have covered some dos and don'ts for effective communication, but remember that it is just talk, unless you back up your words with actions and follow through. Our reputation, credibility and commitment are embedded in our daily communications, so take it seriously, as you reflect on your own interpersonal communications within your own teams.

Research shows that Companies that communicate with courage, innovation and discipline, especially during times of economic challenge and change, are more effective at engaging employees and achieving desired business results. Our research has consistently found the firms that communicate effectively with employees are also the best financial performers. When it comes to communication, successful companies pay close attention to articulating their employee value proposition. In times of change, they use social media and other, time-tested tools to communicate with an increasingly diverse and dispersed audience. These companies treat their managers as a special audience — offering additional communication and training to help them manage. They focus on the customer and use communication programs to drive productivity, quality and safety. 2009/2010 Communication ROI Study Report summarizes the findings of 2009/2010 multiregional study. It identifies what the companies with highly effective communication practices are doing to inform and engage their employees in challenging economic times, and shows how these practices vary around the world.

Key Findings:

- Effective employee communication is a leading indicator of financial performance and a driver of employee engagement. Companies that are highly effective communicators had 47% higher total

returns to shareholders over the last five years compared with firms that are the least effective communicators.

- Despite all of the organizational and benefit changes employers have been making in response to challenging economic conditions, only 14% of the survey participants are explaining the terms of the new employee value proposition (EVP) to their employees.
- The best invest in helping leaders and managers communicate with employees. While only three out of 10 organizations are training managers to deal openly with resistance to change, highly effective communicators are more than three times as likely to do this as the least effective communicators.
- Despite the increased use of social media, companies are still struggling to measure the return on their investment in these tools. Highly effective communicators are more likely than the least effective communicators to report their social media tools are cost-effective (37% vs. 14%).
- Measurement is critical. Companies that are less-effective communicators are three times as likely as highly effective communicators to report having no formal measurements of communication effectiveness.

BIBLIOGRAPHY

1. "Attaining High Performance Communications: A Vertical Approach" Edited by Ada Gavrilovska . *CRC Press*
2. "High-Performance Communication Networks" by Jean Walrand and Pravin Varaiya. *Academic Press*
3. "Quality Pays: Reaching World-class Ranking by Nurturing a High-performance Culture and Meeting Customer Needs" (Hardcover): by Rommell Gunter. *Palgrave Macmillan*
4. "The Habits Of S.U.C.C.E.S.S: Nurturing Intelligence in Every Aspect of Life".By Henry Toi. *Embassy Books*
5. Website. http:// www.larsentoubro.com

PROMOTIONAL EFFORT IN 21ST CENTURY BY INSURANCE COMPANIES

Dr.Biswamohan Dash, Prof.Gopikant Panigrahy, Prof.Nirmal Kumar Routra

Abstract: *This research study focuses on the management of the customer relationship and using the effective communication channels. Here CRM is being considered as the comprehensive integrated approach to improve the customer experience.CRM is the concept and practice which has been very prominent in service sectors. Here the service sector has been considered like insurance sector in Odisha market. The insurance companies are taken into consideration like LIC, AVIVA, BSLI, and ICICI PRUDENTIAL AND RELIANCE and these companies are practicing the CRM. But to experience the loyal profitable and satisfied relationship with customers the insurers are adopting various communication channels. These channels are sales agents, hoardings, TV commercials, web charts, e-mails, websites, telephone etc. This research study facilitates to prove the effectiveness of each communication channel for the sake of creating awareness regarding the insurance products in Odisha market.*

Keywords: Integrated Approach, Loyal, Profitable, Customer Experience and Awareness

1. Introduction of the Study

As a result of globalization of business and evolving recognition of the importance of customer satisfaction and retention, there has been a change in marketing policies. Bose (2002) added that, over the past few years, there has been a shift in relationship between company and customers, focusing on the benefits of long term relationship with the customers. Over the time, there has been a gradual move in marketing thoughts; from mass marketing to market segmentation. Then from market segmentation to Niche marketing and then from niche marketing to customization and personalization, the twenty first century marketing emphasizes more on smaller group of customers. Increasing competitiveness in international economy is forcing the organizations to place larger emphasis on building valuable customer relationship.

Customer Relationship Management (CRM) is the concept of building the philosophy of comprehensive and integrated approach towards the customers. CRM enables the service providers to improve their customers' experience with every interaction by delivering real business benefits. Bradshaw (2004) said that CRM is consistently building improved customer loyalty, increased customer satisfaction and enhanced profitability. In looking for ways to drive growth, insurers need to evaluate their customer management strategy having CRM practices which lead consistent and cost-effective customer service, Customer-aligned products, and enhanced customer loyalty, long-term value and customer retention. Today, more than ever before, the ability to maximize customer loyalty through close relationships is critical to insurers to grow their businesses. As insurers strive to create and manage customer relationships, the companies should adopt several emerging tools to achieve sustainable growth.

2. Customer Relationship Management

CRM is an integrated business approach to create and develop one to one relationship with customers. CRM is the customer –focused strategy to deliver customized service with value. CRM is about managing customer knowledge to better understanding and serve them. It is an umbrella concept that places the customer at the centre of an organization. Customer service is an important component of CRM; however CRM is also concerned with coordinating customer relations across all business functions and points of interaction. The business organizations in general depend on customers for their sustenance and growth.

Every business communicates with their clients in different ways by using various communication channels. CRM acts as a central repository of information on clients – both existing and potential ones. Customer relationship management software and technology are helpful to organize the data. Insurers receive data about customers and record it in an orderly manner. Online and web based CRM software help to understand customer needs and helps to recognize the required processes to achieve business goals. It should be the most acceptable practice for Indian service providers to adopt e-CRM and to get benefits. The essence of CRM is to build customer relationship and trust among the customers which reflect a fundamental change in the ways insurers interact with the customers.

3. Literature Review

Gal breathes and Rogers (1999) stated that, the goal of relationship marketing is the focus on customer loyalty, retention and CRM, which is becoming the foundational corner stone of profitable business. Kotorov (2003) added that many management experts welcomed the concepts of customer relationship management and hurried its implementation in spite of the lack of a clear definition, vision and without an understanding of the extent and complexity of organizational restructuring required for a successful CRM implementation. IT departments within the firms are often unable to provide information and implement the demand. The gap between corporate needs and the limited available resources will keep impelling the great demand for CRM oriented implementation and integration to create better service. Through CRM, firms are able to understand customers from strategic perspective and as a result the CRM ultimately focuses on effectively turning customer information into intelligence to more efficiently manage customer relationship. Kotler (2003) observed that customer relationship management revolves around marketing and begins with a deep analysis of consumer behavior. Bose (2003) stated that CRM is an integration of technologies and business processes used to satisfy the needs of a customer during any given interaction. Chou et al (2004) also have described it as an information industry including software, methodologies and internet capabilities to manage the huge customer data base.

In order to understand CRM, one must understand the changing nature of the customer. Today customers are highly educated, under higher stress, more specialized, living longer and more influenced by the global culture. The emergence of e-business, organizational dynamics and cultural change issues has dramatically shifted organizational functions to focus on the customers. Consequently organizations have recognized the need to develop customer-centric strategies. The practice of planning, creating and managing customer relationships has now a day become the heart of organizational strategy and to lead customer retention. Fayerman (2004) added that, the hype surrounding CRM has only been pervasive within business, technology, media and academic communities since early 1997.It showed the large impact on profitability and increases in customer retention rates. CRM is a concept that enables an organization to tailor specific products or services to each individual customer. In the most advanced scenario, CRM may be used to create a personalized, one-to-one experience that will give the individual customer a sense of being cared for, thus opening up new marketing opportunities based on the preferences and history of the customer. For this purpose insurers must be choosy to select the suitable and effective communication channels to spread the knowledge regarding the insurance product. CRM is also a customer focused business strategy that aims to increase customer satisfaction and customer retention by offering a more responsive and customized service to each customer. Anuroop Tony Singh (2004) stated that selling insurance in India is an attractive opportunity because of the untapped potential but is fraught with challenges such as language and cultural barriers and low purchasing power. Naren Joshi (2004) felt that consumer education is the key to the growth of the insurance industry in India. Viswanadhan (2005), said that banc assurance can be sure a fire way to reach a wide customer base. Rajesh Jhampala (2005) stated that multi-channel distribution and marketing of new insurance products have been the strategy of new players and this trend would continue in the future. Smita Mishra (2005), opined that to constantly differentiate themselves, insurers have to constantly raise the bar of customer service and shredding inefficient practices. Anil Chandok (2006) stated that to have an upper hand over competitors, insurers need to adopt and implement CRM. Sridhar and Allimuthu (2009) stated that banc assurance would have a positive impact on insurance products

distribution if banks and insurance companies understand each other's businesses and will seize the opportunities .

4. Research Objective

The objective of this study is to gain a better understanding of CRM in insurance. The objective is;

To study the impact of CRM implementation in insurance organizations and perception of respondents towards various communication channels for creating maximum product's awareness.

5. Research Hypothesis

Hypothesis of the research study is

H_1: The communication channels like print media, electronic media and Internet along with sales agents are creating maximum awareness regarding product's benefits among the customers.

6. Research Methodology

6.1. Sample Selection

When conducting research, it is often impossible, impractical or too expensive to collect data from all the potential units of analysis included in the research problem. Thus a smaller number of units, a sample, are often choosen to represent the relevant attributes of the whole set of units. This research is purely based in Odisha market, interacting with insurance consumers and insurance officials. More over 284 customers have given their opinions regarding the insurance policies and insurance companies in relation to CRM practices, service standard, and effectiveness of communication channels for product awareness . In order to suit this particular research purpose, the sample collection followed some judgmental criteria. The first sample criterion was that the selected respondents should have at least one life insurance policy and should have knowledge about customer relationship management (CRM) in insurance companies

As far as respondent's profile is concerned, I have taken the demographic characteristics such as, age, education, occupation and income. Then the sampling distribution is prepared. For age, three groups of respondents are there like below 25 years, between 25 to 35 years and above 35 years. For education two groups of respondents are there, like up to graduate and above graduate. For occupation two groups of respondents are there; like service holders and business men. For income three groups are there like; below Rs 20, 000, between 20,000 to 30,000 and above 30,000.

6.2. Data Analysis and the Statistical Techniques Used

Chi square test: since the sampling method is stratified random sampling and the variables under study are each categorical variables, then chi square test can be used to know whether there is a significant relationship between two variables. This method is used to determine goodness of fit. In the hypothesis the dependent variable is product awareness and independent variables are the communication channels. To study the relationship between two variables, probability value (p) has been derived and existence of relationship has been measured

7. Scope of the Study

This study is being conducted by considering five insurance companies in Odisha,who have already implemented the CRM softwares.These companies are; LIC of India. AVIVA Life Insurance, ICICI prudential Insurance, Birla Sun Life Insurance and Reliance Life Insurance. These companies are all operating in Odisha market. For the sake of better service standards, better customer satisfaction, quick digital access, integration. better relation building process with customers. they have all implemented the CRM software Now this study will focus on how these companies have created awareness, customer

satisfaction level and relationship building process in the competitive markets in Odisha to retain the customers.

8. Data Analysis

This chapter deals with primary data collected from the customers through a structured questionnaire. For this purpose five insurance companies are selected. These companies are AVIVA Insurance, Birla Sun Life Insurance, ICICI Prudential Insurance, LIC of India and Reliance Insurance. These five insurance companies have already implemented CRM in their operations. The data were collected from 284 respondents selected among the customers.

9. Respondent Profile

Table 1 *Perception of Respondents across Insurance Organizations*

Sl. No.	Demographic factors	Sample profile	Insurance Organisations					
			LIC	AVIVA	Reliance	ICICI	Birla	Total
1.	Age	Gr.1 (below 25 yrs)	7	6	6	07	08	34
		Gr.2 (25-35)	30	22	20	17	36	125
		Gr.3 (Above 35)	35	22	22	24	22	125
		Total	72	50	48	48	66	284
2.	Education	(Gr.1) up to grad.	30	22	24	21	32	129
		(Gr.2) above grad.	42	28	24	27	34	155
		Total	72	50	48	48	66	284
3	Occupation	Gr. 1(Service holder)	40	31	30	28	41	170
		Gr.2 (Business men)	32	19	18	20	25	114
		Total	72	50	48	48	66	284
4.	Income	Gr.I (below 20000)	26	18	16	21	32	113
		Gr.II (20000-30000)	24	18	18	17	25	102
		Gr.III (Above 30000)	22	14	14	10	19	79
		Total	72	50	48	48	66	284

10. Channels of Communication and Perception of Consumers

Insurance companies under study are using different channels of communication to create awareness. Table 2 depicts the perception of respondents towards different channels of communication in creating awareness regarding products to facilitate the relationship process with target customers.

Table 2. *Perception of Consumers towards Communication Channels across organizations.*

Sl. No.	Comm. Channel	Insurance Organization	Perception					χ^2	P
			1	2	3	4	5		
1.	News Paper	AVIVA		0	4	36	10	137.926	0.0
		BIRLA		0	4	46	16		
		ICICI		0	28	20	0		
		LIC		8	52	12	0		
		RELIANCE		0	14	26	08		
2.	Sales People	AVIVA		0	4	36	10	64.168	0.0
		BIRLA		0	4	46	16		
		ICICI		0	28	20	0		
		LIC		8	52	12	0		
		RELIANCE		0	14	26	8		
3.	Website	AVIVA		14	28	8	0	116.67	0.0
		BIRLA		0	26	38	2		
		ICICI		0	24	24	0		
		LIC		22	44	6	0		
		RELIANCE		0	10	34	4		
4.	Person to person contact	AVIVA		0	16	34	0	70.299	0.0
		BIRLA		0	18	48	0		
		ICICI		4	28	16	0		
		LIC		0	32	40	0		
		RELIANCE		0	10	32	6		
5.	E-mail	AVIVA		0	8	40	2	61.229	0.001
		BIRLA		8	34	24	0		
		ICICI		0	20	28	0		

Sl. No.	Comm. Channel	Insurance Organization	Perception 1	2	3	4	5	χ^2	P
		LIC		0	28	38	6		
		RELIANCE		0	14	34	0		
		AVIVA		4	30	14	2		
		BIRLA		6	36	24	0		
6.	Web-chart	ICICI		4	22	22	0	48.507	0.002
		LIC		0	22	50	0		
		RELIANCE		0	14	30	4		
		AVIVA		6	32	12	0		
		BIRLA		8	38	20	0		
7.	Telephone	ICICI		6	34	8	0	66.977	0.0
		LIC		0	42	30	0		
		RELIANCE		0	12	32	4		

News paper: It is observed that the views of the respondents are mostly in the perceptual groups 3 and 4 indicating higher preference for the media. The customers of LIC have shown news paper as 'sometimes preferred' compared to other companies. The customers of Birla sun life and AVIVA mostly prefer news paper as a medium to create awareness. The chi square value is 137.926 and p=0.0, indicating the statistical significance at 1% level. Hence the difference of perception exists. It indicates news paper advertisements were perceived differently for different organisations.In case of Birla sun life and AVIVA the news paper is perceived to be the most preferred communication channels to spread information, while for other organizations it was sometimes preferred.

Sales people: The opinion of respondents regarding sales people as a medium of communication are also shown in table 4.2 It is observed that the views of respondents are mostly in the perceptual groups 3 and 4,indicating the higher preference for the media. The Chi square value is 64.168 and p= 0.0 ,which is less than 0.05.It means that chi square value is significant at 1% level indicating the difference in perception of consumers. Hence sales people were perceived differently for different organizations. Also in case of all the organizations, sales people are perceived to be the most preferred communication channels to spread information.

Website: It is observed that, the perception of respondents towards website as a medium of creating awareness is similar to the earlier two media. In case of five insurance players, the website is perceived to be the most acceptable communication channels to spread information, since in the five point scale of perception the views of the respondents are mostly in the perceptual group 3 and 4, indicating the higher preference for the media. The Chi square value is 116.67 and p= 0.0 ,which is less than 0.05.It means that chi square value is statistically significant at 1 level indicating the difference in perception consumers. This indicates websi advertisements were perceived differently fo different organizations.

Person to person contact: It is observed tha in case of all five insurance players, thi channel is perceived to be the most acceptable communication channel to spread information since in the five point scale of perception the views of the respondents are mostly in the perceptual group 3 and 4 indicating the higher preference for the media. The Chi square value is 70.299 and p= 0.0 ,which is less than 0.05.It means that chi square value is statistically significant at 1% level indicating the difference in perception of consumers. This indicates person to person contact advertisements were perceived differently for different organizations.

E-mail: In case of five insurance players, this channel is perceived to be the most preferred communication channel to spread information since the views of respondents are mostly in the perceptual group 3 and 4, indicating the higher preference for the media. The Chi square value is 61.229 and p= 0.001, which is less than 0.05.It means that chi square value is statistically significant at 1% level, indicating the difference in perception of consumers Hence e mail advertisements were perceived differently for different organizations.

Web chart: In case of five insurance players the channel is perceived to be the most preferred communication channel to spread information, especially for LIC .It is because the views of the respondents are mostly in the perceptual group 3 and 4, indicating the higher preference for the media. The Chi square value is 48.507 and p= 0.002 ,which is less than 0.05.It means chi square value is statistically significant at 1% level, indicating the difference in perception of consumers. Hence web chart advertisements were perceived differently for different organizations.

Telephone: In case of five insurance players, this channel is perceived to be the most preferred communication channel to spread information, since the views of respondents are mostly in the perceptual group 3 and 4, indicating the higher preference for the media. The Chi square value is 66.977 and p= 0.00, which is less than 0.05 It means that chi square value is statistically significant at 1% level, indicating the difference in perception of consumers. Hence the telephonic advertisements were perceived differently for different organizations

11. Consumer's Perception towards Private and Public Insurers

The table 3 depicts the perception of respondents towards different communication channels in creating awareness relating to CRM across private and public organizations. Those media are website, news paper, sales people, e mail and web chart etc in creating awareness.

***Table 3**. Consumer's Perception towards Private and Public Insurers*

Sl. No.	Comm. Channel	Organization Type	Perception 1	2	3	4	5	χ^2	P
1.	News paper	Private		0	50	128	34	91.334	0.0
		Public		8	52	12	0		
2.	Sales people	Private			50	124	38	25.978	0.00
		Public			36	36	0		
3.	Web site	Private		14	88	104	6	53.817	0.00
		Public		22	44	6	0		
4.	E-mail	Private		8	76	126	2	13.685	0.003
		Public		0	28	38	6		
5.	Web-chart	Private		14	102	90	6	18.503	0.003
		Public		0	22	50	0		

News paper: It is observed that in case of private insurers the news paper is perceived as most preferred communication channel since in five point scale of perception, the views of respondents are mostly in the perceptual group 3, 4 and 5 indicating higher preference for the media. But for the public insurers the views of the respondents are mostly in the perceptual group 3 and 4 indicating as a mostly preferred channel. Chi square value is 91.334 and p= 0.0, which is less than 0.05 It means that the value is statistically significant at 1% level, indicating the difference in perception of consumers. Hence the impact of news paper in creating awareness across different organization is statistically significant. This indicates news papers were perceived differently for different organizations.

Sales people: It is observed that, for private insurers, sales people are perceived to be most preferred channel of communication since in five point scale of perception, the views of respondents are mostly in the perceptual group 3, 4 and 5 indicating higher preference for the media. But for the public sector the views of the respondents are mostly in the perceptual group 3 and 4. Chi square value is 25.978 and P=0.002, which is less than 0.05 .It means the value is statistically significant at 1% level, indicating the difference in perception of consumers. Hence the impact of sales people in creating awareness across different organizations is statistically significant .This indicates sales people were perceived differently for different organizations.

Website: It is observed that, for private insurers, web sites are perceived to be most preferred channel of communication since in five point scale of perception, the views of respondents are mostly in the perceptual group 3 and 4 indicating higher preference for the media. Chi square value is 53.817 and p=0.0, which is less than 0.05 It means the value is statistically significant at 1% level indicating the difference in perception of consumers. Hence the impact of websites in creating awareness across different organizations is statistically significant and were perceived differently for different organizations.

E mail: It is observed that, for private insurers, e mails are perceived to be most preferred channel of communication since in five point scale of perception, the views of respondents are mostly in the perceptual group 3 and 4 indicating higher preference for the media. Chi square value is 13.685 and p=0.003, which is less than 0.05. E mail can be a very confidential source of information. Chi square value is significant at 1% level, indicating the difference in perception of consumers. Hence the impact of e mail in creating awareness across different organization is statistically significant .This indicates e mails were perceived differently for

different organizations.

Web chart: It is observed that, for private insurers, web charts are perceived to be most preferred channel of communication since in five point scale of perception, the views of respondents are mostly in the perceptual group 3 and 4 indicating higher preference for the media. Chi sq value is 18.503 and p= 0.0034,which is less than 0.05.Chi square value is statistically significant at 1% level indicating the difference in perception of consumers. Hence the impact of web chart in creating awareness across different organizations is statistically significant .This indicates web charts were perceived differently for different organizations.

12. Findings

As far as perception of consumers towards communication channels are concerned (from table 2) for news paper, the views of the respondents are mostly in the perceptual group 3 and 4(in a 5 point likert scale of perception) for LIC It shows the consumers perceive that news paper has greater impact for LIC or it is the most preferred channel to spread the information regarding products and its benefits in Odisha market. Also the value of p is less than 0.05, which is statistically significant. It is found that perceptual difference exists and there is relationship between independent variable like news paper and dependent variable like customer awareness. So, news paper has greater impact on creating awareness.

For LIC, Birla and ICICI prudential life insurance, sales people are most influential for product awareness compared to other companies, percentage of total for LIC is highest that is 25.6%, 23.5% for Birla and 18% for ICICI in a five point scale of perception and thus sales people are most preferred channels to spread the information regarding product's benefits. The views of the respondents are mostly in the perceptual group 3 and 4.also the value of p is less than 0.05, which is statistically significant and perceptual difference exists, indicating the relationship between the variables. Hence sales people are preferred to spread the awareness.

As far as the electronic channels are concerned, website, web chart, e mail and telephone are perceived strongly and are the most preferred channels to increase the awareness. For communicating channel like website, consumers perceive each company is using this channel and in five point scale of perception, opinions are coming u perceptual group 4 (mostly preferred). Simi for e mail, web chart and telephone, percep of consumers across the companies reflect for each company the percentages are hig Views of the respondents are also perceptual group3 and 4, indicating hig preference for media and percentage of t for LIC are always above 25% for all electro channels. These channels are preferred T the fact is that, in Odisha market the insur have started to interact with custom electronically by taking the help of electro channels to spread the information regard products. Besides for all the electro channels the p values are less than 0.(which are all statistically significant. It mea the relationship exists between t independent variable like electronic channe and the dependent variable like custom awareness

12.1. Consumer's perception towards private and public insurers

For communicating channel like new papers (from table 3), the consumers percei strongly and it's a preferred channel for bo private and public insurers. The views of th respondents are in perceptual group 3 and 4 five point scale of perception for both privat sectors and public sectors and for eac communicating channel the values of p ar statistically significant, for which the perceptua difference exists. Then it is found that new paper advertisements are adopted for eac company to spread the information, regardin benefits of insurance policies.

For all the electronic channels; like website e-mail and web chart the consumers preferences are strong. Also it is found that the communicating channels like web site and web chart are becoming popular for insurers to create maximum awareness regarding the products. It is because the p values are all less than the significance level and relationship exists between the independent and dependent variable.

13. Conclusion

It is concluded that, for LIC and ICICI prudential life insurance, sales people are most influential and responsible for product awareness compared to other companies. In these two companies sales people or the insurance agents are doing the good job by touching the target customers in time and

maintaining a need based selling. The response for news paper is very strong also as a communicating channel to increase the awareness. Again the responses for all the electronic channels are always preferred. So consumers perceive that the electronic communication channels like, website, mail, webchart and telephone have much more impact to increase the awareness. So it is concluded that, the undertaken five insurance companies are getting success by utilizing the electronic communicating channels, which can help to deliver quick service and convenient on line interaction to convince or sell the products to the potential customers. These companies are also able to create personalization and customization for the customers. These electronic channels help the agents also to motivate the customers and to build integration among customers and officials.

References

[1] Kotler, Keller, Koshy and Jha, (2010); Marketing Management, PHI, New Delhi.

[2] Dyche, Jill, (2002), The CRM hand book, Pearson education, Singapore

[3] Sheth, Jagdish N. and Parvatiyar, (2003), Handbook of relationship marketing, Sage Publication, New Delhi.

[4] Kothari, C.R. (2009), Research methodology, New Age International Publisher, New Delhi. officials and customers.

[5] Chou, C.D. (2004), Adopting Customer Relationship Management Technology, Industrial Management Journal, vol.102, no.8, pp.442-452.

[6] Gal, Breathe. J. Rogers, T. (1999); Customer relationship leadership, TQM Magazines, vol.11, no.3, pp.161-71.

[7] Gefen, D. and Ridings, C.M. (2005); implementation team responsiveness and user evaluation of customer relationship management, journal of management information system, vol.19, no.1, pp.47-69.

[8] Fayerman, M. (2002), Customer relationship management, New Directions for Institutional Research, vol.1, no .113, pp57-67.

[9] Information on customer relationship management and its solution, www.crminfoline.com/crm-articles http://dilbert.iiml.ac.in/crm

[10] Importance of e CRM in marketing management. www.ehow.com

[11] On demand CRM softwares and ERP at its best,www.salesboom.com

[12] Gate way to customer relationship management, www.crm-infosource.com

[13] CRM systems and implementation in office www.acadjournal.com/2008/v22

GREEN HRM FOR BUSINESS SUSTAINABILITY

Dr.Sasmita Nayak, Vikashita Mohanty, (1, 2) Asst.Prof., MBA, GIFT ,BPUT

Abstract: *For globalisation, industrialisation and liberalisation every organisation tries to sustain in competitive business environment. In current scenario companies only sustain by maintaining eco-friendly environment. Natural resources are vital resource for an organisation .It is the responsibility of every organisation to implement a eco-friendly system to create a healthy environment for long term sustainability. One emerging issue Green HRM by which organisation implement policies and procedures for benefit of organisation as well as for society. Green HRM focuses on rules, regulations, recruitment, selection, induction, training, performance appraisal, counselling, safety and welfare concern of employees. Green initiative in HR practice is a corporate social responsibility itself. This paper tries to understand the concept of Green HRM and the role of HRM to create green environment for sustainability of business.*

Key words: Green HRM, sustainability, eco-friendly, corporate social responsibility

Introduction:

Green Human Resource Management is the integration of HR practice with environmental management. For organisational sustainability every organisation are using green practice in their manufacturing process. Now a day's organisations are using HR strategies to create environment friendly product and services for society. By aligning organisational goal with Human Resource Management for business sustainability is known as Green Human Resource Management. Many companies using Green HR practice which helps in reducing carbon foot print through less use of paper, mail communication, video conferencing meeting, E-training, video conferencing interview and encouraging employee to turn off light and computer when they are leaving the desk or in weekend. Green HR is using environment friendly HR practice as well as develops of knowledge capital of employees. It is helpful to employees for their career development as well as organisation sustainability. Measuring employee's performance on green practice is one of key function in Green HRM. HR practices are aligned with organisational strategy that is live with culture and business goal (Boselil, 2001). Green Human Resource management is alignment of HRM practice with the business's environmental goals (Jabbour, 2013). Green HR practice results in greater efficiencies and build an atmosphere of better employee engagement which helps to operate and environmentally sustainable business practice (Meilyy and Susanti, 2013).

Objectives of the Study

- To study the concept of green HRM.
- To study Green HR initiatives taken by organisation

Literature Review

Dechant and Altman (1994) suggested on employee perception of a firm's environmental behaviour. Employees are willing to work in an organisation only when they feel it adds to their value of profile.

A positive relationship between employees and employers facilitate productivity participation and empowerment (Daily & Huarg 2001). There is a positive effect of green HR on corporate environment leading to competitive advantage of firms. Sudin (2011). The compensation and rewards systems in an organisation could contribute to environment management. Rewards motivate and increase commitment from workers to be environmentally responsible. HR practices such as training and development, performance management, compensation management, reward system also concerned for environment management. It increases the ability to adopt change and develop attitudes towards environment issues (Carter & Dresner, 2001). Green HRM initiative in

performance management may be an effective way to enhance environment friendly HR practices (Milliman and Clair, 1996).

Govindarajulu and Daily (2004) have suggested that employee involvement programme may helps the organisation to promote green practices which improve health, safety and welfare of workers. Green HRM is the use of human resource management policies to promote sustainable use of resources within business organisation Madip (2014).

Practices of Green HRM

- Paperless office
- Turn off lights, Computer and Printer after work and on weekends.
- Mail communication.
- Electronic filing.
- Encouraging use of laptop instead of desktop.
- Waste Management.
- Online recruitment.
- Video conferencing meeting.
- Paper less training.
- Performance management on basis of green practices.
- Car pooling
- Job sharing
- Use of brown bagging in the office.
- Loan discount on energy saving home and fuel efficient car.

Components of Green HRM

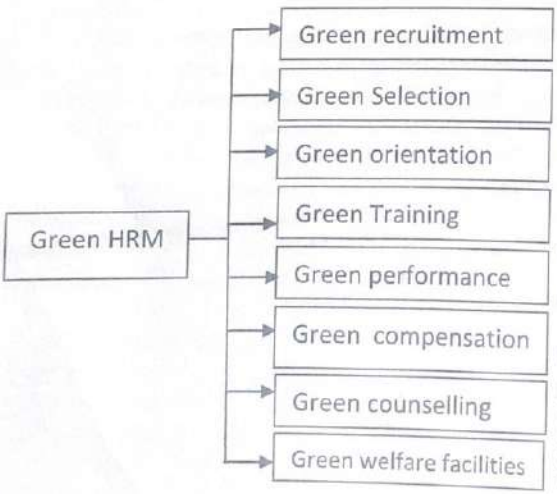

Green Recruitment-

Now organisations are giving their advertisement through their web-site. This method is very fast, cheap and easy to assess. Bauer & Aiman- Smith (1996) identified the impact of pro-environmental factor recruitment that employees are more willing to work in a firm which promotes environmental characteristic. Frank (2003) identified the relationship between ethical behaviour of a company and its impact on employee perception. He suggested employees willing to work for environmentally friendly company.

Green Selection:-

Interviews are conducted by group discussion, personal interview, and different activities and in online test. Candidates could be given preferences that are more environment friendly for an organisation.

Green Orientation:-

Induction and orientation programmes are framed in such a way that facilitates the new comers about green practices. Green issues like health and safety, use of material and cleanness of area in work place etc.

Green Training:-

Training should be given on "increase of green management". Trainer should give their training on presentation or by video conferencing. Trainer should use more soft materials rather than printed handouts to reduce the use of paper. Sarkaris (2010) suggested that employees presented better training on better perception of environment management principles. Daily (2007) suggested training will help employees identify with challenges and opportunities of green management principles.

Green Performance Appraisal:-

In performance appraisal use of green practice should be one of the key performances Area (KPA). Green performance appraisal motivates employees for use of green practices in organisation. Jabbar (2012) studied that human dimensions

impacts the organisational performance as well as environmental management system or organisation.

Green compensation and reward:-

Compensation and reward system should be directly linked to use of green skills. Special bonuses should be given to employees for their effort of less carbon foot print. Forman and Jorgensen (2001) suggested rewards help to improve employee commitment to environment management programmes.

Green Counselling: -

Top level managers and counsellors can take initiative to motivate employees for implementation green practices and business sustainability.

Green Welfare Practices:-

Now a days, many organisations changed the concept of health, safety and welfare of employees to health, safety and environmental management. These companies have continuously giving their effort to reduce stress occupational disease and hazards at work place.

Impact of green HRM

In the first level fully implementation of green HRM is difficult but by continuous effort organisation may create learning environment which adds value to professional and personal life of employees. The impacts of green HRM practices are noted below.

- It increases employee morally.
- It preserves the natural resources.
- It improves the relationship between stake holder, customer, supplier, employees and the media.
- It reduces the overall cost.
- It increases the company's image.
- It develops the knowledge of green HRM.
- It motivates innovation and growth.
- It provides competitive advantage.

Conclusion:-

Green HR practices focused on improving HR practices for business sustainability. Green HR aims at reducing wastages and very much concern for environment. Eco-friendly HR initiatives resulting greater efficiencies and create better developmental climate for business. By doing so, organisations would add value to their brand image. The green recruitment, green selection, green induction, green performance appraisal, green compensation and rewards system are powerful tools in making employees more eco-friendly for business sustainability.

GREEN PRACTICES ADOPTED BY COMPANIES IN INDIA

NAME OF COMPANY	GREEN PRACTICE	IMPACT
LG India	Newly lunched LED E60 and E90 series monitor	40% less energy than conventional LED monitors
HCL	Introduce eco-friendly products HCL ME 40 notebooks	Energy efficiency
Hair India	Lunched Eco life series	Energy efficiency
Samsung India	Eco-Friendly LED backlight in LED TV	40% less use of electricity
Tata Consultancy Services	Initiative of creating technology for agriculture	Community benefits
ONGC	Invention of green crematorium	Less use of Oxygen
Indusind Bank	Sending electrics message without counterfoils in ATM	Saving paper
ITC	Free bleaching technology	Cleaner environment approach
Wipro	Eco-friendly building	Saving energy and preventing waste
MRF Tyres	Eco-friendly tubeless tyre	Offers extra fuel efficiency

*Source: Fiinovation-(http://www.fiinovation.co.in)

Reference:-

1. Boselie, P., Paauwe, J., & Jansen, P. G. W. (2001). Human practice, International conference on Business, Economics, and Accounting Bangkok-Thailand.
2. Milliman, J. and Clair, J. (1996) 'Best Environmental HRM Practices in the US', in Wehrmeyer, W. (ed) (1996), Wehrmeyer, W. (ed) (1996) Greening People: Human Resources and Environmental Management, Sheffield: Greenleaf Publishing.
3. Sarkis, J., Gonzalez-Torre, P., & Adenso-Diaz, B. (2010) Stakeholder pressure and the adoption of environmental practices, the mediating effect of training. Journal of Operations Management, 28(2), 163-176.
4. Sudin, S. (2011) 'Strategic green HRM: a proposed model that supports corporate environmental citizenship', Paper presented at the International Conference on Sociality and Economics Development, Kuala Lumpur, Malaysia, 4–5 June, IPEDR, IACSIT Press, Singapore, Vol. 10.
5. resource management and performance: lessons from the Netherlands. *The International Journal of Human Resource Mana gement*, *12*(7),1107-1125.
6. Bauer, T. N., & Aiman-Smith, L. (1996). career choices: the influences of ecological stance on recruiting. Journal of Business and Psychology, 10(3), 445-458.
7. Carter, C., & Dressner, M. (2001). Purchasing's Role in Environmental Management: Cross functional Development of Grounded Theory. The Journal of Supply Chain Management, 12-27.
8. Daily, B. F. and Huang, S. (2001). Achieving sustainability through attention to human resource factors in environmental management. International Journal of Operations & Production Management, 21(12), 1539-1552.
9. Daily, B. F., Bishop, J., & Steiner, R. (2007). The mediating role of EMS teamwork as it pertains to HR factors and perceived environmental performance. Journal of Applied Business Research, 23(1), 95-109.
10. Dechant, K., & Altman, B. (1994). Environmental leadership: from compliance to competitive advantage.Academy of Management Executive, 8(3), 7-27.
11. Forman, M., & Jorgensen, M. S. (2001). The social shaping of the participation of employees in environmental work within enterprises – experiences from a Danish context. Technology Analysis and Strategic Management, 13(1), 71-90.
12. Frank, R. H. (2003). What Price the Moral High Ground? Ethical Dilemmas in Competitive Environment. Princeton University Press.
13. Govindarajulu, N. and Daily, B.F. (2004) 'Motivating employees for environmental improvement', Industrial Management and Data Systems, vol.104, no.4, pp.364-372.
14. G. Mandip, Green HRM: People management commitment [3]to environmental sustainability. Research Journal of Recent Sciences, 1, 244-252, 2012, accessed on November 02 , 2014, from http://www.isca.in/rjrs/archive/iscsi/38.ISCA-ISC-2011-18CLM-Com-03.pdf .
15. Jabbour Chiappetta, C. J., Jabbou Lopes de Sousa, A. B., Govindan, K., Teixeira, A. A., & Freitas Ricardo de Souza, W. (2012). Environmental management and operational performance in automotive companies in Brazil: The role of human resource management and lean manufacturing, Journal of Cleaner Production.
16. Jabbour, C (2003), Environmental training in organisations: From a literature review to theoretical frame work, resources, conservation and recycling, Vol.12.
17. Maaargaretha, M. And Saragih, S. (2013), Developing New Corporate culture through green human resource

Green Marketing- Its application, scope and future in India

Vikashita Mohanty, Dr.Sasmita Nayak, Asst.Prof, MBA

Abstract: *Green Marketing a major breakthrough in the vast field of marketing has become one of the growing areas and is inviting a lot of attention towards it. In India Green Revolution started as a new revolution in late 1990's .Consumer Preferences and their buying behavior are changing and so is their concern for the society. There has been a change in consumer attitudes towards a green lifestyle. The companies are also actively trying to increase their impact on the environment. There is a paradigm shift from traditional marketing to green marketing; companies these days are facing many new challenges. Organizations and business however have seen this change in consumer attitudes and are trying to gain an edge in the competitive market by exploiting the potential in the green market industry. This paper discusses the initiatives of customers and corporate towards green marketing in India. Though their initiatives are different but the goals are similar and the initiative has resulted in competitive advantage for these organizations and is also a fruitful step towards a green global market.*

Keywords: ***Green Marketing, Green Product, Consumer preferences, Competitive advantage, Green price***

Introduction:

Green Marketing takes into account all those activities that ensure the best of service to the customers and also meeting the needs of the customers in such an efficient and innovative way that ensure that the environment is not under threat in any manner due to the above activities. Green marketing is also known as ecological marketing, sustainable marketing. Due to increase in concerns about the safety and sustainability of environment and society among the consumers the concept of Green Marketing is attracting a lot of attention and application.

Green Marketing is the process of promoting products and services based on their positive impacts on the environment and their benefits to the society. Product may be environmentally friendly in itself or produced in an environmentally friendly way and they are known as Green Products. It is important to identify the products which can be tagged as' Green'. Green products include products:

- Being manufactured in an environmentally sustainable manner
- Energy Efficient and Water Efficient
- They are healthy
- Non toxic materials and not containing ozone-depleting substances
- Can be recycled and/or is produced from recycled material
- Can be made from renewable materials (such as bamboo, cotton etc.)
- Not making use of excessive packaging or using plastic packaging
- Being designed to be repairable and not "throwaway"
- Green products are products that are more durable and efficient

Green Marketing is about holistic marketing in which all the process from procurement of raw materials to consumption of finished goods India and Indian market is marked by a lot of emotional factors. Most Indian consumers are sensitive about the sustenance of a green and healthy environment. Indian consumers and also many Indian corporate are working towards the betterment of a green environment by adopting healthy and innovative ways. The consumers are getting aware and concerned about the environmental issues and are playing their little parts in making a change. Various social Medias are also influencing the consumers by making them aware of the probable hazards due to inappropriate marketing activities. The various social media are also giving platform for educating people about environmentally friendly activities like non usage of plastic bags, usage of bio-degradable bags, generation of

minimum amount waste, using energy efficient electronic appliances. Educating the consumers through various media has shown a remarkable change in the buying pattern of consumers and has helped in making the consumers more environments friendly.

Some Green concepts in Green Marketing:

Green products: Green Products are the ones which are which are recyclable in nature are not harmful to the environment. They are manufactured in an eco friendly manner and are also use eco friendly packaging and promotion.

Green Consumerism: Informing and educating the consumers and thus attracting the consumers to use green products and to recycle the products and motivating them to buy eco friendly products we can involve consumers in the process of Green Marketing. This phenomenon is known as Green Consumerism

Green Pricing /Green pricing Gap : As the manufacturing of genuine green products attracts genuine raw materials which are pure and making them also attracts additional charges in terms of labor and raw materials they are normally charged at a higher price than the normal products .This creates a gap in price between the prevailing non green products and green products. This is known as Green Pricing or Green pricing gap.

Green Promotion: Creating an image of Go green for their products and their brand in the market through appropriately projecting them is known as Green promotion. Through Green promotion the companies tries to create and claim their concern for sustainable business and environment.

Green Place: Green Place with respect to green marketing is creating an environment friendly place. Companies build energy efficient buildings for their offices. Many big and small corporate houses are adopting this strategy of Green Place. Tata's have created a building that runs entirely on solar energy and thus saves electricity.

Application of Green Marketing by Corporate Houses in India:

Various Indian and Multi National Companies are manufacturing Green products and are positively impacting the Indian green marketing sector. Companies like

- **Fab India:** Fab India is a Indian fashion brand with its stores all across the nation. This brand is popular for promoting handloom and hand made products. This brand is into fashion clothing, cosmetics and furniture's. They have been manufacturing the products in a complete eco friendly manner and they claim of using the ingredients without any harmful chemicals. The packaging is also eco friendly and they discourage use of polythene for packaging.

- **Patanjali:** Patanjali is promoted by a person who is face of natural and healthy practices. Swami Baba Ramdev who started Patanjali proudly claims of producing eco friendly and safe products.

- **TATA Group of Companies:** Tata Group is another trendsetter in promoting green marketing in the Indian markets. Tata Group under their flagship produces products which are eco friendly and adopts green ways of marketing its image. The Tata Group companies such as Tata Steel, Tata Motors, Tata Chemicals and Tata Consultancy Services contribute positive results to the environment. Tata Steel said it is currently working on more than 17

CDM i.e. Clean Development mechanism projects to check harmful emission with Ernst & Young and these projects are at various stages of approval at United Nations Framework Convention on Climate Change

- **LG India**: LG India is one of the initial propagators of Green products in India, they have a number of electronic gadgets those are eco friendly in nature. They rarely use halogens or mercury and lead in the manufacturing process. The products do harm the environment and also uses 40% less electricity

- **HCL**: HCL is also adopting the green strategy. It has recently launched HCL ME Notebooks which are eco friendly in nature. These notebooks do not use any polyvinyl chloride or any other harmful chemicals in manufacturing. It has also got a five star rating from the Bureau of energy efficiency

- **Haier**: Haier in its new green initiative has been focusing on eco branding. They have launched Eco life series. Their products are also energy efficient and safe to the environment

- **Samsung India**: They are taking a lot of considerable efforts in the path of promoting and practicing green marketing in the India. Their eco friendly products like LED TV,Air conditioners does not use any harmful chemicals like mercury and lead.Their products also claim to consume 40% less electricity

- **SAIL**: SAIL is one of largest producer of steel in India. SAIL is also engaged in green activities. SAIL in various cities Rourkela and Bhilai has established green crematoriums that serves as a replacement for funeral pyres that emits so much smoke and uses oxygen
- **IndusInd Bank**: IndusInd Bank is one of the first bank to introduce green practices. They discouraged the use of papers in the branches and their ATM's and started sending electronic messages and mails. These practices has helped in saving the environment and also reduced deforestation. Many other banks like ICICI,SBI ,Axis etc. are also following these practices

- **ITC Ltd**: ITC has introduced ozone treated elemental chlorine free bleaching technology and it has impacted the environment positively. They have also adopted a Low Carbon Growth Path and a Cleaner Environment Approach that is creating a better environment

- **Wipro**: Wipro has launched a wide range of eco friendly desktops.Wipro under its green initiatives have undertaken a lot of measures

Strength of Green Marketing

- **Is self sustainable**: Green Marketing is a breakthrough strategy in the current era where the focus is on adopting practices those are safe on the environment i.e. having least or no negative impact on the environment. This helps in creating a more sustainable and healthy surrounding around us

- **Is cost saving**: Green Marketing also saves a lot of cost with respect to its manufacturing, packaging and promotion. As they use eco friendly

products and also practices 3R's i.e. Reduce, Reuse and Recycle these practices cuts down on a lot of expenditure that otherwise could have taken place.

- **Is Innovative**: Green marketing is a new and innovative concept and thus it attracts a lot of consumers towards it. And as it comes with a message of Go Green it is more worthy in the perception of the consumers.
- **Helps in sustainable long term growth**: Green marketing is here to stay. As it is based on an eco friendly process it is sustainable and also ensures long term growth and profit to the organization.
- **A part of CSR activities**: Green Marketing is a part of CSR activities which is practiced by most of the corporate houses. And it is a mandatory activity which strengthens the image of the corporate in society.

Weaknesses of Green Marketing :

Lack of appropriate knowledge: Green Marketing being a new concept many people are not fully aware of it. Many consumers are not educated enough about green produces. And this lack of knowledge is acting as a weakness for the promotion of green marketing.

Highly Priced: As sometimes the manufacturing of the green products are expensive it automatically demands a high selling price that is higher than other contemporary substitutive products this may sometimes discourage the consumers to go for green products until they are green customers.

Beliefs of Consumers: Many consumers are of the belief that the green products are not as efficient as the other competitive products and they also have a perception that the green products are much highly priced.

Lack of Research and Development and Technology: Another barrier in the way of Green marketing is the lack of proper technology to bring about green products in use and also lack of adequate research and development in this field.

Scope of. Opportunity Green Marketing in India:

Consumer Demand:

Indian consumers are emotional buyers, if we study their buying behavior we see that the Indian consumer does a lot of emotional buying. As we see that many Indian consumers are more green product oriented it gives a great scope for the green market to expand. Organization in India has indentified the need of the consumers, they are realizing the need for adoption of an ecological marketing as they are aware that consumers are demanding products that are not only safe for them to consume but should also be same to the environment. Conscious and green customers prefer the organizations that provide environmentally safe products. Companies nowadays have taken green marketing as a competitive advantage.

Corporate Social Responsibility:

Organizations like Tata group, Wipro, have been doing green marketing as a duty towards environment and society. They have been engaging in various activities to promote the green activities. This is also falling in line with the company's corporate social responsibility. Where the companies are discharging their duties towards the environment in which they are operating.

Competition:

One more scope of growth for green marketing comes in disguise of competition from the organizations that are practicing green marketing. Other companies who have not adopted the green marketing strategy are pressurized to adopt the strategy to compete in the industry.

Government Initiations:

Government today is taking a lot of initiatives to promote the activities that are safe for the environment. They have laid various policies and guidelines for the companies to adopt environment safe activities.

Cost Effectiveness:

Green Marketing has a wider scope in the current scenario because of its cost effectiveness. In green marketing activities the focus is on recycle and reuse of materials. The firms use technologies for reduction of waste materials and also for reutilization of materials. These activities are environment safe and also good for the society and are a need of the hour.

Threats In Green Marketing:

Balance between company's profitability and responsibity:

Various companies in today's time are finding it very difficult to strike a balance between the profitability and social responsibility. In today's time both profitability and social responsibility is important to sustain in the market.

Expensive Raw Materials:

Green Products are made up of materials which are natural and safe and can be recycled and reused. These materials attract a lot of costs, and as the manufacturing is costly this also acts as a threat in the way of green marketing.

Threat from competitors:

Many competitors come up with cheaper products as compared to green products and thus they act as a threat because most customers prefer to buy cheaper products.

Green Washing:

Various companies have identified the need of green marketing for sustainability. As not every company is capable of producing green product they pretend to produce green products and try to mislead the consumers. This is known as green washing.

CONCLUSION:

Studies have shown that various Social Medias like the ones given below are creating a lot of awareness among the consumers and is helping in creating and promoting Green marketing:

- Internet
- Commercial Messages
- News Paper and Magazines
- Hoardings and Banners
- Television and Radio
- Friends and Relatives etc

The things to rejoice is that the corporate as well as the consumers are becoming more and more concerned about their roles in building a green environment.

We can thus say that green marketing is much beyond only products that are environment safe. It is also about how the company promotes its sustainable ways of practicing and producing goods which have little or no adverse impact on the environment.

Green Marketing is also facing a lot of challenges in meeting its goals. One of the common challenges faced is striking a balance between the profitability and of a company and its responsibility towards the society and environment. In today's scenario both the things are important to sustain in the market. A company has to be good in business as well as in discharging his duties towards the society and also towards the customers who are concerned about their surroundings.

Reference:

Ottman, J.A. et al, "Avoiding Green Marketing Myopia", Environment, Vol-48, June-2006

Unruh, G. And Ettenson, R. (2010, June). *Growing Green; Three smart paths to developing sustainable products.* Harvard Business Review. Vol. 5(6). Boston

J. M. Ginsberg and P. N. Bloom, —*Choosing the Right Green Marketing Strategy*,‖ MIT Sloan Management Journal, fall 2004: 79–84.

Sustainable Green Marketing the New Imperative. Dutta, B. (2009, January). Marketing Mastermind. Pg 23-26. Hyderabad: The ICFA University Press.

.J. Makower, —*Green Marketing: Lessons from the Leaders*,‖ Two Steps Forward, September 2005,

Chaudhary, Tripathi, Monga. Green Marketing and CSR. International Journal of Research in Finance and Marketing. 2010; 1(6):1–14.

Hybrid Scheduling for Impatient Clients with Reneging and Balking

[1]R.Kavitha, [2]S.Krishna Mohan Rao
[1]Research Scholar, Rayalaseema University, Kurnool, Andhra Pradesh, India
[2]Gandhi Institute For Technology, Bhubaneshwar, Khurda, India

Abstract: *The efficiency of scheduling algorithm lies in providing multimedia applications and web applications with data processing abilities. This paper introduces hybrid scheduling model which efficiently combines push and pull (on-demand) models for heterogeneous environment. The proposed algorithm considers variable sized data items and computes access patterns of data items by dividing the database at the server into two sets, pull and push. In order to deliver data items of push set hashing technique is used and for pull data items M/M/1 and M/M/C queuing models are employed for single pull channel and multiple pull channels respectively. The essence of this algorithm lies in reducing the access time by considering the dynamics of the system. Dynamics of the system considers impatient clients who leave the system before they are served, with the required data item. The proposed algorithm analyzes the system performance in terms of average access time in retention of impatient clients. The analytical model shows that the proposed algorithm performs well in handling impatient clients.*

Index Terms: average access time, balking, client's impatience, renege

I. INTRODUCTION

The advancement in current technology in web has given rise to serve the needy efficiently with the required data. To extract the required data and transmit it there is a need for broadcasting strategies In the mobile computing environment, information dissemination no longer requires a user to maintain a fixed position in the network. The wireless medium enables virtually unrestricted mobility and portability. A mobile computing environment requires two major components: a wireless network, and a portable computing platform. Currently used wireless networks are cellular networks, wireless LAN, wide-area wireless networks and paging networks. Mobile computing platforms include palmtops, Personal Digital Assistants (PDA); and personal computers. There are unique characteristics of wireless networks have significant impact on wireless data management. These include - channel limitation, asymmetry in the communications: the bandwidth of downlink (server-to-client) is greater than the uplink (client-to-server), frequent disconnection and relocation (move from one place to another): mobile users tend to switch their units on and off regularly and, power limitation: most of the portable units use batteries that require frequent recharge.

Information Dissemination is the most important application of mobile computing. In general, there are two basic methods to provide users with information. They are pull [4] and push [1] methods. In this paper, hybrid method is addressed with a variable data item size, which is the combination of both push and pull models.

In a hybrid push-pull environment, popular data items are broadcasted in the form of a broadcast disk, and less popular items are pulled from the server via explicit client requests. To retrieve individual records of interest, mobile users can either monitor the broadcast channels for the arrival of desired data or issue a pull request to the server. The broadcast disk can be viewed as storage on the air or as an extension of the server's memory, which alleviates pull-based requests considerably. Since the wireless broadcast channel is a limited resource in a mobile environment, data distribution should be carefully managed to achieve efficient utilization of the resources. This paper investigates a method to efficiently broadcast data. The existing algorithms [1], [5], [7] and [9] are not capable of handling heterogeneous environments where the data items have different sizes. The algorithm defined in [12] and [13], focuses on these heterogeneous environments but uses single channel for

broadcasting the data items. The above mentioned problem is solved by proposing a scheduling algorithm that is made available not only to the heterogeneous environment where the data items are of variable sized but also reduces the access time by effectively utilizing multiple channels for broadcasting the data items. Multiple channels [14] have capabilities and applications that cannot be mapped on to single channels. As they have several advantages which include better fault tolerance, configurability and scalability.

For achieving optimal average access time, the schedule related to packet fair queuing model discussed in [5] is used. For asymmetric communication, a three-player model [8], defined logically divides the clients, servers and service providers. The authors of [2] and [6] derive a method to be

Figure 1: **Hybrid Scheduling For Reneging Clients**

Adaptive which considers changes in the mobile client's requests, on the other hand many pull algorithms with preemption and non-preemption are proposed in [1], [3] and [5] but lacks in addressing the heterogeneity of data Items, dynamic computation of access patterns (probabilities) of the data items and lack of patience in the clients due to waiting for required data item.

Section II introduces the problems with client's impatience.
Section III starts with modeling the proposed system and ends with defining the algorithm. Simulation results in Section IV show the performance of the proposed algorithm. Finally, Section V concludes the paper with pointing out the future enhancement.

II. Client Impatience

In most of the cases involving practical application, it has been observed that the clients lose patience whilst waiting for the required data item. This, after a certain limit of tolerance, results in the client moving away from the system ensuing in a drop of access requests. This conjectures the performance of the system which in turn reflects the immediate need for corrective behavior. This is profoundly found in cases reflecting the false situation of the system. Considering the scenario where numerous requests for a single data item is received by the server due to client's impatience; in turn increases the access probability, even
when not requested by different clients . The access rate multiplies. In obtainable systems, the server remains unaware
of the information and hence considers the data item as popular and thereby inserts it in the push or pull set at the expense of other popular items.

So as a summary the problems with client impatience are

1) Leaving the system without being severed (Reneging)

2) Does not join the system after finding it as busy

(Balking)

III. Hybrid Scheduling

Hybrid scheduling is obtained by combing push and pull models. This scheduling partitions the database at server into two sets push and pull. The push set (queue) contains the data items to be broadcasted. Hashing technique is applied to broadcast the data items. For pull, M/M/1 queuing model is considered with reneging [10].

HYBRID SCHEDULING FOR RENEGING CLIENTS

While true do
Begin
Phase I:
1. Broadcast the data items according to hashing technique
2. Handling the requests coming in during broadcast
If the request received for push data item
then ignore the request
else
compute the reneging rate(dropping rate) and
decrease the access probability of the data item
update the stretch value of the data items in pull queue;
3. if Q_{pull} not empty
Phase II:
4. extract an item from the Q_{pull} with max stretch
5. if there is a tie
extract the item whose access probability is high
5. clear all the pending requests for that item
Go to step 2
End

A. Modeling the System:

The proposed algorithm uses Hybrid model. Let us specify the parameters and assumptions used in our model:

1) We assume that there are many clients who are been served by a single server. Figure1 shows the asymmetric communication environment where there is a single server and the downlink capacity of the channel is more than that of the uplink channel capacity.
2) The server maintains a database and it is assumed that it consists of N number of data items, each with different lengths (size). Let server push M data items and (N-M) are pulled. The service time is assumed to be dependent on the size of the data item. Larger the size of data item higher its service time. The size of the data item i, is denoted as s_i. The stretch of the data items are calculated as $S(i) = \frac{p_i}{s_i}$.
3) The server supports C channels and each channel has a bandwidth b. Among these channels, C_{pull} are number of on-demand or pull (uplink) channels, for accepting client's requests and C_{push} are the broadcast channels. So, $= C_{push} + C_{pull}$.
4) Clients send requests to the server for their required data item. The requests from the client are accumulated as access probabilities.
5) The access probabilities of data items are skewed and modeled by ZipF distribution, which is typically used to model non-uniform access probabilities [9]. We use the same mathematical formulation for the ZipF distribution. That is, if we label the items in decreasing order of popularity, the probability of particular request for item i is given by $p_i = \frac{(1/i)^\theta}{\sum_{j=1}^{N}(1/j)^\theta}$ where θ is access coefficient.

   As server broadcasts M data items, so the size of Q_{push} is M. And the sizeofQ_{pull} is (N-M). Thus the total access probabilities of data items in $Q_{push}$is $\sum_{i=1}^{M} p_i$and in pull queue is $\sum_{i=M+1}^{N} p_i$
6) The time taken between successive requests and the service times of the server are exponentially distributed. Thus the service rate of Q_{push} is $\mu_{push} = \sum_{i=1}^{M} p_i \times s_i$ and Q_{pull} is$\mu_{pull} = \sum_{i=M+1}^{N} p_i \times s_i$.
7) Let λ be the arrival rate of the system and the requests that are send by the clients be $\lambda_{pull} = (1 - \sum_{i=M+1}^{N} p_i) \times \lambda$
8) Client upon putting request will wait for certain amount of time before the required data item is broadcasted. If not began, client get impatient or reneged and leave the system with probability$q$. The reneging time follows exponential distribution with ξ as parameter. When $\xi = 0$ means that the clients never leave the system before its service. This indicates that it is retention of reneged clients
9) On arriving client finds the server busy and does put request i,e may balk with q' or join with probability $1 -$

q'. If $q' = 0$ represents client join the system.

As hybrid broadcast results from the combination of push and pull models, we will start with formulating the push and pull models and then combine those models to calculate the overall access time for the proposed hybrid algorithm.

B. Analytical Model for Push Model To Minimize Expected Delay

The server has N number of data items where for M items are for broadcasting and remaining N-M are the requests put by the clients. The server picks the data items from the Q_{push} and transmits them on to the C_{push} broadcast channels. The number of data items that have to be broadcasted on to each channel is determined by hashing function. The hashing function is defined as :$f(s_i) = s_i mod C_{push}$ where s_i is the size of the data item i. Store these $f(s_i)$ values and arrange them in ascending order. All data items with same $f(s_i)$ are broadcasted onto the same channel. So as a result there will be m_i, number of data items in each broadcast channel i where $i = 1,2,3,\ldots C_{push}$. These m_i values differ from channel to channel. Each channel has bandwidth, b. As C_{push} channels are used for broadcast, the total bandwidth of these channels is bC_{push}. The average access time for a broadcast data item is the average time spent on waiting for that item. As the bandwidth of each push channel is assumed to be b and the average size of a data item in a channel i, $S_{tot} = \sum_{j=1}^{m_i} s_j$, the propagation time for each data item of a single broadcast channel is equal to S_{tot}/b. The average probe time for all channels is $S_{tot}/2bC_{push}$ In skewed broadcast system the expected waiting time $(E[T_{C_{push}}])$ for a data item in the push channel i given as :

$$E[T_{C_{push}}](i) = \frac{s_i}{b} + \frac{S_{tot}}{2bC_{push}} \quad (1)$$

The Average access time (AAT) of all the push or broadcast channels will be derived as

$$A[T_{C_{push}}] = \sum_{i=1}^{M} pi \times E[T_{C_{push}}](i) \quad (2)$$

$$A[T_{C_{push}}] = \left(\sum_{i=1}^{M} pi \times \frac{s_i}{b}\right) + \frac{S_{tot}}{2bC_{push}} \quad (3)$$

C. Analytical Model for Pull Model to Minimize waiting Time

When Reneging is considered:

For pull, M/M/1 queuing model with reneging is used where n is the number of requests from the clients and N is pull system capacity. According to [10] queuing model with retention of reneged clients with

$$Pr_n = \left[\prod_{k=M+1}^{n} \frac{\lambda_{pull}}{\mu_{pull}+(k-1)\xi q}\right] Pr_0; 1 \le n \le N \quad (4)$$

$$Pr_0 = \frac{1}{1 + \sum_{n=M+1}^{N}\left[\prod_{k=M+1}^{n} \frac{\lambda_{pull}}{\mu_{pull}+(k-1)\xi q}\right]}$$

As the clients become inpatient and leave the system there by dropping the request for the data item and is calculated as

$$R_{drop} = \lambda_{pull} \sum_{n=M+1}^{N} Pr_n - \sum_{n=M+1}^{N} n\mu_{pull}\left[\prod_{k=M+1}^{n} \frac{\lambda_{pull}}{\mu_{pull}+(k-1)\xi q}\right] Pr_0 \quad (5)$$

The above is the model defined for single pull(on-demand) channel .
For multi pull channel M/M/C_{pull} model defined as

$$Pr_n = \frac{1}{n!}\left(\frac{\lambda_{pull}}{\mu_{pull}}\right)^n Pr_0 + \left[\prod_{k=C_{pull}+1}^{n} \frac{\lambda_{pull}}{C_{pull}\mu_{pull}+(k-C_{pull})\xi q}\right] \frac{1}{C_{pull}!}\left(\frac{\lambda_{pull}}{\mu_{pull}}\right)^{C_{pull}} Pr_0; \quad 1 \le n \le N \quad (6)$$

Where

$$Pr_0 = \left[1 + \sum_{n=1}^{C_{pull}} \frac{1}{n!}\left(\frac{\lambda_{pull}}{\mu_{pull}}\right)^n + \sum_{n=C_{pull}+1}^{N} \prod_{k=C_{pull}+1}^{n} \frac{\lambda_{pull}}{C_{pull}\mu_{pull}+(k-C_{pull})\xi p} \frac{1}{C_{pull}!}\left(\frac{\lambda_{pull}}{\mu_{pull}}\right)^{C_{pull}}\right]^{-1}$$

Dropping rate is defined for multi-channel pull system as

$$R_{drop} = \lambda_{pull} \sum_{n=1}^{N} Pr_n - \sum_{n=1}^{C_{pull}} n\mu_{pull} \frac{1}{n!} \left(\frac{\lambda_{pull}}{\mu_{pull}}\right)^n Pr_0 + \left[\sum_{n=C_{pull}}^{N} C_{pull}\, \mu_{pull} \prod_{k=C_{pull}+1}^{n} \frac{\lambda_{pull}}{C_{pull}\mu_{pull}+(k-C_{pull})\xi p}\right] \frac{1}{C_{pull}!} \left(\frac{\lambda_{pull}}{\mu_{pull}}\right)^{C_{pull}} Pr_0;$$

(7)

Where $\sum_{n=1}^{N} Pr_n = 1$

Expected pull system size is obtained as

$$Pull_{SysSize} = \sum_{n=M+1}^{N} nPr_n$$

(8)

If Pr_n is substituted in (4) then the expected size of the pull system for single channel is obtained. If Pr_n is substituted in (6) and expected size for multichannel is derived.

$$E[TR_{pull}] = \frac{Pull_{Syssize}}{\lambda_{pull}} X \sum_{i=M+1}^{N} p_i$$

(9)

The case of retention of clients comes when reneging parameter is set to 0 ($\xi = 0$).

When Balking with reneging is considered:

According to the authors of [10] model the system for retaining impatient clients. The M/M/1 queuing model is considered and devised a convincing method to retain the clients. Thus, there is a probability say, q not to retain in system and (1-q) for retention. An arriving requests from client finds the server busy on arrival, may balk with probability q' or join the system with $1 - q'$

So Pr_0 *and* Pr_n are defined as follows:

$$Pr_n = \frac{\lambda_{pull}}{\mu_{pull}} \left[\frac{(\lambda_{pull} \times q')^{n-1}}{\prod_{k=M+1}^{n-1} \mu_{pull} + k\xi q'}\right] Pr_0 ; 1 \le n \le N$$

and

$$Pr_{n0} = 1 + \frac{\lambda_{pull}}{\mu_{pull}} + \sum_{n=M+1}^{N} \frac{\lambda_{pull}}{\mu_{pull}} \left[\frac{(\lambda_{pull} \times q')^{n-1}}{\prod_{k=M+1}^{n-1} \mu_{pull} + k\xi q'}\right]$$

Expected pull system when balking and reneging is considered is defined as

$$Pull_{SysSizerb} = \sum_{n=M+1}^{N} nPr_n$$

And waiting time is derived as

$$E[TRB_{pull}] = \frac{Pull_{Syssizerb}}{\lambda_{pull}} X \sum_{i=M+1}^{N} p_i$$

(10)

D. Hybrid Model

Thus the expected access time for the proposed hybrid model, $E[T_{hybrid}]$, for any data item can be obtained by the combination of both push and pull models and is given by adding (3) with (9).

□[□ℎ□□□□□] = □[□□□□ℎ] + □[□□□□□□□] for Reneging

□[□ℎ□□□□□] = □[□□□□ℎ] + □[□□□□□□□□] for Reneging and balking

IV SIMULATION AND EXPERIMENTS

This section performs simulation experiments on the proposed system. The only and important goal is to reduce average access time.

The below are the assupmtions and parameters used to evaluate the simulation.

1. Total number of data items or the Database size N=1000
2. The size of the data items vary from 1 to 5
3. The arrival rate □ is varied 1 to 4. □□□□□ is assigned accordingly. The values □□□□ℎ = ∑□□=1 □□ × □□ and □□□□□ = ∑□□=□+1 □□ × □□ are estimted where □□ and □□ are access probabilities and size of data item i.
4. The skew coefficient, □, vary from 0.2 to 1.5
5. The reneging parameter, □, varied from 0.1 -0.5. And when it is set to 0. Probability of reneging set to 0.1 We retain the clients requests.
6. The probability of balking □′ varied from 0.1 to 0.5
7. The number of channels varied from 5 to 20 .
8. To compare the performance with the proposed hybrid system with clients reneging the work proposed in [11] is used , as per our knowledge, this is the algorithm considered client impatience but not how to retain them.

In the following discussion we evaluate the results obtained to show the effiency of our proposed method.

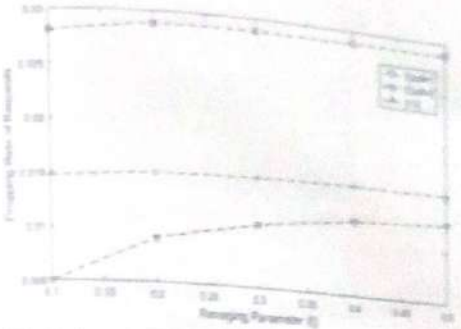

Fig 2: Impact Of Reneging Parameter on Dropping rate

Figure 3 shows that as the reneging parameter increase dropping rate of the requests increase. The algorithm defined in [11] shows the impact of dropping rate on reneging parameter. But the dropping rate of it is more when compared to our proposed algorithm. And it can be also concluded that as the number of channels for pull increase the dropping rate decreases drastically.

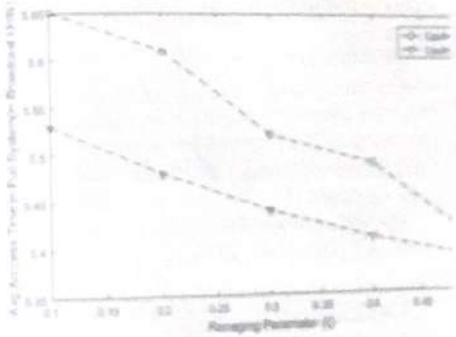

Fig 3: Minimum access Time with variation of reneging Parameter

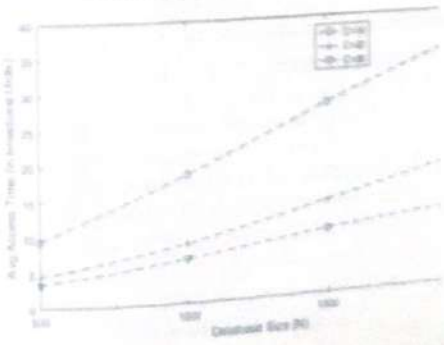

Fig 4 Varying access time with increasing in Database Size

It is observed that the as database size and number of channels increase there will be increase in average access time but increase with slower rate

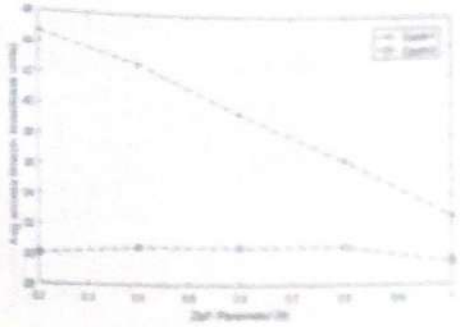

Fig 5: Expected access time with ZipF parameter

As ZipF or Skew Parameter increases the average access time decreases it is depicted in Fig 5.

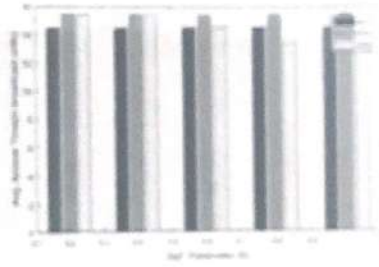

Fig 6: Impact of Arrival times on Avg Access Time

The varying arrival rates of data items have significant affect on the average access time of the system. From Fig 2 it is evident that for different access skewness and with increase in arrival rate the average access time also increases.

Table 1: Values of different parameters when reneging factor is varied

	Pull System Size	Dropping Rate	Avg Access time
0.1	13.4	0.2103	6.64

0.2	6.775	0.2576	3.96
0.3	4.5	0.26	3.7
0.4	3.4	0.2686	2.6
0.5	2.72	0.27	2.62

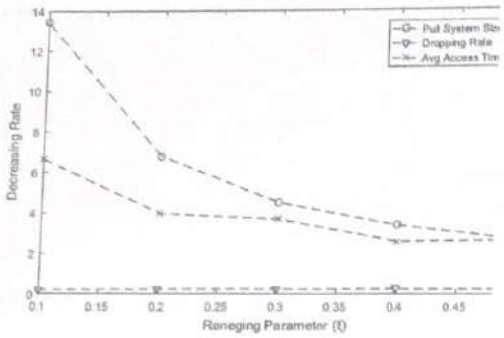

Fig 7:Affect of Reneging Parameter

From Fig 7 and table 1, it can be observed that increasing rate of reneging causes decrease in pull system size. Thus, resulting in increase in dropping rate of requests, it is concluded that more and more requests are dropped. Increase in drop rate will decrease in number of requests causing decrease in average access time.

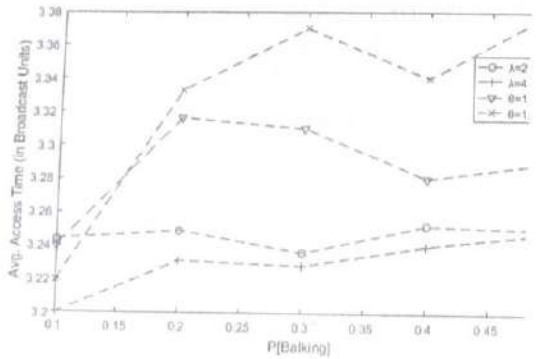

Fig 8: Comparision of Avg Access time with varying arrival rate and skew parameter

For evaluation of balking for the system we have choosen Database size to be , N=100 and M=60. Probability of the balking is varied from 0.1 to 0.5.Skew Parameter varies from 1 to 1.5 and arrival rate varies from 2 to 4.

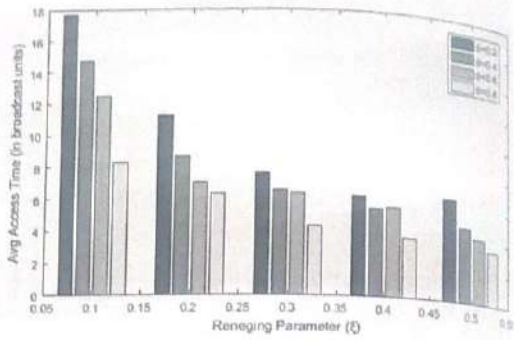

Fig 9: Impact of Reneging parameter

It is concluded from Fig 9 that increase in reneging parameter with varying access coefficient will decrease the access time of the data items requested by the clients.

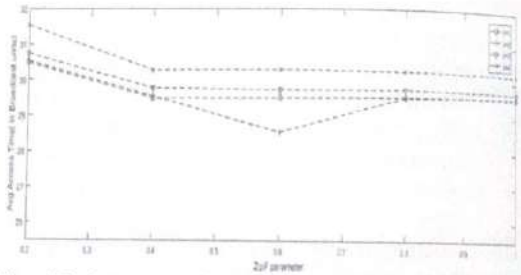

Fig 10 Impact of Retention of Reneged Client's Request

To evaluate the Fig 10 , reneging parameter set to 0 ($\theta = 0$). And it is evident that the avgerage access time decreases with increase in ZipF (skew) parameter reduced to pull model with push as the impatient clients are retained.

Similarly the model reduces to push model if the probability of balking is set to 0.

[Note : ZipF parameter and Skew Parameter are used Interchangeably. Both are one and the same]

V CONCLUSION

It is a tendency of the clients to become impatient while they are waiting for the required data item. They become impatient and leave the system before they are served. This causes changes in the access probabilities and affects the average access time. So this paper has proposed a hybrid scheduling algorithm of to minimize average access time with retention of impatient clients. This work can be extended to handle multiple requests for data item arise from same client.

References :

[1] S. Acharya, R. Alonso, M. Franklin and S. Zdonik. Braodcast Disks: Data Management for Asymmetric Communication Environments. *Proc.of ACM SIGMOD* , San Jose, May 1995

[2] W. C. Peng, J. L. Huang and M. S. Chen. Dynamic Levelling: Adaptive Data Broadcasting in a Mobile Computing Environment. In *Mobile Networks and Applications*, Vol. 8, pages 355-364, 2003.

[3] A. Bar-Noy, B. Patt-Shamir and I. Ziper, "Broadcast Disks with Polynomial Cost Functions", *ACM/Kluwer Wireless Networks*, vol. 10, pp.157-168, 2004.

[4] S. Acharya and S. Muthukrishnan. Scheduling on-demand broadcasts: New metrics and algorithms. In *Proceedings of the 4th Annual ACM/IEEE International Conference on Mobile Computing and Networking (MobiCom'98)*, items 43–54, Dallas, TX, USA, October 1998.

[5] S. Hameed and N. H. Vaidya. Efficient Algorithms for Scheduling Data Broadcast *Wireless Networks*, Vol. 5, pp. 183-193, 1999.

[6] C-L. Hu and M-S Chen, "Adaptive Information Dissemination: An Extended Wireless Data Broadcasting Scheme with Loan-Based Feedback Control, *IEEE Trans. on Mobile Computing*, vol. 2, no. 4, 2003

[7] J. W. Wong. Broadcast delivery. *Proceedings of the IEEE*, 76(12):1566–1577, December 1988.

[8] A. Bar-Noy, J. S. Naor and B. Schieber. Pushing Dependent Data in Clients-Providers-Servers Systems. In *Mobile Networks and Applications*, Vol. 9, pages 421-430, 2003.

[9] D. Aksoy and M. Franklin. R x W: A scheduling approach for large scale on-demand data broadcast. *IEEE/ACM Transactions on Networking*, 7(6):846–860, December 1999.

[10] R.Kumar and S.K.Sharma, "Queuing with reneging, balking and retention of Reneged Customers", International Journal of Mathematical Models and Methods in Applied Sciences, Issue 7,Vol 6, 2012.

[11] N. Saxena and M. C. Pinotti, \A Dynamic Hybrid Scheduling Algorithm with Clients' Departure for Impatient Clients in Heterogeneous Environments" *5th IEEE International Workshop on Algorithms for Wireless, Mobile, Ad Hoc and Sensor Networks (WMAN)* 2005.

[12] S. Acharya and S. Muthukrishnan. Scheduling on-demand broadcasts: New metrics and algorithms. In *Proceedings of the 4th Annual ACM/IEEE International Conference on Mobile Computing and Networking (MobiCom'98)*, items 43–54, Dallas, TX, USA, October 1998.

[13] Yiqiong Wu Guohong Cao , Stretch-optimal scheduling for on-demand data broadcasts , Computer Communications and Networks, 2001. Proceedings. Tenth International Conference, 2001

[14] K Prabhakara, K A Hua and J Oh. Multi-level multi-channel air cache designs for broadcasting in a mobile environment. *Proceedings of the IEEE International Conference on Data Engineering*, 2000.

R.KAVITHA, research scholar in Computer Science bearing registered no PP.COMP.SCI-268, from Rayalaseema University, Andhra Pradesh,India. Her area of interest is Design Analysis and Algorithms, Mobile Computing, Database Management System.
Email: kavitha1611@gmail.com

Dr.S.KRISHNAMOHAN RAO, **Principal**, Gandhi Institute of Technology, Bhubaneshwar, Khurda, India. His areas of specializations are Mobile Computing, MANETS, Adhoc Sensor Networks and Computer Networks.
Email:mohanrao.krishna@gmail.com

An analysis on effects of Demonetization on Cooperative Banks

[1] Nihar Ranjan Swain, [2] Dr. Rashmita Sahoo
[1] Asst. Prof, MBA, GIFT [2] Lecturer, Dept. of Business Administration, UU

Abstract: *This research paper focuses on the effect of demonetization on Banking Industry. We have taken the consideration of Cooperative Banks across the country after demonetization. Demonetization is a generations' memorable experience and is going to be one of the economic events of our time. Its impact is felt by every Indian citizen. Banks work as a lifeline for any economy; any positive or negative effect over them also affects economy of the country to a great extent. Hence, it becomes important to know how recent demonetization will affect the banking industry. This study focuses that demonetization is good but it has to be taken into consideration that most of the black money is kept in the form of land, buildings or gold or kept abroad. Only 4% of the total amount of black money is in cash, on which taxes are not being paid. Out of this, a lot of money is in circulation in everyday transaction. With move to demonetize Rs.500 and Rs.1000 notes by the central government had a strange fall out when Cooperative Banks, which are the backbone of the rural economy, have been paralyzed with the ban of accepting the old currency that are no long legal tender now. Cooperative banks have been the trusted centres to bank for millions of farmers and middle, low-income people for long. These institutions are known to offer them easier loan and deposit products and hence are the favourite institution for the poor. The restriction on the conduct of business after demonetization will have major impacts on these banks.*

Key Words: Demonetization, Taxes, Money Circulation, Legal Tender, Financial Health

Introduction:

Demonetization is the act of stripping a currency unit of its status as legal tender. It is necessary whenever there is a change of national currency. The old unit of currency must be retired and replaced with a new currency unit. In 2016, the Indian government decided to demonetize the 500 and 1000 rupee notes, the two biggest denomination notes. These notes accounted for 86% of the country's cash supply. The government's goal was to eradicate counterfeit currency, fight tax evasion, eliminate black money gotten from money laundering and terrorist financing activities, and promote a cashless economy. By making the larger denomination notes worthless, individuals and entities with huge sums of black money gotten from parallel cash systems were forced to convert the money at a bank which is by law required to acquire tax information from the entity.

The demonetization initiative caused a sudden breakdown in India's commercial ecosystem. Trade across all facets of the economy was disrupted, and cash-centric sectors like agriculture, fishing, and the voluminous informal market were virtually shutdown, with many businesses and livelihoods going under completely - not to mention the economic impact of millions of people standing in line for hours to exchange or deposit canceled banknotes rather than working or doing business.

"The unbanked and informal economy is hard hit," explained Monishankar Prasad, the New Delhi-based author and editor for Alochonaa, an Australian current events publication. "The poor do not have the

access to structural and cultural resources to adapt to shock doctrine economics. The poor were taken totally off guard and the banking infrastructure in the surroundings is rather limited. The tech class has poor exposure to critical social theory in order to understand the impact on the ground. There is an empathy deficit."

If there is any immediate casualty to Prime Minister Narendra Modi's demonetization exercise, announced on 8 November, that could possibly be for the country's cooperative banks, which are struggling to stay afloat. Though inefficient, cooperative banks are still critical for the last mile in rural India. This will continue for at least the next 5 - 10 years till larger banks/payment banks/small finance banks take firm hold in rural India.

Post demonetization, the cooperative banking sector is gasping for breath on account of a severe liquidity crisis. Soon after the demonetization announcement, cooperative banks were asked not to accept the old Rs. 500, Rs 1,000 currency note deposits or exchange those notes with the new currency notes. This meant that these lenders could only deal with permissible denominations of Rs 100 and below or takes deposits in new currencies that are hardly available in the system.

This has effectively left many smaller cooperative banks with a few thousand rupees of funds. "There is practically no business in the bank for last two months or so. It is going to be tough," said an official with one of the primary cooperative banks in Kerala, a state where cooperative banks play a crucial role in taking the banking services to the last mile.

Cooperative banks are particularly important for farmers and lower income groups who want small ticket loans in less time in relation to larger banks. The banking correspondents (BCs) system hasn't worked well so far though. Banking correspondents are agents of banks who operate in areas where there are no bank branches. The BCs collect deposits and offer loan products on behalf of the banks.

According to data from NABARD, there are 32 state cooperative banks, 370 district central cooperative banks (DCCBS) as on 31 March 2015. The number of primary agricultural credit societies (PACS), the smaller ones, as on 31 March 2014, stood at 93042, as per the latest data available.

Why cooperative banks should matter to us?

There are a couple of reasons why the government and the Reserve Bank of India (RBI) did not allow cooperative banks to accept or exchange old notes for the new currency.

First, the checks and balances at these banks aren't perceived to be strong enough to counter efforts to push black money into the banking system. Cooperative Bankers too aren't trained well. These banks aren't as tightly regulated as scheduled commercial banks. Most of these banks are indirectly controlled by politicians or local businessmen. Hence, there is, of course, reason to worry to let these banks participate in such a massive exercise. But, by choking funds to cooperative banks and prolonging the crisis can inflict significant damage to the health of several cooperative banks, which are already on the verge of closure. The small ones are more vulnerable.

The cooperative sector has largely been a failure on account of the accumulated losses, etc, but that situation is beginning to change after an overhaul initiated by the RBI and NABARD in 2010. Many inefficient corrupt banks have been shut and the remaining is good enough to continue.

State cooperative banks across the country have deposits to the tune of Rs. 1,02859 crore as on 31 March 2015 as against Rs

1,04369 crore as on 31 March 2014. They have a total loan outstanding of Rs. 1, 14545 crore as on 31 March 2015 with an impressive loan recovery percentage almost 95 percent.

On the profitability front too, the sector has done relatively well, of late. Of the total, 29 state cooperative banks posted total profit of Rs. 1,105 crore during 2014-15 as against Rs 926 crore by 27 state cooperative banks during 2013-14. Their NPAs stood at 5.02 percent of their total loans and advances outstanding as on 31 March 2015 as compared to 5.53 percent as on 31 March 2014.

In absolute terms, their NPAs stood at Rs. 5,746 crore during 2014-15 as against Rs. 5699 crore during 2013-14. Also, these banks' accumulated losses decreased to Rs 617 crore as on 31 March 2015 from Rs. 696 crore as on 31 March 2014.

Similarly, primary agriculture credit societies (PACS) too have an impressive record of deposit-lending operations, at least in recent years. Total members of PACS as on 31 March 2014 aggregated Rs. 13.01 crore of which, borrowing members at Rs. 4.81 crore constituted around 39 percent. On the deposit side, these banks mobilized Rs. 81,895 crore as on 31 March 2014, indicating a growth rate of 34 percent over the previous year. Currently, all these banks are under stress on account of severe cash crunch and most of them are not functioning.

As mentioned earlier, following restrictions, there has been hardly any business in cooperative banks across the country. Also, since there are no new funds, their lending operations and even ATM services have been hit hard. Even large multi-state cooperative banks, like Mumbai-based Saraswat cooperative bank are struggling to get funds for routine transactions of normal customers.

Second, the whole chaos will takes away the trust of common man from cooperative banks. Customers will think twice again before depositing their hard-earned money or taking a loan against their property from a local cooperative bank.

In states like Kerala, there have been massive protests already. Besides giving a major jolt to the cooperative banking sector, the PM will also risk the wrath of millions of common people - customers, who have deposited money in these banks.

As far as the crisis is concerned, the situation is precarious since most of these banks (especially PACS) are left with very few funds in acceptable denominations. Their credibility has also taken a hit since people will now be scared to park their money in future in these banks due to uncertainty. The current crisis could take the shape of a permanent impairment if cash crunch continues for a few months. It will take a long time for them to recover.

Impact of Demonetization on Cooperative Banking System

The volume of rural credit in India is mainly for short term credit (one year) for production of Kharif and Rabi crops and vegetables and medium term credit (three to five years) for allied sectors such as wells, pump sets, dairy, poultry, horticulture, plantation, etc. A small portion goes to non-agricultural sector such as artisans and tiny business/services.

Total rural credit disbursed by Commercial Banks (CBs), Regional Rural Banks (RRBs) and State/District Central Co-op Banks (SCBs/DCCBs) together in 2014-15 is about Rs. 845329 crore in 854 lakh accounts of which Rs. 346666 crore goes to small and marginal (poor) farmers in 486 lakh accounts. The number of total accounts at 854 lakh is a low number against rural population in crores. Money lenders and traders still play a big role in providing informal production credit plus consumption

credit to rural people at high interest rates. 518 lakh Kishan Credit Cards have been issued by all these credit agencies to farmers with average limit of one lakh rupees which can be used for both agricultural and consumption needs. Outstanding loans against such credit cards are reported to be Rs. 196781 crore as of March 2015. The major chunk of credit goes to Kharif and Rabi operations every year.

The share of co-op banks:

The share in rural credit of SCBs and DCCBs which have not been allowed to accept and exchange old 500 &1000 notes by RBI unlike Urban Co-op Banks (UCBs) which are mainly located in urban and semi-urban areas and has a very limited role in rural credit.

All SCBs and DCCBs are subject to statutory annual and bi-annual inspections under Banking Regulation Act, 1949. They are also subject to banking license, liquidity (cash reserve and statutory deposit) ratios maintenance with RBI and deposit insurance norms. It is therefore; wrong to say that they avoid KYC norms in maintaining deposit and loan accounts. However, they are exempt from income-tax on their profits which are very low in view of loans being given to farmers at lower rate (8 % for crop loans). On the other hand, to attract deposits, they pay higher rate of interest (by 0.5 - 1 %) on deposits compared to other banks, making their profit margin from thin to thinner.

Almost all SCBs have Scheduled Banks' status under the RBI Act, 1935. The SCBs are responsible for the DCCBs' operations. In 19 states, 371 member DCCBs with 14060 branches are extending rural credit to the farmers on behalf of the SCBs (3-Tier system) and in 12 states and UT, the SCBs does it directly through its 1131 branches (2-Tier system). The borrowing members are 92789 primary agricultural and non-agricultural credit societies of the farmers/artisans and also 31 lakh individual farmers/artisans whose societies are ineligible to borrow from the DCCBs or the SCBs due to high overdue percentage. The societies are members of either the DCCB branches in three-tier system or the SCB branches in two-tier system.

During 2014-15, rural credit of Rs. 340392 crore was disbursed by the SCBs/the DCCBs to the farmers and artisans through such co-op societies and also to individuals. Their total deposits are Rs. 436523 crore. The overdue as on March 2015 was 22% in DCCBs and 5 % at the SCB level. Thus, rural people are more honest in repaying their dues. In the event of famine, drought or scarcity, such short term loans are rescheduled payable over 3-5 years so that they do not turn ineligible for next year's crop seasons. There are total 2.60 lakh employees in this 3-tier/ 2-tier system with 1.64 lakh at village level, 0.83 lakh at DCCB level and 0.13 lakh at the SCB level.

(Source: National Federation of Co-op. Banks)

RBI data says 370 DCCBs held deposits of Rs. 236,890 crore as of 2014 while PACS had Rs. 81,900 crore deposits. Operations at 370 district central cooperative banks (DCCBs) and over 93,000 Primary Agricultural Credit Societies (PACS) have been severely hit with the Reserve Bank of India (RBI) slapping restrictions following the demonetization of Rs 500 and Rs. 1,000 notes. Urban cooperative banks (UCBs) too have complained to the RBI that commercial banks are refusing to provide them currency support, affecting their operations. The RBI has not given any reason for the curbs on DCCBs and PACS - these are considered the lifeline of the rural economy, especially for farmers in states like Maharashtra, Kerala, Uttar Pradesh, Gujarat, Tamil Nadu and Karnataka — but banking sources said it could be related to lax KYC (know your customer) norms and money laundering in some cooperative banks. RBI data says 370

DCCBs held deposits of Rs. 236,890 crore as of 2014 while PACS had Rs. 81,900 crore deposits.

The RBI has stipulated that DCCBs and PACS can allow existing customers to withdraw money from their accounts up to Rs. 24,000 per week until November 24. It has said no exchange facility against the specified bank notes (Rs 500 and Rs 1000) or deposit of such notes should be entertained by DCCBs. It has advised all banks to permit withdrawal of cash by DCCBs from their accounts based on need. According to Pramod Karnad, Managing Director, Maharashtra State Cooperative Bank (MSCB), only UCBs and SCBs are allowed to exchange and deposit notes. The Mumbai District Cooperative Bank, chaired by BJP member Pravin Darekar, has filed a petition in the Bombay High Court against the RBI circular preventing cooperative banks from accepting deposits in demonetized currency notes. The petition states that the circular is discriminatory and arbitrary besides violating fundamental rights. "No reason has been given for singling out cooperative banks like this. We act as bankers to other cooperative societies within Mumbai district. If the circular is followed, cooperative societies will not be able to deposit the discontinued currency notes with their banker. This would cause loss to members of such societies,". The petition points out that several hospitals, petrol pumps, medical stores have their accounts with the bank and they too will be affected. It states that there are 103,873 saving accounts being operated by individuals and 12,285 saving accounts of housing societies.

Although over 1,500 UCBs in the country are allowed to exchange and deposit demonetized notes, they said they have been at the receiving end of the demonetization scheme following inadequate remittances from the central bank. "While the apex bank has been making all efforts to provide liquidity for the nationalized and private sector banks, the common man's cooperative banking sector has been ignored with close to 52 cooperative banks being left out with empty hands over the past days," the UCBs said in a letter.

The Maharashtra State Cooperative Banks Federation Ltd, in a letter to RBI Deputy Governor R Gandhi, said, "after the announcement of the scheme of withdrawal of legal tender character of existing Rs. 500 and Rs. 1000 bank notes, commercial banks refused to provide currency support to our UCBs on November 10, 2016, treating us as 'general customers'. Later, in spite of issuance of circular by the RBI that the limit of Rs 10,000 is applicable to general customers and not applicable to cash withdrawal from a bank account by one bank from another bank, these public sector banks, especially SBI and Bank of India refused to adhere to the request of UCBs." "While the RBI did offer some remittances in the first few days, the approach in the past days are far from encouraging for the fraternity, which has been fighting shoulder to shoulder with other bankers to make the national cause of demonetization a great success," the letter said. As many as 1,579 cooperative banks have over 10,000 branches and close to 3,000 operational ATMs across the country and constitute nearly four per cent market share in the banking business mix of the country. UCBs have to depend on local currency chests of public/private sector banks to withdraw or deposit the currency, while many others have partnership of payment systems with the National Payments Corporation of India (NPCI).

Most of these UCBs, the letter stated, are direct members of the RBI for CTS (cheque truncation system) and, therefore, expect good cooperation from the SBI as well as from the other public/private sector banks. "While there are huge queues lined up with public and private sector banks, the

cooperative banks have been left out for want of legal tender adding to the chaos," the letter stated.

Cash deposits in 285 district cooperative banks (DCBs) across India surged six fold in the first four working days after the recall of high-value currency on November 8, as compared to reserves a day before the announcement. An analysis of classified bank transaction data revealed DCBs deposited Rs. 3,051.2 crore with public sector banks between November 8 - when Rs 500 and Rs 1,000 were withdrawn - and November 14, when the Reserve Bank of India (RBI) banned the institutions from accepting cash. This is six times the Rs. 496.88 crore reserves in the DCBs on November 7. All cooperative banks maintain a current account with a public sector bank, where they have to hold their cash deposits.

There are three types of cooperative banks in India, state cooperative bank, urban cooperative banks and district cooperative banks. Only DCBs were banned by RBI after allegations of money laundering. But around 100 urban cooperatives banks are also being probed by the ED. In the first three weeks after demonetization, nearly Rs. 12,000 crore worth high-value cash deposits worth Rs. 80 lakh each were made by 325 urban cooperative banks from remote districts, This is nearly a 25-fold increase in cash balance of these urban cooperative banks compared to their last balance on November 7.

The government and Reserve Bank of India (RBI) are set to bring out tougher norms for cooperative banks, which have come under scanner for alleged discrepancies and irregularities in the wake of the demonetization drive. According to a recent report by the income tax department, most banks have indulged in money laundering after the central government announced ban on high-value bank notes of Rs. 500 and Rs. 1,000 from November 8 midnight.

Many banks accepted and exchanged the old currency notes at a premium and parked large deposits in multiple accounts, the report added. Moreover, several accounts have been opened without following Know-Your-Customer norm, the report pointed out. A senior government official said these banks could become conduits for black money in the future. At present, the scrutiny and vigilance on these banks is not as stringent as that on scheduled commercial banks. "These banks need to be monitored as carefully as any other scheduled commercial banks have been used for a large number of inappropriate activities in the past and these can be used for the same purpose in the future," the official, who did not wish to be identified.

Demonetization: Retaining Credibility of Co-operative Banks:

With move to demonetize Rs. 500 and Rs.1000 notes by the central government had a strange fall out when Cooperative Banks which are the backbone of the rural economy, have been paralyzed with the ban of accepting the old currency that are no long legal tender now.

Operations at 370 district central cooperative banks (DCCBs) and over 93,000 primary agricultural credit societies (PACS) have been severely hit with the Reserve Bank of India (RBI) slapping restrictions following the demonetization of Rs. 500 and Rs. 1,000 notes.

In a direction to the banks, RBI says that they have advised the Urban Cooperative Banks through its Regional Offices and the State Cooperative Banks through National Bank for Agricultural and Rural Development (NABARD) of the need to ensure strict compliance with the instructions issued with regard to exchange of specified bank notes as also deposit of such notes into the accounts of their customers. But there were reports that some cooperative banks were not strictly adhering to the instructions issued

in connection with the withdrawal of legal tender status of the existing Rs. 500 and Rs. 1000 bank notes (specified bank notes).

The Reserve Bank of India's restrictions drive during the demonetization for the Cooperative Banks who have provided credit to farmers and three-tier banking system is one of the largest in the country. Like the Railways, the Cooperative Banks have also been described as the lifeline of the state's economy and there had been protests following the RBI decision and the cooperative sector went on strike last week.

The government must allow Cooperative Banks to function or farmers which have been their source of funds for decades and have suddenly become invalid. Dr. Anand Rai Vyapamm scam whistleblower has rightly pointed out that this step was taken because some cooperative banks are dominated by politicians and were reportedly being used to launder Rs. 500 and Rs. 1000 notes.

The discrimination towards the Cooperative Banks will put the credibility of the banks at stake. The RBI and the Central Government should have taken this into consideration before meting out discriminatory treatment. The whole chaos will takes away the trust of common man from cooperative banks. Customers will think twice again before depositing their hard-earned money or taking a loan against their property from a local cooperative bank. Due to uncertainty, the people will now be scared to park their money in future in these banks due to uncertainty as their credibility has also taken a hit. The current crisis could take the shape of a permanent mutilation if cash crunch continues for a few months and it will take a long time for them to recover. Instead, the government should have tried to strengthen the infrastructure and capabilities of these banks instead of bringing them on the verge of collapse.

Conclusion:

Cash crunch is the new norm for most people after demonetization, and some of the worst impacted are customers of co-operative financial institutes - banks and societies. One problem with the structure of the cooperatives is that there are multiple regulators. The control of the Reserve Bank of India (RBI) on state, district and urban cooperative banks get diluted because of this. Also, cooperative banks and societies chose their management through an election process. Given that cooperative banks are largely controlled by politicians, investors also need to be very careful about their banking practices. If the loans are granted very easily, the deposits will be at risk. Customers should not get lured to banking with a cooperative financial institution just because it does not insist on you giving PAN number, or does not deduct TDS on interest, etc. If you are not comfortable doing the due diligence, then it is best to avoid co-operative banks. Even as things are on the mend, the problems - situational and institutional - are still there. There is surely cause for concern, but experts advise against any panic decisions. They insist that investors need to evaluate whether or not they are banking with strong institutions. "Instead of avoiding cooperative banks altogether, customers need to do stress on due diligence.

References:

[1] Braga, F.D., Isabella G and Mazzon J.A., (2013). Digital wallets as a payment method influence consumer in their buying behaviour, Available at http://www.anpad.org.br/admin/pdf/2013_EnANPAD_MKT1209.pdf

[2] Deodhar, Rahul Prakash, Black Money and Demonetisation (November 14, 2016). Available at SSRN: https://ssrn.com/abstract=2869172

[3] Lee, Jinkook, Fahzy Abdul-Rahman, and Hyungsoo Kim. "Debit card usage: an examination of its impact

on household debt." Financial Services Review. 16.1 (2007): 73.

[4] Mercatanti, Andrea, and Fan Li. (2014). "Do debit cards increase household spending? Evidence from a semiparametric causal analysis of a survey." The Annals of Applied Statistics. 8.4: 2485-2508.

[5] Morewedge, C. K., Holtzman, L., & Epley, N. (2007). Unfixed resources: perceived costs, consumption, and the accessible account effect. Journal of Consumer Research, 34(4), 459–467).

[6] Padmini Sivarajah. (2016, Nov. 11). Demonetisation: Madurai Corporation makes record tax collection on a single day. The Times of India. Retrieved from http://timesofindia.indiatimes.com/city/chennai/Demonetisation-Madurai-Corporation-makes-recordtax-collection-on-a-single-day/articleshow/55374378.cms

PTI. (2016, Nov. 9). Demonetisation will benefit economy in long run: Jaitley. The Hindu Business Line. Retrieved from http://www.thehindubusinessline.com/economy/demonetisation-to-increase-ecosize-enhance-revenue-base-says-jaitley/article9324312.ece

PTI . (2016, Nov. 12). Hyderabad civic body collects Rs 65 crore of property tax. The Indian Express. Retrieved from http://indianexpress.com/article/india/india-news-india/demonetisation-hyderabadcivic-body-collects-rs-65-crore-of-property-tax-4372156/

http://www.businessinsider.in/shocking-more-than-rs-9000crore-deposited-across-cooperative-banks-of-the-country-after-demonetization/articleshow/56046405.cms

★★

★

Enhancing Performance of Detonation Driven Shock Tube

[1]Swagatika Acharya ,[2] Tatwa Prakash Pattsani
[1][2] Gandhi Institute For Technology (GIFT)

Abstract— To produce high enthalpy flow detonation driven shock tube is needed. If a damping section is attached at the end of the driver then it can eliminate the high reflection pressure which is produced by detonation wave, and as a result the backward detonation driver can be employed to generate high enthalpy and high density test flow. By using this apparatus, a strong shock wave is generated by detonating an oxygen-hydrogen mixture. The detonation wave is induced by the expansion of helium or air. A detonation wave is produced by this method which propagates downstream that transition into a shock wave in the driven section.

Index Terms— Shock tube, detonation-driven, high-enthalpy

INTRODUCTION

The shock tube is required to reproduce and direct blast waves at a sensor to simulate actual explosions and their effects. A detonator is a device used to trigger an explosive device .Shock tube produces a moving normal shock wave by sudden bursting of a diaphragm which separates a high pressure section and a low pressure section. This is basically a closed tube divided by a diaphragm into two sections of substantially different pressures. The material used for shock tubes is mostly brass or steel. The diaphragms are made of cellophane, copper, aluminum, or steel depending upon the strength of the shock wave required. The diaphragm is ruptured either by increasing the pressure difference between the sections or by puncturing with a mechanical device. When the diaphragm gets ruptured the gas at high pressure (driver) side acts like a piston and presses the gas at low pressure (driven) side. As a result a shock wave propagates into the driven section and compresses the test gas. A detonator is a device used to trigger an explosive device. A shock tube detonator is a non-electric explosive fuse or initiator in the form of small-diameter hollow plastic tubing used to transport an initiating signal to an explosive charge by means of a percussive wave traveling the length of the tube. It contains a small quantity of high explosive, but safer and more reliable than detonating cord with the same quantity of explosive. A shock tube detonator designed to initiate explosions, generally for the purpose of demolition of buildings and for use in the blasting of rock in mines and quarries. Instead of electric wires, a hollow plastic tube delivers the firing impulse to the detonator, making it immune to most of the hazards associated with stray electric current. It consists of a small diameter, three-layer plastic tube coated on the innermost wall with a reactive explosive compound, which, when ignited, propagates a low energy signal, similar to a dust explosion.

METHODOLOGY

A shock tube detonator is a non-electric explosive fuse or initiator in the form of small-diameter hollow plastic tubing used to transport an initiating signal to an explosive charge by means of a percussive wave traveling the length of the tube. It contains a small quantity of high explosive, but safer and more reliable than detonating cord with the same quantity of explosive. Another early product contained an

Proceedings of IIRAJ International Conference (ICCI-SEM-2K17), GIFT, Bhubaneswar, India, 18th - 19th February 2017, ISBN: 978-93-86352-38-5

enclosed combusting, non-detonating fiber.

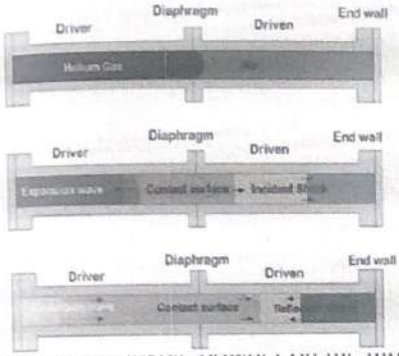

Th c outer
dia ny
dusting of explosive powder on the tubing's inner surface, which detonates down the tube at a speed greater than 6500 feet per second but does not burst the tube. Being non-electrical and nonmetallic, shock tubes are less sensitive to static electricity

aluminum and is pressed into place above the base charge, usually TNT or tetryl in military detonators and PETN in commercial detonators.

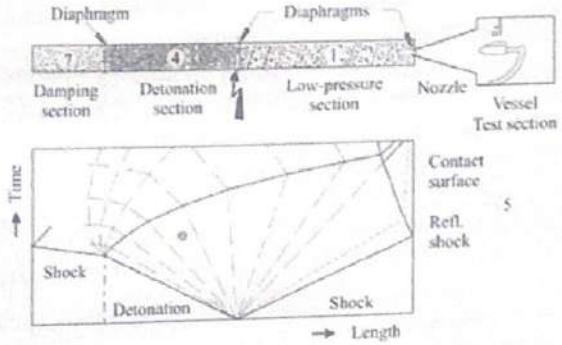

Other materials such as DDNP (diazo dinitro phenol) are also used as the primary charge to

ISSN:2277-
International Journal of Engineering and
Volume 1, Issue 3

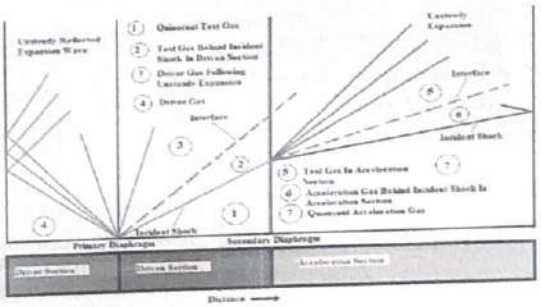

Fig. 2.5. Wave diagram of an expansion tube [11]

pressure. The pressure rise following the detonation wave is constant, but the momentum

and radio frequency energy and thus have replaced many uses of electric detonators and are safer to handle and store than detonating cord. A version containing an explosive gas mixture has the additional advantage of being entirely inert until the tubing is charged with the gas.

One manufacturer estimates that over 2 billion feet of shock tube are used each year worldwide, in commercial blasting, military demolition, theatrical special effects, automobile airbags, aircraft escape systems, IED initiation and professional fireworks.

The commercial use of explosives uses electrical detonators or the capped fuse which is a length of safety fuse to which an ordinary detonator has been crimped. Many detonators' primary explosive is a material called ASA compound. This compound is formed from lead aside, lead styphnate and reduce the amount of lead emitted into the atmosphere by mining and quarrying operations. Old detonators used mercury fulminate as the primary, often mixed with potassium chlorate to yield better performance. Two modes of operation are possible. In the upstream-or backward propagation mode, the ignition source is just upstream of the primary diaphragm between the detonation and driven sections. In this case, the detonation wave propagates upstream.

imparted to the driver gas by the detonation wave is directed upstream, that is, opposite to the main flow. This leads to a reduction of the effective driver performance. Shortly after initiation, the main diaphragm opens and the burnt products exhaust into the low-pressure section, driving the incident shock that compresses and heats the test gas. A Taylor expansion immediately follows the

detonation wave, decelerating the burnt gas to zero velocity along the characteristic labeled. Detonation is a type of combustion involving a supersonic exothermic front accelerating through a medium that eventually drives a shock front propagating directly in front of it. Detonations occur in both conventional solid and liquid explosives, as well as in reactive gases. The velocity of detonation in solid and liquid explosives is much higher than that in gaseous ones, which allows the wave system to be observed with greater detail (higher resolution). An extraordinary variety of fuels may occur as gases, droplet fogs, or dust suspensions. Oxidants include halogens, ozone, hydrogen peroxide and oxides of nitrogen. Gaseous detonations are often associated with a mixture of fuel and oxidant in a composition somewhat below conventional flammability ratios. They happen most often in confined systems, but they sometimes occur in large vapor clouds. A shock wave or shock is a type of propagating disturbance. When a wave moves faster than the local speed of sound in a fluid it is a shock wave. Like an ordinary wave, a shock wave carries energy, and can propagate through a medium; however it is characterized by an abrupt, nearly discontinuous change in pressure, temperature and density of the medium. In supersonic flows, expansion is achieved through an expansion fan also known as a PrandtlMeyer expansion fan.

RESULT

The inputs are as given below.
Pressure in driver section – 15 bar (Helium).
Pressure in driven section – 0.2 bar (Air).
Pressure in the nozzle – 0.00002 bar (Air).
Temperature all three section – 300K. Variation of diameter of shock tunnel, pressure, temperature, velocity can be clearly seen.

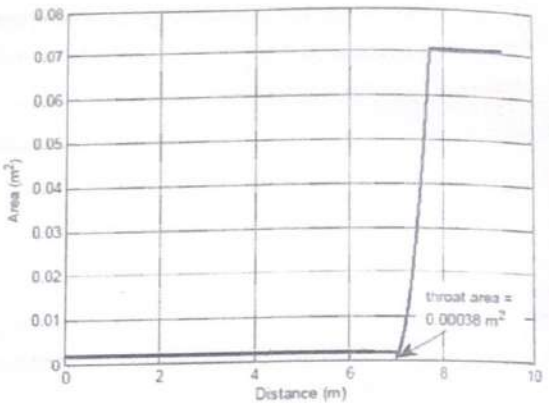

CONCLUSION

This work has been done to design 1D shock tube with one and two diaphragms with help of different numerical solver. A CFD solver was developed for a rectangular CD nozzle having unit width which gives a Mach number 5. A shock tunnel CFD solver was also developed to study the properties variation in a shock tunnel which gives a shock Mach number nearly equal to 6. Two solvers were also developed for calculation of fluid and flow properties across the shock wave and Mach number using EXCEL. Simulation is done to obtain a wide range of Mach number varying the pressure ratio and using different driver gases.

REFERENCE

[1] http://www.aero.iisc.ernet.in/lhsr/history.htm.
[2] http://accessscience.com/content/Hypersonicflight/333400.
[3] Bertin, J. J. (1994). Hypersonic Aerothermodynamics. Washington DC, AIAA.
[4] Hirshel, E. H. (2005). Basics of Aerothermodynamics. Heidelberg, Springer.
[5] http://en.wikipedia.org/wiki/Shock_tube.